Charles University in Prague, Faculty of Science

Department of Organic Chemistry

Vishwas D. Joshi

Synthesis of novel helquats and their properties

PhD. Thesis

Supervisor: Mgr. Filip Teplý, PhD.

Institute of Organic Chemistry and Biochemistry, CAS

Prague-2017

Prohlašuji, že jsem předloženou doktorskou dizertační práci vypracoval samostatně a uvedl všechny použité literární prameny. Dále prohlašuji, že jsem nepředložil tuto práci ani její podstatnou část k získání jiného nebo stejného akademického titulu.

This work was carried out in years 2011-2017 at the IOCB, CAS. I declare that I have done the PhD. thesis independently citing all resources used. I also declare that I did not use this work to get the same or another university degree.

Prague, October 2017

……

Vishwas D. Joshi

Acknowledgment

I would like to acknowledge number of people, who helped me a lot during the completion of my PhD. over last six years. I would like to express my gratitude to my supervisor, Dr. Filip Teplý for giving me an opportunity to join his group as a PhD. student and work on a multidisciplinary project. He assigned me a project, which includes synthesis, characterization, and study of various properties of the compounds in order to explore the application potential. I also like to thank all my former and present group mates for providing a nice and healthy atmosphere in the lab.

I am indebted to Jaroslav Kozak, Erika Kuzmova, and Miroslav Hájek for their help in the designing of biological experiments. I want to express my sincere thanks to Dr. David Šaman (NMR), Dr. Ivana Cisarova (X-ray crystallography), Dr. Lucie Bednárová (CD spectroscopy), and Dr. Pavel Fiedler (IR spectroscopy). In addition, I want to thank the team of mass spectrometry and analytical department of IOCB CAS. I am expressing my sincere thanks to Prof. Vladimír Dohnal (UCT Prague) for allowing me to use instruments in his research group.

I would like to thank Prof. Benjamin Coe and all other co-authors for collaborating with us during the study of nonlinear optical properties of functionalized helquats.

I would like to thank Prof. Pavel Hobza, Martin Lepšík, and Adam Pecina for the theoretical study regarding dsDNA binding properties of one of the functionalized helquat derivatives.

In addition, I would like to thank IOCB CAS, and all relevant research groups from the IOCB for an opportunity to access all the key facilities for the research, Czech Science Foundation and Charles University in Prague for the financial support.

On this occasion, I would like to remember my early mentor at IOCB, late Dr. Illya Lyapkalo, for his teaching and support during my early days at IOCB. I also want to thank the previous team of Dr. Lyapkalo, who helped me a lot during my early days.

I would also like to take this opportunity to thank my early stage mentors, Dr. C. V. Rode, Scientist, National Chemical Laboratory (CSIR), India and Professor U. D. Joshi, Swami Ramanand Teerth Marathwada University, India for inspiring me to choose research as a career and pursuit a PhD. degree in Chemistry.

Finally, I like to thank my family and friends for giving me an emotional support during this time.

Abstrakt

Předmětem této dizertační práce je syntéza nových helquatů, studium jejich vlastností, např. nelineárně-optické vlastnosti, cílově specifické fluorescenční light-up vlastnosti, molekulární rozpoznávání (zahrnující chirální rozpoznávání dvouvláknové DNA s použitím opticky čistých helquatových barviv) a jejich aplikovatelnost založená na těchto vlastnostech.

Byly syntetizovány čtyři nové helquaty obsahující aktivované methylové skupiny a jeden z těchto helquatů byl úspěšně v gramovém měřítku rozštěpen na enantiomery pro následné aplikace. Syntéza funkcionalizovaných helquatových derivátů byla vyvinuta za použití Knoevenagelovy kondenzace helquatu s aktivovanými methylovými skupinami s různě substituovanými aromatickými a heteroaromatickými aldehydy. Tato metodika otevřela snadný přístup ke strukturně rozmanité knihovně více než 500 sloučenin skrze nechromatografické purifikace ve středních až vysokých výtěžcích. Zástupci této knihovny sloučenin byly prozkoumány v následujících směrech: jako nové nelineárně optické chromofory, cílově specifické fluorescenční ligth-up próby pro rozpoznávání cílů jako heparin nebo dvouvláknová DNA. Několik helquatových derivátů vykazovalo fluorescenční light-up v přítomnosti AT bohatých DNA sekvencí. Tato vlastnost byla dále detailně studována s použitím různých spektroskopických technik. Aplikace jedné z těchto sloučenin, **HeliDye1**, jakožto fluorescenční próby pro mikroskopii, gelovou elektroforézu a průtokovou cytometrii byly demonstrovány. Ve spolupráci s teoretickými chemiky jsme byli též schopni identifikovat možné vazebné módy molekul interagujících s dvouvláknovou DNA.

Abstract

The subject of this thesis comprises synthesis of novel helquats, exploration of their different properties, such as nonlinear optical properties, target-specific fluorescence light-up properties, molecular recognition properties (including chiral recognition of dsDNA using enantiopure helquat dyes) and their applicability based on these properties.

Four novel helquats containing activated methyl groups were synthesized and one of the synthesized helquats has been successfully resolved in gram scale into two separate enantiomers for further applications. Synthesis of functionalized helquat derivatives employing Knoevenagel condensation reaction between helquats having activated methyl groups and various substituted aromatic and heteroaromatic aldehydes has been developed. This methodology opened an easy access to a structurally diverse library of more than 500 compounds *via* chromatography-free purifications in moderate to high yield. Members of this compound library have been explored in various directions: as novel nonlinear optical chromophores, target-specific fluorescence light-up probes for recognition of targets like heparin and dsDNA. Few helquat derivatives have shown fluorescence light-up in presence of AT-rich DNA sequences. This feature has been further studied in detail using various spectroscopic techniques. Applications of one of these compounds, **HeliDye1,** as a fluorescent probe for microscopy, gel electrophoresis and flow cytometry has been demonstrated. In collaboration with theoretical chemists, we were also able to identify possible binding modes of the dsDNA interacting compound.

Abbreviations

aq.	aqueous
Ac	acetyl
Bn	benzyl
br	broad
n-Bu,	*n*-butyl
t-Bu	*tert*-butyl
calc.	calculated
cat.	catalytic
COSY	two-dimensional homonuclear correlation NMR spectroscopy
δ	chemical shift in parts per million relative to tetramethylsilane
CAM	cerium ammonium molybdate
d	doublet
DCM	dichloromethane
D-DBT	D-dibenzoyl tartrate
DFT	density functional theory
ds	double stranded
HOMO	highest Occupied Molecular orbital
DME	1,2-dimethoxyethane
DMF	*N*,*N*-dimethylformamide
DMSO	dimethyl sulfoxide
ee	enantiomeric excess
EI	electron impact ionization
ESI	electro-spray ionization
eV	electron volts
esu	electrostatic unit
equiv.	equivalents
EtOAc	ethyl acetate
FACS	Fluorescence-Activated Cell Sorting
h	hours
HMBC	heteronuclear multiple bond correlation
HMQC	heteronuclear multiple quantum correlation
HQ	helquat
HRMS	high-resolution mass spectrometry
HSQC	heteronuclear single quantum correlation
Hz	hertz
i-Pr	isopropyl
IR	infrared spectroscopy
J	coupling constant (in NMR spectrometry)
LUMO	lowest occupied molecular orbital
m	multiplet (spectral); meter(s); mili
M+	parent molecular ion
MeCN	acetonitrile
MHz	megahertz
m.p.	melting point
MS	mass spectrometry

MTBE	methyl tert-butyl ether
m/z	mass-to-charge ratio
NMR	nuclear magnetic resonance
NOESY	nuclear overhauser effect spectroscopy
NLO	nonlinear optics
o	*ortho*
p	para
ppm	part(s) per million
n-PrCN	*n*-propionitrile
PI	propidium iodide
PTC	phase-transfer catalysis/catalyst
Py	pyridine
q	quartet
R_f	retention factor (in chromatography)
ROESY	rotating frame overhauser effect spectroscopy
rt	room temperature
s	singlet (spectral); second(s)
ss	single stranded
S_N2	substitution nucleophilic bi-molecular
TBAB	tetra-*n*-butylammonium bromide
TD-TFT	time-dependent Density Functional Theory
TfOH	triflic acid
TfO^-	trifluoromethanesulfonate
TLC	thin layer chromatography
t	triplet (spectral)

Table of Contents

1. Introduction:

Helquats are a class of synthetic *N*-heteroaromatic cations described by our laboratory in 2009. [1] They possess intrinsic helical chirality like helicenes[2] and extended cationic skeleton similar to diquats.[3] This class of compounds thus embody structural features of both helicenes and Viologens and we expect emerging properties for this class of compounds (Fig. 1).

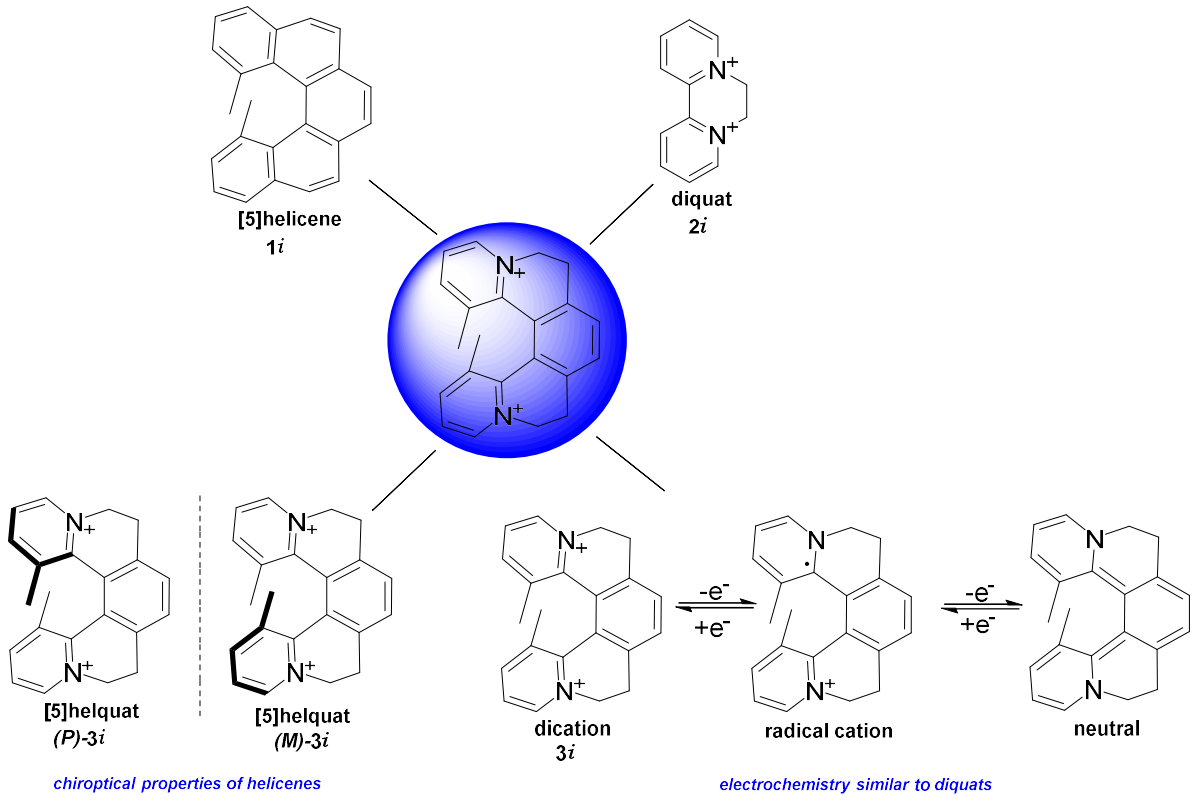

Fig.1: *Structural features of helquats*

So far, our group has reported some interesting features of this class of compounds. Remarkable chiroptical properties like helicenes,[4] SET reduction to radical cation or neutral form similar to diquats,[5] existence of saddlequat lying on helquat racemization pathway,[6] the circulenoid formation and fragmentation by photochemical and thermal process respectively[7] and the functionalization of helquats to give helical cationic styryl dyes *via* Knoevenagel condensation chemistry.[8]

Furthermore, helquats can be used as organocatalysts in organic reactions such as Aldolization and Mannich.[9]

The hypothesis of this thesis is that helquats can be used as novel nonlinear optical materials as well as in recognition exploiting their interactions with cavities and grooves of the biological targets.

One of the main incentives for the introduction of helquats as a novel structural class was fascinating chemistry of helicenes and their application promise. On the other hand, researchers reported number of *N*-heteroaromatic cationic molecules from natural and synthetic sources to have attractive and useful properties.

1.1 Natural and synthetic N-heteroaromatic cations:

Nicotinamide adenine dinucleotide, NAD^+, **4*i*** is a pyridinium based structures and together with its reduced form, NADH, it is known for its key role in cellular metabolism (Fig. 2).[10]

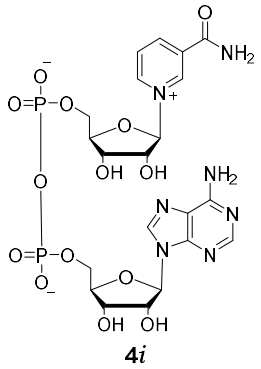

4*i*

Fig. 2: *Nicotinamide adenine dinucleotide.*

Cationic alkaloids containing isoquinolinium and phenanthridinium moieties (Fig. 3) are secondary metabolites which comprise two main groups benzo[*c*]phenanthridines and protoberberines.[11] Berberine **5*i*** is a fluorescent antibiotic used in Ayurveda[12] and also used as a fluorescent stain for heparin in mast cells.[13] Isoquinolinium alkaloids (**5*i*** to **8*i***) are known for their telomeric G-quadruplex binding activity,[14] antifungal activity,[15] antioxidant activity,[16] antimalarial[17] and antidepressant activities.[18]

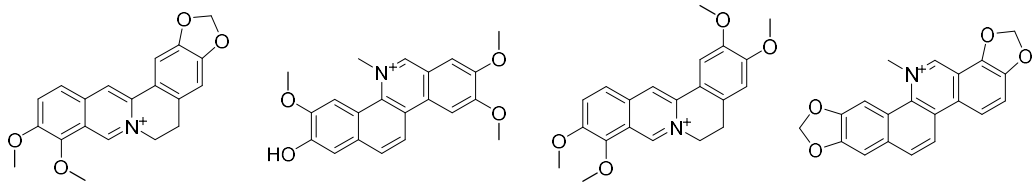

Fig. 3: *Structures of cationic alkaloids.*

N-heteroaromatic cationic molecules are also known for their applications as novel materials, nonlinear optical properties, ionic liquids, as probes for nucleic acids (Fig. 4, **9*i***) and other biological targets. Due to their ionic nature, they usually have good solubility in water. Coralyne (Fig. 4, **10*i***) is a synthetic member of protoberberine family which shows a significant anti-leukemic activity.[19] Various substituted derivatives of berberine are known to interact with G-quadruplex DNA with improved telomerase targeting activity as compared to natural berberine.[20]

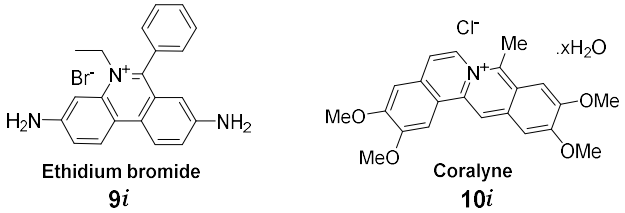

Fig. 4: *Cationic intercalator Ethidium bromide (**9i**) and anti-leukemic drug Coralyne (**10i**).*

$TMPyP_4$ tosylate (**11*i***),[21a] TQMP (**12*i***)[21b] substituted acridine derivative, **13*i*** [21c] and many other synthetic *N*-heteroaromatic cationic molecules (e.g. **14*i*** [21d] and **15*i*** [21e]) are known for their G-quadruplex-DNA stabilizing properties (Fig. 5).

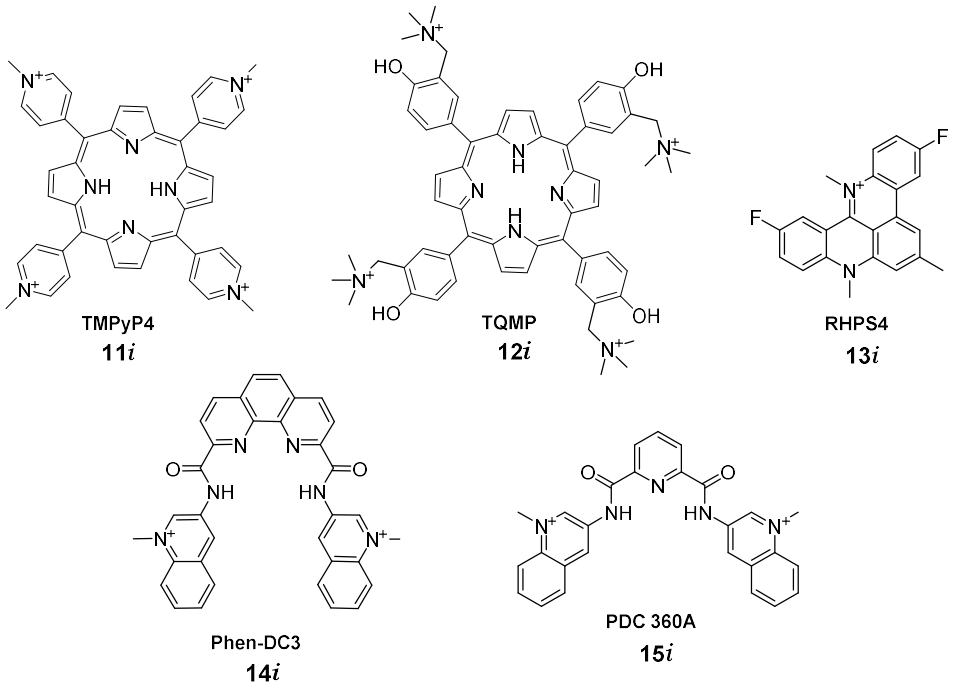

Fig. 5: *G-quadruplex stabilizing ligands.*

Other than biological activities of the *N*-heteroaromatic cationic molecules, such molecules found their uses as novel ionic liquids like **16*i*** or **17*i*** (Fig. 6). Ionic liquids have low melting points and negligible vapour pressure which makes them suitable to be used as solvents for many chemical reactions.[22] Ionic liquids are usually regarded as ‘‘green solvents.’’ All these unique properties of ionic liquids make them applicable in diverse fields such as separation technology,[23] nanotechnology,[24] catalysis[25] and biocatalysis.[26]

Fig. 6: *Cationic ionic liquids.*

Pyridinium and bipyridinium based systems are attractive because of their electron withdrawing properties (pull effect),[27] redox properties,[28] electro-optical and photophysical properties.[29] By virtue of all these properties, they are suitable as electrophores in artificial systems developed for solar energy conversion,[30] components of choice in supramolecular assemblies designed to behave as electron storage systems[31] and as molecular machines.[32]

1.2 Helicenes

Helicene is a specific class of helical molecules formed due to the *o*-fusion of aromatic, heteroaromatic or semi-aromatic rings. The helical arrangement of such molecules is feasible, because it gives a relief from the steric strain. Due to this nonplanar type of arrangement, the molecules become chiral despite of lacking a stereo center and the molecules are called as helically chiral molecules (**18*i*** to **22*i***, Fig. 7).[33]

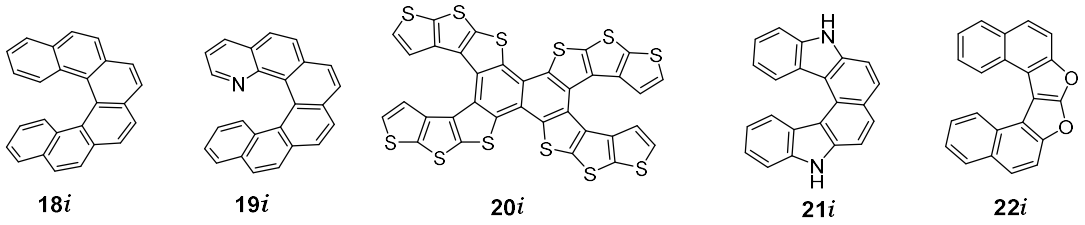

Fig. 7: *Structures of carbo and heterohelicenes.*

According to the rule of helicity (Ingold and Prelong, 1966), a left-handed helix is designated as "minus" and denoted as ''*M*'' and a right-handed one is designated as "plus" and denoted as ''*P*'' (Fig. 8).

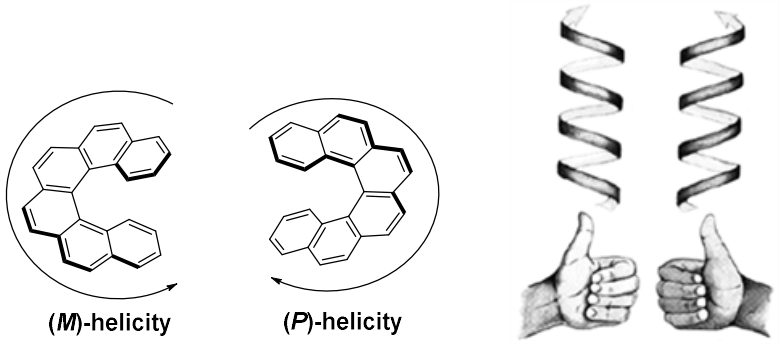

Fig. 8: *Schematic representation of helicity*

Examples of helical chirality in nature are right handed and left handed structures of dsDNA and some of the proteins.

- ***Synthesis of carbo and heterohelicenes:***

Classical synthesis of *racemic* helicenes (for e.g. **24*i***) *via* an oxidative photocyclization of stilbene type precursors (**23*i***) was reported by Martin *et al.* in 1967.[34] Due to the easy availability of stilbene-type precursors prepared by Wittig olefination, many helicene homologues, starting from [5] to [14]helicene and their derivatives were prepared. The main drawback of photochemical synthesis is the use of very high dilute solutions of reaction components in carcinogenic solvents like benzene and formation of isomers. Therefore, in modern methodologies using non-photochemical methods were more encouraged.

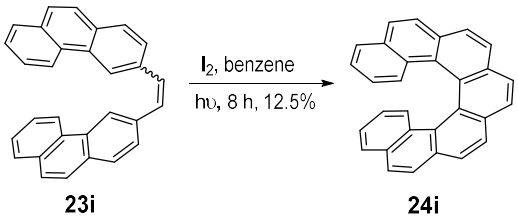

Scheme 1: *Classical way of synthesizing helicene.*

Katz and Liu did the pioneering work to develop one of the modern, convenient and non-photochemical approach for the synthesis of *racemic* helicene bisquinones by Diels-Alder reaction.[35] The other reported approaches are carbenoid coupling,[36] tin-mediated, non-reducing tandem radical cyclization of (*Z,Z*)-1,4-bis(2-iodostyryl)-benzene derivatives[37] and many more.

Collins *et al.* introduced a novel approach in helicene chemistry. A transition metal catalyzed ring closing olefin metathesis of substrate **25*i*** in microwave at 100 °C or by classical heating at 40 °C in a sealed tube[38] gave [5]helicene, **26*i*** (Scheme 2).

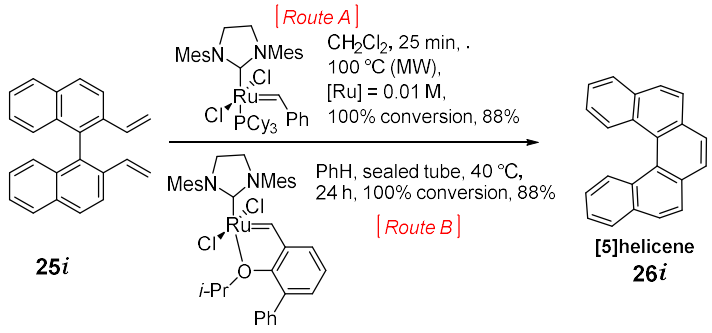

Scheme 2: *Olefin metathesis method for helicene synthesis.*

Guitian *et al.* were the first to introduce an intramolecular [2+2+2] cycloaddition of arynes and alkynes (Scheme 3).[39] In a reaction sequence, a mixture of two regioisomers **31*i*** and **32*i*** were obtained *via* formation of benzyne like intermediate **30*i***. The main drawback of this method was the formation of regioisomers.

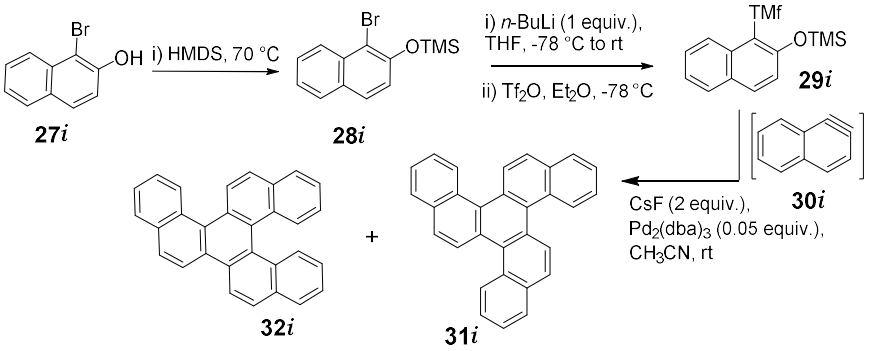

Scheme 3: *[2+2+2] cycloaddition of arynes and alkynes.*

Stary *et al.*[40] developed a novel approach for the synthesis of helicenes in a Co(I) or Ni(0) catalyzed [2+2+2] cyclotrimerization of triyne intermediate. For e.g. triyne **33*i*** was cyclotrimerized to [5]helicene **26*i***. Five, six and seven helicenes were synthesized with ease using this methodology. The main advantage of the methodology is that it is an atom-economy method and three rings are formed in a single step, as compared to classical photocyclization approach. (Scheme 4 and 5).

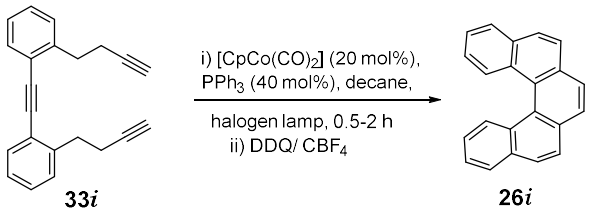

Scheme 4: *Co catalyzed [2+2+2] cyclotrimerization to helicenes.*

When Co(I) catalyst was replaced with Ni(0) catalyst, the reaction can be carried out at an ambient temperature, without irradiation with visible light. The products previously synthesized in Co(I) catalyzed methodology were synthesized with almost similar yields in a Ni(0) catalyzed reaction. (Scheme 5).

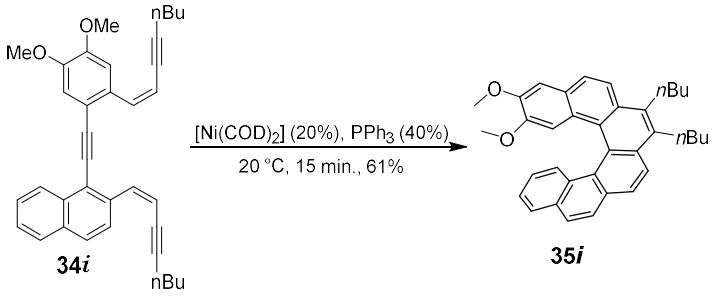

Scheme 5: *Ni catalyzed [2+2+2] cyclotrimerization to helicenes.*

To achieve fully aromatic helicene, dehydrogenation was performed either with DDQ or CBF_4. The methodology is very practical because of its high efficiency (100% atom economy, good to excellent yields, rapid reactions). So that many substituted helicenes and helicene like molecules such as Vollhardt's heliphenes,[41] Tanaka's [9]helicene like molecules,[42] Carbery's helicinoidal DMAP catalysts[43] were synthesized using this approach.

Some research groups also synthesized heteroaromatic helicenes other than carbohelicenes, such as azoniahelicenes (**36*i*** and **37*i***), dioxahelicenes (**38*i***) and thiahelicenes (**39*i***).

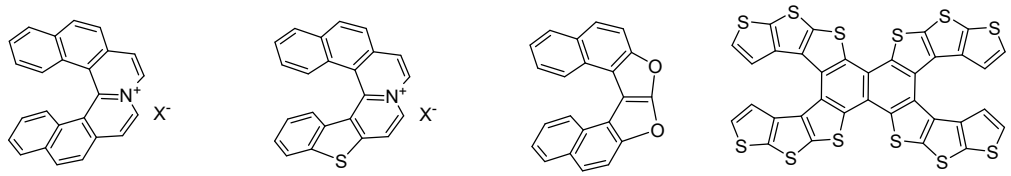

Fig. 9: *Heterohelicenes containing one or more heteroatom.*

Arai *et al.* reported synthesis of first fully aromatic azoniahelicene, **36*i*** *via* photocyclization of styryl intermediate **45*i*** in 4 steps (Scheme 6).[44]

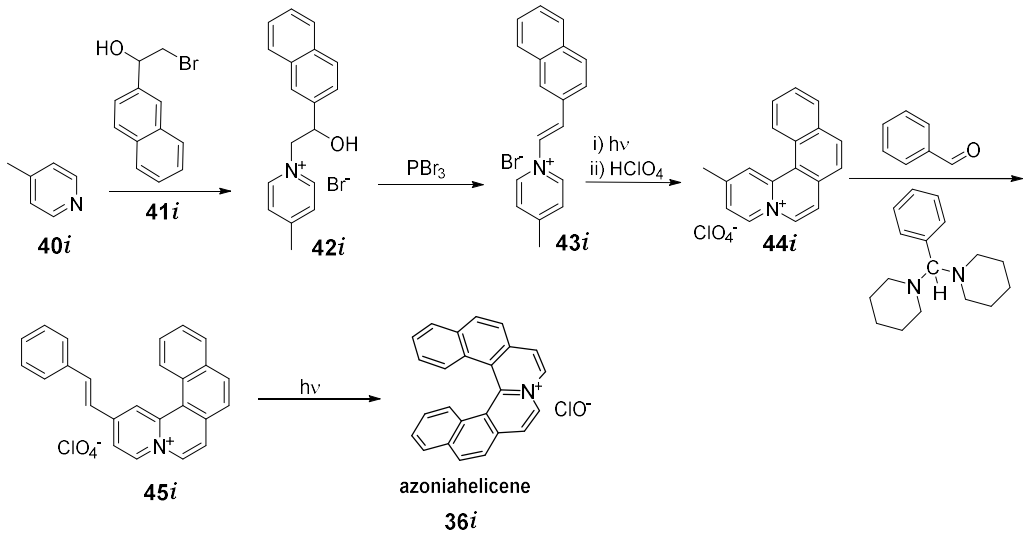

Scheme 6: *Arai's methodology for azoniahelicenes synthesis.*

Other than photochemical cyclization, several modern strategies were developed for the synthesis of azahelicenes. Stabb *et al.* reported Stille-Kelly coupling reaction (Scheme 7)[45] for azahelicene synthesis. Diaza[6]helicene **47*i*** was obtained in 52% yield in a Pd(0)

catalyzed reaction in presence of hexamethyldistannane. A similar method was independently developed by Takenaka *et al.*[46] 1-azahelicene **49*i*** was synthesized in 61% yield in Pd(II) catalyzed reaction in presence of Sn.

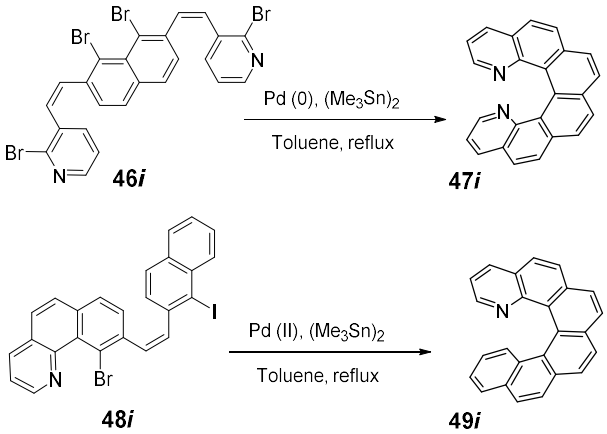

Scheme 7: *Stille-Kelly cross coupling methodology for the synthesis of azahelicenes.*

Due to easily obtained precursors *via* highly *Z*-selective Wittig reaction of halo substituents, the strategy is of considerable practical utility for the synthesis of different helicenes.

Cyclotrimerization approach developed by Stary *et al.* was also successful for the synthesis of azahelicenes (Scheme 8). Triyne precursor of type **52*i***, obtained in two consecutive steps *via* nucleophilic substitution followed by Pd/Cu catalyzed Sonogashira cross-coupling reaction was successfully cyclotrimerized to dihydrohelicene **53*i***. The bottleneck of the synthetic cascade was the final step, in which cyclotrimerized product, **53*i*** was oxidized using MnO_2 in the microwave at 150 °C. Fully aromatic 1,14-diaza[5]helicene was obtained in 41% yield. [47]

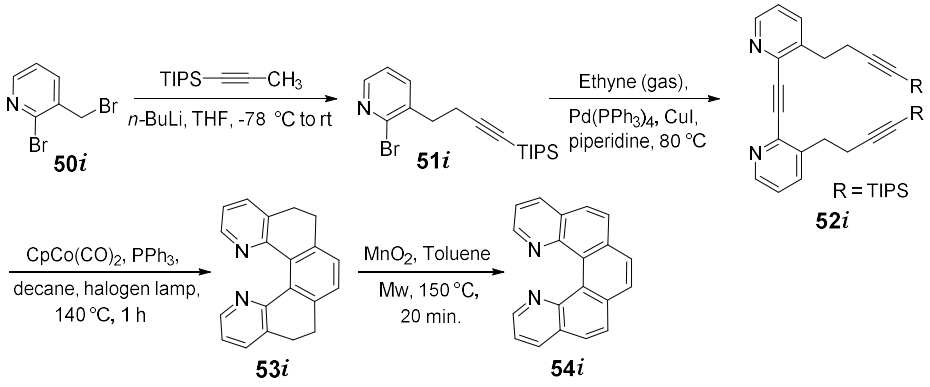

Scheme 8: *Cyclotrimerization approach for azoniahelicenes synthesis.*

Even though all above discussed methods preferentially gave *racemic* helicenes, several methods for the enantiopure synthesis such as CPL-induced asymmetric photocyclization, chemically induced asymmetric photocyclization, metal catalyzed asymmetric synthesis, asymmetric Diels-Alder reactions, asymmetric rearrangements, and synthesis using chiral additives were developed.

Several methods for the optical resolution of helicenes and helicene like molecules, such as recrystallization, direct resolution by HPLC, resolution using chiral auxiliaries, and enzymatic resolutions were developed. In our group, we developed methods for resolution of helquats *via* formation of a diastereomeric mixture from *racemic* helquat *via* anion exchange to chiral counterions such as dibenzoyl tartrate or camphor sulfonate in anion exchange process.

Two diastereomers were separated *via* washings with a preferential solvent such as MeOH or EtOH and respective pure enantiomer was obtained by breaking a pure diastereomeric salt of helquat *via* second anion exchange to achiral counterion such as bromide or triflate.[4] This method of resolution is discussed in section 2 of this thesis.

- **Properties of helicenes:**

The bond lengths between C-C and C=C in helicenes are different in comparison with typical bond length in benzene (1.393 Å).[48] The average bond length of the C-C bonds in the inner helix is lengthened to about 1.430 Å while the average length of the ones on the periphery is shortened to about 1.360 Å.[33b]

As like other aromatic compounds, helicenes are good π-donors and can form charge transfer-complexes with many π-acceptors.[49] As a result, by enthalpy driven charge transfer complex formation with a chiral π-acceptor reagent, the optical resolution of helicenes is achieved. In addition, π-π interaction also plays an important role in determining properties and self-assembly behaviour of helicene in solution and solid state.[50]

Some other interactions in crystals such as Hydrogen bonding,[51] CH-π interactions,[52] S-S interactions,[53] and H-H interactions[54] are also known to be observed in case of helicenes. In case of some helicenes, recrystallization spontaneously affords homochiral conglomerates[55] or enantioenriched crystals.[56]

High 'proton sponge' basicity is one of the property of some azahelicenes (**55*i*** to **59*i***) shown in Fig. 10 by forming linear N---H---N hydrogen bonds.[45]

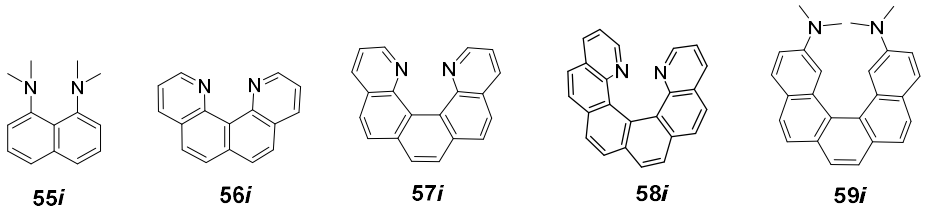

Fig. 10: *Some helical 'proton sponges'.*

The solubility of helicenes is much higher as compared to other planar polycyclic aromatic compounds. The solubility can be improved by introducing appropriate substituents-alkoxy and alkyl groups.[57]

Helicenes show a unique combination of three-dimensionality and remarkable spectral and optical properties. As a result, the considerable attention has been drawn towards their synthesis and their uses especially in the field of enantioselective catalysis,[46] sensing,[58] molecular recognition,[59] self-assembly,[51] nonlinear optics,[50b, 60] liquid crystals[61] and circularly polarized luminescence (CPL)[35] for back lighting in LCD displays.[62] Due to all these properties discussed above, the application potential of helicenes was very well explored in diverse fields such as asymmetric catalysis as chiral auxiliaries in diastereoselective reactions,[63] as organocatalyst,[64] as chiral ligands with metal catalysts for asymmetric synthesis,[65] in the field of developing molecular machines,[66] as dye materials,[67] and many more. All these applications of helicenes are the subjects of many review articles and book chapters.[33] Molecular recognition and Nonlinear optical properties of helicenes are discussed in more in context to this thesis.

- **Molecular recognition properties of helicenes:**

Noncovalent interactions such as hydrogen bonding, metal coordination, hydrophobic forces, Van der Walls forces, π- π interactions, electrostatic or electromagnetic between two or more molecules are known as molecular recognition. In addition to these direct interactions, solvents may also play important role in molecular recognition in solution. The host and guest involved in molecular recognition also possess molecular complementarily.

Chiral recognition is one of the important applications of helicenes. Nakazaki *et al.* demonstrated the use of two optically pure crown ethers **60*i*** and **61*i*** (Fig. 11), both in their *M*-configuration, for the enantiomeric separation of guest molecules in solution *via* chiral recognition.[68] Interestingly, both molecules were showing exactly opposite chiral recognition to each other.

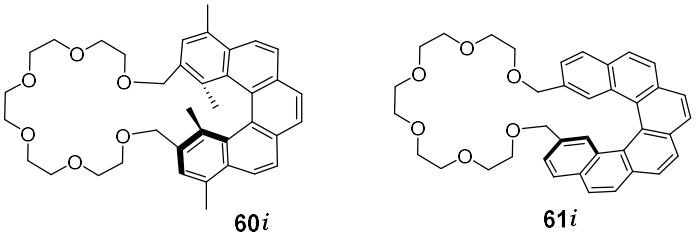

Fig. 11: *Optically pure crown ethers with helicene: showing chiral recognition in solution.*

Katz *et al.* reported a novel method to for the sensing of remote chiral centres by attaching the molecules to the chiral groove of [5]HELOL **62*i*** chlorophosphite (Scheme 9).[59b, 69]

The chiral molecules with reacting groups such as alcohols, amines or carboxylic acids in their *racemic* form were reacted with [5]HELOL chlorophosphite to form different diastereomers, which were analyzed by ^{31}P-NMR. The ratio of the peak integrals for the individual diastereomer directly gave the enantiomeric excess in the previous mixture. This method was efficient because the authors were able to synthesize [5]HELOL **62*i*** substrate on a large scale and were able to employ the method for the broad range of substrates, including alcohols, phenols, amines, and carboxylic acids.

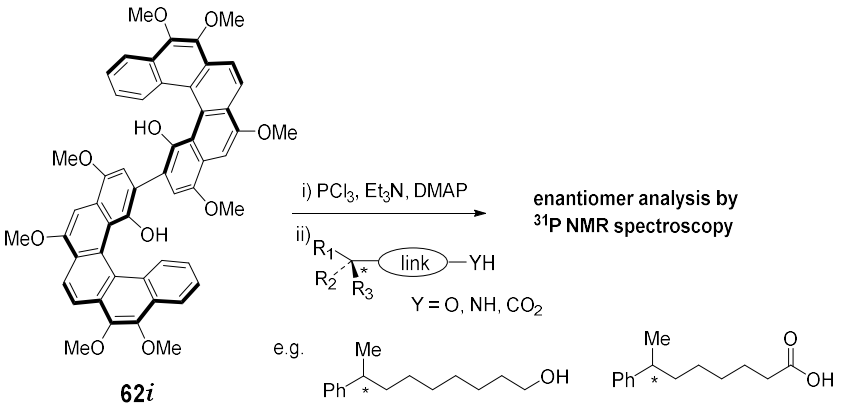

Scheme 9: *Katz method for chiral recognition of remote chiral centers.*

Molecular recognition properties of helicene were studied in the context of chiral recognition of either right-handed (*B*-form) or left-handed (*Z*-form) dsDNA. Vauthey *et al.* reported the binding properties of chiral [4]helicene derivatives **63*i*** to **65*i*** (Scheme 10) with dsDNA by fluorescence spectroscopy and linear dichroism spectroscopy, which shows higher selectivity of *M*-enantiomer over *P*. The binding constant (K_B) depends substantially on the

dye substituents and in all cases was larger in case of *M* than with *P*, by factors ranging from 1.2 to 2.3, depending on the dye (Scheme 10).[70]

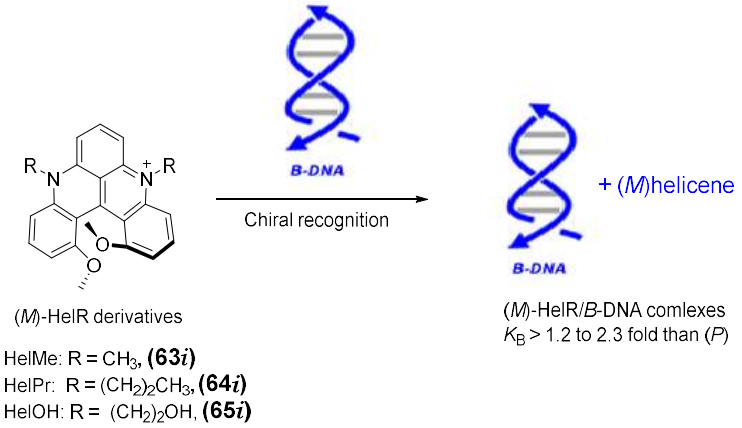

Scheme 10: *Stereo-selective binding of chiral [4]helicene with B-DNA.*

Tanaka *et al.* studied the chiral selection of *Z*-DNA using *P* and *M* enantiomers of **66*i*** (Scheme 11). The ***P*-66*i*** was found to show high selectivity towards *Z*-DNA with a K_B value five times greater than that with *M*-enantiomer. Moreover, it was also observed that the *P*-enantiomer was effectively converting *B*-DNA to *Z*-DNA [71]

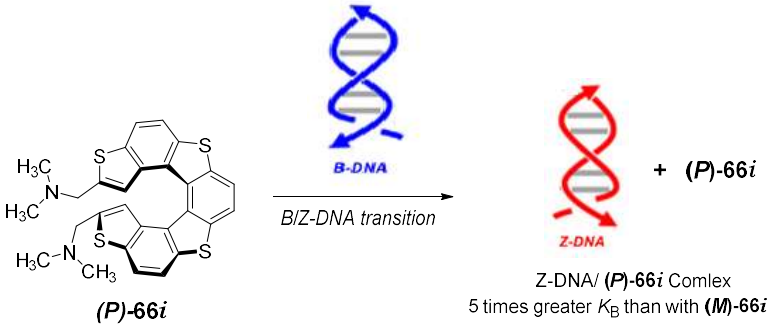

Scheme 11: *Enantiomeric pair of Tanaka's thiahelicenes* ***65i****, showing enantio-selective binding to Z-DNA.*

Sugiyama *et al.* reported another cyclic thiahelicenes molecule (**67*i***) with a short linker. The enantioselective telomerase inhibition and stabilization of G-quadruplex DNA structures was observed. They reported the dose-dependent inhibition of telomeric ladder formation, with the concentrations between 0.2 to 0.5 µM of the ***(M)*-67*i***. In contrast, no inhibition was observed in the presence of ***(P)*-67*i***, even at 10 µM concentration (Fig. 12).[72]

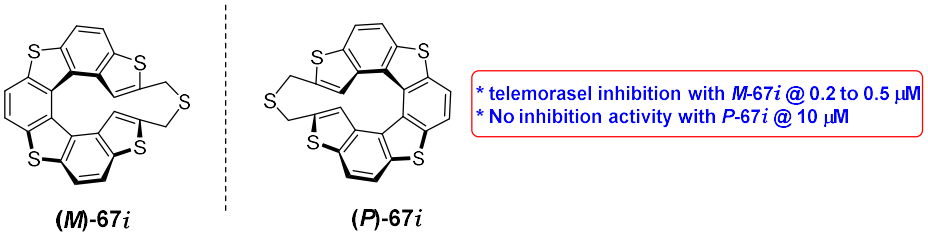

Fig. 12: *Enantiomeric pair of cyclic thiahelicene that showed stabilization of G-quadruplex DNA via selective inhibition of telomerase.*

Very recently, Sasaki *et al.* have shown the synchronized chiral recognition between [5]helicene-Spermine ligand and *B*/*Z*-DNA. The *racemic* **68*i*** was bound to B-DNA (Scheme 12). with an induction of its *P*-chirality together with the *B* to-*Z* helicity change of the duplex

DNA, $[(dC\text{-}dG)_3]_2$. The (*P*)-chirality of the bound **68*i***, in turn, transitioned to the (*M*)-chirality according to the changed chirality of the DNA to *Z* [73]

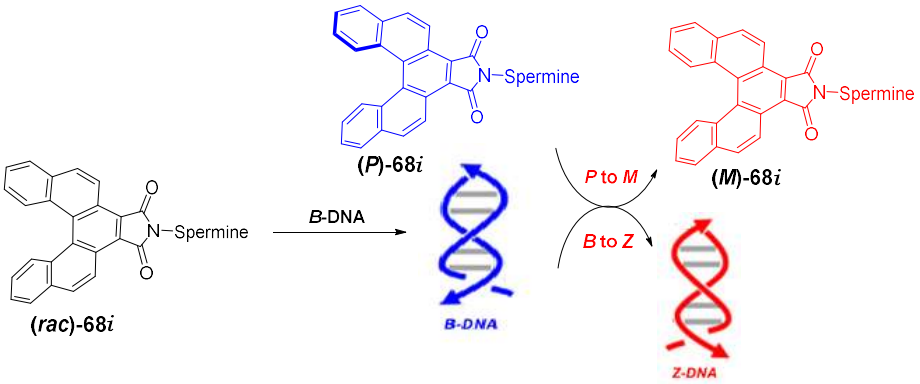

Scheme 12: *Synchronized chiral recognition between [5]helicene-Spermine ligand and B/Z-DNA.*

The field of chiral recognition of DNA, using helicene is relatively new and many developments leading to some potential applications can happen in near future.

- **Nonlinear optical (NLO) properties of helicenes:**

In day-to-day life, the optical properties of the material are independent of the intensity of the light beam. With the light of very high intensity is used, the material properties start to change according to the intensity and other characteristics of that light. The study of changing optical properties of the material after an interaction with such a high-intensity light beam is coming under a relatively young branch of Physics, called as nonlinear optics (NLO).[74, 75] The material which shows such properties due to their particular arrangement of molecular components are called as NLO material. NLO materials based on molecular compounds are of considerable interests because of their applications in advanced optoelectronic and all-optical data processing technology.[76]

In a chemist point of view, at the molecular level NLO phenomenon originated due to an interaction between polarizable electron density within a molecule and a very strong alternating electric field of a laser light beam. As a resultant induced polarization, response (*P*) of a molecule can be expressed as a power series in the applied field (*E*) according to the expression given below:[77]

$$P = \alpha E + \beta E^2 + \gamma E^3 + \ldots\ldots\ldots \qquad (eq.\ 1)$$

With the use of normal low-intensity light originated from non-laser source, the quadratic and cubic terms in eq. 1 can be neglected and a linear optical behaviour is observed. The coefficient α is known as linear molecular polarizability and is related to the refractive index of the material.

However when light originating from high power laser beam is used and the *E* approaches to the magnitude of atomic field strength, the βE^2 and γE^3 terms in equation becomes important and it gives rise to quadratic (second order) and cubic (third order) NLO effects. The coefficients β and γ are termed as molecular hyperpolarizabilities.

The equivalent form of eq. 1 at macroscopic level is given in eq. 2.

$$P = \chi^{(1)}E + \chi^{(2)}E^2 + \chi^{(3)}E^3 + \ldots\ldots\ldots \qquad (eq.\ 2)$$

Majority of molecules, which possess large β values contain three basic components:

1) A powerful σ/π electron donor group (D)

2) A powerful σ/π electron acceptor group (A)

3) A π-conjugated electron bridge connecting (D) to (A)

Few examples of such dipolar molecules[78-81] showing pronounced quadratic NLO activities are shown in Fig. 13.

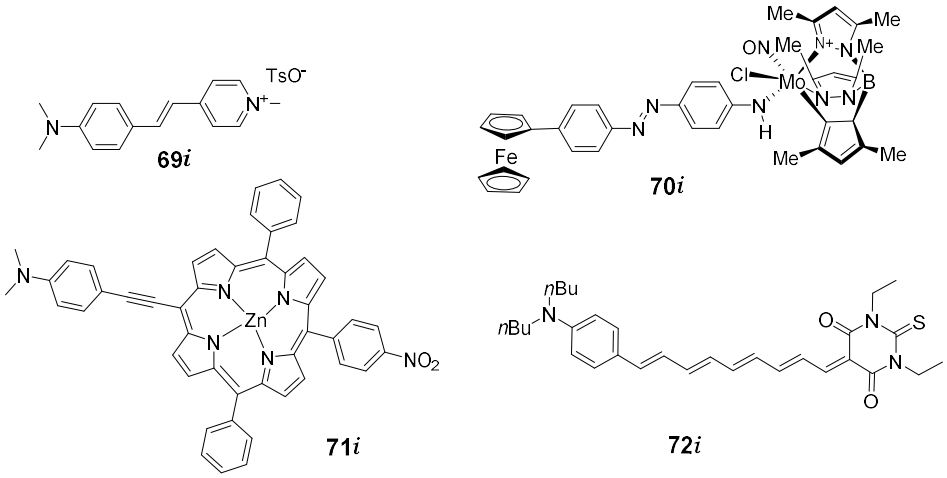

Fig.13: *Few examples of nonlinear optical materials.*

The macroscopic requirement for 2nd order hyperpolarizability, $\chi^{(2)}$ in non-centrosymmetric material featuring some degree of alignment of the dipolar molecular constituents. Therefore, the extent of potentially useful NLO activity depends on not only the structure of the molecule but its crystal packing arrangements.

Even though for the device applications thermal and photochemical stability, processability and many other factors are measured, but for common applications, the quadratic NLO properties of the materials could be adequately measured by techniques like hyper-Rayleigh scattering, second harmonic generation spectroscopy, stark spectroscopy and computational methods.

Although numerous factors must be considered for device applications (e.g., thermal and Photochemical stability, processability, etc.), the quadratic NLO properties of materials are adequately accessed on the basis of β and $\chi^{(2)}$ coefficients. $\chi^{(2)}$ coefficients values are obtained from solid-state SHG experiments, whilst β coefficients are measured in solution, and until recently the only means for achieving this was the electric-field-induced Second Harmonic Generation (EFISHG) technique.[82]

SHG is a nonlinear optical phenomenon, in which certain materials possessing required molecular arrangement and as a result showing nonlinear optical properties can modulate the property of very high-intensity light emitted from a powerful source such as a laser beam. The two light photons of same frequency after passing through such material combine and emitted as a single photon of double the frequency or half of the wavelength.[83]

In SHG spectroscopy, one focus is on measuring the doubled frequency 2ω due to an incoming electric field $E\omega$ in order to reveal information about a surface. The induced second-harmonic dipole per unit volume, $P^2 2\omega$ can be written as

$$E(2\omega) \sim P^2 2\omega = \chi^{(2)} (E\omega)(E\omega) \qquad (eq.\ 3)$$

Where, $\chi^{(2)}$ is known as the nonlinear susceptibility tensor and is a characteristic to the materials at the interface of study.[84] The generated of *E(2ω)* and corresponding $\chi^{(2}$ gives an information about the orientation of molecules at a surface/interface, the interfacial analytical chemistry of surfaces, and chemical reactions at interfaces.

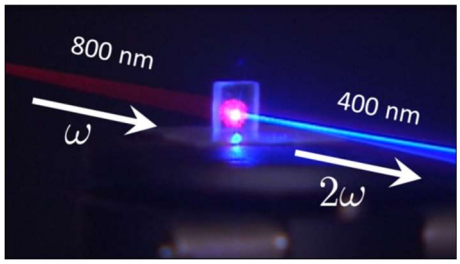

Fig.14: *Illustration of Second harmonic generation.*

Since SHG cannot be observed from an isotropic solution, pooling with a strong external electric field is used to create a partially non-centrosymmetric macroscopic structure, and analysis of the second harmonic light affords the component of β along the dipolar axis. During last few years, the versatile hyper-Rayleigh scattering (HRS) technique has also become available.[85] This relies upon the fact that microscopic anisotropy within a solution can produce incoherent harmonic scattering; this allows the determination of different directional components of β. HRS has certain advantages over EFISHG, for example, it does not require knowledge of molecular dipole moments and is applicable to charged and octopolar compounds that are not amenable to EFISHG study.

Measurements of β are typically made by the use of a 1064 nm NIR Nd^{3+}: YAG laser fundamental (532 nm second harmonic), and the resultant β1064 values are increased by resonance enhancement. By using the two-level model,[86] which is valid for dipolar molecules in which β is primarily associated with a single ICT excitation, we can calculate β_0 values. β_0 is termed the zero-frequency hyperpolarizability and is an estimate of the intrinsic molecular hyperpolarizability in the absence of resonance effects. Applications of molecular NLO materials will generally involve NIR lasers operating in the region about 1000 ± 15 nm, and β_0 values represent molecular quadratic NLO responses at such off-resonance wavelengths. The nonlinear optical properties of styryl dyes containing donor acceptor groups are discussed in section 1.4. In this section, NLO properties of helicenes and few examples are discussed below.

Chirality is an important theme of in NLO.[75] Due to the removal of mirror planes, the symmetry requirements for NLO effects can be slightly relaxed and as a result, the main requirement for NLO activity, such as polar molecular arrangement is no longer strictly necessary. Therefore, any organized bulk structure, polar or apolar with chiral components can in principle show NLO activity with this major advantage over the achiral molecules. Helicenes, which are the intrinsic chiral molecules, show NLO activity. Many groups working in helicene chemistry so far studied the NLO properties of various substituted helicenes based on theoretical studies; as a result, very few practical examples are available.

Verbiest et al. reported a new approach, in which they studied NLO properties of the novel chiral material, **73*i***. The supramolecular organization of chiral helicene material **73*i*** (Fig. 15b) was playing an important role[50b] and they proved that Langmuir-Blodgett films of a chiral helicene composed of supramolecular arrays of the molecules increase the second-order NLO susceptibility about 30 times larger than the same molecule in racemic form. The

Susceptibility components that were allowed only by chirality dominates the second-order NLO response.

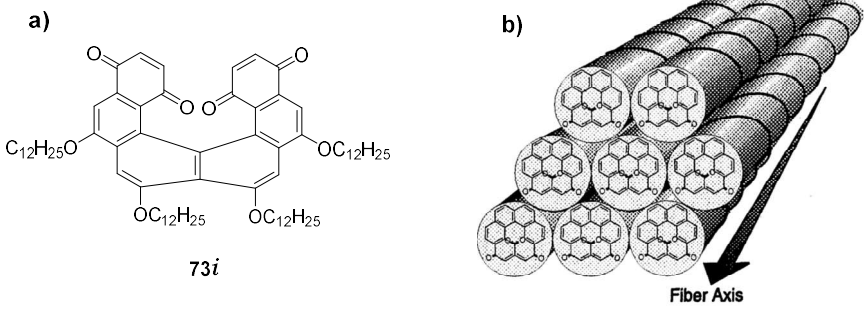

73*i*

Fig. 15: *a) Chemical structure of the helicene molecule; b) Schematic arrangement of molecules as stacked columns in solid material leading to NLO activity.*

Weber et al. reported a theoretical study using both a semi-empirical approach in the case of static and dynamic properties and Density Functional Theory (DFT), in the case of static electric properties. The nonlinear optical (NLO) properties of a set of 10 molecules were investigated to predict the couple of donor-acceptor substituents that could best enhance the optical properties of (*M*)-tetrathia-[7]-helicene, **74*i*** (Fig. 16).[60] Based on their calculations, they have shown that the best nonlinear optical properties were obtained with the nitro NO2 and the amino NH2 pair substituents.

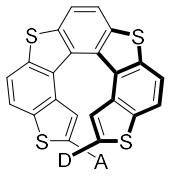

74*i*

A	D	num.
H	H	1
H	NH_2	2
NO_2	H	3
NO_2	NH_2	4
NO_2	OH	5
COOH	H	6
NO_2	Cl	7
CHO	OH	8
CHO	H	9
CF_3	NH_2	10

Fig. 16: *Basic chemical structure of the (M)-tetrathia-[7]helicene,* ***74i*** *with the list of suggested structural modifications.*

Gubler and Bosshard reviewed the molecular engineering strategies that can be used to develop new features in nonlinear optical systems and they proposed Self-assembly based on chiral molecules is one of the important approaches that opens up interesting routes in materials development.[75]

Verbiest et al. reported the second order NLO properties of the single enantiomer of helicene **75*i***, based on the orientation of a lyotropic nematic phase of the molecule by an electric field. Helicene **75*i*** in dodecane solution exhibits second-harmonic generation, the intensity of which was affected by the helicity of the irradiating circularly polarized light and it reverses the sign when the polarity of the orienting electric field reverses (Fig. 17).[87]

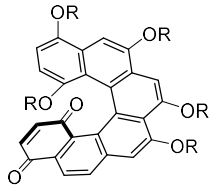

(*M*)-75*i*

Fig. 17: *Helicene* ***(M)-75i*** *studied for the NLO activity under the effect of electric field.*

So far, many research groups studied the NLO properties of helicenes *via* theoretical study and there is a lot of potential in this field to develop.

Our research group recently reported helicene like helquat dyes in their racemic form for their second-order nonlinear optical properties by measuring spectroscopic techniques and DFT calculations.[88] This study is part of this work and will be discussed in the results and discussion section of this thesis.

1.3 Viologens:

The bis-quaternary derivatives of 4,4'-bipyridyl and 2,2'-bipyridyl are known as Viologens.[89] The name originated from intensively blue colored cation radical easily available by reduction. Possibly the best-known Viologens are paraquats (e.g., **76*i***) and diquats (e.g., **77*i***), the world's most widely used herbicides.[90]

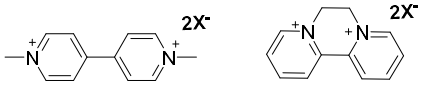

Paraquat **76*i*** Diquat **77*i***

Fig. 18: *Structures of paraquat and diquat.*

Viologens are known for their ability to change colors in solution by single electron reduction processes. A radical cation (**76*i'***) with intense blue color is formed, which may be oxidized in a reversible reaction to give back viologen. Further reduction of radical cation takes place to give a yellow colored quinoid (**76*i''***) (Scheme 13).

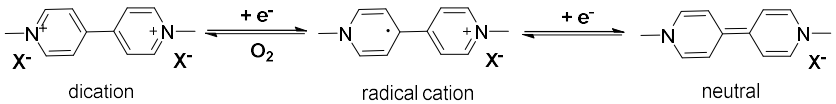

dication **76*i*** radical cation **76*i'*** neutral **76*i''***

Scheme 13: *Single electron reduction of paraquat.*

The stable, reversible redox behaviour of Viologens can be confirmed *via* cyclic voltammetry (CV), having reduction potentials of 1.09 V and -1.52 V in MeCN (vs. Fc/Fc^+, NBu_4PF_6 as supporting electrolyte). These low reductions are ideal for electron-accepting organic materials, relating to the overwhelming interest of viologens and their application to electronics. Although viologens have a variety of interesting properties, they additionally can also be modified to improve their novel electronic and photophysical properties, increasing their versatility for practical applications.[91]

Due to their highly colored, reversible redox states of Viologens makes them promising candidate several machine applications. Three common molecular machine architectures reported for Viologens includes pseudorotaxanes, rotaxanes and catenanes. Pseudorotaxanes typically consist of a rod-like species encircled by one or more

macrocycles. Rotaxanes are similar, however, contain bulky substituents on the end of the rod-like species. Catenanes differ by having interlocked macrocycles, producing a chain-like supramolecular complex. The numerical value [n] describes the number of individual species involved in the overall machine (Fig. 19).[92]

Fig. 19: *General structures of molecular machines.*

Many such molecular machines were reported by well-known research groups and one such example is the formation of pseudorotaxane complexes between curcurbit[n]uril (CB) with and Viologens, which are the suitable host-guest pair with each other. Curcurbit[n]uril (CB) are macrocyclic molecules made of glycoluril (=$C_4H_2N_4O_2$=) monomers linked by methylene bridges (-CH_2-). The oxygen atoms are located along the edges of the band and are tilted inwards, forming a partly enclosed cavity. The name is derived from the resemblance of this molecule with a pumpkin of the family of Cucurbitaceae. Viologens, due to their cationic nature, developing ideal ion-dipole interactions with the CB carbonyl rims. Song et al. synthesized 1,1'-bis[4-(4-pyridinyl)phenyl]-4,4'-bipyridinium chloride (BPPV), which was investigated with the two CBs, CB[6] and CB[7] presented to develop a [2]pseudorotaxane (single ringed) and [3]pseudorotaxane (Fig. 20).[93]

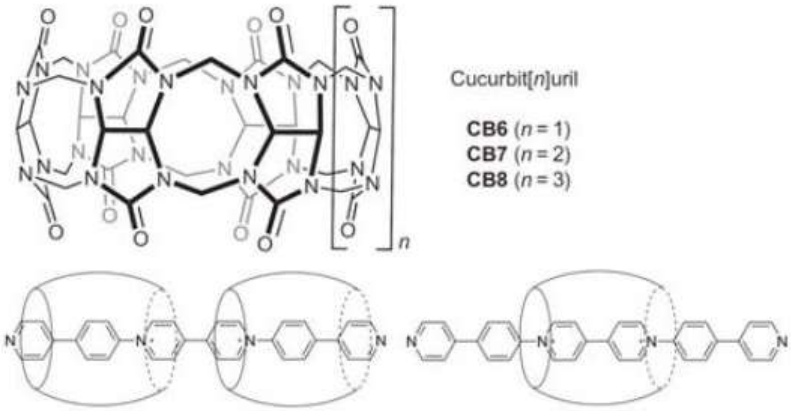

Fig. 20: *Pseudorotaxane formed by encapsulation of 1,1'-bis[4-(4-pyridinyl)phenyl]-4,4'-bipyridinium chloride (BPPV) molecule with curcurbit[n]uril.*

Other applications based on Viologens are as catalysts for direct carbohydrate fuel cells have been reported due to their ability to oxidize glucose and other carbohydrates in alkaline solutions.[94] Viologens were also reported as fast electron-transfer constitutes of data storage materials,[95] building blocks in supramolecular chemistry,[96] energy storage organic materials[97] and bioactive compounds.[98]

1.4: Cationic dyes and their applications:

- **Introduction to dyes:**

A dye is a colored substrate, which has an affinity to the other substrate to which it is being applied.[99] It is generally applied in an aqueous solution and may require a mordant to improve the fastness of the dye on the fibre.

The first human-made organic aniline dye Mauveine A **78*i*** (Fig. 21) was accidentally discovered by William Henry Perkin in 1856 during a failed attempt for the total synthesis of quinine. Other aniline dyes followed, such as fuchsine, safranin, and induline. Thousands of synthetic dyes were synthesized after that discovery.[100]

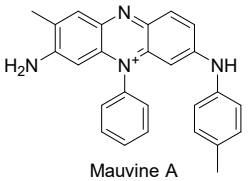

Fig. 21: *Structure of Mauvine A, first human–made organic dye.*

Based on the nature of the chromophore present, organic dyes are classified as below:
1) Azo dyes; 2) Anthraquinone dyes; 3) Indigoid dyes; 4) Polymethine dyes; 5) Pthalocyanine dyes; 6) Cationic dyes

In this thesis, the synthesis, properties and applications of cationic dyes, which are related to the present work are discussed.

- **Cationic dyes:**

Cationic dyes carry a positive charge in their molecule. The salt-forming counterion in most cases is a colorless anion of a low molecular mass inorganic or organic acid. Few examples of organic cationic dyes (**79*i*** to **83*i***)[101-105] are shown in Fig. 22.

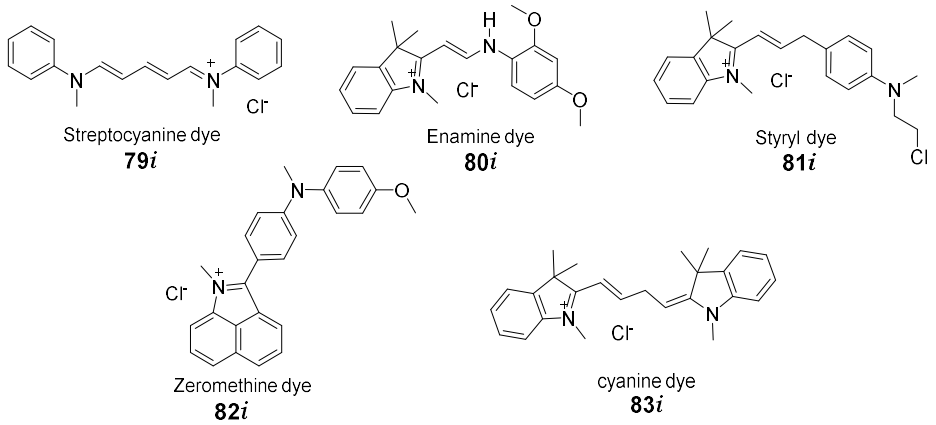

Fig. 22: *Representative examples of cationic dyes.*

a) Cyanine dyes: Cyanine is a non-systematic name of the class of functional dyes from the family of polymethine dyes. The classical cyanine dyes are mostly cationic with two terminal nitrogen heterocyclic subunits, which are separated by a polymethine bridge as shown by the generic structures in Fig. 23a.[106] Common heterocyclic units found in cyanine dyes are shown in Fig. 23b.

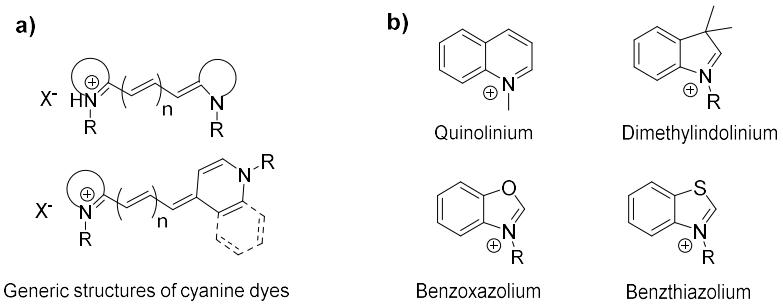

Fig. 23: *Generic structures and common heterocyclic components of cyanine dyes.*

The name cyanine is derived from an English word "cyan" conventionally means a shade of blue-green. These dyes are fluorescent molecules that embody a number of desirable qualities such as high extinction coefficients, tunable absorption/emission spectra, ease of synthesis and moderate to high quantum yields.

Various synthetic methods were reported for the synthesis of sub-classes of these dyes. Some of those methods are reviewed here. Deligeorgiev *et al.* reported the synthesis of monomethine dyes by heating together a mixture of heterocyclic salt containing 2- or 4-methyl group and 2-sulfobetaine derived from a cationic heterocyclic system and a suitable base (Scheme 14a). These are mostly known as nucleic acid binding molecular probes.[107]

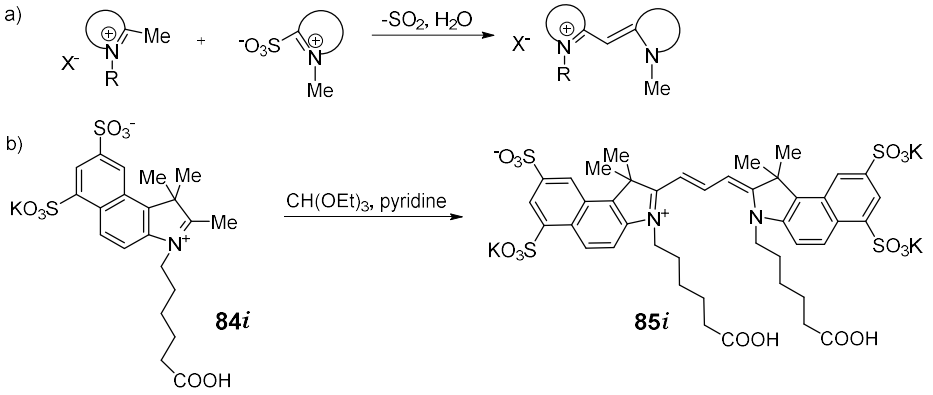

Scheme 14: *Classical approach for the synthesis of mono and trimethine dyes.*

The second approach for the synthesis of trimethine dyes (e.g. **85*i***) is shown in Scheme 14b, the condensation reaction between triethyl orthoformate and quaternary heterocyclic salt, **84*i*** substituted with activated methyl group under basic conditions.

The modern method for the synthesis includes the use of Vilsmeier-type reagent derived from *N*,*N*-dimethylformamide and HBr (Scheme 15).[108] Similarly, more recent approaches for the synthesis of pentamethine dyes are also developed.

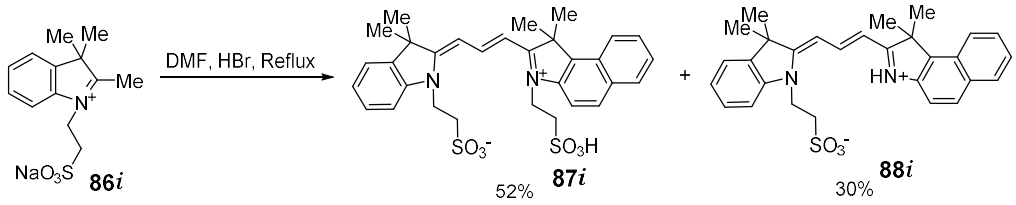

Scheme 15: *Use of Vilsmeier-type reagent for the synthesis of dyes.*

After the discovery of cyanine dyes, their first uses were limited to photographic sensitizers.[109] But other than photography, cyanine dyes now also found their applications in several other fields such as recording media,[110] laser materials,[111] solar cells,[112] and semiconductors.[113]

Currently, cyanine dyes are widely used in biotechnology due to their ability to form fluorescent complexes with nucleic acids. The structure of the dye determines the mode in which it binds to nucleic acids as well as the fluorescence properties of the resulting complexes. In addition, covalent conjugates of cyanine with nucleic acids or with nucleic acid-binding ligands allow fluorescent labelling and probing of DNA/RNA structure and function. Several examples of different types of conjugates and their applications are reported in the literature.

Symmetrical cyanine dyes Cy3 (**89*i***) and Cy5 (**90*i***),[114] which are commonly used as fluorescent DNA labels, unsymmetrical cyanine thiazole orange (**91*i***),[115] TOTO1 (**92*i***),[116] Pinacyanol (**93*i***),[117] DISC3+ (**94*i***)[118] are the common examples shown in Fig. 24.

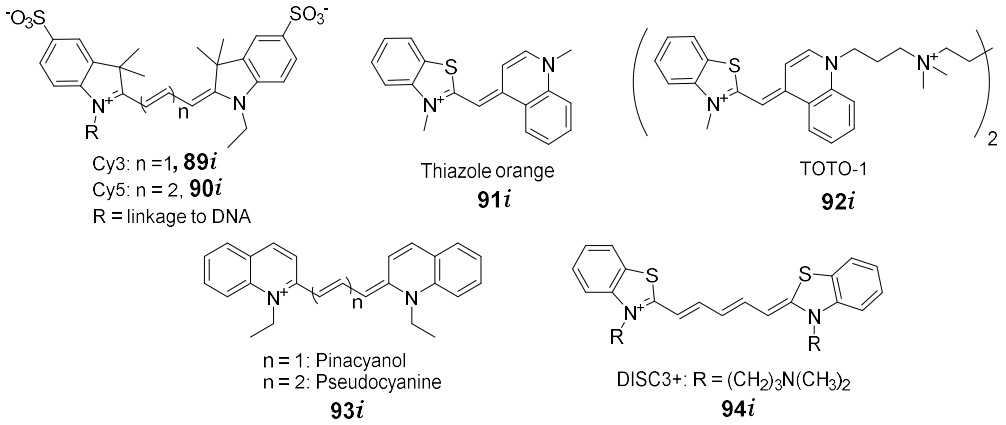

Fig. 24: *DNA binding cyanine dyes.*

Cyanine dyes typically associates noncovalently with dsDNA in one of two ways: (1) intercalation, in which the dye inserts between two adjacent base pairs resulting in a π-stacked sandwich complex, or (2) minor groove binding, in which the dye inserts lengthwise in to the narrower of the two grooves present in the DNA structure. These different dsDNA binding modes are discussed in more detail in section 1.6.

Several near infrared (NIR) cyanine dyes were reported for the fluorescent detection of proteins. Proteins in their neutral form, especially *in vivo* studies, have significant absorption and fluorescence in the visible spectral range. By moving to the longer wavelengths, the detection becomes virtually free from background interference. Such protein probes bind either by covalent or noncovalent interactions. Some common examples[119] are shown in Fig. 25.

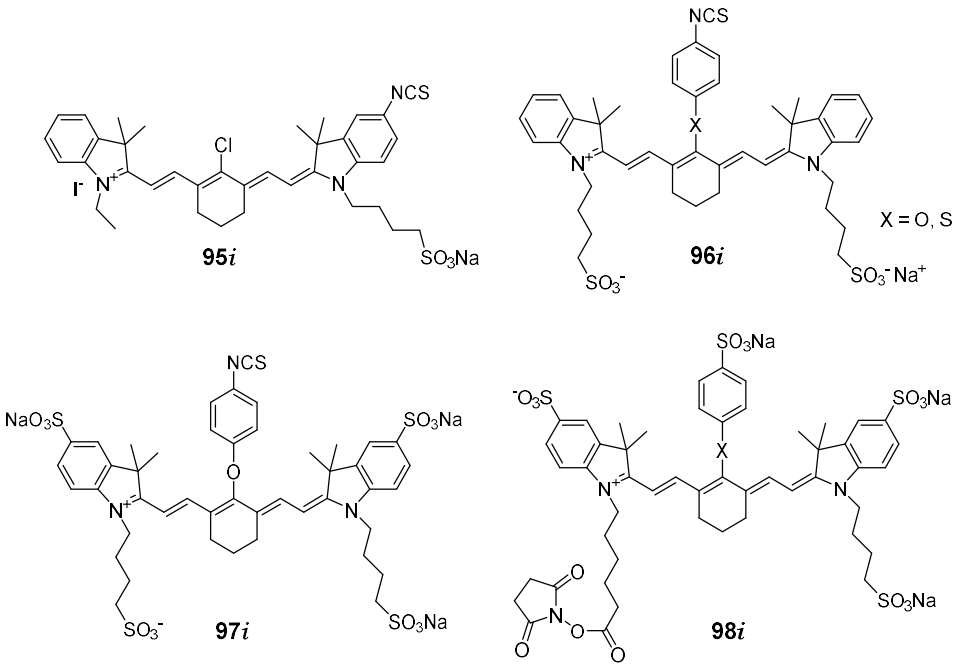

Fig. 25: *NIR cyanine dyes for covalent labeling of proteins at an amino group.*

NIR dyes had also found applications in capillary electrophoresis (CE) of proteins. The most attractive feature of covalent labelling is very low limits of detection (LODs) in CE with laser-induced fluorescence (LIF) detection.[120] Less than an attomole range of detection can be achieved when NIR dyes are used with this technique. In conjunction with immunoassays, CE-LIF is particularly beneficial. An antibody labelled with a NIR dye reduces the LOD for an antigen. The role of antibodies is to introduce specificity for only a particular antigen. The combination of the selectivity of immunoassays with the sensitivity of NIR detection makes combining the two techniques quite desirable for protein analysis.[121] The other applications of NIR emitting dyes substituted with donor-acceptor groups for bio-imaging and monitoring various functions in cells. The ability of these dyes to emit in NIR region through a turn-on activation mechanism makes them promising candidate probes for *in vivo* imaging applications.[122]

b) Styryl dyes: One of the most widely used and important class of functional dyes are the styryl dyes. The univalent radical (C_6H_5-CH=CH-), derived from styrene is called styryl radical. Charged or uncharged dyes in which, styryl moiety became the part of the molecules are called as styryl dyes.

A series of Styrylpyridinium, styrylquinolinium, and styrylbenzothiazolium dyes have been synthesized by the condensation of aryl aldehydes with methyl-substituted cationic hetero-aromatic moiety. These dyes are also referred, as hemicyanine dyes.[111] The transformation (Knoevenagel condensation) is generally reliable, selective, experimentally simple, and versatile. The environment-friendly version of this transformation includes condensation of 2- or 4-methyl substituted pyridinium, quinolinium or benzothiazolium unit with aromatic aldehydes under solvent-free conditions or microwave irradiation, in the presence of different acidic or basic reagents with excellent yields (Scheme 16).[123]

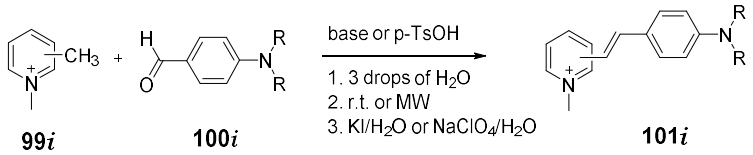

Scheme 16: *Generic scheme for the synthesis of styryl dyes.*

Many styryl dyes were reported for various applications such as novel materials, for biological imaging, dying of textiles and paper, sensitizers in silver halide based photography and many more applications. Many dyes from this class are commercial because of their wide applicability.[100]

FM® dyes are the commercial styryl dyes, which have been used to label and then monitor synaptic vesicles, secretory granules and other endocytic structures in a variety of preparations. Structures of few members of this class are shown in Fig. 26.[124]

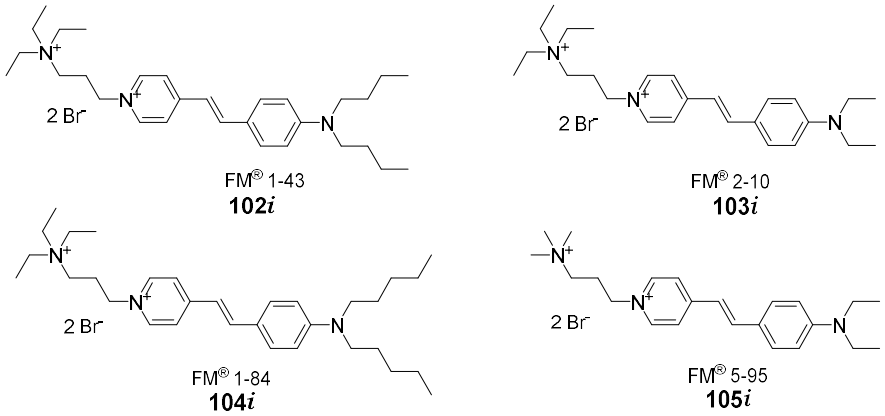

Fig. 26: *FM dye labeled synaptic vesicles in nerve terminals.*

Chang *et al.* reported number of styryl dyes for live cell imaging,[125] DNA selective probes,[126] heparin selective fluorescent chemosensors[127] and RNA selective probes[128] *via* library synthesis of styryl dyes and screening in well plate based fluorescent assay development (Fig. 27).

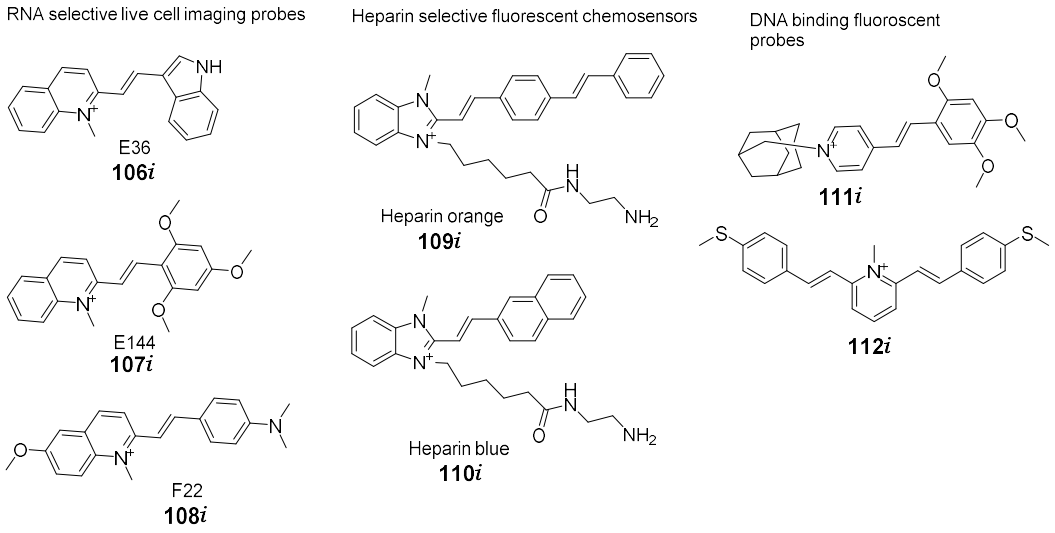

Fig. 27: *Styryl fluorescent probes from Chang's lab.*

Krieg *et al.* reported new highly fluorescent homodimeric stilbene dyes (**113*i*** to **115*i***) for the histochemical evaluation using cryotome sections and Peroxidase-staining protocol. These dyes were reported to be of potential interest because of their excitation with green light. This feature makes them complementary to the other classes of dyes, which are normally excited with either UV or blue light (Fig. 28).[129]

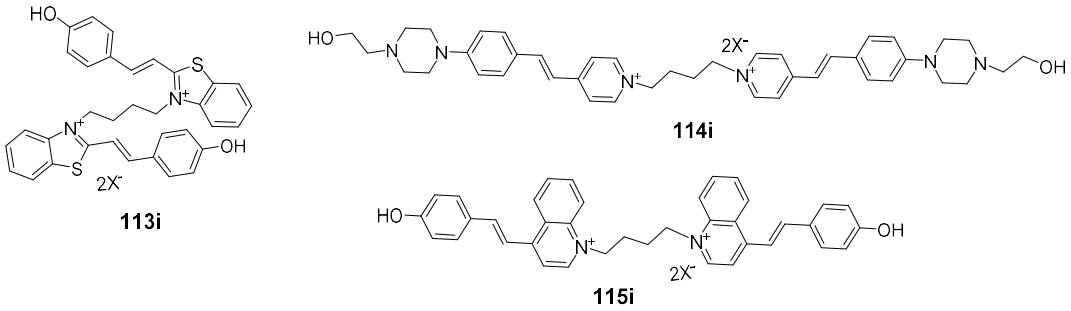

Fig. 28: *Homodimeric styryl fluorescent probes from histochemical evaluation.*

Styryl dyes are also reported to show the spectral changes in response to the voltage changes in cells. Such dyes are called as voltage sensitive dyes or potentiometric dyes (Fig. 29).[130] These voltage sensitive dyes are used for the analysis of neural network because it balances water solubility with good signal, stability, and low phototoxicity for brain tissues.[131] Depending on their chemical modifications, which change their physical properties, they are used for different experimental procedures.[133]

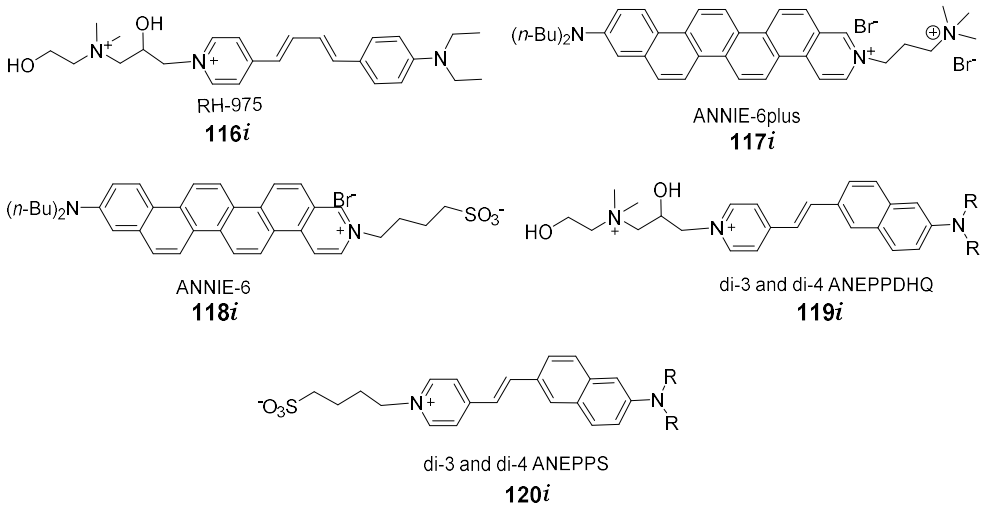

Fig. 29: *Voltage sensitive styryl dyes.*

In addition to applications as fluorescent probes and sensors, other applications of styryl dyes were also reported. Fedorova *et al.* reported a cationic styryl dye with [15]-cown-5 moiety (Fig. 30). The dye was able to sense alkaline earth metal cations *via* crown ether moiety and protons, Ag^+, and Hg^+ *via* heterocyclic moiety.[134]

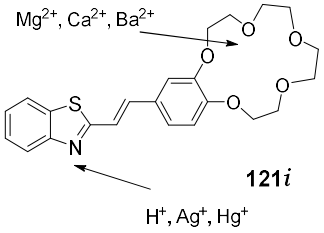

Fig. 30: *Crown ether styryl dyes for small cation sensing.*

The styryl dyes based on helical scaffolds (Fig. 31) were reported in by Arai *et al.* But no synthetic details, properties and applications were studied.[135]

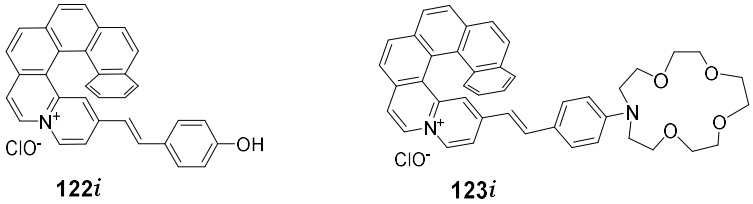

Fig. 31: *Styryl dyes originating from azoniahelicene.*

Recently our group introduced helicene like styryl dyes (Scheme 17), which were resolved into the pure enantiomers and exhibited high magnitude of ECD responses and pH switching.[8]

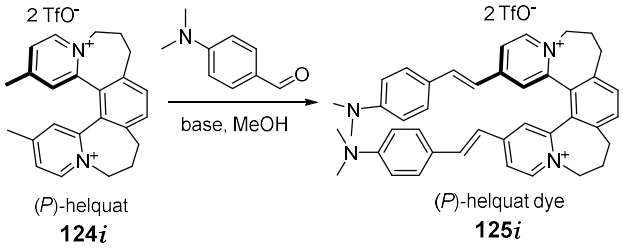

Scheme 17: *Synthesis of enantio-pure helquat dyes.*

Recently we reported G-quadruplex binding properties[136] and nonlinear optical properties of helquat styryl dyes.[88] This study is a part of the present work.

Push-pull type of molecular arrangements in some of the styryl dyes makes them ideal nonlinear optical materials. The Recent success of DAST, *p*-$MeC_6H_4SO_3$ (Fig. 32) with 10^3 higher powder SHG efficiency than urea as well as very large β_0 value from HRS measurement using 1064 nm laser ultimately lead to the fabrication of prototype NLO devices for parametric interactions and electro-optical (EO) modulations.[137] It was also observed that increasing conjugation, the nonlinear optical response of the material was also increased (e.g., **126*i***).[138]

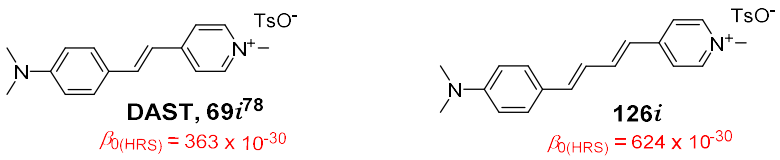

Fig.32: *Few examples of nonlinear optical materials.*

Kim *et al.* prepared an inclusion complex of a stilbazolium dye into the helical cavity of amylose, forming a rigid rod-like supramolecular complex (Fig. 33). Spin-coated thin solid

films of the material were shown to exhibit self-pooling of the chromophore leading to a respectable nonlinearity.[139]

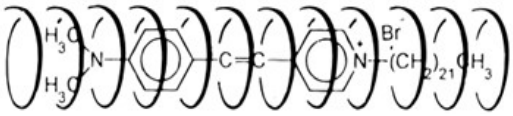

127*i*

Fig.33: *Supramolecular amylose-DASPC$_{22}$ inclusion complex.*

Recently B. *Coe et al.* reported new diquat chromophores containing stilbazolium dyes, showing higher β_0 values than DAST (Fig. 34).[140]

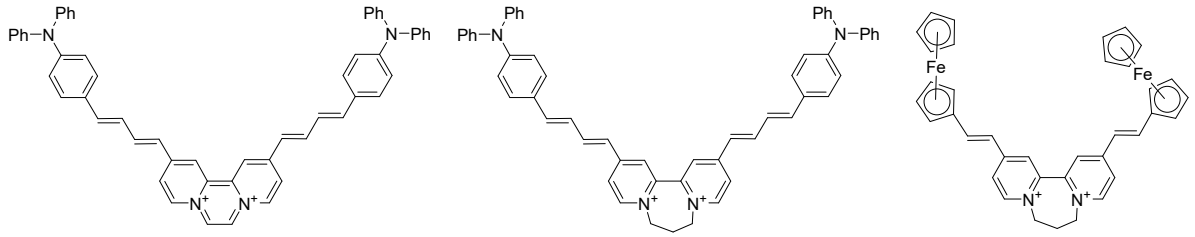

128*i*
β_0 = 876 x 10^{-30} esu

129*i*
β_0 = 916 x 10^{-30} esu

130*i*
β_0 = 206 x 10^{-30} esu

Fig.34: *Nonlinear optical materials based on diquats, showing higher β_0 value that benchmark compound DAST.*

Styryl dyes have a lot of potentials to be used for biological second harmonic imaging microscopy (SHIM). SHG does not involve the excitation of molecules like in other techniques such as fluorescence microscopy. Therefore, the molecules should not suffer the effects of phototoxicity or photobleaching. Also, since many biological structures produce strong SHG signals, the labelling of molecules with exogenous probes is not required which can also alter functions of the way a biological system. By using near infrared (NIR) wavelengths for the incident light, SHIM has the ability to construct three-dimensional images of the specimens by deeper penetration through thick tissues.[141] Structures of Some of the dyes used for SHIM are shown in Fig. 35.

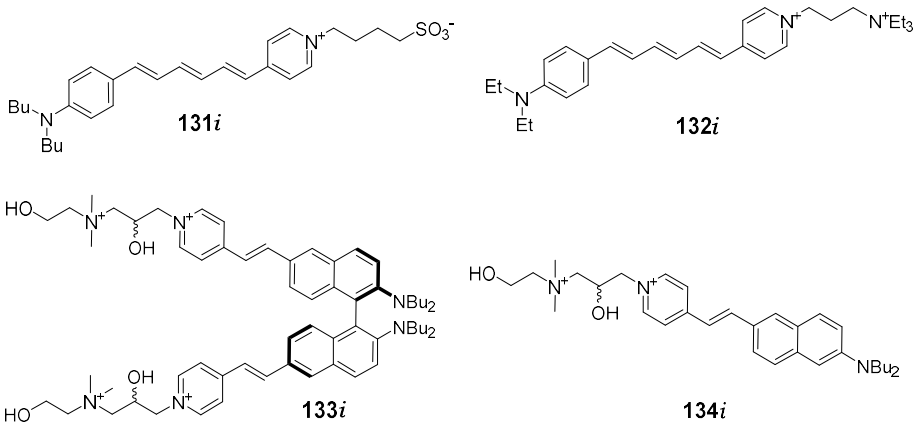

131*i*

132*i*

133*i*

134*i*

Fig.35: *Structures of some dyes used for SHIM.*

Few microscopic images taken using various styryl dyes are shown in Fig. 36 and 37.

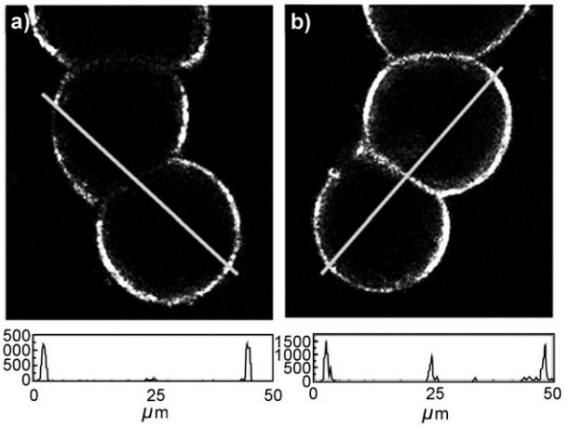

Fig.36: *SHG images of cells stained with (a) racemic dimer (**133i**), and (b) chiral dimer (**133i**) when illuminated with circularly polarized light. Intensity of line scans through cell–cell junctions are shown on plots below, demonstrating that the chiral dye (**133i**) is capable of SHG in a symmetrical bilayer environment whereas the racemate (**133i**) is not.*[142]

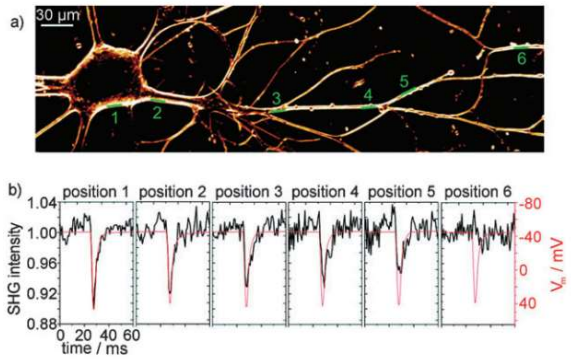

Fig.37: *(a) SHG image of a cultured squid neuron showing six positions of interest at which line scans of SHG intensity took place. (b) SHG intensity for a series of line scans at increasing distance from the soma, the point of greatest SHG response. At larger distances from the soma, SHG signal is lower but action potentials are still easily observed until position 6.*[143]

Due to relatively simple preparations and wide scope for applications of these classes of dyes are often synthesized for developing devices based on these chromophores,[144] for biological imaging and probing etc.

1.5 Heparin and its sensors:

Heparin is one of the oldest known drugs from the glycosaminoglycan (GAG) family and is in clinical use since its discovery in 1916. It was originally isolated from canine liver cells, hence its name (*hepar* or "ήπαρ" is Greek for "liver"; *hepar* + *-in*). The discovery of Heparin was even before an establishment of Food and Drug Administration of the United States in 1916, although it did not enter clinical trials until 1935.[145]

Heparin is a highly sulphated polysaccharide with the highest negative charge density of any known biomacromolecules,[146] known to bind antithrombin with a high affinity, and the binding significantly enhances antithrombin inhibition activity towards thrombin and other coagulation factors.[147] It is a linear polysaccharide consisting predominantly of 1–4 linked uronic acid and glucosamine subunits (Fig. 38).[148]

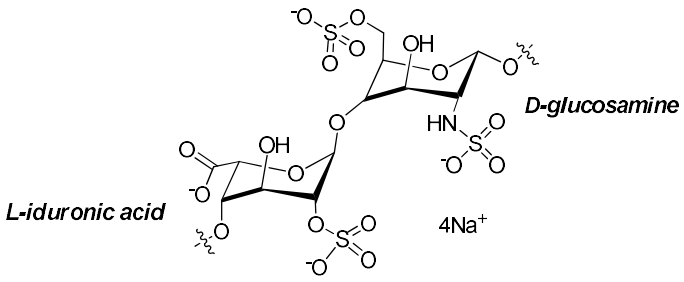

Fig. 38: *Major heparin disaccharide repeating units.*

Due to varying degrees of sulfation in disaccharide components, heparin is one the most complex member the glycosaminoglycan (GAG) family with the polymer M_r spanning ca. 2500–25 000 Da.

Even though the history and widespread use of heparin as an anticoagulant during various surgeries, it is necessary to quantify and control the heparin levels into the bloodstream of a patient. Some of the adverse effects of heparin overdosing include hemorrhages and heparin-induced thrombocytopenia (HIT).[149] To initiate the recovery of a patient, it is important to neutralize the anticoagulant effect of heparin and restore the blood clotting process.

Protamine is only licensed antidote of heparin.[150] It is usually administered to the patient for neutralizing the anticoagulant effect of heparin by electrostatic binding. However, due to nonspecificity for active and inactive forms of heparin, it can cause problems.[151] Due to all these issues there is a significant interest in finding an alternative effective and non-toxic heparin reversal agent, along with an improved methodology for determining blood heparin levels at the point of care.

Traditionally for heparin quantification, some indirect assays are used, which are measuring activated clotting time, such as aPTT or anti-Xa assay etc.[152] All these assays are expensive as well as less accurate and unreliable due to the lack of specificity and potential interference of other factors.[153] Other than clotting time-based assays, employed for this purpose are colorimetric assays, capillary electrophoresis, electrochemical methods, surface enhanced Raman spectroscopy, and unbiased sensor arrays.[154]

Therefore, it is strongly desired to develop an assay for rapid and sensitive heparin detection using an inexpensive instrumentation. In addition, the ideal method should be easily employed at the bedside of the patient and should give an accurate read-out of heparin present. The fluorescence-based techniques are highly sensitive to the environment and there are continuous developments throughout the decades with the discovery of various chemosensors for diverse chemical, biological and medical applications.

Two types of fluorescent chemosensors showing either fluorescence light-up or light-off response in presence of analytes are possible. The pioneering work towards the development of heparin fluorescent chemosensors was reported by Anslyn *et al.*[154d, 155] They reported a tripodal boronic acid-based small molecule **135*i***, which was demonstrated as fluorescence light-off (quencher) probe. (Fig. 39)

Even though it was the first successful fluorescent sensor for heparin detection in serum environment, it suffers from the emission at short wavelength (355 nm) and the auto-fluorescence in the more complex biological samples.

Egawa and co-workers reported fluorescein isothiocyanate-labelled protamine (F-protamine) as a light-off probe, [156] it was able to quantify the heparin in therapeutic level from blood serum, but was suffered from nonspecific fluorescence light-off with serum alone. Nalage *et al.* reported a pyrene functionalized kanamycin A derivative **136*i*** (Fig. 39), which was showing dual detection: either through color changes or through the fluorescence light-off response in EtOH : water (1:3) mixture as a medium.[157]

Smith *et al.* reported Mallard blue **137*i*** (Fig. 39), which was a thionine dye modified with arginine amino acids.[158] This probe was detecting heparin by showing changes in UV-vis. spectra and was reported as one of the successful sensors for detection of heparin in 100% serum.

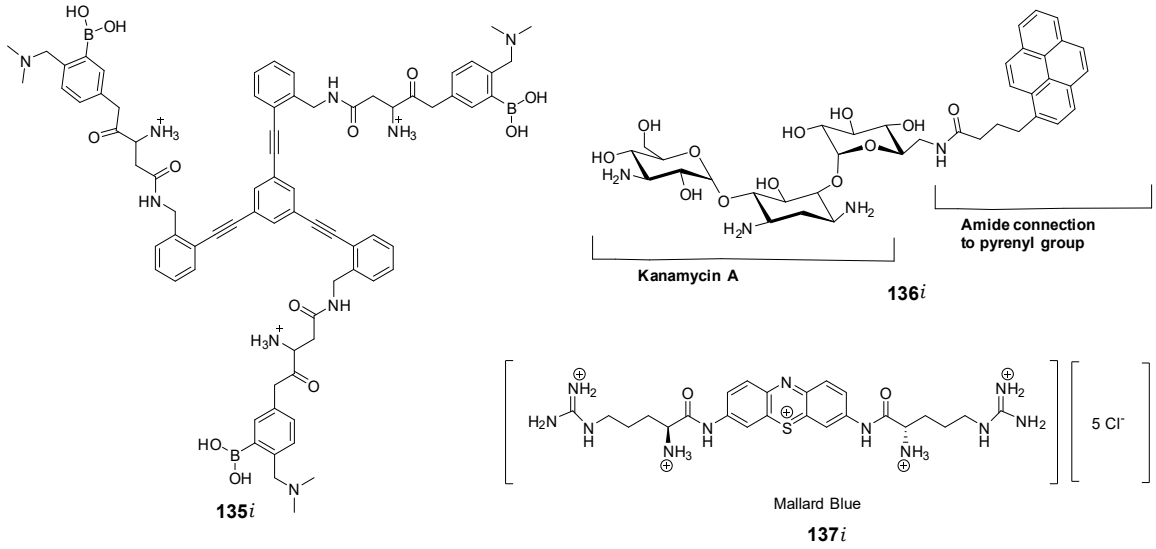

Fig. 39: *Turn-off heparin probes.*

Fluorescence quenching of light-off probe can be affected by many other components of the complex biological medium, as a result, light-up probes should be more reliable than the light-off ones to avoid false positive results.[158] In this regard, the development of sensitive and selective turn-on fluorescent probes for heparin detection is still highly desirable.

Zhang *et al.* reported a ratiometric fluorescent detection of heparin, based on aggregation-caused quenched emission (ACQ) and aggregation-induced emission (AIE) features of anthracene **138*i*** and tetraphenylethene **139*i*.**[159] This ratiometric fluorescence method was used to distinguish heparin from its analogues and quantify heparin in serum (Fig. 40).

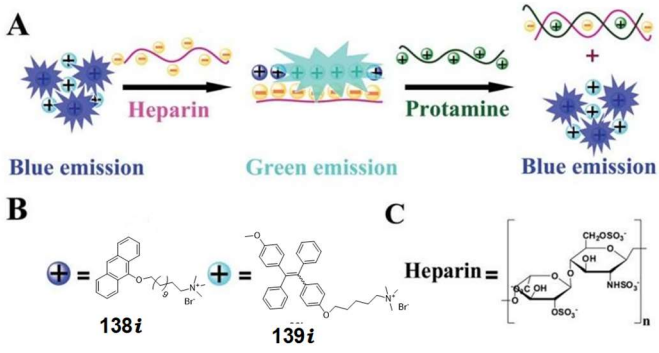

Fig. 40: *(A) Illustration of the design rationale for the fluorescence ratiometric detection of heparin based on the combination of the ACQ feature of compound **138i** and the AIE feature of compound **139i**, and the potential application to study the interaction between heparin and protamine. (B) Chemical structures of **138i** and **139i**. (C) Chemical structure of the major unit of heparin*

Wang *et al.* reported a new quinine derivative **140*i***, bearing pyrene as a fluorophore for heparin detection in an aqueous medium.[160] **140*i*** exhibits good selectivity and sensitivity for heparin over other biological molecules. Upon binding with heparin, **140*i*** shows a typical excimer emission at 489 nm along with a weak monomer emission at 376 nm. The probe can detect heparin from diluted serum (Fig. 41).

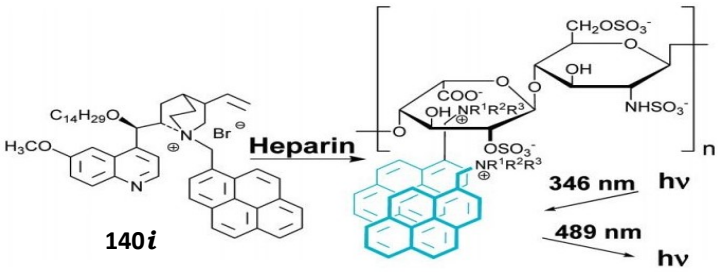

Fig. 41: *Heparin detection with quinine derivative bearing pyrene fluorophore.*

Kramer *et al.* reported a perylene diimide based dye **141*i***, with emission at long wavelength (485 nm) to overcome the problem of serum auto-fluorescence. They achieved meaningful detection of low molecular weight heparin in the presence of up to 20 vol% of serum or plasma (Fig. 42).[161]

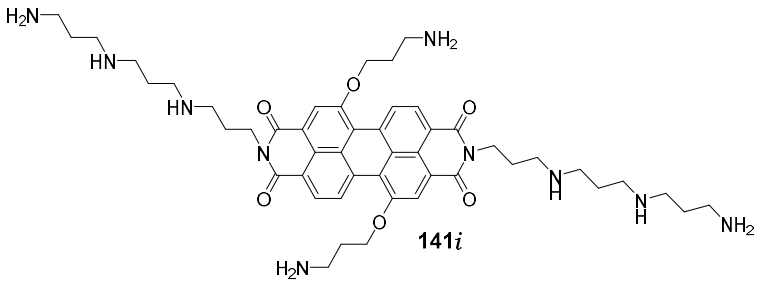

Fig. 42: *Perylene diimide based heparin probe.*

A versatile conjugated polyelectrolyte compound **142*i***, reported by Liu and co-workers, shows dual detection upon binding with heparin, either *via* fluorescence light-up or by direct colorimetric or ratiometric fashion.[162] This probe shows high selectivity for heparin over other GAGs and differentiates between heparin and other GAGs by color changes after interactions (Fig. 43).

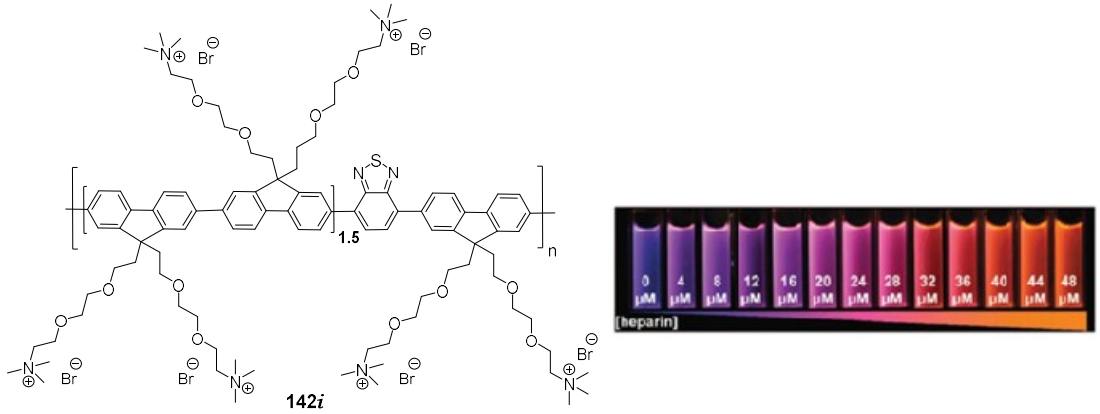

Fig. 43: *Liu's versatile probe, dual detection of heparin via fluorescence light up, as well as with naked eye detection by color changes.*

Chang and co-workers developed a high-throughput approach in search of optimized heparin chemosensors from their library of benzimidazolium dyes. They reported highly selective heparin probes heparin blue and heparin orange, which can detect and quantify UFH (Unfractionated heparin) and LMWH (Low Molecular Weight Heparin) in a clinically relevant range in 20 vol% diluted human plasma. These two probes show high selectivity for heparin over other GAGs as well as plasma proteins such as albumins, and many other analytes (Fig. 44).[163]

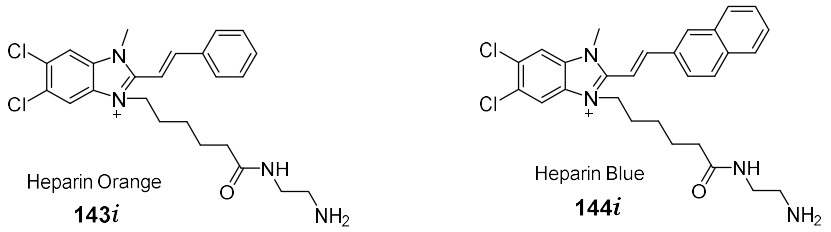

Fig. 44: *Heparin orange and heparin blue, found through a high-throughput fluorescence screening.*

Although some of the approaches detailed so far are able to respond somewhat to the presence of heparin in biological media, many of the non-colorimetric fluorescence-based assays quickly become plagued by the problem of serum auto-fluorescence. The hydrophobic regions of serum can exhibit fluorescence following excitation with shorter wavelength light and can prevent procedures from being used at high (>5%) serum levels.

There is a huge demand for simple commercially relevant systems which can achieve switch-on ratiometric sensing and operate in human serum/plasma, or even better in whole blood. Ideally, such systems should be robust and exhibit long-term stability, so that they can be built into commercial sensing systems, which can be applied at the bedside in surgery for instant read-out of heparin levels in human blood. The devices developed should be as simple as possible, in terms of use and calibration, in order to facilitate their uptake in clinical practice. In this respect, there is a huge scope in modifying currently identified fluorophores and dyes, so as they can emit even in far red or near infrared region, so that, there will be no problem of plasma/ serum autofluorescence.

1.5 dsDNA binding small molecules:

Deoxyribonucleic acid (DNA) is a molecule that carries the genetic information required for the growth, development, functioning and reproduction of all living organisms and many viruses. James Watson and Francis Crick originally elucidated the double helical anti-parallel structure of eukaryotic DNA in 1953.[164] The double-stranded helical structure is made up of the repeating units called as nucleotides, which further contains the nucleobase (Fig. 45b, blue), the deoxyribose sugar (Fig. 45b, red), and the phosphate backbone (Fig. 45b, black). The only variation found among the four DNA nucleotides is at the nucleobase part. Two types of nucleotides comprising purines (adenosine, A and guanosine, G) and pyrimidines (thymidine, T and cytosine, C). In dsDNA, the hydrogen bonding occurs between purines and pyrimidines bases, i.e. AT or GC. Although hydrogen bonding is usually a weak noncovalent bonding force, the summation of hydrogen bonding interactions along the length of DNA anti-parallel strands provides a strong and stable force keeping the strands together.

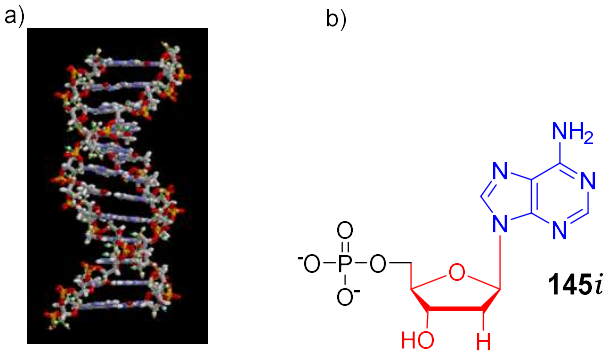

Fig. 45: *a) Double helical structure of DNA; b) structure of monomeric repeating unit (nucleotide) consisting of nucleobase (blue), deoxyribose sugar (red) and phosphate backbone (black).*

Even though B-DNA (right-handed conformation) is the most prevalent form in eukaryotic animals, the double helical structures can adopt two more conformations i.e. *A*-DNA and *Z*-DNA (Fig. 46a).[165] The conformation that the DNA adopts is depending upon many factors such as the hydration level, DNA sequence, the amount and direction of super coiling, chemical modifications of the bases, the type and concentration of metal ions, and the presence of polyamines in solution.[166]

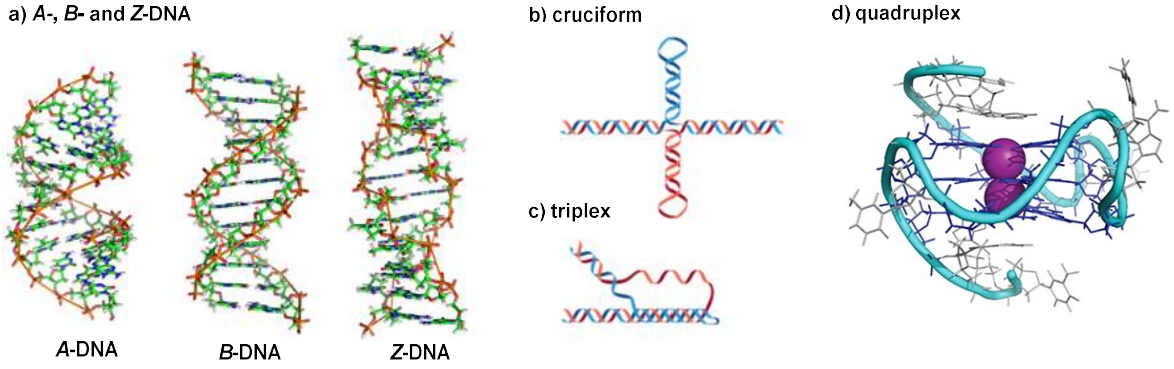

Fig. 46: *Various secondary structures of DNA.*

Depending upon particular sequences and interaction with protein, DNA can acquire a variety of alternative conformations. These secondary structures such as cruciform (Fig. 46b), triplex (Fig. 46c), and G-quadruplex (Fig. 46d) are known to exist under relevant physiological conditions. *In vivo,* functional roles of all these structures are also known.[167] This study is not the part of the present work.

Even before the secondary DNA structures and their roles in physiological and biological processes were known, the molecules interacting with dsDNA were very widely researched and are known for their therapeutic potential. For predicting the physiological/therapeutic consequences of DNA-small molecule interactions, it is necessary to understand the type of possible modes of interactions between these two partners.

DNA alkylation or covalent binding ligands are widely known in cancer chemotherapy, which are preferentially forming covalent bonds at *N*-7 position of guanine or *N*-3 of adenine. These ligands either cause the fragmentation of DNA by repair enzymes in order to replace the modified bases or can form a crosslink between two nucleobases through two binding sites, preventing further synthesis or transcription or in another mechanism, causing mutations to the DNA due to crosslinking of nucleobases. Few examples of anticancer DNA alkylating agents are shown in Fig. 47.[168-170]

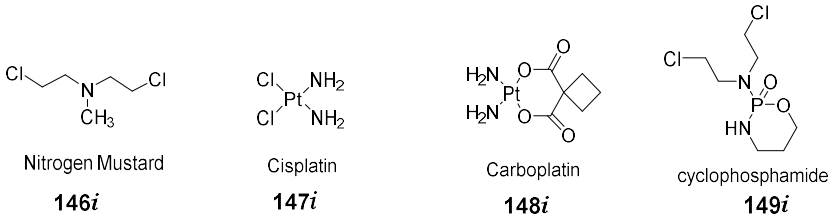

Fig 47: *DNA alkylating agents.*

Intercalation is a noncovalent type of interaction between DNA and its ligands, characterized by insertion of planar aromatic rings in between the DNA base pairs. This kind of interaction is quite strong, even though high energy is consumed for the unwinding of DNA helix and is usually independent of base pair sequences. Intercalators can affect the protein-DNA interactions because they cause severe distortion in the native conformation of the DNA. Two major types of intercalations are possible. Classical intercalation is usually seen in case of some DNA stains like ethidium bromide **9*i*** and antimalarial quinacrine **150*i*** (Fig. 48). These molecules intercalate by stacking of heteroaromatic rings present in their structure with the DNA base pairs.[171] These molecules show less sequence specificity.

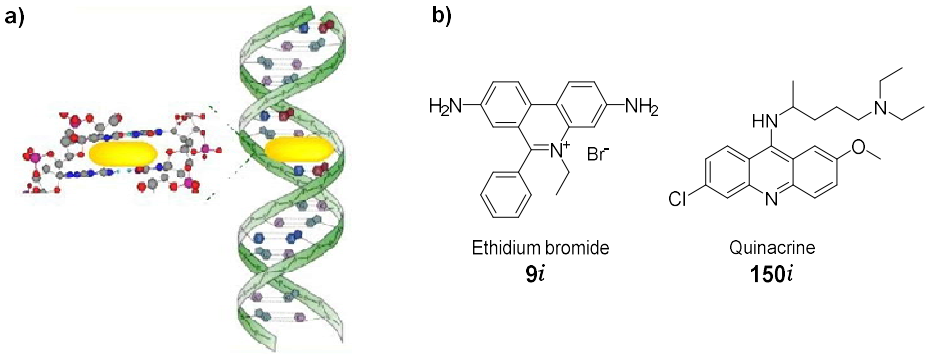

Fig. 48: *Intercalative mode of dsDNA binding: a) Pictorial illustration with a model; b) Two examples of classical DNA intercalators.*

Due to easy unstacking of the sequences in GC region, some molecules like anthracyclins, actinomycin, nogalamycin **151*i*** and daunomycin **152*i*** (Fig. 49) show preferential intercalation into the GC-rich regions.[172] Such intercalators typically have two side chains on opposite sides of planar aromatic systems. The mode of intercalation is quite complicated. The planar aromatic part is intercalated whereas the side chains interact with both minor and major groove.

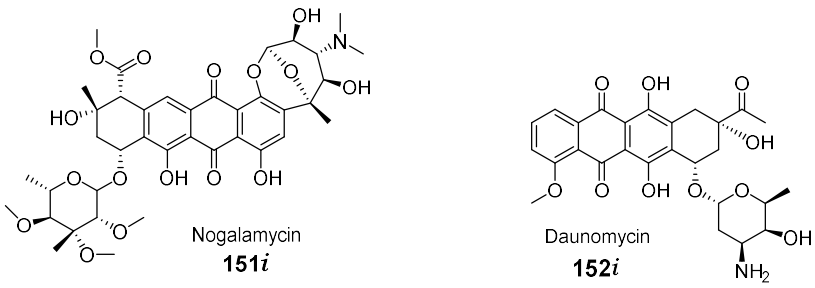

Fig. 49: *DNA intercalator molecules showing threading intercalation.*

The major and minor grooves of dsDNA are the sites for the binding of various small molecule DNA ligands. As the name suggests, the major groove is wider in comparison to a minor. Most of the small molecules interacting with dsDNA are minor groove binders and

major groove is specialized for the DNA binding proteins. Therefore, a non-protein structure containing molecules interacting with major groove are rear. Due to the evolution of minor groove binding antibiotics targeting DNA of competing organisms, a lot of attention was drawn towards minor groove binding small molecules.[173] As compared to intercalators, minor groove binders (e.g. Fig. 50b)[174] show high sequence specificity and affinity and can be neutral, mono-charged or multiply charged.

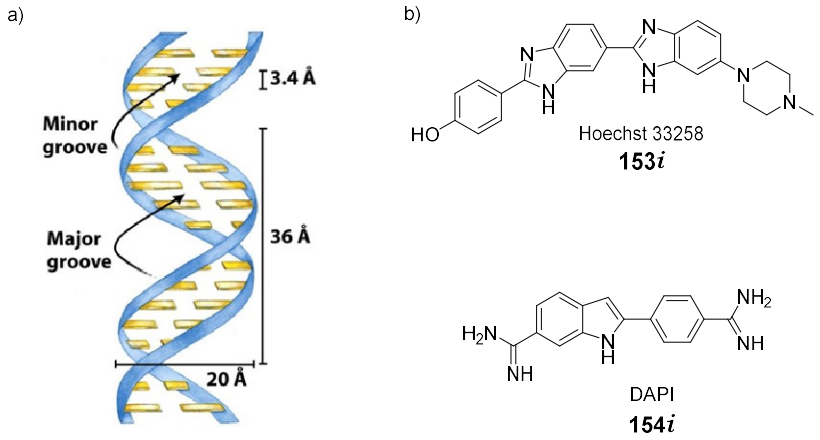

Fig. 50: *a) A dsDNA model showing major and minor grooves of dsDNA; b) Minor groove binding small molecules.*

The forces that dominate small molecule-minor groove binding interactions are electrostatic, Van der Waals, hydrophobic and hydrogen bonding forces. Most of the minor groove binding molecules are crescent shaped with a complementary shape to the groove. They usually show AT-selectivity, due to the higher electrostatic potential at AT sites as compared to GC.

More recently, the hybrid molecules with combined structural features of Intercalators and minor groove binder were introduced and getting recognition as combilexins. Such compounds showed even better sequence specificity and affinity than classical intercalators and minor groove binders. Even though these are synthetic molecules, some natural combilexin such as echinomycin,[175] actinomycin-D[176] and doxorubicin[177] were also found to behave as combilexin.

The main guiding principle behind the synthetic design of combilexin with therapeutic or DNA probing activity was to combine the AT-specificity of groove binder with the GC-specificity of an intercalator. For e.g. Bailey *et al.* reported a molecule with a combination of netropsin, a minor groove binder with an aminoacridine, an intercalator (**155*i***, Fig. 51).[178a] Few other examples of synthetic combilexin are shown in Fig. 51.[178]

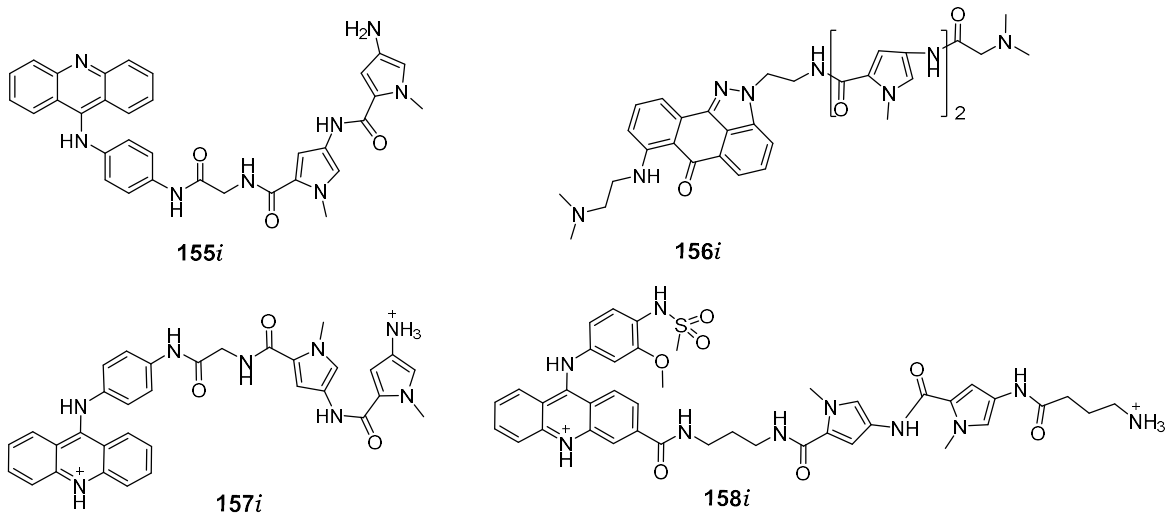

Fig. 51: *Synthetic combilexin.*

Even before the discovery of its double-stranded helical structure, DNA was a target of anticancer drug discovery. The compounds previously identified as anticancer agents were later found to target DNA either directly or through an inhibition of enzymes responsible for controlling the integrity of DNA or providing building blocks for DNA synthesis. There were several established therapeutic modalities targeting DNA: antimetabolites, which deplete nucleotides, including folic acid antagonists such as methotrexate; alkylation agents, which cause direct DNA damage, such as nitrogen mustard and its derivatives; and intercalators such as actinomycins, which bind DNA and inhibit the activity of many enzymes that use DNA as a substrate. Among the most widely and successfully used anticancer agents today are nonspecific DNA-damaging chemicals, including inhibitors of topoisomerases (TOPO) I and II, antimetabolites, alkylating agents and agents causing covalent modification of DNA (mitomycin C and platinum compounds), as well as γ-irradiation, for which the main target is also DNA.

In addition to cancer treatment, dsDNA interacting molecules also found their therapeutic uses against infectious diseases. For example, dsDNA binding small molecules such as DAPI, ethidium bromide, netropsin, and Nogalamycin efficiently inhibits the helicase and ATPase activity of *Plasmodium falciparum* helicase PfD66 and therefore can act as antimalarial drugs.[179]

In addition to therapeutic uses, dsDNA binding fluorescent probes are widely used for various microscopic and cytometry applications. Therefore, it is highly desirable to develop small molecule ligands interacting with dsDNA and other secondary structures with minimal side effects for advanced therapeutic practice as well as for diagnostic purposes such as fluorescent probes with minimal cytotoxicity and environmental friendly properties are desired.

2. Aims of the thesis:

The present thesis aims to fulfil the following tasks:

A. Synthesis of four novel *racemic* helquats **6**, **10**, **14** and **16** (Fig. 52) containing one or two active methyl groups next to the quaternary nitrogen centre and scale-up of the synthesis to accumulate these compounds on a gram scale in order to study the properties and applications.

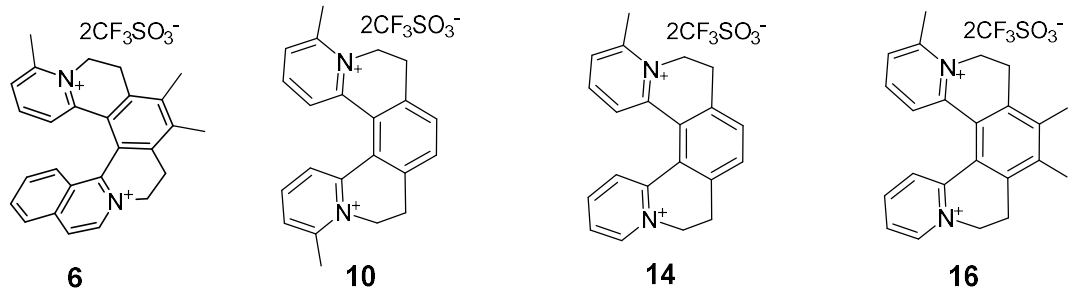

Fig. 52: *Target helquats containing active methyl groups next to quaternary center.*

B. Resolution of [6]helquat **6** and scale up the resolution in order to produce pure enantiomers (*P* and *M*) in gram scale for further explorations towards applications.

C. Synthesis of a library of helquat derivatives *via* Knoevenagel condensation between activated methyl groups attached to helquat scaffolds and various diversely substituted aromatic and heteroaromatic aldehydes. The aim of the synthesis was to run property screens with the generated library of compounds towards various directions such as in search of novel 3D nonlinear optical materials, to identify molecular recognition through fluorescence light-up with various biological targets, such as heparin and dsDNA (Scheme 18).

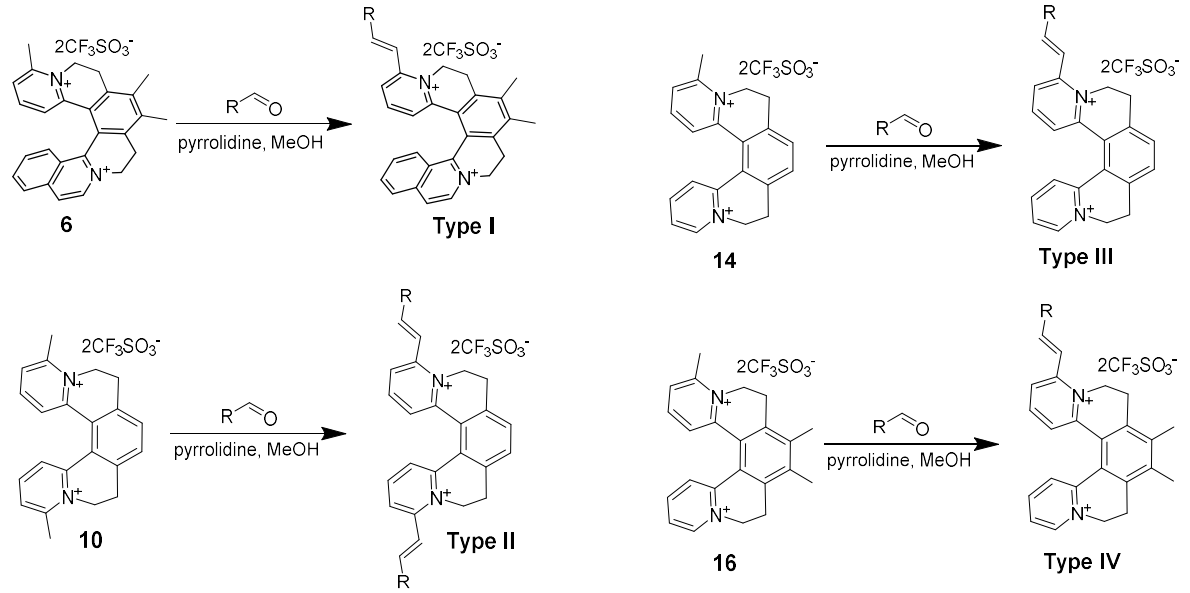

Scheme 18: *Synthesis of library of helquat dyes.*

D. Synthesize prototypical push-pull styryl dyes containing helquat **6**, substituted with electron donating aromatic or heteroaromatic chromophores for investigation of nonlinear optical properties (Fig. 53).

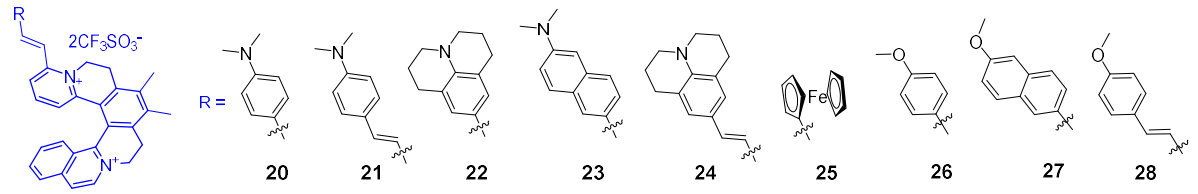

Fig. 53: *Targeted push-pull styryl dyes containing [6]helquat core.*

E. Analyze helquat derivatives of **Type I** and **II** for their molecular recognition properties towards biological targets like heparin and DNA, by selectively lighting-up fluorescence in presence of target (Fig. 54).

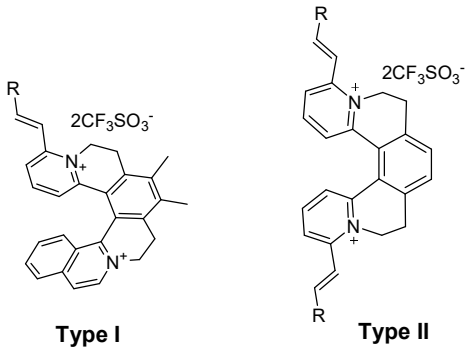

Fig. 54: *General structure of dyes screened in search of heparin chemosensors.*

3. Results and discussion:

3.1 Synthesis of helquats and helquat derivatives:

- **General Points about synthesis:**

Synthesis of four new helquats **6, 10, 14** and **16** containing activated methyl groups at position 2 with respect to quaternary nitrogen was accomplished by following previously developed three-step methodology in our group.[180]

Sonogashira cross-coupling reaction between terminal alkynes **1**, **11** or gaseous acetylene and 2-bromo-6-methylpyridine was catalyzed by Pd/Cu(I) catalyst system to give internal alkynes **3**, **7** and **12** in good to optimal yields (Scheme 19, 22 and 25).

Triyne **5**, **9**, **13** and **15** were synthesized from internal alkynes **3**, **7** and **12** respectively by S_N2 displacement of triflate from alkynyl side chains **4** and **8** (Scheme 20, 23 and 26).[180] Due to the sensitivity of alkynyl triflates and triynes to ambient light, these reactions were carried out in dark.

Helquats **6**, **10**, **14** and **16** were obtained through the final step, in which [2+2+2] cyclotrimerization of triynes 5, 9, 13 and 15 was carried out under Rh(I) catalysis (Scheme 21, 24 and 26).

Library synthesis of helquat dyes of **Type I**, **II**, **III** and **IV** was accomplished by a Knoevenagel condensation reaction between respective helquat scaffolds **6**, **10**, **14** and **16** with various substituted aromatic and heteroaromatic aldehydes in presence of alicyclic secondary amine in good to optimal yield.

The planar controls of helquat dyes of **Type V** and **VI** were synthesized by Knoevenagel condensation of respective methyl pyridinium substrates **17** and **18** with various aromatic and heteroaromatic aldehydes.

- **Synthesis of [6]helquat 6 containing active methyl group:**

The aim of this synthesis was to incorporate an activated methyl group at position 2 relative to the quaternary nitrogen atom in [6]helquat core for further functionalization using Knoevenagel condensation reaction (Fig. 55).

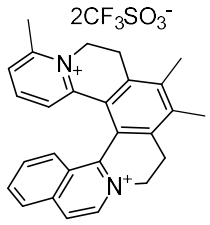

6

Fig. 55: *Structure of the [6]helquats* ***6.***

The first step in the synthesis was Pd/Cu(I) catalyzed Sonogashira cross coupling reaction between 1-ethynylisoquinoline and 2-bromo-6-methylpyridine in triethylamine as a base and high boiling solvent (Scheme 19). The study for the optimization of reaction conditions is summarized in Table 1.

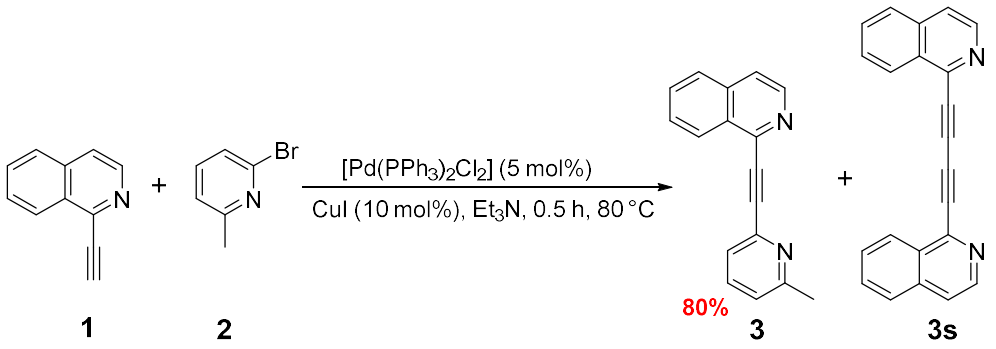

Scheme 19: *Sonogashira coupling reaction between terminal alkyne,* ***1*** *and 2-bromo-6-methylpyridine,* ***2****.*

Sr. No.	*Reaction temperature*	*Product 3 (%)*	*Recovered alkyne 1 (%)*	*Side product 3s (%)*
1.	rt	-	~ 100	-
2.	55 °C	43	~ 30	27
3.	80 °C	80	-	17

Table 1: *Optimization of reaction conditions for Sonogashira coupling.*

The reaction does not proceed at rt and after 24 h of stirring, only starting materials **1** and **2** were detected by TLC analysis (mobile phase: 50% EtOAc in *n*-hexane). After heating the reaction mixture at 55 °C for 4 h, the reaction was not completed and starting material **1** was still present according to TLC analysis. After the workup and purification by column chromatography using 50% EtOAc in *n*-hexane as a mobile phase, an internal alkyne **3** was isolated in only 43% yield with the recovery of ~30% of unreacted alkyne **1** and 27% of **3s**. In a successful attempt, complete consumption of starting material **1** takes place, when the reaction was carried out at 80 °C. Within 30 minutes, complete consumption of terminal alkyne **1** was confirmed by TLC analysis (50% EtOAc in *n*-hexane).

Attempted purification techniques involved recrystallization, trituration with solvents (boiling in *n*-heptane) and precipitation from EtOAc solution by the dropwise addition of *n*-hexane. However, only column chromatography led to pure samples of product **3.** After optimization of above-mentioned reaction conditions, heating for 30 minutes at 80 °C followed by purification of internal alkyne product **3** by column chromatography using 50% EtOAc in *n*-hexane gave the desired product in 80% yield and side product **3s** in in 17% yield.

Triyne **5** was synthesized from compound **3** (Scheme 20). Nucleophilic nitrogen atoms of **3**, displaces triflate leaving group from alkynyl side chain **4** in a S_N2 substitution reaction. As alkyne **3** is unsymmetrical, the rate of alkylation at both nitrogen is different. Due to the steric hindrance caused by methyl substituent next to the nitrogen atom of the pyridine ring, the rate of alkylation at this nitrogen was lower than the alkylation at nitrogen atom from the isoquinoline ring. The reaction proceeds through the formation of mono-quaternary product **5s**. The first alkylation takes place at the nitrogen atom from isoquinoline ring. The nucleophilicity of the nitrogen from the pyridine ring was further decreased after the formation of electron deficient isoquinolinium product **5s**. Often this reaction never goes to complete conversion to form the triyne product (**5**) and the mixture

of mono (**5s**) and bis-quaternary product (**5**) was obtained. The reaction rate was slightly increased by heating the reaction mixture to reflux in a Carius tube.

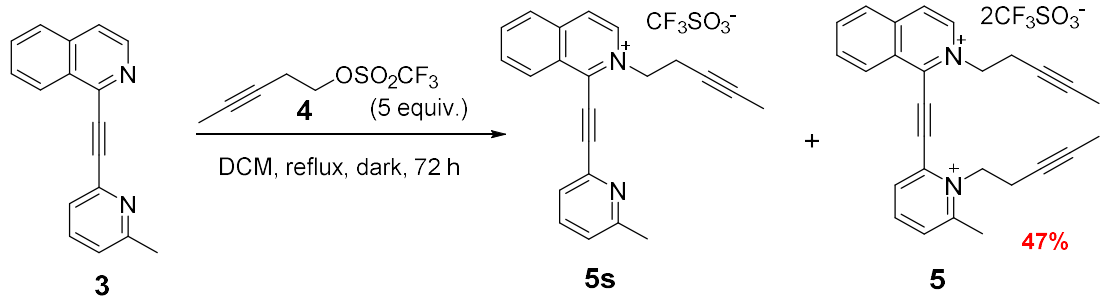

Scheme 20: *Synthesis of triyne* ***5****.*

The progress of the reaction was monitored after each 24 h by TLC analysis (mobile phase: Stoddart's magic mixture) and ^{1}H-NMR. By TLC analysis, the alkyne **3** was completely consumed, but from the spectroscopic analysis, the reaction does not proceed further, after the formation of approximately 1:1 ratio of products **5s** and **5**. Even after 72 h of reflux, the complete conversion to bis-quaternary product **5** does not take place. Due to this reason, we decided to stop the reaction, and solve the purification problem. After evaporation of volatiles, washing of the residue with various solvent combinations resulted in non-purified triyne **5**. Finally, product **5** was separated from rest of the impurities by biphasic extraction in the DCM-water system. Exclusively bis-quaternary product goes to the aqueous phase, leaving impure side product **5s** and other impurities in DCM phase. For effective separation of two phases, centrifugation was used and pure triyne **5** was obtained in 47% yield by evaporating aqueous layer on rotatory evaporator followed by trituration of yellowish brown oil with Et_2O. The attempted purifications are summarized in Table 2.

Sr.No.	*Method of purification*	*Nature/ color of the product*	*Purity by ^{1}H-NMR*
1.	EtOAc	Black, sticky residue	Impure
2.	50% EtOAc in Et_2O	Black, sticky residue	Impure
3.	THF	Black, sticky residue	Impure
4.	DCM : water extraction	Light brown sticky solid was obtained after evaporation of water layer followed by trituration with Et_2O	Pure

Table 2: *Optimization of purification procedure of triyne* ***5****.*

The final step in the synthesis of helquat **6** was [2+2+2] cyclotrimerization of triyne **5**, which was catalyzed by Wilkinson's catalyst to afford a cyclized product (Scheme 21). The workup of this step was relatively simple as compared to other steps. After completion of the reaction (analyzed by TLC analysis using Stoddart's magic mixture as a mobile phase), DMF was evaporated under reduced pressure and pure product was obtained after repeated washings with THF, until solid becomes free flowing and the THF layer after each sonication became colorless. Rh(I) catalyst goes to THF, leaving pure helquat as a solid. Finally, solid was washed several times with Et_2O and dried under high vacuum to give [6]helquat **6** as off-white solid.

The structure of helquat **6** was confirmed by spectroscopic analysis (^{1}H and ^{13}C-NMR, IR, ESI and HRMS). X-ray quality crystals of helquat **6** were grown by slow diffusion of MTBE into the methanolic solution of helquat and X-ray diffraction study of the obtained single crystals gave an idea about the structure. X-ray crystal structure of (*rac*)-helquat **6** is shown in Scheme 21.

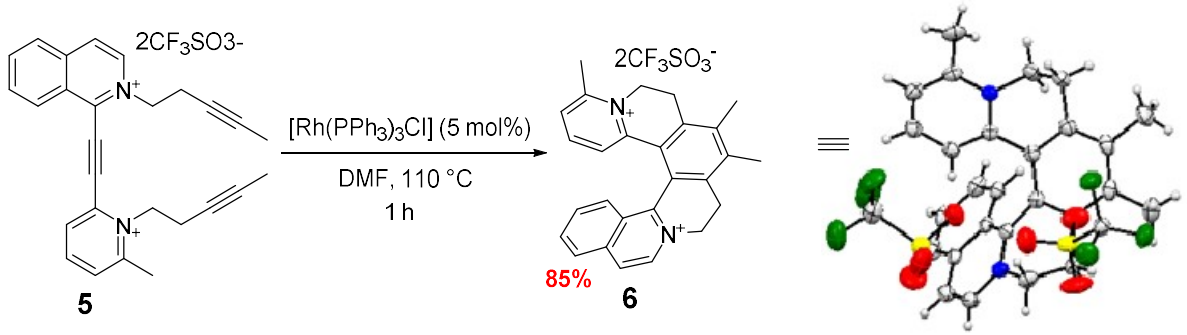

Scheme 21: *Synthesis of helquat* ***6****. Structure of the compound was confirmed by X-ray crystallography*

- **Synthesis of [5]helquats containing activated methyl groups:**

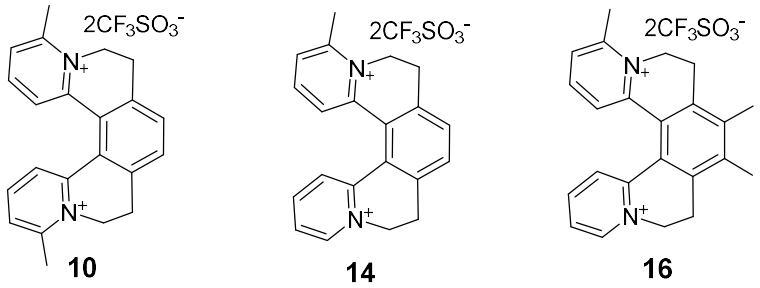

Fig. 56: *Derivatives of [5]helquat containing activated methyl groups.*

The methylated variants of [5]helquat (Fig. 56) were synthesized as new scaffolds for the library synthesis of helquat derivatives with diverse structures. The synthesized library of helquat derivatives was screened in various property screens and successful candidates were identified, which may lead us towards the application of the identified derivatives as fluorescence probe specific for specific biological targets. In addition to fluorescence library screening, the compounds were also checked for their G-quadruplex stabilizing activity as well as in live cell imaging applications in collaboration with biologists.

Alkyne **7** was prepared and purified according to the reported procedure[8] in 79% yield in a Sonogashira cross-coupling reaction between 2-bromo-6-methylpyridine **2** and gaseous acetylene catalyzed by Pd(0)/Cu(I) catalyst system (Scheme 22).

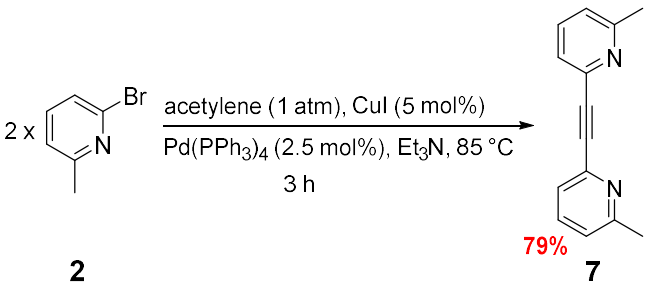

Scheme 22: *Synthesis of alkyne* ***7****.*

Triyne **9** was prepared by bis-quaternization of alkyne **7** with an excess of alkynyl triflate **8** (Scheme 23)**.** After 48 h of reflux in a Carius tube, complete conversion to triyne was observed by ^{1}H-NMR analysis.

Purification of the triyne **9** was easier as compared to triyne **5**. The solid was readily precipitated out from the reaction mixture. Excess of alkylating reagent was separated from the solid product by addition of EtOAc to the suspension followed by sonication and centrifugation of suspended solid. After first sonication and centrifugation, the dark brown supernatant was separated. Resulting solid was repeatedly washed with EtOAc *via* sonication and separation of supernatants after centrifugation. After the final washing, solid was vacuum dried and triyne **9** was obtained as an off-white solid in 83% yield.

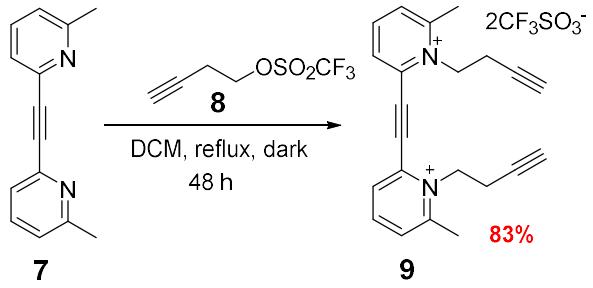

Scheme 23: *Synthesis of triyne* ***9****.*

Triyne **9** was cyclotrimerized to helquat **10** by heating DMF solution of triyne **9** in presence of Wilkinson's catalyst, [Rh(PPh$_3$)$_3$Cl] (Scheme 24). The workup of this reaction was relatively simple, similar to cyclotrimerization in case of [6]helquat **6**. After purification similar to [6]helquat **6**, [5]helquat **10** was obtained in its pure form in 73% yield.

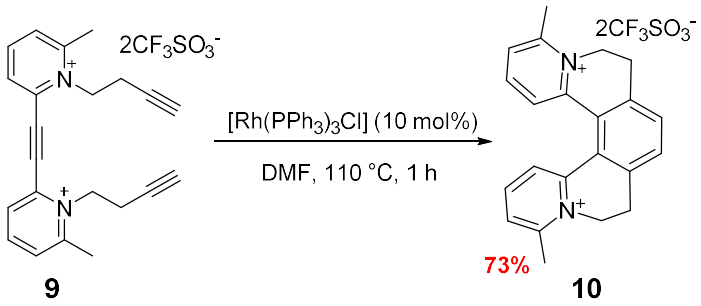

Scheme 24: *Synthesis of helquats* ***10****.*

Helquat **14** and **16** were synthesized analogously to helquat **10** in three steps.

Sonogashira cross-coupling reaction between terminal alkyne **11** and 2-bromo-6-methylpyridine **2** using previously optimized reaction conditions for the preparation and purification of alkyne **3**. Internal alkyne **12** was obtained as a brown, low melting solid in 74% yield (Scheme 25)**.**

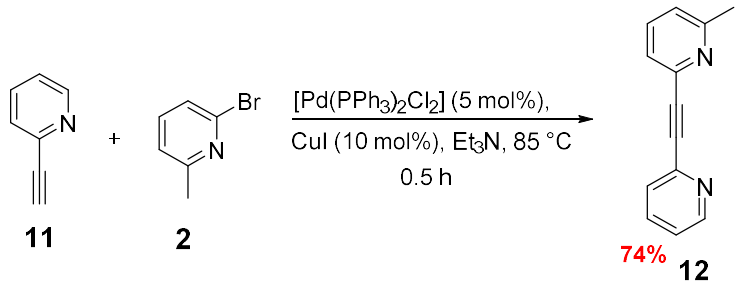

Scheme 25: *Synthesis of internal alkyne* ***12****.*

The reaction conditions for quaternization and [2+2+2] cyclotrimerization from the synthesis of helquat **10** were adopted and two new [5]helquats **14** and **16** were obtained in 69% and 59% respective overall yields over the two steps (Scheme 26).

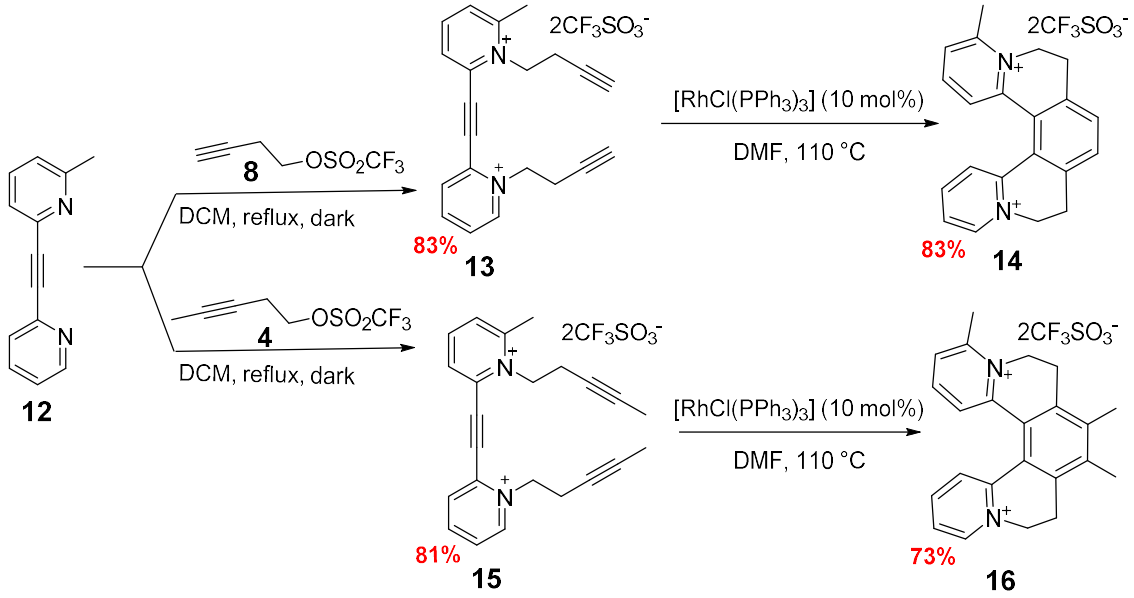

Scheme 26: *Synthesis of helquat* ***14*** *and* ***16****.*

- **Synthesis of Type I, II, III and IV helquat derivatives:**

In order to expand the existing library of helical dicationic molecules for studying their properties leading towards successful applications, a single step structure diversification protocol was developed.[8] Helquat derivatives originating from *racemic* parent helquat scaffolds **6**, **10**, **14** and **16** were synthesized by a single Knoevenagel condensation reaction. In a condensation reaction between activated methyl groups from respective parent helquats and varyingly substituted aromatic or heteroaromatic aldehydes in presence of base, helquat derivatives of **Type I**, **II**, **III** and **IV** were obtained in good to optimum yields (Scheme 27).

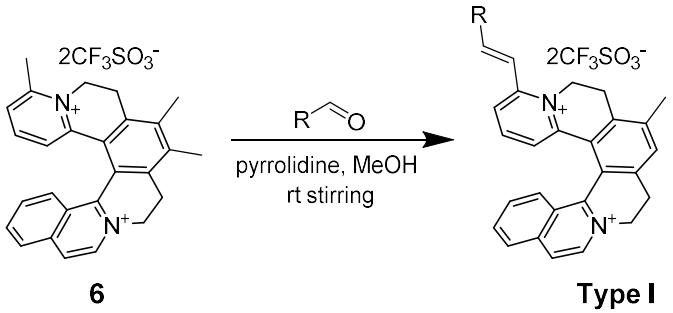

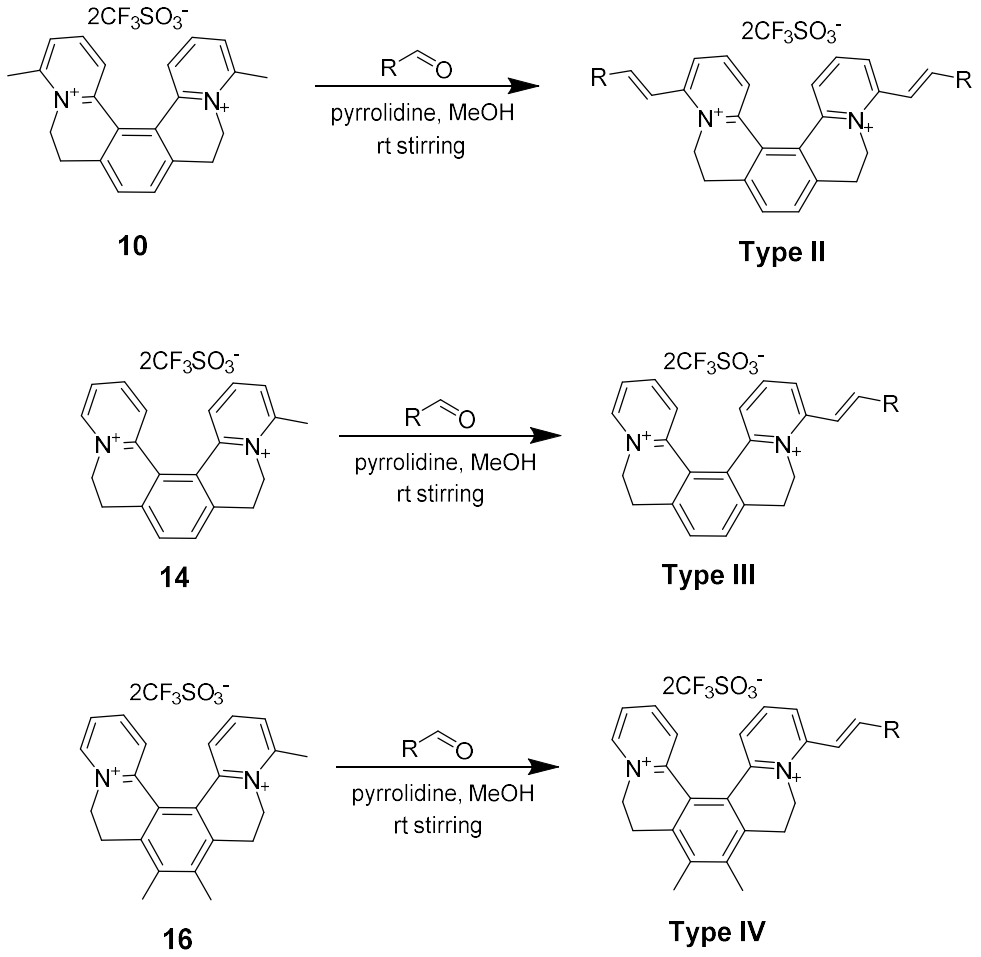

Scheme 27: *Helquat derivatization by single Knoevenagel condensation.*

Initially, all helquat derivatives of all types were synthesized in their *racemic* form and were explored in various property screens. If some specific property of the derivative was identified, then it was further explored towards finding of applications.

If needed, such compounds were synthesized in their enantiopure form as both enantiomers and were tested in comparison with the original compound.

The key characteristics of this methodology are - i) in a single step, reliable methodology, various functionalities can be attached to the helquat core; ii) products are purified by a chromatography-free method, usually by precipitation; iii) yields are moderate to high, typically more than 70% (exceptions are few dimethyl amino substituted derivatives).

Overall, it opens a very straightforward access to a structurally diverse library of helquat derivatives, which offers itself for various property screens. Number of helquat derivatives originating from **6** and **10** (**Type I** and **II**) were extensively synthesized (~ 200 and ~ 200, respectively), whereas derivatives originating from helquats **14** and **16** were mostly prepared and studied as controls or structural variant for **Type I** and **II** derivatives identified in the screens (~ 35 and ~ 15, respectively).

The reaction conditions, suitable amine catalyst and the purification process for the synthesis of **Type I** helquat derivatives were optimized by performing a model reaction of helquat **6** with 4-(*N*,*N*-dimethylamino)benzaldehyde **19** (Scheme 28) were successfully followed for the synthesis of all types of helquat derivatives with slight modifications,

depending upon the type of substrate and aldehyde. The optimized reaction and purification conditions are listed below.

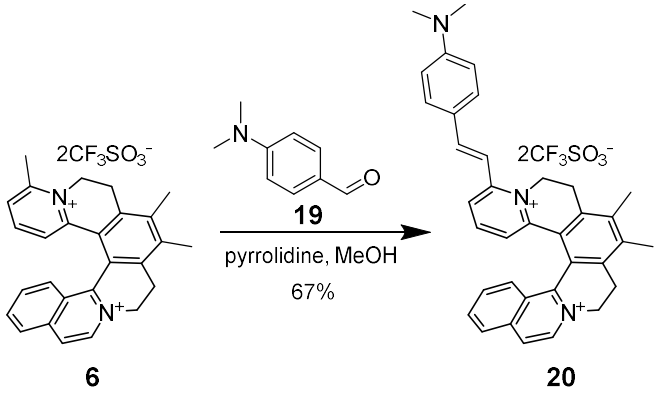

Scheme 28: *Synthesis of helquat derivatives of* ***Type I****.*

All reactions were preferentially performed at rt, while protected from ambient light and under dry conditions of solvents and glassware. Out of three screened bases (pyridine, piperidine and pyrrolidine), an excess of pyrrolidine up to 12.0 equiv. with respect to starting helquat was successful for better conversion and purity of the dye product. Even though, helquat derivatization reactions with some electron-rich aldehydes were successful using 3-5 equiv. excess of aldehyde and 1.5-3.0 equiv. of the base and it was also possible to achieve the pure products in reasonable yields, but it required reaction time up to several hours. From our previous observations, parent helquats themselves were not very stable in the strongly basic environment for a longer time and tends to get decomposed. Therefore, we decided to use an excess of base and aldehyde to shorten the reaction time from several hours to few minutes in several cases and 2-3 h in case of few alkoxy substituted and non-substituted aldehydes.

Initial attempts to purify the desired product by preparative TLC using a mixture of acetone, water and saturated KNO_3 (87.5:10:2.5) as mobile phase and the major purple dark spot was isolated but it was the impure product. Probably the product was not stable to the acidic surface of the silica.

In the next attempt, purification of the expected product by precipitation with a nonpolar solvent like Et_2O was successful when the proper ratio between MeOH and Et_2O was adjusted. It was also observed that by addition of 8 volumes higher amount of Et_2O to that of MeOH gave the product with good purity (according to ^{1}H-NMR analysis). To obtain the dye products with high purity, it was necessary to take following precautions:

1. Due to *cis-trans* isomerization of styryl double bond (as observed in case of few alkoxy substituted helquat dyes), all reactions were essentially carried out in dark, while protecting them with Alufoil cover and under argon atmosphere in dry MeOH as a solvent.

2. If the reaction time was increased, few unknown impurities were formed during the course of the reaction. It was also observed that using a large excess of aldehyde (12 equiv.); the reaction time can be minimized. Therefore many reactions were carried out under these optimized conditions.

3. For the effective purification of dye products from the unwanted impurities, complete dissolution of solid before addition of Et_2O was important.

Above optimized reaction conditions and purification protocol were used for the synthesis of **Type I** helquat derivatives. The helquat derivative **20** was fully characterized by spectroscopic analysis (^{1}H-NMR, ^{13}C-NMR, IR, ESI and HRMS analysis). The structure of the compound **20** was also confirmed by X-ray crystallography. The single crystal suitable for X-ray diffraction analysis was grown by slow diffusion of *i*-Pr_2O into the acetone solution of helquat dye **20** (Fig. 57). The conformation of styryl double bond was found to be exclusively *E* and it is in agreement with NMR spectroscopy (coupling constant, *J* = 15.9 Hz). For the condensation with few aldehydes, further optimization was needed to obtain the respective helquat derivatives in their pure form.

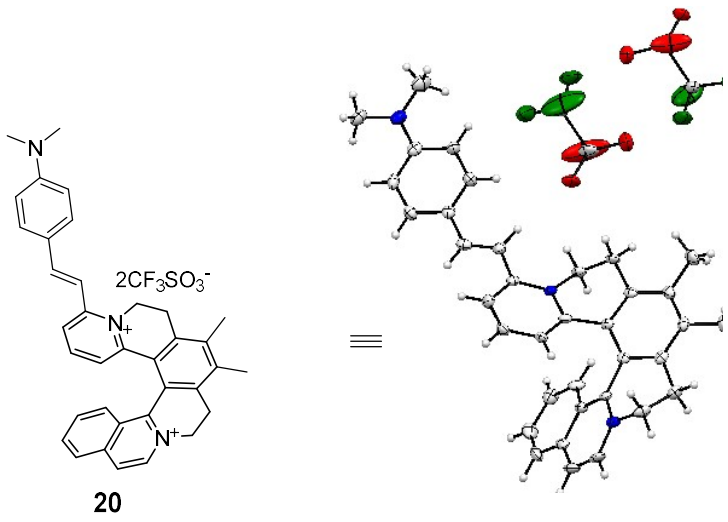

Fig. 57: *X-ray crystal structure of helquat derivative* ***20****.*

Few representative examples of **Type I** derivatives with their respective yields are shown in Fig. 58.

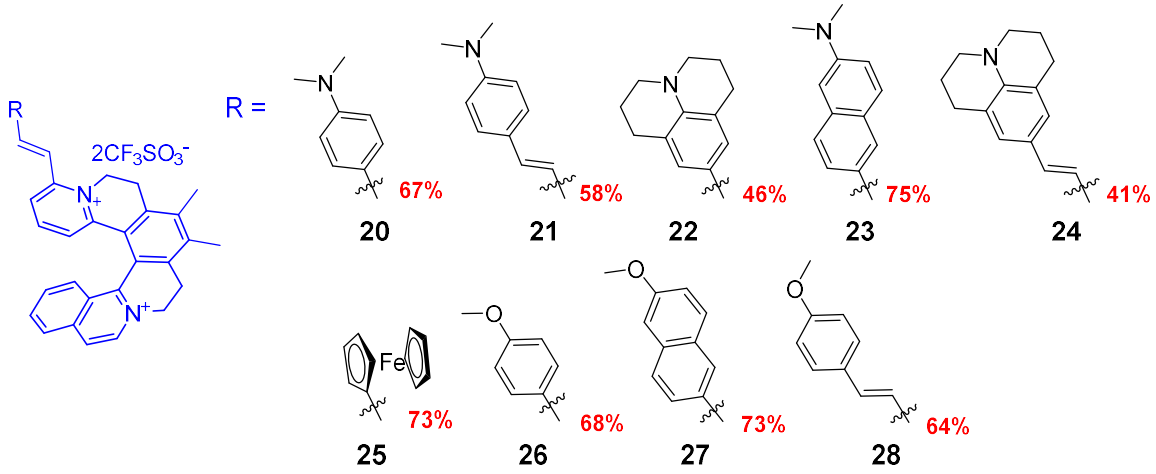

Fig. 58: *Generic structure of* ***Type I*** *derivatives (blue). Various R-group were connected to [6]helquat core with their respective yields mentioned in red.*

Helquat derivatives of **Type II**, **III** and **IV**, originating from helquat scaffolds **10**, **14** and **16**, respectively were synthesized by slightly tuning the reaction conditions and modifications in the purification procedure (Table 3).

Derivative type	Base (equiv.)	Aldehyde (equiv.)	Modifications in purification procedure
Type II	15	15	i) For few of them, MeOH was replaced with MeCN for re-dissolution of the solid during re-precipitation and purification. Less volume of Et_2O was used during precipitation. ii) For few derivatives, reaction times were higher due to the presence of two reactive methyl groups.
Type III	15	15	-
Type IV	15	15	-

Table 3: *Fine tuning of reaction conditions and purification methods to achieve* ***Type II****,* ***III*** *and* ***IV*** *helquat derivatives.*

Type II helquat derivatives originating from helquat **10** were extensively synthesized and were screened for their target-specific fluorescence light-up properties and applications based on these properties, such as fluorescent probes were developed.

For the synthesis of helquat derivatives of **Type II**, the Knoevenagel condensation methodology was successfully extended to achieve bischromophoric dyes, according to finely tuned reaction conditions and purification method described in Table 3. Reactions using a lower amount of base and aldehyde were usually sluggish, which led to longer reaction times and less clean reaction mixtures.

The generic reaction and few representative examples of **Type II** helquat derivatives with their respective yields are shown in Scheme 29.

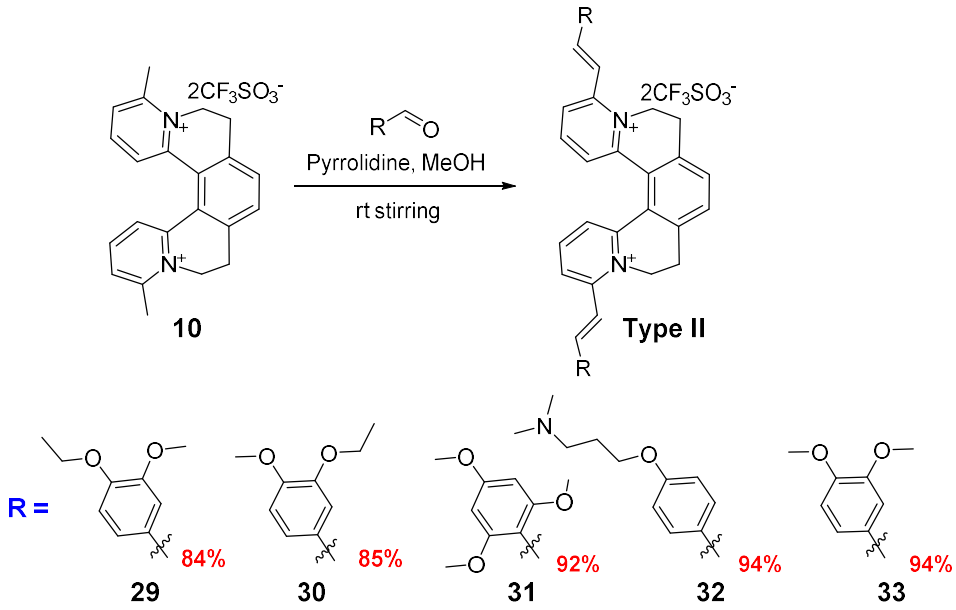

Scheme 29: *Generic scheme and few representative examples of* ***Type II*** *derivatives with their respective yields.*

Using above methodology, more than 200 derivatives of **Type II** were synthesized; some representative examples are shown in Scheme 29 with their respective yields.

Helquat derivatives of **Type III** and **IV** were synthesized from the respective substrates **14** and **16** by following reaction conditions summarized above. A small library of more than 50 compounds was synthesized (~ 35 and ~ 15, respectively).

Representative examples of these two series are shown in Scheme 30.

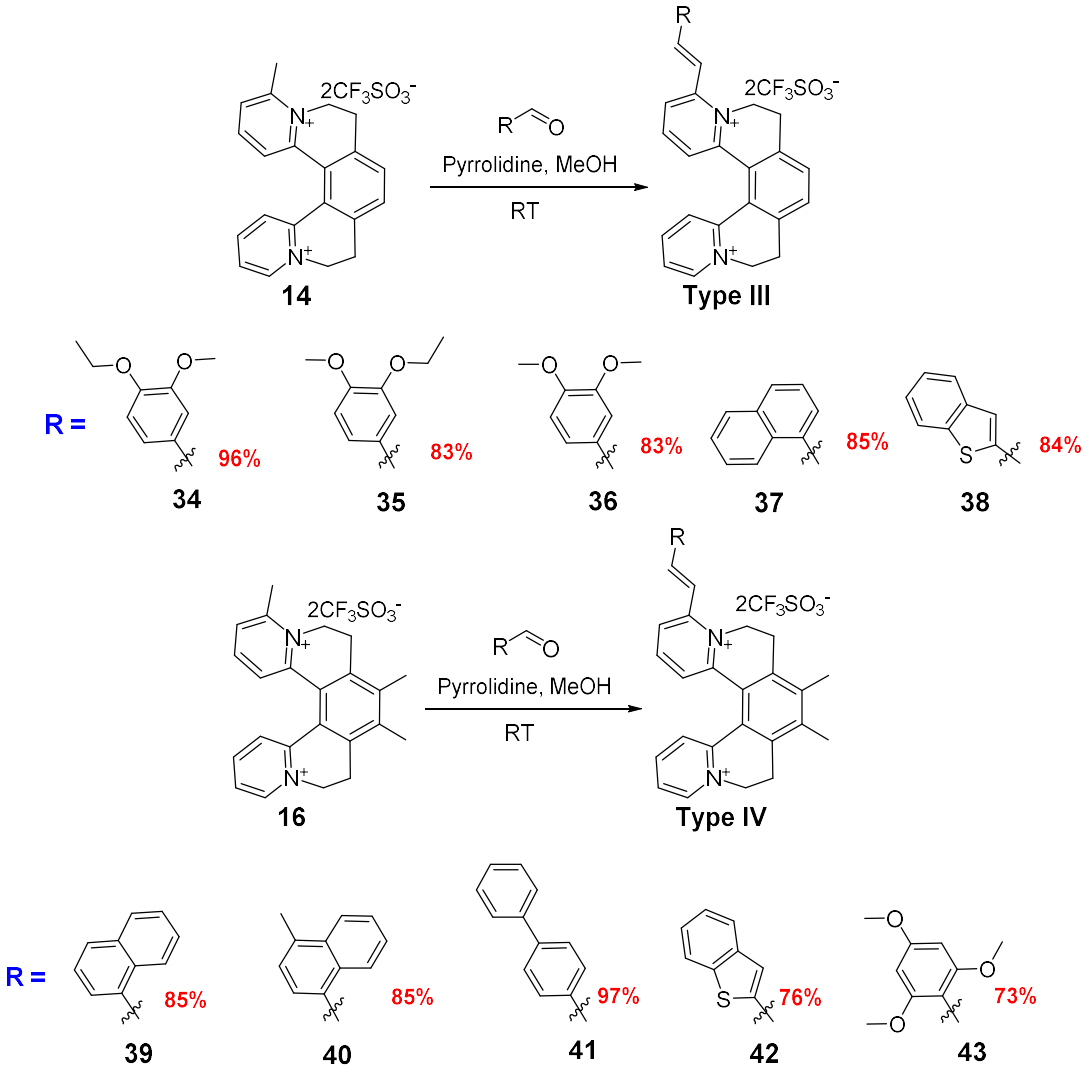

Scheme 30: *Generic scheme and representative examples of* ***Type III*** *and* ***IV*** *derivatives.*

- **Planar cationic dyes, representing controls of helquat derivatives:**

Planar dyes originating from two pyridinium substrates **17** and **18** were synthesized and screened in various experiments as controls of their helical counterparts. These dyes were prone to formation of unknown side products with increasing reaction time. Therefore, the reaction rate was increased either by refluxing EtOH solution of all reaction components in dark or in microwave reactor at 70 °C (Scheme 31).

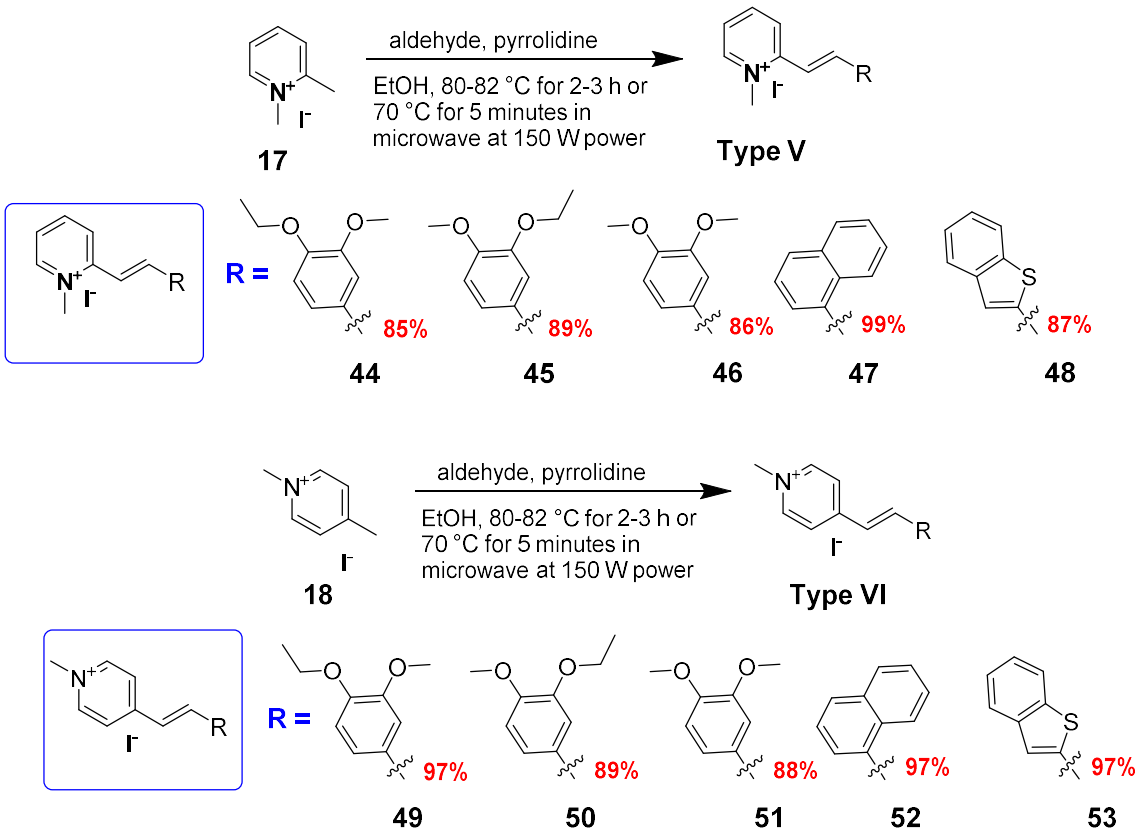

Scheme 31: *Synthesis of planar dyes of* ***Type V*** *and* ***VI****.*

3.2 Properties of helquats and their derivatives:

- **Chiroptical Properties of helquats:**

The key feature of helquats is their helical chirality. Helquats can be resolved into separate enantiomers. Our group has studied the chiral properties of helquats and developed some successful procedures for their resolutions to isolate enantiopure helquat samples in multigram scale. Out of all the helquats reported in this thesis only [6]helquat **6** can be resolved into pure enantiomers.

In our group, successful resolution of resolvable diquats (unpublished results) was achieved by direct precipitation of only one diastereomer with an addition of sodium salt of L-DBT into the aqueous solution of *racemic* dication. The second diastereomer goes to water and precipitated diastereomer was further purified by repeated washings with MeOH or EtOH. Diastereomer thus separated *via* very direct and practical protocol followed by second anion exchange from L-DBT to achiral anions (triflate or bromide) to give pure enantiomer was applied for the resolution of resolvable helquat **6**, but no diastereomer precipitation was achieved by this direct precipitation approach (Scheme 32).

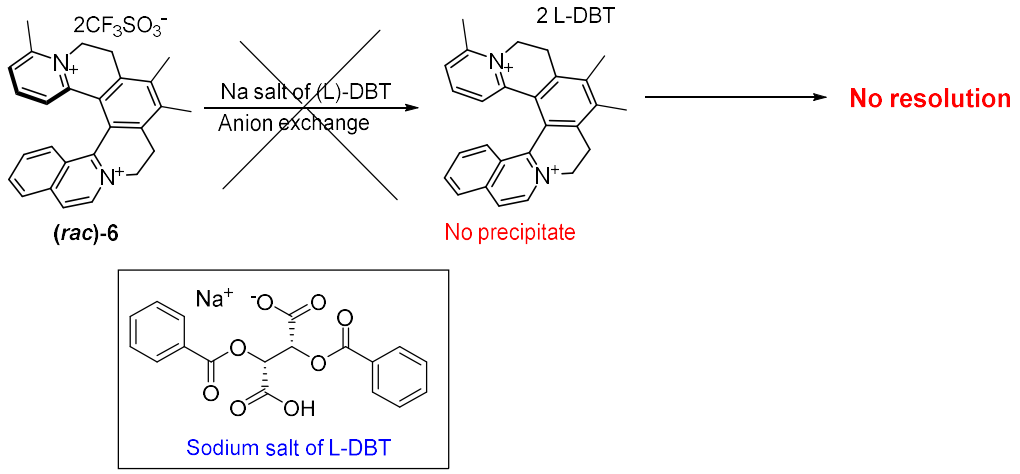

Scheme 32: *Failure of the resolution of helquat* ***6*** *by direct precipitation.*

In our group, other diquats were successfully resolved by another method, in which diastereomeric mixture was precipitated by addition of sodium borate salt of *R*-mandelic acid into the ethanolic solution of diquat. Diastereomers were separated from the mixture by EtOH washings and pure enantiomers were obtained by exchanging chiral anion to achiral anions (TfO^-, Cl^-).

In case of resolution of helquat **6**, a sticky solid was precipitated out from the ethanolic solution after 12 h of addition of the borate salt, which was analyzed by capillary electrophoresis (CE) and found to be the diastereomeric mixture. However, after several washings with EtOH, separation of diastereomers did not take place, resulting in unsuccessful resolution (Scheme 33).

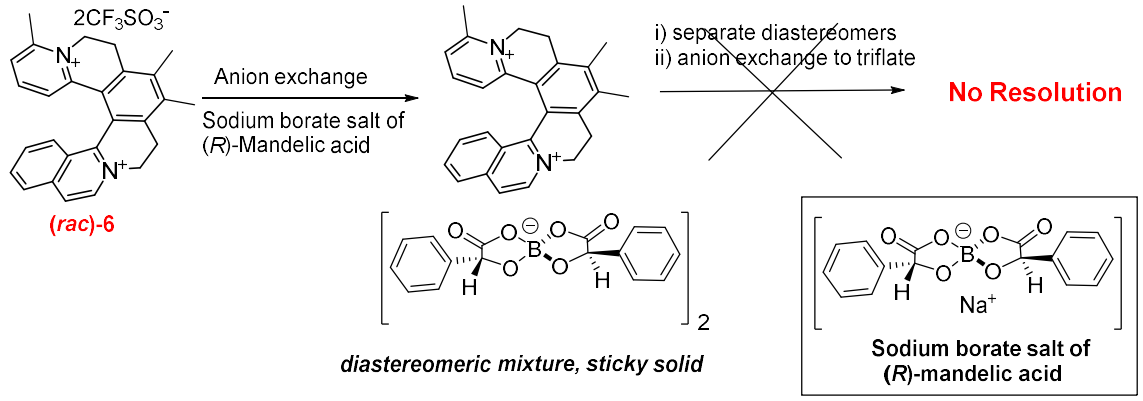

Scheme 33: *Failure of the resolution of helquat* ***6****.*

The successful resolution was achieved by following the reported procedure with other helquat scaffolds.[181]

A mixture of diastereomeric salts of both enantiomers of [6]helquat **6** was obtained by passing a methanolic solution of *racemic* helquat through a resin (anion exchange resin) column pre-loaded with L-DBT anions (Scheme 34). After confirming complete anion exchange by fluorine NMR, the attempts were made for successful separation of diastereomers.

In an initial attempt, obtained mixture of diastereomers was purified by trituration with EtOH. No separation of diastereomers was achieved using this method.

In next attempt, the diastereomeric mixture was purified using MeOH, by trituration of the mixture of the two diastereomeric salts with MeOH, which involves sonication leading to the dissolution of one diastereomeric salt in MeOH and the second diastereomer was left undissolved.

The success of the resolution was decided after analyzing the results of chiral capillary electrophoresis of final solid. The obtained solid was sufficiently enantiopure (*ee* > 98%).

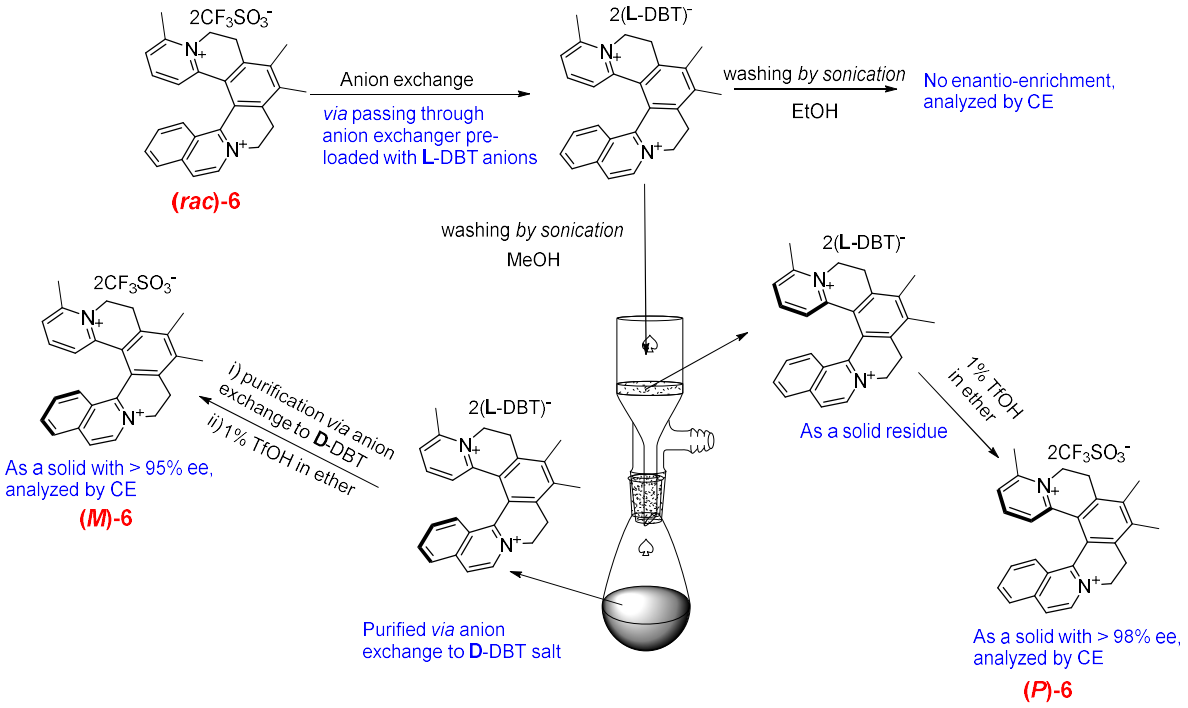

Scheme 34: *Resolution of helquat* ***6*** *via anion exchange and separation of the resulting diastereomeric salts.*

Respective pure enantiomers were obtained by breaking diastereomeric salt of pure enantiomer by second anion exchange from chiral, L-DBT counterion to achiral counterion such as triflate. The enantiopurity of obtained pure enantiomer was accessed by chiral CE analysis using cyclodextrins as chiral selectors (Fig. 59).

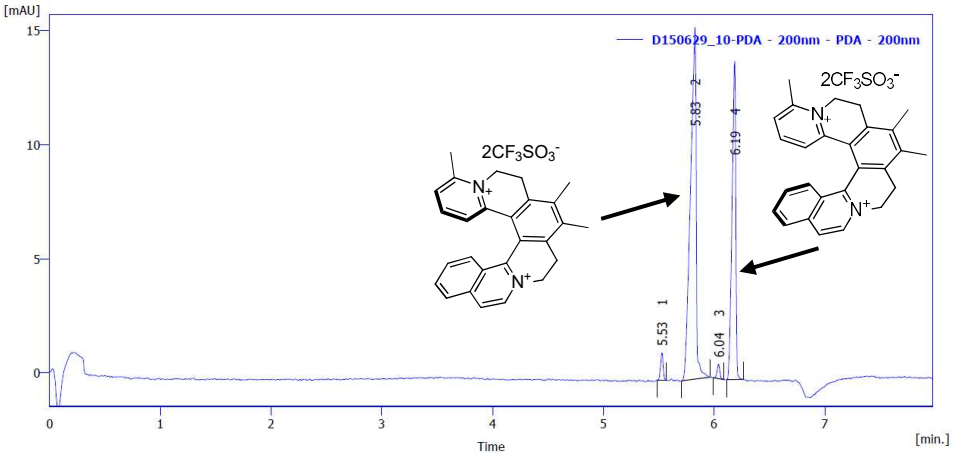

Result Table (Uncal - D150629_10-PDA - 200nm - PDA - 200nm)

	Migr. Time [min]	Area [mAU.s]	Height [mAU]	Area [%]	A/t% [%]	Efficiency [th.pl]	Resolution [-]	w [s]
1	5.529	1.9	1.2	2.09	2.25	199093		1.75
2	5.829	55.6	15.4	61.04	62.28	55321	4.046	3.50
3	6.042	1.1	0.6	1.21	1.19	237711	2.866	1.75
4	6.188	32.5	14.0	35.67	34.28	122169	2.429	2.50
	Total	91.1	31.2	100.00				9.50

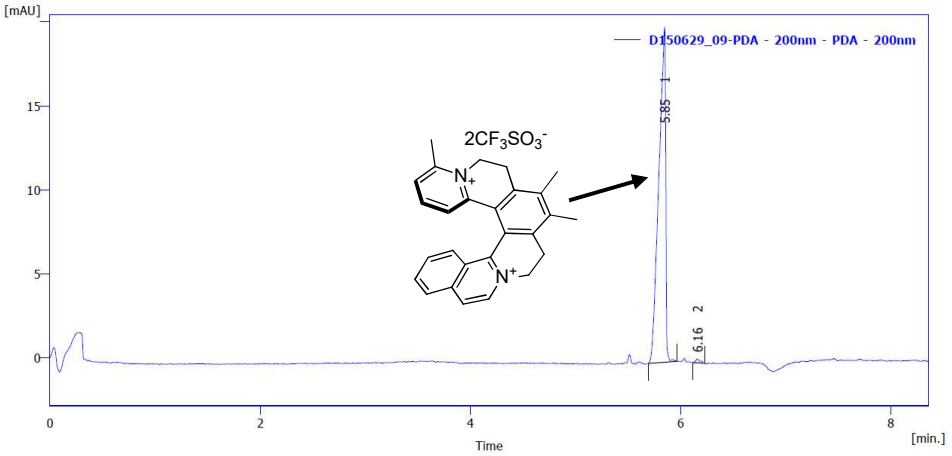

Result Table (Uncal - D150629_09-PDA - 200nm - PDA - 200nm)

	Migr. Time [min]	Area [mAU.s]	Height [mAU]	Area [%]	A/t% [%]	Efficiency [th.pl]	Resolution [-]	w [s]
1	5.846	89.8	19.9	99.21	99.25	30208		4.75
2	6.158	0.7	0.2	0.79	0.75	121020	3.052	2.50
	Total	90.5	20.2	100.00				7.25

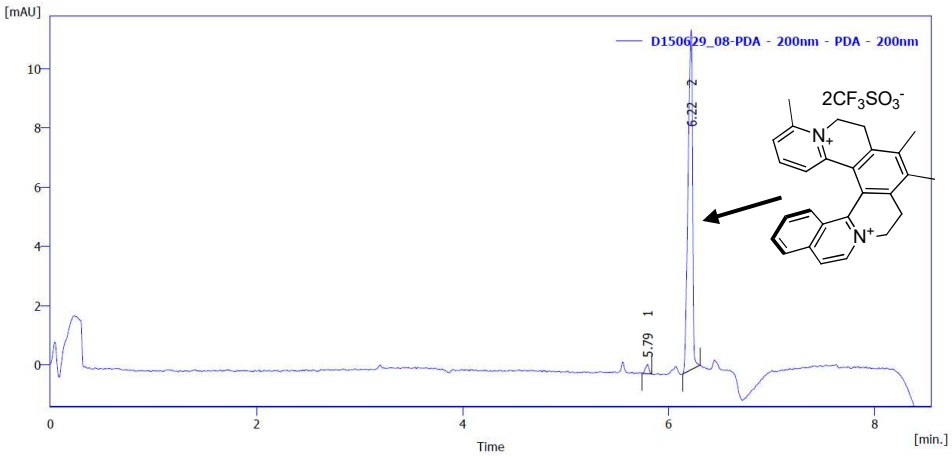

Result Table (Uncal - D150629_08-PDA - 200nm - PDA - 200nm)

	Migr. Time [min]	Area [mAU.s]	Height [mAU]	Area [%]	A/t% [%]	Efficiency [th.pl]	Resolution [-]	w [s]
1	5.792	0.8	0.3	2.16	2.32	88461		2.75
2	6.217	34.7	11.5	97.84	97.68	85642	5.233	3.00
	Total	35.4	11.8	100.00				5.75

Fig. 59: *Capillary electrophoresis charts for a)* ***(rac)-6****; b)* ***(P)-6*** *and c)* ***(M)-6*** *helquat bistriflate.*

The pure diastereomer obtained from an anion exchange to (L-DBT) was re-exchanged to the achiral, diiodide salt. The enantiopurity of this material was accessed by CE (>98%) and the X-ray quality crystals of the pure enantiomer thus obtained were grown by slow diffusion of MTBE into the MeCN solution of the enantiopure **6** diiodide. From the X-ray diffraction study of enantiopure helquat diiodide, obtained by above-mentioned root, the absolute configuration was assigned to be *P* (plus).

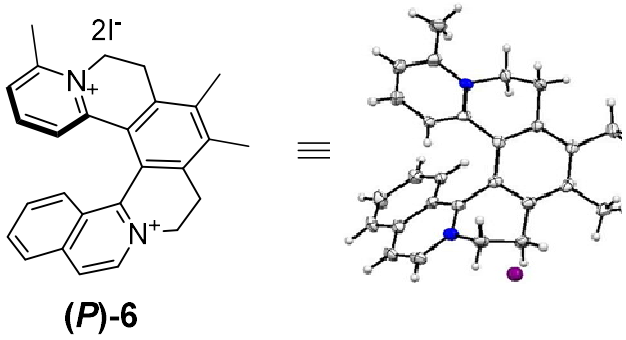

(*P*)-6

Fig. 60: *X-ray crystal structure of pure enantiomer, as a proof for the absolute configuration.*

The racemization energy and temperature of helquat **6** were determined by heating DMSO solution of 1.0 mg of pure **(*P*)-6** (0.5 mL) at 120 °C. The racemization process was monitored by chiral CE analysis of the samples taken after every 20 minutes. The decrease in *ee* of the major enantiomer with time follows the first order kinetics. When the kinetic law is transformed into the logarithmic form, the graph is linearized and the slope of the line corresponds to the desired rate constant of racemization 2k (Fig. 62). From this value, half-life of the racemization was calculated as

$$T_{1/2} = (ln\ 2)/2k \qquad \textit{(eq. 4)}$$

According to the theory of transition state, rate constant *k* can be transformed into activation Gibbs energy. This is the barrier of interconversion of one enantiomer into the other.

$$k = \frac{k_B T}{h} e^{-\Delta G^{\#}/RT} \qquad \textit{(eq. 5)}$$

Where k_B is Boltzmann constant (1.3806504 X 10^{-23} Jk^{-1}), *R* is the universal gas constant (8.314472 $Jk^{-1}mol^{-1}$), *h* is Planck constant (6.62606896 X 10^{-34} Js) *T* is thermodynamic temperature (in Kelvin).

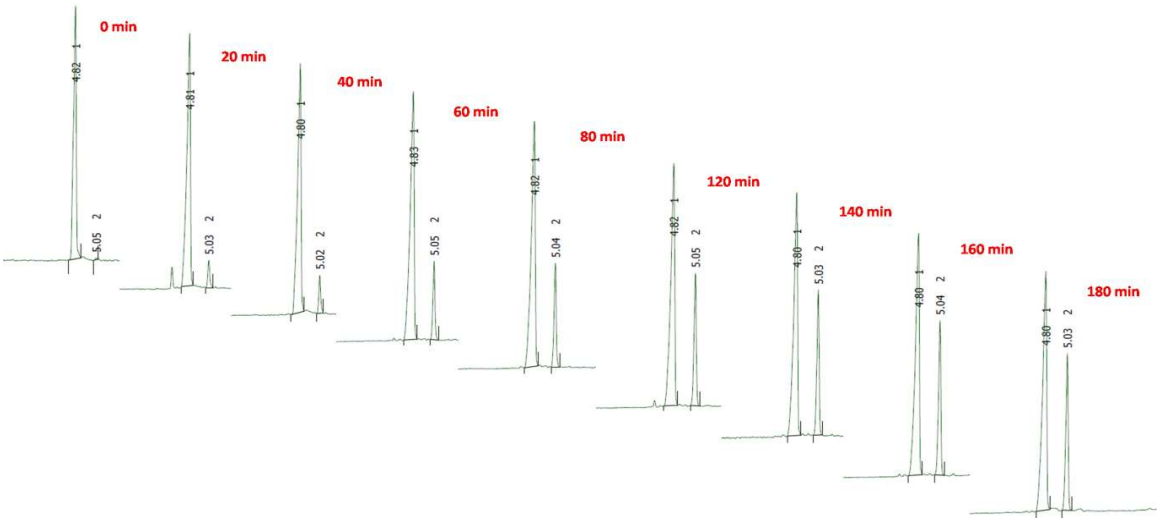

Fig. 61: *Monitoring of racemization progress at 120 °C, with increasing time %ee of major enantiomer was decreased.*

Time (minutes)	Peak 1	Peak 2	ee (%)	ln (ee %)
0	99.6	0.4	99.2	4.597
20	98.1	1.9	96.2	4.566
40	94.6	5.4	89.2	4.491
60	92.5	7.5	85.0	4.443
80	86.4	13.6	72.8	4.288
100	81.2	18.8	62.4	4.134
120	76.6	23.4	53.2	3.974
140	74.7	25.3	49.4	3.900
160	73.5	26.5	47.0	3.850
180	72.1	29.9	42.2	3.738

Table 4: *Data from CE measurement, during the racemization of helquat* ***(P)-6*** *at 120 °C.*

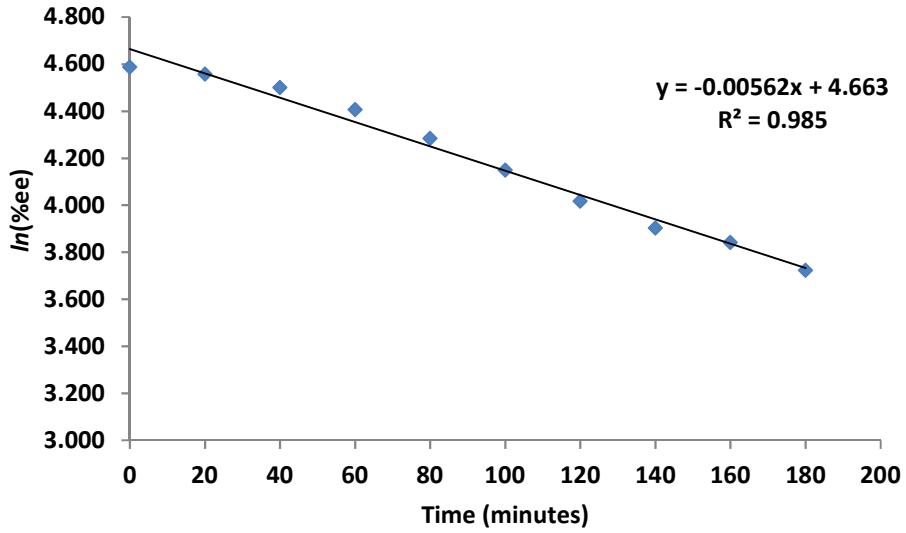

Fig. 62: *Racemization chart for* ***(P)-6*** *bis-triflate over time.*

Gibbs free energy $\Delta G^{\ddagger}$ (racemization barrier)			
$\Delta G^{\ddagger}$ (kJ/mol)	k (min^{-1})	k (s^{-1})	$T_{1/2}$ [h]
129.794	0.0028	5e-05	2.06

Table 5: *Results of racemization study of* ***(P)-6*** *bistriflate in DMSO-d_6 at 120° C.*

From the analysis of this data, we got the value of the activation free energy, $\Delta G^{\ddagger}$ = 129.8 kJ.mol^{-1} and racemization half-life at 120 °C, $T_{1/2}$ = 2 h.

- **Nonlinear optical properties of Type I helquat derivatives:**

Nonlinear optical properties of derivatives **20**–**28** were studied by Electronic spectroscopy, Hyper-Rayleigh scattering (HRS), Stark spectroscopy, and density functional theory (DFT) to assess their second-order NLO responses.

DFT and TD-DFT calculations were performed mainly to predict the molecular electronic structures and optical properties of the new cations characterized by experimental techniques. UV-vis. absorption spectra of derivatives **20**-**28** (Fig. 63) show an intense low energy absorption band due to charge transfer (ICT) from the amino/alkoxy unit to helquat fragment and less intense high-energy absorption band. By increasing conjugation between an acceptor and the donor part, the intense ICT band is shifted even higher towards the low energy region. This shifting of ICT band also depends upon the structure of donor part.

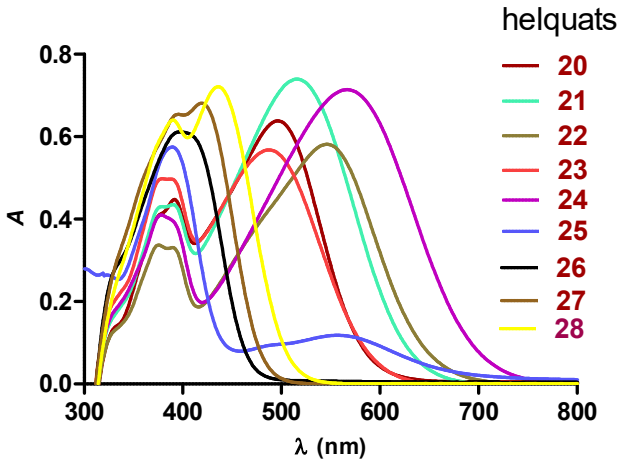

Fig.63: *UV-vis. spectra of helquat derivatives* ***20-28****.*

Helquat structure	Color	λ_{max} (nm)	ε (l.mol-1.cm^{-1})
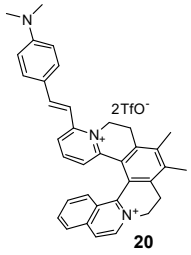 20	Purple	386 502	21674 31678
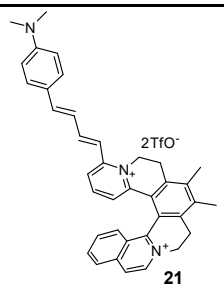 21	Purple	386 490	24842 28359
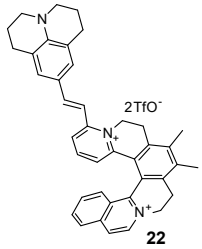 22	Purple	386 546	16461 29080

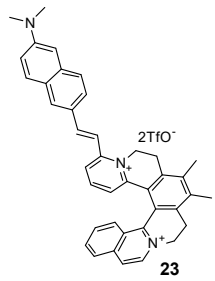 23	Red	386 523	21604 36690
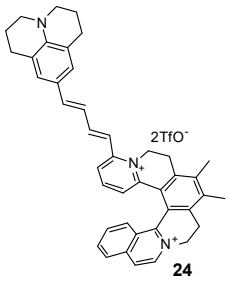 24	Deep blue	385 574	20136 35500
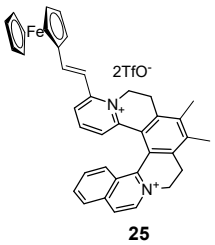 25	Blue	393 570	28504 5762
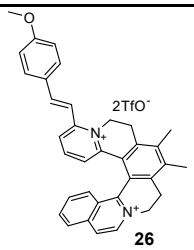 26	Yellow	391 419	30000 28000
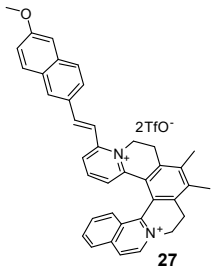 27	Lemon yellow	396 422	32000 34000
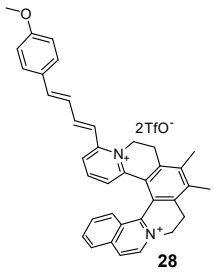 28	Orange	392 438	31000 36000

Table 6: *UV-vis. absorption properties of helquat dyes* ***20-28.***

The simulated UV-vis. spectra for dication **21** using above DFT TD-DFT method when compared with the experimental spectra confirms the above-mentioned behaviour of helquat chromophores (Fig. 64).

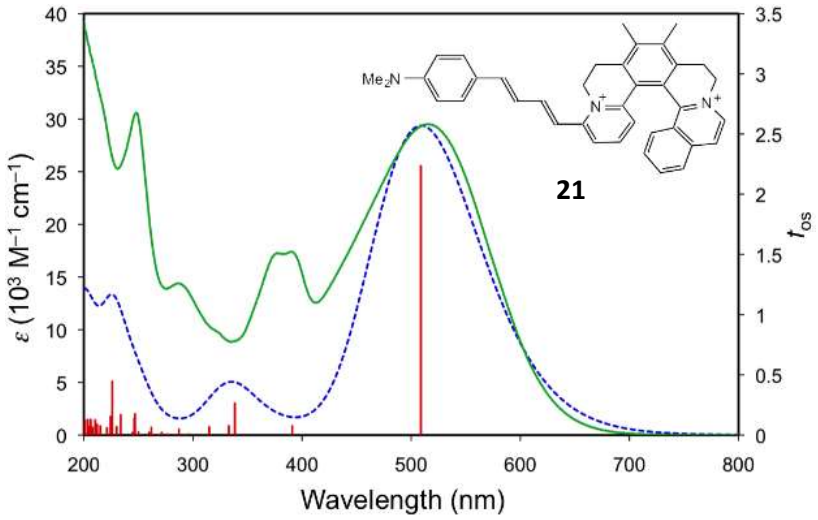

Fig. 64: *Experimental UV-vis. absorption spectra of helquat **21** (green line), with the CAM-B3LYP6-311G(d) calculated spectra. The ε-axes refer to the experimental data only and the vertical axes of the calculated data are scaled to match the main experimental absorptions. The f_{os}-axes refer to the individual calculated transitions (red).*

Molecular quadratic nonlinear optical (NLO) responses of all helquat derivatives **20**-**28** have been determined directly by using hyper-Rayleigh scattering (HRS) with 800 nm laser. The results of 800 nm *f*sHRS measurements[182] of resonant β values and β_0 (derived using the two-state model)[183] for cations **20–28** in MeCN are shown in Table 7 together with data reported for [DAS]PF_6.[184] The DFT and TD-DFT results confirm that the new chromophores are described adequately as two-state systems, i.e., a single low energy electronic transition is expected to dominate the NLO response. Helquat derivatives **20**-**28**, shows an increase in β_0[H] in the order **28** < **20** < **23** ≤ **22** < **21** ≤ **24**. The magnitude of β_0 increases either on extending the π-conjugation length or replacing a methoxy with a tertiary amino electron donor substituent. Thus the methoxy-substituted helquats show weak NLO responses than analogously substituted helquat with tertiary amino groups, possibly due to the weak electron donating strength of a methoxy group.

We have used Stark (electroabsorption) spectroscopy in PrCN glasses at 77 K to derive $\Delta\mu_{12}$ values for the low energy ICT bands of cations **20**-**28**. The results of stark spectroscopy[185] for salts **20**-**28**, along with DAS^+PF6^- are summarized in Table 7, and their representative spectra for **22**, **24** and **26** are shown below (Fig. 65).

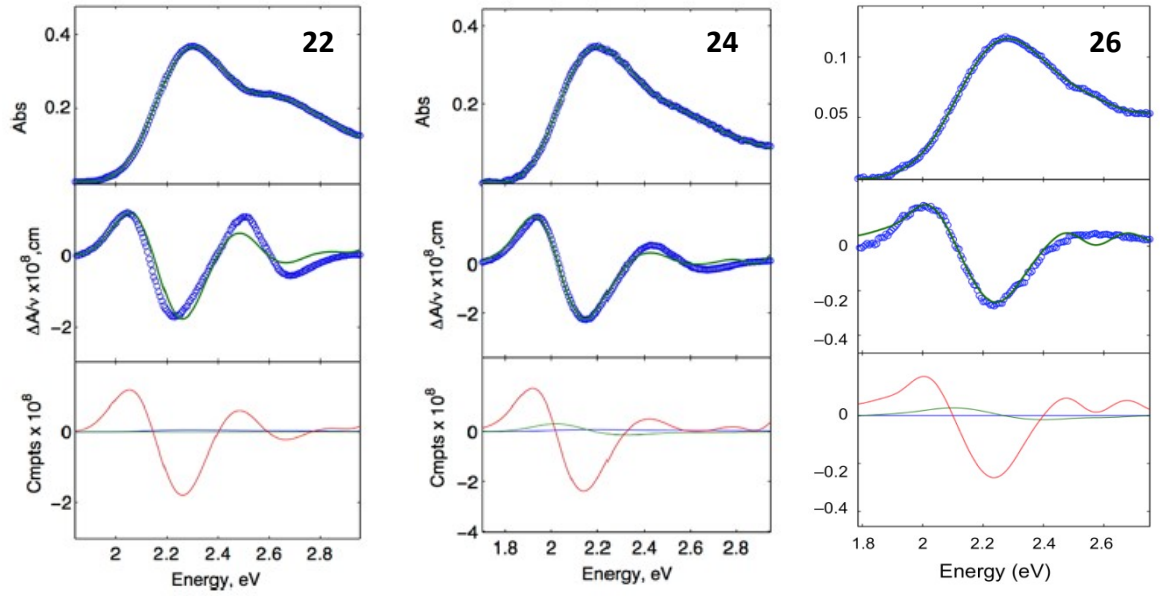

Fig. 65: *Spectral and calculated fits for salts* ***22***, ***24*** *and* ***26****. Top panel: UV–vis absorption spectrum; middle panel: electro absorption spectrum, experimental (blue), and fits (green) according to the Liptay equation[185b] and bottom panel: contribution of 0th (blue), 1st (green), and 2nd (red) derivatives of the absorption spectrum to the calculated fits.*

Salt	$\lambda_{max}{}^{a}$ *(nm)*	$\lambda_{max}{}^{b}$ *(nm)*	$E_{max}{}^{b}$ *(ev)*	$f_{os}{}^{b,c}$	$\mu_{12}{}^{b,d}$ *(D)*	$\Delta\mu_{12}{}^{b,e}$ *(D)*	$\beta_0[S]^{f}$ *(10^{-30} esu)*	$\beta_{800}{}^{g}$ *(10^{-30} esu)*	$\beta_0[H]^{h}$ *(10^{-30} esu)*
20	496	498	2.49	0.56	7.8	22.5	252	171±12	57±4
21	516	533	2.33	0.82	9.7	21.1	424	401±43	156±17
22	538	537	2.31	0.71	9.0	20.2	364	209 ±6	93±3
23	485	493	2.52	0.46	7.0	29.5	260	302±13	90±4
24	564	564	2.20	0.78	9.7	26.1	588	376±32	187±16
25	557	544	2.28	0.09	3.2	14.5	36	208±21[j]	-[i]
26	396	427	2.90	0.07	2.5	15.4	14	-[i]	-[i]
		407	3.05	0.17	3.9	13.6	26		
		383	3.24	0.11	3.0	6.0	6		
27	417	433	2.86	0.15	3.7	14.7	28	-[i]	-[i]
		412	3.01	0.17	3.9	12.8	26		
		384	3.23	0.21	4.7	0.0	2		
28	436	455	2.73	0.23	4.7	15.8	54	199±8	26±1
		428	2.90	0.34	5.6	13.0	56		
		382	3.25	0.35	5.3	8.5	28		
[DAS^{+}]^{i} PF_6^{-}	470	470	2.58	0.8	9.1	16.3	236	440±30	110±7

Table 7: *ICT absorption, Stark spectroscopic, and HRS data for salts* ***20–28****.*

[a]In MeCN at 295 K. [b]In PrCN at 77 K. [c]Obtained from $(4.32 \times 10^{-9}$ M cm$^2)\varepsilon_{max} \times fw_{1/2}$, where ε_{max} is the maximal molar extinction coefficient and $fw_{1/2}$ is the full width at half height (in wavenumbers). [d]Calculated from **eq 1.** [e]Calculated from $f_{int}\Delta\mu_{12}$ using $f_{int} = 1.33$. [f]Calculated from **eq 2.** The quoted cgs units (esu) can be converted to SI units (C^3 m^3 J^{-2}) by dividing by 2.693×10^{20} or into atomic units by dividing by 0.8640×10^{-32}. [g]Obtained from HRS measurements with an 800 nm Ti^{3+}:sapphire laser and MeCN solutions at 295 K. [h]Derived from β_{800} by application of the two-state model. [i] Could not be measured due to weak HRS signals.

In case of methoxy-substituted derivatives (**26**-**28)**, the ICT bands show almost no change on moving from MeCN to PrCN. However, small red shifts were observed in case of amino-substituted helquats (**20**-**25**) on moving from MeCN solutions to PrCN glasses. The decreases

in E_{max} on extending a vinyl to 1,3-butadienyl bridge or replacing a 4-(dimethylamino)-phenyl with julolidinyl group are maintained at 77 K. The μ_{12} values determined using eq. 6 below:

$$|\mu_{12}| = \left(\frac{f_{os}}{1.08 \times 10^{-5} E_{max}}\right)^{1/2} \quad (eq.\ 6)$$

All values were falling into a relatively narrow range with small increases on conjugation extension. In general, $\Delta\mu_{12}$ also increases in the same manner and as expected, although the value for **23** was unexpectedly low.

The β_0[S] values determined using the eq. 7 below:

$$\beta_0\,[S] = \frac{3\Delta\mu_{12}(\mu_{12})^2}{(E_{max})^2} \quad (eq.\ 7)$$

β_0 values were in order, **26 < 27 < 25 < 28 < 20 ⩽ 23 < 22 < 21 < 24** matches the HRS trend exactly. The expected increases in the NLO response on enhancing the electron donor strength or extending the conjugation are thus also shown by most of the Stark-derived data. However, the difference is within the estimated error limit of ±20%. Also, as for the HRS data, changing the helquat unit leads to variations in β_0[S] that are generally not statistically significant.

The electronic structure of the molecule **20** was predicted using DFT calculations (Fig. 65). MOs of compound **20**, were determined from gas phase transition, whereas DFT and TD-DFT calculations show the lowest energy transition from HOMO -> LUMO and HOMO -> LUMO+1. HOMO is located on the 4-(dimethylamino)styryl fragment whereas LUMO is mostly based on the helquat unit and the LUMO+1 spread over the whole molecule (Fig. 66).

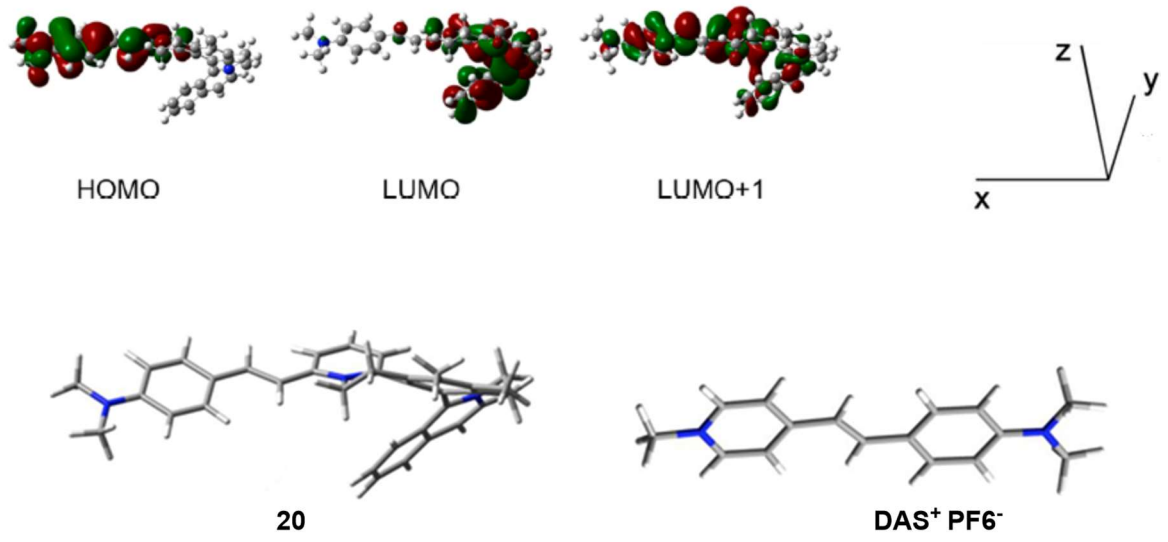

Fig. 66: *CAM-B3LYP/6-311G(d)-derived contour surface diagrams of the frontier MOs for cation **20** (isosurface value 0.03 au), optimized structures of the cation **20** and DAS+, with the axis convention used in the hyperpolarizability calculations.*

Cation	ΔE (ev)	λ (nm)	f_{os}	Major contributions
20	2.76	449	1.570	H → L (43%), H → L+1 (48%)
	3.37	368	0.136	H–1 → L (10%), H → L (37%), H → L+1 (38%)
	3.67	338	0.297	H–2 → L (28%), H–1 → L (54%)
	3.87	320	0.055	H → L+2 (73%)
	4.00	310	0.069	H–3 → L (14%), H–2 → L (49%), H–1 → L
	4.29	289	0.042	H–5 → L (35%), H–3 → L (35%)
	4.54	273	0.049	H–2 → L+1 (24%), H–1 → L+1 (34%)
	4.82	257	0.022	H → L+3 (72%)
	4.90	253	0.123	H–3 → L+1 (12%), H–2 → L+2 (20%), H–1 → L+2 (23%)
	5.04	246	0.070	H–4 → L (15%), H–4 → L+1 (35%), H → L+5 (14%), H → L+6 (23%)
	5.12	242	0.016	H–1 → L+1 (28%), H–1 → L+2 (21%)
	5.23	237	0.101	H–5 → L (20%), H–3 → L (21%), H–2 → L+2 (12%)
	5.25	236	0.075	H → L+4 (11%), H → L+5 (32%), H → L+7 (19%)
	5.32	233	0.169	H–5 → L+1 (17%), H–3 → L+2 (16%), H–2 → L+2 (17%), H–1 → L+4 (10%)
	5.37	231	0.173	H–5 → L (10%), H–5 → L+2 (12%), H–3 → L+1 (49%)
	5.51	225	0.491	H–6 → L (25%), H–5 → L+1 (14%), H–1 → L+3 (19%)
	5.58	222	0.184	H–1 → L+3 (17%), H → L+4 (30%), H → L+5 (12%)
	5.79	214	0.032	H–5 → L+1 (27%), H–3 → L+2 (17%), H → L+7 (10%)
	5.85	212	0.027	H–5 → L+3 (13%), H–2 → L+3 (32%), H–1 → L+3 (14%)
	5.93	209	0.018	H–3 → L+2 (12%), H–2 → L+3 (10%), H → L+7 (14%)
	5.96	208	0.153	H–2 → L+4 (10%), H–1 → L+4 (23%)
	6.02	206	0.058	H–9 → L (16%), H–5 → L+2 (19%)
	6.05	205	0.044	H–8 → L (11%), H–3 → L+3 (19%), H–2 → L+3 (10%)
	6.08	204	0.183	H–9 → L (10%), H–8 → L (32%), H–8 → L+1 (12%)

6.14	202	0.127	H–2 → L+4 (27%)
6.26	198	0.065	H–11 → L (16%), H–7 → L (19%), H–6 → L+2 (11%)
6.26	198	0.078	H–6 → L+1 (39%), H–6 → L+2 (16%)
6.36	195	0.087	H–12 → L (13%), H–7 → L+1 (12%), H–6 → L+3 (12%)
6.42	193	0.262	H–12 → L (19%), H–11 → L (15%), H–6 → L+3 (11%)
6.46	192	0.015	H–10 → L (12%), H–10 → L+1 (38%)
6.46	192	0.030	H → L+11 (56%), H → L+13 (16%)
6.53	190	0.015	H–6 → L+2 (14%)
6.53	190	0.124	H–12 → L (13%), H–8 → L+1 (19%)

Table 8: *Selected TD-DFT-calculated data for cation* ***20****.*

Note: Geometry optimizations and TD-DFT calculations used the CAM-B3LYP functional with the 6-311G(d) basis set, and a CPCM MeCN solvent model was included for TD-DFT. Only the main transitions within each absorption band are included. H = HOMO, L = LUMO.

atom	*x*	*y*	*z*
N	8.938623	0.17543	–0.569128
C	–1.467294	–0.645551	1.835076
H	–2.475991	–0.830667	2.173323
C	–0.389445	–1.339288	2.401899
H	–0.568716	–2.079859	3.172115
C	0.87875	–1.108696	1.958783
H	1.701071	–1.697778	2.3369
C	1.14195	–0.129418	0.975948
N	0.061826	0.591662	0.517569
C	0.269922	1.798879	–0.30703
H	0.152943	1.54192	–1.363423
H	1.288891	2.135343	–0.147571
C	–0.693994	2.896799	0.1012
H	–0.460887	3.239683	1.115219
H	–0.519047	3.743266	–0.561647
C	–2.117585	2.421636	0.002491
C	–3.177903	3.280825	–0.310579
C	–4.479914	2.769816	–0.393714
C	–4.698626	1.40977	–0.162021
C	–6.084138	0.824974	–0.050543
H	–6.788663	1.576447	0.30291
H	–6.464019	0.4605	–1.010993
C	–6.048416	–0.299107	0.965745
H	–5.724544	0.063711	1.9437
H	–7.016458	–0.780784	1.076713
N	–5.089417	–1.325069	0.498947
C	–5.452478	–2.64582	0.559874
H	–6.401234	–2.850537	1.034067

C	–4.652664	–3.607297	0.052937
H	–4.947374	–4.645841	0.131248
C	–3.474	–3.242358	–0.640819
C	–2.678155	–4.20488	–1.296248
H	–2.945761	–5.251849	–1.21663
C	–1.60634	–3.814294	–2.048495
H	–1.00767	–4.554577	–2.565512
C	–1.297992	–2.445379	–2.189819
H	–0.483378	–2.148636	–2.839268
C	–2.029658	–1.494269	–1.538114
H	–1.806993	–0.44824	–1.690834
C	–3.12434	–1.866201	–0.717962
C	–3.926166	–0.91204	–0.027005
C	–3.626714	0.533986	0.05583
C	–2.333625	1.066218	0.241808
C	–1.235647	0.290916	0.865082
C	2.439561	0.107062	0.443156
H	2.512098	0.604147	–0.513734
C	3.596725	–0.284889	1.067595
H	3.509927	–0.726301	2.056945
C	4.928874	–0.153122	0.609533
C	5.987392	–0.565757	1.450524
H	5.75365	–0.975732	2.427868
C	7.298165	–0.464695	1.080024
H	8.06357	–0.795478	1.766423
C	7.65407	0.067202	–0.188523
C	6.591031	0.481411	–1.044182
H	6.811342	0.88763	–2.020585
C	5.289038	0.373502	–0.653016
H	4.521147	0.700124	–1.345289
C	10.011352	–0.252936	0.320558
H	10.002561	0.313043	1.254694
H	10.967402	–0.083373	–0.164524
H	9.935049	–1.317778	0.551675
C	9.284704	0.720924	–1.875658
H	8.866968	0.116057	–2.683723
H	10.364463	0.724823	–1.986064
H	8.932837	1.749311	–1.984422
C	–2.934583	4.752804	–0.507418
H	–2.047658	5.099899	0.018031
H	–3.769387	5.347548	–0.141869
H	–2.807795	4.996233	–1.566974
C	–5.629666	3.680117	–0.73665
H	–6.480862	3.13746	–1.142014
H	–5.340337	4.413096	–1.488114
H	–5.977508	4.237997	0.138027

Table 9: *DFT-optimized coordinates for cation* ***20****.*

The β_{tot} value obtained *via* DFT for dyes **20** and **21** were showing an increase while moving from the gas phase to MeCN and are in correlation to the data obtained by HRS and Stark spectroscopy. β_{tot} increases substantially from 214 (for **20**) to 345 (for **21**) in the gas phase

with increasing the π-conjugation system in each pair. Whereas, by moving from gas phase to MeCN, the β_{tot} value for cation **20** was increased from 214 -> 472 and for cation **21**, it was changed from 345 to 1069.

Comparing the β_0 values for helquat dyes **20**-**28** with those of [DAS]PF_6 reveals that a number of the new dye salts show a similar level of NLO activity and that several compare favourably. In particular, **21**, and **24** show β_0[S] responses twice as large or even greater when compared with this benchmark compound. These enhancements are due to a combination of decreasing E_{max} and increasing $\Delta\mu_{12}$. These observations provide a strong incentive to pursue further crystalline materials as well as pure enantiomers (*P* and *M*) incorporating these new helquat cations in which large bulk NLO effects can be anticipated.

For this reason, the pure enantiomers of helquat **6** were synthesized and multigram quantity. Pure enantiomers of helquat dyes **20-28** will be synthesized and screened for their nonlinear optical properties in solution as well as in crystalline form.

- **Target-specific fluorescence light-up properties: search of heparin chemosensors:**

A chemical compound, recognizing the presence of a particular analyte of interest by remarkable changes in color or spectroscopic properties after interaction as compared to the sensor alone are widely studied. Such molecules are known as chemosensors and the much-desired quality of such a chemosensor must be its specificity and selectivity for the particular target of interest. Quantification of a particular analyte of interest in the complicated environment is much-desired application area of such sensors.

We were interested to screen our dyes with various important biological targets. As our dyes are cationic in nature, we expected to have electrostatic interactions with targets, which are highly negatively charged. Heparin is a member of glycosaminoglycan family and is known as a highly negatively charged molecule. It is used as an anticoagulant drug during cardiovascular surgery and many more complicated medical procedures. Taking an inspiration from the diversity-oriented approach (DOFLA)[163] developed by Chang *et al.* in search of fluorescent chemosensors, we decided to develop an assay using the experimental setup is described in the experimental section. The simple setup comprising a 96 or 384-well plate, a device for identification of preliminary hits by observing the changes that are visible with naked eyes after irradiation with UV-transilluminator and a plate reader for confirming the visually identified hits by spectroscopic measurements.

As heparin is administered at therapeutic dosing levels of 2-8 U/mL (17–67 μM) during cardiovascular surgery and 0.2–1.2 U/mL (1.7–10 μM) in post-operative and long-term care[186]. As reported in previously developed assays, for the preliminary screening 10 μM of each dye was mixed with 10 μM of heparin in HEPES (2-(4-(2-hydroxyethyl)piperazine-1-yl)ethane sulphonic acid) buffer, 10 mM (pH 7).[162, 163]The fluorescence response of each dye in absence and presence of heparin was monitored.

Before starting actual screening, the solubility of dyes containing various functional groups was determined. As most of our dyes were insoluble in HEPES buffer (pH 7), we decided to use 1 mM DMSO stock solutions of the dyes and dilute them inside the well to appropriate DMSO %, which was determined by checking the solubility of few representative dyes under four different conditions summarized in Table 10. Based upon the results, we decided to go with 10% DMSO for all preliminary screening experiments.

Structure	Solubility conditions (with % DMSO in HEPES buffer (pH 7.0)			
	0	1	5	10
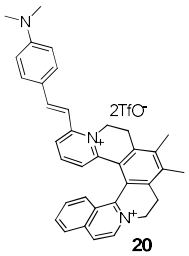 20	insoluble	soluble	soluble	soluble
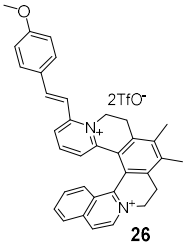 26	insoluble	soluble	soluble	soluble
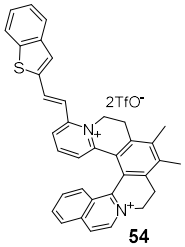 54	insoluble	insoluble	soluble	soluble
 33	insoluble	insoluble	insoluble	soluble
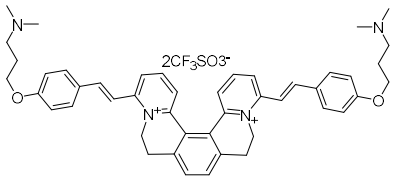 32	insoluble	insoluble	soluble	soluble
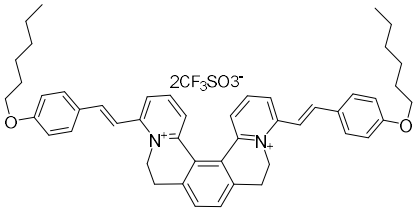 69	insoluble	insoluble	insoluble	Soluble

Table 10: *Screening of solubility conditions for helquat dyes.*

A high-throughput assay was a need to screen a library of compounds under the identical conditions in multiplicates. To identify the compounds, which shows selective florescence light-up in presence of heparin alone, two separate wells were produced for each compound, with one containing a solution of heparin in the buffer and the other for the dye alone (in absence of heparin). Each experiment was performed at least in duplicate to remove possible experimental error during the experiment preparation. After giving proper

interaction time to both the interaction partners, the preliminary assessment of the hits was performed by recording the fluorescent photograph of the whole experiment under irradiation of UV light in UV-transilluminator (commonly used device for visualization of gels). It was also observed that many compounds also show color changes in interaction with heparin. After primary identification of the compound as a preliminary hit, the result was further confirmed by measuring their relative emission spectra in presence and absence of heparin. After the preliminary screening was over, all hits were organized based on their relative fluorescence intensity increase in presence of heparin.

Entry	*Structure*	*Emission spectra*	*Relative fluorescence intensity increase*
1.	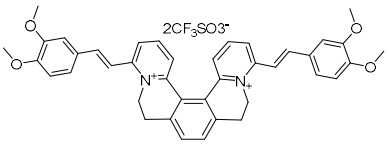 33	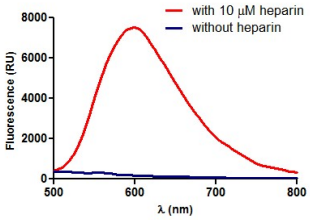	49.50
2.	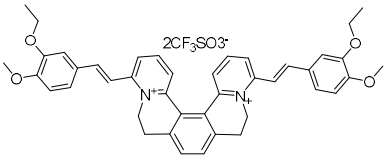 30	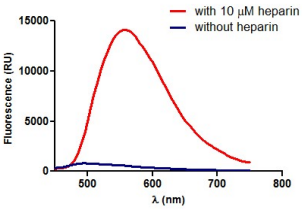	26.09
3.	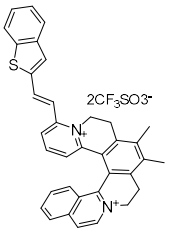 54	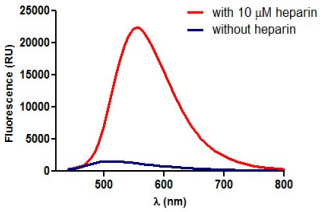	18.77
4.	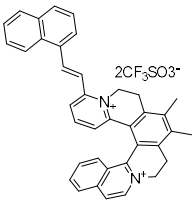 55	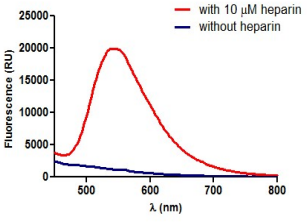	17.88
5.	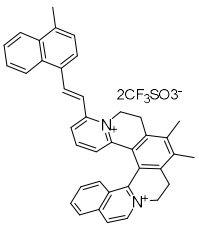 56	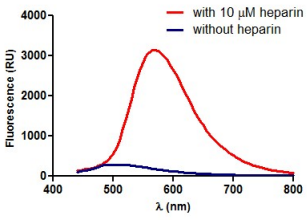	17.45

6.	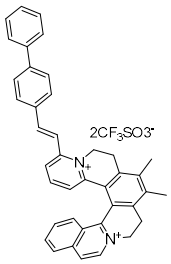 57	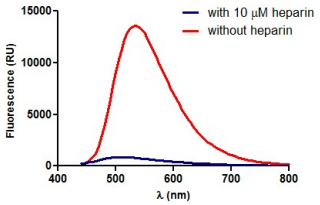	16.99
7.	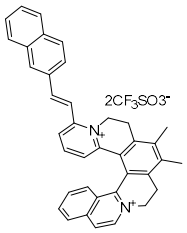 58	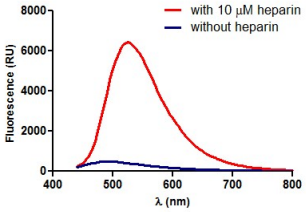	15.86
8.	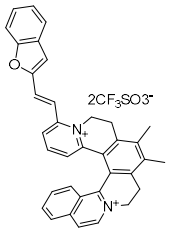 59	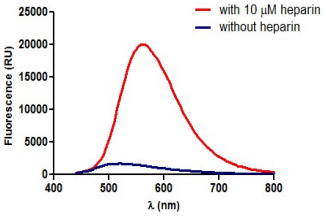	14.95
9.	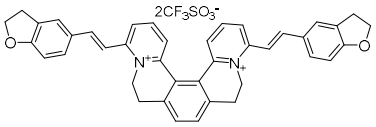 60	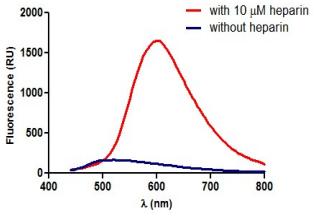	14.72
10.	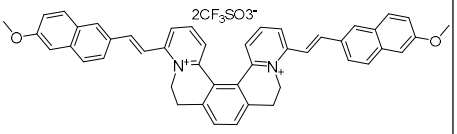 61	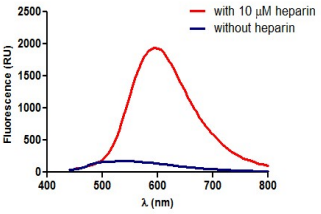	14.00
11.	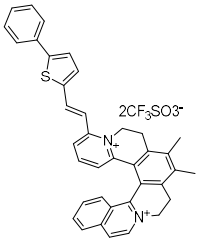 62	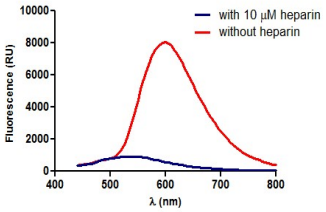	13.95

12.	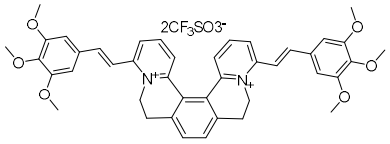 63	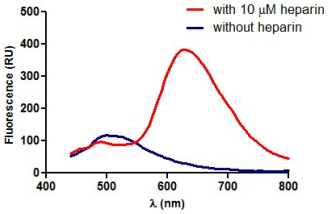	13.75
13.	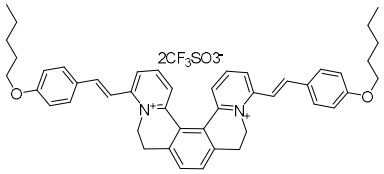 64	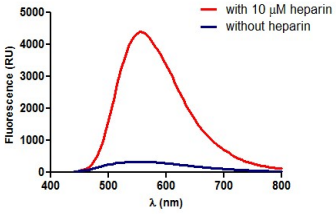	13.24
14.	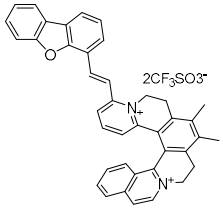 65	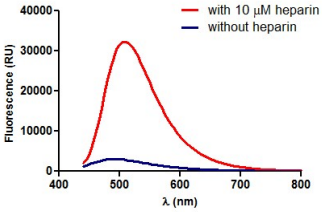	11.42
15.	 66	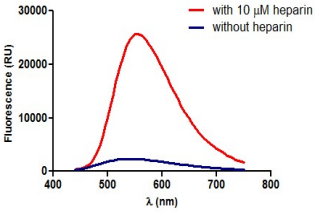	11.30
16.	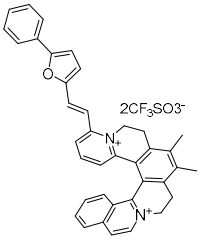 67	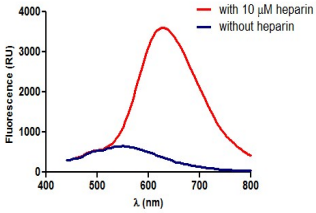	10.45
17.	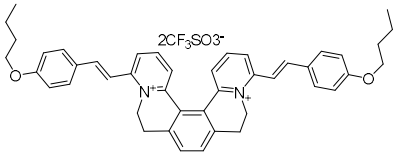 68	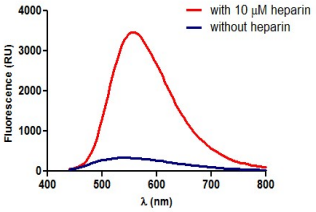	10.44
18.	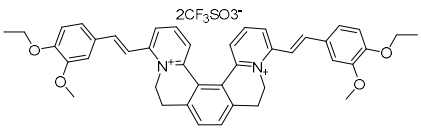 29	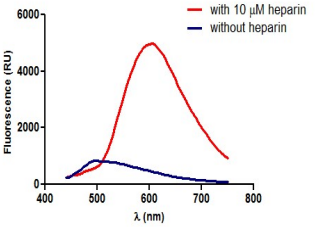	10.00

19.	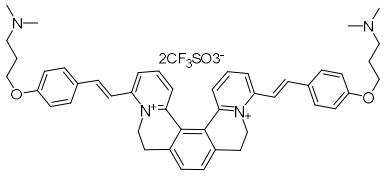 32	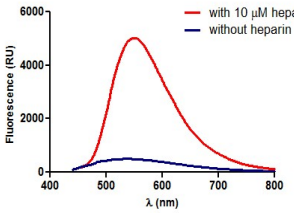	10.00
20.	 69	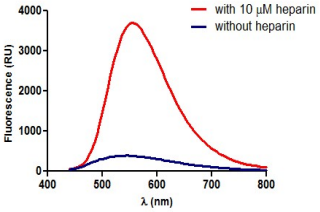	9.55
21.	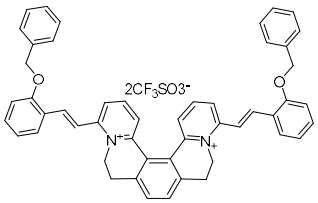 70	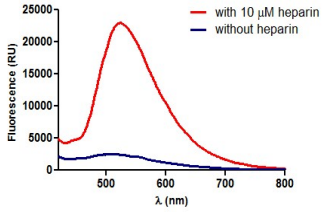	9.41
22.	 71	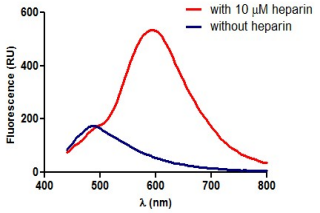	9.27
23.	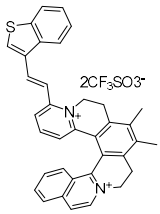 72	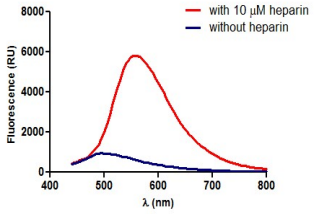	9.14
24.	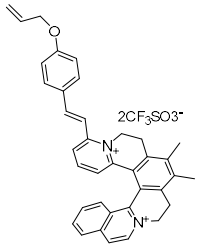 73	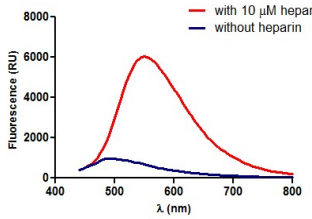	9.00

Table 11: *Hits arranged according to relative fluorescence intensity increase.*

The ideal chemosensors must interact with its target specifically, even in presence of other analytes. For this purpose, we carefully selected the analytes such as sulphated glycosaminoglycan (GAGs), which are structurally related to heparin, DNA, nucleotides, 20 % human serum, serum albumins, and many others. Out of 24 hits, two Compounds were identified to show selective fluorescence light up in presence of heparin over other analytes and accidentally found one of the hit, showing selective fluorescence light up in presence of

DNA. DNA binding properties and applications of DNA chemo-sensor obtained through the fluorescent library screening approach mentioned above were discussed in detail in the following section (Fig. 67).

In addition, few compounds show two times higher fluorescence light up in presence of chondroitin sulphate, which is another member of glycosaminoglycan family with a lot of structural similarity to heparin. In future, such compounds can be used as fluorescent probes for identification and quantification of chondroitin sulphate and oversulphated chondroitin sulphate, which are the commonly found impurities in the pharmaceutical formulations of heparin. Such a study is beyond the scope of this thesis due to some practical reasons.

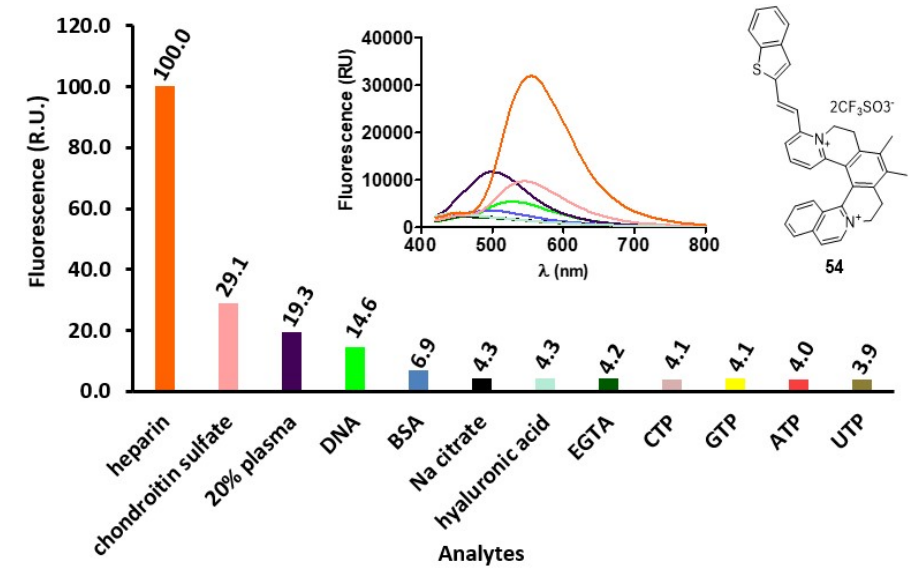

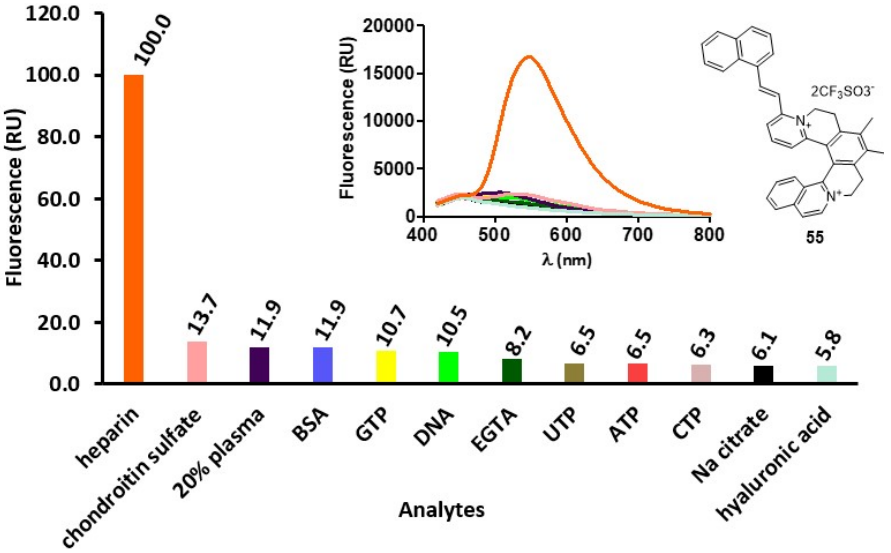

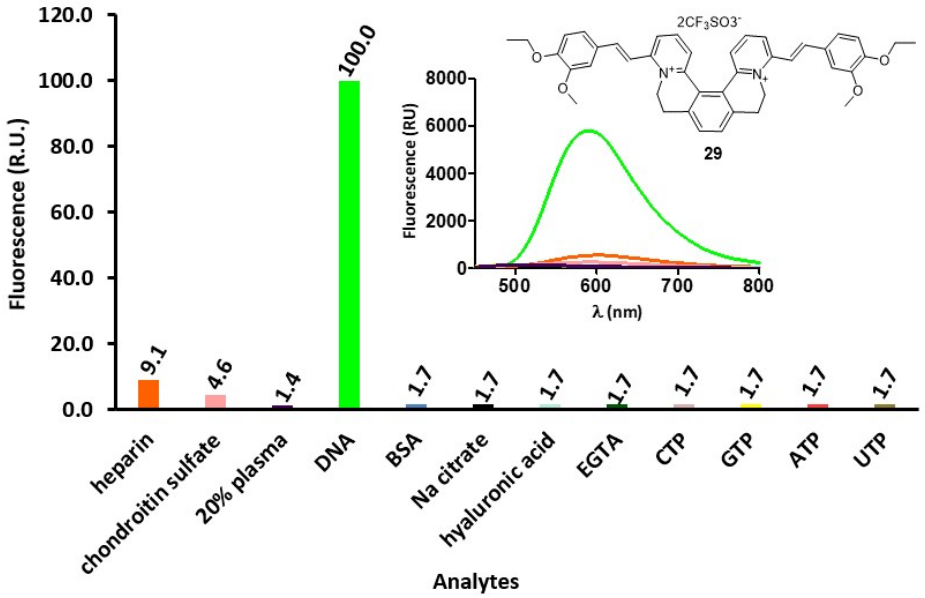

Fig. 67: *Selectivity charts of two heparin sensors,* ***54*** *and* ***55*** *and DNA sensor* ***29****.*

The next step in the assay development was to calibrate both heparin chemosensors *vs.* heparin concentrations in plasma or serum.

The plasma and serum are the complex mixtures of many components with the huge auto-fluorescence response, due to which it was quite difficult to recognize the small changes in fluorescence intensity due to the added amount of heparin. From initial calibration experiments, it was realized that, if the plasma/serum diluted, the autofluorescence could be reduced. For this reason, initially, we tested the various dilutions of the plasma and came to the conclusion with less than 20% of dilution of plasma as reported in other articles before,[163] we were able to develop the calibration with our fluorescent probes for detection of heparin present in plasma in the clinically relevant range.

In order to cope with this problem, we prepared the samples of plasma spiked with the actual concentrations observed in clinical range and then to prepare the calibration curve, with 10 times diluted samples. Therefore, the concentrations seen at calibration curves are lower by 10 times than actual. The calibration curves clearly show the potential of both probes in the quantification of UFH and LMWH in a clinical range in diluted plasma with the Lowest Limit of Detection (LOD) = 0.2 μM using both probes (Fig. 68A and 68B).

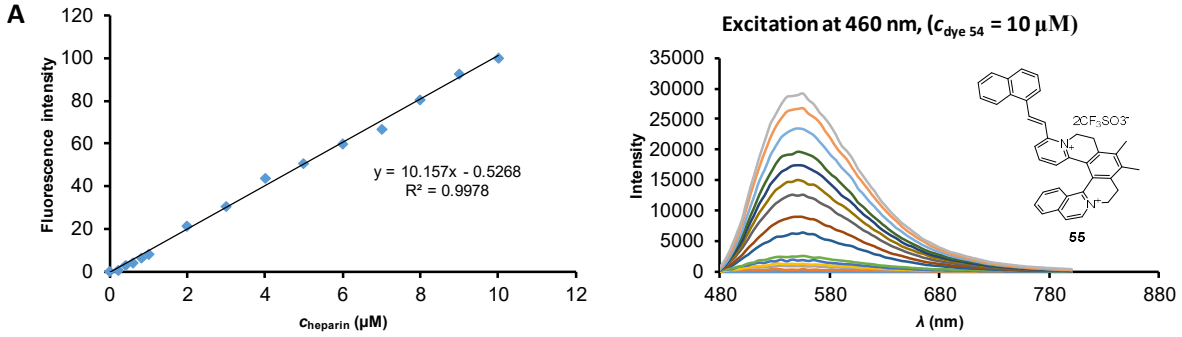

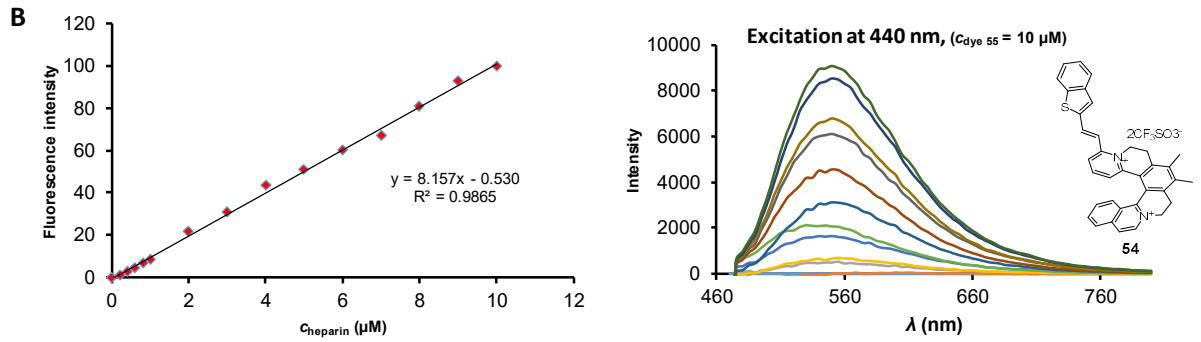

Fig. 68: *A) Calibration curve for chemosensors* ***54****; B) calibration curve for chemosensor* ***55*** *in clinically relevant concentrations of heparin.*

A small library of helquat and planar variants of two chemosensors were analyzed in search of other possible hits, but most of them show no fluorescence light up in presence as well as the absence of heparin or show nonselective fluorescence light up in presence and absence of heparin. All these results are summarized in Fig. 69.

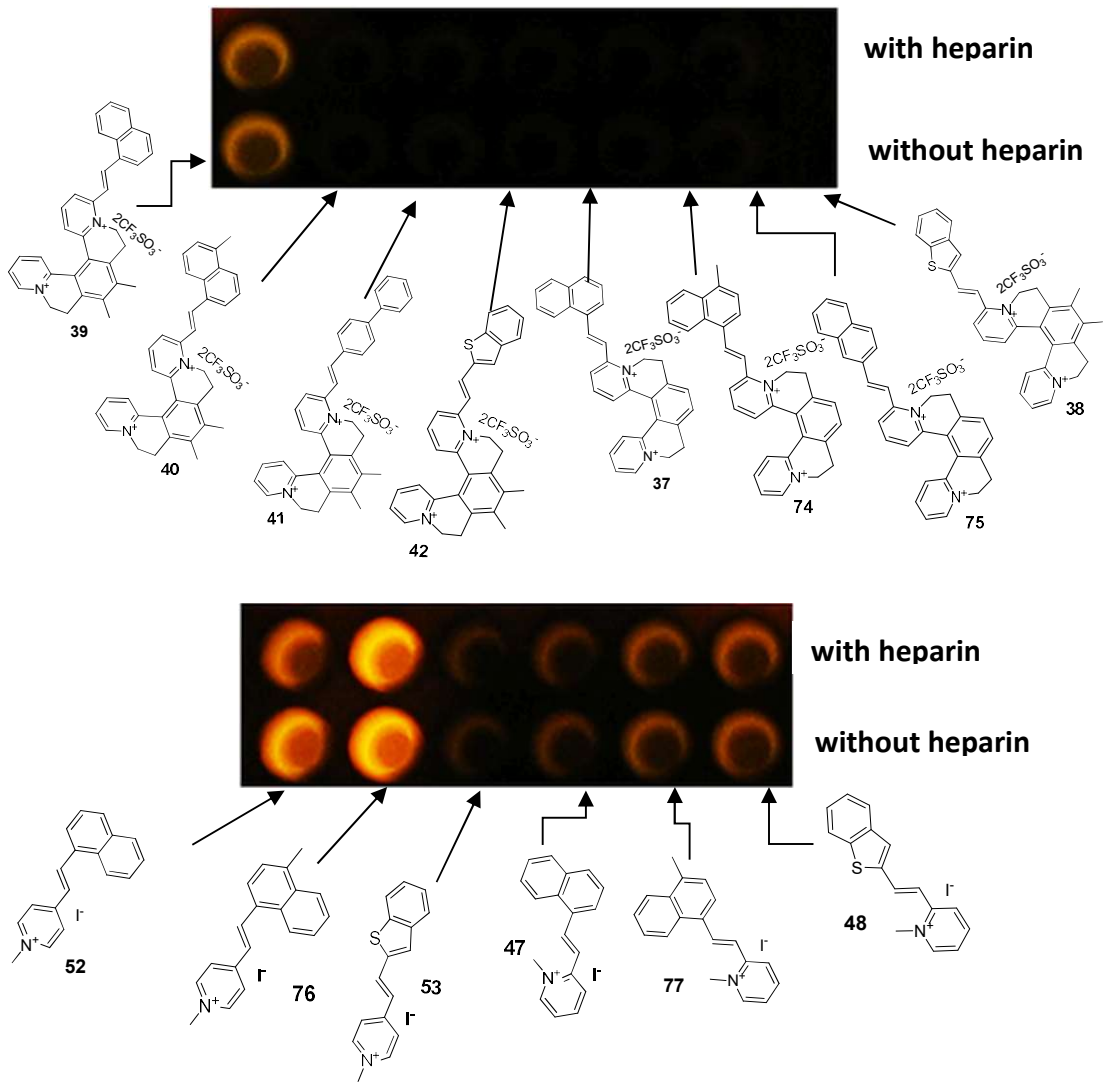

Fig. 69: *Structure Activity Relationship (SAR) study around the two chemosensor.*

We believe the molecular recognition properties of the helquat dyes with heparin are not purely due to the electrostatic interactions of the doubly positive helquat molecules and highly negative heparin molecules. Because if it would be so, the fluorescence light-up should have been observed in case of all the helquat dyes. Therefore, it needs to be inspected more deeply in collaboration with other research groups, which got expertize in the field.

Even though, at this moment, we were not able to go further with this project for actual quantification of heparin from the patient's plasma samples. However, we are in search for the research partners associated with medical hospitals, which can develop the method using our probes and can compare them with existing methods for heparin quantification.

- **Molecular Recognition: Sequence specific recognition of dsDNA, properties and applications:**

During the fluorescent library screening with various biological targets (Fig. 67), a helquat dye **29** was found. This compound was showing selective fluorescence light-up in presence of dsDNA (Fig. 70). When the quantitative fluorescence spectra of the dye in presence and absence of model DNA duplex was measured, the dye gave an emission spectra with huge increase in fluorescence intensity (λ_{max} = 590 nm) in presence of ds26 DNA, whereas very weak fluorescence response was obtained for dye alone (Fig. 73a, orange and black continuous lines respectively, for presence and absence of dsDNA). In UV-vis. absorption spectroscopy, red shifting of absorption maxima of the dye from 417 nm (unbound state) to 438 nm (in complex with dsDNA) was also observed. These two primary observations were sufficient to decide that, the dye was interacting with dsDNA. DNA binding properties of dye **29** were deeply studied using emission spectroscopy, UV-vis. spectroscopy, ECD spectroscopy, hydrodynamic study and computational methods. Due to the helical shape of the molecule, we named it as **HeliDye1**.

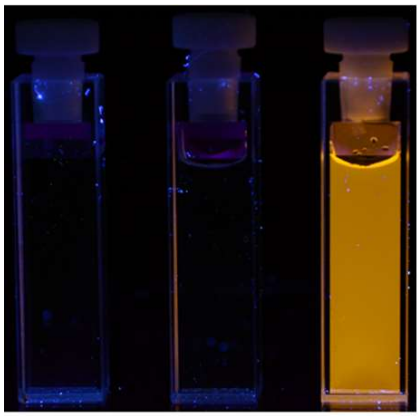

29 (HeliDye1)

Fig. 70: *Selective orange fluorescence light-up of* ***HeliDye1*** *(10 µM) in presence of ds26 (CAATCGGATCGAATTCGATCCGATTG) oligonucleotide (5 µM).*

The binding stoichiometry of **HeliDye1** : ds26 interaction was found to be in the range of 1:0.5 to 1:1. Therefore, in most of our future experiments, we used this ratio of dye : DNA as a basis.

The Structure Activity Relationship (SAR) study revealed an importance of bischromophoric helical structure with specific attachments of two alkoxy substituents, because on swapping

relative positions of ethoxy and methoxy substituents (dye **30**) or by replacing ethoxy substituent with methoxy substituent (dye **31**) the fluorescence light-up was completely lost (Fig. 71). In addition, monochromophoric helquat dyes were also inactive for fluorescence light-up in presence of dsDNA (dye **34**-**36**, Fig. 71). Planar variants of helical dyes (**44**-**46** and **49**-**51**) were completely nonselective for their light-up responses.

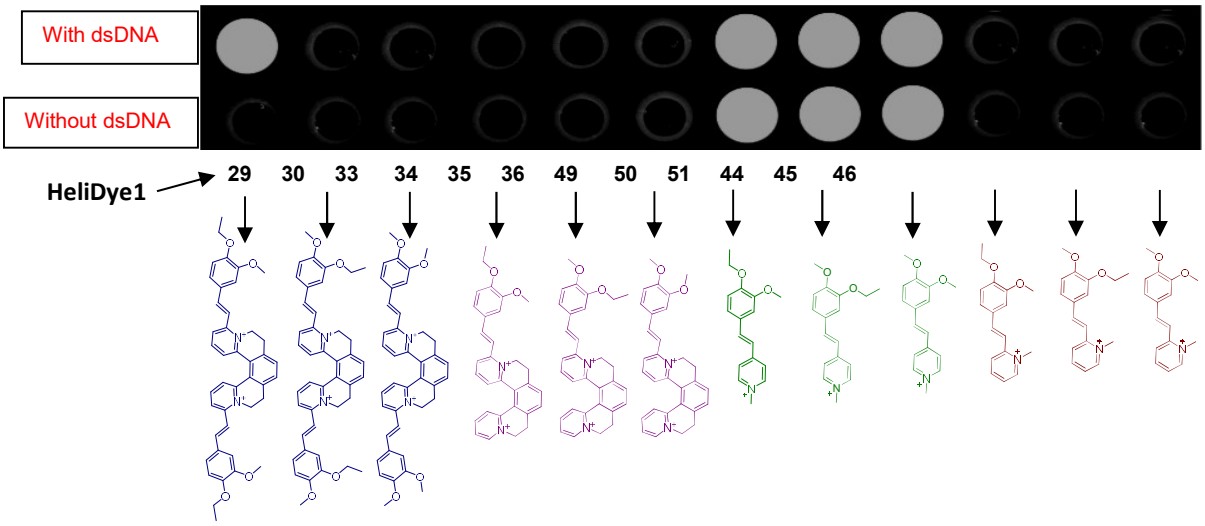

Fig. 71: *1st generation Structure Activity Relationship (SAR) study around the structure of* ***HeliDye1****.*

The fluorescence light up response of **HeliDye1** was selective towards AT-base pair containing dsDNA sequences. No fluorescence light-up was observed for **HeliDye1** alone or in presence of dsDNA lacking AT-pairs, ssDNA and total RNA (RNA isolated from cells, which may contain unknown sequences of single and double-stranded RNA templates) (Fig. 72).

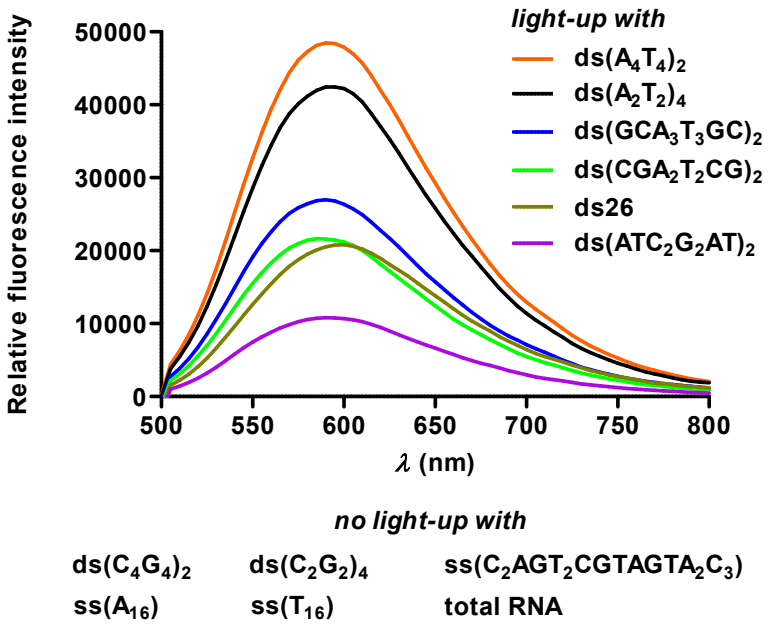

Fig. 72: *Selectivity of* ***HeliDye1*** *towards AT-rich dsDNA over GC-rich dsDNA sequences, ssDNA and RNA*

The dissociation constants of interactions between **HeliDye1** and various self-complementary and hairpin forming dsDNA sequences were determined by fluorescence titration method and are summarized in Table 12**.** An inverse relationship was observed

between the number of AT-pairs contained in the sequence and K_D value, indicating more tight binding with AT-rich dsDNA sequences.

	Sequence (5' - 3')	K_D (μM)	Number of AT pairs
	Part A: self-complementary dsDNA sequences		
1	ds(AAAATTTTAAAATTTT)	2.9 ± 0.04	8
2	ds(AATTAATTAATTAATT)	3.5 ± 0.20	8
3	ds(GCAAATTTGCGCAAATTTGC)	4.7 ± 0.20	6
4	ds(CGAATTCGCGAATTCG)	5.7 ± 0.20	4
5	ds(CGCGAATTCGCGCGCGAATTCGCG)	6.0 ± 0.10	4
6	ds(ATCCGGATATCCGGAT)	15.1± 0.10	4
	Part B: hairpin-forming dsDNA sequences		
7	ds(CAATCGGATCGAATTCGATCCGATTG)	5.9 ± 0.20	7
8	ds(GGCAAAAACGCGGTCCGCGTTTTTGCC)	9.7 ± 0.10	5
9	ds(GGCAAAACCGCGGTCCGCGGTTTTGCC)	11.2 ± 0.03	4
10	ds(GGCAAAGCCGCGGTCCGCGGCTTTGCC)	16.1 ± 0.20	3
11	ds(GGCAACGCCGCGGTCCGCGGCGTTGCC)	26.5 ± 0.30	2
12	ds(GGCAGCGCCGCGGTCCGCGGCGCTGCC)	48.2 ± 0.50	1

Table 12: *K_D values for interaction of dye **HeliDye1** with various DNA duplexes (c_{dsDNA} = 1 μM).*

The red shifting of absorption maxima was also found to be more sequences dependent and maximum shifting by 42 nm was observed in presence of ds$(A_4T_4)_2$ oligonucleotide sequence (Fig. 73C). Absorption and emission spectral changes of **HeliDye1** (10 μM) with (w) and without (w/o) different oligonucleotide sequences (5 μM) are shown in Fig. 73 and spectral properties are summarized in Table 13. The fluorescence quantum yield of **HeliDye1** in presence of various dsDNA sequences was determined using Coumarin 153 as a standard.[186]

	λ_{abs} (nm)	λ_{em} (nm)	φ^a	ϵ (l.mol^{-1}cm^{-1})
w ds26	438	590	0.010 ± 0.004	19534
w ds$(GCA_3T_3GC)_2$	435	590	0.016 ± 0.004	20578
w ds$(A_4T_4)_2$	458	590	0.030 ± 0.004	20471
w/o dsDNA	417	-	-	22921

Table 13: *Spectroscopic properties of **HeliDye1** in presence and absence of different dsDNA oligonucleotides at dye : DNA ratio 2:1 ($c_{HeliDye1}$ = 10 μM and c_{dsDNA} = 5 μM)*

[a] Coumarin 153 was used as the reference for quantum yield.[186]

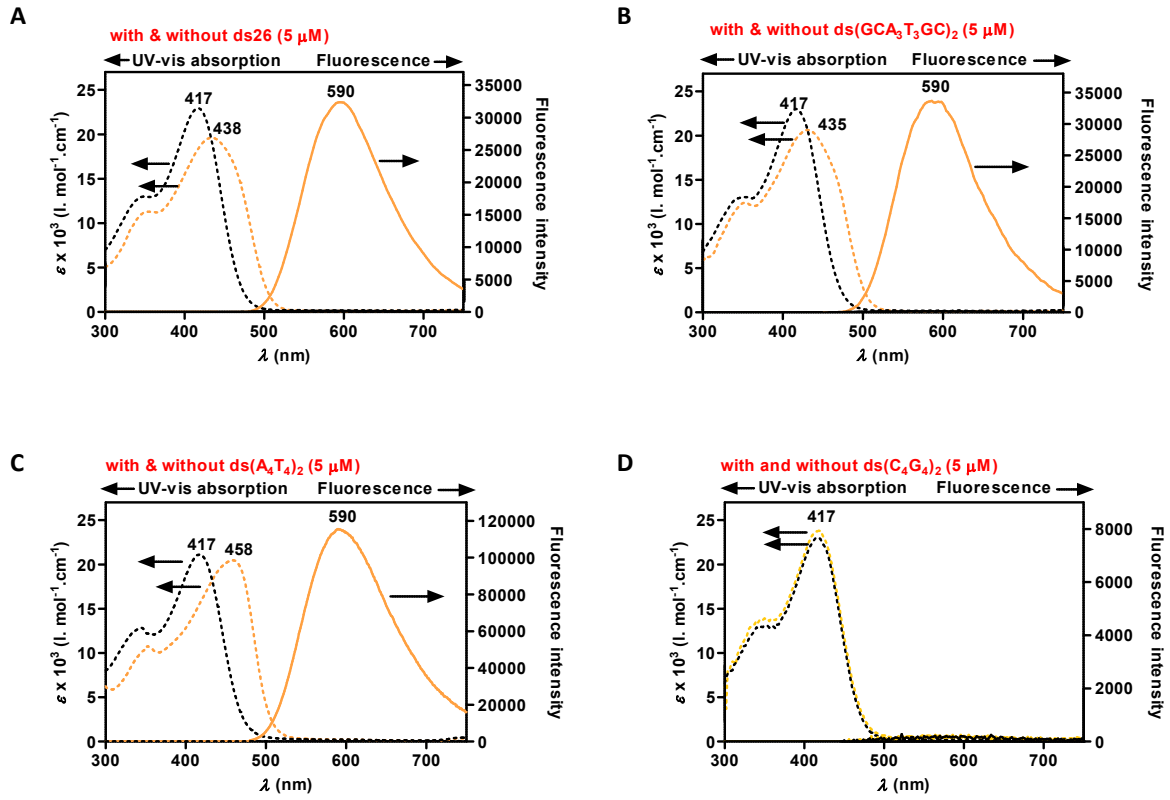

Fig. 73: *UV-Vis. absorption (left) and emission (right) spectra of* ***HeliDye1*** *(10 µM) in presence (orange line) and absence (black line) of A ds26; B ds(GCA₃T₃GC)₂; C ds(A₄T₄)₂ and D ds(C₄G₄)₂ oligonucleotides (5 µM).*

For the practical applicability of the probe, the sequence specificity of **HeliDye1** was compared with three established DNA probes, **propidium iodide (PI)**, **Hoechst-33258** and **DAPI** in a fluorescence light-up assay (Fig. 74A). Quantitative fluorescence spectra of all three probes at their respective excitation wavelengths[187] were measured in presence and absence of ds$(A_4T_4)_2$, ds$(C_4G_4)_2$, ssDNA, ssRNA, dsRNA as analytes. This experiment has proven the high specificity of **HeliDye1** as compared to **PI** and **Hoechst 33258** (Fig. 74A and B). The specificity of DAPI was also high as compared to remaining two probes, but it was showing week fluorescence response with RNA, in this respect **HeliDye1** is superior over **DAPI**.

A

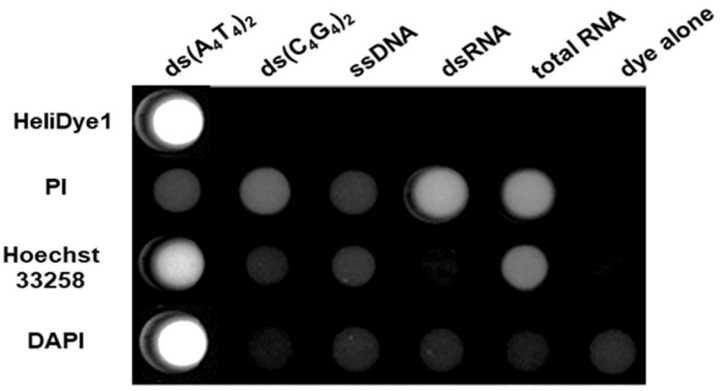

B

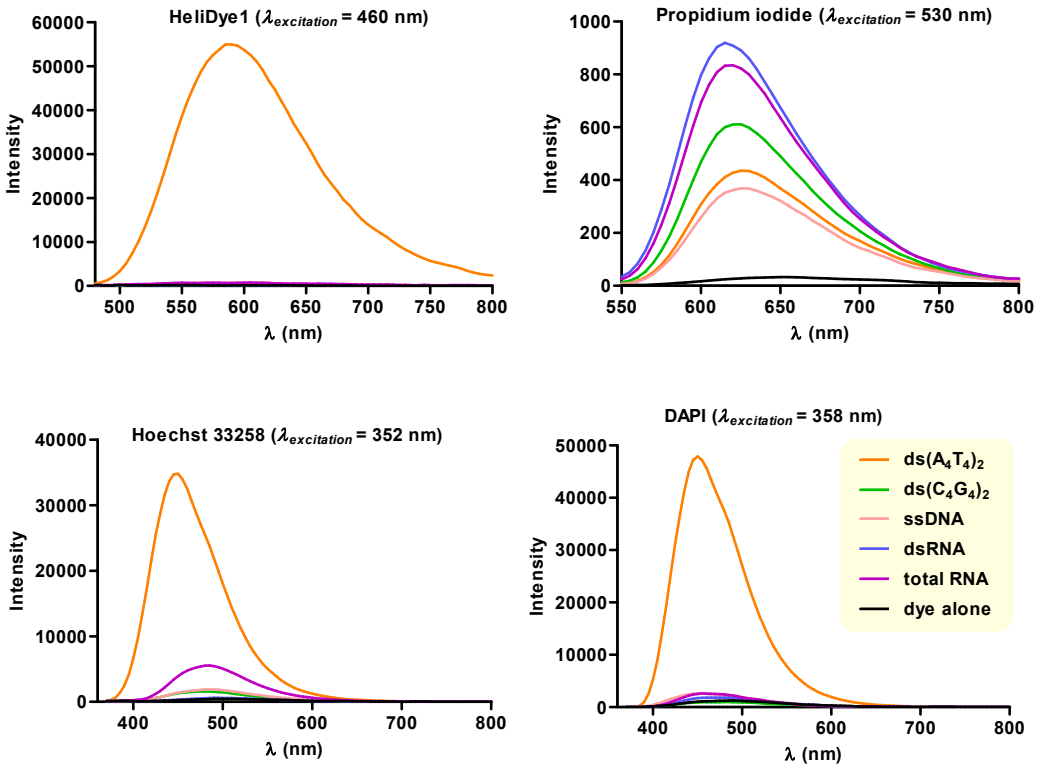

Fig. 74: *A) Picture of the well plate showing comparison in fluorescence light-up of* ***HeliDye*** *with established probes (irradiation at 365 nm UV light); B) Quantitative fluorescence spectra of* ***HeliDye1*** *and all three established probes in presence and absence of analytes at dye:DNA ratio 2:1 (c_{dye} = 10 μM and c_{dsDNA} = 5 μM).*
Note: ssDNA: ss($C_2AGT_2CGTAGTA_2C_3$); dsRNA: ds($CA_2UCG_2AUCGA_2U_2CGAUC_2GAU_2G$); total RNA: RNA isolated from cells using standard RNA isolation kit.[188]

In addition, the ability of **HeliDye1** to detect DNA duplexes bands of only specific sequences was compared with **GelRed™** stain in nondenaturing gel electrophoresis (Fig. 75).

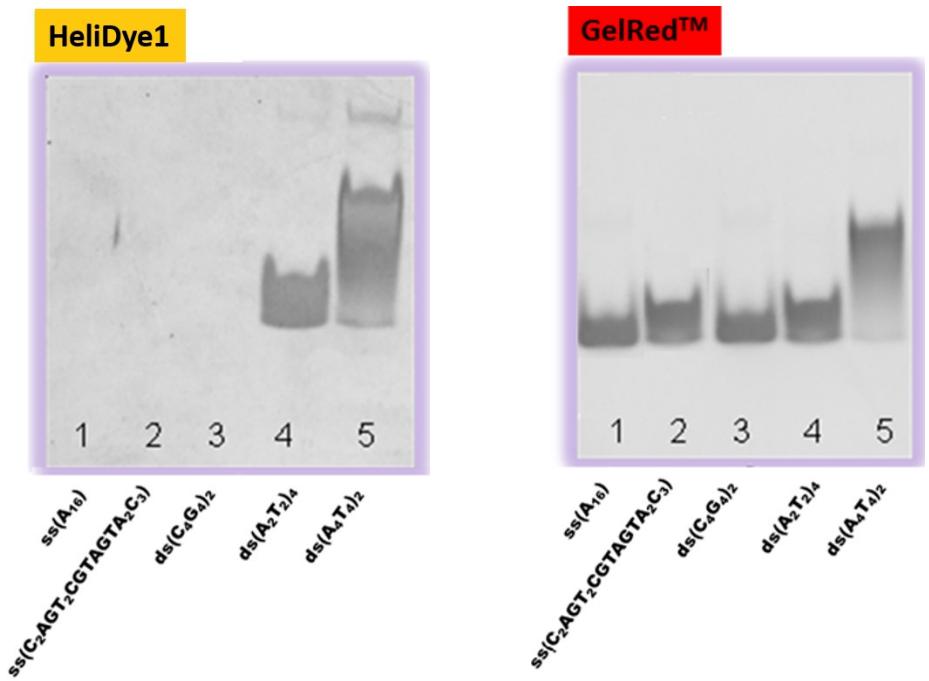

Fig. 75: *Selective staining of nucleic acid bands with* ***HeliDye1*** *(1 μM) in comparison with* ***GelRed™****.*

Electronic Circular Dichroism (ECD) spectroscopy is a technique used to study the interactions of small molecule ligands with biological targets such as proteins and nucleic acids. From our previous study, we knew that symmetrical **HeliDye1** undergoes rapid helix inversion in solution at a rate of 31 s^{-1}. Therefore, it exists as a racemate and gives no net signal in ECD spectroscopy. We measured the experimental ECD spectra of **HeliDye1** alone (10 µM), the dye : DNA complex ($c_{\mathbf{HeliDye1}}$ = 10 µM and c_{dsDNA} = 5 µM) and ds26 (5 µM) alone (Fig. 76A). (see Table 13, entry 7 for ds26 sequence). As expected, no ECD spectrum was obtained from **HeliDye1** solution in absence of DNA (magenta line). **HeliDye1** : dsDNA complex (2:1) solution gave intense induced bisignate ECD signal positioned in the visible spectral region (orange line). As DNA has no spectral contribution to ECD signal above 300 nm (blue line), the ECD bands in the visible region can be attributed exclusively to the **HeliDye1**. In order to see which enantiomer of **HeliDye1** was preferentially interacting with DNA, we computed the ECD spectra of *M*-enantiomer using DFT calculations (Fig. 76B, using BMK functional[189] with 6-31+G* basis set.[181]). By its correlation with experimental spectra, we were able to conclude that *M*-enantiomer of **HeliDye1** was preferentially interacting at this particular dye : DNA ratio.

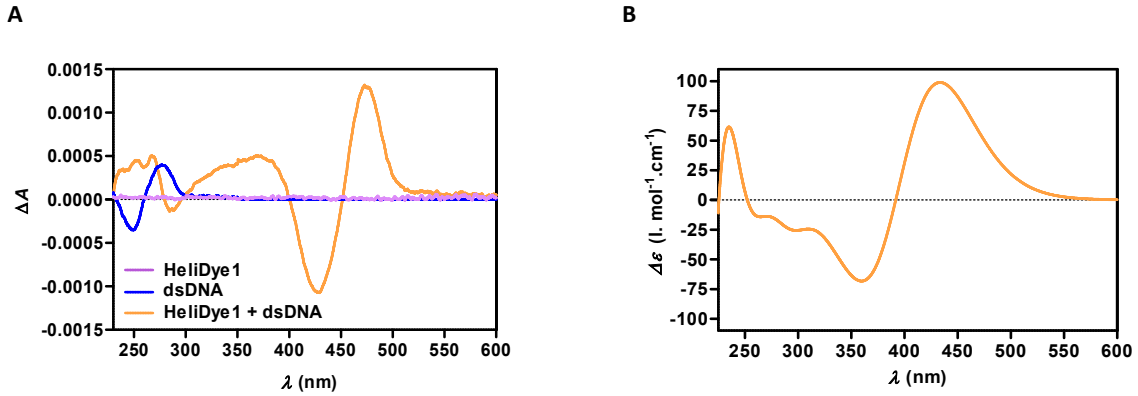

Fig. 76: *Comparison of A) experimental and B) simulated ECD spectra of* ***HeliDye1****.*

In order to study the binding mode in more details, we performed an ECD titration experiment with increasing concentrations of ds26 DNA (from 0 to 400 µM) at fixed concentration of **HeliDye1** (10 µM) (Fig. 77A) as per the previous report from Chaires *et al.*[190] Within all concentrations, the ds26 DNA existed in its most naturally abundant form (B-DNA, right-handed helix) as proven by inspecting UV region of the ECD spectra, where the ECD bands appeared with increasing DNA concentration (Fig. 77B). Therefore ECD spectral changes in the visible region should be explained only by ligand reconfiguration. From dye : DNA ratio 1:0.5 to 1:10, we could observe a decrease of ECD signal, which could be attributed possibly to the change in **HeliDye1** configuration (*M* → *P*) at higher DNA concentration, thus indicating binding of both enantiomers at two different dye : DNA ratios. At extreme ratios (> 1:20), a transition in the ECD spectral behaviour of the **HeliDye1** : DNA complex occurred. The bisignate nature of induced ECD spectrum with a positive band centered at 472 nm was transformed into a monosignate ECD negative band centered at 443 nm. Some other effects accompanied by a transition from *M* → *P* Configuration of **HeliDye1** must be responsible for such a behaviour, which we need to study more deeply.

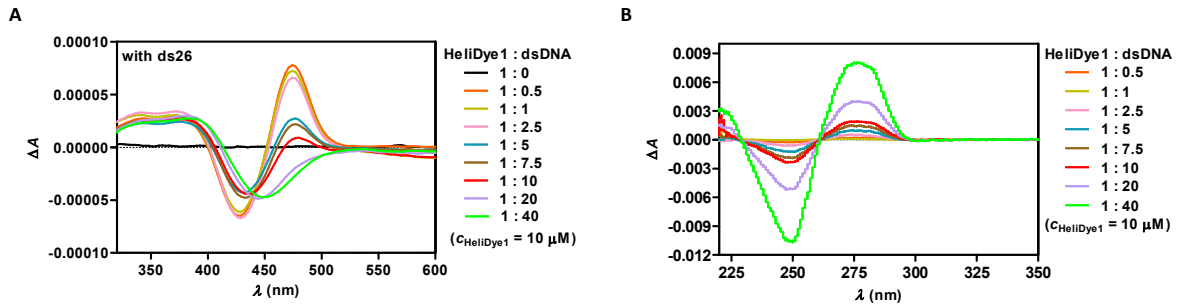

Fig. 77: *ECD titration of HeliDye1 (10 µM) with increasing concentrations of ds26 DNA (0-400 µM) in BPES buffer, A) ECD spectral region of* ***HeliDye1****,showing differential spectral behavior of P and M-enantiomers of* ***HeliDye1*** *at two extreme concentrations of ds26; B) ECD spectral region of ds26DNA, showing no conformational change in the structure of ds26 DNA.*

The consistent ECD spectral behaviour of **HeliDye1** was also observed in ECD titration experiments with different dsDNA oligonucleotide sequences. (Fig. 78A and B).

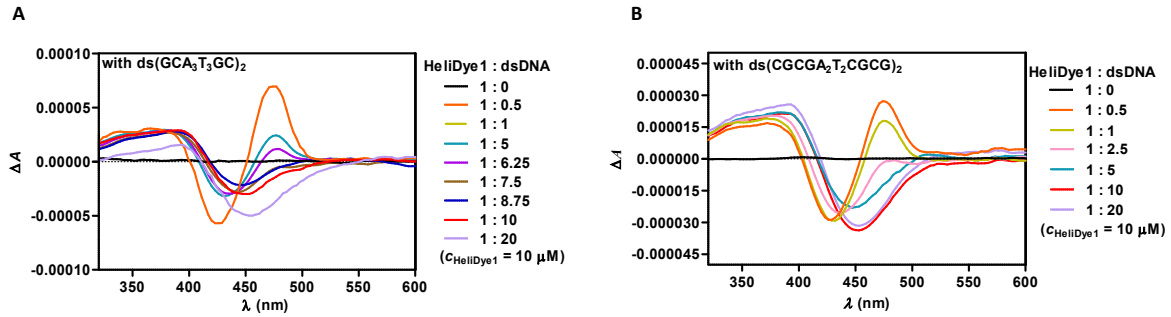

Fig. 78: *ECD titration of* ***HeliDye1*** *(10 µM) with increasing concentrations (0-200 µM) of A) ds(GCA3T3GC)2 and B) titration with ds(CGCGA2T2CGCG)2 DNA.*

Hydrodynamic study (viscosity measurement) is a classical experiment described for proposing a mode of interaction of DNA binding molecules to DNA. The Previous study reported that the viscosity of DNA solutions in complex with classical intercalator ethidium bromide increases if the concentration of ethidium was increased keeping the DNA concentration constant.[191a] It is also known that intercalators disturbs the native conformation of DNA causing lengthening of the DNA strand in the longitudinal direction, which eventually leads to an increase in the viscosity of the DNA solution. Minor groove binders, as they do not disturb the native conformation of DNA and thus have the negligible effect of their increasing concentrations on the viscosity of the DNA solutions.[191]

Effects of increasing **HeliDye1**, **PI** and **DAPI** concentrations (0-200 µM) in a set of dye : DNA complex solutions (individual set of solutions for each dye) containing 100 µM BP (base pair molarity) of calf-thymus DNA (ctDNA) were studied.

As compared to **PI**, **HeliDye** and **DAPI** affected very less the viscosity of DNA solutions with their increasing concentrations (Fig. 79). This experiment is suggesting no intercalative binding of **HeliDye1** similar to **PI**, but indicating the possibility of similar minor groove binding to that of **DAPI**.

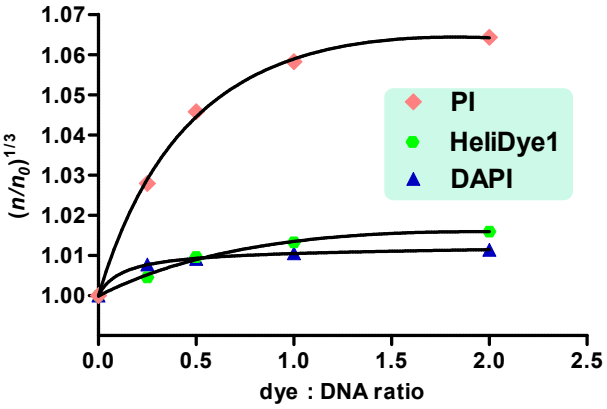

Fig. 79: *Viscosity measurements of DNA duplex (ctDNA, 100 μM BP) solution containing increasing concentrations of* ***HeliDye1****, propidium iodide (****PI****) and* ***DAPI*** *(0-200 μM).*

As the ECD titration experiments discussed above (Fig. 77) suggesting differential binding of *M* and *P*-enantiomers at different dye : dsDNA ratios, molecular docking of optimized structures of both enantiomers of **HeliDye1** with model DNA duplex ds$(GCA_3T_3GC)_2$ gave more insight into the possible mode of binding. Both intercalation and groove binding possibilities were inspected. Molecular docking was carried out to obtain potential ligand binding poses using AutoDock Vina, version 1.1.2.[192] The intercalation possibility was studied in a model where an intercalation site was formed between A5-T6, by doubling the step-to-step distance (from 3.4 to 6.8 Å) and optimization of the phosphate backbone.

The experimental results and the computational results can be correlated with each other in this way and explained with the help of Fig. 80A – D:
a) Most of the docking solutions, obtained in case of intercalation model were found to be clustered into the intercalation site, with the *M*-enantiomer of the dye was positioned in the center of the intercalation site (Fig. 80A) and the *P*-enantiomer was found to be slightly shifted to the side of the intercalation site (Fig. 80B). However, no classical intercalation was observed. Further, in molecular dynamics, this artificially created intercalation site disappeared and proposed model A and B was converted to model C and D respectively, suggesting no such binding possible.

b) In case of the model expected to check the possibility of groove binding, all obtained docking posses were clustured into the minor groove, showing a strong preference for the minor groove binding. The *M*-enantiomer of the dye fitted snugly into the groove (Fig. 80C), whereas half of the *P*-enantiomer was fitted into the groove and half of the molecule was protruded into the solvent (Fig. 80D).

The hydrodynamic behaviour and AT-sequence specificity of **HeliDye1,** similar to the known DNA minor groove binding dye DAPI opposed to known intercalator dye propidium iodide (PI) is in agreement with minor groove binding of **HeliDye1**.

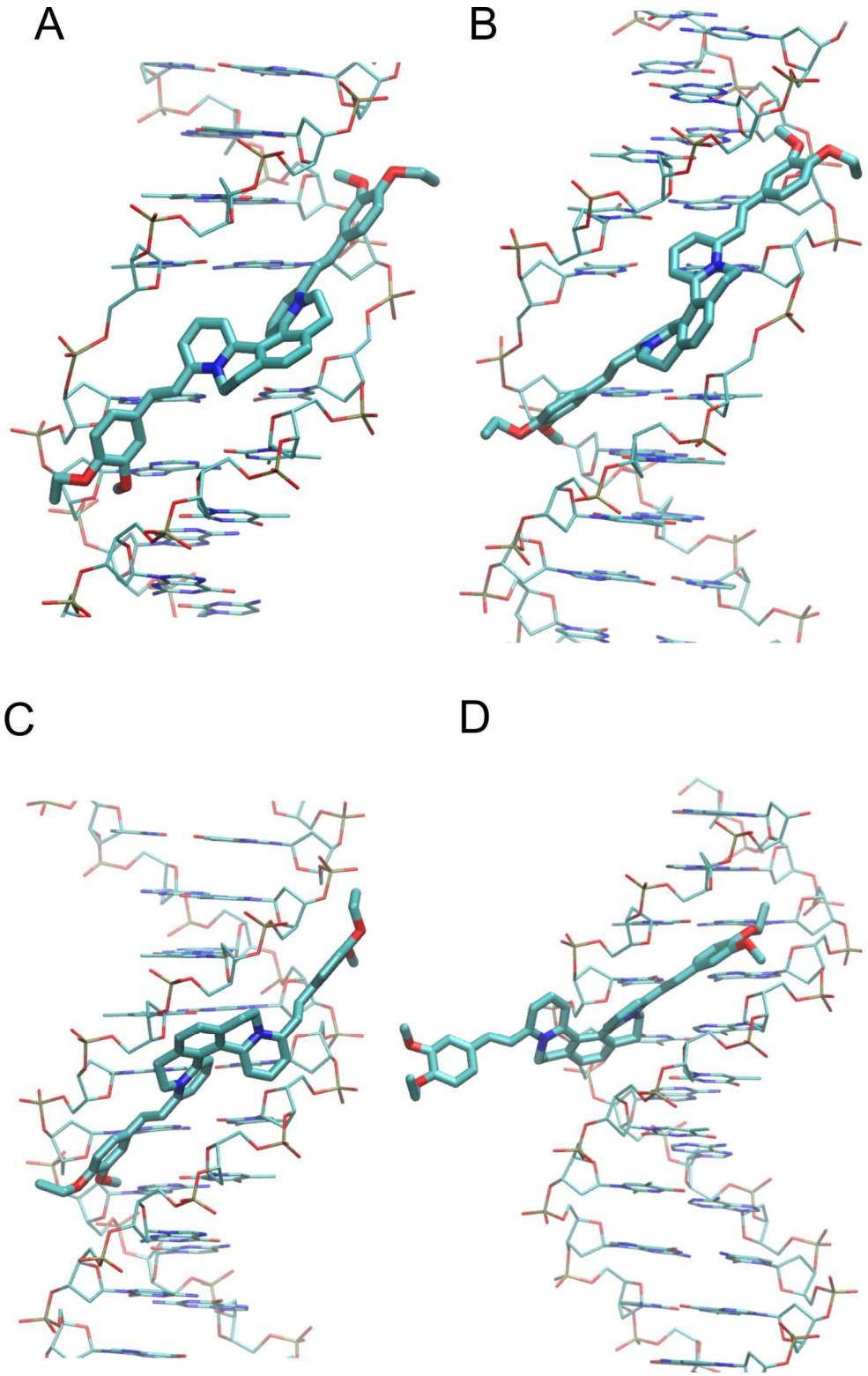

Fig. 80: *Representative binding modes of* ***HeliDye1*** *(in sticks) in AT-rich dsDNA structure as obtained from molecular docking. Panels A and C: M-enantiomer of* ***HeliDye1****. Panels B and D: P- enantiomer of* ***HeliDye1****. Panels A, B: intercalation model. Panels C, D: groove binding model. Color-coding cyan – carbon, red – oxygen, blue – nitrogen, and gold – phosphorus. Figure prepared with VMD, version 1.9.3.*[193]

Based on docking solutions, new helical dyes containing following two types of modifications in the structure of HeliDye1 were done and a short library of new helquat dyes was synthesized and tested for their DNA binding fluorescence light-up properties.

A) Modification in styryl part, while keeping helquat part intact (**78**-**80**, Fig. 81).

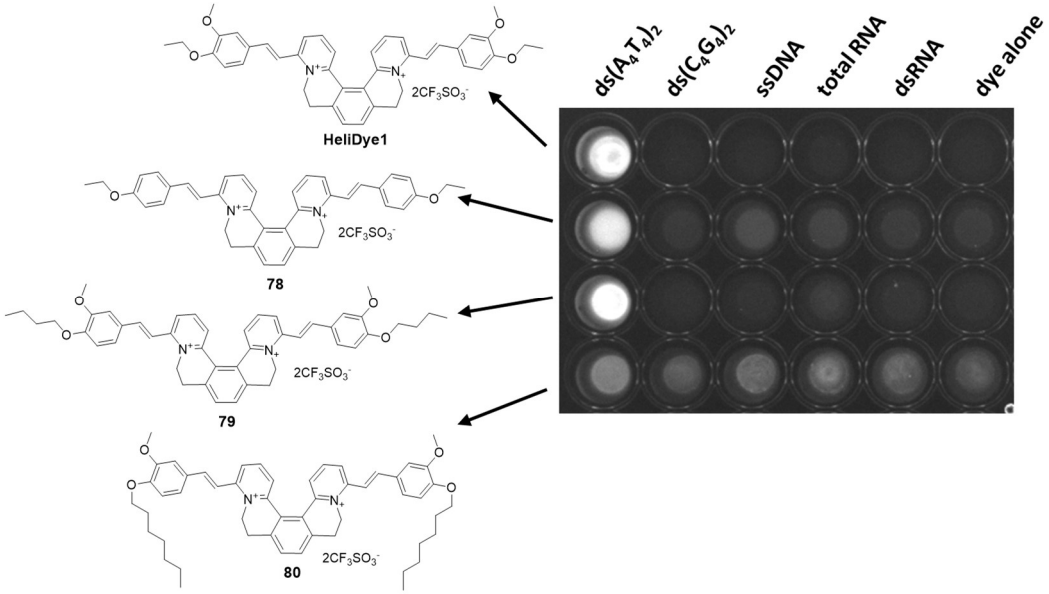

Fig. 81: *SAR study with molecules containing modifications in styryl chromophore.*

B) Helquat dyes **86**-**90** originating from various helquat cores **81**–**85**, with no modifications in styryl chromophore were synthesized (Fig. 82).

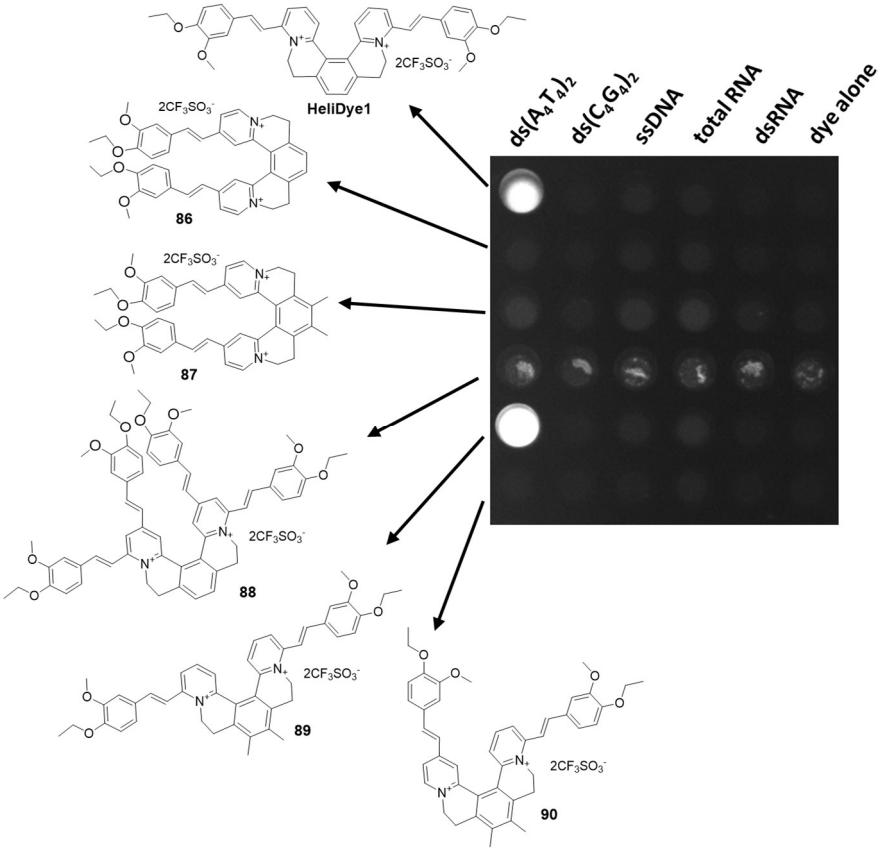

Fig. 82: *SAR study with molecules containing modifications in helical structure.*

All these modifications were screened for their performance in fluorescence light-up assay with various nucleic acid sequences. Modifications in styryl part (Fig. 81) were somehow showing similar AT-selectivity either by removing one of the methoxy substituent from the styryl chromophore (dye **78**) or by increasing the length of alkoxy chain of one of the

substituents from ethoxy to *n*-butyloxy (dye **79**), but the selectivity was completely lost in case of compound **80**, which contains *n*-heptyloxy modification in the styryl part (Fig. 81). In addition, it is important to mention that the solubility in an aqeous buffer was also getting worse with increasing the length of alkoxy side chain. Therefore, we decided to keep the basic chromophore of **HeliDye1** intact and keep our focus towards modifications in helquat cores (Fig. 82). All these helquat cores were ready in our group, which were attached with the basic styryl chromophore from **HeliDye1** through a Knoevenagel condensation reaction. However, out of all these modifications, only small modification in helquat core such as in dye **89**, in which helquat core was modified by the addition of two methyl substituents to the central aromatic ring (Fig. 82). This derivative showed strong fluorogenic response comparable to **HeliDye1** as well as similar selectivity for AT-rich dsDNA sequence. The compound **89** exhibited 2.7 times increase in fluorescence quantum yield after binding to AT-rich DNA, in comparison to **HeliDye1** (Table 14). The K_D value of interaction of dye **89** with ds(A_4T_4) was also comparable with **HeliDye1** (Table 14, last column).

In order to prove our hypothesis of chiral recognition of dsDNA target by helquat dyes, 3rd generation SAR study was performed, by synthesizing new helical dyes, in which the same styryl chromophore was present and size of ring 2 and 4 of [5]helquat skeleton was increased from six to seven carbon atoms (Fig. 83). Due to these changes, the molecule gets conformational stability[8] and two enantiomers of the new compound were obtained with *ee* > 95% (by capillary electrophoresis).

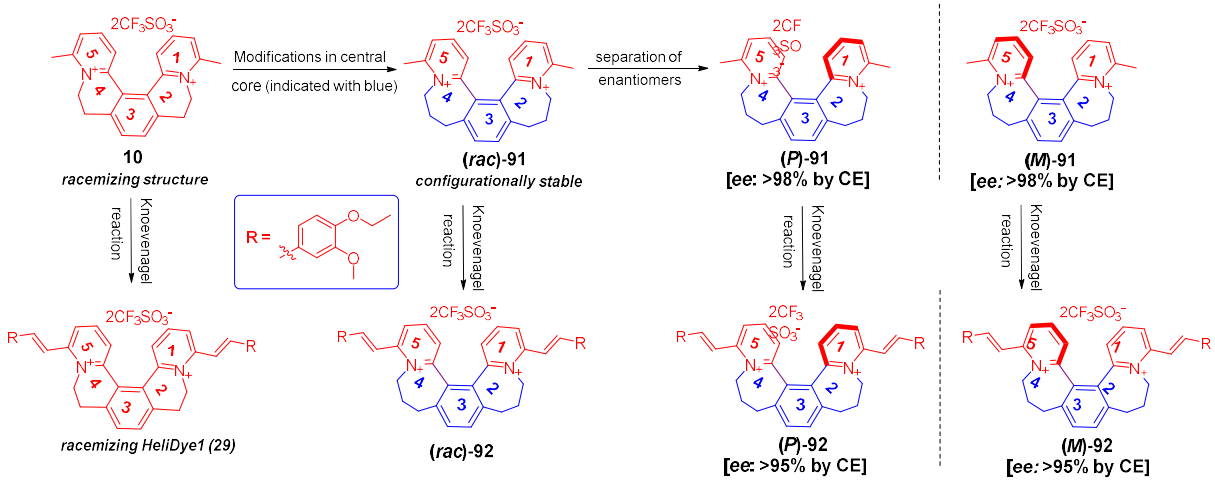

Fig. 83: *Structural modifications to the helical core of* ***HeliDye1*** *to obtain confirmationally stable helquats.*

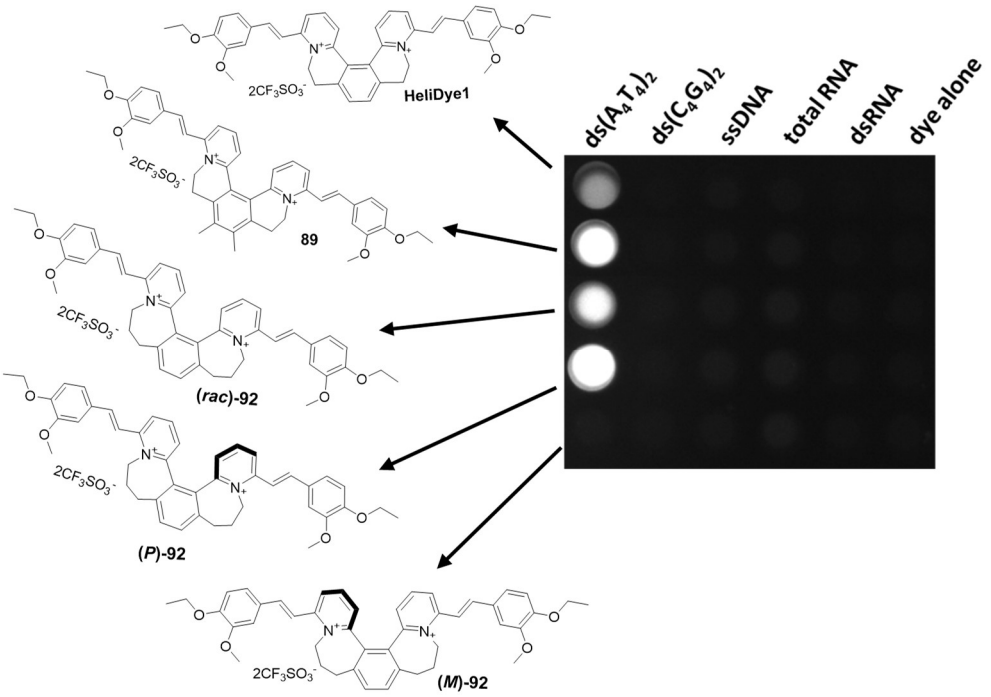

Fig. 84: *3rd generation SAR study stronger fluorescence light-up with* ***(P)-92*** *than* ***HeliDye1, 89*** *and* ***(rac)-92.*** *No fluorescence light-up of* ***(M)-92*** *with any of the analyte.*

Based on the fluorescence light-up experiment (Fig. 84), chiral recognition by *P*-enantiomer of dye **92** was observed, whereas the *M*-enantiomer, showing no fluorescence light-up in presence of any of the analyte included in the experiment.

Even though obtained results with enantiopure helquat dye **92** are contradictory to those obtained in case of **HeliDye1**, they are in strong favour of one of the hypotheses given at the beginning of this thesis, that novel specificities will be expected by the interaction of the molecules of this class with the cavities/ grooves of biological targets.

Compound	$ds(A_4T_4)_2$	λ_{abs} (nm)	λ_{em} (nm)	φ	ϵ ($l.mol^{-1}cm^{-1}$)	K_D (μM)
HeliDye1	**w**	458	590	0.030 ± 0.004	20471	2.9 ± 0.12
	w/o	417	-	-	21127	
89	**w**	455	575	0.081 ± 0.004	19220	3.2 ± 0.10
	w/o	420	-	-	21790	
(*rac*)-92	**w**	420	555	0.055 ± 0.004	19820	5.3 ± 0.10
	w/o	410	-	-	22580	
(*P*)-92	**w**	440	555	0.13 ± 0.004	21620	2.0 ± 0.10
	w/o	410	-	-	22140	
(*M*)-92	**w**	410	555	-	22330	-
	w/o	410	-	-	22970	

Table 14: *Comparison between spectroscopic properties of* ***HeliDye1****, dye* ***89****,* ***(rac)-92****,* ***(P)-92****) and* ***(M)-92*** *(all probes 10 μM) in interaction with (w) and without (w/o) $ds(A_4T_4)_2$ (5 μM). Last column with K_D (in μM) for the interaction of all these chemical modifications with $ds(A_4T_4)_2$ (1 μM), obtained by fluorescence titration.*

Currently, we are investigating in detail the possible mode of binding of dye **89** and **92** (in its *racemic* and enantiomeric form) as well other biological properties and the study will be performed, which can be considered as an outlook of the work reported in this thesis.

DNA duplex binding fluorescent molecules are useful as probes for microscopy and cell cytometry applications. Our initial microscopy experiments (Fig. 85) with **HeliDye1** (10 µM) revealed that dead cells are stained selectively leaving live cells unstained. Colocalization with GelRed™ (1:10000 as per the protocol from the supplier), an established dead cell probe, confirmed this staining pattern (Fig. 86). In addition, dot plots from flow cytometry with HGC-27 cells stained with **HeliDye1** allow to differentiate a population of dead cells that have high fluorescence as compared to a population of live cells (Fig. 86). These flow cytometry data were consistent with our findings from microscopy and thus further demonstrate the usefulness of **HeliDye1** for live/dead cell exclusion experiments.

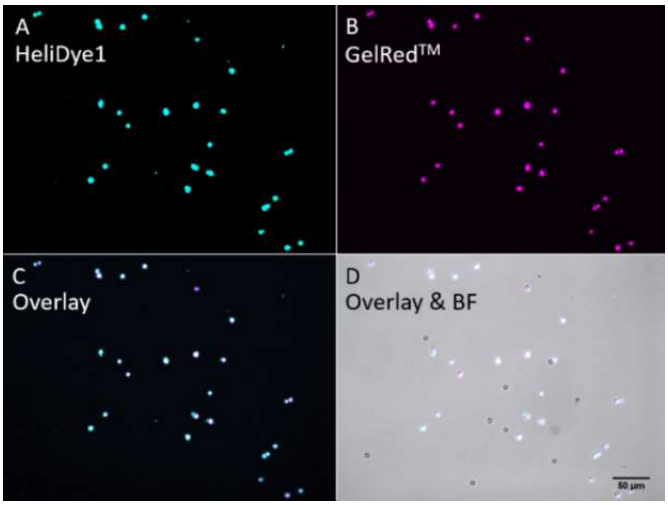

Fig. 85: *Selective staining of dead cells over live cells with* ***HeliDye1*** *(10 µM). HGC-27 cells co-stained with* ***HeliDye1*** *and* ***GelRed™****. Panel A:* ***HeliDye1*** *fluorescence channel. Panel B:* ***GelRed™*** *channel. Panel C: Overlay image obtained from* ***GelRed™*** *and* ***HeliDye1*** *fluorescence channels showing co-localization of bright spots corresponding to dead cells. Panel D: Combination of bright field (BF) image and overlay of two fluorescence channels A and B. Bright spots correspond to dead cells and dark spots to live cells.*

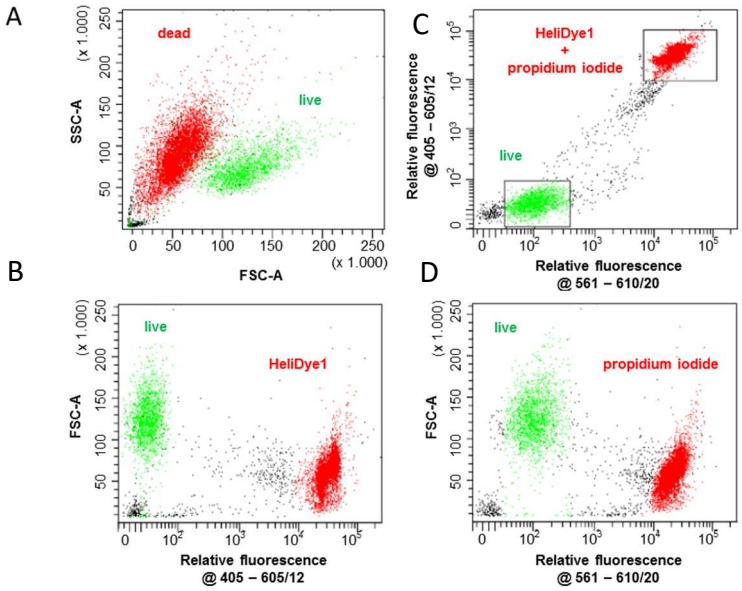

Fig. 86: *Fluorescence Activated Cell Sorting of live and dead cells (HGC-27), by* ***HeliDye1*** *(10 µM) in comparison with* ***PI*** *(1.5 µM).*

In confocal microscopy of U2OS cells (fixed cells), selective nuclei staining was observed at 1 µM concentration of **HeliDye1**. Colocalization study with **DAPI** (1 µM), confirms the selective nuclei staining (Fig. 87).

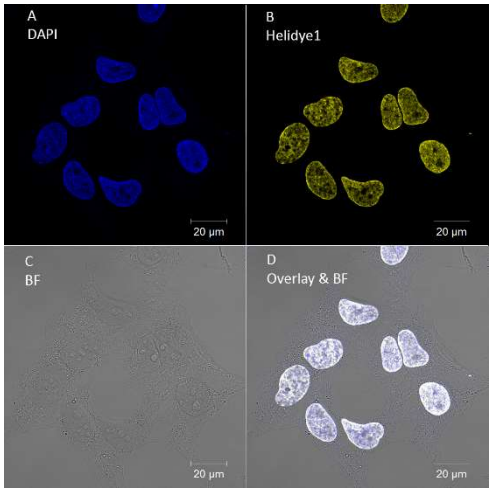

Fig. 87: *Selective nuclei staining in fixed U2OS cells using* ***HeliDye1*** *(1 µM) in colocalization with DAPI (1 µM).*

Propidium iodide (**PI**) is widely used stain for DNA quantification in flow cytometry. As it was seen that, the selectivity of **HeliDye1** towards DNA was higher than for RNA as compared to PI (Fig. 74), the use of **HeliDye1** could be advantageous for cell cycle analysis. Due to this feature of **HeliDye1**, we were able to avoid the RNase treatment completely, which is typically required in case of **PI** in order to have nice cell cycle analysis. The results are presented in Fig. 88.

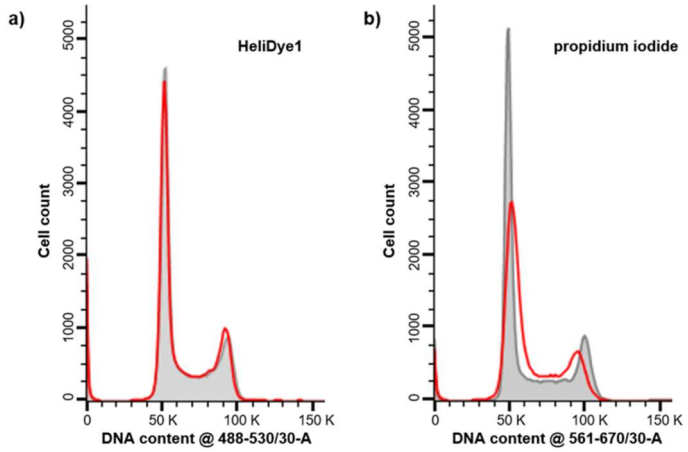

Fig. 88: *Cell cycles of HeLa cells analyzed using a)* ***HeliDye1*** *(10 µM); b)* ***PI*** *(1.5 µM). Brown histogram was obtained by standard RNase treatment prior staining with both probes. Red histogram was obtained without any RNase treatment.*

If the cell cycle analysis using **PI** was two times worse in absence of RNase treatment (Coefficient of Variation, CV value was almost double in absence of RNase treatment). Whereas, in case of cell cycle analysis using **HeliDye1**, which was mostly unaffected, even in presence and absence of RNase treatment (CV value was almost comparable).

Treatment /Cell cycle phases	G1	S2	G2/ M	G1 CV
HeliDye1 w/o RNase	43	31.1	13.4	5.5
HeliDye1 w RNase	43.9	31.2	12.3	5.7
PI w/o RNase	47	31	12.8	10.2
PI w RNase	44.7	32	12.8	5.21

Table 15: *Cell cycle analysis using HeliDye1 (10 µM) and PI (1.5 µM) as staining reagents with (w) and without (w/o) RNase treatment.*

HeliDye1 was evaluated for cytotoxic activity *in vitro* against a panel of human cancer and two non-tumour fibroblasts cell lines by using the standard 3-day MTS test. The cancer cell lines were derived from acute T-lymphoblastic leukemia CCRF-CEM, chronic myeloid leukemia K562 and their multidrug-resistant counterparts (CEM-DNR, K562-TAX) expressing the LRP and P-glycoprotein (P-gp) transporter proteins involved in tumour resistance, respectively. Additionally, solid tumour cell lines, including lung (A549) and colon (HCT116, HCT116p53-/-) adenocarcinomas, an osteosarcoma cell line (U2OS), and for comparison, two human non-cancer fibroblasts (BJ, MRC-5) and one endothelial (HUVEC) cell lines were included in the study. Importantly, **HeliDye1** showed very low cytotoxicity activity (IC_{50} > 50 µM) with all tested cell lines. Showing usefulness of the probe for most of the cell-based assays.

4. Conclusions:

Following aims of this thesis were fulfilled:

A. Helquats **6, 10, 14,** and **16** containing activated methyl groups next to quaternary nitrogen centers were successfully synthesized in multi-gram scale (Fig. 89).

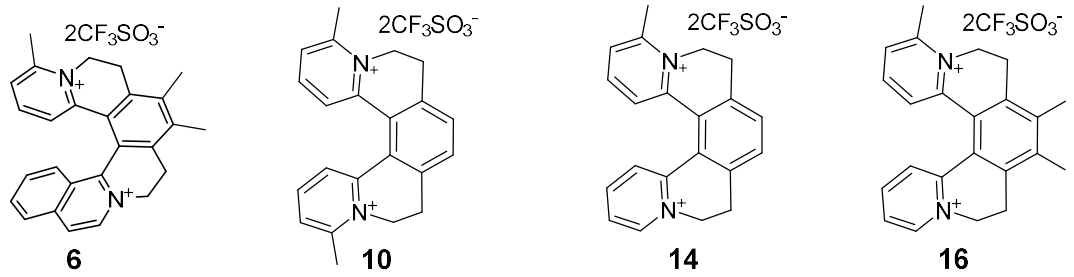

Fig. 89: *Activated methyl group containing novel helquats*

B. Resolution of methyl [6]helquat has been accomplished *via* anion exchange to form a mixture of two diastereomeric salts, which were separated by simple washing with methanol. Pure enantiomers (*P* and *M*) were obtained in multi-gram quantity by exchanging the tartrate salt to triflate (Scheme 35). The enantio-purity was determined by capillary electrophoresis and absolute configuration was determined by X-ray crystallography.

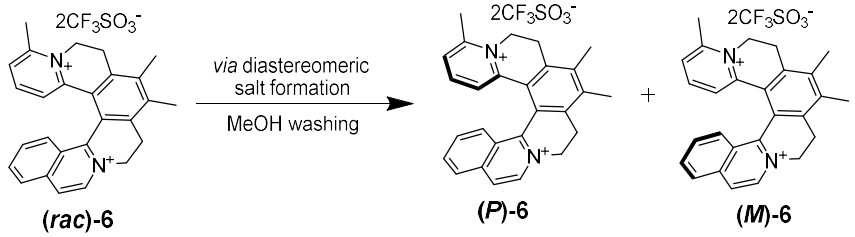

Scheme 35: *Resolution of helquat* ***6*** *via diastereomeric salt formation.*

C. A library of more than 500 compounds with diverse structures were synthesized from four different helquat scaffolds (Fig. 90) and evaluation of biological properties, to identify the therapeutic or diagnostic potential of these novel class of compounds is under investigation.

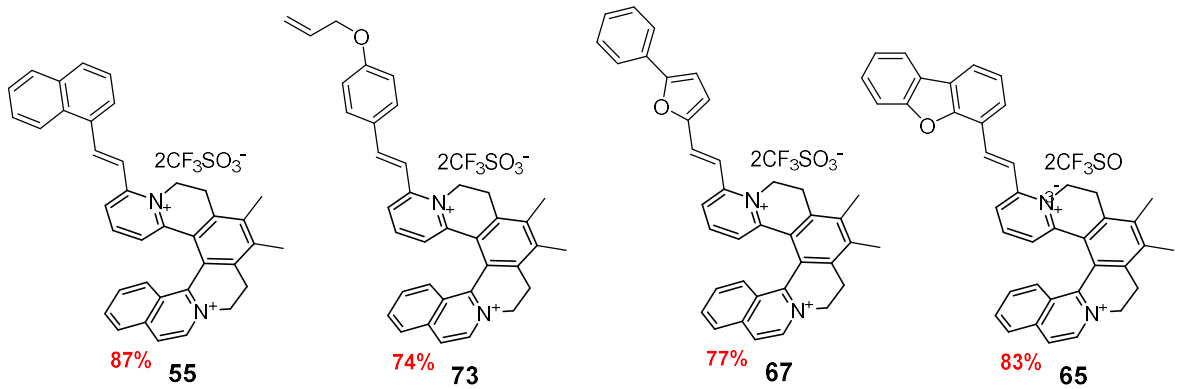

Type I derivatives

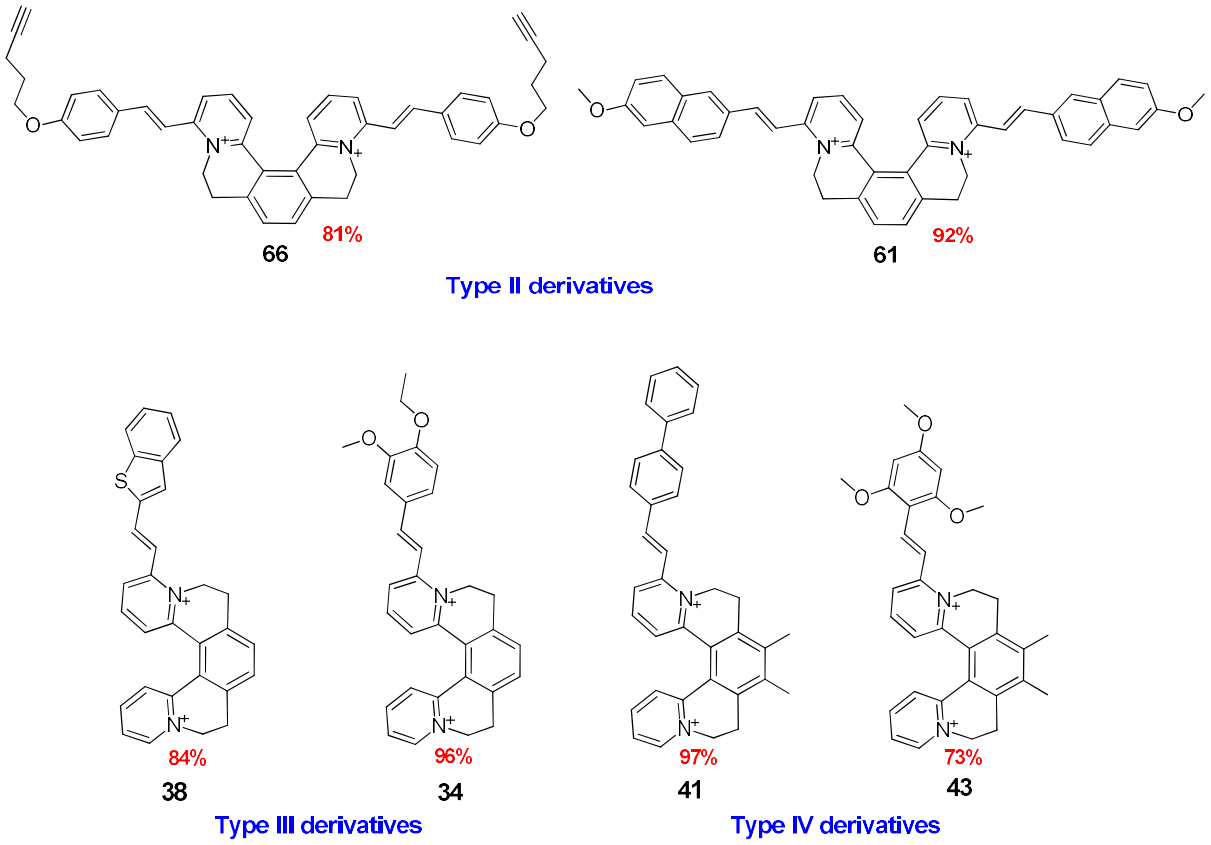

Fig. 90: *Representative examples from a library of helquat dyes.*

D. Nine compounds from **Type I** dye series were investigated for their second-order nonlinear optical responses in *racemic* forms, they were found to be better than the commercial compound DAST, with their second-order nonlinear optical responses. We will further explore the nonlinear optical properties of individual enantiomers of those nine compounds in solution and in a crystalline state (Fig. 91).

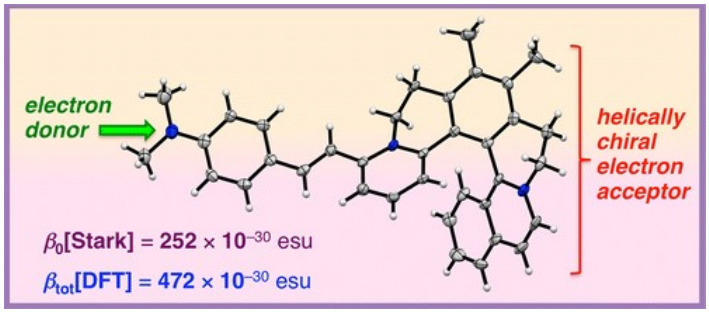

Fig. 91: *Nonlinear optical helquats.*

E. Dyes of **Type I** and **II** were screened in a high-throughput fluorescence-based assay in search of heparin chemosensors.

- Twenty four compounds were identified as preliminary hits, some of the representative examples are shown in Fig. 92:

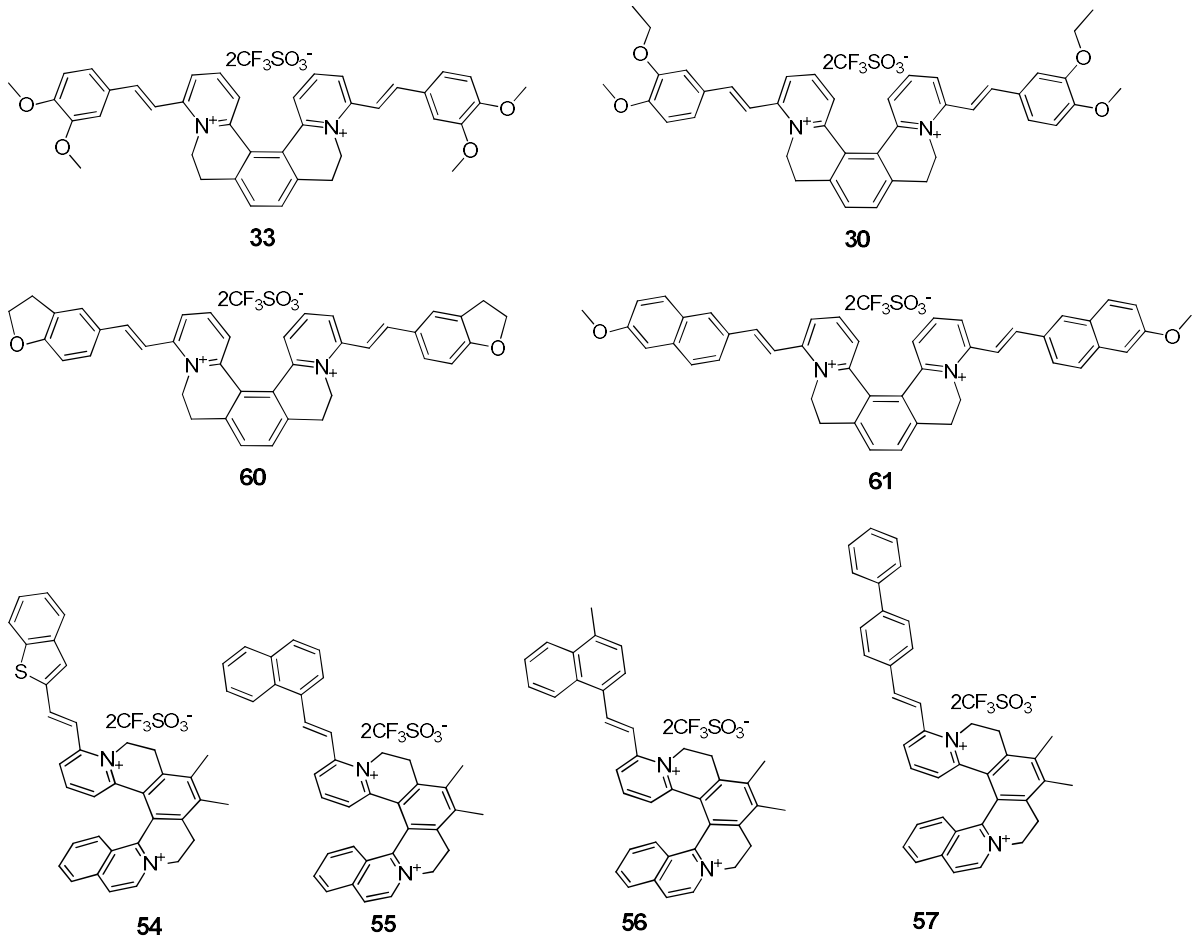

Fig. 92: *Preliminary hits for heparin chemosensors.*

- Two compounds were found to be selective for heparin over other analytes (Fig. 93).

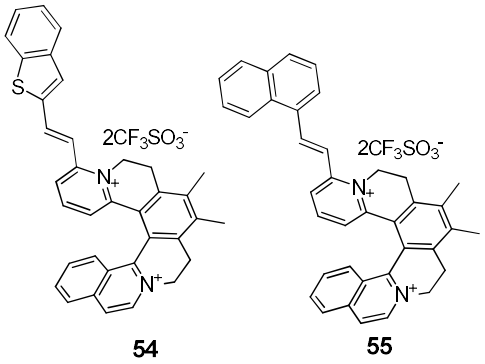

Fig. 93: *Heparin selective fluorescent probes*

- Two heparin selective fluorescent probes were validated for their capacity to quantify heparin in theoropatic and post-operative dosing level in highly competitive media such as blood plasma and serum.
- dsDNA binding dye **HeliDye1** have been discovered during the heparin screen and found to be selective for AT-rich dsDNA sequences over GC-rich sequences, ssDNA, ssRNA and dsRNA. During the SAR analysis around the structure of **HeliDye1**, three more compounds were identified to show similar selectivity and improved spectroscopic properties as compared to **HeliDye1** probe (Table 14, the fluorescence quantum yield of compound **82**, **(*rac*)-92** and **(*P*)-92** was 2.8 fold, 1.8 fold and 4.3 fold more, respectively as compared to **HeliDye1** in interaction with ds$(A_4T_4)_2$ DNA

sequence) (Fig. 94). Compound **92** was showing chiral recognition with *P*-enantiomer (K_D = 2.0 μM, Table 14), whereas *M*-enantiomer was not interacting. The biological properties and mode of interaction of newly discovered compounds will be studied in more detail.

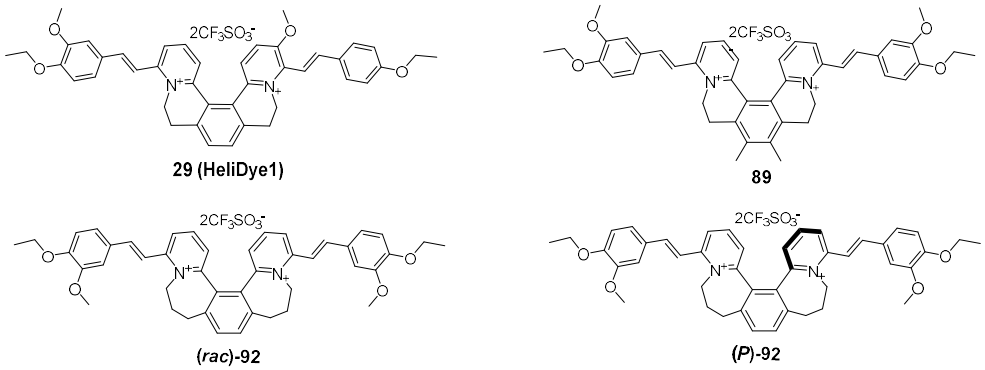

Fig. 94: *B-DNA binding helquat probes with improved spectroscopic properties.*

- DNA duplex binding properties of **HeliDye1** and other compounds were studied by UV-vis., emission, CD-spectroscopy and hydrodynamic study.
- Stereospecific recognition of minor groove of B-DNA using helquat dyes was confirmed by synthesizing enantiopure variants **(*P*)-92** and **(*M*)-92** of **HeliDye1**. Only *rac* and *P*-form of dye were found to show selective fluorescence light up in presence of AT-rich dsDNA sequences, whereas *M*-enantiomer was found to show no fluorogenic response in presence of any of the analytes, suggesting either no binding or binding with less affinity.
- A Computational study has proven the novel type of minor groove recognition of B-DNA by **HeliDye1** and binding modes of other variants are under investigation.
- Following potential applications of **HeliDye1** were successfully demonstrated
    - Nuclei staining probe in fixed cells at 1 μM concentration
    - Selectively staining of nucleic acid bands in gel electrophoresis
    - Fluorescent probe for live/dead cells exclusion
    - Fluorescent probe for cell cycle analysis

5. Experimental:

5.1 General information:

All reactions were carried out under an inert atmosphere of dry argon. Glassware was dried in an oven or by heat-gun in vacuum shortly before the experiments. Liquids and solutions were transferred *via* needle and syringe under inert atmosphere unless stated otherwise. Melting points were determined on a Wagner & Munz PolyTherm A micro melting point apparatus and are uncorrected. Thin-layer chromatography (TLC) analysis was performed on silica gel plates (Silica gel 60 F_{254}-coated aluminum sheets, Merck, cat. no. 1.05554.0001) and visualized by UV (UV lamp 254/365 nm, Spectroline® Model ENF-240C/FE). TLC analysis of dications was achieved using Stoddart's magic mixture (MeOH : NH_4Cl aq. (2 M) : $MeNO_2$, 7:2:1) as eluent on silica gel plates. Sonication was conducted with a BANDELIN SONOREX sonicator. Chemical shifts are given in δ-scale as parts per million (ppm); coupling constants (*J*) are given in Hertz (Hz). Peaks in ^1H and ^{13}C NMR spectra in acetone-d_6 were referenced relative to the solvent residual peak (CHD_2COCD_3, δ_H = 2.09 ppm) and CD_3COCD_3 (δ_C = 29.80 ppm); in $CDCl_3$ relative to the solvent peak δ_H = 7.26 ppm and δ_C = 77.00 ppm; and in DMSO-d_6 δ_H = 2.50 ppm and δ_C = 39.50 ppm. IR spectra were recorded on a Bruker EQUINOX55 (IFS55) spectrometer in KBr pellets. Abbreviations for intensities of IR bands are as follows: s for strong, vs for very strong, m for medium, w for weak, vw for very weak, br for broad, sh for shoulder. Mass spectral data were obtained at the Mass Spectrometry Facility operated by the Institute of Organic Chemistry and Biochemistry, Czech Academy of Sciences (IOCB CAS). ESI mass spectra were recorded using a Thermo Scientific LCQ Fleet mass spectrometer equipped with an electrospray ion source and controlled by Xcalibur software. The mobile phase consisted of MeOH : water (9:1) at a flow rate of 200 µL/min. The sample was dissolved, diluted with the mobile phase and injected using a 5 µL loop. Spray voltage, capillary voltage, tube lens voltage and capillary temperature were 5.5 kV, 5 V, 80 V and 275 °C, respectively. HRMS spectra were obtained with the ESI instrument.

The instruments used are listed below:

- NMR spectrometers: Bruker Avance 600 (600 MHz for ^1H, 151 MHz for ^{13}C) or Bruker Avance 400 (400 MHz for ^1H, 100.6 MHz for ^{13}C)
- For imaging of well plates: QUANTUM ST4-1100 (Viber Lourmat) imaging device
- For fluorescent imaging in cuvettes: 3UV™ transilluminator equipped with three wavelengths, 254, 312 and 365 nm.
- Microplate reader: TECAN infinite M1000 series
- UV-vis. and fluorescence spectrometer: Varian Cary 5000 series UV-vis spectrometer; Fluoromax-4 spectrofluorometer (HORIBA Scientific)
- Cell cytometry: BD FACS Aria™ cell sorter
- Fluorescence microscopy: Zeiss Axio Observer A1, 10x objective microscope; Zeiss LSM 780 confocal microscope
- Viscometer: Lovis 2000 M/ME rolling-ball viscometer, Anton Paar GmbH
- Centrifuge: Biosan LMC3000 series
- CD spectroscopy: Jasco-815 spectropolarimeter
- IR spectroscopy: Nicolet 6700
- Visualization of gels: Typhoon FLA 9500 fluorescence scanner, GE Healthcare, USA
- *NanoDrop*™ 1000 spectrophotometer, Thermo Scientific

5.2 Experimental procedures:

a) General procedure for Sonogashira coupling reaction (for internal alkyne 3 and 12):

A mixture of $[Pd(PPh_3)_2Cl_2]$ (1.6 mmol, 5 mol %), CuI (3.3 mmol, 10 mol %), and terminal alkyne **1** or **11** (32.6 mmol, 1.0 equiv.) was placed under argon into an oven-dried Schlenk flask. Freshly distilled Et_3N (6 mL/mmoL), followed by 2-bromo-6-methylpyridine (39.1 mmol, 1.2 equiv.) was added to the reaction mixture at rt. The reaction mixture was heated at 80-82 °C for 1 h until complete disappearance of **1** or **11** was detected (TLC analysis in 50% EtOAc in hexane, starting material (**1** or **11**) R_f = 0.5, product R_f = 0.25). Cooling of the reaction mixture at rt, filtration through a Celite pad, repetitive washings of Celite bed with EtOAc until no product was detected in the eluent (TLC analysis) followed by evaporation of volatiles under reduced pressure gave Sonogashira coupling product **3** or **12** in crude form. Purified product **3** or **12** was obtained by chromatographing the crude product through a column of silica gel using 1:1 mixture of hexane/EtOAc as a mobile phase. Purified products were obtained as brown solids.

b) Procedure for the synthesis of triyne 9, 13 and 15:

Internal alkynes **7** or **12** (4.8 mmol, 1.0 equiv.) was charged under argon into an oven dried Carius tube. Dry DCM (25 mL) and respective alkylating agent **4** or **8** (24 mmol, 5.0 equiv.) was added to a Carius tube at rt. The resulting solution was heated to reflux for 40 h in dark. The progress of the reaction was monitored by TLC (mobile phase Stoddart's magic mixture, starting material R_f = 0.85, product R_f = 0.48), as well as by ^{1}H-NMR analysis. After cooling, volatiles were evaporated under reduced pressure on a rotatory evaporator and resulting residue was sonicated with Et_2O (25 mL). After separation of the supernatant, the residue was sonicated in EtOAc (3 x 25 mL) and each time the supernatant was separated by centrifugation of the suspension. After drying of the solid under high vacuum, pure triynes **9**, **13** or **15** were obtained as off-white solid.

c) General procedure for the synthesis of helquat 6, 10, 14 and 16:

Cyclotrimerization of triynes **5**, **9**, **13** or **15** (2.848 mmol, 1.0 equiv.) takes place under $[Rh(PPh_3)_3Cl]$ (0.142 mmol, 5 mol %) catalysis under argon atmosphere in dry-degassed DMF in an oven dried Schlenk flask under heating at 110-112 °C. After 1 h, reaction progress was monitored by TLC analysis for complete consumption of respective triyne (mobile phase: Stoddart's magic mixture). After cooling of the reaction to rt, the reaction mixture was transferred to a round bottom flask and DMF was evaporated under reduced pressure at 50 °C water bath temperature. Brown residue obtained after evaporation of DMF was triturated with Et_2O (2 x 25 mL) and THF (3 x 25 mL) by sonication, followed by separation of supernatant by centrifugation and drying of final solid under high vacuum gave respective helquat **6**, **10**, **14** or **16** as off-white to light brown amorphous solid.

d) Procedure for the resolution of [6]helquat:

Resolution of Trimethyl[6]helquat **6** was carried out by modifying the previously described procedure.[181]

- **Procedure to prepare anion exchange resin in OH^- cycle:**

Strongly basic anion exchange resin in Cl^- cycle (soaked in water for overnight) was loaded into a column equipped with a Teflon tap and sinter s0 at the bottom of the column. For the uninterrupted smooth flow of liquid through the ion-exchange column equipped with a sinter or a piece of cotton wool plug in the bottom part of the column was used. Amount of

resin, which was used for each experiment, was measured in terms of volume of resin (in Cl^- cycle) in water (bed volume). Switching from Cl^- cycle to OH^- cycle was done by passing 2 M aq. solution of NaOH through the resin. Sufficient amount of 2 M solution of NaOH for complete exchange of chloride anions is 18 ml per 1 ml of bed volume of the resin. The fact that the exchange is complete, the absence of Cl^- anions was checked by taking a few drops of out coming basic solution to a small vial. This sample was acidified with few drops of aq. solution of HNO_3 (1:1), until the universal pH-paper test detected acidic reaction. Finally, two drops of 0.1M aq. solution of $AgNO_3$ was added. Completely clear solution (absence of AgCl precipitate) indicated the absence of Cl^- anions in the outcoming basic solution. At that point, pure water was run through the resin until the neutral reaction of out coming liquid was detected (universal pH paper test). Subsequently, water was expelled from the resin by applying small overpressure and MeOH was placed instead of it. All bubbles were removed by mixing the resin with a long needle or by stoppering the column and turning it gently upside down and back, so that all beads of the resin nicely mixed with MeOH and no bubble remained.

- **Procedure to prepare diastereomeric mixture *via* anion exchange**

A column of outer diameter 2.5 cm was put to OH- cycle. The solvent was subsequently exchanged for MeOH, then 0.2 M solution of (*R*,*R*)-(-)-*O*,*O'*-dibenzoyl-L-tartaric acid in MeOH was passed through the column until pH of the eluent becomes fairly acidic. For rough pH assessment the following method is recommended: a drop of pure MeOH is spotted on a universal pH-paper and, next to it, a drop of eluting solution is spotted. If the drop of eluting solution is more red than the drop of pure MeOH, the eluting solution is considered acidic. Overall, 85 mL of this solution was passed. Then the column was stoppered, and turned up and down repeatedly, so as to remove air bubbles and create a uniform bed of resin. Then pure MeOH was passed through the column until the pH of the eluent becomes neutral.

A methanolic solution of [*rac*-**6**][TfO^-]$_2$ (1.000 g, 1.478 mmol) (250 mL) was passed through the resin column pre-loaded with (*R*,*R*)-(-)-O,O'-dibenzoyl-L-tartrate anions. The column was repeatedly washed with pure MeOH. After regular intervals, the spot of the eluted MeOH was spotted on TLC and was observed under UV lamp for its UV response. Once no UV response was observed to the new spot on TLC, it was confirmed that complete helquat, loaded on the column was eluted and was exchanged to bis-(*R*,*R*)-(-)-*O*,*O'*-dibenzoyl-L-tartrate anions.

The combined eluent was evaporated to dryness to obtain an oily residue, which was triturated with Et_2O. Precipitated solid was filtered. After vacuum drying, the absence of fluorine signal in the ^{19}F-NMR spectrum of the solid confirms the complete exchange of bis triflate salt to diastereomeric (*R*,*R*)-(-)-*O*,*O'*-dibenzoyl-L-tartrate salt.

Two diastereomers were separated by simple washings with MeOH. The obtained mixture of diastereomeric salts was sonicated with MeOH (10 x 5 mL) and after each washing, the suspension was centrifuged, which help to separate supernatant from the solid. Each time supernatant and residual solid were sampled for CE analysis. After 10 washings, the residual solid was vacuum dried to give 924 mg of pure diastereomer with >97% ee.

The enantiopurity of the purified material was accessed by chiral capillary electrophoresis analysis. Pure enantiomer was obtained from the purified diastereomer by breaking the diastereomeric salt by anion exchange to achiral anion such as triflate.

The opposite diastereomer was recovered from the supernatant by passing it through the resin column pre-loaded with D-dibenzoyl tartrate anions and by following the similar procedure used for the isolation of the previous enantiomer in its enantiopure form, the opposite enantiomer was also obtained with satisfactory enantiopurity.

- **Procedure for anion exchange to triflate, and isolation of pure enantiomers:**

A pure diastereomeric salt of trimethyl[6]helquat, **6** with (*R*,*R*)-(-)-*O*,*O'*-dibenzoyl-L-tartrate anions (0.924 g, 0.8451 mmol) was transferred into a 50 mL centrifuge tube and dissolved in a solution of TfOH [2.3% in MeOH] (2 mL). Complete dissolution was ensured by sonication. Et_2O (40 mL) was added, the resulting solution becomes turbid and after sonication for 2-3 minutes, a dark brown oily residue was accumulated at the base of the centrifuge tube. The supernatant was separated from the residue after centrifugation of the resulting solution for 5 minutes. The dissolution, addition of Et_2O (40 mL), sonication and centrifugation was repeated for two more times, to ensure complete anion exchange. After complete anion exchange, the brownish oily residue was dissolved in MeOH (2 mL), and was re-precipitated by addition of Et_2O (40 mL). This re-dissolution and re-precipitation was repeated for two more times, still the precipitated solid becomes free flowing powder. The Obtained residue was vacuum dried as a pale yellow powder. Yield: 382 mg (76.4%).

The opposite enantiomer was obtained by following the similar procedure as a pale yellow powder. Yield: 397 mg (79.4%)

- **Racemization study with [*P*-6][TfO^-]:**

[*P*-6][TfO^-](2.5 mg, 0.004) was dissolve in DMSO (0.5 mL) in an NMR tube and was immersed in an oil bath pre-heated at 120 °C. Before heating, approximately 10 µL of the solution was taken with the help of capillary into an eppendorf for the capillary electrophoresis measurement. After commencing heating, approximately 10 µL of the sample from the NMR tube was withdrawn at an interval of 20 minutes for chiral capillary electrophoresis analysis. After analysis of all samples by CE, a racemization curve between time *vs. ln*(%*ee*) of major enantiomer and by performing some arithmetic (described in Results and discussion section), the halflife of racemization ($T_{1/2}$) and racemization barrier of interconversion of one enantiomer to other (ΔG) was determined.

e) General procedure for the synthesis of helquat dyes:

Under an argon atmosphere, helquat dye precursors **6, 10, 14,** or **16** and various aromatic, hetero-aromatic or metalloaromatic aldehydes (5 to 15 equiv.) were charged into a Schlenk flask and were placed under argon. Dry MeOH (0.1 mL/mg) followed by pyrrolidine (12 equiv.) was added to the reaction mixture. The flask was covered with Alufoil and until complete consumption of helquat dye precursor **6**, **10**, **14** or **16** analyzed by TLC analysis (mobile phase: Stoddart's magic mixture), the reaction was maintained under stirring at rt. The reaction was quenched by addition of Et_2O (8 x vol. of MeOH) into the reaction mixture. The suspension was sonicated for 2 min. and then centrifuged. The supernatant was separated from the solid. For further purification, obtained crude solid was completely dissolved in MeOH or MeCN and then precipitated by addition of Et_2O (6-8 vol. to the vol. of MeOH or MeCN). The suspension was sonicated, centrifuged and the supernatant was separated. This dissolution, precipitation procedure was repeated two more times. After drying under high vacuum, cationic styryl dyes were obtained as colored solids.

f) General procedure for the synthesis of planar dyes:

Method 1: Planar dye precursors **17 or 18** (30 mg, 0.128 mmol, 1.0 equiv.) and various aromatic, heteroaromatic or metalloaromatic aldehydes (0.640 mmol, 5.0 equiv.) were charged into a Schlenk flask under an argon atmosphere. Dry EtOH followed by pyrrolidine (15.8 μL, 13.7 mg, 0.192 mmol, 1.5 equiv.) was added to the reaction mixture. The flask was covered with Alufoil and the reaction mixture was heated at reflux until complete disappearance of the starting pyridinium substrate by TLC analysis (mobile phase: Stoddart's magic mixture). The reaction was quenched by addition of Et_2O (8 x vol. of MeOH) into the reaction mixture. The suspension was sonicated for 2 min. and then centrifuged. The supernatant was separated from the solid. The solid was further cleaned by washing with MeOH (3 x 0.5 mL) by sonication. Every time supernatant was separated from the solid and finally washed with Et_2O. Resulting solid was dried under high vacuum to give respective pyridinium dye in high yields.

Method 2: Planar dye precursor **17** or **18** (0.128 mmol, 1.0 equiv.), aromatic or heteroaromatic aldehydes (0.640 mmol, 5.0 euiv.), EtOH (1.0 ml) followed by pyrrolidine (14.7 mg, 17 μL, 0.207 mmol, 1.6 equiv.) were mixed together in a microwave glass tube and heated for 5 minutes in a microwave at microwave power 150 w. After 5 minutes complete starting consumption was confirmed by TLC analysis (eluent: Stoddart's magic mixture) and Et_2O (8 mL) was added. Precipitated solid was transferred to the storage vials and centrifuged. The supernatant was separated and solid was washed two times with MeOH (2 x 0.5 mL) and the supernatant was separated and finally with Et_2O (2 x 5 mL). Resulting solid was dried under high vacuum to give respective pyridinium dye in high yields.

g) General procedure for high-throughput fluorescence light-up assay:

A high-throughput fluorescence light up assay was designed for screening a library of helquat dyes. The experimental setup for the screening is shown in Fig. 95. In order to screen number of helquat dyes at a time, the screening was performed in a 96/384 well plate. The Well plate experiment also allows us to perform high-throughput screening of many compounds with repetition in multiplicates using a small quantity of sample as well as analytes.

DMSO stock solution (1 mM) of each dye was prepared. For screening, 1 mM DMSO stock solution of dyes and 1 mM aqueous stock solution of analyte were mixed together in a buffer in different ratios, in such a way that each well contains only one dye in presence of respective analyte. The final volume of DMSO into the test well was controlled between 1 to 10% depending upon the solubility of the dye in aqueous buffer environment. A blank well for each compound, i.e. dye alone (at the same concentration in presence of analyte) was also prepared. The well plate was protected from light. After preparing the well plate, contents were mixed together by shaking for 5 min. at rt and 500 rpm speed on a thermoshaker device and centrifuged at high speed for 30-50 seconds. At this stage, the well plate was placed inside the cabinet of an imaging device equipped with a camera at the top, the well plate was illuminated at 312 nm or 365 nm, and the picture of the well plate was recorded, while irradiating with UV light. By the visual observation of fluorescence light-up response of the dye, in presence and absence of analyte, the preliminary hits were identified. The quantitative measurement of fluorescence light up of the identified hits in presence and absence of analyte was measured at optimized excitation of the compound by using Tecan infinite® M1000 well plate reader, which confirms recognition of the analyte by the identified hit by showing fluorescence light-up in presence of analyte as compared to dye alone.

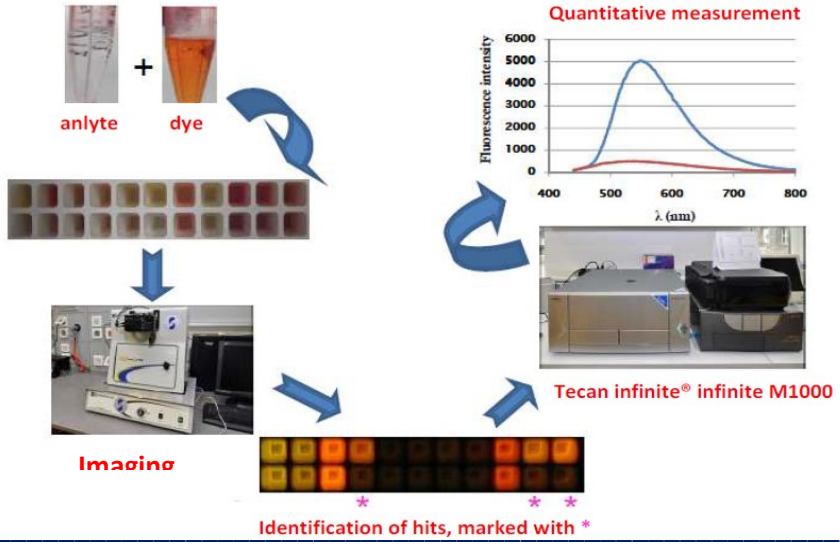

Fig. 95: *Experimental setup for fluorescence light-up experiment*

h) Procedure for determination of selectivity of identified hits for heparin or dsDNA:

The selectivity of all preliminary hits for various targets was analyzed in a competitive fluorescence light up experiment, where a solution of each analyte was mixed with each of the analyte mentioned below in a separate well.

All nucleotide triphosphates, EGTA, Na_2SO_4, glucose, Na Citrate were at 50 µM in 10 mM HEPES buffer (pH = 7.4). DNA was at 0.025 mg mL^{-1} (~50 µM). Bovine serum albumin (BSA) was at 0.5 mg mL^{-1}. Heparin, hyaluronic acid and chondroitin sulphate were at 6.5 µg mL^{-1} (~10 µM). 20% plasma solution was prepared by dilution of pooled normal human plasma in 10mM HEPES buffer (pH = 7.4). Control was 10 mM HEPES buffer (pH = 7.4).

Fluorescence light up response of each compound for each analyte was measured and the selectivity for that particular compound was decided on the basis of comparison of relative fluorescence light up intensity in each case of every analyte at maxima.

By following this general procedure, two heparin selective helquat dyes were identified as well as a dsDNA binding dye was also identified. All these identified hits were further developed for finding useful applications.

i) Procedure for blood plasma isolation:

Approximately 20 mL of blood was drawn with the help of a nurse or the general practitioner and transferred into the capillary blood collection tubes (5 mL vol., BD Vacutainer Seditainer, Catalogue number 366016). Vacutainer tubes were inverted carefully 10 times to mix blood and the anticoagulant and stored at rt until centrifugation.

The samples were centrifuged immediately by transferring the blood into sterile Falcon tubes with 10 mL volume for 15–20 minutes at 1500–1700 RCF at room temperature. The supernatant (plasma) was separated at room temperature and inspected for turbidity (if there was some turbidity, the samples were centrifuged for 15–20 min. at 1500 RCF and supernatant was filtered through the sterile filter of pore size 0.22 micron (Millipore, Catalogue Number: SLGVR25LS). The isolated plasma was aliquot to 3-4 times into the 1.5 mL sterile Eppendorf tubes with vol. for further use. Remaining aliquots were stored at 0-5 °C into the fridge.

j) Procedure for the calibration of heparin chemosensors for heparin quantification:

For developing a calibration curve for heparin quantification from plasma/serum, a concentration series from 0 µM to 100 µM was prepared by spiking 100% plasma/serum with the desired amount of heparin. The samples prepared in the previous step were diluted to achieve 10% diluted plasma (now the amount of heparin became 10 times less than the original, and these concentrations can be seen at calibration curve) were mixed with 10 µM of heparin probe **54** or **55** and fluorescence spectra from each well were recorded and the calibration curve was prepared by plotting intensity of fluorescence spectra at maxima *Vs.* heparin concentration in respective well.

k) UV-vis. absorption and fluorescence spectroscopy:

All UV-vis. and fluorescence spectra were measured in semi-micro quartz fluorescence cuvettes (Hellma Analytics) of path length 1 cm. The individual samples were prepared with or without oligonucleotide using 1 mM **HeliDye1** stock solution and 1 mM oligonucleotide stock solution as follows:

1. with oligonucleotide: Mixing of 1mM oligonucleotide stock solution (5 µL) + BPES buffer (985 µL) + **HeliDye1** 1mM stock solution (10 µL) in a 1.5 mL Eppendorf tube.

2. without oligonucleotide: Mixing of 1 mM **HeliDye1** stock solution (10 µL) + BPES buffer (990 µL) in a 1.5 mL Eppendorf tube.

UV-vis. absorption spectrum of each sample was measured in between 300–750 nm range with reference to the corresponding blank solution. For **HeliDye1** in absence of oligonucleotide, BPES buffer containing 1% DMSO was used as a reference. For each sample of HeliDye1 with oligonucleotides, respective 5 µM oligonucleotide solution in BPES buffer (containing 1% DMSO) was used as a reference solution.

After measurements of absorption spectra of each solution, fluorescence spectra of each sample was recorded at $\lambda_{excitation}$ = 460 nm. UV-vis. and fluorescence spectra for **HeliDye1** with and without respective oligonucleotide were plotted. The spectroscopic properties of **HeliDye1** in presence of various DNA oligonucleotide sequences are listed in Table 12.

l) Determination of fluorescence quantum yield (Table 12 for HeliDye1 and Table 15 for dye 90 and 93) :

Determination of the fluorescence quantum yields[186] (Φ_f) was performed using coumarin 153 (Φ_f = 0.53 at 25° C) as a standard in spectroscopy grade EtOH as a solvent. Measurements were performed in semi-micro quartz fluorescence cuvettes (Hellma Analytics) on a Fluoromax-4 spectrofluorometer equipped with a thermostated cuvette holder at 25° C. The excitation wavelength was 435 nm and the recorded spectral range was 455-750 nm for compounds and coumarin 153. The absorbance of the sample solution and the standard at the excitation wavelength were kept below 0.08. The quantum yields were calculated using the following equation:

$$\emptyset_{f,x} = \emptyset_{f,st}\, X\, \frac{F_x}{F_{st}}\, X\, \frac{1-10^{-Absst}}{1-10^{-Absx}}\, X\, \frac{n_x^2}{n_{st}^2} \qquad \textit{(eq. 8)}$$

The quantum yield, *F* is the integrated fluorescence intensity, *Abs* is the absorbance of the solution at the excitation wavelength, *n* is the refractive index of solvent; the subscripts *x*

and *st* stands for the sample and standard, respectively. Quantum yield measurements were done in triplicate with a standard deviation of ± 0.04.

m) Sequence specificity of DNA interacting dyes:

Light-up properties of DNA interacting dyes were studied with various dsDNAs, ssDNAs and RNA sequences, to determine their sequence specificity. All test nucleic acids were dissolved in nuclease-free water at 1 mM concentration and all dyes were dissolved in pure DMSO at 1 mM concentration.

In a 96 well plate, each well, 1 mM stock solution of respective nucleic acid (0.75 µL) and 1 mM DMSO stock solution of each dye (1.5 µL) were mixed with 147.75 µL of BPES buffer, to achieve 5 µM final respective nucleic acid concentrations and 10 µM final concentration of the respective dye. Fluorescence spectra of each dye at their respective excitation wavelengths[187] were measured in presence of all analytes after 5 minutes of mixing and from the fluorogenic response of each probe with all possible analytes, the sequence specificity was determined.

n) K_D values of interaction of dye 6a and various dsDNA sequences

The dissociation constants (K_D) of the interaction between **HeliDye1** and various example DNA duplexes were determined by fluorescence titration method. Each oligonucleotide (1 µM) was titrated with increasing concentrations of dye **HeliDye1** from 0 to 200 µM in BPES buffer. The dissociation curves were best-fitted using 1:1 binding with Hill slope model (nonlinear regression least square method) from Graph pad prism 5.[194] The dissociation constants for each of the dsDNA sequence are summarized in Table 13. An inverse relationship was found between number of AT-pairs and K_D.

o) Hydrodynamic study

Hydrodynamic study of drug-DNA interactions is a sensitive technique to probe the DNA duplex/ligand binding mode.[193] Viscosity measurements were performed using Rolling Ball Viscometer Lovis 2000 M/ME series, from Anton Parr GmbH. Following solutions with five different ratios of dye **HeliDye1** : dsDNA solutions were prepared, while keeping the concentration of dsDNA constant at 100 µM bp. Base pair molarity of the ctDNA stock solution was determined as follows. Concentration value of the DNA stock solution (in ng/µL) was determined by *NanoDrop*™ 1000 spectrophotometer. The base pair molarity of DNA stock solution was determined by putting the obtained value of ng/µL to the DNA calculator at molbiotools webpages.[195]

	c_{dye} (µM)	c_{dsDNA} (µM)	Ratio (dye/dsDNA)
1.	0	100	0
2.	25	100	0.25
3.	50	100	0.5
4.	100	100	1
5.	200	100	2

Table 16: *Solutions of different dye : dsDNA ratios used for viscosity measurement.*

Viscosity of each solution was measured four times, and a graph presenting $(n/n_o)^{1/3}$ *vs.* dye **HeliDye1** : dsDNA ratio was plotted. Similar experiment was performed for propidium iodide

(PI), which is a typical intercalator, and was used as a positive control. DAPI, a minor groove binder was used as a negative control.

5.3 Analytical data:

1-((6-methylpyridin-2-yl)ethynyl)isoquinoline (3)

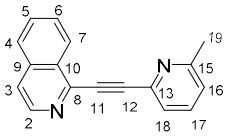

$(C_{17}H_{12}N_2)$
[244.3]

The synthesis of the compound **3** was accomplished by following *general procedure 5.2.a*.
A brown crystalline solid was obtained.
Yield: 6.370 g, 80%.
m.p. 113-116 °C. **^{1}H-NMR (600 MHz, acetone-d_6):** δ 2.61 (s, 3H, H-19), 7.39 (d, J = 7.8 Hz, 1H, H-16), 7.69 (d, J = 7.6 Hz, 1H, H-18), 7.83 (t, J = 7.7 Hz, 1H, H-17), 7.86 (ddd, J = 1.2, 6.7, 8.2 Hz, 1H, H-6), 7.89 (ddd, J = 1.4, 6.7, 8.3 Hz, 1H, H-5), 7.92 (dd, J = 1.3, 5.6 Hz, 1H, H-3), 8.08 (ddt, J = 0.8, 1.3, 8.3 Hz, 1H, H-4), 8.62 (ddd, J = 0.8, 1.4, 8.2 Hz, 1H, H-7), 8.63 (d, J = 5.6 Hz, 1H, H-2). **^{13}C-NMR (151 MHz, acetone-d_6):** δ 24.5 (C-19), 85.8 (C-11), 93.5 (C-12), 122.0 (C-3), 124.4 (C-16), 125.8 (C-18), 127.2 (C-7), 128.1 (C-4), 129.4 (C-6), 130.3 (C-10), 131.7 (C-5), 136.7 (C-9), 137.6 (C-17), 142.6 (C-13), 144.0 (C-2), 144.2 (C-8), 160.2 (C-15). **IR (KBr): ν (cm^{-1})** 1495, 1552, 1566, 1581, 1619, 2212, 3009, 3054. **MS (ESI) *m/z* (%):** 245.1 (M + 1) (100), 246.1 (20), 267.1 (10). **HRMS ESI *m/z*:** (M + 1) [$(C_{17}H_{13}N_2)^+$] calc. 245.1073, found 245.1072.

1-((6-methyl-1-(pent-3-yn-1-yl)pyridin-1-ium-2-yl)ethynyl)-2-(pent-3-yn-1-yl)isoquinolin-2-ium trifluoromethanesulfonate (5)

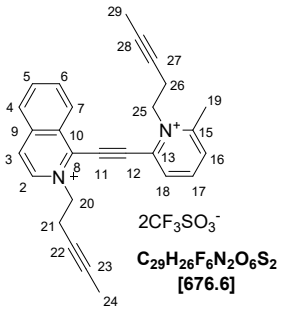

$2CF_3SO_3^-$
$C_{29}H_{26}F_6N_2O_6S_2$
[676.6]

Into an oven dried Carius tube, alkyne **3** (1.000 g, 4.093 mmol, 1.0 equiv.) and DCM (40 mL) was charged under argon. Pent-3-yn-1-yl trifluoromethanesulfonate (4.450 g, 20.586 mmol, 5.0 equiv.) was added to the reaction mixture at rt. The reaction mixture in a Carius tube was immersed into an oil bath and was heated to reflux for 65 h (reaction was monitored by ^{1}H-NMR analysis after each 24 h). The set-up was completely covered with Alufoil during the whole operation. After cooling at rt, the reaction mixture was transferred into a round bottom flask and solvent was evaporated on a rotary evaporator. The Washing of the residual containt in a flask with Et_2O (3 x 20 mL) followed by biphasic extraction in 1:0.6 water/DCM mixture (65 mL x 3), all triyne product was extracted into the aqueous phase. Evaporation of combined aqueous portion on rotatory evaporator, followed by trituration of residual oil with Et_2O (2 x 25 mL), gave **5** as a brown gummy solid.
Yield: 1.3 g, 47 %.
m.p. 151-154 °C. **^{1}H-NMR (600 MHz, acetone-d_6):** δ 1.74 (t, J = 2.6 Hz, 3H, H-29), 1.77 (t, J = 2.6 Hz, 3H, H-24), 3.27–3.30 (m, 4H, H-21 & H-27), 3.31 (s, 3H, H-19), 5.44 (t, J = 6.6 Hz, 2H, H-25), 5.50 (t, J = 6.6 Hz, 2H, H-20), 8.33 (ddd, J = 1.2, 7.0, 8.5 Hz, 1H, H-6), 8.46 (ddd, J = 1.1, 7.0, 8.4 Hz, 1H, H-5), 8.46 (dd, J = 1.6, 7.9 Hz, 1H, H-16), 8.59 (dt, J = 1.2, 8.4 Hz, 1H, H-4),

8.81 (t, *J* = 7.9 Hz, 1H, H-17), 8.90 (dd, *J* = 1.6, 7.9 Hz, 1H, H-18), 8.93 (dd, *J* = 0.8, 6.8 Hz, 1H, H-3), 9.09 (dq, *J* = 1.0, 8.5 Hz, 1H, H-7), 9.20 (d, *J* = 6.8 Hz, 1H, H-2). **^{13}C-NMR (151 MHz, acetone-d_6):** δ 3.2 (C-24), 3.2 (C-29), 20.0 (C-19), 21.8 (C-26), 22.0 (C-21), 56.5 (C-25), 61.2 (C-20), 74.2 (C-28), 74.3 (C-23), 82.0 (C-27), 82.2 (C-22), 90.1 (C-11), 99.4 (C-12), 128.6 (C-3), 129.3 (C-4), 130.0 (C-7), 131.0 (C-10), 133.6 (C-16), 134.1 (C-18), 134.4 (C-6), 136.3 (C-13), 138.5 (C-2), 138.5 (C-5), 138.6 (C-9), 138.9 (C-8), 146.3 (C-17), 160.7 (C-15). **IR (KBr): *v* (cm^{-1})** 518, 574, 639, 1031, 1172, 1265, 1491, 1509, 1564, 1581, 1602, 1611, 1619, 2223, 2291, 3092. **MS (ESI) *m/z* (%):** 295.1 (4), 296.1 (15), 311.1 (36), 312.1 (10), 377.2 (100), 378.2 (31), 395.2 (13), 527.1 [(M − $CF_3SO_3^-$)$^+$] (11). **HRMS ESI *m/z*:** calc. for [(M − $CF_3SO_3^-$)$^+$] [($C_{28}H_{26}O_3N_2F_3S$)$^+$] 527.1611, found 527.1612.

6,7,11-trimethyl-4,5,8,9-tetrahydroisoquinolino[1,2-a]pyrido[1,2-k][2,9]phenanthroline-3,10-diium trifluoromethanesulfonate (6)

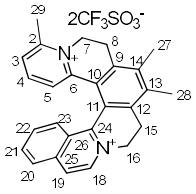

$C_{29}H_{26}F_6N_2O_6S_2$
[676.6]

Synthesis of [6]helquat **6** was accomplished by following *general procedure 5.2.c.* An off-white amorphous solid was obtained.

Yield: 1.630 g, 85 %.

m.p. 241-243 °C. **^{1}H-NMR (600 MHz, acetone-d_6):** δ 2.66 (s, 6H, H-27 & 28), 3.16 (s, 3H, H-29), 3.38 (dt, *J* = 4.8, 15.7 Hz, 1H, H-8a), 3.48 (dt, *J* = 4.5, 15.3 Hz, 1H, H-15a), 3.81 (ddd, *J* = 1.7, 3.6, 17.0 Hz, 1H, H-15b), 3.83 (ddd, *J* = 1.9, 3.7, 17.0 Hz, 1H, H-8b), 5.10 (dt, *J* = 3.7, 14.4 Hz, 1H, H-7b), 5.17 (dt, *J* = 3.6, 14.0 Hz, 1H, H-16a), 5.39 (ddd, *J* = 1.7, 4.5, 14.0 Hz, 1H, H-16b), 5.59 (ddd, *J* = 1.9, 4.8, 14.2 Hz, 1H, H-7a), 7.48 (dd, *J* = 2.7, 6.8 Hz, 1H, H-5), 7.74 (t, *J* = 7.4 Hz, 1H, H-4), 7.76 (dd, *J* = 2.7, 7.8 Hz, 1H, H-3), 7.83 (ddd, *J* = 1.2, 6.9, 8.7 Hz, 1H, H-22), 7.99 (ddd, *J* = 1.1, 6.9, 8.1 Hz, 1H, H-21), 8.09 (dq, *J* = 0.8, 8.7 Hz, 1H, H-23), 8.29 (d, *J* = 8.1 Hz, 1H, H-20), 8.55 (d, *J* = 6.7 Hz, 1H, H-19), 9.03 (d, *J* = 6.7 Hz, 1H, H-18). **^{13}C-NMR (151 MHz, acetone-d_6):** δ 16.8 (C-27), 17.0 (C-28), 21.4 (C-29), 26.0 (C-8), 26.9 (C-15), 50.2 (C-7), 56.2 (C-16), 123.8 (C-13), 125.9 (C-19), 127.0 (C-26), 128.7 (C-23), 128.8 (C-14), 128.9 (C-3), 129.2 (C-5), 129.2 (C-20), 132.8 (C-22), 136.2 (C-21), 137.6 (C-18), 138.9 (C-10), 140.0 (C-25), 141.1 (C-9), 142.0 (C-12), 142.6 (C-11), 144.4 (C-4), 148.9 (C-6), 151.7 (C-24), 157.0 (C-2). **IR (KBr): *v* (cm^{-1})** 518, 638, 1031, 1154, 1265, 1491, 1509, 1564, 1581, 1602, 1611, 1619, 3080. **MS (ESI) *m/z* (%):** 181.6 (4), 377.2 (100), 378.2 (34), 527.2 [($C_{28}H_{26}F_3N_2O_3S$)$^+$] (4). **HRMS ESI *m/z*:** calc. for [(M − $CF_3SO_3^-$)$^+$] [($C_{28}H_{26}F_3N_2O_3S$)$^+$] 527.1611, found 527.1612

1,2-bis(6-methylpyridin-2-yl)ethyne (7)

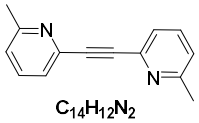

$C_{14}H_{12}N_2$
[208.3]

Synthesis was accomplished as described in literature.[8]

To the reaction mixture containing [$Pd(PPh_3)_4$] (2.85 g, 2.47 mmol, 2.5 mol%) and CuI (942 mg, 4.95 mmol, 5 mol%) in a Schlenk flask under argon was added dry Et_3N (200 mL). 2-Bromo-6- methylpyridine, **2** (11.3 mL, 17.0 g, 98.8 mmol) was added to the stirring reaction mixture *via* needle and syringe. Finally argon atmosphere was exchanged for acetylene

atmosphere by connecting a balloon with acetylene gas to the Schlenk flask and by piercing the septum with a needle for 10 seconds. The reaction mixture was stirred for 3 h at 80-82 °C. The progress of the reaction was monitored by TLC (mobile phase: 50% EtOAc in hexane, starting material, R_f = 0.88, product, R_f = 0.24). After filtration through a sinter with Celite® 512 layer and washing with EtOAc (500 mL), the volatiles were removed on a rotary evaporator and the residue was transferred to a 250 mL round-bottomed flask (using acetone for rinsing). After removing the acetone on a rotary evaporator, cyclohexane (4 x 150 mL) was added to the solid residue and the mixture was heated at 80 °C on a rotary evaporator without applying vacuum. After 1 min of rotation and heating, the insoluble residue was decanted and the hot solution was fast and carefully transferred to a new flask to complete the crystallization at rt. Crystals were separated from supernatant by vacuum filtration gave compound **7** as a yellow crystalline powder.

Yield: 8.17 g, 79%

m.p. 135-137 °C. **^{1}H-NMR (600 MHz, acetone-d_6):** δ 2.55 (bs, 6H), 7.32 (qdd, *J* = 0.6, 1.0, 7.7 Hz, 2H), 7.50 (qdd, *J* = 0.7, 1.0, 7.7 Hz, 2H), 7.77 (t, *J* = 7.7 Hz, 2H). **^{13}C-NMR (151 MHz, acetone-d_6):** δ 23.5, 87.3, 123.0, 124.6, 136.6, 141.9, 159.1. **IR (KBr):** *v* (cm^{-1}) 736, 743, 793, 1090, 1154, 1231, 1242, 1373, 1452, 1458, 1565, 1584, 2220, 2959, 2987, 3054, 3069. **MS (ESI) *m/z* (%):** 209 (100). **HRMS ESI *m/z*:** [$(C_{14}H_{13}N_2)^+$] calc.: 209.1073, found 209.1073.

6,6'-(ethyne-1,2-diyl)bis(1-(but-3-yn-1-yl)-2-methylpyridin-1-ium)trifluoromethane-sulfonate (9)

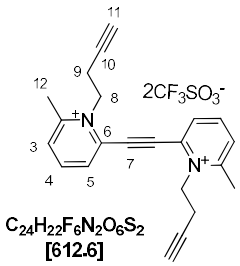

Synthesis of triyne **9** was accomplished by following the procedure *general procedure 5.2.b.* Triyne **9** was obtained as an off-white solid.

Yield: 2.4 g, 83%.

m.p. 176-178 °C. **^{1}H-NMR (600 MHz, acetonitrile-d_3):** δ 2.46 (t, 2H, H-11), 2.98 (s, 6H, H-12), 3.04 (dt, *J* = 2.7, 7.0, 7.0 Hz, 4H, H-9), 4.99 (t, *J* = 7.0 Hz, 4H, H-8), 8.06 (dd, *J* = 1.5, 8.1 Hz, 2H, H-5), 8.33(dd, *J* = 1.5, 7.9 Hz, 2H, H-3), 8.49 (t, *J* = 8.0 Hz, 2H, H-4). **^{13}C-NMR (151 MHz, acetonitrile-d_3):** 19.5 (C-9), 22.4 (C-12), 55.5 (C-8), 75.0 (C-11), 79.1 (C-10), 92.8 (C-7), 133.4 (C-5), 133.6 (C-3), 136.4 (C-6), 146.4 (C-4), 160.5 (C-2). **IR (KBr):** *v* (cm^{-1}) 632, 1025, 1128, 1157, 1195, 1220, 1252, 1272, 1282, 1435, 1468, 1526, 1574, 1629, 3069, 3099, 3251. **MS (ESI) *m/z* (%):** 261.2 (44), 313.2 (100), 314.2 (28), 345.3 (15), 463.2 (12). **HRMS ESI *m/z*:** calc. for [$(M - 2CF_3SO_3^-)^{+2}$] [$(C_{22}H_{22}N_2)^{+2}$] 157.0886, found 157.0886.

4,13-dimethyl-6,7,10,11-tetrahydrodipyrido[2,1-a:1',2'-k][2,9]phenanthroline-5,12-diium trifluoromethanesulfonate (10)

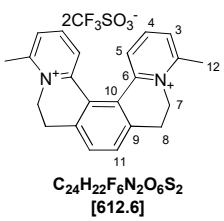

Synthesis of [5]helquat **10** was accomplished by following the *general procedure* 5.2.c. [5]helquat **10** was obtained as an off-white amorphous solid.**Yield:** 0.73 g, 73%.
m.p. 248-252 °C. **^{1}H-NMR (600 MHz, acetonitrile-d_3):** δ 2.93 (bs, 6H, H-12), 3.13-3.23 (m, 2H, H-8a), 3.27-3.38 (m, 2H, H-8b), 4.33-4.45 (m, 2H, H-7a), 5.03-5.13 (m, 2H, H-7b), 7.69 (dd, *J* = 1.0, 8.1 Hz, 2H, H-5), 7.70 (s, 2H, H-11), 7.77 (dd, *J* = 1.0, 7.9 Hz, 2H, H-3), 7.99 (t, *J* = 8.0 Hz, 2H, H-4). **^{13}C-NMR (151 MHz, acetonitrile-d_3):** δ 22.1 (C-12), 28.0 (C-8), 50.2 (C-7), 128.1 (C-10), 129.5 (C-3), 129.8 (C-5), 132.8 (C-11), 141.6 (C-9), 144.5 (C-4), 148.5 (C-6), 157.3 (C-2). **IR (KBr):** ν (cm^{-1}) 642, 831, 866, 1026, 1035, 1152, 1227, 1262, 1458, 1515, 1571, 1633, 2869, 2935, 3043, 3097, 3159. **MS (ESI) *m/z* (%):** 157.1 (33), 313.2 [$(M - 2CF_3SO_3^-)^{2+}$] (100), 463.2 [$(M - CF_3SO_3^-)^+$] (71). **HRMS ESI *m/z*:** calc. for [$(M - 2CF_3SO_3^-)^{2+}$] [$(C_{22}H_{22}N_2)^{2+}$] 157.0885, found 157.0886.

2-methyl-6-(pyridin-2-ylethynyl)pyridine (12)

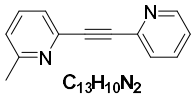

$C_{13}H_{10}N_2$
[194.2]

Synthesis of an internal alkyne **12** was accomplished by following *general procedure 5.2.a*. An internal alkyne **12** was obtained as a dark brown sticky solid.
Yield: 0.69 g, 74%.
m.p. 46-48 °C. **^{1}H-NMR (400 MHz, acetonitrile-d_3):** δ 2.52 (s, 3H), 7.24 (dd, *J* = 0.5, 7.8 Hz, 1H), 7.36 (dddd, *J* = 1.2, 7.8 Hz, 1H), 7.43 (dd, *J* = 0.5, 7.7 Hz, 1H), 7.61 (dt, *J* = 1.2, 7.8 Hz, 1H), 7.67 (t, *J* = 7.8 Hz, 1H), 7.79 (td, *J* = 1.8, 7.7 Hz, 1H), 8.61 (dt, *J* = 1.2, 5.0, 1H). **^{13}C-NMR (101 MHz, acetonitrile-d_3):** δ 24.6, 87.9, 88.6, 118.3, 124.7, 125.7, 128.6, 137.5, 137.7, 142.4, 143.4, 151.3, 160.3. **IR (KBr):** *v* (cm^{-1}) 572, 630, 737, 778, 791, 990, 1045, 1090, 1153, 1245, 1282, 1317, 1429, 1449, 1465, 1566, 1584, 2215, 2923, 3055. **MS (ESI) *m/z* (%):** 195.1 (100), 196.1 (13), 217.1 (8), 254.2 (5), 389.2 (20), 390.2 (6). **HRMS ESI *m/z*:** calc. for [$(C_{13}H_{11}N_2)^+$] 195.0917, found 195.0916.

1-(but-3-yn-1-yl)-2-((1-(but-3-yn-1-yl)pyridin-1-ium-2-yl)ethynyl)-6-methylpyridin-1-ium trifluoromethanesulfonate (13)

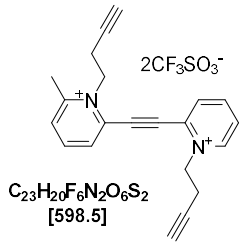

$C_{23}H_{20}F_6N_2O_6S_2$
[598.5]

Synthesis of triyne **13** was accomplished by following *general procedure 5.2.b*. Triyne **13** was obtained as an off-white amorphous powder.
Yield: 2.4 g, 83%.
m.p. 131-133 °C. **^{1}H-NMR (400 MHz, acetonitrile-d_3):** δ 2.46-2.49 (m, 2H), 2.98 (s, 3H), 3.02-3.07 (m, 4H), 4.96-5.02 (m, 4H), 8.08 (dd, *J* = 1.6, 8.0 Hz, 1H), 8.20 (dddd, *J* = 2.6, 6.2 Hz, 1H), 8.35 (dd, *J* = 1.3, 8.0 Hz, 1H), 8.49 (dd, *J* = 0.5, 8.0 Hz, 1H), 8.50 (t, *J* = 8.0 Hz, 1H), 8.70 (td, *J* = 1.4, 8.0 Hz, 1H), 8.97 (dd, J = 0.3, 6.2 Hz, 1H). **^{13}C-NMR (101 MHz, acetonitrile-d_3):** δ 19.4, 21.0, 22.3, 55.4, 59.9, 74.9, 75.3, 78.9, 79.1, 91.6, 93.4, 130.4, 133.4, 133.6, 135.2, 135.7, 136.1, 146.3, 147.5, 148.6, 160.5. **IR (KBr):** *v* (cm^{-1}) 518, 547, 573, 638, 732, 792, 814, 929, 1029, 1158, 1197, 1225, 1255, 1273, 1322, 1385, 1453, 1469, 1486, 1515, 1582, 1613, 2122, 3065, 3095, 3241, 3436. **MS (ESI) *m/z* (%):** 274.2 (32), 299.2 (50), 300.2 (22), 449.2 [(M −

$CF_3SO_3^-)^+$] (100), 450.2 (47) 451.3 (10). **HRMS ESI *m/z*:** calc. for [(M − $CF_3SO_3^-)^+$] [$(C_{22}H_{20}O_3N_2F_3S)^+$] 449.1141, found 449.1141.

4-methyl-6,7,10,11-tetrahydrodipyrido[2,1-a:1',2'-k][2,9]phenanthroline-5,12-diium trifluoromethanesulfonate (14)

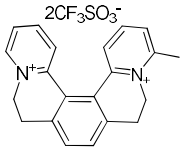

$C_{23}H_{20}F_6N_2O_6S_2$
[598.5]

Synthesis of [5]helquat **14** was accomplished by following *general procedure 5.2.c.* [5]helquat **14** was obtained as an off-white amorphous powder.

Yield: 0.83 g, 83%.

m.p. 227-229 °C. **^{1}H-NMR (400 MHz, acetonitrile-d_3):** δ 3.01 (s, 3H), 3.28-3.45 (m, 4H), 5.01-5.17 (m, 2H), 5.14-5.35 (m, 2H), 7.76 (s, 2H), 7.91 (dd, *J* = 1.4, 7.8 Hz, 1H), 7.97 (dddd, J = 1.6, 6 Hz, 1H), 8,08 (t, *J* = 7.9 Hz, 1H), 8.15 (dd, *J* = 1.3, 8.2 Hz, 1H), 8.21 (dddd, *J* = 1.6, 8.3 Hz, 1H), 8.26 (dd, *J* = 1.5, 8.3 Hz, 1H), 9.11 (dd, *J* = 0.6, 6.0 Hz, 1H). **^{13}C-NMR (101 MHz, acetonitrile-d_3):** δ 21.0, 26.9, 27.1, 49.1, 55.1, 119.5, 122.7, 126.2, 126.5, 127.0, 128.9, 130.2, 132.2, 140.6, 140.7, 143.6, 144.8, 145.7, 147.0, 147.1, 156.5. **IR (KBr):** ν (cm^{-1}) 517, 573, 632, 794, 863, 1027, 1140, 1249, 1266, 1277, 1495, 1509, 1620, 1675, 3012. **MS (ESI) *m/z* (%):** 150.1 (100), 150.6 (24), 166.1 (19), 239.1 (6), 299.2 (14), 331.2 (5), 449.1 (9). **HRMS ESI *m/z*:** calc. for [(M − $CF_3SO_3^-)^+$] [$(C_{22}H_{20}O_3N_2F_3S)^+$] 449.1141, found 449.1141.

2-methyl-1-(pent-3-yn-1-yl)-6-((1-(pent-3-yn-1-yl)pyridin-1-ium-2-yl)ethynyl)pyridin-1-ium trifluoromethanesulfonate (15)

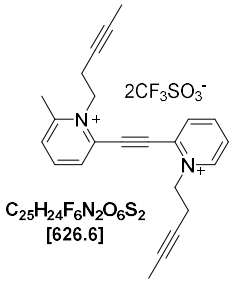

$C_{25}H_{24}F_6N_2O_6S_2$
[626.6]

Synthesis of triyne **15** was accomplished by following the *general procedure 5.2.b.* Triyne **15** was obtained as an off-white amorphous solid.

Yield: 1.3 g, 81%.

m.p. 139-141 °C. **^{1}H-NMR (400 MHz, acetonitrile-d_3):** δ 1.69 (t, *J* = 2.6 Hz, 3H), 1.71 (t, *J* = 2.6 Hz, 3H), 2.94-2.97 (m, 4H), 2.98 (s, 3H), 4.91 (t, *J* = 6.4 Hz, 2H), 4.94 (t, *J* = 6.4 Hz, 2H), 8.07 (dd, *J* = 1.6, 8.1 Hz, 1H), 8.21 (ddd, *J* = 1.5, 6.2, 7.8 Hz, 1H), 8.34 (dd, *J* = 1.5, 7.9 Hz, 1H), 8.45 (dd, *J* = 1.5, 6.6 Hz, 1H), 8.48 (t, *J* = 8.0 Hz, 1H), 8.67 (td, *J* = 1.4, 8.0 Hz, 1H), 8.94 (ddd, *J* = 0.5, 1.5, 6.1 Hz, 1H). **^{13}C-NMR (101 MHz, acetonitrile-d_3):** δ 3.3, 19.8, 21.5, 22.2, 22.2, 56.0, 60.5, 73.6, 73.9, 82.2, 82.8, 91.4, 93.2, 120.5, 123.7, 130.3, 133.3, 133.5, 135.1, 146.2, 147.4, 148.5, 160.4. **IR (KBr):** *v* (cm^{-1}) 518, 575, 640, 758, 1015, 1032, 1168, 1198, 1226, 1262, 1487, 1514, 1579, 1616, 2222, 2238, 3085. **MS (ESI) *m/z* (%):** 261.2 (10), 304.3 (8), 359.2 (22), 477.2 (13), 509.2 (100), 510.2 (27), 511.2 (11). **HRMS ESI *m/z*:** calc. for [(M – $2CF_3SO_3^-)^{2+}$]] [$(C_{23}H_{24}N_2)^{2+}$] 164.0964, found 164.0964.

4,8,9-trimethyl-6,7,10,11-tetrahydrodipyrido[2,1-a:1',2'-k][2,9]phenanthroline-5,12-diium trifluoromethanesulfonate (16)

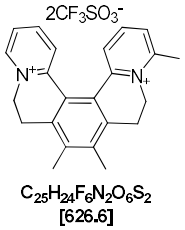

Synthesis of [5]helquat **16** was accomplished by following *general procedure 5.2.c.* [5]helquat **16** was obtained as an off-white amorphous solid.

Yield: 0.75 g, 73%.

m.p. 231-233 °C. **^{1}H-NMR (400 MHz, acetonitrile-d_3):** 2.52 (s, 6H), 3.10 (s, 3H), 3.22-3.39 (m, 2H), 3.61-3.72 (m, 2H), 4.69 (t, *J* = 14.1 Hz, 1H), 5.07 (t, *J* = 14.1 Hz, 1H), 5.28 (d, *J* = 13.2 Hz, 1H), 5.43 (d, *J* = 13.2 Hz, 1H), 7.93- 7.98 (m, 1H), 8.02 (td, *J* = 2.3, 6.4 Hz, 1H), 8.12 (s, 1H), 8.13 (d, *J* = 1.6 Hz, 1H), 8.22-8.29 (m, 2H), 9.17 (d, *J* = 6.1 Hz, 1H). **^{13}C-NMR (101 MHz, acetonitrile-d_3):** 16.8, 21.8, 21.8, 26.1, 26.3, 49.8, 55.6, 125.1, 125.9, 126.8, 129.2, 129.6, 131.5, 140.4, 140.4, 141.2, 141.2, 144.3, 145.4, 146.1, 148.8, 148.9, 156.8. **IR (KBr):** ν (cm^{-1}) 518, 574, 636, 755, 1030, 1165, 1225, 1259, 1282, 1400, 1495, 1509, 1560, 1584, 1625. **MS (ESI) *m/z* (%):** 164.1 [$(M - 2CF_3SO_3^-)^{2+}$] (100), 164.6 (25), 327.2 (4), 477.1 (3). **HRMS ESI *m/z*:** calc. for [$(M - 2CF_3SO_3^-)^{2+}$] [$(C_{23}H_{24}N_2)^{2+}$] 164.0964, found 164.0964.

(*E*)-11-(4-(dimethylamino)styryl)-6,7-dimethyl-4,5,8,9-tetrahydroisoquinolino[1,2-a]pyrido [1,2-k][2,9]phenanthroline-3,10-diium trifluoromethanesulfonate (20)

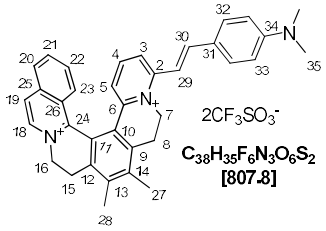

Synthesis and purification of [6]helquat dye **20** was accomplished by following *general procedure 5.2.e*, using helquat dye precursor **6** (70 mg, 0.103 mmol, 1.0 equiv.), 4-dimethylaminobenzaldehyde (48 mg, 0.322 mmol, 3.1 equiv.), pyrrolidine (100 μL, 87 mg, 1.223 mmol, 11.8 equiv.) in dry MeOH (7.0 mL) and dye **20** was obtained as a purple solid.

Yield: 0.056 g, 67%.

m.p. >350 °C. **^{1}H-NMR (600 MHz, acetone-d_6):** δ 2.66 (s, 3H, H-27), 2.66 (s, 3H, H-28), 3.15 (s, 6H, H-35), 3.34 (bddd, *J* = 4.2, 14.4, 17.3 Hz, 1H, H-8a), 3.48 (bdt, *J* = 4.0, 16.2, 16.2 Hz, 1H, H-15a), 3.82 (bdt, *J* = 3.7, 16.8, 16.8 Hz, 1H, H-8b), 3.82 (bdt, *J* = 3.5, 16.8, 16.8 Hz, 1H, H-15b), 5.12 (bdt, *J* = 3.7, 14.2, 14.2 Hz, 1H, H-7a), 5.17 (bdt, *J* = 3.5, 14.7, 14.7 Hz, 1H, H-16a), 5.40 (bdd, *J* = 4.0, 13.5 Hz, 1H, H-16b), 5.68 (bddd, *J* = 1.6, 4.2, 13.3 Hz, 1H, H-7b), 6.87- 6.90 (m, 2H, H-33), 7.3 (d, *J* = 8.0 Hz, 1H, H-5), 7.63 (t, *J* = 8.1 Hz, 1H, H-4), 7.68 (d, *J* = 15.6 Hz, 1H, H-29), 7.77-7.80 (m, 2H, H-32), 7.82 (d, *J* = 15.6 Hz, 1H, H-30), 7.84 (ddd, *J* = 1.2, 7.0, 8.5 Hz, 1H, H-22), 7.99 (bdd, *J* = 7.0, 8.2 Hz, 1H, H-21), 8.07 (bd, *J* = 8.2 Hz, 1H, H-3), 8.13 (d, *J* = 8.5 Hz, 1H, H-23), 8.29 (bd, *J* = 8.2 Hz, 1H, H-20), 8.55 (bd, *J* = 6.7 Hz, 1H, H-19), 9.04 (bd, *J* = 6.7 Hz, 1H, H-18). **^{13}C-NMR (151 MHz, acetone-d_6)**: δ 16.8 (C-28), 16.9 (C-27), 26.2 (C-8), 26.8 (C-15), 40.1 (C-35), 49.9 (C-7), 56.2 (C-16), 111.9 (C-29), 112.8 (C-33), 123.4 (C-31), 123.6 (C-13), 124.3 (C-3), 125.7 (C-19), 126.9 (C-26), 127.6 (C-5), 128.8 (C-23), 129.1 (C-20),129.2 (C-14), 131.8 (C-32), 132.6 (C-22), 136.1 (C-21), 137.4 (C-18), 138.6 (C-10), 139.8 (C-25), 140.5(C-9), 141.7 (C-12), 142.3 (C-11), 142.5 (C-4), 146.5 (C-30), 147.6 (C-6), 151.9 (C-24),

153.7 (C-34), 155.9 (C-2). **IR (KBr):** *v* (cm^{-1}) 517, 573, 638, 1030, 1164, 1269, 1530, 1555, 1591, 3076. **MS (ESI) *m/z* (%):** 194.0 (7), 247.6 (8), 254.6 (100), 255.1 (20), 375.2 (3), 508.3 (10), 658.2 [(M − $CF_3SO_3^-$)$^+$] (5). **HRMS ESI *m/z*:** calcd for [(M − $CF_3SO_3^-$)$^+$] [($C_{37}H_{35}O_3N_3F_3S$)$^+$] 658.2346, found 658.2344.

11-((1*E*,3*E*)-4-(4-(dimethylamino)phenyl)buta-1,3-dien-1-yl)-6,7-dimethyl-4,5,8,9-tetrahydro isoquinolino[1,2-a]pyrido[1,2-k][2,9]phenanthroline-3,10-diium trifluoromethanesulfonate (21)

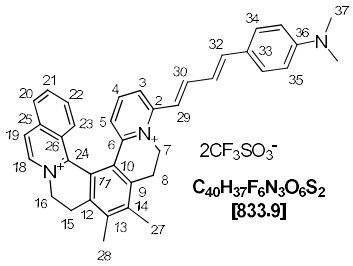

Synthesis and purification of [6]helquat dye **21** was accomplished by following *general procedure 5.2.e*, using helquat dye precursor **6** (100 mg, 0.148 mmol, 1.0 equiv.), (*E*)-3-(4-(dimethylamino)phenyl)acrylaldehyde (80 mg, 0.457 mmol, 3.1 equiv.), pyrrolidine (143 μL, 124 mg, 1.746 mmol, 11.8 equiv.) in dry MeOH (10.0 mL) and dye **21** was obtained as a purple solid.

Yield: 0.072 g, 58%.

m.p. >350 °C. **^{1}H-NMR (600 MHz, acetone-d_6):** *δ* 2.66 (s, 3H, H-27), 2.67 (s, 3H, H-28), 3.10 (s, 6H, H-37), 3.35 (bddd, *J* = 4.8, 14.8, 17.4 Hz, 1H, H-8a), 3.49 (ddd, *J* = 4.5, 14.8, 17.2 Hz, 1H, H-15a), 3.82 (ddd, *J* = 1.8, 3.7, 17.2 Hz, 1H, H-15b), 3.86 (ddd, *J* = 2.0, 3.7, 17.4 Hz, 1H, H-8b), 5.07 (dt, *J* = 3.7, 14.5, 14.5 Hz, 1H, H-7a), 5.18 (bdt, *J* = 3.7, 14.4, 14.4 Hz, 1H, H-16a), 5.40 (ddd, *J* = 1.8, 4.5, 14.0 Hz, 1H, H-16b), 5.60 (ddd, *J* = 2.0, 4.8, 13.7 Hz, 1H, H-7b), 6.81-6.84 (m, 2H, H-35), 7.16 (d, *J* = 15.3 Hz, 1H, H-32), 7.21 (dd, *J* = 10.0, 15.3 Hz, 1H, H-31), 7.30 (dd, *J* = 1.3, 8.0 Hz, 1H, H-5), 7.34 (d, *J* = 14.9 Hz, 1H, H-29), 7.52-7.55 (m, 2H, H-34), 7.64 (t, *J* = 8.1 Hz, 1H, H-4), 7.75 (dd, *J* = 10.0, 14.9 Hz, 1H, H-30), 7.81 (ddd, *J* = 1.2, 6.9, 8.8 Hz, 1H, H-22), 8.01 (ddd, *J* = 1.1, 6.9, 8.1 Hz, 1H, H-21), 8.04 (dd, *J* = 1.3, 8.2 Hz, 1H, H-3), 8.14 (dq, *J* = 0.9, 0.9, 0.9, 8.8 Hz, 1H, H-23), 8.29 (bd, *J* = 8.1 Hz, 1H, H-20), 8.55 (bd, *J* = 6.7 Hz, 1H, H-19), 9.03 (d, *J* = 6.7 Hz, 1H, H-18). **^{13}C-NMR (151 MHz, acetone-d_6):** δ 16.9 (C-27), 16.8 (C-28), 26.2 (C-8), 26.9 (C-15), 40.2 (C-37), 49.8 (C-7), 56.3 (C-16), 113.0 (C-35), 117.6 (C-29), 123.6 (C-31), 123.7 (C-13), 124.4 (C-3), 124.7 (C-33), 125.8 (C-19), 127.0 (C-26), 128.0 (C-5), 128.9 (C-23), 129.2 (C-20), 129.2 (C-14), 130.4 (C-34), 132.5 (C-22), 136.2 (C-21), 137.5 (C-18), 138.6 (C-10), 140.0 (C-25), 140.7 (C-9), 141.9 (C-12), 142. 5 (C-11), 147.6 (C-30), 142.7 (C-4), 145.1 (C-32), 147.9 (C-6), 152.0 (C-24), 152.9 (C-36), 155.3 (C-2). **IR (KBr):** ν (cm^{-1}) 518, 573, 638, 1031, 1153, 1263, 1483, 1527, 1552, 1583, 1626, 3076. **MS (ESI) *m/z* (%):** 194.1 (21), 267.7 (100), 268.2 (43), 362.3 (8), 377.3 (10), 401.4 (17), 402.4 (12), 534.5 (40), 535.5 (13), 684.5 [(M − $CF_3SO_3^-$)$^+$] (7). **HRMS ESI *m/z*:** [(M − $CF_3SO_3^-$)$^+$] [($C_{39}H_{37}O_3N_3F_3S$)$^+$] calc. 684.25022, found 684.24999.

(*E*)-11-(2-(1,2,3,5,6,7-hexahydropyrido[3,2,1-ij]quinolin-9-yl)vinyl)-6,7-dimethyl-4,5,8,9-tetrahydroisoquinolino[1,2-a]pyrido[1,2-k][2,9]phenanthroline-3,10-diium trifluoromethane- sulfonate (22)

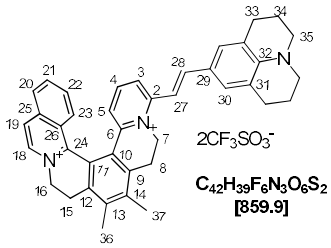

Synthesis and purification of [6]helquat dye **22** was accomplished by following *general procedure 5.2.e*, using helquat dye precursor **6** (70 mg, 0.103 mmol, 1.0 equiv.), 9-julolidinecarboxaldehyde (147 mg, 0.731 mmol, 7.1 equiv.), pyrrolidine (100 μL, 87 mg, 1.223 mmol, 11.8 equiv.) in dry MeOH (7.0 mL) and dye **22** was obtained as a purple solid.
Yield: 0.041 g, 46%.
m.p. >350 °C. **^{1}H-NMR (600 MHz, acetone-d_6):** δ 1.98-2.03 (m, 4H, H-34), 2.65 (s, 3H, H-36), 2.66 (s, 3H, H-37), 2.79-2.83 (m, 4H, H-33), 3.30 (bddd, *J* = 3.7, 14.2, 17.0 Hz, 1H, H-8a), 3.38-3.41 (m, 4H, H-35), 3.47 (bddd, *J* = 3.7, 14.5, 17.0 Hz, 1H, H-15a), 3.80 (ddd, *J* = 1.9, 4.7, 17.0 Hz, 1H, H-15b), 3.82 (ddd, *J* = 1.9, 4.9, 17.0 Hz, 1H, H-8b), 5.04 (dt, *J* = 3.7, 14.0, 14.0 Hz, 1H, H-7a), 5.16 (dt, *J* = 3.7, 14.3, 14.3 Hz, 1H, H-16a), 5.39 (ddd, *J* = 1.9, 4.7, 14.0 Hz, 1H, H-16b), 5.60 (ddd, *J* = 1.9, 4.9, 13.8 Hz, 1H, H-7b), 7.20 (dd, *J* = 1.2, 8.0 Hz, 1H, H-5), 7.34 (s, 2H, H-30), 7.55 (t, *J* = 8.1 Hz, 1H, H-4), 7.73 (d, *J* = 15.5 Hz, 1H, H-28), 7.82 (ddd, *J* = 1.2, 6.9, 8.8 Hz, 1H, H-22), 7.84 (d, *J* = 15.5 Hz, 1H, H-27), 7.98 (ddd, 1H, *J* = 1.1, 6.9, 8.1 Hz, 1H, H-21), 8.01 (dd, *J* = 1.2, 8.2 Hz, 1H, H-3), 8.11 (dq, *J* = 0.9, 0.9, 0.9, 8.8 Hz, 1H, H-23), 8.28 (bd, *J* = 8.1 Hz, 1H, H-20), 8.53 (bd, *J* = 6.8 Hz, 1H, H-19), 9.02 (d, *J* = 6.8 Hz, 1H, H-18). **^{13}C-NMR (151 MHz, acetone-d_6):** δ 16.7 (C-36), 16.9 (C-37), 22.1 (C-34), 26.2 (C-8), 26.8 (C-15), 28.3 (C-33), 49.6 (C-7),50.6 (C-35), 56.2 (C-16), 110.1 (C-27), 122.1 (C-31), 122.5 (C-29), 123.6 (C-13), 123.8 (C-3), 125.6 (C-19), 126.9 (C-5), 126.9 (C-26), 128.8 (C-23), 129.1 (C-20), 129.4 (C-14), 129.7 (C-30), 132.5 (C-22), 136.1 (C-21), 137.4 (C-18), 138.6 (C-9), 139.8 (C-25), 140.3 (C-12), 141.7 (C-10), 141.9 (C-4), 142.2 (C-11), 147.0 (C-32), 147.1 (C-28), 147.3 (C-6), 152.0 (C-24), 156.0 (C-2). **IR (KBr):** ν (cm^{-1}) 517, 573, 638, 1030, 1163, 1260, 1484, 1524, 1553, 1588, 1627, 3074. **MS (ESI) *m/z* (%):** 217.1 (4), 280.7 (100), 362.3 (7), 453.4 (10), 475.4 (6), 561.4 (7), 710.4 [(M − $CF_3SO_3^-$)$^+$] (14). **HRMS ESI *m/z*:** calc. for [(M − $CF_3SO_3^-$)$^+$] [($C_{41}H_{39}N_3O_3F_3S$)$^+$] 710.2659, found 710.2653.

(*E*)-11-(2-(6-(dimethylamino)naphthalen-2-yl)vinyl)-6,7-dimethyl-4,5,8,9-tetrahydroiso-quinoline[1,2-a]pyrido[1,2-k][2,9]phenanthroline-3,10-diium trifluoromethanesulfonate (23)

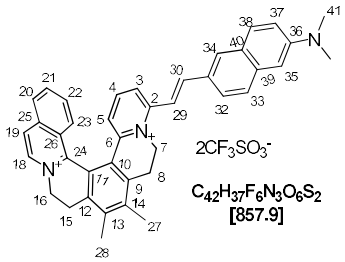

Synthesis and purification of [6]helquat dye **23** was accomplished by using helquat dye precursor **6** (75 mg, 0.111 mmol, 1.0 equiv.), 6-dimethylamino-2-naphthylaldehyde (66.3 mg, 0.333 mmol, 3.0 equiv.), pyrrolidine (108 μL, 93.2 mg, 1.310 mmol, 11.8 equiv.) in dry MeOH (7.5 mL) and dye **23** was obtained as a red solid.

Yield: 71 mg, 75%.

m.p. >350 °C. **^{1}H-NMR (600 MHz, acetonitrile-d_3):** δ 2.53 (s, 3H, H-27), 2.55 (s, 3H, H-28), 3.05 (bddd, *J* = 4.8, 14.3, 17.3 Hz, 1H, H-8a), 3.11 (s, 6H, H-41), 3.16 (bddd, *J* = 4.5, 15.1, 17.0 Hz, 1H, H-15a), 3.54 (ddd, *J* = 1.8, 3.5, 17.0 Hz, 1H, H-15b), 3.58 (bdt, *J* = 2.0, 3.8, 17.3 Hz, 1H, H-8b), 4.71 (dt, *J* = 3.8, 14.0, 14.0 Hz, 1H, H-7a), 4.79 (dt, *J* = 3.5, 14.5, 14.5 Hz, 1H, H-16a), 5.01 (ddd, *J* = 1.8, 4.5, 13.8 Hz, 1H, H-16b), 5.38 (ddd, *J* = 2.0, 4.8, 13.7 Hz, 1H, H-7b), 6.82 (dd, *J* = 1.3, 8.0 Hz, 1H, H-3), 7.01 (bd, *J* = 2.7 Hz, 1H, H-38), 7.28 (dd, *J* = 2.7, 9.0 Hz, 1H, H-37), 7.49 (t, *J* = 8.1 Hz, 1H, H-4), 7.58 (d, *J* = 15.8 Hz, 1H, H-29), 7.65 (ddd, *J* = 1.2, 6.9, 8.8 Hz, 1H, H-22), 7.74 (d, *J* = 15.8 Hz, 1H, H-30), 7.77 (d, *J* = 8.7 Hz, 1H, H-33), 7.80 (dq, *J* = 1.0, 8.8 Hz, 1H, H-23), 7.82 (bd, *J* = 9.0 Hz, 1H, H-35), 7.83 (dd, *J* = 1.3, 8.2 Hz, 1H, H-5), 7.86 (dd, *J* = 1.9, 8.7 Hz, 1H, H-32), 7.88 (ddd, *J* =1.1, 6.9, 8.1 Hz, 1H, H-21), 8.02 (bd, *J* = 1.9 Hz, 1H, H-34), 8.12 (bdt, *J* = 0.8, 0.8, 1.2, 8.1 Hz, 1H, H-20), 8.30 (bd, *J* = 6.8 Hz, 1H, H-19), 8.60 (d, *J* = 6.8 Hz, 1H, H-18). **^{13}C-NMR (151 MHz, acetonitrile-d_3):** δ 17.1 (C-27), 17.2 (C-28), 26.1 (C-8), 26.8 (C-15), 40.7 (C-41), 50.3 (C-7), 56.1 (C-16), 106.6 (C-38), 106.6 (C-39), 115.6 (C-29), 117.7 (C-36), 123.5 (C-13), 125.0 (C-32), 125.2 (C-5), 125.3 (C-20), 126.0 (C-19), 127.1 (C-26), 128.1 (C-33),128.3 (C-14), 128.3 (C-3), 128.6 (C-23), 129.1 (C-31), 131.0 (C-35), 132.4 (C-34), 132.8 (C-22), 136.5 (C-21), 137.0 (C-18), 137.9 (C-40), 138.7 (C-10), 140.0 (C-25), 141.1 (C-11), 142.3 (C-9), 142.4 (C-12), 143.1 (C-4), 146.3 (C-30), 148.1 (C-6), 151.4 (C-37), 151.9 (C-24), 155.5 (C-2). **IR (KBr):** ν (cm^{-1}) 518, 573, 639, 1031, 1154, 1263, 1484, 1508, 1560, 1599, 1622, 3081. **MS (ESI) *m/z* (%):** 194.2 (7), 279.7 (100), 280.2 (48), 375.3 (7), 558.5 (50), 559.5 [(M − $2CF_3SO_3^-$)$^{2+}$] (25), 708.5 [(M − $CF_3SO_3^-$)$^+$] (68). **HRMS ESI *m/z*:** calc. for [(M − $CF_3SO_3^-$)$^+$] [($C_{41}H_{37}O_3N_3F_3S$)$^+$] 708.2502, found 708.2505.

11-((*1E*,*3E*)-4-(1,2,3,5,6,7-hexahydropyrido[3,2,1-ij]quinolin-9-yl)buta-1,3-dien-1-yl)-6,7-dimethyl-4,5,8,9-tetrahydroisoquinolino[1,2-a]pyrido[1,2-k][2,9]phenanthroline-3,10-diium trifluoromethanesulfonate (24)

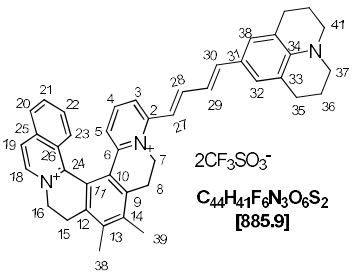

Synthesis ans purification of [6]helquat dye **24** was accomplished by following *general procedure 5.2.e*, using helquat dye precursor **6** (70 mg, 0.103 mmol, 1.0 equiv.), (*E*)-3-(1,2,3,5,6,7-hexahydropyrido[3,2,1-ij]quinolin-9-yl)acrylaldehyde (70.5 mg, 0.310 mmol, 3.0 equiv.), pyrrolidine (100 µL, 86.6 mg, 1.218 mmol, 11.8 equiv.) in dry MeOH (7.0 mL) and [6]helquat dye **24** was obtained as a blue solid.

Yield: 37.6 mg, 41%.

m.p. >350 °C. **^{1}H-NMR (600 MHz, acetone-d_6):** δ 1.96-2.01 (m, 4H, H-36), 2.65 (s, 3H, H-38), 2.66 (s, 3H, H-39), 2.77 (bt, *J* = 6.4 Hz, 4H, H-35), 3.32-3.35 (m, 4H, H-37), 3.33 (ddd, *J* = 4.8, 14.5, 17.2 Hz, 1H, H-8a), 3.47 (bddd, *J* = 4.6, 14.2, 17.0 Hz, 1H, H-15a), 3.80 (ddd, *J* = 1.8, 3.5, 17.0 Hz, 1H, H-15b), 3.84 (ddd, *J* = 1.9, 3.5, 17.2 Hz, 1H, H-8b), 5.04 (bdt, *J* = 3.5, 14.2, 14.2 Hz, 1H, H-7a), 5.16 (bdt, *J* = 3.5, 14.0, 14.0 Hz, 1H, H-16a), 5.39 (ddd, *J* = 1.8, 4.6, 13.8 Hz, 1H, H-16b), 5.55 (bddd, *J* = 1.9, 4.8, 13.9 Hz, 1H, H-7b), 7.05 (bd, *J* = 15.1 Hz, 1H, H-30), 7.08 (bd, *J* = 0.6 Hz, 2H, H-32), 7.14 (ddd, *J* = 0.7, 10.7, 15.1 Hz, 1H, H-29), 7.26 (dd, *J* = 1.3, 7.9 Hz, 1H, H-5), 7.26 (bd, *J* = 14.8 Hz, 1H, H-27), 7.59 (t, *J* = 8.1 Hz, 1H, H-4), 7.74 (dd, *J* = 10.7, 14.8 Hz, 1H, H-28), 7.80 (ddd, *J* = 1.3, 7.0, 8.8 Hz, 1H, H-22), 8.00 (ddd, *J* = 1.1, 7.0, 8.1 Hz, 1H, H-21),

8.01 (dd, *J* = 1.3, 8.4 Hz, 1H, H-3), 8.29 (ddt, *J* = 0.7, 0.7, 1.3, 8.1 Hz, 1H, H-20), 8.29 (dq, *J* = 0.9, 0.9, 0.9, 8.8 Hz, 1H, H-23), 8.54 (dd, *J* = 0.9, 6.7 Hz, 1H, H-19), 9.03 (d, *J* = 6.7 Hz, 1H, H-18). **^{13}C-NMR (151 MHz, acetone-d_6):** *δ* 16.8 (C-38), 16.9 (C-39), 22.3 (C-36), 26.1 (C-8), 26.8 (C-15), 28.3 (C-35), 49.5 (C-7), 50.5 (C-37), 56.2 (C-16), 116.4 (C-27), 121.3 (C-31), 122.1 (C-33), 122.6 (C-30), 123.6 (C-13), 124.1 (C-3), 127.5 (C-5), 125.7 (C-19), 126.9 (C-26), 128.2 (C-32), 128.8 (C-23), 129.1 (C-20), 129.2 (C-14), 132.5 (C-22), 136.1 (C-21), 137.4 (C-18), 138.5 (C-9), 139.8 (C-25), 140.4 (C-12), 141.7 (C-10), 142.2 (C-11), 142.3 (C-4), 145.9 (C-29), 145.9 (C-34), 147.6 (C-6), 147.9 (C-28), 151.9 (C-24), 155.2 (C-2). **IR (KBr):** ν (cm^{-1}) 517, 573, 638, 1030, 1163, 1260, 1484, 1524, 1553, 1588, 1627, 3074. **MS (ESI) *m/z* (%):** 186.2 (8), 194.1 (22), 279.7 (22), 293.7 (100), 294.2 (50), 401.2 (11), 586.4 (42), 736.3 [(M − $CF_3SO_3^-$)$^+$] (43). **HRMS ESI *m/z*:** calc. for [(M − $CF_3SO_3^-$)$^+$] ($C_{43}H_{41}N_3O_3F_3S$) 736.2815, found 736.2653.

(*E*)-11-(ferrocene-2-yl) vinyl)-6,7-dimethyl-4,5,8,9-tetrahydroisoquinolino[2,1-*k*]pyrido [2,1-*a*][2,9] phenanthroline-3,10-diium trifluoromethanesulfonate (25)

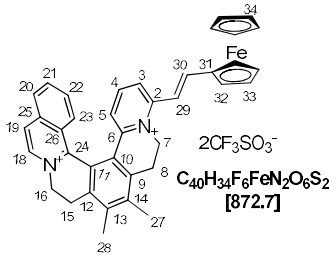

Synthesis and purification of [6]helquat dye **25** was accomplished by following *general procedure 5.2.e*, using helquat dye precursor **6** (75 mg, 0.111 mmol, 1.0 equiv.), ferrocenecarboxaldehyde (71.3 mg, 0.333 mmol, 3.0 equiv.), pyrrolidine (108 μL, 93.2 mg, 1.310 mmol, 11.8 equiv.) in dry MeOH (7.5 mL) and dye **25** was obtained as a blue solid.
Yield: 70.6 g, 73%.
m.p. >350 °C. **^{1}H-NMR (600 MHz, acetone-d_6):** *δ* 2.66 (s, 3H, H-27), 2.67 (s, 3H, H-28), 3.31-3.37 (m, 1H, 15a), 3.48 (bdt, *J* = 4.5, 15.9, 15.9 Hz, 1H, H-8a), 3.79-3.87 (m, 2H, H-8b and H-15b), 4.29 (s, 5H, H-34), 4.70 (bs, 2H, H-33), 4.92 (bs, 1H, H-32a), 4.96 (bs, 1H, H-32b), 5.12 (bdt, *J* = 3.3, 14.0, 14.0 Hz, 1H, H-7a), 5.18 (bdt, *J* = 3.5, 14.5, 14.5 Hz, 1H, H-16a), 5.39 (bdd, *J* = 4.0, 13.6 Hz, 1H, H-16b), 5.60 (bdd, *J* = 4.5, 13.7 Hz, 1H, H-7b), 7.36 (bd, *J* = 7.8 Hz, 1H, H-5), 7.54 (d, *J* = 15.4 Hz, 1H, H-29), 7.68 (bt, *J* = 7.9 Hz, 1H, H-4), 7.85 (d, *J* = 15.4 Hz, 1H, H-30), 7.86 (bt, *J* = 8.1 Hz, 1H, H-22), 8.01 (bt, *J* = 7.7 Hz, 1H, H-21), 8.07 (bd, *J* = 8.1 Hz, 1H, H-3), 8.12 (bd, *J* = 8.7 Hz, 1H, H-23), 8.29 (bd, *J* = 8.1 Hz, 1H, H-20), 8.54 (bd, *J* = 6.7 Hz, 1H, H-19), 9.02 (bd, *J* = 6.7 Hz, 1H, H-18). **^{13}C-NMR (151 MHz, acetone-d_6):** *δ* 16.8 (C-27), 16.9 (C-28), 26.1 (C-8), 26.9 (C-15), 50.2 (C-7), 56.3 (C-16), 70.1 (C-32a), 70.5 (C-32b), 70.9 (C-34), 73.0 (C-33), 80.6 (C-31), 114.7 (C-29), 123.7 (C-13), 124.8 (C-3), 125.8 (C-19), 127.0 (C-26), 128.1 (C-5), 128.9 (C-23), 129.1 (C-14), 129.2 (C-20), 132.6 (C-22), 136.1 (C-21), 137.5 (C-18), 138.7 (s, C-10), 140.0 (C-25), 140.7 (C-9), 141.8 (C-12), 142.5 (C-11), 143.1 (C-4), 147.9 (C-6), 148.1 (C-30), 151.9 (C-24), 155.3 (C-2). **IR (KBr):** *v* (cm^{-1}) 518, 573, 637, 1030, 1105, 1154, 1262, 1412, 1487, 1508, 1558, 1605, 1622, 3085. **MS (ESI) *m/z* (%):** 194.2 (12), 286.7 (17), 287.2 (100), 287.7 (47), 377.3 (17), 453.4 (15), 573.4 (40), 574.4 [(M – 2$CF_3SO_3^-$)$^{2+}$] (20), 723.5 [(M – $CF_3SO_3^-$)$^+$] (45). **HRMS ESI *m/z*:** calc. for [(M – $CF_3SO_3^-$)$^+$] [($C_{39}H_{34}O_3N_2F_3FeS$)$^+$] 723.1586; found 723.1583.

(*E*)-11-(4-Methoxystyryl)-6,7-dimethyl-4,5,8,9-tetrahydroisoquinolino[1,2-*a*]pyrido[1,2-*k*][2,9] phenanthroline-3,10-diium Trifluoromethanesulfonate (26)

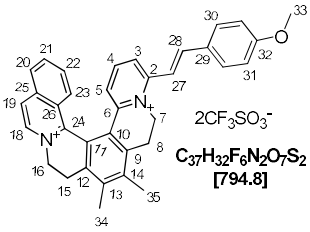

Synthesis and purification of [6]helquat dye **26** was accomplished by following *general procedure 5.2.e*, using [6]helquat dye precursor **6** (35 mg, 0.052 mmol, 1.0 equiv.), 4-methoxybenzaldehyde (354 mg, 2.6 mmol, 50.0 equiv.), pyrrolidine (53 μL, 45.9 mg, 0.645 mmol, 12.4 equiv.) in dry MeOH (3.5 mL) and [6]helquat dye **26** was obtained as a lemon yellow solid.

Yield: 28 mg, 68%.

m.p. > 350 °C. **^{1}H-NMR (600 MHz, acetone-d_6):** δ 2.66 (s, 3H, H-34), 2.66 (s, 3H, H-35), 3.38 (bddd, *J* = 4.7, 14.6, 16.8 Hz, 1H, H-8a), 3.50 (ddd, *J* = 4.6, 14.3, 16.8 Hz, 1H, H-15a), 3.84 (ddd, *J* = 1.9, 3.6, 16.8 Hz, 1H, H-8b), 3.84 (ddd, *J* = 1.9, 3.6, 16.8 Hz, 1H, H-15b), 3.94 (s, 3H, H-33), 5.18 (dt, *J* = 3.6, 14.3, 14.4 Hz, 1H, H-7a), 5.20 (dt, *J* = 3.6, 14.2, 14.2 Hz, 1H, H-16a), 5.41 (ddd, *J* = 1.9, 4.6, 14.1 Hz, 1H, H-16b), 5.74 (ddd, *J* = 1.9, 4.7, 13.7, 1H, H-7b), 7.11-7.17 (m, 2H, H-31), 7.44 (dd, *J* = 1.3, 8.0 Hz, 1H, H-5), 7.75 (t, *J* = 8.1 Hz, 1H, H-4), 7.83 (d, *J* = 15.9 Hz, 1H, H-28), 7.85 (ddd, *J* = 1.2, 6.9, 8.7 Hz, 1H, H-22), 7.88-7.91 (m, 2H, H-30), 7.90 (d, *J* = 15.9 Hz, 1H, H-27), 8.00 (ddd, *J* = 1.1, 6.9, 8.1 Hz, 1H, H-21), 8.11 (dd, *J* = 1.3, 8.2 Hz, 1H, H-3), 8.14 (dq, *J* = 0.9, 0.9, 0.9, 8.7 Hz, 1H, H-23), 8.30 (bddt, *J* = 0.7, 0.7, 1.2, 8.1 Hz, 1H, H-20), 8.57 (bd, *J* = 6.7 Hz, 1H, H-19), 9.05 (d, *J* =6.7 Hz, 1H, H-18). **^{13}C-NMR (151 MHz, acetone-d_6):** δ 16.8 (C-34), 16.9 (C-35), 26.0 (C-8), 26.7 (C-15), 50.4 (C-7), 55.9 (C-33), 56.1 (C-16), 115.4 (C-31), 116.1 (C-27), 123.7 (C-13), 125.2 (C-4), 125.8 (C-19), 126.9 (C-26), 128.6 (C-29), 128.7 (C-23), 128.8 (C-5), 128.9 (C-14), 129.1 (C-20), 131.5 (30), 132.7 (C-22), 136.1 (C-21), 137.5 (C-18), 138.7 (C10), 139.9 (C-25), 140.8 (C-9), 141.8 (C-12), 142.4 (C-11), 143.5 (C-4), 145.1 (C-28), 148.2 (C-6), 151.7 (C-24), 155.4 (C-3), 163.2 (C-32). **IR (KBr):** $\tilde{\nu}$ (cm^{-1}) 1029, 1155, 1175, 1256, 1271, 1441, 1599, 1625, 2851, 3074. **MS (ESI) *m/z* (%):** 248.1 [(M – 2 $CF_3SO_3^-$)$^{2+}$] (100), 495.2 [(M – 2$CF_3SO_3^-$)$^{2+}$] (5), 645.2 [(M – $CF_3SO_3^-$)$^+$] (5). **HRMS ESI *m/z*:** calc. for [(M – $CF_3SO_3^-$)$^+$] [($C_{36}H_{32}O_4N_2F_3S$)$^+$] 645.2029, found 645.2013.

(*E*)-11-(2-(6-Methoxynaphthalen-2-yl)vinyl)-6,7-dimethyl-4,5,8,9-tetrahydroisoquinolino-[1,2-*a*]pyrido[1,2-*k*][2,9]phenanthroline-3,10-diium Trifluoromethanesulfonate (27)

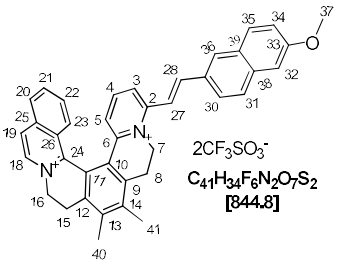

The synthesis and purification of [6]helquat dye **27** was accomplished by following *general procedure 5.2.e*, using helquat dye precursor **6** (75 mg, 0.111 mmol, 1.0 equiv.), 6-methoxy-2-naphthylaldehyde (146.7 mg, 0.788 mmol, 7.1 equiv.), pyrrolidine (108 μL, 93.5 mg, 1.315 mmol, 11.8 equiv.) in dry MeOH (7.0 mL) and [6]helquat dye **27** was obtained as a yellow amorphous solid.

Yield: 68.3 mg (73%).

m.p. > 350 °C. **^{1}H-NMR (600 MHz, acetonitrile-d_3):** δ 2.54 (s, 3H, H-40), 2.55 (s, 3H, H-41), 3.07 (ddd, *J* = 4.9, 14.8, 17.2 Hz, 1H, H-8a), 3.18 (ddd, *J* = 4.5, 14.8, 17.2 Hz, 1H, H-15a), 3.56 (ddd, *J* = 1.8, 3.6, 17.2 Hz, 1H, H-15b), 3.60 (ddd, *J* = 1.8, 3.8, 17.2 Hz, 1H, H-8b), 3.96 (s, 3H), 4.77 (dt, *J* = 3.8, 14.4, 14.4 Hz, 1H, H-7a), 4.84 (ddd, *J* = 3.6, 14.3, 14.3 Hz, 1H, H-16a), 5.04 (ddd, *J* = 1.8, 4.5, 13.8 Hz, 1H, H-16b), 5.41 (ddd, *J* = 1.8, 4.9, 14.0 Hz, 1H, H-7b), 6.92 (dd, *J* = 1.1, 8.0 Hz, 1H, H-5), 7.24 (dd, *J* = 2.6, 8.8 Hz, 1H, H-34), 7.35 (d, *J* = 2.6 Hz, 1H, H-32), 7.55 (t, *J* = 8.1 Hz, 1H, H-4), 7.68 (ddd, *J* = 1.2, 6.9, 8.7 Hz, 1H, H-22), 7.69 (d, *J* = 15.9 Hz, 1H, H-27), 7.74 (d, *J* = 15.9 Hz, 1H, H-28), 7.82 (dq, *J* =1.0, 1.0, 1.0, 8.7 Hz, 1H, H-23), 7.84 (dd, *J* = 1.1, 8.2 Hz, 1H, H-3), 7.88 (ddd, *J* =1.1, 6.9, 8.1 Hz, 1H, H-21), 7.90 (d, *J* = 8.8 Hz, 1H, H-35), 7.92 (d, *J* =8.6 Hz, 1H, H-31), 7.95 (dd, *J* = 1.8, 8.6 Hz, 1H, H-30), 8.12 (bd, *J* =8.1 Hz, 1H, H-20), 8.16 (d, *J* = 1.8 Hz, 1H, H-36), 8.30 (bd, *J* = 6.7 Hz, 1H, H-19), 8.62 (d, *J* = 6.7 Hz, 1H, H-18). **^{13}C-NMR (151 MHz, acetonitrile-d_3):** δ 16.0 (C-40), 16.1 (C-41), 25.0 (C-15), 25.8 (C-8), 49.6 (C-7), 55.1 (C-16), 55.3 (C-37), 106.6 (C-32), 116.6 (C-27), 119.6 (C-34), 122.6 (C-13), 124.4 (C-3), 124.6 (C-31), 124.9 (C-19), 126.0 (C-26), 127.5 (C-5), 127.7 (C-39), 127.8 (C-23), 128.2 (C-30), 128.7 (C-20), 130.3 (C-14), 130.4 (C-29), 130.4 (C-35), 130.4 (C-36), 131.8 (C-22), 135.5 (C-21), 136.0 (C-38), 136.3 (C-18), 137.6 (C-9), 139.0 (C-25), 140.2 (C-12), 141.4 (C-10), 141.4 (C-4), 142.6 (C-11), 144.7 (C-28), 147.3 (C-6), 150.8 (C-24), 154.2 (C-2), 159.6 (C-33). **IR (KBr):** $\tilde{\nu}$ (cm^{-1}) 518, 573, 638, 1031, 1154, 1266, 1482, 1506, 1562, 1608, 1623, 2841, 3077. **MS ESI *m/z* (%):** (15) 273.1 [(M – $CF_3SO_3^-$)$^+$] (100), 545.3 [(M – $2CF_3SO_3^-$)$^{2+}$] (25), 695.3 [(M – $CF_3SO_3^-$)$^+$]. **HRMS ESI *m/z*:** calc. for [(M – $CF_3SO_3^-$)$^+$] [($C_{40}H_{34}O_4N_2F_3S$)$^+$] 695.2186, found 695.2180.

11-((1*E*,3*E*)-4-(4-Methoxyphenyl)buta-1,3-dienyl)-6,7-dimethyl-4,5,8,9-tetrahydroisoquinolino[1,2-a]pyrido[1,2-k][2,9]phenanthroline-3,10-diium Trifluoromethanesulfonate (28)

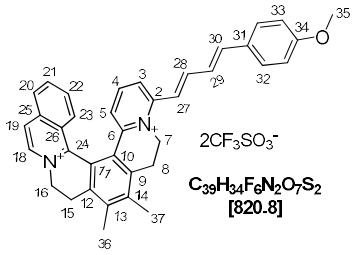

The synthesis and purification of [6]helquat dye **28** was accomplished by following the *general procedure 5.2.e*, using dye precursor **6** (100 mg, 0.148 mmol, 1.0 equiv.), 4-methoxycinnamaldehyde (170.5 mg, 1.051 mmol, 7.1 equiv.), pyrrolidine (143 μL, 124 mg, 1.744 mmol, 11.8 equiv.) in dry MeOH (10 mL) and [6]helquat dye **28** was obtained as an orange solid.

Yield: 77.6 mg (64%).

m.p. 167-169 °C. **^{1}H NMR (600 MHz, acetone-d_6):** δ 2.66 (s, 3H, H-27), 2.67 (s, 3H, H-28), 3.35 (bddd, *J* = 4.8, 14.8, 17.4 Hz, 1H, H-8a), 3.49 (ddd, *J* = 4.5, 14.8, 17.2 Hz, 1H, H-15a), 3.82 (ddd, *J* = 1.8, 3.7, 17.2 Hz, 1H, H-15b), 3.86 (ddd, *J* = 2.0, 3.7, 17.4 Hz, 1H, H-8b), 3.86 (s, 3H, H-37), 5.07 (dt, *J* = 3.7, 14.5, 14.5 Hz, 1H, H-7a), 5.18 (bdt, *J* = 3.7, 14.4, 14.4 Hz, 1H, H-16a), 5.40 (ddd, *J* = 1.8, 4.5, 14.0 Hz, 1H, H-16b), 5.60 (ddd, *J* = 2.0, 4.8, 13.7 Hz, 1H, H-7b), 6.81-6.84 (m, 2H, H-35), 7.16 (d, *J* = 15.3 Hz, 1H, H-32), 7.21 (dd, *J* = 10.0, 15.3 Hz, 1H, H-31), 7.30 (dd, *J* = 1.3, 8.0 Hz, 1H, H-5), 7.34 (d, *J* = 14.9 Hz, 1H, H-29), 7.52-7.55 (m, 2H, H-34), 7.66 (t, 1H, *J* = 8.1 Hz, 1H, H-4), 7.75 (dd, *J* = 10.0, 14.9 Hz, 1H, H-30), 7.81 (ddd, *J* = 1.2, 6.9, 8.8 Hz, 1H, H-22), 8.01 (ddd, *J* = 1.1, 6.9, 8.1 Hz, 1H, H-21), 8.04 (dd, *J* = 1.3, 8.2 Hz, 1H, H-3), 8.14 (dq, *J* = 0.9, 0.9, 0.9, 8.8 Hz, 1H, H-23), 8.29 (bd, *J* = 8.1 Hz, 1H, H-20), 8.55 (bd, *J* = 6.7 Hz, 1H, H-19), 9.03 (d, *J* = 6.7 Hz, 1H, H-18). **^{13}C NMR (151 MHz, acetone-d_6):** δ 16.8 (C-36), 16.9 (C-37), 26.0 (C-15), 26.8 (C-8), 50.1 (C-7), 55.8 (C-35), 56.2 (C-16), 115.4 (C-33), 120.1 (C-27), 123.7 (C-13), 124.8 (C-30), 125.7 (C-3), 126.4 (C-19), 126.9 (C-26), 128.7 (C-5), 128.7

(C-23), 129.0 (C-31), 129.1 (C-20), 129.7 (C-14), 130.1 (C-32), 132.6 (C-22), 136.1 (C-21), 137.5 (C-18), 138.6 (C-9), 139.9 (C-25), 140.7 (C-12), 141.8 (C-10), 142.4 (C-11), 143.0 (C-4), 143.2 (C-29), 146.4 (C-28), 148.1 (C-6), 151.7 (C-24), 154.8 (C-2), 162.1 (C-34). **IR (KBr):** $\tilde{\nu}$ (cm^{-1}) 517, 573, 638, 1030, 1155, 1259, 1485, 1577, 1589, 1626, 2483, 3074. **MS (ESI) *m/z* (%):** 261.1 [(M – $2CF_3SO_3^-$)$^{2+}$] (100), 521.2 [(M – $2CF_3SO_3^-$)$^{2+}$] (13), 671.2 [(M – $CF_3SO_3^-$)$^+$] (12). **HRMS ESI *m/z*:** calc. for [(M – $CF_3SO_3^-$)$^{2+}$] [($C_{38}H_{34}O_4N_2F_3S$)$^{2+}$] 671.2186, found 671.2183.

4,13-bis((*E*)-4-ethoxy-3-methoxystyryl)-6,7,10,11-tetrahydrodipyrido[2,1-a:1',2'-k][2,9] phenanthroline-5,12-diium trifluoromethanesulfonate (29)

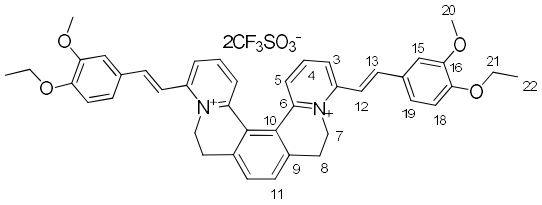

$C_{44}H_{42}F_6N_2O_{10}S_2$
[936.9]

The synthesis and purification of the [5]helquat dye **29** was accomplished by following *general procedure 5.2.e*, using helquat dye precursor **10** (50 mg, 0.082 mmol, 1.0 equiv.), 4-ethoxy-3-methoxybenzaldehyde (221.6 mg, 1.230 mmol, 15.0 equiv.), pyrrolidine (100 µL, 86.6 mg, 1.218 mmol, 14.9 equiv.) in dry MeOH (5.0 mL) and [5]helquat dye **29** was obtained as an orange solid.

Yield: 64.3 mg, 84%.

m.p. 263-265 °C. **^{1}H-NMR (600 MHz, DMSO-d_6):** δ 1.38 (t, *J* = 7.0 Hz, 6H, H-22), 3.23 (ddd, *J* = 4.5, 14.0, 17.1, 2H, H-8a), 3.36 (ddd, *J* = 2.0, 3.5, 17.1, 2H, H-8b), 3.90 (s, 6H, H-20), 4.12 (q, *J* = 7.0 Hz, 4H, H-21), 4.50 (dt, *J* = 3.5, 13.6, 13.6 Hz, 2H, H-7a), 5.40 (bdd, *J* = 2.0, 4.5, 13.4 Hz, 2H, H-7b), 7.11 (d, *J* = 8.0 Hz, 2H, H-19), 7.45 (dd, *J* = 2.1, 8.5 Hz, 2H, H-18), 7.55 (d, *J* = 2.1 Hz, 2H, H-15), 7.68 (d, *J* = 15.8 Hz, 2H, H-12), 7.79 (s, 2H), 7.85 (d, *J* = 15.8 Hz, 2H, H-13), 7.98 (dd, *J* = 1.3, 8.0 Hz, 2H, H-5), 8.15 (t, *J* = 7.9 Hz, 2H, H-4), 8.34 (dd, *J* = 1.3, 7.8 Hz, 2H, H-3). **^{13}C-NMR (151 MHz, DMSO-d_6):** δ 14.6 (C-22), 26.9 (C-8), 49.1 (C-7), 55.8 (C-20), 63.9 (C-21), 110.8 (C-15), 112.5 (C-19), 115.7 (C-12), 123.7 (C-18), 124.7 (C-3), 127.1 (C-10), 127.7 (C-14), 127.7 (C-5), 131.0 (C-11), 139.9 (C-9), 142.0 (C-4), 143.8 (C-13), 146.2 (C-6), 149.2 (C-16), 150.7 (C-17), 153.8 (C-2). **IR (KBr):** *v* (cm^{-1}) 637, 813, 822, 962, 1029, 1141, 1171, 1230, 1259, 1425, 1475, 1490, 1513, 1563, 1597, 1610, 1622, 2928, 2983, 3075. **MS (ESI) *m/z* (%):** 185.1 (23), 227.1 (91), 251.1 (17), 319.2 [(M – $2CF_3SO_3^-$)$^{2+}$] (100), 319.7 (45), 320.2 (10), 413.3 (5), 637.3 (5), 787.3 (3). **HRMS ESI *m/z*:** calc. for [(M – $2CF_3SO_3^-$)$^{2+}$] [($C_{42}H_{42}O_4N_2$)$^{2+}$] 319.1567, found 319.1566.

4,13-bis((*E*)-3-ethoxy-4-methoxystyryl)-6,7,10,11-tetrahydrodipyrido[2,1-a:1',2'-k][2,9] phenanthroline-5,12-diium trifluoromethanesulfonate (30)

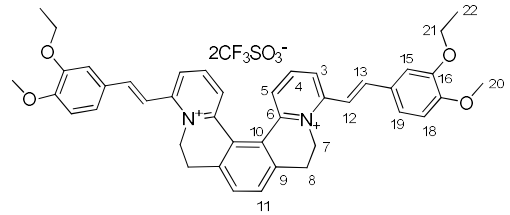

$C_{44}H_{42}F_6N_2O_{10}S_2$
[936.9]

The synthesis and purification of the [5]helquat dye **30** was accomplished by following *general procedure 5.2.e*, using helquat dye precursor **10** (50 mg, 0.082 mmol, 1.0 equiv.), 3-

ethoxy-4-methoxybenzaldehyde (221.6 mg, 1.230 mmol, 15.0 equiv.), pyrrolidine (100 µL, 86.6 mg, 1.218 mmol, 14.9 equiv.) in dry MeOH (5.0 mL) and [5]helquat dye **30** was obtained as an orange solid.

Yield: 65 mg, 85%.

m.p. 268-270 °C. **^{1}H-NMR (400 MHz, DMSO-d_6):** δ 1.40 (t, *J* = 7.0 Hz, 6H, H-22), 3.23 (ddd, *J* = 4.5, 14.0, 17.1 Hz, 2H, H-8a), 3.36 (ddd, *J* = 2.0, 3.5, 17.1, 2H, H-8b), 3.86 (s, 6H, H-20), 4.12 (q, *J* = 7.0 Hz, 4H, H-21), 4.50 (dt, *J* = 3.5, 13.6, 13.6 Hz, 2H, H-7a), 5.40 (bdd, *J* = 2.0, 4.5, 13.4 Hz, 2H, H-7b), 7.12 (d, *J* = 8.5 Hz, 2H, H-19), 7.45 (dd, *J* = 1.8, 7.4 Hz, 2H, H-18), 7.55 (d, *J* = 1.8 Hz, 2H, H-15), 7.68 (d, *J* = 15.8 Hz, 2H, H-12), 7.79 (s, 2H, H-11), 7.85 (d, *J* = 15.8 Hz, 2H, H-13), 7.98 (dd, *J* = 1.0, 8.0 Hz, 2H, H-5), 8.15 (t, *J* = 8.1 Hz, 2H, H-4), 8.34 (dd, *J* = 1.1, 8.4 Hz, 2H, H-3). **^{13}C-NMR (101 MHz, DMSO-d_6):** δ 14.7 (C-22), 26.9 (C-8), 49.2 (C-7), 55.7 (C-20), 64.1 (C-21), 111.7 (C-22), 111.8, 115.7 (C-12), 123.7 (C-18), 124.7 (C-3), 127.1 (C-10), 127.7 (C-13), 127.8 (C-14), 131.0 (C-11), 140.0 (C-9), 142.0 (C-4), 143.8 (C-13), 146.5 (C-6), 148.3 (C-16), 151.6 (C-17), 153.9 (C-3). IR (KBr): *v* (cm^{-1}) 639, 1031, 1261, 1490, 1513, 1562, 1596, 1610, 2929, 2979, 3403. **MS (ESI) *m/z* (%):** 305.1 (10), 319.2 [(M – $2CF_3SO_3^-$)$^{2+}$] (100), 319.7 (46), 320.2 (11), 637.3 (4), 787.3 (15), 788.3(10). **HRMS ESI *m/z*:** calc. for [(M – $2CF_3SO_3^-$)$^{2+}$] [($C_{42}H_{42}O_4N_2$)$^{2+}$] 319.1567, found 319.1567.

4,13-bis((*E*)-2,4,6-trimethoxystyryl)-6,7,10,11-tetrahydrodipyrido[2,1-a:1',2'-k][2,9] phenanthroline-5,12-diium trifluoromethanesulfonate (31)

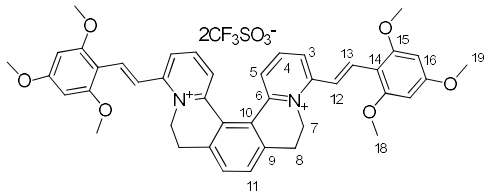

The synthesis and purification of the [5]helquat dye **31** was accomplished by following *general procedure 5.2.e*, using helquat dye precursor **10** (50 mg, 0.082 mmol, 1.0 equiv.), 2,4,6-trimethoxybenzaldehyde (241.3 mg, 1.230 mmol, 15.0 equiv.), pyrrolidine (100 µL, 86.6 mg, 1.218 mmol, 14.9 equiv.) in dry MeOH (5.0 mL) and [5]helquat dye **31** was obtained as a yellow solid.

Yield: 72.8 mg, 92%.

m.p. 314-316 °C. **^{1}H-NMR (600 MHz, DMSO-d_6):** 3.18 (ddd, *J* = 4.3, 14.0, 17.0 Hz, 2H, H-8a), 3.30 (ddd, *J* = 1.9, 3.4, 17.0 Hz, 2H, H-8b), 3.90 (s, 12H, H-18), 3.95 (s, 6H, H-19), 4.48 (dt, *J* = 3.4, 13.6 Hz, 2H, H-7a), 5.06 (ddd, *J* = 1.9, 4.3, 13.3 Hz, 2H, H-7b), 6.41 (s, 4H, H-16), 7.76 (s, 2H, H-11), 7.76 (d, *J* = 16.0 Hz, 2H, H-12), 7.83 (d, *J* = 16.0 Hz, 2H, H-13), 7.94 (dd, *J* = 1.4, 8.1 Hz, 2H, H-5), 8.08 (t, *J* = 8.1 Hz, 2H, H-4), 8.19 (dd, *J* = 1.4, 8.1 Hz, 2H). **^{13}C-NMR (151 MHz, DMSO-d_6):** 26.9 (C-8), 49.9 (C-7), 55.7 (C-19), 56.3 (C-18), 91.2 (C-16), 105.3 (C-14), 117.4 (C-12), 124.7 (C-3), 127.0 (C-5), 127.2 (C-10), 130.8 (C-11), 134.2 (C-13), 139.8 (C-9), 141.9 (C-4), 146.2 (C-6), 155.4 (C-2), 160.8 (C-15), 163.6 (C-17). **IR (KBr):** *v* (cm^{-1}) 637, 808, 1029, 1124, 1156, 1270, 1456, 1473, 1552, 1560, 1575, 1660, 3076. **MS (ESI) *m/z* (%):** 335.2 (100), 336.2 (13), 819.3 (20), 820.3 (10). **HRMS ESI *m/z*:** calc. for [(M – $2CF_3SO_3^-$)$^{2+}$] [($C_{42}H_{42}O_6N_2$)$^{2+}$] 335.1516, found 335.1517.

4,13-bis((*E*)-4-(3-(dimethylamino)propoxy)styryl)-6,7,10,11-tetrahydrodipyrido[2,1-a:1',2'-k][2,9]phenanthroline-5,12-diium trifluoromethanesulfonate (32)

$C_{48}H_{52}F_6N_4O_8S_2$
[991.1]

The synthesis and purification of the [5]helquat dye **32** was accomplished by following *general procedure 5.2.e*, using helquat dye precursor **10** (50 mg, 0.082 mmol, 1.0 equiv.), 4-(3-(dimethylamino)propoxy)benzaldehyde (255 mg, 1.230 mmol, 15.0 equiv.), pyrrolidine (100 µL, 86.6 g, 1.218 mmol, 14.9 equiv.) in dry MeOH (5.0 mL) and [5]helquat dye **32** was obtained as a yellow solid.

Yield: 76 mg, 94%.

m.p. 315-317 °C. **^{1}H-NMR (acetontrile-d_3, 400 MHz):** 1.89-1.98 (m, 4H), 2.20 (s, 12H), 2.41 (t, *J* = 7.0 Hz, 4H), 3.12-3.34 (m, 4H), 4.12 (t, *J* = 6.4 Hz, 4H), 4.41-4.50 (m, 2H), 5.21-5.26 (m, 2H), 7.06 (dd, *J* = 2.0, 6.8 Hz, 4H), 7.43 (d, *J* = 15.9 Hz, 2H), 7.65 (d, *J* = 15.8 Hz, 2H), 7.67 (dd, *J* = 7.6, 6.2 Hz, 2H), 7.70 (s, 2H), 7.78 (dd, *J* = 2.0, 6.8 Hz, 4H), 8.01 (t, *J* = 8.1 Hz, 2H), 8.11 (dd, *J* = 8.3, 1.4 Hz, 2H). **^{13}C-NMR (acetontrile-d_3, 101 MHz):** 28.1, 28.1, 45.7, 50.6, 56.7, 67.5, 116.2, 116.2, 126.3, 128.1, 128.4, 129.1, 131.4, 132.5, 141.2, 143.6, 144.9, 147.8, 156.0, 162.7. **IR (KBr):** *v* (cm^{-1}) 637, 813, 822, 962, 1029, 1141, 1171, 1230, 1259, 1425, 1475, 1490, 1513, 1563, 1597, 1610, 1622, 2928, 2983, 3075. **MS (ESI) *m/z* (%):** 281.5 (7), 303.7 (57), 346.2 (100), 346.7 (49), 347.2 (13), 521.2 (40), 522.2 (15), 606.3 (18), 607.3 (7), 692.4 (5), 841.4 (6). **HRMS ESI *m/z*:** calc. for $[(M - 2CF_3SO_3^-)^{2+}]$ $[(C_{46}H_{52}O_2N_4)^{2+}]$ 346.2040, found 346.2035.

4,13-bis((E)-3,4-dimethoxystyryl)-6,7,10,11-tetrahydrodipyrido[2,1-a:1',2'-k][2,9]phenanthroline-5,12-diium trifluoromethanesulfonate (33)

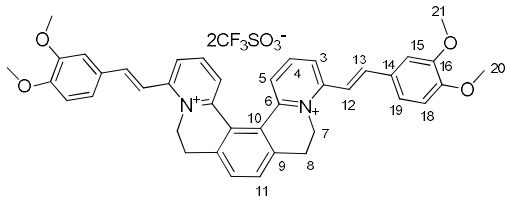

$C_{42}H_{38}F_6N_2O_{10}S_2$
[908.9]

The synthesis and purification of the [5]helquat dye **33** was accomplished by following *general procedure 5.2.e*, using helquat dye precursor **10** (50 mg, 0.082 mmol, 1.0 equiv.), 3,4-dimethoxybenzaldehyde (204.4 mg, 1.230 mmol, 15.0 equiv.), pyrrolidine (100 µL, 86.6 mg, 1.218 mmol, 14.9 equiv.) in dry MeOH (5.0 mL) and [5]helquat dye **33** was obtained as a yellow solid.

Yield: 69.7 mg, 94%.

m.p. 264-266 °C. **^{1}H-NMR (400 MHz, DMSO-d_6):** δ 3.23 (ddd, *J* = 4.5, 14.0, 17.1 Hz, 2H, H-8a), 3.36 (ddd, *J* = 2.0, 3.5, 17.1 Hz, 2H, H-8b), 3.86 (s, 6H, H-20), 3.90 (s, 6H, H-21), 4.50 (dt, *J* = 3.5, 13.6, 13.6 Hz, 2H, H-7a), 5.40 (bdd, *J* = 2.0, 4.5, 13.4 Hz, 2H, H-7b), 7.12 (d, *J* = 8.5 Hz, 2H, H-19), 7.46 (dd, *J* = 1.9, 8.5 Hz, 2H, H-18), 7.56 (d, *J* = 1.9 Hz, 2H, H-15), 7.70 (d, *J* = 15.8 Hz, 2H, H-12), 7.79 (s, 2H, H-11), 7.86 (d, *J* = 15.8 Hz, 2H, H-13), 7.99 (td, *J* = 0.3, 8.1 Hz, 2H, H-5), 8.15 (t, *J* = 8.1 Hz, 2H, H-4), 8.34 (dd, *J* = 1.3, 8.1 Hz, 2H, H-3). **^{13}C-NMR (101 MHz, DMSO-d_6):** δ 26.2 (C-8), 49.2 (C-7), 55.7 (C-20), 55.9 (C-21), 110.7 (C-15), 111.7 (C-19), 115.8 (C-12), 123.7 (C-18), 124.7 (C-3), 127.1 (C-10), 127.7 (C-14), 127.8 (C-5), 131.1 (C-11), 140.0

(C-9), 142.0 (C-4), 143.8 (C-13), 146.5 (C-6), 149.1 (C-16), 151.5 (C-17), 153.9 (C-2). **IR (KBr):** *v* (cm^{-1}) 639, 1031, 1143, 1262, 1424, 1473, 1491, 1514, 1563, 1623, 2840, 3076, 3434. **MS (ESI) *m/z* (%):** 231.2 (22), 305.2 [$(M - 2CF_3SO_3^-)^{2+}$] (100), 305.8 (58), 306.3, 461.4 (29), 462.4 (12), 609.5 (19), 611.5 (21), 612.5 (9), 723.6 (21), 759.5 (74), 760.6 (35). **HRMS ESI *m/z*:** calc. for [$(M - 2CF_3SO_3^-)^{2+}$] [$(C_{40}H_{38}O_4N_2)^{2+}$] 305.1410, found 305.1410.

(*E*)-4-(4-ethoxy-3-methoxystyryl)-6,7,10,11-tetrahydrodipyrido[2,1-a:1',2'-k][2,9] phenanthroline-5,12-diium trifluoromethanesulfonate (34)

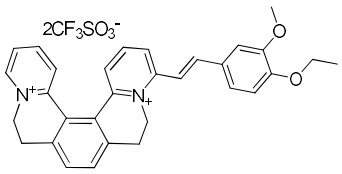

$C_{33}H_{30}F_6N_2O_8S_2$
[760.7]

The synthesis and purification of the [5]helquat dye **34** was accomplished by following *general procedure 5.2.e*, using helquat dye precursor **14** (50 mg, 0.084 mmol, 1.0 equiv.), 4-ethoxy-3-methoxybenzaldehyde (227.1 mg, 1.260 mmol, 15.0 equiv.), pyrrolidine (103 µL, 89.2 mg, 1.254 mmol, 14.9 equiv.) in dry MeOH (5.0 mL) and [5]helquat dye **34** was obtained as a yellow solid.

Yield: 61.1 mg, 96%.

m.p. 231-233 °C. **^{1}H-NMR (400 MHz, DMSO-d_6):** δ 1.37 (t, *J* = 7.0 Hz, 3H), 3.23 (ddd, *J* = 4.5, 14.0, 17.1, 2H), 3.36 (ddd, *J* = 2.0, 3.5, 17.1, 2H), 3.90 (s, 3H), 4.12 (q, *J* = 7.0 Hz, 2H), 4.45 (dt, *J* = 3.5, 13.6, 13.6 Hz, 1H), 4.83 (dt, *J* = 3.5, 13.6, 13.6 Hz, 1H), 5.04 (bdd, *J* = 2.0, 4.5, 13.4 Hz, 1H), 5.40 (bdd, *J* = 2.0, 4.5, 13.4 Hz, 1H), 7.10 (d, *J* = 8.4 Hz, 1H), 7.45 (dd, *J* = 1.9, 8.4 Hz, 1H), 7.55 (d, *J* = 1.9 Hz, 1H), 7.69 (d, *J* = 15.8 Hz, 1H), 7.77 (d, *J* = 7.8 Hz, 1H), 7.80 (d, *J* = 7.9 Hz, 1H), 7.87 (d, *J* = 15.8 Hz, 1H), 8.01-8.06 (m, 2H), 8.17 (t, *J* = 8.2 Hz, 1H), 8.20 (d, *J* = 8.2 Hz, 1H), 8.28 (t, *J* = 8.0 Hz, 1H), 8.36 (d, *J* = 8.2 Hz, 1H), 9.19 (d, *J* = 6.1 Hz, 1H). **^{13}C-NMR (101 MHz, DMSO-d_6):** 14.6, 26.9, 49.2, 54.4, 55.82, 63.9, 110.8, 112.5, 115.7, 119.1, 122.3, 123.7, 124.9, 126.1, 126.3, 127.1, 127.6, 127.7, 129.6, 131.5, 131.6, 140.1, 142.2, 143.9, 144.1, 145.8, 146.1, 146.6, 149.7, 150.7, 154.0. **IR (KBr):** *v* (cm^{-1}) 638, 1031, 1156, 1261, 1425, 1478, 1490, 1512, 1564, 1596, 1625, 2986, 3078, 3499. **MS (ESI) *m/z* (%):** 217.1 (9), 231.1 [$(M - 2CF_3SO_3^-)^{2+}$] (100), 231.6 (35), 232.1 (5), 461.2 (8), 611.2 (100), 612.2 (35). **HRMS ESI *m/z*:** calc. for [$(M - 2CF_3SO_3^-)^{2+}$] [$(C_{31}H_{30}O_2N_2)^{2+}$] 231.1148, found 231.1149.

(*E*)-4-(3-ethoxy-4-methoxystyryl)-6,7,10,11-tetrahydrodipyrido[2,1-a:1',2'-][2,9] phenanthroline-5,12-diium trifluoromethanesulfonate (35)

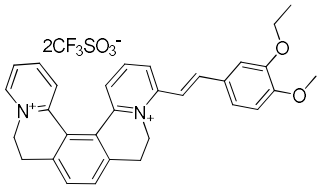

$C_{33}H_{30}F_6N_2O_8S_2$
[760.7]

The synthesis and purification of the [5]helquat dye **35** was accomplished by following *general procedure 5.2.e*, using helquat dye precursor **14** (50 mg, 0.084 mmol, 1.0 equiv.), 3-ethoxy-4-methoxybenzaldehyde (227.1 mg, 1.260 mmol, 15.0 equiv.), pyrrolidine (103 µL, 89.2 mg, 1.254 mmol, 14.9 equiv.) in dry MeOH (5.0 mL) and [5]helquat dye **35** was obtained as a yellow solid.

Yield: 52.8 mg, 83%.

m.p. 260-262 °C. **^{1}H-NMR (400 MHz, DMSO-d_6):** δ 1.40 (t, *J* = 7.0 Hz, 3H), 3.23 (ddd, *J* = 4.5, 14.0, 17.1 Hz, 2H), 3.36 (ddd, *J* = 2.0, 3.5, 17.1 Hz, 2H), 3.86 (s, 3H), 4.12 (q, *J* = 7.0 Hz, 2H), 4.45 (dt, *J* = 3.5, 13.6, 13.6 Hz, 1H), 4.83 (dt, *J* = 3.5, 13.6, 13.6 Hz, 1H), 5.04 (bdd, *J* = 2.0, 4.5, 13.4 Hz, 1H), 5.40 (bdd, *J* = 2.0, 4.5, 13.4 Hz, 1H),7.12 (d, *J* = 8.5 Hz, 1H), 7.45 (dd, *J* = 2.0, 8.5 Hz, 1H), 7.55 (d, *J* = 2.0 Hz, 1H), 7.68 (d, *J* = 15.8 Hz, 1H), 7.77 (d, *J* = 7.8 Hz, 1H), 7.81 (d, *J* = 7.8 Hz, 1H), 7.86 (d, *J* = 15.8 Hz, 1H), 8.02-8.07 (m, 2H), 8.16 (t, *J* = 8.1 Hz, 1H), 8.20 (dd, *J* = 1.3, 8.3 Hz, 1H), 8.28 (td, *J* = 1.4, 8.0 Hz, 1H), 8.36 (dd, *J* = 1.4, 8.3 Hz, 1H), 9.19 (dd, *J* = 1.0, 6.3 Hz, 1H). **^{13}C-NMR (101 MHz, DMSO-d_6):** δ 14.7, 26.8, 26.9, 49.2, 54.3, 55.7, 64.1, 111.7, 111.8, 115.7, 122.3, 123.8, 124.9, 126.1, 126.3, 127.1, 127.6, 127.8, 129.6, 131.5, 131.5, 140.1, 142.2, 143.9, 144.1, 145.7, 146.1, 146.6, 148.3, 151.6, 154.0. **IR (KBr):** *v* (cm^{-1}) 518, 640, 1031, 1143, 1162, 1261, 1436, 1478, 1490, 1513, 1564, 1596, 1612, 1625, 2984, 3076, 3438. **MS (ESI) *m/z* (%):** 231.1 [$(M - 2CF_3SO_3^-)^{2+}$] (100), 231.6 (35), 232.1 (5), 461.2 (8), 611.2 (100), 612.2 (35). **HRMS ESI *m/z*:** calc. for [$(M - 2CF_3SO_3^-)^{2+}$] [$(C_{31}H_{30}O_2N_2)^{2+}$] 231.1148, found 231.1149.

(*E*)-4-(3,4-dimethoxystyryl)-6,7,10,11-tetrahydrodipyrido[2,1-a:1',2'-k][2,9]phenanthroline -5,12-diium trifluoromethanesulfonate (36)

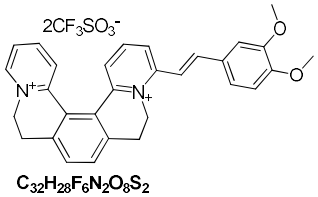

$C_{32}H_{28}F_6N_2O_8S_2$
[746.7]

The synthesis and purification of the [5]helquat dye **36** was accomplished by following *general procedure 5.2.e*, using helquat dye precursor **14** (50 mg, 0.084 mmol, 1.0 equiv.), 3,4-methoxybenzaldehyde (209.4 mg, 1.260 mmol, 15.0 equiv.), pyrrolidine (103 µL, 89.2 mg, 1.254 mmol, 14.9 equiv.) in dry MeOH (5.0 mL) and [5]helquat dye **36** was obtained as a yellow solid.

Yield: 51.8 mg, 83%.

m.p. 272-273 °C. **^{1}H-NMR (400 MHz, DMSO-d_6):** δ 3.23 (ddd, *J* = 4.5, 14.0, 17.1 Hz, 2H), 3.36 (ddd, *J* = 2.0, 3.5, 17.1 Hz, 2H), 3.86 (s, 3H), 3.90 (s, 3H), 4.45 (dt, *J* = 3.5, 13.6, 13.6 Hz, 1H), 4.83 (dt, *J* = 3.5, 13.6, 13.6 Hz, 1H), 5.04 (bdd, *J* = 2.0, 4.5, 13.4 Hz, 1H), 5.40 (bdd, *J* = 2.0, 4.5, 13.4 Hz, 1H), 7.12 (d, *J* = 8.0 Hz, 1H), 7.47 (dd, *J* = 2.0, 8.4 Hz, 1H), 7.56 (d, *J* = 2.0 Hz, 1H), 7.70 (d, *J* = 15.9 Hz, 1H), 7.77 (d, *J* = 7.8 Hz, 1H), 7.81 (d, *J* = 7.8 Hz, 1H), 7.88 (d, *J* = 15.9 Hz, 1H), 8.02-8.07 (m, 2H), 8.16 (d, *J* = 8.1 Hz, 1H), 8.20 (dd, *J* = 1.8, 8.8 Hz, 1H), 8.28 (ddd, *J* = 1.4, 7.7, 8.6 Hz, 1H), 8.37 (dd, *J* = 1.4, 8.3 Hz, 1H), 9.19 (dd, *J* = 1.4, 6.2 Hz, 1H). **^{13}C-NMR (101 MHz, DMSO-d_6):** δ 26.8, 26.9, 49.2, 54.4, 55.7, 55.9, 110.7, 111.7, 115.8, 116.8, 123.8, 124.9, 126.1, 126.3, 127.1, 127.6, 127.8, 129.6, 131.5, 131.6, 140.1, 142.2, 143.9, 144.1, 145.8, 146.1, 146.6, 149.1, 151.5, 154.0. **IR (KBr):** *v* (cm^{-1}) 519, 640, 1032, 1162, 1232, 1262, 1425, 1478, 1490, 1513, 1564, 1596, 1625, 2837, 3074, 3439. **MS (ESI) *m/z* (%):** 202.1 (5), 216.1 (14), 224.1 [$(M - 2CF_3SO_3^-)^{+2}$] (100), 224.6 (31), 225.1 (7), 447.2 (25), 448.2 (12), 479.2 (7), 597.2 (62), 598.2 (22). **HRMS ESI *m/z*:** calc. for [$(M - 2CF_3SO_3^-)^{+2}$] [$(C_{30}H_{28}O_2N_2)^{2+}$] 224.1070, found 224.1070.

(*E*)-4-(2-(naphthalen-1-yl)vinyl)-6,7,10,11-tetrahydrodipyrido[2,1-a:1',2'-k][2,9]phenanthroline-5,12-diium trifluoromethanesulfonate (37)

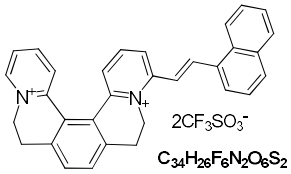

$C_{34}H_{26}F_6N_2O_6S_2$
[736.7]

The synthesis and purification of the [5]helquat dye **37** was accomplished by following *general procedure 5.2.e*, using helquat dye precursor **14** (50 g, 0.084 mmol, 1.0 equiv.), 1-naphthylaldehyde (196.8 mg, 1.260 mmol, 15.0 equiv.), pyrrolidine (103 µL, 89.2 mg, 1.254 mmol, 14.9 equiv.) in dry MeOH (5.0 mL) and [5]helquat dye **37** was obtained as a yellow solid.

Yield: 52.3 mg, 85%.

m.p. 249-251 °C. **^{1}H-NMR (acetonitrile-d_3, 400 MHz):** δ 3.15-3.37 (m, 4H), 4.48-4.60 (m, 1H), 4.82-4.91 (m, 2H), 5.27-5.31 (m, 1H), 7.62-7.71 (m, 4H), 7.73 (s, 2H), 7.84 (d, *J* = 8.0 Hz, 1H), 7.90 (ddd, *J* = 7.7, 6.1, 1.4 Hz, 1H), 7.98 (d, *J* = 8.4 Hz, 1H), 8.02 (dd, *J* = 1.4, 7.8 Hz, 1H), 8.09 (d, *J* = 8.2 Hz, 1H), 8.15 (t, *J* = 8.1, 1H), 8.12 (d, *J* = 7.3 Hz, 1H), 8.20 (td, *J* = 8.0, 1.4 Hz, 1H), 8.31 (dd, *J* = 8.2, 1.3 Hz, 1H), 8.37 (d, *J* = 8.6 Hz, 1H), 8.49 (d, *J* = 15.7 Hz, 1H), 8.81 (d, *J* = 6.2 Hz, 1H). **^{13}C-NMR (acetonitrile-d_3, 101 MHz):** δ 28.0, 28.1, 51.0, 56.1, 121.9, 124.3, 126.8, 126.8, 127.1, 127.5, 127.5, 127.6, 128.1, 128.3, 129.8, 129.9, 131.2, 132.2, 132.3, 133.0, 133.1, 133.2, 134.8, 141.5, 141.6, 141.9, 144.3, 145.9, 146.8, 147.7, 148.0, 155.5.

IR: *v* (cm^-) 804, 841, 963, 1031, 1157, 1225, 1261, 1274, 1479, 1491, 1511, 1565, 1580, 1595, 1611, 1625. **MS (ESI) *m/z* (%):** 219.2 (8), 449.4 (8), 587.5 [$(M - CF_3SO_3^-)^+$] (100), 588.5 (39), 589.5 (10), 759.5 (5). **HRMS ESI *m/z*:** calc. for [$(M - 2CF_3SO_3^-)^{2+}$] [$(C_{32}H_{26}N_2)^{2+}$] 219.1043, found 219.1044.

(*E*)-4-(2-(benzo[b]thiophen-2-yl)vinyl)-6,7,10,11-tetrahydrodipyrido[2,1-a:1',2'-k][2,9]phenanthroline-5,12-diium trifluoromethanesulfonate (38)

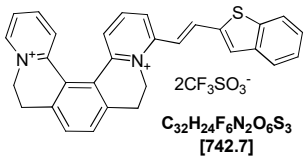

$C_{32}H_{24}F_6N_2O_6S_3$
[742.7]

The synthesis and purification of the [5]helquat dye **38** was accomplished by following *general procedure 5.2.e*, using helquat dye precursor **14** (50 mg, 0.084 mmol, 1.0 equiv.), benzo[*b*]thiophene-2-carbaldehyde (204.4 mg, 1.260 mmol, 15.0 equiv.), (103 µL, 89.2 mg, 1.254 mmol, 14.9 equiv.) in dry MeOH (5.0 mL) and [5]helquat dye **38** was obtained as a yellow solid.

Yield: 52.1 mg, 84%.

m.p. 223-225 °C. **^{1}H-NMR (acetonitrile-d_3, 400 MHz):** δ 3.21-3.43 (m, 4H), 4.49-4.56 (m, 2H), 4.81-4.90 (m, 2H), 7.38 (d, *J* = 15.7 Hz, 1H), 7.44 (ddd, *J* = 1.4, 1.4, 0.8 Hz, 1H), 7.48 (ddd, *J* = 1.6, 1.6, 0.8 Hz, 1H), 7.72 (s, 2H), 7.79 (dd, *J* = 1.4, 7.9 Hz, 1H), 7.82 (s, 1H), 7.89 (ddd, *J* = 1.4, 6.1, 7.6 Hz, 1H), 7.92-7.95 (m, 2H), 7.98 (dd, *J* = 15.7 Hz, 1H), 7.96-7.99 (m, 1H), 8.09 (t, *J* = 8.1 Hz, 1H), 8.16 (dd, *J* = 1.5, 8.3 Hz, 1H), 8.18 (dd, *J* = 1.5, 8.3 Hz, 1H), 8.80 (d, *J* = 0.8, 6.2 Hz, 1H). **^{13}C-NMR (acetonitrile-d_3, 101 MHz):** δ 28.0, 28.1, 50.9, 56.1, 119.8, 123.6, 126.0, 126.4, 126.9, 127.1, 127.5, 128.0, 128.0, 129.7, 131.2, 131.2, 133.1, 133.2, 138.2, 140.7, 140.8, 141.4, 141.5, 141.6, 144.2, 145.8, 146.7, 147.8, 148.0, 154.8. **IR:** *v* (cm^-) 726, 757, 826, 951, 1031, 1158, 1226, 1261, 1274, 1422, 1456, 1479, 1489, 1508, 1563, 1579, 1607, 1622.

MS (ESI) *m/z* (%): 222.1 (100), 593.1 (96), 594.1 (35), 595.1 (7). **HRMS ESI *m/z*:** calc. for [(M – $2CF_3SO_3^-$)$^{2+}$] [($C_{30}H_{24}N_2S$)$^{2+}$] 222.08246, found 222.08263.

(*E*)-8,9-dimethyl-4-(2-(naphthalen-1-yl)vinyl)-6,7,10,11-tetrahydrodipyrido[2,1-a:1',2'-k][2,9]phenanthroline-5,12-diium trifluoromethanesulfonate (39)

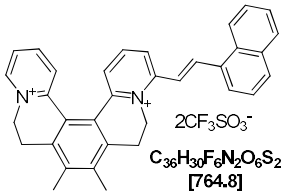

The synthesis and purification of the [5]helquat dye **39** was accomplished by following *general procedure 5.2.e*, using helquat dye precursor **16** (50 mg, 0.080 mmol, 1.0 equiv.), 1-naphthylaldehyde (187.4 mg, 1.200 mmol, 15.0 equiv.), pyrrolidine (98.5 µL, 85.3 mg, 1.200 mmol, 15.0 equiv.) in dry MeOH (5.0 mL) and [5]helquat dye **39** was obtained as a yellow solid.

Yield: 51.9 mg, 85%.

m.p. 283-285 °C. **^{1}H-NMR (acetonitrile-d_3, 400 MHz):** δ 2.44 (s, 6H), 2.99-313 (m, 2H), 3.41-3.50 (m, 2H), 4.50 (t, *J* = 14.1 Hz, 1H), 4.76 (t, *J* = 14.3 Hz, 1H), 4.95 (d, *J* = 13.3 Hz, 1H), 5.33 (d, *J*= 13.4 Hz, 1H), 7.62-7.72 (m, 5H), 7.83-7.87 (m, 2H), 8.02 (d, *J* = 7.8 Hz, 1H), 8.07-8.17 (m, 4H), 8.26 (dd, *J* = 1.3, 8.1 Hz, 1H), 8.38 (d, *J* = 8.4 Hz, 1H), 8.48 (d, *J* = 15.7 Hz, 1H), 8.76 (d, *J* = 6.8 Hz, 1H). **^{13}C-NMR (acetonitrile-d_3, 101 MHz):** δ 17.0, 17.2, 25.9, 26.7, 50.6, 56.0, 119.4, 120.6, 123.5, 125.7, 125.9, 126.4, 126.9, 128.1, 128.4, 129.2, 131.4, 132.8, 136.4, 137.0, 138.3, 138.6, 139.9, 140.6, 140.8, 141.3, 141.5, 142.3, 142.4, 143.7, 148.5, 149.5, 151.6, 154.0. **IR:** *v* (cm^-) 801, 810, 959, 1030, 1151, 1160, 1224, 1263, 1276, 1403, 1488, 1508, 1558, 1579, 1610, 1625. **MS (ESI) *m/z* (%):** 233.3 (7), 615.6 [(M – $CF_3SO_3^-$)$^+$] (100), 616.6 (40), 617.6 (10), 787.7 (5). **HRMS *m/z*:** calc. for [(M – $2CF_3SO_3^-$)$^{2+}$] [($C_{34}H_{30}N_2$)$^{2+}$] calc. 233.1199, found 233.1201.

(*E*)-8,9-dimethyl-4-(2-(4-methylnaphthalen-1-yl)vinyl)-6,7,10,11-tetrahydrodipyrido[2,1-a:1',2'-k][2,9]phenanthroline-5,12-diium trifluoromethanesulfonate (40)

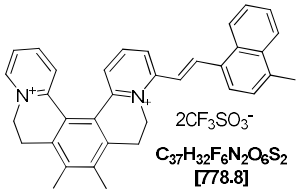

The synthesis and purification of the [5]helquat dye **40** was accomplished by following *general procedure 5.2.e*, using helquat dye precursor **16** (50 mg, 0.080 mmol, 1.0 equiv.), 4-methyl-1-naphthylaldehyde (204.2 mg, 1.200 mmol, 15.0 equiv.), pyrrolidine (98.5 µL, 85.3 mg, 1.200 mmol, 15.0 equiv.) in dry MeOH (5.0 mL) and [5]helquat dye **40** was obtained as a yellow solid.

Yield: 52.8 mg, 85%.

m.p. 242-244 °C. **^{1}H-NMR (acetonitrile-d_3, 400 MHz):** δ 2.44 (s, 6H), 2.79 (s, 3H), 2.97-3.14 (m, 2H), 3.41-3.51 (m, 2H), 4.47 (t, *J* = 13.9 Hz, 1H), 4.74 (t, *J* = 14.1 Hz, 1H), 4.93 (d, *J* = 13.4 Hz, 1H), 5.25 (d, *J* = 13.4 Hz, 1H), 7.54 (d, *J* = 7.4 Hz, 1H), 7.64-7.72 (m, 4H), 7.80 (dd, *J* = 1.0, 8.2 Hz, 1H), 7.83 (ddd, *J* = 1.5, 6.2 Hz, 1H), 8.03 (d, *J* = 7.4 Hz, 1H), 8.07 (t, *J* = 8.1 Hz, 1H), 8.14 (td, *J* = 8.1, 1.5 Hz, 1H), 8.18-8.20 (m, 1H), 8.26 (dd, *J* = 8.2, 1.3 Hz, 1H), 8.37-8.41 (m, 1H), 8.49 (d, *J* = 15.7 Hz, 1H), 8.74 (dd, *J* = 0.8, 6.2 Hz, 1H). **^{13}C-NMR (acetonitrile-d_3, 101 MHz):** δ 16.8, 16.9, 20.0, 26.2, 26.4, 50.6, 55.6, 120.7, 124.8, 125.1, 126.0, 126.1, 126.6, 126.7, 126.9, 127.4, 127.6, 127.9, 129.9, 131.3, 131.5, 132.3, 133.7, 139.6, 140.3, 140.4,

141.2, 141.3, 142.0, 143.9, 145.4, 146.1, 148.4, 148.8, 155.1. **IR:** *v* (cm^{-}) 765, 1031, 1166, 1225, 1260, 1273, 1485, 1508, 1558, 1576, 1611, 1623. **MS (ESI) *m/z* (%):** 240.3 (10), 629.5 [$(M - CF_3SO_3^-)^+$] (100), 630.5 (38), 631.6 (12), 801.6 (4). **HRMS *m/z*:** calc. for [$(M - 2CF_3SO_3^-)^{2+}$] [$(C_{35}H_{32}N_2)^{2+}$] 240.1277, found 240.1278.

(*E*)-4-(2-([1,1'-biphenyl]-4-yl)vinyl)-8,9-dimethyl-6,7,10,11-tetrahydrodipyrido[2,1-a:1',2'-k][2,9]phenanthroline-5,12-diium trifluoromethanesulfonate (41)

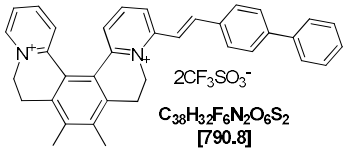

The synthesis and purification of the [5]helquat dye **41** was accomplished by following *general procedure 5.2.e*, using helquat dye precursor **16** (50 mg, 0.080 mmol, 1.0 equiv.), [1,1'-biphenyl]-4-carbaldehyde (218.6 mg, 1.200 mmol, 15.0 equiv.), pyrrolidine (98.5 µL, 85.3 mg, 1.200 mmol, 15.0 equiv.) in dry MeOH (5.0 mL) and [5]helquat dye **41** was obtained as a yellow solid.

Yield: 61.2 g, 97%.

m.p. 269-273 °C. **^{1}H-NMR (acetonitrile-d_3, 400 MHz):** δ 2.44 (s, 3H), 2.45 (s, 3H), 2.96-3.13 (m, 2H), 3.41-3.49 (m, 2H), 4.46 (t, *J* = 14.0 Hz, 1H), 4.73 (t, *J* = 14.1 Hz, 1H), 4.93 (d, *J* = 13.4 Hz, 1H), 5.32 (d, *J* = 13.6 Hz, 1H), 7.42-7.46 (m, 1H), 7.50-7.55 (m, 2H), 7.63 (dd, *J* = 8.1, 1.3 Hz, 1H), 7.64 (d, *J* = 16.0 Hz, 1H), 7.72-7.77 (m, 3H), 7.79 (dd, J = 1.2, 8.3 Hz, 1H), 7.82 (d, *J* = 8.6 Hz, 1H), 7.83-7.85 (m, 2H), 7.91-7.94 (m, 2H), 8.04 (t, J = 8.1 Hz, 1H), 8.10 (dd, *J* = 1.5, 8.5 Hz, 1H), 8.12 (dd, *J* = 8.4, 1.4 Hz, 1H), 8.74 (dd, J = 0.7, 6.2 Hz, 1H). **^{13}C-NMR (acetonitrile-d_3, 101 MHz):** δ 16.8, 16.9, 26.2, 26.3, 50.5, 55.6, 118.9, 125.1, 126.0, 126.3, 126.8, 128.0, 128.6, 129.2, 129.9, 130.1, 131.5, 135.0, 140.3, 140.4, 140.7, 141.1, 141.2, 143.9, 144.2, 144.3,145.4, 146.1, 148.5, 148.8, 155.1. **IR:** *v* (cm^{-}) 699, 833, 1006, 1030, 1160, 1224, 1261, 1275, 1412, 1450, 1488, 1509, 1577, 1559, 1603, 1610, 1625. **MS (ESI) *m/z* (%):** 246.1 (100), 246.6 (40), 247.1 (7), 491.2 (8), 641.2 (100), 642.2 (41), 643.2 (9). **HRMS ESI *m/z*:** calc. for [$(M - 2CF_3SO_3^-)^{2+}$] [$(C_{36}H_{32}N_2)^{2+}$] 246.1277, found 246.1277.

(*E*)-4-(2-(benzo[b]thiophen-2-yl)vinyl)-8,9-dimethyl-6,7,10,11-tetrahydrodipyrido[2,1-a:1',2'-k][2,9]phenanthroline-5,12-diium trifluoromethanesulfonate (42)

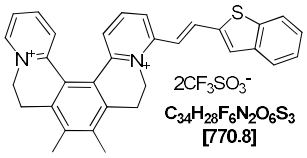

The synthesis and purification of the [5]helquat dye **42** was accomplished by following *general procedure 5.2.e*, using helquat dye precursor **16** (50 mg, 0.080 mmol, 1.0 equiv.), benzo[*b*]thiophene-2-carbaldehyde (194.6 mg, 1.200 mmol, 15.0 equiv.), pyrrolidine (98.5 µL, 85.3 mg, 1.200 mmol, 15.0 equiv.) in dry MeOH (5.0 mL) and [5]helquat dye **42** was obtained as a yellow solid.

Yield: 46.7 mg, 76%.

m.p. 309-311 °C. **^{1}H-NMR (acetonitrile-d_3, 400 MHz):** δ 2.43 (s, 3H), 2.44 (s, 3H), 2.96-3.13 (m, 2H), 3,43-3.50 (m, 2H), 4.47 (t, *J* = 13.9 Hz, 1H), 4.74 (t, *J* = 14.1 Hz, 1H), 4.93 (d, *J* = 13.4 Hz, 1H), 5.25 (d, *J* = 13.4 Hz, 1H), 7.39 (d, *J* = 15.7 Hz, 1H), 7.44-7.52 (m, 2H), 7.66 (dd, *J* = 8.0, 1.4 Hz, 1H), 7.84 (ddd, *J* = 7.6, 6.1, 1.4 Hz, 1H), 7.81 (s, 1H), 7.79 (ddd, *J* = 8.4, 1.5, 0.5 Hz, 1H), 7.92-8.01 (m, 3H), 8.04 (t, *J* = 8.1, 1H), 8.10 (td, *J* = 1.52, 7.98 Hz, 1H), 8.12 (dd, *J* = 1.4, 8.2 Hz, 1H), 8.74 (dd, *J* = 0.9, 6.2 Hz, 1H). **^{13}C-NMR (acetonitrile-d_3, 101 MHz):** δ 16.8, 16.9,

26.2, 26.3, 50.6, 55.6, 119.7, 123.6, 125.1, 126.0, 126.3, 126.4, 126.9, 128.0, 130.1, 131.1, 131.5, 131.5, 138.0, 140.3, 140.4, 140.7, 140.8, 141.2, 141.3, 141.5, 143.9, 145.4, 146.1, 148.6, 148.7, 154.2. **IR:** *v* (cm^{-}) 728, 757, 832, 1031, 1158, 1224, 1261, 1272, 1401, 1457, 1485, 1508, 1556, 1577, 1621. **MS (ESI) *m/z* (%):** 236.1 [$(M - 2CF_3SO_3^-)^{2+}$] (100), 236.6 (35), 237.1 (4), 593.1 (7), 621.1 (75), 622.1 (27), 623.1 (5). **HRMS *m/z:*** calc. for [$(M - 2CF_3SO_3^-)^{2+}$] [$(C_{32}H_{28}N_2S)^{2+}$] 236.0981, found 236.0982.

(*E*)-8,9-dimethyl-4-(2,4,6-trimethoxystyryl)-6,7,10,11-tetrahydrodipyrido[2,1-a:1',2'-k][2,9]phenanthroline-5,12-diium trifluoromethanesulfonate (43)

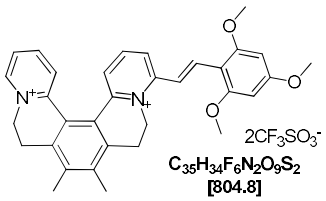

The synthesis and purification of the [5]helquat dye **43** was accomplished by following *general procedure 5.2.e*, using helquat dye precursor **16** (50 mg, 0.080 mmol, 1.0 equiv.), 2,4,6-trimethoxybenzaldehyde (235.4 mg, 1.200 mmol, 15.0 equiv.), pyrrolidine (98.5 µL, 85.3 mg, 1.200 mmol, 15.0 equiv.) in dry MeOH (5.0 mL) and [5]helquat dye **43** was obtained as a yellow solid.

Yield: 46.9 mg, 73.2%.

m.p. 315-317 °C. **^{1}H-NMR (acetonitrile-d_3, 400 MHz):** δ 2.43 (s, 3H), 2.44 (s, 3H), 2.96-3.13 (m, 2H), 3,43-3.50 (m, 2H), 3.90 (s, 3H), 3.97 (s, 6H), 4.47 (t, *J* = 13.9 Hz, 1H), 4.74 (t, *J* = 14.1 Hz, 1H), 4.93 (d, *J* = 13.4 Hz, 1H), 5.25 (d, *J* = 13.4 Hz, 1H), 6.33 (s, 2H), 7.50 (dd, *J* = 1.3, 7.9 Hz, 1H), 7.74 (dd, *J* = 1.3, 8.4 Hz, 1H), 7.82 (ddd, *J* = 1.4, 6.2, 7.6 Hz, 1H), 7.86 (d, *J* = 16.0 Hz, 1H), 7.91 (d, *J* = 8.1 Hz, 1H), 7.96 (d, *J* = 16.0 Hz, 1H), 8.04 (dd, *J* = 1.4, 8.3 Hz, 1H), 8.09 (td, *J* = 1.5, 8.1 Hz, 1H), 8.73 (dd, *J* = 1.4, 6.2 Hz, 1H). **^{13}C-NMR (acetonitrile-d_3, 101 MHz):** δ 16.8, 26.3, 26.4, 49.8, 55.6, 56.4, 57.0, 92.0, 106.8, 117.8, 120.1, 125.0, 125.4, 126.3, 126.8, 128.6, 131.4, 136.3, 140.2, 140.3, 140.8, 141.1, 143.1, 145.3, 146.0, 147.8, 148.9, 157.5, 162.5, 165.3. **IR:** *v* (cm^{-}) 517, 573, 637, 856, 1030, 1157, 1223, 1261, 1440, 2844. **MS (ESI) *m/z* (%):** 253.1 (59), 253.6 (20), 505.2 (18), 655.2 (100), 656.2 (32). **HRMS ESI *m/z***: calc. for [$(M - 2CF_3SO_3^-)^{2+}$] [$(C_{33}H_{33}N_2O_3)^{2+}$] 505.24857, found 505.24835.

(*E*)-4-(4-ethoxy-3-methoxystyryl)-1-methylpyridin-1-ium iodide (44)

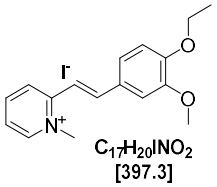

The synthesis and purification of pyridinium dye **44** was accomplished using *general procedure 5.2.f. method 1*. Pyridinium dye **44** was obtained as a yellow amorphous solid.

Yield: 43.1 mg, 85%.

m.p. 235-237 °C. **^{1}H-NMR (400 MHz, DMSO- d_6):** δ 1.36 (t, *J* = 7.0 Hz, 3H), 3.87 (s, 3H), 4.10 (q, *J* = 7.0 Hz, 2H), 4.37 (s, 3H), 7.07 (d, *J* = 8.4 Hz, 1H), 7.38 (dd, *J* = 2.0, 8.4 Hz, 1H), 7.45 (d, *J* = 15.9 Hz, 1H), 7.49 (d, *J* = 2.0 Hz, 1H), 7.85 (td, *J* = 2.2, 6.5 Hz, 1H), 7.91 (d, *J* = 15.9 Hz, 1H), 8.43-8.50 (m, 2H), 8.86 (dt, *J* = 0.9, 6.2 Hz, 1H). **^{13}C-NMR (101 MHz, DMSO- d_6):** δ 14.6, 46.0, 55.8, 63.9, 110.7, 112.4, 114.7, 123.7, 124.4, 124.4, 127.6, 143.4, 143.9, 145.8, 149.1, 150.7, 152.8. **IR (KBr) *v* (cm^{-1}):** 517, 537, 569, 643, 800, 921, 1032, 1145, 1185, 1233, 1427, 1442, 1459, 1484, 1516, 1565, 1577, 1539, 1613, 1631, 2832, 3033, 3428. **MS (ESI) *m/z* (%):** 270.2

(100), 271.2 (19), 450.2 (5). **HRMS ESI *m/z*:** calc. for [(M – I^-)$^+$] [($C_{17}H_{20}O_2N$)$^+$] 270.1489, found 270.1489.

(*E*)-4-(3-ethoxy-4-methoxystyryl)-1-methylpyridin-1-ium iodide (45)

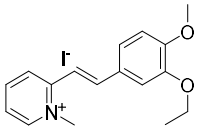

$C_{17}H_{20}INO_2$
[397.3]

The synthesis and purification of pyridinium dye **45** was accomplished using *general procedure 5.2.f. method 1*. Pyridinium dye **45** was obtained as a yellow amorphous solid.
Yield: 45.1 mg, 89%.
m.p. 233-235 °C. **^{1}H-NMR (400 MHz, DMSO-d_6):** δ 1.38 (t, *J* = 7.0 Hz, 3H), 3.84 (s, 3H), 4.11 (q, *J* = 7.0 Hz, 2H), 4.36 (s, 3H), 7.09 (d, *J* = 8.4 Hz, 1H), 7.39 (dd, *J* = 2.0, 8.4 Hz, 1H), 7.44 (d, *J* = 15.9 Hz, 1H), 7.48 (d, *J* = 2.0 Hz, 1H), 7.85 (td, *J* = 2.8, 6.2 Hz, 1H), 7.90 (d, *J* = 15.9 Hz, 1H), 8.41-8.51 (m, 2H), 8.86 (dt, *J* = 0.9, 6.2 Hz, 1H). **^{13}C-NMR (101 MHz, DMSO- d_6):** δ 14.7, 46.0, 55.7, 64.0, 111.7, 111.8, 114.7, 123.7, 124.4, 124.4, 127.7, 143.4, 143.9, 145.8, 148.3, 151.6, 152.8. **IR (KBr):** *v* (cm^{-1}): 543, 637, 773, 814, 855, 900, 974, 1022, 1041, 1148, 1171, 1181, 1238, 1268, 1331, 1440, 1461, 1514, 1566, 1577, 1592, 1616, 1631, 2036, 2838, 2931, 2980, 3034, 3070, 3431. **MS (ESI) *m/z* (%):** 270.2 (100), 271.2 (22), 539.3 (5), 667.2 (3). **HRMS ESI *m/z*:** calc. for [(M – I^-)$^+$] [($C_{17}H_{20}O_2N$)$^+$] 270.1489, found 270.1489.

(*E*)-4-(3,4-dimethoxystyryl)-1-methylpyridin-1-ium iodide (46)

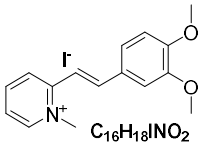

$C_{16}H_{18}INO_2$
[383.2]

The synthesis and purification of pyridinium dye **46** was accomplished using *general procedure 5.2.f. method 1*. Pyridinium dye **46** was obtained as a yellow amorphous solid.
Yield: 42.1 g, 86%.
m.p. 235-237 °C. **^{1}H-NMR (400 MHz, DMSO- d_6):** δ 3.84 (s, 3H), 3.87 (s, 3H), 4.36 (s, 3H), 7.09 (d, *J* = 8.4 Hz, 1H), 7.40 (dd, *J* = 2.0, 8.4 Hz, 1H), 7.46 (d, *J* = 15.9 Hz, 1H), 7.49 (d, *J* = 2.0 Hz, 1H), 7.85 (td, *J* = 2.5, 6.4 Hz, 1H), 7.91 (d, *J* = 15.9 Hz, 1H), 8.40-8.53 (m, 2H), 8.86 (dt, *J* = 0.9, 6.2 Hz, 1H). **^{13}C-NMR (101 MHz, DMSO- d_6):** δ 46.0, 55.7, 55.9, 110.6, 111.7, 114.8, 123.7, 124.4, 124.4, 127.7, 143.4, 143.93, 145.82, 149.06, 151.43, 152.77. **IR (KBr):** *v* (cm^{-1}) 543, 589, 617, 637, 773, 814, 900, 1022, 1041, 1109, 1148, 1171, 1181, 1238, 1268, 1331, 1401, 1440, 1461, 1514, 1566, 1577, 1592, 1616, 1631, 2036, 2836, 2931, 2971, 2980, 3034, 3070, 3142, 3431**. MS (ESI) *m/z* (%):** 256.2 (100), 257.2 (22). **HRMS ESI *m/z*:** calc. for [(M – I^-)$^+$] [($C_{16}H_{18}O_2N$)$^+$] 256.13321, found 256.13323.

(*E*)-1-methyl-2-(2-(naphthalen-1-yl)vinyl)pyridin-1-ium iodide (47)

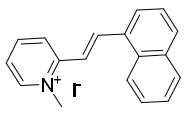

$C_{18}H_{16}IN$
[373.2]

The synthesis and purification of pyridinium dye **47** was accomplished using *general procedure 5.2.f. method 2*. Pyridinium dye **47** was obtained as a yellow amorphous solid.
Yield: 47.1 mg, 99%.

m.p. 254-256 °C. **^{1}H-NMR (DMSO-d_6, 400 MHz):** δ 4.43 (s, 3H), 7.60-7.73 (m, 4H), 7.97 (ddd, *J* = 1.5, 6.2, 7.6 Hz, 1H), 8.01-8.06 (m, 1H), 8.10 (d, *J* = 8.2 Hz, 1H), 8.22 (dt, *J* = 0.8, 7.3 Hz, 1H), 8.53-8.56 (m, 1H), 8.58 (dd, *J* = 1.4, 7.9 Hz, 1H), 8.74 (d, *J* = 15.8 Hz, 1H), 8.84 (dd, *J* = 1.4, 8.2 Hz, 1H), 8.96 (dt, *J* = 0.8, 6.2 Hz, 1H). **^{13}C-NMR (DMSO-d_6, 101 MHz):** δ 46.1, 120.1, 121.4, 123.7, 125.4, 125.7, 125.7, 126.5, 127.1, 128.7, 131.0, 131.0, 131.9, 133.3, 139.3, 144.4, 146.1, 152.1.
IR (KBr): *v* (cm^{-1}) 794, 832, 1143, 1170, 1459, 1510, 1517, 1575, 1597, 1638**. MS (ESI) *m/z* (%):** 246.1 (100), 247.1 (21), 491.3 (5). **HRMS ESI *m/z*:** calc. for [(M – I^-)$^+$] [($C_{18}H_{16}N$)$^+$] 246.1277, found 246.1277.

(*E*)-2-(2-(benzo[b]thiophen-2-yl)vinyl)-1-methylpyridin-1-ium iodide (48)

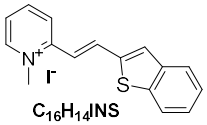

The synthesis and purification of pyridinium dye **48** was accomplished using *general procedure 5.2.f. method 2*. Pyridinium dye **48** was obtained as a yellow amorphous solid.
Yield: 42.1 g, 87%.
m.p. 221-223 °C. **^{1}H-NMR (DMSO-d_6, 400 MHz):** δ 4.39 (s, 3H), 7.31 (d, *J* = 15.7 Hz, 1H), 7.40-7.52 (m, 2H), 7.89-7.99 (m, 3H), 8.00-8.08 (m, 2H), 8.29 (d, *J* = 15.8 Hz, 1H), 8.45-8.57 (m, 2H), 8.94 (d, *J* = 6.7 Hz, 1H). **^{13}C-NMR (DMSO-d_6, 101 MHz):** δ 46.0, 118.5, 122.8, 125.0, 121.1, 125.3, 125.4, 126.7, 129.5, 136.0, 139.3, 139.8, 139.9, 144.4, 146.2, 151.5. **IR:** *v* (cm^-) 491, 509, 708, 725, 745, 1129, 1152, 1177, 1259, 1456, 1505, 1520, 1588, 1609, 1627. **MS (ESI) *m/z* (%):** 252.1 (100), 253.1 (24), 254.1 (10), 414.4 (5). **HRMS ESI *m/z*:** calc. for [(M - I^-)$^+$] [($C_{16}H_{14}NS$)$^+$] 252.0842, found 252.0842.

(*E*)-4-(4-ethoxy-3-methoxystyryl)-1-methylpyridin-1-ium iodide (49)

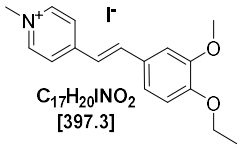

The synthesis and purification of pyridinium dye **49** was accomplished using *general procedure 5.2.f. method 1*. Pyridinium dye **49** was obtained as a yellow amorphous solid.
Yield: 49.2 mg, 97%.
m.p. 268-271 °C. **^{1}H-NMR (400 MHz, DMSO-d_6):** δ 1.35 (t, *J* = 7.0 Hz, 3H), 3.85 (s, 3H), 4.09 (q, *J* = 7.0 Hz, 2H), 4.23 (s, 3H), 7.05 (d, *J* = 8.4 Hz, 1H), 7.27 (d, *J* = 2.0, 8.4 Hz, 1H), 7.39 (d, *J* = 2.0 Hz, 2H), 7.42 (d, *J* = 16.3 Hz, 1H), 7.96 (d, *J* = 16.3 Hz, 1H), 8.15 (d, *J* = 6.8 Hz, 2H), 8.80 (d, *J* = 6.8 Hz, 1H). **^{13}C-NMR (101 MHz, DMSO-d_6):** δ 14.6, 46.7, 55.6, 63.8, 110.0, 112.5, 120.7, 122.9, 123.1, 127.8, 141.0, 144.9, 149.1, 150.4, 152.9. **IR (KBr):** *v* (cm^{-1}) 514, 616, 803, 867, 1036, 1141, 1168, 1268, 1426, 1474, 1519, 1579, 1594, 1616, 1645, 2910, 3002, 3028. **MS (ESI) *m/z* (%):** 270.2 (100), 271.2 (13). **HRMS ESI *m/z*:** calc. for [(M - I^-)$^+$] [($C_{17}H_{20}O_2N$)$^+$] calc. 270.14886, found 270.14889.

(*E*)-4-(3-ethoxy-4-methoxystyryl)-1-methylpyridin-1-ium iodide (50)

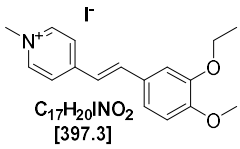

The synthesis and purification of pyridinium dye **50** was accomplished using *general procedure 5.2.f. method 1*. Pyridinium dye **50** was obtained as a yellow amorphous solid.
Yield: 45.1 mg, 89%.
m.p. 263-265 °C. **^{1}H-NMR (400 MHz, DMSO-d_6):** δ 1.37 (t, *J* = 7.0 Hz, 3H), 3.83 (s, 3H), 4.10 (q, *J* = 7.0 Hz, 2H), 4.22 (s, 3H), 7.07 (d, *J* = 8.4 Hz, 1H), 7.28 (dd, *J* = 2.0, 8.4 Hz, 1H), 7.37 (d, *J* = 2.0 Hz, 1H), 7.41 (d, *J* = 16.3 Hz, 1H), 7.94 (d, *J* = 16.3 Hz, 1H), 8.13 (d, *J* = 6.8 Hz, 2H), 8.79 (d, *J* = 6.8 Hz, 2H). **^{13}C-NMR (101 MHz, DMSO-d_6):** δ 14.7, 46.7, 55.6, 63.9, 111.0, 111.8, 120.8, 122.9, 123.1, 128.0, 141.0, 144.9, 148.3, 151.2, 152.9. **IR (KBr):** *v* (cm^{-1}) 516, 614, 978, 1043, 1140, 1265, 1314, 1432, 1469, 1517, 1580, 1594, 1616, 1643, 2929, 2977, 3028, 3439. **MS (ESI) *m/z* (%):** 270.1 (100), 271.2 (22). **HRMS ESI *m/z*:** calc. for $[(M - I^-)^+]$ $[(C_{17}H_{20}O_2N)^+]$ 270.14886, found 270.14891.

(*E*)-4-(3,4-dimethoxystyryl)-1-methylpyridin-1-ium iodide (51)

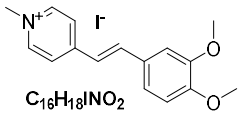

The synthesis and purification of pyridinium dye **51** was accomplished using *general procedure 5.2.f. method 1*. Pyridinium dye **51** was obtained as a yellow amorphous solid.
Yield: 43 mg, 88%.
m.p. 265-267 °C. **^{1}H-NMR (400 MHz, DMSO-d_6):** δ 3.83 (s, 3H), 3.85 (s, 3H), 4.23 (s, 3H), 7.07 (d, *J* = 8.4 Hz, 1H), 7.29 (dd, *J* = 2.0, 8.4 Hz, 1H), 7.40 (d, *J* = 2.0 Hz, 1H), 7.45 (d, *J* = 16.2 Hz, 1H), 7.96 (d, *J* = 16.2 Hz, 1H), 8.15 (d, *J* = 6.5 Hz, 2H), 8.81 (d, *J* = 6.5 Hz, 2H). **^{13}C-NMR (101 MHz, DMSO-d_6):** δ 46.8, 55.6, 55.7, 109.9, 111.7, 120.8, 122.9, 123.1, 128.0, 141.0, 144.9, 149.1, 151.1, 152.9. **IR (KBr):** *v* (cm^{-1}) 514, 618, 766, 829, 865, 968, 1020, 1142, 1163, 1186, 1209, 1238, 1271, 1423, 1446, 1487, 1517, 1595, 1615, 1644, 2831, 2911, 2988, 3075, 3439. **MS (ESI) *m/z* (%):** 256.2 $[(M - I^-)]$ (100), 257.2 (20). **HRMS ESI *m/z*:** calc. for $[(M - I^-)^+]$ $[(C_{16}H_{18}O_2N)^+]$ 256.1332, found 256.1332.

(*E*)-1-methyl-4-(2-(naphthalen-1-yl)vinyl)pyridin-1-ium iodide (52)

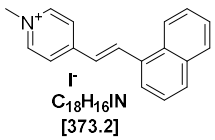

The synthesis and purification of pyridinium dye **52** was accomplished using *general procedure 5.2.f. method 2*. Pyridinium dye **52** was obtained as a yellow amorphous solid.
Yield: 46.2 mg, 97%.
m.p. 289-291 °C. **^{1}H-NMR (DMSO-d_6, 400 MHz):** δ 4.29 (s, 3H), 7.60-7.70 (m, 4H), 8.02 (dd, *J* = 8.0, 1.4 Hz, 1H), 8.06 (d, *J* = 8.1 Hz, 1H), 8.10 (dd, *J* = 7.4, 1.1 Hz, 1H), 8.45 (d, *J* = 6.9 Hz, 2H), 8.59 (d, *J* = 8.5 Hz, 1H), 8.82 (d, *J* = 16.1 Hz, 1H), 8.92 (d, *J* = 6.6 Hz, 2H).
^{13}C-NMR (DMSO-d6, 101 MHz): δ 47.0, 123.7, 124.0, 124.9, 125.8, 125.8, 126.4, 127.0, 128.7, 130.7, 131.0, 132.1, 133.4, 136.8, 145.1, 152.3. **IR:** *v* (cm^-) 744, 798, 826, 1142, 1188, 1459, 1511, 1519, 1571, 1618, 1639. **MS (ESI) *m/z* (%):** 246.1 $[(M - I^-)]$ (100), 247.1 (21). **HRMS ESI *m/z:*** calc. for $[(M - I^-)]$ $[(C_{18}H_{16}N)^+]$ 246.1277, found: 246.1278.

(*E*)-4-(2-(benzo[b]thiophen-2-yl)vinyl)-1-methylpyridin-1-ium iodide (53)

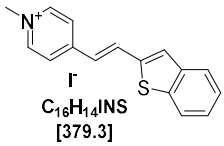

The synthesis and purification of pyridinium dye **53** was accomplished using *general procedure 5.2.f. method 2*. Pyridinium dye **53** was obtained as a yellow amorphous solid.
Yield: 47.0 mg, 97%.
m.p. 254-256 °C. **^{1}H-NMR (DMSO-d_6, 400 MHz):** δ 4.26 (s, 3H), 7.25 (d, *J* = 16.0 Hz, 1H), 7.38-7.49 (m, 2H), 7.81 (s, 1H), 7.89-7.97 (m, 1H), 7.98-8.07 (m, 1H), 8.27 (d, *J* = 6.9 Hz, 2H), 8.35 (d, *J* = 16.1 Hz, 1H), 8.88 (d, *J* = 6.9 Hz, 2H). **^{13}C-NMR (DMSO-d_6, 101 MHz):** δ 47.0, 122.8, 123.6, 124.5, 124.8, 125.2, 126.6, 129.1, 134.1, 139.4, 139.6, 140.4, 145.1, 151.7. **IR:** *v* (cm^-) 707, 726, 752, 1147, 1454, 1504, 1523, 1587, 1613, 1641. **MS (ESI) *m/z* (%):** 252.1 [$(M - I^-)^+$] (100), 253.1 (18), 414.1 (3). **HRMS ESI *m/z*:** calc. for [$(M - I^-)^+$] [$(C_{16}H_{14}NS)^+$] 252.0842, found 252.0842.

(*E*)-11-(2-(benzo[b]thiophen-2-yl)vinyl)-6,7-dimethyl-4,5,8,9-tetrahydroisoquinolino[1,2-a]pyrido[1,2-k][2,9]phenanthroline-3,10-diium trifluoromethanesulfonate (54)

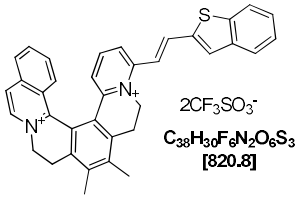

The synthesis and purification of [6]helquat dye **54** was accomplished by following the *general procedure 5.2.e*, using helquat dye precursor **6** (20 mg, 0.030 mmol, 1.0 equiv.), benzo[*b*]thiophene-2-carbaldehyde (73 mg, 0.450 mmol, 15.0 equiv.), pyrrolidine (30 µL, 26 mg, 0.366 mmol, 12.2 equiv.) in dry MeOH (2.0 mL) and dye **54** was obtained as a yellow solid.
Yield: 19 mg, 78%.
m.p. 216-218 °C. **^{1}H-NMR (acetonitrile-d_3, 400 MHz):** δ 2.54 (s, 3H), 2.55 (s, 3H), 3.05 (ddd, *J* = 4.9, 14.3, 17.1 Hz, 1H), 3.16 (ddd, *J* = 4.6, 14.6, 17.2 Hz, 1H), 3.54 (ddd, *J* = 1.8, 3.5, 17.2 Hz, 1H), 3.58 (ddd, *J* = 1.9, 3.8, 17.1 Hz, 1H), 4.70 (dt, *J* = 3.8, 14.0 Hz, 1H), 4.79 (dt, *J* = 3.5, 14.3 Hz, 1H), 5.01 (ddd, *J* = 1.8, 4.6, 13.9 Hz, 1H), 5.38 (ddd, *J* = 1.9, 4.9, 13.8 Hz, 1H), 6.92 (dd, *J* = 1.2, 8.2 Hz, 1H), 7.42 (d, *J* = 15.6 Hz, 1H), 7.45-7.53 (m, 2H), 7.55 (t, *J* = 4.1, 1H), 7.67 (ddd, *J* = 1.3, 6.9, 8.6 Hz, 1H), 7.77 (dq, *J* = 1.3, 8.2 Hz, 1H), 7.79 (s, 2H), 7.86-7.94 (m, 3H), 7.99 (ddd, *J* = 0.7, 1.6, 7.3 Hz, 1H), 8.12 (dd, *J* = 1.1, 8.3 Hz, 1H), 8.31 (d, *J* = 6.7 Hz, 1H), 8.61 (d, *J* = 6.7 Hz, 1H). **^{13}C-NMR (acetonitrile-d_3, 101 MHz):** 17.0, 17.2, 25.9, 26.7, 50.6, 56.0, 119.4, 120.6, 123.5, 123.7, 125.7, 125.9, 126.4, 126.9, 128.1, 128.4, 129.2, 129.2, 131.4, 132.8, 136.4, 137.0, 138.3, 138.6, 139.9, 140.6, 140.8, 141.3, 141.5, 142.3, 142.4, 143.7, 148.5, 149.5, 151.6, 154.0. **IR (KBr):** *v* (cm^{-1}) 728, 757, 828, 1031, 1157, 1226, 1265, 1379, 1410, 1457, 1484, 1507, 1554, 1563, 1574, 1606, 1622. **MS (ESI) *m/z* (%):** 261.1 (100), 261.6 (42), 262.1 [$(M - CF_3SO_3^-)^{2+}$] (6), 521.2 [$(M - CF_3SO_3^-)^{2+}$] (9), 671.2 [$(M - CF_3SO_3^-)^+$] (55), 672.2 (23). **HRMS ESI *m/z*:** calc. for [$(M - 2CF_3SO_3^-)^{2+}$] [$(C_{36}H_{30}N_2S)^{2+}$] 261.1059, found 261.1060.

(*E*)-6,7-dimethyl-11-(2-(naphthalen-1-yl)vinyl)-4,5,8,9-tetrahydroisoquinolino[1,2-a]pyrido[1,2-k][2,9]phenanthroline-3,10-diium trifluoromethanesulfonate (55)

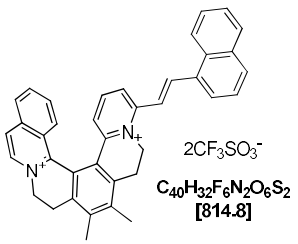

The synthesis and purification of [6]helquat dye **55** was accomplished by *general procedure 5.2.e*, using helquat dye precursor **6** (20 mg, 0.030 mmol, 1.0 equiv.), 1-naphthylaldehyde (70.3 mg, 0.450 mmol, 15.0 equiv.), pyrrolidine (30 µL, 26 mg, 0.366 mmol, 12.2 equiv.) in dry MeOH (2.0 mL) and helquat dye **55** was obtained as a yellow solid.

Yield: 21 mg, 87%.

m.p. > 350 °C. **^{1}H-NMR (600 MHz, acetone-d_6):** δ 2.63 (s, 3H), 2.64 (s, 3H), 3.34 (ddd, *J* = 4.2, 14.4, 17.3 Hz, 1H), 3.48 (dt, *J* = 4.0, 16.2 Hz, 1H), 3.82 (dt, *J* = 3.7, 16.8 Hz, 1H), 3.82 (dt, *J* = 3.5, 16.8 Hz, 1H), 5.12 (dt, *J* = 3.7, 14.2 Hz, 1H), 5.17 (dt, *J* = 3.5, 14.7 Hz, 1H), 5.40 (dd, *J* = 4.0, 13.5 Hz, 1H), 5.68 (ddd, *J* = 1.6, 4.2, 13.3 Hz, 1H), 7.52 (d, *J* = 8.0 Hz, 1H), 7.61-7.66 (m, 2H), 7.68 (t, *J* = 7.7 Hz, 1H), 7.82 (t, *J* = 8.0 Hz, 1H), 7.84 (ddd, *J* = 3.3, 8.7 Hz, 1H), 7.98 (ddd, *J* = 1.04, 7.0 Hz, 1H), 8.03-8.05 (m, 1H), 8.10 (dd, *J* = 0.28, 5.6 Hz, 1H), 8.13 (d, *J* = 2.0 Hz, 1H), 8.14 (dd, *J* = 0.9, 8.7 Hz, 1H), 8.27 (d, *J* = 7.7 Hz, 1H), 8.28 (d, *J* = 8.6 Hz, 1H), 8.33 (dd, *J* = 1.1, 8.1 Hz, 1H), 8.42 (d, *J* = 7.7 Hz, 1H), 8.55 (d, *J* = 6.6 Hz, 1H), 8.64 (d, *J* = 15.7 Hz, 1H), 9.03 (d, *J* = 6.7 Hz, 1H). **^{13}C-NMR (151 MHz, acetone-d_6):** δ 16.9, 17.0, 26.1, 26.8, 50.8, 56.2, 121.5, 123.8, 124.2, 125.9, 126.3, 126.6, 126.7, 127.0, 127.4, 128.1, 128.8, 128.9, 129.2, 129.6, 129.8, 132.2, 132.4, 132.8, 132.9, 134.8, 136.2, 137.6, 138.7, 140.0, 141.0, 141.6, 141.9, 142.6, 144.1, 148.6, 151.6, 154.8. **IR:** *v* (cm^-) 517, 573, 638, 1030, 1168, 1264, 1484, 1524, 1553, 1588, 1627, 3074. **MS (ESI) *m/z* (%):** 258.1 (100), 258.6 (42), 258.1 (9), 377.2 (6), 413.3 (13), 515.2 (6), 516.2 [$(M - 2CF_3SO_3^-)^{2+}$] (2), 665.2 [$(M - CF_3SO_3^-)^+$] (4). **HRMS ESI *m/z*:** calc. for [$(M - CF_3SO_3^-)^+$] [$(C_{39}H_{32}O_3N_2F_3S)^+$] 665.2080, found 665.2079.

(*E*)-6,7-dimethyl-11-(2-(4-methylnaphthalen-1-yl)vinyl)-4,5,8,9-tetrahydroisoquinolino[1,2-a] pyrido[1,2-k][2,9]phenanthroline-3,10-diium trifluoromethanesulfonate (56)

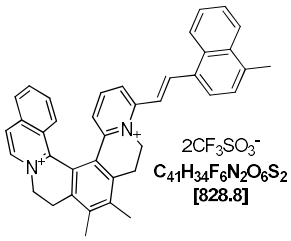

The synthesis and purification of [6]helquat dye **56** was accomplished by following the *general procedure 5.2.e*, using helquat dye precursor **6** (20 mg, 0.030 mmol, 1.0 equiv.), 4-methyl-1-naphthylaldehyde (76.6 mg, 0.450 mmol, 15.0 equiv.), pyrrolidine (30 µL, 26 mg, 0.366 mmol, 12.2 equiv.) in dry MeOH (2.0 mL) and [6]helquat **56** was obtained as a yellow solid.

Yield: 14.9 g, 61%.

m.p. 314-316 °C. **^{1}H-NMR (400 MHz, acetonitrile-d_3):** δ 2.54 (s, 3H), 2.55 (s, 3H), 2.79 (s, 3H), 3.05 (ddd, *J* = 4.9, 14.3, 17.1 Hz, 1H), 3.16 (ddd, *J* = 4.6, 14.6, 17.2 Hz, 1H), 3.54 (ddd, *J* = 1.8, 3.5, 17.2 Hz, 1H), 3.58 (ddd, *J* = 1.9, 3.8, 17.1 Hz, 1H), 4.70 (dt, *J* = 3.8, 14.0 Hz, 1H), 4.79 (dt, *J* = 3.5, 14.3 Hz, 1H), 5.01 (ddd, *J* = 1.8, 4.6, 13.9 Hz, 1H), 5.38 (ddd, *J* = 1.9, 4.9, 13.8 Hz, 1H), 6.95 (dd, *J* = 8.0 Hz, 1H), 7.56 (d, *J* = 8.1 Hz, 1H), 7.60 (d, *J* = 8.1 Hz, 1H), 7.67-7.71 (m, 4H), 7.82 (dd, *J* = 1.0, 8.8 Hz, 1H), 7.90 (ddd, *J* = 1.1, 6.9, 8.2 Hz, 1H), 7.95 (dd, *J* = 1.3, 8.2 Hz, 1H), 8.05 (d, *J* = 7.4 Hz, 1H), 8.13 (d, *J* = 8.3 Hz, 1H), 8.16-8.20 (m, 1H), 8.31-8.36 (m, 2H), 8.39 (d, *J* = 15.7 Hz, 1H), 8.62 (d, *J* = 6.7 Hz, 1H). **^{13}C-NMR (101 MHz, acetonitrile-d_3):** δ 17.0, 17.1, 20.1, 25.9, 26.7, 50.6, 56.1, 120.4, 123.5, 124.7, 125.9, 126.1, 126.2, 126.6, 126.7, 127.0, 127.4, 127.6, 128.0, 128.5, 128.6, 129.0, 129.2, 131.3, 132.3, 132.8, 133.7, 136.4, 137.0, 138.6, 139.7, 139.9, 141.2, 142.3, 142.4, 143.7, 148.2, 151.6, 154.9. **IR:** *v* (cm^-) 517, 573, 639, 743, 771, 804, 961, 1031, 1159, 1223, 1245, 1272, 1488, 1507, 1562, 1576, 1611, 1628. **MS (ESI) *m/z* (%):** 265.1 [$(M - 2CF_3SO_3^-)^{2+}$] (100), 265.6 (41), 529.3 (25), 679.2 (72), 680.2 (30),

697.2 (10). **HRMS ESI *m/z*:** calc. for [(M – $2CF_3SO_3^-)^{2+}$] [$(C_{39}H_{33}N_2)^{2+}$] 529.2638, found 529.2638.

(*E*)-11-(2-(biphenyl-4-yl)vinyl)-6,7-dimethyl-4,5,8,9-tetrahydroisoquinolino[1,2-a]pyrido-[1,2-k][2,9]- phenanthroline-3,10-diiumbistrifluoromethanesulfonate (57)

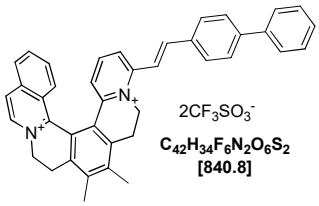

The synthesis and purification of [6]helquat dye **57** was accomplished by following the *general procedure 5.2.e*, using helquat dye precursor **6** (20 mg, 0.030 mmol, 1.0 equiv.), [1,1'-biphenyl]-4-carbaldehyde (82 mg, 0.450 mmol, 15.0 equiv.), pyrrolidine (30 µL, 26 mg, 0.366 mmol, 12.2 equiv.) in dry MeOH and [6]helquat dye **57** was obtained as a yellow solid.
Yield: 22.9 mg, 92%.
m.p. 311-313 °C. **^{1}H-NMR (600 MHz, acetonitrile-d_3):** δ 2.54 (s, 3H), 2.55 (s, 3H), 3.05 (ddd, *J* = 4.9, 14.3, 17.1 Hz, 1H), 3.16 (ddd, *J* = 4.6, 14.6, 17.2 Hz, 1H), 3.54 (ddd, *J* = 1.8, 3.5, 17.2 Hz, 1H), 3.58 (ddd, *J* = 1.9, 3.8, 17.1 Hz, 1H), 4.70 (dt, *J* = 3.8, 14.0 Hz, 1H), 4.79 (dt, *J* = 3.5, 14.3 Hz, 1H), 5.01 (ddd, *J* = 1.8, 4.6, 13.9 Hz, 1H), 5.38 (ddd, *J* = 1.9, 4.9, 13.8 Hz, 1H), 6.91 (d, *J* = 8.0 Hz, 1H), 7.42-7.55 (m, 4H), 7.57-7.68 (m, 3H), 7.71-7.91 (m, 9H), 8.12 (d, *J* = 8.3 Hz, 1H), 8.31 (d, *J* = 6.8 Hz, 1H), 8.61 (d, *J* = 6.8 Hz, 1H). **^{13}C–NMR (151 MHz, acetonitrile-d_3):** δ 17.1, 17.2, 26.0, 26.8, 50.6, 56.1, 121.1, 123.2, 123.6, 125.7, 126.0, 127.0, 128.0, 128.5, 128.7, 128.7, 129.1, 129.2, 129.3, 130.2, 132.9, 134.9, 136.5, 137.1, 138.7, 140.0, 140.7, 142.3, 142.4, 142.5, 143.8, 144.4, 144.8, 148.4, 151.7, 155.0. **IR:** *v* (cm^-) 517, 573, 638, 756, 770, 826, 1006, 1031, 1151, 1262, 132, 1379, 1411, 1436, 1447, 1508, 1562, 1610, 1628, 3081, 3435. **MS (ESI) *m/z* (%):** 235.6 (6), 268.2 (7), 271.1 (100), 271.6 (44), 541.3 (12), 542.3 [(M – $2CF_3SO_3^-)^{2+}$] (5), 691.2 [(M – $CF_3SO_3^-)^+$] (6). **HRMS ESI *m/z*:** calc. for [(M – $CF_3SO_3^-)^+$] [$(C_{41}H_{34}O_3N_2F_3S)^+$] 691.2237, found 691.2235.

(*E*)-6,7-dimethyl-11-(2-(naphthalen-2-yl)vinyl)-4,5,8,9-tetrahydroisoquinolino[1,2-a]pyrido [1,2-k][2,9]phenanthroline-3,10-diium trifluoromethanesulfonate (58)

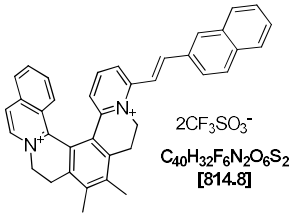

The synthesis and purification of [6]helquat dye **58** was accomplished by following the *general procedure 5.2.e*, using helquat dye precursor **6** (20 mg, 0.030 mmol, 1.0 equiv.), 2-naphthylaldehyde (70.3 mg, 0.450 mmol, 15.0 equiv.), pyrrolidine (30 µL, 26 mg, 0.366 mmol, 12.2 equiv.) in dry MeOH (2.0 mL) and [6]helquat dye **58** was obtained as a yellow solid.
Yield: 21 mg, 87%.
m.p. 312-313 °C. **^{1}H-NMR (acetonitrile-d_3, 600 MHz):** δ 2.54 (s, 3H), 2.55 (s, 3H), 3.05 (ddd, *J* = 4.9, 14.3, 17.1 Hz, 1H), 3.16 (ddd, *J* = 4.6, 14.6, 17.2 Hz, 1H), 3.54 (ddd, *J* = 1.8, 3.5, 17.2 Hz, 1H), 3.58 (ddd, *J* = 1.9, 3.8, 17.1 Hz, 1H), 4.70 (dt, *J* = 3.8, 14.0 Hz, 1H), 4.79 (dt, *J* = 3.5, 14.3 Hz, 1H), 5.01 (ddd, *J* = 1.8, 4.6, 13.9 Hz, 1H), 5.38 (ddd, *J* = 1.9, 4.9, 13.8 Hz, 1H), 6.91 (d, *J* = 8.1 Hz, 1H), 7.56 (t, *J* = 8.1 Hz, 1H), 7.61 (dd, *J* = 2.5, 9.6 Hz, 1H), 7.63 (t, *J* = 3.7 Hz, 1H), 7.68 (dd, *J* = 7.1, 1.3 Hz, 1H), 7.76 (s, 2H), 7.81 (d, *J* = 8.7 Hz, 1H), 7.87 (td, *J* = 1.2, 7.1 Hz, 1H), 7.89

(dd, *J* = 1.0, 7.0 Hz, 1H), 7.97-8.06 (m, 4H), 8.13 (d, *J* = 8.2 Hz, 1H), 8.23 (d, *J* = 1.5 Hz, 1H), 8.31 (d, *J* = 6.7 Hz, 1H), 8.61 (d, *J* = 6.7 Hz, 1H). **^{13}C-NMR (acetonitrile-*d*$_3$, 151 MHz):** *δ* 17.0, 17.4, 26.0, 26.8, 50.6, 56.1, 118.9, 120.5, 123.6, 124.6, 125.7, 125.9, 126.9, 128.2, 128.5, 128.6, 128.9 128.9, 129.0, 129.2, 129.7, 130.0, 131.6, 132.8, 133.4, 134.3, 135. 136.4, 137.0, 138.6, 139.9, 141.2, 142.3, 143.7, 145.2, 148.3, 151.7, 154.9. **IR:** *v* (cm^{-}) 517, 573, 638, 756, 770, 826, 1006, 1031, 1151, 1262, 1329, 1379, 1411, 1436, 1447, 1508, 1562, 1610, 1628, 3081, 3435. **MS (ESI) *m/z* (%):** 258.1 (100), 258.6 (42), 258.1 (9), 377.2 (6), 413.3 (13), 515.2 (6), 516.2 [(M – 2$CF_3SO_3^-$)$^{2+}$] (2), 655.2 [(M – $CF_3SO_3^-$)$^+$] (4). **HRMS ESI *m/z*:** calc. for [(M – $CF_3SO_3^-$)$^+$] [($C_{39}H_{32}O_3N_2F_3S$)$^+$] 665.2080, found 665.2079.

(*E*)-11-(2-(benzofuran-2-yl)vinyl)-6,7-dimethyl-4,5,8,9-tetrahydroisoquinolino[1,2-a]pyrido[1,2-k][2,9]phenanthroline-3,10-diium trifluoromethanesulfonate (59)

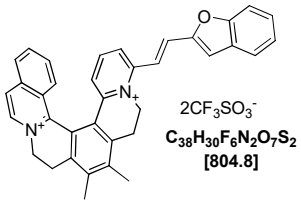

The synthesis and purification of [6]helquat dye **59** was accomplished by following the *general procedure 5.2.e*, using helquat dye precursor **6** (20 mg, 0.030 mmol, 1.0 equiv.), benzofuran-2-carbaldehyde (65.7 mg, 0.450 mmol, 15.0 equiv.), pyrrolidine (30 µL, 26 mg, 0.366 mmol, 12.2 equiv.) in dry MeOH (2.0 mL) and helquat dye **59** was obtained as a yellow solid.

Yield: 18.1 mg, 76%.

m.p. 321-323 °C. **^{1}H-NMR (acetonitrile-*d*$_3$, 400 MHz):** *δ* 2.54 (s, 3H), 2.55 (s, 3H), 3.05 (ddd, *J* = 4.9, 14.3, 17.1 Hz, 1H), 3.16 (ddd, *J* = 4.6, 14.6, 17.2 Hz, 1H), 3.54 (ddd, *J* = 1.8, 3.5, 17.2 Hz, 1H), 3.58 (ddd, *J* = 1.9, 3.8, 17.1 Hz, 1H), 4.70 (dt, *J* = 3.8, 14.0 Hz, 1H), 4.79 (dt, *J* = 3.5, 14.3 Hz, 1H), 5.01 (ddd, *J* = 1.8, 4.6, 13.9 Hz, 1H), 5.38 (ddd, *J* = 1.9, 4.9, 13.8 Hz, 1H), 6.94 (dd, *J* = 1.3, 8.0 Hz, 1H), 7.31 (s, 1H), 7.36 (ddd, *J* = 1.0, 7.3, 8.1 Hz, 1H), 7.50 (ddd, *J* = 1.3, 7.3, 8.4 Hz, 1H), 7.55 (t, *J* = 8.08, 1H), 7.57 (d, *J* = 15.6 Hz, 1H), 7.63 (dq, *J* = 0.9, 8.4 Hz, 1H), 7.65 (ddd, *J* = 1.23, 6.9 Hz, 1H), 7.67 (d, *J* = 15.6 Hz, 1H), 7.74-7.77 (m, 1H), 7.78-7.81 (m, 2H), 7.88 (ddd, *J* = 1.2, 6.9, 8.2 Hz, 1H), 8.12 (d, *J* = 8.4 Hz, 1H), 8.31 (d, *J* = 6.7 Hz, 1H), 8.62 (d, *J* = 6.7 Hz, 1H).

^{13}C-NMR (acetonitrile-*d*$_3$, 101 MHz): *δ* 17.0, 17.1, 25.8, 26.7, 50.6, 56.0, 106.0, 112.2, 113.9, 114.0, 120.5, 123.5, 123.7, 124.9, 128.4, 128.5, 128.5, 129.2, 129.2, 129.3, 129.5, 131.5, 132.9, 136.4, 137.0, 138.5, 139.9, 141.3, 142.3, 142.5, 143.7, 148.5, 151.6, 153.5, 154.0, 156.7. **IR (KBr):** *v* (cm^{-1}) 518, 573, 638, 755, 888, 1031, 1100, 1157, 1224, 1263, 1276, 1349, 1379, 1411, 1449, 1485, 1507, 1551, 1565, 1607, 1627. **MS (ESI) *m/z* (%):** 253.1 [(M – 2$CF_3SO_3^-$)$^{2+}$] (100), 253.6 (40), 254.1 (7), 655.2 [(M – $CF_3SO_3^-$)$^+$] (23), 656.2 (7). **HRMS ESI *m/z*:** calc. for [(M – 2$CF_3SO_3^-$)$^{2+}$] [($C_{36}H_{30}ON_2$)$^{2+}$] 253.1174, found 253.1174.

4,13-bis((*E*)-2-(2,3-dihydrobenzofuran-5-yl)vinyl)-6,7,10,11-tetrahydrodipyrido[2,1-a:1',2'-k] [2,9]phenanthroline-5,12-diium trifluoromethanesulfonatetrifluoromethanesulfonate (60)

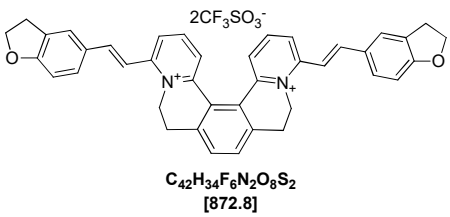

The synthesis and purification of the [5]helquat dye **60** was accomplished according to *general procedure 5.2.e*, using helquat dye precursor **10** (50 mg, 0.082 mmol, 1.0 equiv.), 2,3-dihydrobenzofuran-5-carbaldehyde (182.3 mg, 1.230 mmol, 15.0 equiv.), pyrrolidine (100 µL, 86.6 mg, 1.218 mmol, 14.9 equiv.) in dry MeOH (5.0 mL) and [5]helquat dye **60** was obtained as a yellow solid.

Yield: 64.1 g, 90%.

m.p. 204-206 °C. **^{1}H-NMR (acetonitrile-d_3, 400 MHz):** δ 3.16-3.19 (m, 4H), 3.29 (t, *J* = 8.5 Hz, 4H), 4.45-4.53 (m, 2H), 4.67 (t, *J* = 8.5 Hz, 4H), 5.18-5.26 (m, 2H), 6.89 (d, *J* = 8.3 Hz, 2H), 7.40 (d, *J* = 15.9 Hz, 2H), 7.58 (dd, *J* = 1.9, 8.3 Hz, 2H), 7.64 (d, *J* = 15.9 Hz, 2H), 7.69 (s, 2H), 7.72 (dd, *J* = 1.4, 8.1 Hz, 2H), 7.76 (d, *J* = 1.7 Hz, 2H), 8.00 (t, *J* = 8.1 Hz, 2H), 8.11 (dd, *J* = 1.4, 8.3 Hz, 2H). **^{13}C-NMR (acetonitrile-d_3, 101 MHz):** δ 28.2, 29.7, 50.5, 73.2, 110.6, 115.6, 126.2, 128.1, 128.7, 129.0, 130.3, 131.3, 131.4, 132.4, 141.2, 143.5, 145.4, 147.7, 156.0, 164.1. **IR (KBr):** *v* (cm^{-1}) 935, 1031, 1154, 1231, 1260, 1276, 1326, 1473, 1493, 1561, 1588, 1601, 1625. **MS (ESI) *m/z* (%):** 287.1 [$(M - 2CF_3SO_3^-)^{2+}$] (100), 287.6 (43), 288.1 (8), 723.2 [$(M - CF_3SO_3^-)^+$] (6). **HRMS ESI *m/z*:** calc. for [$(M - 2CF_3SO_3^-)^{2+}$] [$(C_{40}H_{34}O_2N_2)^{2+}$] 287.13047, found 287.13055.

4,13-bis((*E*)-2-(6-methoxynaphthalen-2-yl)vinyl)-6,7,10,11-tetrahydrodipyrido[2,1-a:1',2'-k] [2,9]phenanthroline-5,12-diium trifluoromethanesulfonate (61)

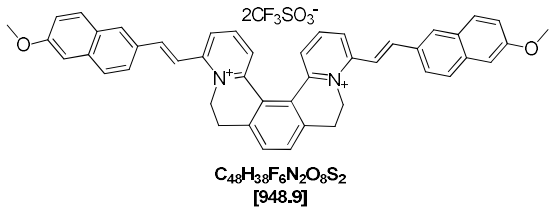

The synthesis and purification of the [5]helquat dye **61** was accomplished according to *general procedure 5.2.e*, using helquat dye precursor **10** (50 mg, 0.082 mmol, 1.0 equiv.), 6-methoxy-2-naphtylaldehyde (229.0 mg, 1.230 mmol, 15.0 equiv.), pyrrolidine (100 µL, 86.6 mg, 1.218 mmol, 14.9 equiv.) in dry MeOH (5.0 mL) and [5]helquat dye **61** was obtained as a yellow solid.

Yield: 71.2 mg, 92%.

m.p. 264-266 °C. **^{1}H-NMR (acetonitrile-d_3, 400 MHz):** δ 3.12-3.34 (m, 4H), 3.95 (s, 6H), 4.48-4.56 (m, 2H), 5.26-5.34 (m, 2H), 7.25 (dd, *J* = 9.0, 2.5 Hz, 2H), 7.36 (d, *J* = 2.5 Hz, 2H), 7.66 (d, *J* = 15.9 Hz, 2H), 7.72 (d, *J* = 4.1 Hz, 2H), 7.74 (dd, *J* = 1.32, 8.0 Hz, 2H), 7.85 (d, *J* = 15.9 Hz, 2H), 7.91 (d, *J* = 3.8 Hz, 2H), 7.93 (d, *J* = 3.4 Hz, 2H), 7.97-8.01 (m, 2H), 8.07 (t, *J* = 8.1 Hz, 2H), 8.19 (d, *J* = 1.6 Hz, 2H), 8.20 (dd, *J* = 1.3, 8.2 Hz, 2H). **^{13}C-NMR (acetonitrile-d_3, 101 MHz):** δ 28.1, 50.7, 56.2, 56.3, 107.3, 120.7, 125.4, 126.6, 128.1, 128.8, 129.5, 129.6, 131.2, 131.3, 131.4, 132.6, 137.2, 141.3, 143.8, 145.3, 147.9, 155.7, 160.4. **IR (KBr):** *v* (cm^{-1}) 812, 965, 1030, 1156, 1224, 1265, 1272, 1392, 1441, 1474, 1482, 1502, 1563, 1600, 1608, 1619, 2841. **MS (ESI) *m/z* (%):** 241.1 (18), 325.1 [$(M - 2CF_3SO_3^-)^{2+}$] (100), 325.6 (50), 326.1 (13), 481.2 (8), 649.3 (13), 799.2 [$(M - CF_3SO_3^-)^+$] (93), 800.2 (47), 801.3 (10). **HRMS ESI *m/z*:** calc. for [$(M - 2CF_3SO_3^-)^{2+}$] [$(C_{46}H_{38}O_2N_2)^{2+}$] calc. 325.14612, found 325.14632.

(*E*)-6,7-dimethyl-11-(2-(5-phenylthiophen-2-yl)vinyl)-4,5,8,9-tetrahydroisoquinolino[1,2-a] pyrido[1,2-k][2,9]phenanthroline-3,10-diium trifluoromethanesulfonate (62)

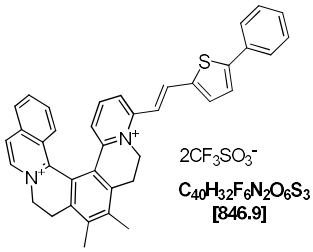

The synthesis and purification of [6]helquat dye **62** was accomplished according to the *general procedure 5.2.e* using [6]helquat dye precursor **6** (20 mg, 0.030 mmol, 1.0 equiv.), 5-phenylthiophene-2-carbaldehyde (84.7 mg, 0.450 mmol, 15.0 equiv.), pyrrolidine (30 µL, 26 mg, 0.366 mmol, 12.2 equiv.) in dry MeOH (2.0 mL) and [6]helquat dye **62** was obtained as a yellow solid.

Yield: 17.8 mg, 72%.

m.p. 329-331 °C. **^{1}H-NMR (400 MHz, acetonitrile-d_3):** δ 2.53 (s, 3H), 2.54 (s, 3H), 3.05 (ddd, *J* = 4.9, 14.3, 17.1 Hz, 1H), 3.16 (ddd, *J* = 4.6, 14.6, 17.2 Hz, 1H), 3.54 (ddd, *J* = 1.8, 3.5, 17.2 Hz, 1H), 3.58 (ddd, *J* = 1.9, 3.8, 17.1 Hz, 1H), 4.70 (dt, *J* = 3.8, 14.0 Hz, 1H), 4.79 (dt, *J* = 3.5, 14.3 Hz, 1H), 5.01 (ddd, *J* = 1.8, 4.6, 13.9 Hz, 1H), 5.38 (ddd, *J* = 1.9, 4.9, 13.8 Hz, 1H), 6.87 (dd, *J* = 1.5, 8.3 Hz, 1H), 7.36 (d, *J* = 15.6 Hz, 1H), 7.41-7.43 (m, 1H), 7.48-7.56 (m, 5H), 7.66 (ddd, *J* = 1.3, 6.9, 7.2 Hz, 1H), 7.76-7.80 (m, 5H), 7.88 (ddd, J = 1.3, 6.9, 7.2 Hz, 1H), 8.12 (d, *J* = 8.4 Hz, 1H), 8.30 (d, *J* = 6.7 Hz, 1H), 8.61 (d, J = 6.7 Hz, 1H). **^{13}C-NMR (101 MHz, acetonitrile-d_3):** δ 17.0, 17.1, 25.9, 26.7, 50.4, 56.0, 116.6, 120.5, 123.4, 123.7, 125.2, 125.9, 126.1, 126.9, 128.4, 128.6, 128.7, 129.2, 130.0, 130.3, 132.8, 134.1, 135.2, 136.4, 137.0, 137.7, 138.5, 139.9, 140.1, 141.1, 141.8, 142.2, 142.4, 143.3, 148.2, 149.9, 151.6, 154.5. **IR:** *v* (cm^-) 1032, 1163, 1227, 1264, 1412, 1432, 1571, 1610, 1629, 2363, 3090. **MS (ESI) *m/z* (%):** 274.1 (100), 274.6 (43), 547.2 [$(M - 2CF_3SO_3^-)^{2+}$] (45), 548.2 (20), 697.2 [$(M - CF_3SO_3^-)^+$] (10). **HRMS *m/z*:** calc. for [$(M - 2CF_3SO_3^-)^{2+}$] [$(C_{38}H_{31}N_2S)^{2+}$] 547.22025, found 547.22017.

4,13-bis((*E*)-3,4,5-trimethoxystyryl)-6,7,10,11-tetrahydrodipyrido[2,1-a:1',2'-k][2,9] phenanthroline-5,12-diium trifluoromethanesulfonate (63)

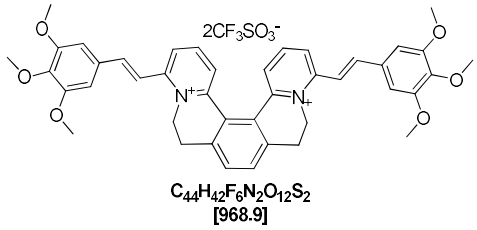

The synthesis and purification of [5]helquat dye **63** was accomplished according to *general procedure 5.2.e*, using helquat dye precursor **10** (50 mg, 0.082 mmol, 1.0 equiv.), 3,4,5-trimethoxybenzaldehyde (241.3 mg, 1.230 mmol, 15.0 equiv.), pyrrolidine (100 µL, 86.6 mg, 1.218 mmol, 14.9 equiv.) in dry MeOH (5 mL) and [5]helquat dye **63** was obtained as a yellow solid.

Yield: 74.4 mg, 94%.

m.p. 280-282 °C. **^{1}H-NMR (acetonitrile-d_3, 400 MHz):** δ 3.14-3.36 (m, 4H), 3.83 (s, 6H), 3.93 (s, 12H), 4.52 (t, *J* = 13.8 Hz, 2H), 5.28 (d, *J* = 13.2 Hz, 2H), 7.12 (s, 4H), 7.55 (d, *J* = 15.9 Hz, 2H), 7.62 (d, *J* = 15.9 Hz, 2H), 7.72 (s, 2H), 7.75 (dd, *J* = 1.5, 7.9 Hz, 2H), 8.06 (t, *J* = 8.0 Hz, 2H), 8.12 (dd, *J* = 1.5, 8.2 Hz, 2H). **^{13}C-NMR (acetonitrile-d_3, 101 MHz):** δ 28.1, 50.9, 57.0, 61.1, 107.1, 126.6, 128.1, 129.5, 131.4, 132.6, 141.3, 141.7, 143.9, 145.1, 147.9, 154.8, 154.8, 155.7. **IR (KBr):** *v* (cm^{-1}): 518, 573, 638, 756, 1031, 1158, 1231, 1262, 1272, 1405,

1431, 1479, 1489, 1510, 1565, 1589, 1608, 1623, 1962. **MS (ESI) *m/z* (%):** 253.1 (7), 335.2 [(M – $2CF_3SO_3^-)^{2+}$] (100), 335.7 (42), 336.2 (10), 669.3 [(M – $2CF_3SO_3^-)^{2+}$] (5), 819.3 [(M – $CF_3SO_3^-)^+$] (27), 820.3 (15). **HRMS ESI *m/z*:** calc. for [(M – $2CF_3SO_3^-)^{2+}$] [$(C_{42}H_{42}O_6N_2)^{2+}$] 335.1516, found 335.1517.

4,13-bis((*E*)-4-(pentyloxy)styryl)-6,7,10,11-tetrahydrodipyrido[2,1-a:1',2'-k][2,9]phenanthroline-5,12-diium trifluoromethanesulfonate (64)

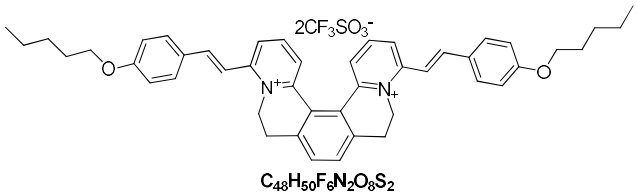

The synthesis and purification of [5]helquat dye **64** was accomplished according to *general procedure 5.2.e*, using [5]helquat dye precursor **10** (50 mg, 0.082 mmol, 1.0 equiv.), 4-(pentyloxy)benzaldehyde (236.5 mg, 1.230 mmol, 15.0 equiv.), pyrrolidine (100 µL, 86.6 mg, 1.218 mmol, 14.9 equiv.) in dry MeOH (5 mL) and [5]helquat dye **64** was obtained as a yellow solid.

Yield: 62.7 mg, 80.4%.

m.p. 289-291 °C. **^{1}H-NMR (acetonitrile-d_3, 400 MHz):** δ 0.95 (t, *J* = 7.1 Hz, 6H), 1.34-1.51 (m, 8H), 1.77-1.84 (m, 4H), 3.12-3.33 (m, 4H), 4.08 (t, *J* = 6.6 Hz, 4H), 4.57 (m, 2H), 5.22-5.26 (m, 2H), 7.04 (dd, *J* = 2.0, 6.8 Hz, 4H), 7.43 (d, *J* = 15.9 Hz, 2H), 7.65-7.70 (m, 6H), 7.77 (dd, *J* = 2.0, 6.8 Hz, 4H), 8.02 (t, *J* = 8.1 Hz, 2H), 8.11 (dd, *J* = 8.3, 1.4 Hz, 2H). **^{13}C-NMR (acetonitrile-d_3, 101 MHz):** δ 14.3, 23.1, 28.1, 28.9, 29.6, 50.6, 69.3, 116.1, 116.2, 126.3, 128.1, 128.3, 129.1, 131.4, 132.5, 141.2, 143.6, 144.9, 147.8, 156.0, 162.7. **IR (KBr):** *v* (cm^{-1}) 518, 573, 639, 755, 828, 968, 1031, 1156, 1176, 1230, 1256, 1277, 1427, 1473, 1490, 1512, 1563, 1600, 1623. **MS (ESI) *m/z* (%):** 331.4 (70), 331.9 (37), 661.8 (4), 811.9 [(M – $CF_3SO_3^-)^+$] (100), 812.9 (50), 813.9 (15). **HRMS ESI *m/z*:** calc. for [(M – $2CF_3SO_3^-)^{2+}$] [$(C_{46}H_{50}O_2N_2)^{2+}$] 331.1931, found 331.1933.

(*E*)-11-(2-(dibenzo[b,d]furan-4-yl)vinyl)-6,7-dimethyl-4,5,8,9-tetrahydroisoquinolino[1,2-a]pyrido[1,2-k][2,9]phenanthroline-3,10-diium trifluoromethanesulfonate (65)

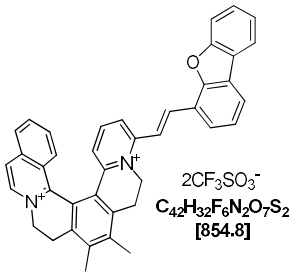

The synthesis and purification of [6]helquat dye **65** was accomplished according to *general procedure 5.2.e*, using dye precursor **6** (20 mg, 0.030 mmol, 1.0 equiv.), dibenzo[*b*,*d*]furan-4-carbaldehyde (88.3 mg, 0.450 mmol, 15.0 equiv.), pyrrolidine (30 µL, 26 mg, 0.366 mmol, 12.2 equiv.) in dry MeOH (2.0 mL) and dye **65** was obtained as a yellow solid.

Yield: 21 mg, 83%.

m.p. 312-314 °C. **^{1}H-NMR (acetonitrile-d_3, 400 MHz):** δ 2.55 (s, 3H), 2.56 (s, 3H), 3.05 (ddd, *J* = 4.9, 14.3, 17.1 Hz, 1H), 3.16 (ddd, *J* = 4.6, 14.6, 17.2 Hz, 1H), 3.54 (ddd, *J* = 1.8, 3.5, 17.2 Hz, 1H), 3.58 (ddd, *J* = 1.9, 3.8, 17.1 Hz, 1H), 4.70 (dt, *J* = 3.8, 14.0 Hz, 1H), 4.79 (dt, *J* = 3.5, 14.3 Hz, 1H), 5.01 (ddd, *J* = 1.8, 4.6, 13.9 Hz, 1H), 5.38 (ddd, *J* = 1.9, 4.9, 13.8 Hz, 1H), 6.98 (dd, *J*= 1.3, 8.0 Hz, 1H), 7.48-7.57 (m, 2H), 7.58-7.66 (m, 2H), 7.69 (ddd, *J* = 1.23, 6.9 Hz, 1H), 7.81-

7.86 (m, 4H), 7.88 (dd, *J* = 1.23, 5.2 Hz, 1H), 7.90 (dd, *J* = 1.22, 5.26 Hz, 1H), 8.14 (d, *J* = 8.3 Hz, 1H), 8.17 (ddd, *J* = 0.7, 1.4, 7.8, Hz, 1H), 8.22 (dd, *J* = 1.2, 7.7 Hz, 1H), 8.28 (d, *J* = 16.1 Hz, 1H), 8.33 (d, *J* = 6.7 Hz, 1H), 8.63 (d, *J* = 6.7 Hz, 1H). **^{13}C-NMR (acetonitrile-*d*$_3$, 101 MHz):** *δ* 17.0, 17.2, 25.9, 26.7, 50.7, 56.1, 112.8, 120.5, 120.9, 121.9, 122.4, 123.5, 123.7, 124.4, 124.6, 124.8, 125.8, 126.0, 126.1, 126.2, 127.0, 128.5, 128.5, 129.2, 129.7, 132.9, 136.4, 137.0, 138.4, 138.6, 139.8, 140.0, 141.3, 142.3, 142.5, 143.9, 148.4, 151.6, 155.0, 157.1. **IR:** *v* (cm^{-}) 761, 832, 1031, 1157, 1188, 1224, 1263, 1275, 1380, 1411, 1455, 1475, 1485, 1507, 1560, 1574, 1609, 1625**. MS (ESI) *m/z* (%):** 278.1 [$(M - 2CF_3SO_3^-)^{2+}$] (100), 278.6 (44), 279.1 (7), 376.2 (12), 376.7 (7), 705.2 [$(M - CF_3SO_3^-)^+$] (8). **HRMS *m/z*:** calc. for [$(M - 2CF_3SO_3^-)^{2+}$] [$(C_{40}H_{32}ON_2)^{2+}$] 278.1252, found 278.1253.

4,13-bis((*E*)-4-(pent-4-yn-1-yloxy)styryl)-6,7,10,11-tetrahydrodipyrido[2,1-a:1',2'-k][2,9] phenanthroline-5,12-diium trifluoromethanesulfonate (66)

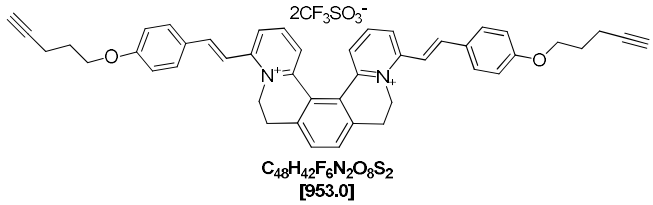

The synthesis and purification of [5]helquat dye **66** was accomplished by following *general procedure 5.2.e*, using [5]helquat dye precursor **10** (50 mg, 0.082 mmol, 1.0 equiv.), 4-(pent-4-yn-1-yloxy)benzaldehyde (231.5 mg, 1.230 mmol, 15.0 equiv.), pyrrolidine (100 µL, 86.6 mg, 1.218 mmol, 14.9 equiv.) in dry MeOH (5 mL) and [5]helquat dye **66** was obtained as a yellow solid.

Yield: 63 mg, 81%.

m.p. 213-215 °C. **^{1}H-NMR (acetonitrile-*d*$_3$, 400 MHz):** *δ* 2.00 (p, *J* = 6.4 Hz, 4H), 2.22 (t, *J* = 2.7 Hz, 2H), 2.41 (td, *J* = 7.1, 2.7 Hz, 4H), 3.12-3.33 (m, 4H), 4.17 (t, *J* = 6.2 Hz, 4H), 4.43-4.51 (m, 2H), 5.23-5.27 (m, 2H), 7.05-7.10 (dd, *J* = 2.0, 6.8 Hz, 4H), 7.44 (d, *J* = 15.9 Hz, 2H), 7.65 (d, *J* = 15.9 Hz, 2H), 7.68 (d, *J* = 7.8 Hz, 2H), 7.70 (s, 2H), 7.77-7.80 (dd, *J* = 2.2, 6.8 Hz, 4H), 8.02 (t, *J* = 8.1 Hz, 2H), 8.12 (dd, *J* = 8.3, 1.4 Hz, 2H). **^{13}C-NMR (acetonitrile-*d*$_3$, 101 MHz):** *δ* 15.5, 28.1, 28.8, 50.6, 67.6, 70.3, 84.3, 116.2, 116.4, 126.3, 128.1, 128.5, 129.2, 131.4, 132.5, 141.2, 143.6, 144.9, 147.8, 155.9, 162.4. **IR (KBr):** *v* (cm^{-1}) 650, 828, 968, 1031, 1156, 1176, 1230, 1257, 1276, 1427, 1474, 1490, 1512, 1563, 1600, 1625, 2116, 3260. **MS (ESI) *m/z* (%):** 327.2 [$(M - 2CF_3SO_3^-)^{2+}$] (100), 327.7 (37), 328.2 (13), 653.3 (8), 803.3 (50), 804.3 [$(M - CF_3SO_3^-)^+$] (25), 805.3 (5). **HRMS ESI *m/z*:** calc. for [$(M - 2CF_3SO_3^-)^{2+}$] [$(C_{46}H_{42}O_2N_2)^{2+}$] 327.1618, found 327.1620.

(*E*)-6,7-dimethyl-11-(2-(5-phenylfuran-2-yl)vinyl)-4,5,8,9-tetrahydroisoquinolino[1,2-a] pyrido [1,2-k][2,9]phenanthroline-3,10-diium trifluoromethanesulfonate (67)

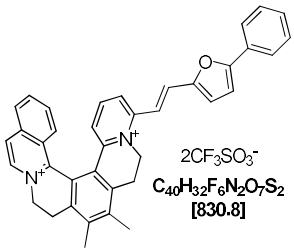

The synthesis and purification of helquat dye **67** was accomplished according to *general procedure 5.2.e*, using [6]helquat dye precursor **6** (20 mg, 0.030 mmol, 1.0 equiv.), 5-phenylfuran-2-carbaldehyde (77.5 mg, 0.450 mmol, 15.0 equiv.), pyrrolidine (30 µL, 26 mg,

0.366 mmol, 12.2 equiv.) in dry MeOH (2.0 mL) and [6[helquat dye **67** was obtained as a yellow solid.

Yield: 18.9 mg, 77%.

m.p. 230-232 °C. **^{1}H-NMR (acetonitrile-d_3, 400 MHz):** δ 2.55 (s, 3H), 2.56 (s, 3H), 3.05 (ddd, *J* = 4.9, 14.3, 17.1 Hz, 1H), 3.16 (ddd, *J* = 4.6, 14.6, 17.2 Hz, 1H), 3.54 (ddd, *J* = 1.8, 3.5, 17.2 Hz, 1H), 3.58 (ddd, *J* = 1.9, 3.8, 17.1 Hz, 1H), 4.70 (dt, *J* = 3.8, 14.0 Hz, 1H), 4.79 (dt, *J* = 3.5, 14.3 Hz, 1H), 5.01 (ddd, *J* = 1.8, 4.6, 13.9 Hz, 1H), 5.38 (ddd, *J* = 1.9, 4.9, 13.8 Hz, 1H), 6.86 (dd, *J* = 1.3, 8.1 Hz, 1H), 7.05 (s, 2H), 7.42-7.49 (m, 2H), 7.50-7.57 (m, 4H), 7.66 (ddd, *J* = 1.2, 6.9, 8.5 Hz, 1H), 7.76 (dd, *J* = 8.3, 1.3 Hz, 1H), 7.78 (dq, *J* = 0.9, 8.7 Hz, 1H), 7.88 (ddd, *J* = 1.1, 6.9, 8.2 Hz, 1H), 7.95-7.97 (m, 2H), 8.12 (dt, *J* = 0.8, 8.4 Hz, 1H), 8.29 (d, *J* = 7.6 Hz, 1H), 8.61 (d, *J* = 6.7 Hz, 1H). **^{13}C-NMR (acetonitrile-d_3, 101 MHz):** δ 17.0, 17.1, 25.9, 26.7, 50.3, 56.0, 110.1, 115.0, 120.9, 123.4, 124.9, 125.5, 125.6, 125.9, 126.9, 128.5, 128.5, 128.7, 129.2, 130.1, 130.5, 130.8, 132.8, 136.4, 136.5, 137.0, 138.5, 139.9, 141.1, 142.2, 142.3, 143.1, 148.2, 151.7, 154.6, 158.2. **IR:** *v* (cm^-) 518, 573, 638, 695, 1031, 1156, 1224, 1262, 1366, 1379, 1411, 1475, 1484, 1507, 1519, 1562, 1581, 1607, 1625. **MS (ESI) *m/z* (%):** 266.1 [(M – $2CF_3SO_3^-)^{2+}$] (100), 266.6 (43), 267.1 (7), 681.2 [(M – $2CF_3SO_3^-)^{2+}$] (5). **HRMS *m/z*:** calc. for [(M – $2CF_3SO_3^-)^{2+}$] [$(C_{38}H_{32}ON_2)^{2+}$] 266.1252, found 266.1253.

4,13-bis((*E*)-4-butoxystyryl)-6,7,10,11-tetrahydrodipyrido[2,1-a:1',2'-k][2,9] phenanthroline-5,12-diium trifluoromethanesulfonate (68)

$C_{46}H_{46}F_6N_2O_8S_2$
[933.0]

The synthesis and purification of [5]helquat dye **68** was accomplished according to *general procedure 5.2.e*, using dye precursor **10** (50 mg, 0.082 mmol, 1.0 equiv.), 4-butoxybenzaldehyde (219.2 mg, 1.230 mmol, 15.0 equiv.), pyrrolidine (100 µL, 86.6 mg, 1.218 mmol, 14.9 equiv.) in dry MeOH (5 mL) and [5]helquat dye **68** was obtained as a yellow solid.

Yield: 57.2 mg, 75%.

m.p. 231-233 °C. **^{1}H-NMR (acetonitrile-d_3, 400 MHz):** δ 0.99 (t, *J* = 7.4 Hz, 6H), 1.46-1.55 (m, 4H), 1.78 (p, *J* = 7.0 Hz, 4H), 3.08-3.34 (m, 4H), 4.09 (t, *J* = 6.5 Hz, 4H), 4.41-4.50 (m, 2H), 5.21-5.25 (m, 2H), 7.06 (dd, *J* = 2.0, 6.8 Hz, 4H), 7.43 (d, *J* = 15.9 Hz, 2H), 7.65 (d, *J* = 15.8 Hz, 2H), 7.67 (dd, *J* = 0.8, 8.0 Hz, 2H), 7.70 (s, 2H), 7.78 (dd, *J* = 2.0, 6.8 Hz, 4H), 8.01 (t, *J* = 8.1 Hz, 2H), 8.11 (dd, *J* = 8.2, 1.3 Hz, 2H). **^{13}C-NMR (acetonitrile-d_3, 101 MHz):** δ 14.1, 19.9, 28.1, 31.9, 50.6, 69.0, 116.1, 116.2, 126.3, 128.1, 128.3, 129.1, 131.4, 132.5, 141.2, 143.6, 144.9, 147.8, 156.0, 162.7. **IR (KBr):** *v* (cm^{-1}) 828, 970, 1031, 1156, 1176, 1227, 1257, 1277, 1427, 1474, 1490, 1512, 1563, 1600, 1623. **MS (ESI) *m/z* (%):** 185.1 (50), 227.1 (86), 228.1 (10), 317.2 [(M – $2CF_3SO_3^-)^{2+}$] (100), 317.7 (50), 318.2 (11), 783.3 [(M – $2CF_3SO_3^-)^{2+}$] (21), 784.3 (10). **HRMS ESI *m/z*:** calc. for [(M – $2CF_3SO_3^-)^{2+}$] [$(C_{44}H_{46}O_2N_2)^{2+}$] 317.17742, found 317.17716.

4,13-bis((*E*)-4-(hexyloxy)styryl)-6,7,10,11-tetrahydrodipyrido[2,1-a:1',2'-k][2,9]phenanthroline-5,12-diium trifluoromethanesulfonate (69)

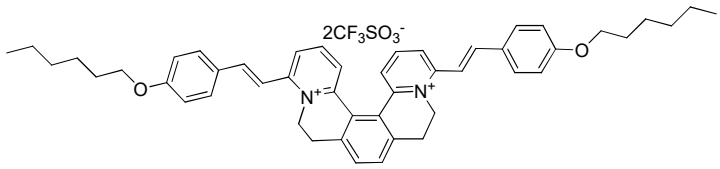

$C_{50}H_{54}F_6N_2O_8S_2$
[989.1]

The synthesis and purification of [5]helquat dye **69** was accomplished according to *general procedure 5.2.e*, using dye precursor **10** (50 mg, 0.082 mmol, 1.0 equiv.), 4-hexyloxybenzaldehyde (253.7 mg, 1.230 mmol, 15.0 equiv.), pyrrolidine (100 µL, 86.6 mg, 1.218 mmol, 14.9 equiv.) in dry MeOH (5 mL) and [5]helquat dye **69** was obtained as a yellow solid.

Yield: 61.3 mg, 76%.

m.p. 267-269 °C. **^{1}H-NMR (acetonitrile-d_3, 400 MHz):** δ 0.92 (t, J = 7.1 Hz, 6H), 1.29-1.54 (m, 12H), 1.79 (p, J = 6.8 Hz, 4H), 3.08-3.34 (m, 4H), 4.08 (t, J = 6.6 Hz, 4H), 4.41-4.50 (m, 2H), 5.21-5.25 (m, 2H), 7.04 (d, J = 6.8 Hz, 2H), 7.06 (d, J = 6.8 Hz, 2H), 7.43 (d, J = 15.9 Hz, 2H), 7.65-7.69 (m, 4H), 7.70 (s, 2H), 7.76 (d, J = 6.8, 2H), 7.78 (d, J = 6.8 Hz, 2H), 8.01 (t, J = 8.1 Hz, 2H), 8.11 (dd, J = 1.4, 8.3 Hz, 2H). **^{13}C-NMR (acetonitrile-d_3, 101 MHz):** δ 14.3, 23.3, 26.4, 28.1, 29.8, 32.3, 50.6, 69.3, 116.1, 116.2, 126.3, 128.3, 129.1, 131.4, 131.5, 132.5, 141.2, 143.6, 145.0, 147.8, 156.0, 162.7. **IR (KBr):** ν (cm^{-1}) 513, 573, 639, 755, 828, 969, 1031, 1156, 1176, 1229, 1256, 1276, 1427, 1474, 1490, 1513, 1563, 1600, 1623, 1870, 2934, 2954.

MS (ESI) *m/z* (%): 261.1 (5), 303.2 (5), 345.2 [$(M - 2CF_3SO_3^-)^{2+}$] (100), 345.7 (53), 346.2 (14), 689.4 [$(M - 2CF_3SO_3^-)^{2+}$] (4), 839.4 [$(M - CF_3SO_3^-)^{+}$] (45), 840.4 (25), 841.4 (7). **HRMS ESI *m/z*:** calc. for [$(M - 2CF_3SO_3^-)^{2+}$] [$(C_{48}H_{54}O_2N_2)^{2+}$] 345.2087, found 345.2088.

4,13-bis((*E*)-2-(benzyloxy)styryl)-6,7,10,11-tetrahydrodipyrido[2,1-a:1',2'-k][2,9]phenanthroline-5,12-diium trifluoromethanesulfonate (70)

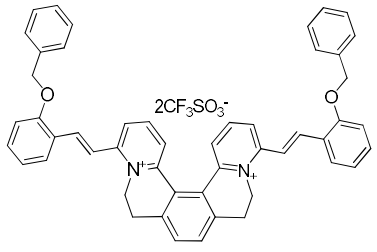

$C_{52}H_{42}F_6N_2O_8S_2$
[1001.0]

The synthesis and purification of [5]helquat dye **70** was accomplished according to *general procedure 5.2.e*, using dye precursor **10** (50 mg, 0.082 mmol, 1.0 equiv.), 2-benzyloxybenzaldehyde (261.0 mg, 1.230 mmol, 15.0 equiv.), pyrrolidine (100 µL, 86.6 mg, 1.218 mmol, 14.9 equiv.) in dry MeOH (5 mL) and [5]helquat dye **70** was obtained as a lemon yellow solid.

Yield: 76.0 mg, 93%.

m.p. 311-313 °C. **^{1}H-NMR (acetonitrile-d_3, 400 MHz):** δ 2.83–3.28 (m, 4H), 4.14-4.22 (m, 2H), 4.91-4.96 (m, 2H), 5.28 (s, 4H), 7.13 (td, J = 0.9, 7.5 Hz, 2H), 7.25 (dd, J = 0.9, 8.5 Hz, 2H), 7.37-7.52 (m, 8H), 7.57-7.60 (m, 4H), 7.64 (d, J = 7.8 Hz, 2H), 7.70 (s, 2H), 7.73 (d, J = 16.0 Hz, 2H), 7.76 (dd, J = 1.6, 7.7 Hz, 2H), 7.83 (d, J = 16.0 Hz, 2H), 8.00 (t, J = 8.1 Hz, 2H), 8.08 (dd, J = 1.4, 8.2 Hz, 2H). **^{13}C-NMR (acetonitrile-d_3, 101 MHz):** δ 28.0, 50.3, 71.6, 114.1, 120.2, 122.3, 124.5, 126.4, 127.6, 129.3, 129.4, 129.4, 129.8, 131.8, 132.6, 133.5, 137.7, 140.9,

141.0, 143.9, 147.8, 156.1, 158.9. **IR (KBr):** *v* (cm^{-1}) 513, 573, 639, 755, 828, 969, 1031, 1156, 1176, 1229, 1256, 1276, 1427, 1474, 1490, 1513, 1563, 1600, 1623, 1870, 2934, 2954. **MS (ESI) *m/z* (%):** 185.1 (25), 227.1 (86), 228.1 (8), 351.2 [$(M - 2CF_3SO_3^-)^{2+}$] (100), 351.7 (52), 352.2 (14), 701.3 (5), 851.3 [$(M - CF_3SO_3^-)^+$] (21), 852.3 (11). **HRMS ESI *m/z*:** calc. for [$(M - 2CF_3SO_3^-)^{2+}$] [$(C_{50}H_{42}O_2N_2)^{2+}$] 351.16177, found 351.16200.

4,13-bis((*E*)- 2,4,5-trimethoxystyryl -6,7,10,11-tetrahydrodipyrido[2,1-a:1',2'-k][2,9] phenanthroline-5,12-diium trifluoromethanesulfonate (71)

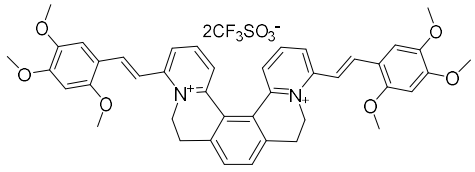

$C_{44}H_{42}F_6N_2O_{12}S_2$
[968.9]

The synthesis and purification of [5]helquat dye **71** was accomplished according to *general procedure 5.2.e*, using dye precursor **10** (50 mg, 0.082 mmol, 1.0 equiv.), 2,4,5-trimethoxybenzaldehyde (241.3 mg, 1.230 mmol, 15.0 equiv.), pyrrolidine (100 µL, 86.6 mg, 1.218 mmol, 14.9 equiv.) in dry MeOH (5 mL) and [5]helquat dye **71** was obtained as a yellow solid.

Yield: 67.2 mg, 85%.

m.p. 298-300 °C. **^{1}H-NMR (acetonitrile-d_3, 400 MHz):** δ 3.10-3.33 (m, 4H), 3.89 (s, 6H), 3.94 (s, 6H), 3.96 (s, 6H), 4.42-4.51 (m, 2H), 5.20-5.23 (m, 2H), 6.74 (s, 2H), 7.34 (s, 2H), 7.52 (d, *J* = 15.9 Hz, 2H), 7.64 (dd, *J* = 1.3, 8.0 Hz, 2H), 7.69 (s, 2H), 7.91 (d, *J* = 15.9 Hz, 2H), 7.98 (t, *J* = 8.1 Hz, 2H), 8.09 (dd, *J* = 8.3, 1.4 Hz, 2H). **^{13}C-NMR (101 MHz, acetonitrile-d_3):** δ 28.2, 50.4, 56.8, 57.2, 57.3, 98.4, 112.5, 115.7, 116.1, 126.1, 128.2, 128.7, 132.4, 140.1, 141.2, 143.3, 144.7, 147.6, 154.7, 155.7, 156.5. **IR (KBr):** *v* (cm^{-1}) 969, 1031, 1152, 1230, 1265, 1440, 1458, 1472, 1489, 1510, 1558, 1602, 1621, 2837. **MS (ESI) *m/z* (%):** 227.1 (5), 320.1 (5), 335.2 [$(M - 2CF_3SO_3^-)^{2+}$] (100), 335.7 (46), 819.3 [$(M - CF_3SO_3^-)^+$] (18), 820.3 (8). **HRMS ESI *m/z*:** calc. for [$(M - 2CF_3SO_3^-)^{2+}$] [$(C_{42}H_{42}O_6N_2)^{2+}$] 335.15160, found 335.15164.

(*E*)-11-(2-(benzo[b]thiophen-3-yl)vinyl)-6,7-dimethyl-4,5,8,9-tetrahydroisoquinolino[1,2-a] pyrido[1,2-k][2,9]phenanthroline-3,10-diium trifluoromethanesulfonate (72)

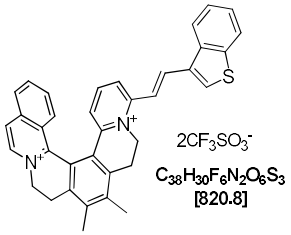

$C_{38}H_{30}F_6N_2O_6S_3$
[820.8]

The synthesis and purification of [6]helquat dye **72** was accomplished by using helquat dye precursor **6** (20 mg, 0.030 mmol, 1.0 equiv.), benzo[b]thiophene-3-carbaldehyde (73 mg, 0.450 mmol, 15.0 equiv.), pyrrolidine (30 µL, 26 mg, 0.366 mmol, 12.2 equiv.) in dry MeOH (2.0 mL) and helquat dye **72** was obtaind as a yellow solid.

Yield: 16 mg, 66%.

m.p. 286-288 °C. **^{1}H-NMR (400 MHz, acetonitrile-d_3):** δ 2.54 (s, 3H), 2.55 (s, 3H), 3.05 (ddd, *J* = 4.9, 14.3, 17.1 Hz, 1H), 3.16 (ddd, *J* = 4.6, 14.6, 17.2 Hz, 1H), 3.54 (ddd, *J* = 1.8, 3.5, 17.2 Hz, 1H), 3.58 (ddd, *J* = 1.9, 3.8, 17.1 Hz, 1H), 4.70 (dt, *J* = 3.8, 14.0 Hz, 1H), 4.79 (dt, *J* = 3.5, 14.3 Hz, 1H), 5.01 (ddd, *J* = 1.8, 4.6, 13.9 Hz, 1H), 5.38 (ddd, *J* = 1.9, 4.9, 13.8 Hz, 1H), 6.93 (dd, *J* =

1.3, 8.1 Hz, 1H), 7.50 (ddd, *J* = 1.2, 6.9 Hz, 1H), 7.57 (dd, *J* = 1.1, 7.1 Hz, 1H), 7.59 (dd, *J* = 1.1, 7.1 Hz, 1H), 7.68 (ddd, *J* = 1.2, 7.0 Hz, 1H), 7.72 (d, *J* = 16.0 Hz, 1H), 7.80 (dq, *J* = 1.0, 8.7 Hz, 1H), 7.87 (d, *J* = 0.8 Hz, 1H), 7.89-7.90 (m, 1H), 7.91 (dd, *J* = 1.2, 3.8 Hz, 1H), 8.05 (dq, *J* = 0.7, 8.06 Hz, 1H), 8.13 (d, *J* = 8.3 Hz, 1H), 8.22 (dt, *J* = 1.0, 7.8 Hz, 1H), 8.29 (d, *J* = 6.6 Hz, 1H), 8.31 (d, *J* = 6.6 Hz, 1H), 8.62 (d, *J* = 6.8 Hz, 1H). **^{13}C-NMR (101 MHz, acetonitrile-d_3):** δ 17.0, 17.2, 25.9, 26.7, 50.6, 56.0, 119.4, 120.6, 123.5, 123.7, 125.7, 125.9, 126.4, 126.9, 128.1, 128.4, 129.2, 129.2, 131.4, 132.8, 136.4, 137.0, 138.3, 138.6, 139.9, 140.6, 140.8, 141.3, 141.5, 142.3, 142.4, 143.7, 148.5, 149.5, 151.6, 154.0. **IR:** *v* (cm^-) 735, 818, 1031, 1157, 1224, 1263, 1379, 1411, 1461, 1483, 1505, 1556, 1573, 1608, 1625. **MS (ESI) *m/z* (%):** 261.1 [(M – $2CF_3SO_3^-$)$^{2+}$] (100), 261.6 (43), 262.1 (5), 521.2 (10), 671.2 [(M – $CF_3SO_3^-$)$^+$] (55), 672.2 (23), 673.3 (5). **HRMS *m/z*:** calc. for [(M – $2CF_3SO_3^-$)$^{2+}$] [($C_{36}H_{30}N_2S$)$^{2+}$] 261.1059, found 261.1060.

(*E*)-11-(4-(allyloxy)styryl)-6,7-dimethyl-4,5,8,9-tetrahydroisoquinolino[1,2-a]pyrido[1,2-k][2,9] phenanthroline-3,10-diium trifluoromethanesulfonate (73)

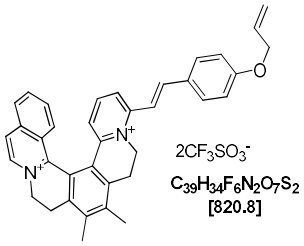

The synthesis and purification was accomplished according to *general procedure 5.2.e,* using [6]helquat dye precursor **6** (20 mg, 0.030 mmol, 1.0 equiv.), 4-(allyloxy)benzaldehyde (73 mg, 0.450 mmol, 15.0 equiv.), pyrrolidine (30 µL, 26 mg, 0.366 mmol, 12.2 equiv.) in dry MeOH (2.0 mL) and [6]helquat dye **73** was obtained as a yellow solid.
Yield: 18 mg, 74%.
m.p. 234-236 °C. **^{1}H-NMR (400 MHz, acetonitrile-d_3):** δ 2.54 (s, 3H), 2.55 (s, 3H), 3.05 (ddd, *J* = 4.9, 14.3, 17.1 Hz, 1H), 3.16 (ddd, *J* = 4.6, 14.6, 17.2 Hz, 1H), 3.54 (ddd, *J* = 1.8, 3.5, 17.2 Hz, 1H), 3.58 (ddd, *J* = 1.9, 3.8, 17.1 Hz, 1H), 4.67 (t, *J* = 1.5, 5.3 Hz, 2H), 4.70 (dt, *J* = 3.8, 14.0 Hz, 1H), 4.79 (dt, *J* = 3.5, 14.3 Hz, 1H), 5.01 (ddd, *J* = 1.8, 4.6, 13.9 Hz, 1H), 5.32 (dq, *J* = 1.5, 11.0 Hz, 1H), 5.38 (ddd, *J* = 1.9, 4.9, 13.8 Hz, 1H), 5.45 (dq, *J* = 1.7, 17.0 Hz, 1H), 6.06-6.15 (m, 1H), 6.81-6.86 (m, 1H), 7.09 (dd, *J* = 2.2, 6.7 Hz, 2H), 7.45-7.52 (m, 2H), 7.56 (d, *J* = 16.0 Hz, 1H), 7.61-7.66 (m, 1H), 7.75-7.79 (m, 4H), 7.87 (ddd, *J* = 1.1, 6.9, 8.2 Hz, 1H), 8.11 (d, *J* = 8.3 Hz, 1H), 8.30 (d, *J* = 6.7 Hz, 1H), 8.60 (dd, *J* = 3.9, 6.8 Hz, 1H). **^{13}C-NMR (acetonitrile-d_3, 101 MHz):** δ 17.0, 17.2, 25.9, 26.7, 50.3, 56.0, 69.8, 116.0, 116.4, 123.4, 125.2, 125.9, 126.9, 128.4, 128.5, 128.6, 128.7, 129.2, 131.4, 132.7, 134.2, 136.4, 136.9, 138.6, 139.9, 141.0, 142.2, 142.3, 143.3, 145.1, 148.1, 151.7, 155.3, 162.2. **IR:** *v* (cm^-) 735, 818, 1031, 1157, 1224, 1263, 1379, 1411, 1461, 1483, 1505, 1556, 1573, 1608, 1625. **MS (ESI) *m/z* (%):** 240.6 (58), 261.6 (22), 521.3 (40), 522.3 [(M – $2CF_3SO_3^-$)$^{2+}$] (16), 671.2 [(M – $CF_3SO_3^-$)$^+$] (100), 672.3 (40), 673.2 (10). HRMS m/z: calc. for [(M – $2CF_3SO_3^-$)$^{2+}$] [($C_{37}H_{33}ON_2$)$^{2+}$] 521.2587, found 521.2587.

(*E*)-4-(2-(4-methylnaphthalen-1-yl)vinyl)-6,7,10,11-tetrahydrodipyrido[2,1-a:1',2'-k][2,9] phenanthroline-5,12-diium trifluoromethanesulfonate (74)

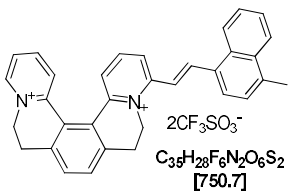

The synthesis and purification of [5]helquat dye **74** was accomplished according to *general procedure 5.2.e*, using dye precursor **14** (50 mg, 0.084 mmol, 1.0 equiv.), 4-methyl-1-naphthylaldehyde (214.4 mg, 1.260 mmol, 15.0 equiv.), pyrrolidine (103.4 µL, 89.6 mg, 1.260 mmol, 15.0 equiv.) in dry MeOH (5.0 mL) and dye **74** was obtained as a yellow solid.
Yield: 52.0 mg, 83%.
m.p. 294-296 °C. **^{1}H-NMR (acetonitrile-d_3, 400 MHz):** δ 2.78 (s, 3H), 3.23-3.33 (m, 4H), 4.50-4.54 (m, 1H), 4.82-4.90 (m, 2H), 5.28-5.31 (m, 1H), 7.54 (d, *J* = 7.4 Hz, 1H), 7.66-7.72 (m, 3H), 7.73 (s, 2H), 7.81 (dd, *J* = 8.1, 1.4 Hz, 1H), 7.90 (ddd, *J* = 7.7, 6.1, 1.4 Hz, 1H), 7.95 (dd, *J* = 1.2, 8.3 Hz, 1H), 8.04 (d, *J* = 7.4 Hz, 1H), 8.13 (t, *J* = 8.1 Hz, 1H), 8.17 (dd, *J* = 1.9, 7.8 Hz, 1H), 8.20 (dd, *J* = 1.9, 7.8 Hz, 1H), 8.31 (dd, *J* = 8.2, 1.4 Hz, 1H), 8.37-8.41 (m, 1H), 8.49 (d, *J* = 15.6 Hz, 1H), 8.80 dd, *J* = 0.9, 6.2 Hz, 1H). **^{13}C-NMR (acetonitrile-d_3, 101 MHz):** δ 20.0, 28.0, 28.1, 50.1, 56.1, 120.9, 124.8, 126.1, 126.7, 127.1, 127.4, 127.4, 127.5, 127.6, 128.0, 128.1, 129.6, 131.2, 131.3, 132.3, 133.1, 133.1, 133.7, 139.6, 141.5, 141.5, 142.2, 144.2, 145.8, 146.7, 147.7, 148.0, 155.7. **IR:** *v* (cm^-) 763, 836, 1031, 1160, 1226, 1259, 1272, 1478, 1490, 1511, 1565, 1580, 1595, 1612, 1624. **MS (ESI) *m/z* (%):** 226.1 [$(M - 2CF_3SO_3^-)^{2+}$] (100), 226.6 (37), 227.1 (23), 451.2 [$(M - 2CF_3SO_3^-)^{2+}$] (8), 601.2 [$(M - CF_3SO_3^-)^+$] (55), 602.2 (21). **HRMS *m/z*:** calc. for [$(M - 2CF_3SO_3^-)^{2+}$] [$(C_{33}H_{28}N_2)^{2+}$] 226.1121, found 226.1122.

(*E*)-4-(2-(naphthalen-2-yl)vinyl)-6,7,10,11-tetrahydrodipyrido[2,1-a:1',2'-k][2,9] phenanthroline-5,12-diium trifluoromethanesulfonate (75)

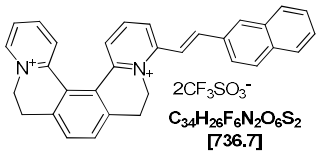

A reaction mixture of helquat dye precursor **14** (25 mg, 0.042 mmol, 1.0 equiv.), 2-naphthylaldehyde (32.8 mg, 0.210 mmol, 5.0 equiv.), EtOH (1 mL) and pyrrolidine (10.4 µL, 9.0 mg, 0.126 mmol, 3.0 equiv.) was placed into a sealed microwave glass tube and was heated in a microwave reactor at 70 °C 5 minutes (microwave power = 150 W). After 5 minutes, TLC analysis (mobile phase: Stoddart's magic mixture) has shown complete consumption of starting helquat **14.** The reaction was quenched by addition of Et_2O (8.0 mL). After centrifugation for 5 minutes, supernatant was separated and the compound was further purified according to the *general procedure 5.2.e*. After drying of the solid under high vacuum, helquat dye **75** was obtained as a greenish yellow solid.
Yield: 27.1 mg, 88.0%.
m.p. 294-296 °C. **^{1}H-NMR (DMSO-d_6, 400 MHz):** δ 3.20-3.29 (m, 2H), 3.34-3.41 (m, 2H), 4.52 (t, *J* = 13.9 Hz, 1H), 4.85 (t, *J* = 13.5 Hz, 1H), 5.05 (d, *J* = 13.0 Hz, 1H), 5.47 (d, *J* = 13.3 Hz, 1H), 7.63 (t, *J* = 9.4 Hz, 1H), 7.65 (dd, *J* = 1.4, 7.4 Hz, 1H), 7.79 (d, *J* = 7.9 Hz, 1H), 7.82 (d, *J* = 7.9 Hz, 1H), 7.97-8.11 (m, 6H), 8.13 (dd, *J* = 1.3, 8.1 Hz, 1H), 8.18-8.38 (m, 5H), 8.47 (dd, *J* = 1.4, 8.2 Hz, 1H), 9.20 (d, *J* = 5.9 Hz, 1H). **^{13}C-NMR (DMSO-d_6, 101 MHz):** δ 26.8, 28.9, 49.4, 54.3, 118.1, 119.1, 122.3, 124.1, 125.3, 126.2, 126.3, 127.1, 127.7, 127.8, 128.2, 128.6, 128.7, 129.6, 130.3, 131.6, 131.7, 132.6, 132.9, 133.9, 140.2, 142.6, 143.4, 144.1, 145.8, 146.4, 146.5, 153.6. **IR:** *v* (cm^-) 518, 573, 637, 755, 793, 825, 1031, 1177, 1260, 1363, 1436, 1509, 1564, 1595, 1624. **MS (ESI) *m/z* (%):** 219.1 [$(M - 2\ CF_3SO_3^-)^{2+}$] (100), 219.6 (42), 437.2 (35), 438.3 (16), 469.2 (10), 587.2 (11). **HRMS ESI *m/z*:** calc. for [$(M - 2\ CF_3SO_3^-)^{2+}$] [$(C_{32}H_{26}N_2)^{2+}$] 219.1043, found 219.1043.

(*E*)-1-methyl-4-(2-(naphthalen-1-yl)vinyl)pyridin-1-ium iodide (76)

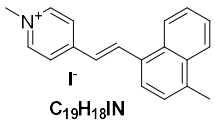

$C_{19}H_{18}IN$
[387.3]

Synthesis and purification of dye **76** as a dark yellow solid was accomplished using *general procedure 5.2.f. method 2.*

Yield: 43 mg, 87%.

m.p. 239-241 °C. **^{1}H-NMR (DMSO-d_6, 400 MHz):** δ 2.72 (s, 3H), 4.28 (s, 3H), 7.51 (dd, *J* = 1.0, 7.5 Hz, 1H), 7.58 (d, *J* = 16.0 Hz, 1H), 7.63-7.72 (m, 2H), 8.01 (d, *J* = 7.5 Hz, 1H), 8.08-8.14 (m, 1H), 8.42 (d, *J* = 6.6 Hz, 2H), 8.55-8.64 (m, 1H), 8.81 (d, *J* = 16.0 Hz, 1H), 8.89 (d, *J* = 6.4 Hz, 2H). **^{13}C-NMR (DMSO-d_6, 101 MHz):** δ 19.5, 46.9, 123.8, 124.2, 124.7, 124.8, 124.9, 126.4, 126.7, 130.4, 130.7, 131.1, 132.3, 137.0, 137.5, 145.0, 152.5. **IR:** *v* (cm^-) 757, 820, 1158, 1189, 1442, 1519, 1595, 1575, 1617, 1640. **MS (ESI) *m/z* (%):** 260.1 (100), 261.2 (25). **HRMS ESI *m/z*:** calc. for $[(M - I^-)^+]$ $[(C_{19}H_{18}N)^+]$: 260.1434, found: 260.1432.

(*E*)-1-methyl-2-(2-(naphthalen-1-yl)vinyl)pyridin-1-ium iodide (77)

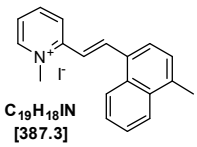

$C_{19}H_{18}IN$
[387.3]

Synthesis and purification of dye **77** as a lemon yellow solid was accomplished using *general procedure 5.2.f. method 2.*

Yield: 43 mg, 87%.

m.p. 271-273 °C. **^{1}H-NMR (DMSO-d_6, 400 MHz):** δ 2.74 (s, 3H), 4.42 (s, 3H), 7.54 (d, *J* = 7.5 Hz, 1H), 7.63 (d, *J* = 15.8 Hz, 1H), 7.65-7.71 (m, 2H), 7.94 (ddd, *J* = 1.4, 6.1, 7.6 Hz, 1H), 8.05-8.21 (m, 2H), 8.48-8.60 (m, 2H), 8.74 (d, *J* = 15.7 Hz, 1H), 8.83 (dd, *J* = 1.4, 8.4 Hz, 1H), 8.94 (dd, *J* = 1.4, 6.3 Hz, 1H). **^{13}C-NMR (DMSO- d_6, 101 MHz):** δ 19.5, 46.9, 119.1, 124.2, 124.9, 125.2, 125.5, 125.6, 126.4, 126.6, 126.8, 130.2, 131.1, 132.3, 137.8, 139.4, 144.2, 146.0, 152.2. **IR:** *v* (cm^-) 741, 803, 1148, 1178, 1462, 1511, 1575, 1610, 1618, 1640. **MS (ESI) *m/z* (%):** 260.1 $[(M - I^-)^+]$ (100), 261.2 (23). **HRMS ESI *m/z*:** calc. for $[(M - I^-)^+]$ $[(C_{19}H_{18}N)]$ 260.1434, found 260.1435.

4,13-bis((*E*)-4-ethoxystyryl)-6,7,10,11-tetrahydrodipyrido[2,1-a:1',2'-k][2,9] phenanthroline-5,12-diium trifluoromethanesulfonate (78)

$C_{42}H_{38}F_6N_2O_8S_2$
[876.9]

Synthesis and purification of [5]helquat dye **78** following *general procedure 5.2.e*, using dye precursor **10** (50 mg, 0.082 mmol, 1.0 equiv.), 4-ethoxybenzaldehyde (184.7 mg, 1.230 mmol, 15.0 equiv.), pyrrolidine (100 µL, 86.6 mg, 1.218 mmol, 14.9 equiv.) in dry MeOH (5 mL) gave **78** as a yellow solid after purification and drying of the solid.

Yield: 63 mg, 88%.

m.p. 213-215 °C. **^{1}H-NMR (acetonitrile-d_3, 400 MHz):** δ 1.41 (t, *J* = 7.0 Hz, 6H), 3.03-3.36 (m, 4H), 4.14 (q, *J* = 7.0 Hz, 4H), 4.43-4.50 (m, 2H), 5.21-5.26 (m, 2H), 7.03 (dd, *J* = 2.0, 6.7 Hz, 2H), 7.05 (dd, *J* = 2.0, 6.7 Hz, 2H), 7.44 (d, *J* = 15.9 Hz, 2H), 7.66 (d, *J* = 15.9 Hz, 2H), 7.67-7.69

(m, 2H), 7.70 (s, 2H), 7.77 (dd, *J* = 2.0, 6.7 Hz, 2H), 7.79 (dd, *J* = 2.0, 6.7 Hz, 2H), 8.02 (t, *J* = 8.1 Hz, 2H), 8.11 (dd, *J* = 1.4, 8.2 Hz, 2H). **^{13}C-NMR (acetonitrile-*d*$_3$, 101 MHz):** *δ* 15.0, 28.1, 50.6, 64.8, 116.1, 116.2, 122.7, 126.3, 128.1, 128.3, 129.1, 131.4, 132.5, 141.2, 145.0, 147.8, 156.0, 162.5. **IR:** *v* (cm^{-}) 518, 573, 638, 755, 827, 1031, 1155, 1177, 1225, 1230, 1256, 1276, 1427, 1475, 1490, 1513, 1564, 1600, 1624, 3074. **MS (ESI) *m/z* (%):** 246.1 (5), 261.1 (24), 275.1 (29), 289.1 [(M – 2$CF_3SO_3^-$)$^{2+}$] (100), 289.6 (43), 290.1 (8), 577.3 (8), 727.2 [(M – $CF_3SO_3^-$)$^{+}$] (36) 728.2 (15). **HRMS ESI *m/z*:** calc. for [(M – 2$CF_3SO_3^-$)$^{2+}$] [($C_{40}H_{38}O_2N_2$)$^{2+}$] 289.14612, found 289.14627.

4,13-bis((*E*)-4-butoxy-3-methoxystyryl)-6,7,10,11-tetrahydrodipyrido[2,1-a:1',2'-k][2,9] phenanthroline-5,12-diium trifluoromethanesulfonate (79)

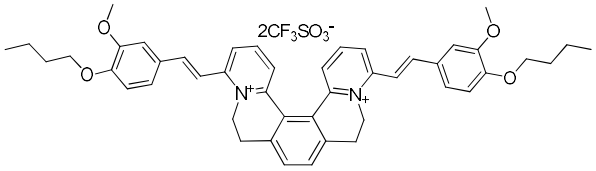

$C_{48}H_{50}F_6N_2O_{10}S_2$
[993.0]

Synthesis and purification of dye **79** using dye precursor **10** (25 mg, 0.041 mmol, 1.0 equiv.), 4-butyloxy-3-methoxybenzaldehyde (128.1 mg, 0.615 mmol, 15.0 equiv.), pyrrolidine (50 µL, 43.3 mg, 0.609 mmol, 14.9 equiv.) in dry MeOH (2.5 mL) was accomplished and [5]helquat dye **79** was obtained as a lemon yellow solid.

Yield: 14.2 mg, 35%.

m.p. 219-221 °C. **^{1}H-NMR (acetonitrile-*d*$_3$, 400 MHz):** *δ* 0.99 (t, *J* = 7.4 Hz, 6H), 1.42-1.58 (m, 4H), 1.79 (dq, *J* = 6.6, 8.5 Hz, 4H), 3.03-3.38 (m, 4H), 3.94 (s, 6H), 4.09 (t, *J* = 6.6 Hz, 4H), 4.43-4.50 (m, 2H), 5.21-5.26 (m, 2H), 7.05 (d, *J* = 8.4 Hz, 2H), 7.34 (dd, *J* = 2.1, 8.4 Hz, 2H), 7.43 (d, *J* = 2.1 Hz, 2H), 7.46 (d, *J* = 15.9 Hz, 2H), 7.65 (d, *J* = 15.9 Hz, 2H), 7.69 (d, *J* = 1.3 Hz, 2H), 7.71 (s, 2H), 8.02 (t, *J* = 8.1 Hz, 2H), 8.12 (dd, *J* = 8.3, 1.4 Hz, 2H). **^{13}C-NMR (acetonitrile-*d*$_3$, 101 MHz):** *δ* 14.1, 20.0, 28.1, 31.9, 50.6, 56.7, 69.5, 111.4, 113.6, 116.3, 124.8, 126.3, 128.1, 128.5, 129.1,132.5, 141.3, 143.6, 145.3, 147.8, 150.8, 152.7, 156.0. **IR:** *v* (cm^{-}) 518, 573, 638, 755, 827, 1031, 1155, 1177, 1225, 1230, 1256, 1276, 1427, 1475, 1490, 1513, 1564, 1600, 1624, 3074. **MS (ESI) *m/z* (%):** 347.2 [(M – 2$CF_3SO_3^-$)$^{2+}$] (100), 347.7 (57), 348.2 (15), 807.4 (8), 843.3 [(M – $CF_3SO_3^-$)$^{+}$] (29), 844.4 (15). **HRMS ESI *m/z*:** calc. for [(M – 2$CF_3SO_3^-$)$^{2+}$] [($C_{46}H_{50}O_4N_2$)$^{2+}$] 347.18798, found 347.18807.

4,13-bis((*E*)-4-heptyloxy-3-methoxystyryl)-6,7,10,11-tetrahydrodipyrido[2,1-a:1',2'-k][2,9] phenanthroline-5,12-diium trifluoromethanesulfonate (80)

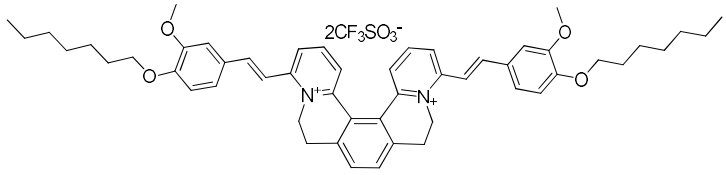

$C_{54}H_{62}F_6N_2O_{10}S_2$
[1077.2]

Synthesis and purification of dye **80** using dye precursor **10** (25 mg, 0.041 mmol, 1.0 equiv.), 4-heptyloxy-3-methoxybenzaldehyde (154 mg, 0.615 mmol, 15.0 equiv.), pyrrolidine (50 µL, 43.3 mg, 0.609 mmol, 14.9 equiv.) in dry MeOH (5 mL) was accomplished according to *general procedure 5.2.e* and [5]helquat dye **80** was obtained as a yellow solid.

Yield: 15 mg, 34%.

m.p. 219-221 °C. **^{1}H-NMR (acetonitrile-*d*$_3$, 400 MHz):** *δ* 0.90 (t, *J* = 7.4 Hz, 6H), 1.27-1.53 (m, 16H), 1.73-1.87 (m, 4H), 3.03-3.38 (m, 4H), 3.94 (s, 6H), 4.09 (t, *J* = 6.6 Hz, 4H), 4.43-4.50 (m,

2H), 5.21-5.26 (m, 2H), 7.05 (d, *J* = 8.4 Hz, 2H), 7.34 (dd, *J* = 2.1, 8.4 Hz, 2H), 7.43 (d, *J* = 2.1 Hz, 2H), 7.46 (d, *J* = 15.9 Hz, 2H), 7.65 (d, *J* = 15.9 Hz, 2H), 7.69 (d, *J* = 1.3 Hz, 2H), 7.71 (s, 2H), 8.02 (t, *J* = 8.1 Hz, 2H), 8.12 (dd, *J* = 8.3, 1.4 Hz, 2H). **^{13}C-NMR (acetonitrile-d_3, 101 MHz):** *δ* 14.4, 23.3, 26.7, 28.1, 29.7, 29.9, 32.5, 50.6, 56.7, 69.8, 111.4, 113.6, 116.3, 124.8, 126.3, 128.1, 128.5, 129.1,132.5, 141.3, 143.6, 145.3, 147.8, 150.8, 152.7, 156.0. **IR:** *v* (cm^-) 518, 573, 638, 755, 827, 1031, 1155, 1177, 1225, 1230, 1256, 1276, 1427, 1475, 1490, 1513, 1564, 1600, 1624, 3074. **MS (ESI) *m/z* (%):** 389.2 [$(M - 2CF_3SO_3^-)^{2+}$] (100), 389.7 (67), 390.2 (23), 891.5 [$(M - 2CF_3SO_3^-)^{2+}$] (10), 927.4 [$(M - CF_3SO_3^-)^+$] (14). **HRMS *m/z*:** calc. for [$(M - 2CF_3SO_3^-)^{+2}$] [$(C_{52}H_{62}O_4N_2)^{2+}$] 389.2349, found 389.2351.

2,15-bis((E)-4-ethoxy-3-methoxystyryl)-6,7,10,11-tetrahydrodipyrido[2,1-a:1',2'-k][2,9] phenanthroline-5,12-diium trifluoromethanesulfonate (86)

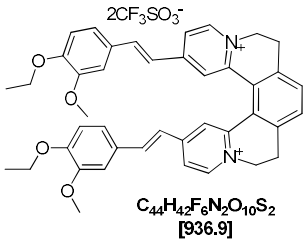

Synthesis and purification of dye **86** using dye precursor **81** (50 mg, 0.082 mmol, 1.0 equiv.), 4-ethoxy-3-methoxybenzaldehyde (221.6 mg, 1.230 mmol, 15.0 equiv.), pyrrolidine (100 µL, 86.6 mg, 1.218 mmol, 14.9 equiv.) in dry MeOH (5 mL) was accomplished according to *general procedure 5.2.e* and [5]helquat dye **86** was obtained as lemon yellow solid.
Yield: 0.052 g, 68.0%.
m.p. 280-282 °C. **^{1}H-NMR (DMSO-d_6, 400 MHz):** *δ* 1.33 (t, *J* = 7.0 Hz, 6H), 3.33-3.36 (m, 4H), 3.76 (s, 6H), 4.04 (q, *J* = 7.0 Hz, 4H), 4.66-4.74 (m, 2H), 4.93-4.99 (m, 2H), 6.98 (d, *J* = 1.0 Hz, 4H), 7.03 (d, *J* = 16.0 Hz, 2H), 7.06 (d, *J* = 1.2 Hz, 2H), 7.34 (d, *J* = 16.2 Hz, 2H), 7.79 (s, 2H), 8.08 (dd, *J* = 2.0, 6.6 Hz, 2H), 8.31 (d, *J* = 2.0 Hz, 2H), 9.08 (d, *J* = 6.6 Hz, 2H). **^{13}C-NMR (DMSO-d_6, 101 MHz):** *δ* 53.2, 66.8, 93.1, 94.6, 103.4, 149.1, 151.6, 159.2, 160.5, 162.5, 164.8, 165.6, 166.8, 171.6, 179.6, 180.8, 184.3, 185.4, 188.7, 190.4, 192.7. **IR:** *v* (cm^-) 517, 573, 638, 859, 1030, 1106, 1161, 1224, 1256, 1424, 1481, 1560, 1615, 1628, 2830. **MS (ESI) *m/z* (%):** 290.1 (10), 319.2 (53), 319.7 (23), 637.3 [$(M - 2CF_3SO_3^-)^{2+}$] (14), 787.3 [$(M - CF_3SO_3^-)^+$] (100), 788.3 (43), 815.3 (14). **HRMS *m/z*:** calc. for [$(M - 2CF_3SO_3^-)^{2+}$] [$(C_{42}H_{41}O_4N_2)^{2+}$] 638.30608, found 638.30624.

2,15-bis((E)-4-ethoxy-3-methoxystyryl)-8,9-dimethyl-6,7,10,11-tetrahydrodipyrido[2,1-a:1',2'-k][2,9]phenanthroline-5,12-diium trifluoromethanesulfonate (87)

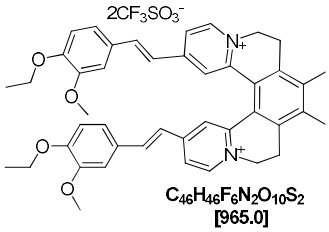

A reaction mixture containing helquat dye precursor **82** (25 mg, 0.039 mmol, 1.0 equiv.), 4-ethoxy-3-methoxybenzaldehyde (35.2 mg, 0.195 mmol, 5.0 equiv.), EtOH (1 mL) and pyrrolidine (9.6 µL, 8.3 mg, 0.117 mmol, 3.0 equiv.) was heated at 70 °C in a microwave reactor for 5 minutes (microwave power = 150 W). After 5 minutes, TLC analysis (mobile phase: Stoddart's magic mixture) has shown complete consumption of starting helquat **82.** The reaction was quenched by addition of Et_2O (8.0 mL). After centrifugation for 5 minutes,

supernatant was separated and the compound was further purified by *general procedure 5.2.e,* followed by drying under high vacuum gave **87** as a yellow solid.

Yield: 29 mg, 77.0%.

m.p. 280-282 °C. **^{1}H-NMR (DMSO-d_6, 400 MHz):** δ 1.37 (t, J = 7.0 Hz, 6H), 2.45 (s, 6H), 3.00-3.16 (m, 2H), 3.32-3.55 (m, 2H), 3.81 (s, 6H), 4.07 (q, J = 7.0 Hz, 4H), 4.68 (td, J = 3.7, 13.7, 14.1 Hz, 1H), 4.70 (td, J = 14.1, 13.7, 3.7 Hz, 1H), 4.84 (dd, J = 13.4, 4.6 Hz, 1H), 4.86 (dd, J = 13.4, 4.6 Hz, 1H), 6.92 (d, J = 8.3 Hz, 2H), 6.98 (d, J = 16.2 Hz, 2H), 7.04 (dd, J = 2.1, 8.3 Hz, 2H), 7.09 (d, J = 2.0 Hz, 2H), 7.31 (d, J = 16.2 Hz, 2H), 7.76 (d, J = 1.9 Hz, 2H), 7.85 (dd, J = 2.0, 6.6 Hz, 2H), 8.59 (d, J = 6.6 Hz, 2H). **^{13}C-NMR (DMSO-d_6, 101 MHz):** δ 14.6, 16.4, 25.3, 52.9, 55.5, 63.8, 110.0, 112.5, 120.4, 122.3, 122.7, 124.3, 125.5, 127.5, 138.8, 139.4, 140.8, 144.6, 146.6, 149.1, 150.4, 152.1. **IR:** v (cm$^-$) 518, 573, 638, 735, 1030, 1143, 1226, 1265, 1424, 1467, 1476, 1512, 1565, 1612, 1631, 2855. **MS (ESI) *m/z* (%):** 333.2 [(M – $2CF_3SO_3^-$)$^{+2}$] (100), 333.8 (67), 334.3 (18), 665.5 [(M – $2CF_3SO_3^-$)$^{2+}$] (5), 815.6 (10). **HRMS *m/z*:** calc. for [(M – $2CF_3SO_3^-$)$^{2+}$] ($C_{44}H_{45}N_2O_4$) calc. 665.3374, found 665.3375.

2,4-bis((E)-4-ethoxy-3-methoxystyryl)-6,7,10,11-tetrahydrodipyrido[2,1-a:1',2'-k][2,9] phenanthroline-5,12-diium trifluoromethanesulfonate (88)

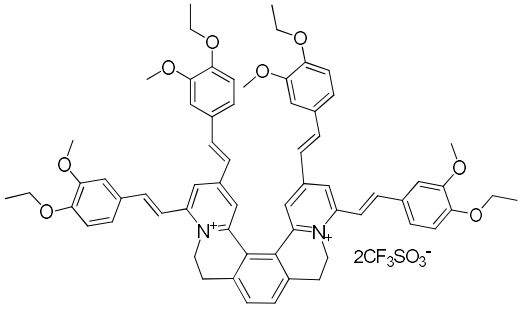

Synthesis and purification of dye **88** using dye precursor **83** (20 mg, 0.031 mmol, 1.0 equiv.), 4-ethoxy-3-methoxybenzaldehyde (167.6 mg, 0.930 mmol, 30.0 equiv.)**,** pyrrolidine (50 µL, 43.3 mg, 0.609 mmol, 19.6 equiv.) in dry MeOH (2 mL) was accomplished according to *general procedure 5.2.e* and [5]helquat dye **88** was obtained as yellow solid.

Yield: 35.9 mg, 89.0%.

m.p. > 350 °C. **^{1}H-NMR (DMSO-d_6, 400 MHz):** δ 1.31 (t, J = 6.9 Hz, 6H), 1.39 (t, J = 6.9 Hz, 6H), 3.22-3.40 (m, 4H), 3.67 (s, 6H), 3.92 (s, 6H), 4.02 (q, J = 7.0 Hz, 4H), 4.14 (q, J = 7.0 Hz, 4H), 4.44-4.52 (m, 2H), 5.30-5.36 (m, 2H), 6.96 (d, J = 8.3 Hz, 2H), 7.00-7.03 (m, 4H), 7.03 (d, J = 16.0 Hz, 2H), 7.13 (d, J = 8.5 Hz, 2H), 7.38 (d, J = 16.2 Hz, 2H), 7.45 (dd, J = 8.4, 1.9 Hz, 2H), 7.54 (d, J = 2.0 Hz, 2H), 7.68 (d, J = 15.8 Hz, 2H), 7.82 (s, 2H), 7.89 (d, J = 15.7 Hz, 2H), 8.04 (d, J = 1.7 Hz, 2H), 8.36 (d, J = 1.8 Hz, 2H). **^{13}C-NMR (DMSO-d_6, 101 MHz):** δ 14.6, 14.7, 27.2, 48.5, 55.3, 55.8, 63.8, 63.9, 110.3, 110.6, 112.6, 112.6, 116.1, 119.9, 120.5, 121.8, 123.4, 127.4, 127.6, 127.7, 131.0, 132.8, 137.0, 139.7, 140.2, 142.8, 146.0, 149.0, 149.2, 150.2, 150.6, 153.3. **IR:** v (cm$^-$) 763, 836, 1031, 1160, 1226, 1259, 1272, 1478, 1490, 1511, 1565, 1580, 1595, 1612, 1624. **MS (ESI) *m/z* (%):** 414.2 (10), 495.2 (100), 495.7 (70), 496.2 (22), 815.3 (5), 1139.4 [(M – $CF_3SO_3^-$)$^+$] (10). **HRMS *m/z*:** calc. for [(M – $2CF_3SO_3^-$)$^{2+}$] [($C_{64}H_{65}O_8N_2$)$^{2+}$] 989.4735, found 989.4738.

4,13-bis((*E*)-4-ethoxy-3-methoxystyryl)-8,9-dimethyl-6,7,10,11-tetrahydrodipyrido[2,1-a:1',2'-k][2,9]phenanthroline-5,12-diium trifluoromethanesulfonate (89)

$C_{46}H_{46}F_6N_2O_{10}S_2$
[965.0]

Synthesis and purification of dye **89** using dye precursor **84** (50 mg, 0.078 mmol, 1.0 equiv.), 4-ethoxy-3-methoxybenzaldehyde (210.8 mg, 1.170 mmol, 15.0 equiv.), pyrrolidine (96 µL, 83.2 mg, 1.170 mmol, 15.7 equiv.) in dry MeOH (5 mL) was accomplished according to *general procedure 5.2.e* and [5]helquat dye **89** was obtained as a lemon yellow solid.
Yield: 60.2 mg, 80.0%.
m.p. 341-343 °C. **^{1}H-NMR (DMSO-d_6, 400 MHz):** δ 1.38 (t, *J* = 6.9 Hz, 6H), 2.43 (s, 6H), 3.00-3.10 (m, 2H), 3.38-3.49 (m, 2H), 3.89 (s, 6H), 4.12 (q, *J* = 6.9 Hz, 4H), 4.43-4.51 (m, 2H), 5.40-5.46 (m, 2H), 7.11 (d, *J* = 8.4 Hz, 2H), 7.44 (dd, *J* = 2.0, 8.4 Hz, 2H), 7.55 (d, *J* = 2.0 Hz, 2H), 7.70 (d, *J* = 15.9 Hz, 2H), 7.84 (d, *J* = 15.8 Hz, 2H), 7.88 (d, *J* = 1.3 Hz, 2H), 8.09 (t, *J* = 8.1 Hz, 2H), 8.29 (dd, *J* = 1.3, 8.3 Hz, 2H). **^{13}C-NMR (DMSO-d_6, 101 MHz):** δ 14.6, 16.1, 25.2, 48.9, 55.8, 63.9, 110.7, 112.5, 115.6, 123.6, 124.1, 125.1, 127.7, 128.0, 138.5, 138.7, 141.8, 143.5, 147.2, 149.2, 150.7, 153.3. **IR:** *v* (cm^-) 763, 836, 1031, 1160, 1226, 1259, 1272, 1478, 1490, 1511, 1565, 1580, 1595, 1612, 1624. **MS (ESI) *m/z* (%):** 318.1 (10), 333.2 (76), 333.7 (37), 334.2 (7), 665.3 [$(M - 2CF_3SO_3^-)^{2+}$] (14), 787.3 (7), 815.3 [$(M - 2CF_3SO_3^-)^+$] (100), 816.3 (47), 817.3 (11). **HRMS *m/z*:** calc. for [$(M - 2CF_3SO_3^-)^{2+}$] [$(C_{44}H_{45}O_4N_2)^{2+}$] 665.3374, found 665.3375.

2,4-bis((E)-4-ethoxy-3-methoxystyryl)-6,7,10,11-tetrahydrodipyrido[2,1-a:1',2'-k][2,9] phenanthroline-5,12-diium trifluoromethanesulfonate (90)

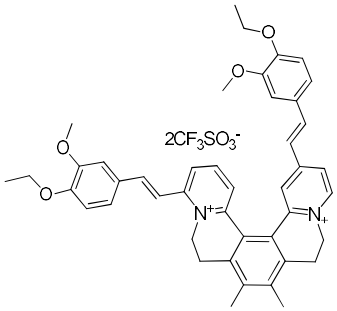

$C_{46}H_{46}F_6N_2O_{10}S_2$
[965.0]

Synthesis and purification of dye **90** using dye precursor **85** (50 mg, 0.078 mmol, 1.0 equiv.), 4-ethoxy-3-methoxybenzaldehyde (210.8 mg, 1.170 mmol, 15.0 equiv.), pyrrolidine (96.1 µL, 83.2 mg, 1.170 mmol, 15.0 equiv.) in dry MeOH (5 mL) was accomplished according to *general procedure 5.2.e* and [5]helquat dye **90** was obtained as a golden yellow solid.
Yield: 51.2 mg, 68.0%.
m.p. 318-320 °C. **^{1}H-NMR (DMSO-d_6, 400 MHz):** δ 1.31 (t, *J* = 6.9 Hz, 3H), 1.38 (t, *J* = 7.0 Hz, 3H), 2.42 (s, 3H), 2.43 (s, 3H), 2.99-3.13 (m, 2H), 3.47 (dd, *J* = 15.1, 18.6 Hz, 1H), 3.49 (dd, *J* = 15.1, 18.6 Hz, 1H), 3.68 (s, 3H), 3.91 (s, 3H), 4.03 (q, *J* = 7.0 Hz, 2H), 4.13 (q, *J* = 7.0 Hz, 2H), 4.44-4.58 (m, 1H), 4.68 (t, *J* = 13.5 Hz, 1H), 4.94 (d, *J* = 12.3 Hz, 1H), 5.48 (d, *J* = 13.2 Hz, 1H), 6.98 (d, *J* = 8.4 Hz, 1H), 7.03 (d, *J* = 8.8 Hz, 1H), 7.06 (d, *J* = 5.4 Hz, 1H), 7.10 (dd, *J* = 2.0, 8.4 Hz, 1H), 7.13 (d, *J* = 8.4 Hz, 1H), 7.36 (d, *J* = 16.2 Hz, 1H), 7.45 (dd, *J* = 8.4, 2.1 Hz, 1H), 7.55

(d, *J* = 2.1 Hz, 1H), 7.72 (d, *J* = 15.9 Hz, 1H), 7.89 (d, *J* = 1.9 Hz, 1H), 7.93 (d, *J* = 15.8 Hz, 1H), 8.02 (dd, *J* = 2.0, 6.7 Hz, 1H), 8.03 (dd, *J* = 1.2, 7.9 Hz, 1H), 8.14 (t, *J* = 8.1 Hz, 1H), 8.37 (dd, *J* = 1.3, 8.3 Hz, 1H), 8.99 (d, *J* = 6.6 Hz, 1H). **^{13}C-NMR (DMSO-d_6, 101 MHz):** *δ* 14.6, 14.7, 16.3, 25.2, 49.1, 52.8, 55.4, 55.8, 63.8, 63.9, 110.6, 110.8, 112.5, 112.7, 115.6, 119.1, 120.5, 120.9, 122.0, 122.3, 123.7, 123.9, 124.4, 125.0, 125.5, 127.5, 127.7, 127.9, 138.7, 138.7, 138.9, 139.1, 141.0, 141.7, 143.4, 144.4, 146.5, 147.3, 149.0, 149.2, 150.3, 150.7, 152.0, 153.5. **IR:** *v* (cm^-) 763, 836, 1031, 1160, 1226, 1259, 1272, 1478, 1490, 1511, 1565, 1580, 1595, 1612, 1624. **MS (ESI) *m/z* (%):** 333.2 (100), 333.7 [$(M - 2CF_3SO_3^-)^{2+}$] (60), 334.2 (18), 665.4 [$(M - 2CF_3SO_3^-)^{2+}$] (8), 815.3 [$(M - CF_3SO_3^-)^+$] (10). **HRMS *m/z*:** calc. for [$(M - 2CF_3SO_3^-)^{2+}$] [$(C_{44}H_{45}O_4N_2)^{2+}$] 665.3374, found 665.3375.

4,15-Bis((*E*)-4-ethoxy-3-methoxystyryl)-6,7,8,11,12,13-hexahydrodipyrido[1,2-a:1', 2'-a'] benzo[2,1-c:3,4-c']bisazepindiium trifluoromethansulfonate [(*rac*)-92]

$C_{46}H_{46}F_6N_2O_{10}S_2$
965.0

Synthesis and purification of dye (***rac*)-92** using dye precursor **(*rac*)-91** (20 mg, 0.031 mmol, 1.0 equiv.), 4-ethoxy-3-methoxybenzaldehyde (83.8 mg, 0.465 mmol, 15.0 equiv.)**,** pyrrolidine (38 µL, 33.0 mg, 0.464 mmol, 15.0 equiv.) in dry MeOH (1.0 mL) was accomplished according to *general procedure 5.2.e* and [5]helquat dye **(*rac*)-92** was obtained as lemon yellow solid.

Yield: 26.2 mg, 87.0%.

m.p. 280-282 °C. **^{1}H-NMR (DMSO-d_6, 400 MHz):** *δ* 1.37 (t, *J* = 6.9 Hz, 6H), 2.24-2.45 (m, 4H), 2.66-2.77 (m, 2H), 3.03 (dd, *J* = 6.1, 13.5 Hz, 1H), 3.05 (dd, *J* = 6.1, 13.5 Hz, 1H), 3.89 (s, 6H), 4.12 (q, *J* = 7.0 Hz, 4H), 4.32-4.41 (m, 2H), 5.17-5.22 (m, 2H), 7.10 (d, *J* = 8.4 Hz, 2H), 7.39 (dd, *J* = 1.3, 7.8 Hz, 2H), 7.48 (dd, *J* = 2.0, 8.5 Hz, 2H), 7.54 (d, *J* = 15.7 Hz, 2H), 7.57 (d, *J* = 1.0 Hz, 2H), 7.77 (s, 2H), 7.90 (d, *J* = 15.7 Hz, 2H), 8.12 (t, *J* = 8.1 Hz, 2H), 8.41 (dd, *J* = 1.3, 8.6 Hz, 2H). **^{13}C-NMR (DMSO-d_6, 101 MHz):** *δ* 14.6, 28.2, 30.5, 52.5, 55.9, 63.9, 111.2, 112.5, 115.0, 123.8, 125.3, 127.6, 128.7, 131.1, 132.5, 138.5, 142.8, 144.8, 149.1, 150.9, 151.5, 154.1. **IR:** *v* (cm^-) 763, 836, 1031, 1160, 1226, 1259, 1272, 1478, 1490, 1511, 1565, 1580, 1595, 1612, 1624. **MS (ESI) *m/z* (%):** 333.1 (100), 333.6 (73), 334.1 (20), 503.2 (5), 815.3 (17), 816.3 (10). **HRMS *m/z*:** calc. for [$(M - 2CF_3SO_3^-)^{2+}$] [$(C_{44}H_{46}O_4N_2)^{2+}$] 333.1723, found 333.1726.

4,15-Bis((*E*)-4-ethoxy-3-methoxystyryl)-6,7,8,11,12,13-hexahydrodipyrido[1,2-a:1', 2'-a'] benzo[2,1-c:3,4-c']bisazepindiium trifluoromethansulfonate (*P*)- 92

$C_{46}H_{46}F_6N_2O_{10}S_2$
965.0

Synthesis and purification of dye **(*P*)-92** using dye precursor **(*P*)-91** (20 mg, 0.031 mmol, 1.0 equiv.), 4-ethoxy-3-methoxybenzaldehyde (83.8 mg, 0.465 mmol, 15.0 equiv.), pyrrolidine (38 µL, 33.0 mg, 0.464 mmol, 15.0 equiv.) in dry MeOH (1.0 mL) was accomplished according to *general procedure 5.2.e* and [5]helquat dye **(*P*)-92** was obtained as a yellow solid.

Yield: 25 mg, 83.0%.

m.p. 280-282 °C. **^{1}H-NMR (DMSO-d_6, 400 MHz):** δ 1.37 (t, *J* = 6.9 Hz, 6H), 2.24-2.45 (m, 4H), 2.66-2.77 (m, 2H), 3.03 (dd, *J* = 6.1, 13.5 Hz, 1H), 3.05 (dd, *J* = 6.1, 13.5 Hz, 1H), 3.89 (s, 6H), 4.12 (q, *J* = 7.0 Hz, 4H), 4.32-4.41 (m, 2H), 5.17-5.22 (m, 2H), 7.10 (d, *J* = 8.4 Hz, 2H), 7.39 (dd, *J* = 1.3, 7.8 Hz, 2H), 7.48 (dd, *J* = 2.0, 8.5 Hz, 2H), 7.54 (d, *J* = 15.7 Hz, 2H), 7.57 (d, *J* = 1.0 Hz, 2H), 7.77 (s, 2H), 7.90 (d, *J* = 15.7 Hz, 2H), 8.12 (t, *J* = 8.1 Hz, 2H), 8.41 (dd, *J* = 1.3, 8.6 Hz, 2H). **^{13}C-NMR (DMSO-d_6, 101 MHz):** δ 14.6, 28.2, 30.5, 52.5, 55.9, 63.9, 111.2, 112.5, 115.0, 123.8, 125.3, 127.6, 128.7, 131.1, 132.5, 138.5, 142.8, 144.8, 149.1, 150.9, 151.5, 154.1. **IR:** *v* (cm^-) 763, 836, 1031, 1160, 1226, 1259, 1272, 1478, 1490, 1511, 1565, 1580, 1595, 1612, 1624. **MS (ESI) *m/z* (%):** 333.1 (100), 333.6 (73), 334.1 (20), 503.2 (5), 815.3 (17), 816.3 (10). **HRMS *m/z*:** calc. for $[(M - 2\ CF_3SO_3^-)^{2+}]$ $[(C_{44}H_{46}O_4N_2)^{2+}]$ 333.1723, found 333.1726. **Chiral purity:** >95% *ee* by CE (Capillary electrophoresis).

4,15-Bis((*E*)-4-ethoxy-3-methoxystyryl)-6,7,8,11,12,13-hexahydrodipyrido[1,2-a:1', 2'-a'] benzo[2,1-c:3,4-c']bisazepindiium trifluoromethansulfonate (*M*)- 92

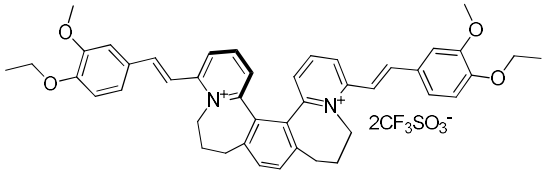

$C_{46}H_{46}F_6N_2O_{10}S_2$
[965.0]

Synthesis and purification of dye **(*M*)-92** using dye precursor **(*M*-91)** (20 mg, 0.031 mmol, 1.0 equiv.), 4-ethoxy-3-methoxybenzaldehyde (83.8 mg, 0.465 mmol, 15.0 equiv.), pyrrolidine (38 µL, 33.0 mg, 0.464 mmol, 15.0 equiv.) in dry MeOH (1.0 mL) was accomplished according to *general procedure 5.2.e* and [5]helquat dye **(*M*)-92** was obtained as a yellow solid.

Yield: 22 g, 73.0%.

m.p. 280-282 °C. δ 1.37 (t, *J* = 6.9 Hz, 6H), 2.24-2.45 (m, 4H), 2.66-2.77 (m, 2H), 3.03 (dd, *J* = 6.1, 13.5 Hz, 1H), 3.05 (dd, *J* = 6.1, 13.5 Hz, 1H), 3.89 (s, 6H), 4.12 (q, *J* = 7.0 Hz, 4H), 4.32-4.41 (m, 2H), 5.17-5.22 (m, 2H), 7.10 (d, *J* = 8.4 Hz, 2H), 7.39 (dd, *J* = 1.3, 7.8 Hz, 2H), 7.48 (dd, *J* = 2.0, 8.5 Hz, 2H), 7.54 (d, *J* = 15.7 Hz, 2H), 7.57 (d, *J* = 1.0 Hz, 2H), 7.77 (s, 2H), 7.90 (d, *J* = 15.7 Hz, 2H), 8.12 (t, *J* = 8.1 Hz, 2H), 8.41 (dd, *J* = 1.3, 8.6 Hz, 2H). **^{13}C-NMR (DMSO-d_6, 101 MHz):** δ 14.6, 28.2, 30.5, 52.5, 55.9, 63.9, 111.2, 112.5, 115.0, 123.8, 125.3, 127.6, 128.7, 131.1, 132.5, 138.5, 142.8, 144.8, 149.1, 150.9, 151.5, 154.1. **IR:** *v* (cm^-) 763, 836, 1031, 1160, 1226, 1259, 1272, 1478, 1490, 1511, 1565, 1580, 1595, 1612, 1624. **MS (ESI) *m/z* (%):** 333.1 (100), 333.6 (73), 334.1 (20), 503.2 (5), 815.3 (17), 816.3 (10). **HRMS *m/z*:** calc. for $[(M - 2\ CF_3SO_3^-)^{2+}]$ $[(C_{44}H_{46}O_4N_2)^{2+}]$ 333.1723, found 333.1726. **Chiral purity:** >95% *ee* by CE.

5.4 X-ray crystallography:

Crystallographic data were collected on a diffractometer equipped with a CCD detector using a monochromatized MoKα radiation (λ = 0.71073 Å) at a temperature of 150(2) K. The structure was solved by direct methods (SHELXS){ref} and refined by full matrix least squares based on F 2 (SHELXL97).){ref} The hydrogen atoms on carbons were fixed into idealized positions (riding model) and assigned temperature factors either Hiso(H) = 1.2 Ueq(pivot atom) or Hiso(H) = 1.5 Ueq for methyl moiety.

5.4.1 X-ray data for [6]helquat 6.

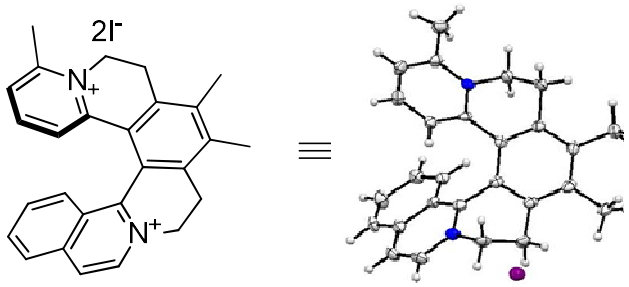

Crystal data for [(*P*)-6][I]$_2$: $C_{27}H_{26}N_2$•2(I), M_r = 632.30; Monoclinic, space group $P2_{1/n}$ (No 14), *a* = 7.8813 (2) Å, *b* = 16.2049 (4) Å, *c* = 19.5829 (5) Å, *β* = 99.067 (1)°; V = 2469.79 (11) Å3 , Z = 4, D_x = 1.700 Mg m-3 ; dimensions of yellow bar 0.44 × 0.12 × 0.11 mm, ϑ_{max} = 27.5°; numerical absorption correction (μ = 2.56 mm^{-1}) T_{min} = 0.401, T_{max} = 0.769; 31665 diffractions collected, 5678 independent (R_{int} =0.025) and 5069 observed according to the $I > 2\sigma(I)$ criterion. The refinement converged (Δ/σ_{max}= 0.002) to *R* = 0.022 for observed reflections and wR(F^2) = 0.047, *GOF* = 1.02 for 283 parameters and all 5678 reflections. The final difference map displayed no peaks of chemical significance ($\Delta\rho_{max}$ =1.02, $\Delta\rho_{min}$ -0.83 e.Å^{-3}).

5.4.2 X-ray data for [6]helquat dye 20:

CCDC 1012247

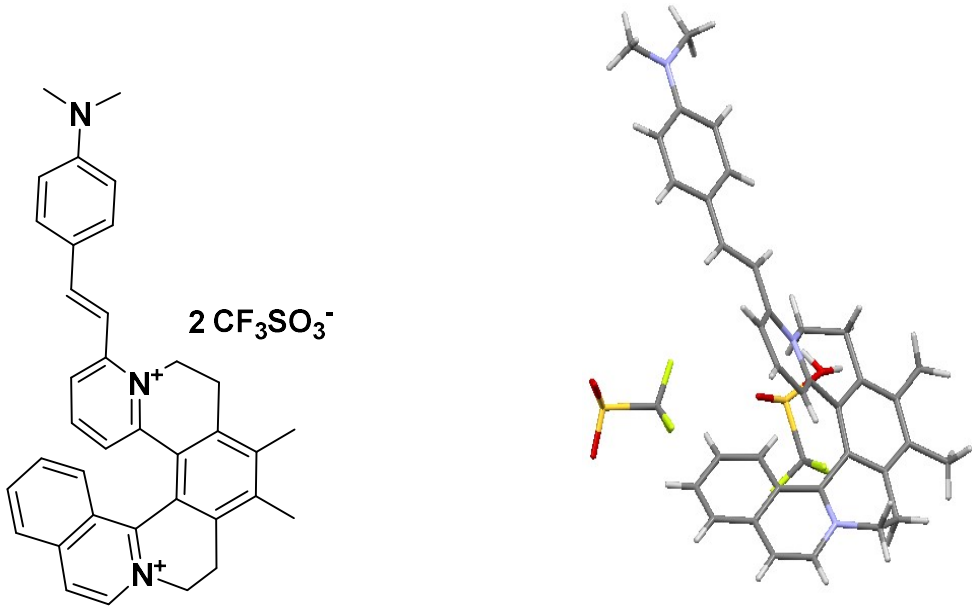

[6]Helquat dye **6** (2 mg) was dissolved in acetone (0.2 mL). Single crystals suitable for X-ray analysis were grown *via* slow diffusion of *i*-Pr2O into the solution at room temperature (22–25 °C) in the dark over 10 days.

Crystal data for CCDC 1012247: 2($C_{36}H_{35}N_3$)•4(CF_3O_3S)•H_2O, *M*r = 1633.64; Triclinic, *P*1 (No 1), *a* = = 9.7985(3) Å, *b* = 10.1396(4) Å, *c* = 19.4403(7) Å, *α* = 89.593(1)°, *β* = 83.894(1)° , *γ* = 68.851(1) °, *V* = 1790.12(11) Å3 , Z = 1, *D*x = 1.515 Mg m–3, red plate of dimensions 0.51 ×

0.43 × 0.17 mm, multi-scan absorption correction (μ = 0.24 mm–1) *T*min = 0.890, *T*max = 0.962; a total of 44178 measured reflections (θmax= 27.5˚), from which 16387 were unique (*R*int = 0.026) and 14165 observed according to the $I > 2\sigma(I)$ criterion. The refinement converged (Δ/σmax= 0.001) to *R* = 0.071 for observed reflections and *wR*(*F*2) = 0.201, GOF = 1.01 for 1001 parameters and all 16387 reflections. The final difference Fourier map displayed no peaks of chemical significance; positive ones are in the vicinity of the triflate moiety, due to its disorder (Δρmax = 1.70, Δρmin = –0.61 eÅ–3). S5

The structure was refined in the noncentrosymmetric space group *P*1, however two helquat cations follow closely the centrosymmetric space group *P*-1 (both enantiomers are present). In this space group, the triflate anions would appeared to be vastly disordered; therefore, low symmetry was selected for final refinement. One isolated peak of positive electron density was assigned to a water molecule, but its hydrogen atoms could not be found on the difference map and were therefore placed in positions suitable for hydrogen bonds.

5.4.3 X-ray data for [6]helquat dye 28:

CCDC 1532598

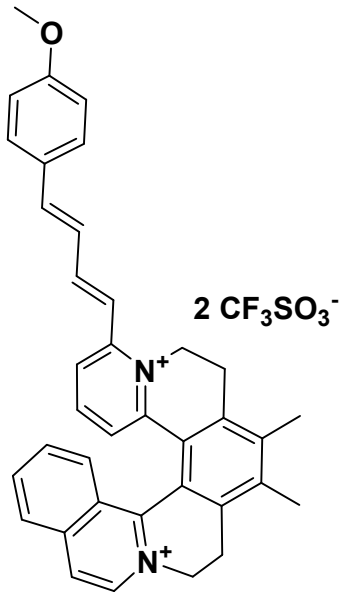

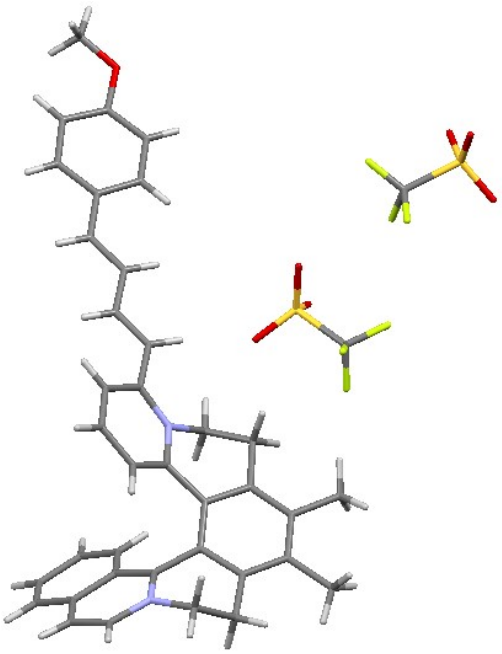

The solid (2 mg) was dissolved in MeOH (0.2 ml). Single crystals suitable for X-ray analysis were grown *via* slow diffusion of *i*-Pr_2O into MeOH solution at room temperature (22-25°C) in dark at within 8 -10 days.

Crystal data for 1532598: , M_r = 820.80; Triclinic, *P-1* (No 2), *a* = 8.1458 (13) Å, *b* = 14.503 (3) Å, *c* = 15.696 (3) Å, α = 89.660 (5) °, *β* = 89.057 (6)°, γ = 76.492 (6), *V* = 1802.8 (5) $Å^3$, Z = 2, D_x = 1.512 Mg m^{-3}, yellow plate of dimensions 0.30 × 0.24 × 0.12 mm, multi-scan absorption correction (μ = 0.23 mm^{-1}), T_{min} = 0.93, T_{max} = 0.97; a total of 13233 measured reflections (ϑ_{max}= 25˚), from which 6369 were unique (R_{int} = 0.072) and 4063 observed according to the $I > 2\sigma(I)$ criterion. The refinement converged (Δ/σ_{max}= 0.003) to *R* = 0.073 for observed reflections and *wR*(F^2) = 0.206, GOF = 1.03 for 508 parameters and all 6369 reflections. The final difference Fourier map displayed no peaks of chemical significance, ($\Delta\rho_{max}$ = 0.51, $\Delta\rho_{min}$ = -0.35 e.$Å^{-3}$).

5.4.4 X-ray data for HeliDye1 (29)

CCDC 1412114

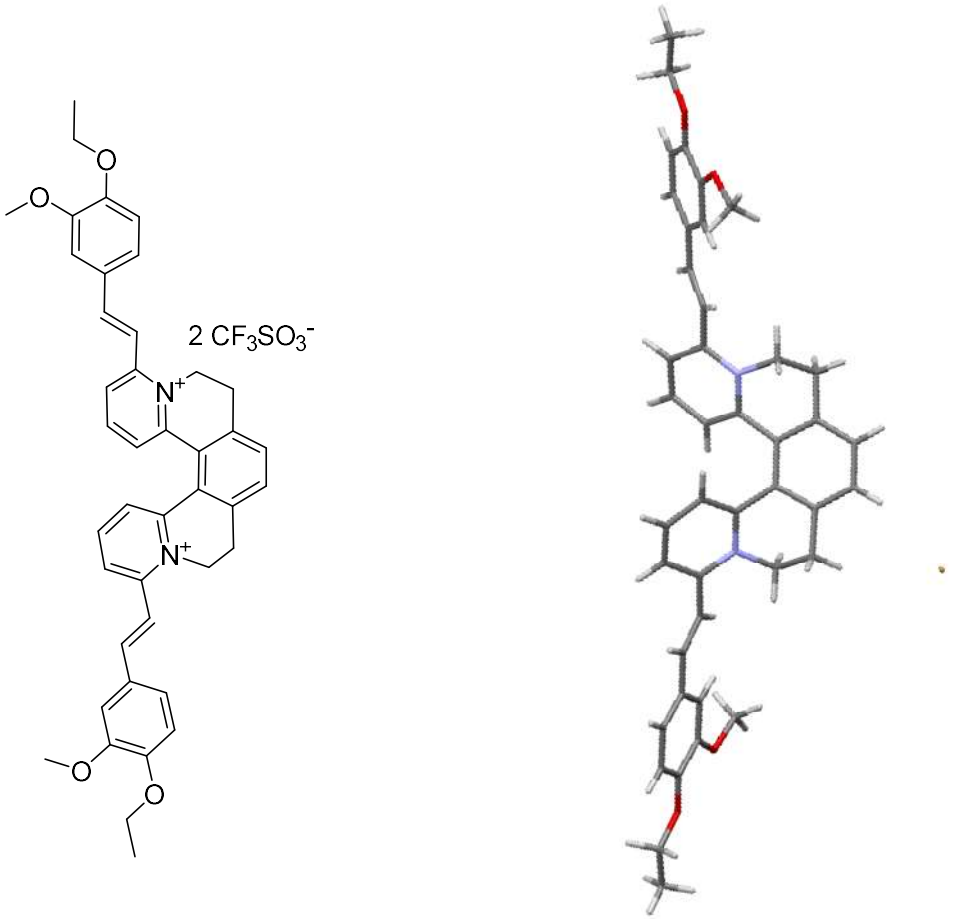

The displacement ellipsoids in this illustration were set to 50% probability level.

Dibromide salt of **29** (2 mg) was dissolved in MeOH (0.2 mL). Single crystals suitable for X-ray analysis were grown *via* slow diffusion of *i*-Pr_2O into the methanolic solution at rt (22-25°C) in the dark within 8-10 days.

CCDC 1412114. Crystal data: $C_{42}H_{42}N_2O_4 \bullet 2Br$, M_r = 798.60, Monoclinic, *C*2/*c* (No 15), *a* = 45.657 (4) Å, *b* = 12.2162 (12) Å, *c* = 7.4051 (6) Å, *β* = 93.046 (3)°, *V* = 4124.4 (7)Å^3, Z = 4, D_x = 1.286 Mg m^{-3}, yellow plate of dimensions 0.38 × 0.18 × 0.06 mm, numerical absorption correction (μ = 2.01 mm^{-1}) T_{min} = 0.515, T_{max} = 0.896, a total of 13287 measured reflections (ϑ_{max}= 26˚), from which 4050 were unique (R_{int} = 0.039) and 2859 observed according to the $I > 2\sigma(I)$ criterion. The refinement converged (Δ/σ_{max}= 0.001) to *R* = 0.048 for observed reflections and $wR(F^2)$ = 0.116, GOF = 1.01 for 228 parameters and all 4050 reflections. The final difference Fourier map displayed no peaks of chemical significance, ($\Delta\rho_{max}$ = 0.74, $\Delta\rho_{min}$ = -0.34 e.Å^{-3}). PLATON/ SQUEEZE procedure was used to correct the diffraction data for the presence of the disordered methanol solvent.

6. References:

1 L. Adriaenssens, L. Severa, T. Salova, I. Cisarova, R. Pohl, D. Saman, S. V. Rocha, N. S. Finney, L. Pospisil, P. Slavicek and F. Teply, *Chem. Eur. J.*, 2009, **15**, 1072.

2 R. H. Martin, *Angew. Chem. Int. Ed.*, 1974, **13**, 649.

3 (a) H. Weidel and M. Russo, *Monatshefte für Chemie und verwandte Teile anderer Wissenschaften*, **3**, 850; (b) L. Michaelis, *Biochem. Zeitschrift*, 1932, **250**, 564; (c) L. A. Summers, *The Bipyridinium Herbicides*, Academic Press, 1980; (d) P. Monk, *viologens*, Wiley, 1998.

4 (a) J. Vavra, L. Severa, P. Svec, I. Cisarova, D. Koval, P. Sazelova, V. Kasicka and F. Teply, *Eur. J. Org. Chem.,* 2012, 489; (c) J. Vavra, L. Severa, I. Cisarova, B. Klepetarova, D. Saman, D. Koval, V. Kasicka and F. Teply, *J. Org. Chem.*, 2013, **78**, 1329.

5 L. Pospisil, F. Teply, M. Gal, L. Adriaenssens, M. Horacek and L. Severa, *Phys. Chem. Chem. Phys.*, 2010, **12**, 1550.

6 L. Adriaenssens, L. Severa, D. Koval, I. Cisarova, M. M. Belmonte, E. C. Escudero-Adan, P. Novotna, P. Sazelova, J. Vavra, R. Pohl, D. Saman, M. Urbanova, V. Kasicka and F. Teply, *Chem. Sci.*, 2011, **2**, 2314.

7 L. Severa, M. Oncak, D. Koval, R. Pohl, D. Saman, I. Cisarova, P. E. Reyes-Gutierrez, P. Sazelova, V. Kasicka, F. Teply and P. Slavicek, *Angew. Chem. Int. Ed.*, 2012, **51**, 11972.

8 P. E. Reyes-Gutierrez, M. Jirasek, L. Severa, P. Novotna, D. Koval, P. Sazelova, J. Vavra, A. Meyer, I. Cisarova, D. Saman, R. Pohl, P. Stepanek, P. Slavicek, B. J. Coe, M. Hajek, V. Kasicka, M. Urbanova and F. Teply, *Chem. Commun.*, 2015, **51**, 1583.

9 M. R. Sonawane, in *Faculty of Science: Department of Organic Chemistry* Charles University in Prague, Prague, 2014, p. 242.

10 (a) P. Belenky, K. L. Bogan and C. Brenner, *Trends Biochem. Sci.*, 2007, **32**, 12; (b) A. D. Vinogradov, *Biochim. Biophys. Acta.*, 2008, **1777**, 729.

11 (a) Cicero A. F., Baggioni A., Adv. Exp. Med. Biol., 2016, **928**, 27; (b) Yin J., Xing H., Ye J., Metabolism, 2008, **57**, 712.

12 L. Grycová, J. Dostál and R. Marek, *Phytochemistry*, 2007, **68**, 150.

13 F. R. Stermitz, P. Lorenz, J. N. Tawara, L. A. Zenewicz and K. Lewis, *Proc. Natl. Acad. Sci. U.S.A.*, 2000, **97**, 1433.

14 Wu H. L.; Hsu C. Y.; Liu W. H.; Yung B. Y. *Int. J. Cancer*, 1999, **81**, 923.

15 M. Freile, F. A. Giannini, M. Sortino, M. Zamora, A. Juárez, S. Zacchino and R. D. Enriz, *Acta Farmacéutica Bonaerense,* 2006, **25**, 83.

16 A. Shirwaikar, A. Shirwaikar, K. Rajendran and I. S. R. Punitha, *Biol. Pharm. Bull.,* 2006, **29**, 1906.

17 J. L. Vennerstrom and D. L. Klayman, *J. Med. Chem.*, 1988, **31**, 1084.

18 S. K. Kulkarni and A. Dhir, *European J. Pharmacol.*, 2008, **589**, 163.

19 (a) R. K.Y. Zee-Cheng, K. D. Paull and C. C. Cheng, *J. Med. Chem.*, 1974, **17**, 347; (b) R. K. Y. Zee-Cheng and C. C. Cheng, *J. Med. Chem.*, 1976, **19**, 882.

20 (a) M. Franceschin, L. Rossetti, A. D'Ambrosio, S. Schirripa, A. Bianco, G. Ortaggi, M. Savino, C. Schultes and S. Neidle, *Bioorg. Med. Chem. Lett.*, 2006, **16**, 1707; (b) W.-J. Zhang, T.-M. Ou, Y.-J. Lu, Y.-Y. Huang, W.-B. Wu, Z.-S. Huang, J.-L. Zhou, K.-Y. Wong and L.-Q. Gu, *Bioorg. Med. Chem. Lett.*, 2007, **15**, 5493.

21 (a) B. Zamiri, K. Reddy, R. B. Jr. Macgregor, C. E. Pearson, *J. Biol. Chem.*, 2014, **289**, 4653; (b) L. Aixiao, M. Francois, B. Florent, D. Michel, W. Baoshan, Z. Xiang, W. Ping, *Eur. J. Med. Chem.*, 2010, **45**, 983; (c) E. Salvati, C. Leonetti, A. Rizzo , M. Scarsella, M. Mottolese, R. Galati, I. Sperduti, M. F. Stevens, M. D'Incalci, M. Blasco, G. Chiorino, S. Bauwens, B. Horard, E. Gilson, A. Stoppacciaro, G. Zupi, A. Biroccio, *J. Clin. Invest.*, 2007, **117**, 3236; (d) W. J. Chung, B. Heddi, F. Hamon, M. P. Teulade-Fichou, A. T. Phan, *Angew. Chem. Int. Ed.*, 2014, **53**, 999; (e) D. Verga, F. Hamon, F. Poyer, S. Bombard, M. P. Teulade-Fichou, *Angew. Chem. Int. Ed.*, 2014, **53**, 994.

22 M. Earle, P. Wasserscheid, P. Schulz, H. Olivier-Bourbigou, F. Favre, M. Vaultier, A. Kirschning, V. Singh, A. Riisager, R. Fehrmann and S. Kuhlmann, in *Ionic Liquids in Synthesis*, Wiley-VCH Verlag GmbH & Co. KGaA, 2008, pp. 265.

23 J.-f. Liu, G.-b. Jiang, J.-f. Liu and J. Å. Jönsson, *Trends Anal. Chem.; TrAC*, 2005, **24**, 20.

24 M. Antonietti, D. Kuang, B. Smarsly and Y. Zhou, *Angew. Chem. Int. Ed.*, 2004, **43**, 4988.

25 (a) P. Wasserscheid and W. Keim, *Angew. Chem. Int. Ed.*, 2000, **39**, 3772; (b) R. Sheldon, *Chem. Commun.*, 2001, 2399; (c) V. I. Pârvulescu and C. Hardacre, *Chem. Rev.*, 2007, **107**, 2615.

26 (a) C. E. Song, *Chem. Commun.*, 2004, 1033; (b) P. Domínguez de María, *Angew. Chem. Int. Ed.*, 2008, **47**, 6960.

27 C. Reichardt, *Chem. Rev.*, 1994, **94**, 2319.

28 C. L. Bird and A. T. Kuhn, *Chem. Soc. Rev.*, 1981, **10**, 49.

29 M. I. Knyazhanskii, Y. R. Tymyanskii, V. M. Feigelman and A. R. Katritzky, *Heterocycles*, 1987, **26**, 2963.

30 (a) C. R. Bock, T. J. Meyer and D. G. Whitten, *J. Am. Chem. Soc.*, 1974, **96**, 4710; (b) H. Dürr and S. Bossmann, *Acc. Chem. Res.*, 2001, **34**, 905.

31 C. M. Ronconi, J. F. Stoddart, V. Balzani, M. Baroncini, P. Ceroni, C. Giansante and M. Venturi, *Chem. Eur. J.*, 2008, **14**, 8365.

32 Z. Gan, A. Okui, Y. Kawashita and M. Hayashi, *Chem. Lett.*, 2008, **37**, 1302.

33 (a) H. Wynberg, *Acc. Chem. Res.*, 1971, **4**, 65; (b) W. H. Laarhoven and W. J. C. Prinsen, in *Stereochemistry*, eds. F. Vögtle and E. Weber, Springer Berlin Heidelberg, Berlin, Heidelberg, 1984, pp. 63; (c) F. Vögtle, *Fascinating molecules in organic chemistry*, John Wiley & Sons Inc, 1992; (d) Y. Shen and C.-F. Chen, *Chem. Rev.*, 2012, **112**, 1463.

34 M. Flammang-Barbieux, J. Nasielski and R. H. Martin, *Tetrahedron Lett.*, 1967, **8**, 743.

35 K. E. S. Phillips, T. J. Katz, S. Jockusch, A. J. Lovinger and N. J. Turro, *J. Am. Chem. Soc.*, 2001, **123**, 11899.

36 (a) M. Gingras and F. Dubois, *Tetrahedron Lett.*, 1999, **40**, 1309; (b) A. Rajca, H. Wang, M. Pink and S. Rajca, *Angew. Chem.,* 2000, **112**, 4655; (c) A. Rajca, H. Wang, M. Pink and S. Rajca, *Angew. Chem. Int. Ed.*, 2000, **39**, 4481.

37 (a) D. C. Harrowven, M. I. T. Nunn and D. R. Fenwick, *Tetrahedron Lett.,* 2002, **43**, 7345; (b) D. C. Harrowven, M. I. T. Nunn and D. R. Fenwick *Tetrahedron Lett.*, 2002, **43**, 3189.

38 S. K. Collins, A. Grandbois, M. P. Vachon and J. Côté, *Angew. Chem. Int. Ed.*, 2006, **45**, 2923.

39 (a) C. Romero, D. Peña, D. Pérez and E. Guitián, *J. Org. Chem.*, 2008, **73**, 7996; (b) D. Peña, D. Pérez, E. Guitián and L. Castedo, *Org. Lett.*, 1999, **1**, 1555; (c) D. Peña, A. Cobas, D. Pérez, E. Guitián and L. Castedo, *Org. Lett.*, 2003, **5**, 1863; (d) D. Peña, A. Cobas, D. Pérez, E. Guitián and L. Castedo, *Org. Lett.*, 2000, **2**, 1629.

40 (a) F. Teplý, I. G. Stará, I. Starý, A. Kollárovič, D. Šaman, L. Rulíšek and P. Fiedler, *J. Am. Chem. Soc.*, 2002, **124**, 9175; (b) I. G. Stara, I. Stary, A. Kollarovic, F. Teply, D. Saman and P. Fiedler, *Collect. Czech. Chem. Commun.*, 2003, **68**, 917; (c) F. Teplý, I. G. Stará, I. Starý, A. Kollárovič, D. Šaman, Š. Vyskočil and P. Fiedler, *J. Am. Chem. Soc.*, 2003, **68**, 5193.

41 (a) S. Han, D. R. Anderson, A. D. Bond, H. V. Chu, R. L. Disch, D. Holmes, J. M. Schulman, S. J. Teat, K. P. C. Vollhardt and G. D. Whitener, *Angewandte Chemie International Edition*, 2002, **41**, 3227; (b) S. Han, A. D. Bond, R. L. Disch, D. Holmes, J. M. Schulman, S. J. Teat, K. P. C. Vollhardt and G. D. Whitener, *Angew. Chem. Int. Ed.*, 2002, **41**, 3223.

42 K. Tanaka, N. Fukawa, T. Suda and K. Noguchi, *Angew. Chem. Int. Ed.*, 2009, **48**, 5470.

43 M. R. Crittall, H. S. Rzepa and D. R. Carbery, *Org. Lett.*, 2011, **13**, 1250.

44 S. Arai, M. Ishikura and T. Yamagishi, *J. Chem. Soc., Perkin Trans.*, 1998, 1561.

45 H. A. Staab, M. Diehm and C. Krieger, *Tetrahedron Lett.*, 1994, **35**, 8357.

46 (a) N. Takenaka, R. S. Sarangthem and B. Captain, *Angew. Chem. Int. Ed.*, 2008, **47**, 9708; (b) J. Chen and N. Takenaka, *Chem. Eur. J.*, 2009, **15**, 7268; (c) M. Šámal, J. Míšek, I. G. Stará and I. Starý, *Collect. Czech. Chem. Commun.*, 2009, **74**, 1151; (d) A. Terfort, H. Görls and H. Brunner, *Synthesis*, 1997, **1997**, 79; (e) M. T. Reetz and S. Sostmann, *J. Organomet.*

Chem., 2000, **603**, 105; (f) M. T. Reetz, E. W. Beuttenmüller and R. Goddard, *Tetrahedron Lett.*, 1997, **38**, 3211.

47 J. Misek, F. Teply, I. G. Stara, M. Tichy, D. Saman, I. Cisarova, P. Vojtisek and I. Stary, *Angew Chem. Int. Ed.*, 2008, **47**, 3188.

48 F. H. Allen, O. Kennard, D. G. Watson, L. Brammer, A. G. Orpen and R. Taylor, *J. Chem. Soc., Perkin Trans. 2*, 1987, S1.

49 (a) M. S. Newman, W. B. Lutz and D. Lednicer, *J. Am. Chem. Soc.*, 1955, **77**, 3420; (b) J. M. Brown, I. P. Field and P. J. Sidebottom, *Tetrahedron Lett.*, 1981, **22**, 4867.

50 (a) B. Busson, M. Kauranen, C. Nuckolls, T. J. Katz and A. Persoons, *Phy. Rev. Lett.*, 2000, **84**, 79; (b) T. Verbiest, S. V. Elshocht, M. Kauranen, L. Hellemans, J. Snauwaert, C. Nuckolls, T. J. Katz and A. Persoons, *Science*, 1998, **282**, 913; (c) R. Amemiya and M. Yamaguchi, *Chem. Rec.,* 2008, **8**, 116; (d) R. Amemiya and M. Yamaguchi, *Org. Biomol. Chem.*, 2008, **6**, 26.

51 E. Murguly, R. McDonald and N. R. Branda, *Org. Lett.*, 2000, **2**, 3169.

52 (a) Y. Kitahara and K. Tanaka, *Chem. Commun.*, 2002, 932; (b) J. E. Field, T. J. Hill and D. Venkataraman, *J. Org. Chem.*, 2003, **68**, 6071.

53 T. Caronna, R. Sinisi, M. Catellani, L. Malpezzi, S. V. Meille and A. Mele, *Chem. Commun.*, 2000, 1139.

54 D. J. Wolstenholme, C. F. Matta and T. S. Cameron, *J. Phy. Chem. A*, 2007, **111**, 8803.

55 (a) J. Vávra, L. Severa, I. Císařová, B. Klepetářová, D. Šaman, D. Koval, V. Kašička and F. Teplý, *J. Org. Chem.*, 2013, **78**, 1329; (b) R. H. Martin and M. J. Marchant, *Tetrahedron*, 1974, **30**, 343.

56 (a) H. Wynberg and M. B. Groen, *J. Am. Chem. Soc.*, 1968, **90**, 5339; (b) R. H. Martin, M. Flammang-Barbieux, J. P. Cosyn and M. Gelbcke, *Tetrahedron Lett.*, 1968, **9**, 3507.

57 (a) T. J. Katz, L. Liu, N. D. Willmore, J. M. Fox, A. L. Rheingold, S. Shi, C. Nuckolls and B. H. Rickman, *J. Am. Chem. Soc.*, 1997, **119**, 10054; (b) K. Paruch, L. Vyklický, D. Z. Wang, T. J. Katz, C. Incarvito, L. Zakharov and A. L. Rheingold, *J. Org. Chem.*, 2003, **68**, 8539.

58 M. T. Reetz and S. Sostmann, *Tetrahedron*, 2001, **57**, 2515.

59 (a) L. Owens, C. Thilgen, F. Diederich and C. B. Knobler, *Helv. Chimica Acta*, 1993, **76**, 2757; (b) D. J. Weix, S. D. Dreher and T. J. Katz, *J. Am. Chem. Soc.*, 2000, **122**, 10027.

60 C. A. Daul, I. Ciofini and V. Weber, *Int. J. Quantum Chem.*, 2003, **91**, 297.

61 C. Nuckolls and T. J. Katz, *J. Am. Chem. Soc.*, 1998, **120**, 9541.

62 A. Montali, C. Bastiaansen, P. Smith and C. Weder, *Nature*, 1988, **392**, 261.

63 (a) B. B. Hassine, M. Gorsane, J. Pecher and R. H. Martin, *Bull. Soc. Chim. Belg.*, 1985, **94**, 597; (b) B. B. Hassine, M. Gorsane, J. Pecher and R. H. Martin, *Bull. Soc. Chim. Belg.*, 1985, **94**, 759; (c) B. B. Hassine, M. Gorsane, F. Geerts-Evrard, J. Pecher, R. H. Martin and D. Castelet, *Bull. Soc. Chim. Belg.*, 1986, **95**, 547; (d) B. B. Hassine, M. Gorsane, J. Pecher and R. H. Martin, *Bull. Soc. Chim. Belg.*, 1986, **95**, 557; (e) B. B. Hassine, M. Gorsane, J. Pecher and R. H. Martin, *Bull. Soc. Chim. Belg.*, 1987, **96**, 801.

64 S. D. Dreher, T. J. Katz, K.-C. Lam and A. L. Rheingold, *J. Org. Chem.*, 2000, **65**, 815.

65 (a) I. G. Sanchez, M. Samal, J. Nejedly, M. Karras, J. Klivar, J. Rybacek, M. Budesinsky, L. Bednarova, B. Seidlerova, I. G. Stara and I. Stary, *Chem. Commun.*, 2017, **53,** 4370; (b) Z. Krausova, P. Sehnal, B. P. Bondzic, S. Chercheja, P. Eilbracht, I. G. Stara, D. Saman and I. Stary, *Eur. J. Org. Chem.* 2011, 3849; (c) K. Yamamoto, T. Shimizu, K. Igawa, K. Tomooka, G. Hirai, H. Suemune and K. Usui, *Sci. Rep.*, 2016, **6**, 36211.

66 (a) K. Tanaka, *Chem. Commun.*, 1998, 1141; (b) K. Tanaka, H. Osuga and Y. Kitahara, *J. Chem. Soc., Perkin Trans., 2*, 2000, 2492; (c) *J. Org. Chem.*, 2002, **67**, 1795; (c) J.-i. Nishida, T. Suzuki, M. Ohkita and T. Tsuji, *Angew. Chem. Int. Ed.*, 2001, **40**, 3251; (d) T. Suzuki, Y. Ishigaki, T. Iwai, H. Kawai, K. Fujiwara, H. Ikeda, Y. Kano and K. Mizuno, *Chem. Eur. J.*, 2009, **15**, 9434.

67 (a) Y. Ooyama, G. Ito, H. Fukuoka, T. Nagano, Y. Kagawa, I. Imae, K. Komaguchi and Y. Harima, *Tetrahedron*, 2010, **66**, 7268; (b) Y. Ooyama, A. Ishii, Y. Kagawa, I. Imae and Y. Harima, *New J. Chem.*, 2007, **31**, 2076; (c) Y. Ooyama, Y. Shimada, Y. Kagawa, I. Imae and Y. Harima, *Org. Biomol. Chem.*, 2007, **5**, 2046; (d) Y. Ooyama, Y. Shimada, Y. Kagawa, Y. Yamada, I. Imae, K. Komaguchi and Y. Harima, *Tetrahedron Lett.*, 2007, **48**, 9167.

68 M. Nakazaki, K. Yamamoto, T. Ikeda, T. Kitsuki, Y. Okamoto, *J. Chem. Soc., Chem. Commun.*, 1983, 787.

69 D. Z. Wang and T. J. Katz, *J. Org. Chem.*, 2005, **70**, 8497.

70 O. Kel, A. Fürstenberg, N. Mehanna, C. Nicolas, B. Laleu, M. Hammarson, B. Albinsson, J. Lacour and E. Vauthey, *Chem. Eur. J.*, 2013, **19**, 7173.

71 (a) Y. Xu, Y. X. Zhang, H. Sugiyama, T. Umano, H. Osuga and K. Tanaka, *J. Am. Chem. Soc.*, 2004, **126**, 6566; (b) Y. Xu, H. Sugiyama, K. Tanaka and H. Osuga, *Nucleic Acids Symp. Ser.*, 2004, **48**, 87.

72 (a) K.-i. Shinohara, Y. Sannohe, S. Kaieda, K.-i. Tanaka, H. Osuga, H. Tahara, Y. Xu, T. Kawase, T. Bando and H. Sugiyama, *J. Am. Chem. Soc.*, 2010, **132**, 3778; (b) Y. Xu, S. Yamazaki, H. Osuga and H. Sugiyama, *Nucleic Acids Symp. Ser.*, 2006, **50**, 183.

73 K. Kawara, G. Tsuji, Y. T. and S. Sasaki, *Chem. Eur. J.*, 2017, **23**, 1763.

74 T. Verbiest and A. Persoons, in Materials Chirality: Topics in Stereochemistry, Eds. M. M. Green, R. J. M. Nolte, E. W. Meijer, S. E. Denmark, J. Siegel, Wiley: New York, 2003; Vol. 24, pp 519−570.

75 U. Gubler and C. Bosshard, *Nat. Mater.*, 2002, **1**, 209.

76 (a) *Nonlinear optical properties of organic molecules and crystals*, D. S. Chemla and J. Zyss, Eds., 1987; Vol. 1 and 2; (b) *Molecular Nonlinear Optics: Materials, Physics and Devices*; J. Zyss, Ed.: Academic Press: Boston, 1994; (c) *Nonlinear Optics*, C. Bosshard, K. Sutter, P. Pretre, J. Hulliger, M. Florsheimer, P. Kaatz, P. Gunter, Eds., Gordon & Breach: Amsterdam, The Netherlands, 1995; Vol. 1; (c) *Nonlinear Optics of Organic Molecules and Polymers*, H. S. Nalwa, S. Miyatra, Eds., CRC Press: BocaRaton, FL., 1997.

77 B. J. Coe, *Chem. Eur. J.*, 1999, **5**, 2464.

78 S. R. Marder, J. W. Perry, W. P. Schaefer, *Science*, 1989, **245**, 626.

79 B. J. Coe, J. -D. Foulon, T. A. Hamor, C. J. Jones, J. A. McCleverty, D. Bloor, G. H. Cross, T. L. Axon, *J. Chem. Soc., Dalt. Trans.*, 1994, **23**, 3427.

80 S. M. LeCours, H. –W. Guan, S. G. DiMagno, C. H. Wang, M. J. Therien, *J. Am. Chem. Soc.*, 1996, **118**, 1497.

81 M. Blanchard-Desce, V. Alain, P. V. Bedworth, S. R. Marder, A. Fort, C. Runser, M. Barzoukas, S. Lebus, R. Wortmann, *Chem. Eur. J.*, 1997, **3**, 1091.

82 G. R. Meredith, *Rev. Sci. Instruments*, 1982, **53**, 48.

83 P. Franken, A. Hill, C. Peters, G. Weinreich, *Phys. Rev. Lett.*, 1961, **7**, 118.

84 Y. R. Shen, Nature, 1989, **337**, 519.

85 E. Hendrickx, K. Clays, A. Persoons, *Acc. Chem. Res*., 1998, **31**, 675.

86 J. L. Oudar, J. Zyss, *Phys. Rev. A*, 1982, **26**, 2016.

87 T. Verbiest, S. Sioncke, A. Persoons, L. VyKlicky, T. J. Katz, *Angew. Chem. Int. Ed.*, 2002, **41**, 3882

88 (a) L. E. R. Buckley, B. J. Coe, D. Rusanova, V. D. Joshi, S. Sanchez,́ M. Jirasek,́ J. Vavra,́ D. Khobragade, L. Severa, I. Císarovaˇ, D. Šaman, R. Pohl, K. Clays, G. Depotter, B. S. Brunschwig and F. Teply, *J. Phys. Chem. A*, 2017, **121**, 5842; (b) B. J. Coe, D. Rusanova, V. D. Joshi, S. Sanchez,́ J. Vavra,́ D. Khobragade, L. Severa, I. Císarovaˇ, D. Šaman, R. Pohl, K. Clays, G. Depotter, B. S. Brunschwig and F. Teply, *J. Org. Chem.*, 2016, **81**, 1912; (c) L. E. R. Buckley, B. J. Coe, D. Rusanova, V. D. Joshi, S. Sanchez,́ J. Vavra,́ D. Khobragade, L. Severa, M. Jirasek,́ I. Císarovaˇ, D. Šaman, R. Pohl, K. Clays, G. Depotter, B. S. Brunschwig and F. Teply, *Dalton Trans.*, 2017, **46**, 1052.

89 N. M., J. J. and K. B. 2006., eds., *Viologens, IUPAC Compendium of Chemical Terminology (Online Ed.). doi:10.1351/goldbook.V06624*, 2006.

90 R. C. Brian, R. F. Homer, J. Stubbs and R. L. Jones, *Nature*, 1958, **181**, 446.

91 L. Striepe and T. Baumgartner, *Chem. Eur. J.*, 2017, Doi: 10.1002/chem.201703348.

92 E. A. Neal, S. M. Goldup, *Chem. Commun.*, 2014, **50**, 5128.

93 Y. Song, X. Huang, H. Hua, Q. Wang, *Dyes Pigm.*, 2017, **137**, 229.

94 D. R. Wheeler, J. Nichols, D. Hansen, M. Andrus, S. Choi and G. D. Watt, *J. Electrochem. Soc.*, 2009, **156**, B1201.

95 B. L. Allwood, F. H. Kohnke, A. M. Z. Slawin, J. F. Stoddart and D. J. Williams, *J. Chem. Soc., Chem. Commun.*, 1985, 311.

96 M. Lahav, K. T. Ranjit, E. Katz and I. Willner, *Chem. Commun.*, 1997, 259.

97 (a) J. Winsberg, T. Hagemann, T. Janoschka, M. D. Hager, U. S. Schubert, *Angew. Chem. Int. Ed*., 2017, **56**, 686; (b) A. Ghosh, S. Mitra, *RSC Adv.*, 2015, **5**, 105632.

98 S. Asaftei and E. De Clercq, *J. Med. Chem.*, 2010, **53**, 3480.

99 H. Mustroph, in *Ullmann's Encyclopedia of Industrial Chemistry*, Wiley-VCH Verlag GmbH & Co. KGaA, 2000.

100 K. Hunger, *Industrial dyes: chemistry, properties, applications*, John Wiley & Sons, 2007.

101 A. E. Siegrist: .Die Anwendung optischer Aufheller in der Papierindustrie., *Papier (Darmstadt),* 1954*,* **8**, 109.

102 R. Zweidler: .Einführung in die Chemie der optischen Aufheller., *Textilveredlung*, 1969, **4,** 75.

103 T. Förster: *Fluoreszenz organischer Verbindungen*, Vandenhoek und Ruprecht, Göttingen, 1951.

104 F. P. Schäfer: *Dye Lasers*, Springer Verlag, Berlin 1973.

105 (a) H. Gold: ‘‘Fluorescent Brightening Agents’’ K. Venkataraman (ed.) in ‘‘*The Chemistry of Synthetic Dyes’’*, vol. V, Academic Press, New York.London 1971, 535; (b) M. Zahradnik: *The Production and Application of Fluorescent Brightening Agents*, John Wiley & Sons, Chichester 1982.

106 L. Strekowski, *Heterocyclic polymethine dyes: synthesis, properties and applications*, Springer, 2008.

107 T. G. Deligeorgiev, D. A. Zaneva, H. E. Katerinopoulos and V. N. Kolev, *Dyes Pigm.*, 1999, **41**, 49.

108 (a) S. R. Mujumdar, R. B. Mujumdar, C. M. Grant and A. S. Waggoner, *Bioconjug. Chem.*, 1996, **7**, 356; (b) B. Chipon, G. Clavé, C. Bouteiller, M. Massonneau, P.-Y. Renard and A. Romieu, *Tetrahedron Lett.*, 2006, **47**, 8279.

109 T. Tani, *J. Imaging sci. Technol.*, 1995, **39**, 31.

110 Z. Dai, L. Qun and B. Peng, *Dyes Pigm.*, 1998, **36**, 243.

111 R. Reisfeld, A. Weiss, T. Saraidarov, E. Yariv and A. Ishchenko, *Polymers Adv. Tech.*, 2004, **15**, 291.

112 (a) M. Liang, W. Xu, F. Cai, P. Chen, B. Peng, J. Chen and Z. Li, *J. Phy. Chem. C*, 2007, **111**, 4465; (b) Q. Zhang, C. S. Dandeneau, X. Zhou and G. Cao, *Adv. Mater.*, 2009, **21**, 4087.

113 (a) C. Nasr, S. Hotchandani, P. V. Kamat, S. Das, K. G. Thomas and M. George, *Langmuir*, 1995, **11**, 1777; (b) F. Tang, H. Shi, D. Gu, X. Tang and F. Gan, in *Optical Science, Engineering and Instrumentation'97*, International Society for Optics and Photonics, 1997, pp. 210.

114 R. B. Mujumdar, L. A. Ernst, S. R. Mujumdar, C. J. Lewis and A. S. Waggoner, *Bioconjug. Chem.*, 1992, **4**, 105.

115 L. G. Lee, C. H. Chen and L. A. Chiu, *Cytometry*, 1986, **7**, 508.

116 T. Deligeorgiev, I. Timcheva, V. Maximova, N. Gadjev, A. Vassilev, J.-P. Jacobsen and K.-H. Drexhage, *Dyes Pigm.*, 2004, **61**, 79.

117 B. Nordén and F. Tjerneld, *Biophys. Chem.*, 1976, **6**, 31.

118 H. Ihmels and D. Otto, in *Supermolecular dye chemistry*, Springer, 2005, pp. 161.

119 R. J. Williams, M. Lipowska, G. Patonay and L. Strekowski, *Anal. Chem.*, 1993, **65**, 601;

120 M. J. Baars and G. Patonay, *Anal. Chem.*, 1999, **71**, 667.

121 J. Sowell, R. Parihar and G. Patonay, *J. Chromatogr. B: Biomed. Sci. Appl.*, 2001, **752**, 1.

122 N. Karton-Lifshin, L. Albertazzi, M. Bendikov, P. S. Baran and D. Shabat, *J. Am. Chem. Soc.*, 2012, **134**, 20412.

123 (a) W. König, *J. Prakt. Chem.*, 1912, **86**, 166; (b) H. Barbier and *Bull. Soc. Chim. Fr.*, 1920, **27**, 427.

124 A. Vasilev, T. Deligeorgiev, N. Gadjev, S. Kaloyanova, J. J. Vaquero, J. Alvarez-Builla and A. G. Baeza, *Dyes Pigm.*, 2008, **77**, 550.

125 (a) M. A. Gaffield and W. J. Betz, *Nat. Protoc.*, 2007, **1**, 2916; (b) S. O. Rizzoli, D. A. Richards and W. J. Betz, *J. Neurocytol.*, 2003, **32**, 539;

(c) https://tools.thermofisher.com/content/sfs/manuals/mp34653.pdf, 2005.
126 G. R. Rosania, J. W. Lee, L. Ding, H.-S. Yoon and Y.-T. Chang, *J. Am. Chem. Soc.*, 2003, **125**, 1130.
127 (a) J. W. Lee, M. Jung, G. R. Rosania and Y.-T. Chang, *Chem. Commun.*, 2003, 1852; (b) S. Feng, Y. Kyung Kim, S. Yang and Y.-T. Chang, *Chem. Commun.*, 2010, **46**, 436.
128 S. Wang and Y.-T. Chang, *Chem. Commun.* 2008, 1173.
129 Q. Li, Y. Kim, J. Namm, A. Kulkarni, G. R. Rosania, Y.-H. Ahn and Y.-T. Chang, *Chem. Biol.*, 2006, **13**, 615.
130 R. Krieg, A. Eitner and K.-J. Halbhuber, *Acta Histochem.*, 2011, **113**, 682.
131 L. M. Loew, *Pure Appl. Chem.*, 1996, **68**, 1405.
132 A. Obaid, L. Loew, J. Wuskell and B. Salzberg, *J. Neurosci. Methods*, 2004, **134**, 179.
133 P. Yan, C. D. Acker, W.-L. Zhou, P. Lee, C. Bollensdorff, A. Negrean, J. Lotti, L. Sacconi, S. D. Antic and P. Kohl, *Proc. Natl. Acad. Sci. U.S.A.*, 2012, **109**, 20443.
134 Y. V. Fedorov, O. A. Fedorova, E. N. Andryukhina, S. P. Gromov, M. V. Alfimov, L. G. Kuzmina, A. V. Churakov, J. A. K. Howard and J. J. Aaron, *New J. Chem.*, 2003, **27**, 280.
135 *Cyclophane Chemistry for the 21st Century*, 2002.
136 F. Teply, M. Hajek, E. Kuzmova, J. Kozak, V. Komarova, P. Hubalkova, P. E. Reyes-Gutierrez, M. Jirasek, M. R. Sonawane and V. D. Joshi, WO/2015/180701, 2015.
137 (a) F. Pan, G. Knöpfle, C. Bosshard, S. Follonier, R. Spreiter, M. S. Wong, P. Günter, *Appl. Phys. Lett.*, 1996, **69**, 13; (b) U. Meier, M. Bösch, C. Bosshard, F. Pan, P. Günter, *J. Appl. Phys.*, 1998, **83**, 3486; (c) M. Thakur, J. J. Xu, A. Bhowmik, L. G. Zhou, *Appl. Phys. Lett.*, 1999, **74**, 635; (d) F. Pan, K. McCallion, M. Chiapetta, *Appl. Phys. Lett.*, 1999, **74**, 492; e) A. K. Bhowmik, S. Tan, A. C. Ahyi, A. Mishra, M. Thakur, *Polym. Mater. Sci. Eng.*, 2000, **83**, 169.
138 T. Verbiest, S. Houbrechts, M. Kauranen, K. Clays and A. Persoons, *J. Mater. Chem.*, 1997, **7**, 2175.
139 O. -K. Kim, L. -S. Choi, H. -Y. Zhang, X. H. He and Y. -H. Shih, *J. Am. Chem. Soc.*, 1996, **118**, 12220.
140 (a) B. J. Coe, J. Fielden, S. P. Foxon, I. Asselberghs, K. Clays, V. Cleuvenbergen, B. Brunschwig, *Organometallics*, 2011, **30**, 5731; (b) B. J. Coe, J. Fielden, S. P. Foxon, M. Helliwell, B. S. Brunschwig, I. Asselberghs, K. Clays, J. Olesiak, K. Matczyszyn, M. J. Samoc, *Phys. Chem. A*, 2010, **114**, 12028; (c) B. J. Coe, J. Fielden, S. P. Foxon, M. Helliwell, M. Helliwell, B. S. Brunschwig, I. Asselberghs, K. Clays, J. Garín, J. J. Orduna, *J. Am. Chem. Soc.*, 2010, **132**, 10498; (d) B. J. Coe, J. A. Harris, B. S. Brunschwig, J. Garín, J. J. Orduna, *J. Am. Chem. Soc.*, 2005, **127**, 3284.
141 J. E. Reeve, H. L. Anderson and K. Clays, *Phys. Chem. Chem. Phys.*, 2010, **12**, 13484.
142 P. Yan, A. C. Millard, M. Wei and L. M. Loew, *J. Am. Chem. Soc.*, 2006, **128**, 11030.
143 L. Sacconi, D. A. Dombeck and W. W. Webb, *Proc. Natl. Acad. Sci. U. S. A.*, 2006, **103**, 3124.
144 http://www.rainbowphotonics.com/prod_dast.php
145 R. J. Linhardt, *Chemistry and industry*, 1991.
146 (a) I. Capila and R. J. Linhardt, *Angew. Chem. Int. Ed.*, 2002, **41**, 390; (b) J. R. Bishop, M. Schuksz and J. D. Esko, *Nature*, 2007, **446**, 1030; (c) C. Guo, B. Wang, L. Wang and B. Xu, *Chem. Commun.*, 2012, **48**, 12222.
147 (a) J. D. Esko and S. B. Selleck, *Annu. Rev. Biochem.*, 2002, **71**, 435; (b) C. Guo, X. Fan, H. Qiu, W. Xiao, L. Wang and B. Xu, *Phys. Chem. Chem. Phy.*, 2015, **17**, 13301.
148 (a) R. Barbucci, A. Magnani, S. Lamponi and A. Albanese, *Polymers Adv. Tech.*, 1996, **7**, 675; (b) D. L. Rabenstein, *Nat. Prod. Rep.*, 2002, **19**, 312; (c) S. Middeldorp, *Thromb. Res.*, 2008, **122**, 753.
149 (a) B. Girolami and A. Girolami, in *Seminars in thrombosis and hemostasis*, Copyright© 2006 by Thieme Medical Publishers, Inc., 333 Seventh Avenue, New York, NY 10001, USA., 2006, pp. 803; (b) T. E. Warkentin, M. N. Levine, J. Hirsh, P. Horsewood, R. S. Roberts, M. Gent and J. G. Kelton, *N. Engl. J. Med.*, 1995, **332**, 1330.
150 R. Balhorn, *Genome Biol.*, 2007, **8**, 227.

151 (a) M. Nybo and J. Madsen, *J.-J. Cai, D.-C. Jiang, D. Jia, S.-Y. Yan and Y.-Q. Wang, Clin. Ther.*, 2010, **32**, 1729; (b) Y.-Q. Chu, L.-J. Cai, D.-C. Jiang, D. Jia, S.-Y. Yan and Y.-Q. Wang, *Clin. Ther.*, 2010, **32**, 1729.

152 (a) G. J. Despotis, G. Gravlee, K. Filos and J. Levy, *J. Am. Soc. Anesthesiol.*, 1999, **91**, 1122; (b) P. Raymond, M. Ray, S. Callen and N. Marsh, *Perfusion*, 2003, **18**, 269; (c) J. W. Vandiver and T. G. Vondracek, *Pharmacotherapy: J. Human Pharmacol. Drug Ther.*, 2012, **32**, 546.

153 M. N. Levine, J. Hirsh, M. Gent, A. G. Turpie, M. Cruickshank, J. Weitz, D. Anderson and M. Johnson, *Arch. Intern. Med.*, 1994, **154**, 49.

154 (a) H. Qi, L. Zhang, L. Yang, P. Yu and L. Mao, *Anal. Chem.*, 2013, **85**, 3439; (b) J. Guo and S. Amemiya, *Anal. Chem.*, 2006, **78**, 6893; (c) G. Qu, G. Zhang, Z. Wu, A. Shen, J. Wang and J. Hu, *Biosens. Bioelectron.*, 2014, **60**, 124; (d) Z. Zhong and E. V. Anslyn, *J. Am. Chem. Soc.*, 2002, **124**, 9014; (e) G. A. Crespo, M. G. Afshar and E. Bakker, *Angew. Chem. Int. Ed.*, 2012, **51**, 12575.

155 A. T. Wright, Z. Zhong and E. V. Anslyn, *Angew. Chem. Int. Ed.*, 2005, **44**, 5679.

156 Y. Egawa, R. Hayashida, T. Seki and J.-i. Anzai, *Talanta*, 2008, **76**, 736.

157 S. V. Nalage, S. V. Bhosale, S. K. Bhargava and S. V. Bhosale, *Tetrahedron Lett.*, 2012, **53**, 2864.

158 S. M. Bromfield, A. Barnard, P. Posocco, M. Fermeglia, S. Pricl and D. K. Smith, *J. Am. Chem. Soc.*, 2013, **135**, 2911.

159 X. Gu, G. Zhang and D. Zhang, Analyst, 2012, **137**, 365.

160 L. Zeng, P. Wang, H. Zhang, X. Zhuang, Q. Dai and W. Liu, *Org. Lett.*, 2009, **11**, 4294.

161 H. Szelke, S. Schubel, J. Harenberg and R. Kramer, *Chem. Commun.*, 2010, **46**, 1667.

162 K.-Y. Pu and B. Liu, *Macromolecules*, 2008, **41**, 6636.

163 S. Wang and Y. –T. Chang, *Chem. Commun.*, 2008, **0**, 1173.

164 J. D. Watson and F. H. C. Crick, *Nature*, 1953, **171**, 737.

165 A. Ghosh and M. Bansal, *Acta Cryst. D*, 2003, **59**, 620.

166 H. S. Basu, B. G. Feuerstein, D. A. Zarling, R. H. Shaffer and L. J. Marton, *J. Biomol. Struct. Dyn.*, 1988, **6**, 299.

167 M. L. Bochman, K. Paeschke and V. A. Zakian, *Nat. Rev. Genet.*, 2012, **13**, 770.

168 G. B. Bauer and L. F. Povirk, *Nucleic Acids Res.*, 1997, **25**, 1211.

169 L. H. Hurley, *Nat. Rev. Cancer*, 2002, **2**, 188.

170 J. Reedijk, *Proc. Natl. Acad. Sci. USA*, 2003, **100**, 3611.

171 B. Clement and F. Jung, *Drug Metab. Dispos.*, 1994, **22**, 486.

172 L. D. Williams, M. Egli and Q. Gao, *Proc. Natl. Acad. Sci. USA*, 1990, **87**, 2225.

173 M. Palumbo, *Advances in DNA Sequence-Specific Agents*, Elsevier, 1997.

174 a) S. A Latt, G. Stetten, L. A. Juergens, H. F. Willard and C. D. Scher, *J. Histochem. Cytochem.*, 1975, **23**, 493; (b) J. Kapuscinski and W. Szer, *Nucleic Acids Res.*, 1979, **6**, 3519.

175 C. Bailly and J. P. Henichart, *Bioconjugate Chem.*, 1991, **2**, 379.

176 S. Kamitori and F. Takusagawa, *J. Am. Chem. Soc.*, 1994, **116**, 4154.

177 C. A. Frederick, L. D. Williams, G. Ughetto, G. A. Van der Marel, J. H. Van Boom, A. Rich and A. H. J. Wang, *Biochemistry*, 1990, **29**, 2538.

178 (a) C. Bailly, M. Collyn-D'Hooghe, D. Lantoine, C. Fournier, B. Hecquet, P. Fosse, J.-M. Saucier, P. Colson, C. Houssier and J. -P. Henichar, *Biochem. Pharmacol.*, 1992, **43**, 457; (b) R. Zhanga, X. Wua, L. J. Guziecb, F. S. Guziec Jr.b, G. –L. Cheea, J. C. Yalowichc and B. B. Hasinoff, *Bioorg. Med. Chem.*, 2010, **18**, 3974; (c) C. Bourdouxhe-Housiaux, P. Colson, C. Houssier, M. J. Waring and C. Bailly, *Biochemistry,* 1996, **35***,* 14.

179 Z. Zhenyu and H. Piet, *Curr. Med. Chem.*, 2001, **8**, 517.

180 (a) L. Adriaenssens, L. Severa, T. Salova, I. Cisarova, R. Pohl, D. Saman, S. V. Rocha, N. S. Finney, L. Pospisil, P. Slavicek and F. Teply, *Chem. Eur. J.*, 2009, **15**, 1072; (b) F. Teply, *Chem. Listy*, 2011, **105**, 506; (c) L. Severa, L. Adriaenssens, J. Vavra, D. Saman, I. Cisarova, P. Fiedler and F. Teply, *Tetrahedron*, 2010, **66**, 3537.

181 L. Severa, D. Koval, P. Novotna, M. Oncak, P. Sazelova, D. Saman, P. Slavicek, M. Urbanova, V. Kasicka and F. Teply, *New J.Chem.*, 2010, **34**, 1063.
182 G. Olbrechts, K. Clays and A. Persoons, *J. Opt. Soc. Am. B*, 2000, **17**, 1867.
183 J. L. Oudar and D. S. Chemla, *J. Chem. Phy.*, 1977, **66**, 2664.
184 (a) K. Clays and B. J. Coe, *Chem. Mater.*, 2003, **15**, 642; (b) B. J. Coe, J. A. Harris, I. Asselberghs, K. Wostyn, K. Clays, A. Persoons, B. S. Brunschwig, S. J. Coles, T. Gelbrich, M. E. Light, M. B. Hursthouse and K. Nakatani, *Adv. Funct. Mat.*, 2003, **13**, 347.
185 (a) G. U. Bublitz and and S. G. Boxer, *Annu. Rev. Phys. Chem.*, 1997, **48**, 213; (b) W. Liptay, *Excited states*, 1974, **1**, 129.
185 (a) J. C. Sauceda, R. M. Duke and M. Nitz, *ChemBioChem*, 2007, **8**, 391; (b) J. C. van Kerkhof, P. Bergveld and R. B. M. Schasfoort, *Biosens. Bioelectron.*, 1995, **10**, 269.
186 C. Würth, M. Grabolle, J. Pauli, M. Spieles and U. Resch-Genger, *Nat. Protoc.*, 2013, **8**, 1535.
187 https://www.thermofisher.com/cz/en/home/references/molecular-probes-the-handbook.html
188 *RNeasy Mini Handbook*, 2012, 23.
189 A. D. Boese and J. M. L. Martin, *J. Chem. Phys.*, 2004, **121**, 3405.
190 N. C. Garbett, P. A. Ragazzon and J. B. Chaires, *Nat. Protoc.*, 2007, **2**, 3166.
191 (a) P. C. Dedon, in *Curr. Protoc. Nucleic Acid Chem.*, 2001, ed. S. L. Beaucage, Chapter 8, Unit 8.1; (b) D. Suh and J. B. Chaires, *Bioorg. Med. Chem.*, 1995, **3**, 723.
192 O. Trott and A. J. Olson, *J. Comput. Chem.*, 2010, **31**, 455.
193 W. Humphrey, A. Dalke and K. Schulten, *J. Mol. Graph.*, 1996, **14**, 33.
194 G. Prism, *San Diego, CA, USA*, 1994.
195 http://www.molbiotools.com/dnacalculator.html.

Charles University in Prague, Faculty of Science

Department of Organic Chemistry

Vishwas D. Joshi

Synthesis of novel helquats and their properties

PhD. Thesis

Supervisor: Mgr. Filip Teplý, PhD.

Institute of Organic Chemistry and Biochemistry, CAS

Prague-2017

Prohlašuji, že jsem předloženou doktorskou dizertační práci vypracoval samostatně a uvedl všechny použité literární prameny. Dále prohlašuji, že jsem nepředložil tuto práci ani její podstatnou část k získání jiného nebo stejného akademického titulu.

This work was carried out in years 2011-2017 at the IOCB, CAS. I declare that I have done the PhD. thesis independently citing all resources used. I also declare that I did not use this work to get the same or another university degree.

Prague, October 2017

……

Vishwas D. Joshi

Acknowledgment

I would like to acknowledge number of people, who helped me a lot during the completion of my PhD. over last six years. I would like to express my gratitude to my supervisor, Dr. Filip Teplý for giving me an opportunity to join his group as a PhD. student and work on a multidisciplinary project. He assigned me a project, which includes synthesis, characterization, and study of various properties of the compounds in order to explore the application potential. I also like to thank all my former and present group mates for providing a nice and healthy atmosphere in the lab.

I am indebted to Jaroslav Kozak, Erika Kuzmova, and Miroslav Hájek for their help in the designing of biological experiments. I want to express my sincere thanks to Dr. David Šaman (NMR), Dr. Ivana Cisarova (X-ray crystallography), Dr. Lucie Bednárová (CD spectroscopy), and Dr. Pavel Fiedler (IR spectroscopy). In addition, I want to thank the team of mass spectrometry and analytical department of IOCB CAS. I am expressing my sincere thanks to Prof. Vladimír Dohnal (UCT Prague) for allowing me to use instruments in his research group.

I would like to thank Prof. Benjamin Coe and all other co-authors for collaborating with us during the study of nonlinear optical properties of functionalized helquats.

I would like to thank Prof. Pavel Hobza, Martin Lepšík, and Adam Pecina for the theoretical study regarding dsDNA binding properties of one of the functionalized helquat derivatives.

In addition, I would like to thank IOCB CAS, and all relevant research groups from the IOCB for an opportunity to access all the key facilities for the research, Czech Science Foundation and Charles University in Prague for the financial support.

On this occasion, I would like to remember my early mentor at IOCB, late Dr. Illya Lyapkalo, for his teaching and support during my early days at IOCB. I also want to thank the previous team of Dr. Lyapkalo, who helped me a lot during my early days.

I would also like to take this opportunity to thank my early stage mentors, Dr. C. V. Rode, Scientist, National Chemical Laboratory (CSIR), India and Professor U. D. Joshi, Swami Ramanand Teerth Marathwada University, India for inspiring me to choose research as a career and pursuit a PhD. degree in Chemistry.

Finally, I like to thank my family and friends for giving me an emotional support during this time.

Abstrakt

Předmětem této dizertační práce je syntéza nových helquatů, studium jejich vlastností, např. nelineárně-optické vlastnosti, cílově specifické fluorescenční light-up vlastnosti, molekulární rozpoznávání (zahrnující chirální rozpoznávání dvouvláknové DNA s použitím opticky čistých helquatových barviv) a jejich aplikovatelnost založená na těchto vlastnostech.

Byly syntetizovány čtyři nové helquaty obsahující aktivované methylové skupiny a jeden z těchto helquatů byl úspěšně v gramovém měřítku rozštěpen na enantiomery pro následné aplikace. Syntéza funkcionalizovaných helquatových derivátů byla vyvinuta za použití Knoevenagelovy kondenzace helquatu s aktivovanými methylovými skupinami s různě substituovanými aromatickými a heteroaromatickými aldehydy. Tato metodika otevřela snadný přístup ke strukturně rozmanité knihovně více než 500 sloučenin skrze nechromatografické purifikace ve středních až vysokých výtěžcích. Zástupci této knihovny sloučenin byly prozkoumány v následujících směrech: jako nové nelineárně optické chromofory, cílově specifické fluorescenční ligth-up próby pro rozpoznávání cílů jako heparin nebo dvouvláknová DNA. Několik helquatových derivátů vykazovalo fluorescenční light-up v přítomnosti AT bohatých DNA sekvencí. Tato vlastnost byla dále detailně studována s použitím různých spektroskopických technik. Aplikace jedné z těchto sloučenin, **HeliDye1**, jakožto fluorescenční próby pro mikroskopii, gelovou elektroforézu a průtokovou cytometrii byly demonstrovány. Ve spolupráci s teoretickými chemiky jsme byli též schopni identifikovat možné vazebné módy molekul interagujících s dvouvláknovou DNA.

Abstract

The subject of this thesis comprises synthesis of novel helquats, exploration of their different properties, such as nonlinear optical properties, target-specific fluorescence light-up properties, molecular recognition properties (including chiral recognition of dsDNA using enantiopure helquat dyes) and their applicability based on these properties.

Four novel helquats containing activated methyl groups were synthesized and one of the synthesized helquats has been successfully resolved in gram scale into two separate enantiomers for further applications. Synthesis of functionalized helquat derivatives employing Knoevenagel condensation reaction between helquats having activated methyl groups and various substituted aromatic and heteroaromatic aldehydes has been developed. This methodology opened an easy access to a structurally diverse library of more than 500 compounds *via* chromatography-free purifications in moderate to high yield. Members of this compound library have been explored in various directions: as novel nonlinear optical chromophores, target-specific fluorescence light-up probes for recognition of targets like heparin and dsDNA. Few helquat derivatives have shown fluorescence light-up in presence of AT-rich DNA sequences. This feature has been further studied in detail using various spectroscopic techniques. Applications of one of these compounds, **HeliDye1,** as a fluorescent probe for microscopy, gel electrophoresis and flow cytometry has been demonstrated. In collaboration with theoretical chemists, we were also able to identify possible binding modes of the dsDNA interacting compound.

Abbreviations

aq.	aqueous
Ac	acetyl
Bn	benzyl
br	broad
n-Bu,	*n*-butyl
t-Bu	*tert*-butyl
calc.	calculated
cat.	catalytic
COSY	two-dimensional homonuclear correlation NMR spectroscopy
δ	chemical shift in parts per million relative to tetramethylsilane
CAM	cerium ammonium molybdate
d	doublet
DCM	dichloromethane
D-DBT	D-dibenzoyl tartrate
DFT	density functional theory
ds	double stranded
HOMO	highest Occupied Molecular orbital
DME	1,2-dimethoxyethane
DMF	*N*,*N*-dimethylformamide
DMSO	dimethyl sulfoxide
ee	enantiomeric excess
EI	electron impact ionization
ESI	electro-spray ionization
eV	electron volts
esu	electrostatic unit
equiv.	equivalents
EtOAc	ethyl acetate
FACS	Fluorescence-Activated Cell Sorting
h	hours
HMBC	heteronuclear multiple bond correlation
HMQC	heteronuclear multiple quantum correlation
HQ	helquat
HRMS	high-resolution mass spectrometry
HSQC	heteronuclear single quantum correlation
Hz	hertz
i-Pr	isopropyl
IR	infrared spectroscopy
J	coupling constant (in NMR spectrometry)
LUMO	lowest occupied molecular orbital
m	multiplet (spectral); meter(s); mili
M+	parent molecular ion
MeCN	acetonitrile
MHz	megahertz
m.p.	melting point
MS	mass spectrometry

MTBE	methyl tert-butyl ether
m/z	mass-to-charge ratio
NMR	nuclear magnetic resonance
NOESY	nuclear overhauser effect spectroscopy
NLO	nonlinear optics
o	*ortho*
p	para
ppm	part(s) per million
n-PrCN	*n*-propionitrile
PI	propidium iodide
PTC	phase-transfer catalysis/catalyst
Py	pyridine
q	quartet
R_f	retention factor (in chromatography)
ROESY	rotating frame overhauser effect spectroscopy
rt	room temperature
s	singlet (spectral); second(s)
ss	single stranded
S_N2	substitution nucleophilic bi-molecular
TBAB	tetra-*n*-butylammonium bromide
TD-TFT	time-dependent Density Functional Theory
TfOH	triflic acid
TfO^-	trifluoromethanesulfonate
TLC	thin layer chromatography
t	triplet (spectral)

Table of Contents

1. Introduction:

Helquats are a class of synthetic *N*-heteroaromatic cations described by our laboratory in 2009. [1] They possess intrinsic helical chirality like helicenes[2] and extended cationic skeleton similar to diquats.[3] This class of compounds thus embody structural features of both helicenes and Viologens and we expect emerging properties for this class of compounds (Fig. 1).

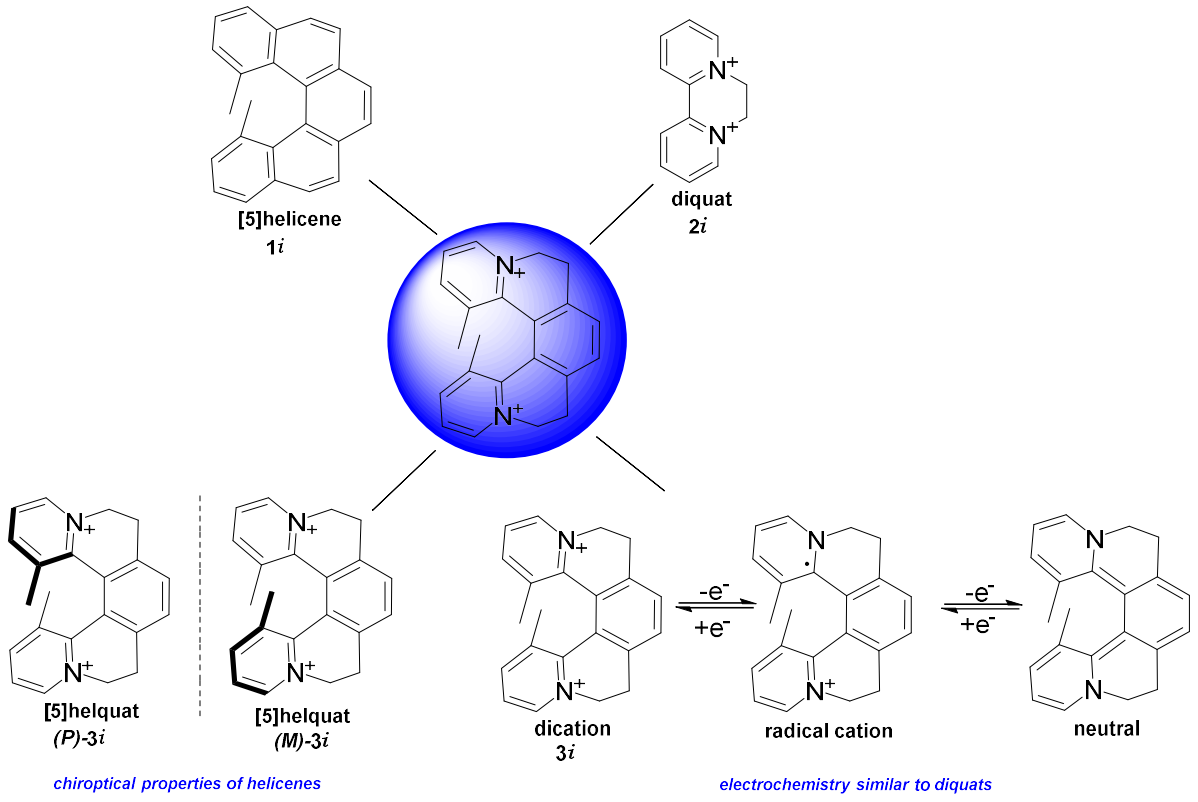

Fig.1: *Structural features of helquats*

So far, our group has reported some interesting features of this class of compounds. Remarkable chiroptical properties like helicenes,[4] SET reduction to radical cation or neutral form similar to diquats,[5] existence of saddlequat lying on helquat racemization pathway,[6] the circulenoid formation and fragmentation by photochemical and thermal process respectively[7] and the functionalization of helquats to give helical cationic styryl dyes *via* Knoevenagel condensation chemistry.[8]

Furthermore, helquats can be used as organocatalysts in organic reactions such as Aldolization and Mannich.[9]

The hypothesis of this thesis is that helquats can be used as novel nonlinear optical materials as well as in recognition exploiting their interactions with cavities and grooves of the biological targets.

One of the main incentives for the introduction of helquats as a novel structural class was fascinating chemistry of helicenes and their application promise. On the other hand, researchers reported number of *N*-heteroaromatic cationic molecules from natural and synthetic sources to have attractive and useful properties.

1.1 Natural and synthetic N-heteroaromatic cations:

Nicotinamide adenine dinucleotide, NAD^+, **4*i*** is a pyridinium based structures and together with its reduced form, NADH, it is known for its key role in cellular metabolism (Fig. 2).[10]

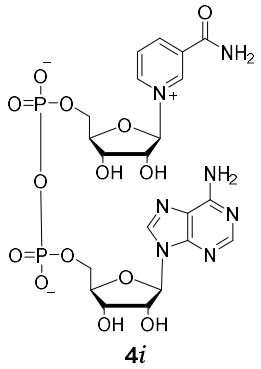

4*i*

Fig. 2: *Nicotinamide adenine dinucleotide.*

Cationic alkaloids containing isoquinolinium and phenanthridinium moieties (Fig. 3) are secondary metabolites which comprise two main groups benzo[*c*]phenanthridines and protoberberines.[11] Berberine **5*i*** is a fluorescent antibiotic used in Ayurveda[12] and also used as a fluorescent stain for heparin in mast cells.[13] Isoquinolinium alkaloids (**5*i*** to **8*i***) are known for their telomeric G-quadruplex binding activity,[14] antifungal activity,[15] antioxidant activity,[16] antimalarial[17] and antidepressant activities.[18]

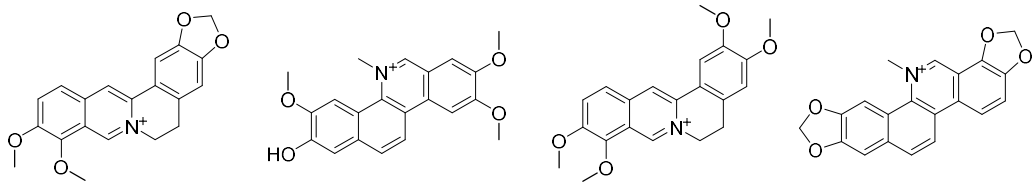

Fig. 3: *Structures of cationic alkaloids.*

N-heteroaromatic cationic molecules are also known for their applications as novel materials, nonlinear optical properties, ionic liquids, as probes for nucleic acids (Fig. 4, **9*i***) and other biological targets. Due to their ionic nature, they usually have good solubility in water. Coralyne (Fig. 4, **10*i***) is a synthetic member of protoberberine family which shows a significant anti-leukemic activity.[19] Various substituted derivatives of berberine are known to interact with G-quadruplex DNA with improved telomerase targeting activity as compared to natural berberine.[20]

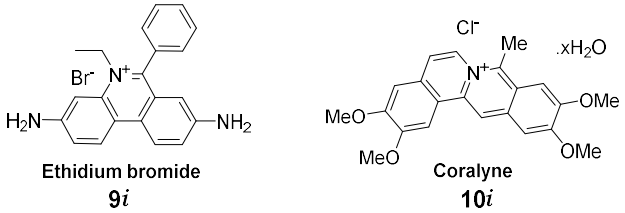

Fig. 4: *Cationic intercalator Ethidium bromide (**9i**) and anti-leukemic drug Coralyne (**10i**).*

$TMPyP_4$ tosylate (**11*i***),[21a] TQMP (**12*i***)[21b] substituted acridine derivative, **13*i*** [21c] and many other synthetic *N*-heteroaromatic cationic molecules (e.g. **14*i*** [21d] and **15*i*** [21e]) are known for their G-quadruplex-DNA stabilizing properties (Fig. 5).

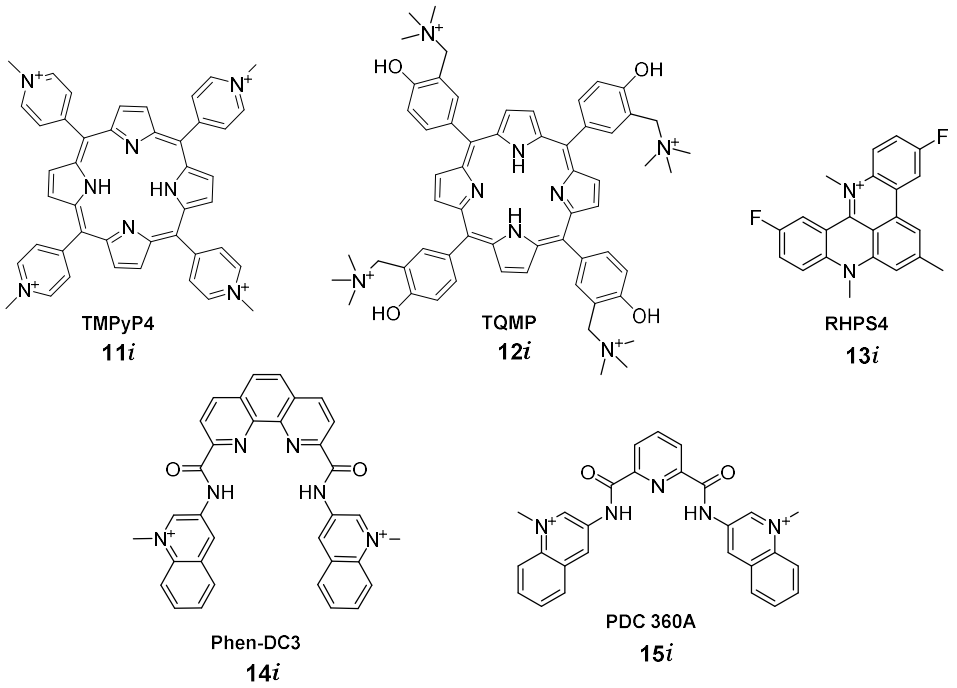

Fig. 5: *G-quadruplex stabilizing ligands.*

Other than biological activities of the *N*-heteroaromatic cationic molecules, such molecules found their uses as novel ionic liquids like **16*i*** or **17*i*** (Fig. 6). Ionic liquids have low melting points and negligible vapour pressure which makes them suitable to be used as solvents for many chemical reactions.[22] Ionic liquids are usually regarded as ‘‘green solvents.’’ All these unique properties of ionic liquids make them applicable in diverse fields such as separation technology,[23] nanotechnology,[24] catalysis[25] and biocatalysis.[26]

Fig. 6: *Cationic ionic liquids.*

Pyridinium and bipyridinium based systems are attractive because of their electron withdrawing properties (pull effect),[27] redox properties,[28] electro-optical and photophysical properties.[29] By virtue of all these properties, they are suitable as electrophores in artificial systems developed for solar energy conversion,[30] components of choice in supramolecular assemblies designed to behave as electron storage systems[31] and as molecular machines.[32]

1.2 Helicenes

Helicene is a specific class of helical molecules formed due to the *o*-fusion of aromatic, heteroaromatic or semi-aromatic rings. The helical arrangement of such molecules is feasible, because it gives a relief from the steric strain. Due to this nonplanar type of arrangement, the molecules become chiral despite of lacking a stereo center and the molecules are called as helically chiral molecules (**18*i*** to **22*i***, Fig. 7).[33]

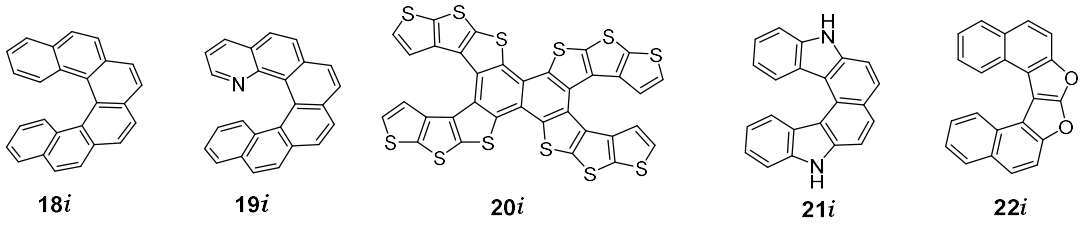

Fig. 7: *Structures of carbo and heterohelicenes.*

According to the rule of helicity (Ingold and Prelong, 1966), a left-handed helix is designated as "minus" and denoted as ''*M*'' and a right-handed one is designated as "plus" and denoted as ''*P*'' (Fig. 8).

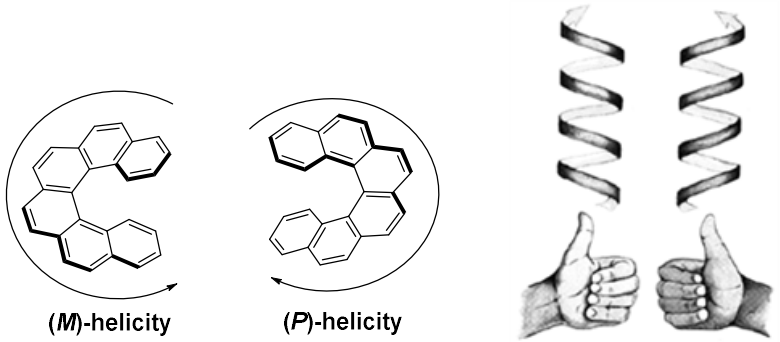

Fig. 8: *Schematic representation of helicity*

Examples of helical chirality in nature are right handed and left handed structures of dsDNA and some of the proteins.

- ***Synthesis of carbo and heterohelicenes:***

Classical synthesis of *racemic* helicenes (for e.g. **24*i***) *via* an oxidative photocyclization of stilbene type precursors (**23*i***) was reported by Martin *et al.* in 1967.[34] Due to the easy availability of stilbene-type precursors prepared by Wittig olefination, many helicene homologues, starting from [5] to [14]helicene and their derivatives were prepared. The main drawback of photochemical synthesis is the use of very high dilute solutions of reaction components in carcinogenic solvents like benzene and formation of isomers. Therefore, in modern methodologies using non-photochemical methods were more encouraged.

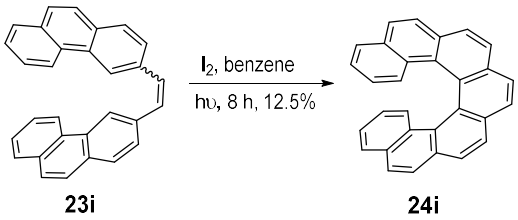

Scheme 1: *Classical way of synthesizing helicene.*

Katz and Liu did the pioneering work to develop one of the modern, convenient and non-photochemical approach for the synthesis of *racemic* helicene bisquinones by Diels-Alder reaction.[35] The other reported approaches are carbenoid coupling,[36] tin-mediated, non-reducing tandem radical cyclization of (*Z,Z*)-1,4-bis(2-iodostyryl)-benzene derivatives[37] and many more.

Collins *et al.* introduced a novel approach in helicene chemistry. A transition metal catalyzed ring closing olefin metathesis of substrate **25*i*** in microwave at 100 °C or by classical heating at 40 °C in a sealed tube[38] gave [5]helicene, **26*i*** (Scheme 2).

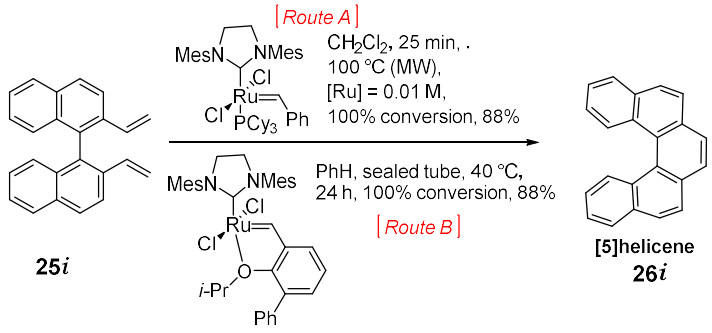

Scheme 2: *Olefin metathesis method for helicene synthesis.*

Guitian *et al.* were the first to introduce an intramolecular [2+2+2] cycloaddition of arynes and alkynes (Scheme 3).[39] In a reaction sequence, a mixture of two regioisomers **31*i*** and **32*i*** were obtained *via* formation of benzyne like intermediate **30*i***. The main drawback of this method was the formation of regioisomers.

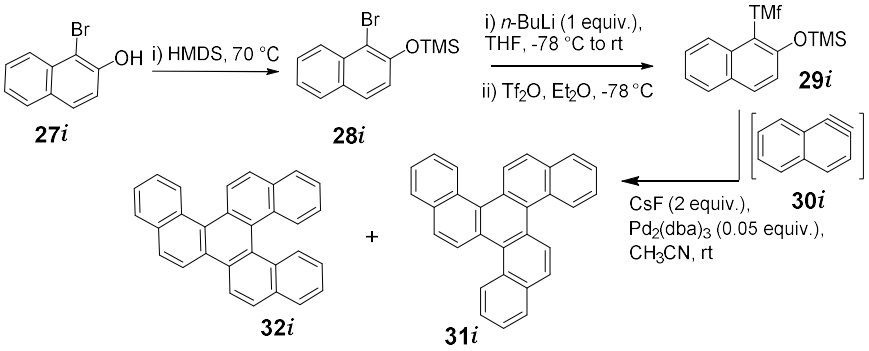

Scheme 3: *[2+2+2] cycloaddition of arynes and alkynes.*

Stary *et al.*[40] developed a novel approach for the synthesis of helicenes in a Co(I) or Ni(0) catalyzed [2+2+2] cyclotrimerization of triyne intermediate. For e.g. triyne **33*i*** was cyclotrimerized to [5]helicene **26*i***. Five, six and seven helicenes were synthesized with ease using this methodology. The main advantage of the methodology is that it is an atom-economy method and three rings are formed in a single step, as compared to classical photocyclization approach. (Scheme 4 and 5).

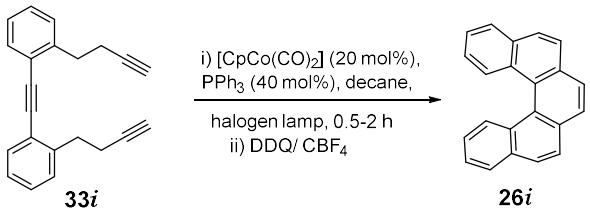

Scheme 4: *Co catalyzed [2+2+2] cyclotrimerization to helicenes.*

When Co(I) catalyst was replaced with Ni(0) catalyst, the reaction can be carried out at an ambient temperature, without irradiation with visible light. The products previously synthesized in Co(I) catalyzed methodology were synthesized with almost similar yields in a Ni(0) catalyzed reaction. (Scheme 5).

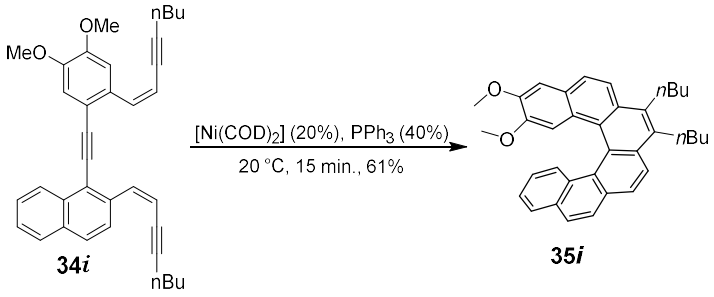

Scheme 5: *Ni catalyzed [2+2+2] cyclotrimerization to helicenes.*

To achieve fully aromatic helicene, dehydrogenation was performed either with DDQ or CBF_4. The methodology is very practical because of its high efficiency (100% atom economy, good to excellent yields, rapid reactions). So that many substituted helicenes and helicene like molecules such as Vollhardt's heliphenes,[41] Tanaka's [9]helicene like molecules,[42] Carbery's helicinoidal DMAP catalysts[43] were synthesized using this approach.

Some research groups also synthesized heteroaromatic helicenes other than carbohelicenes, such as azoniahelicenes (**36*i*** and **37*i***), dioxahelicenes (**38*i***) and thiahelicenes (**39*i***).

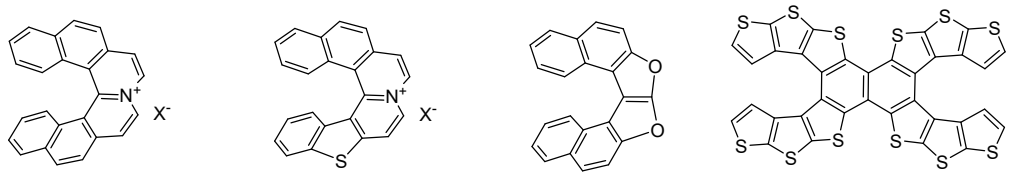

Fig. 9: *Heterohelicenes containing one or more heteroatom.*

Arai *et al.* reported synthesis of first fully aromatic azoniahelicene, **36*i*** *via* photocyclization of styryl intermediate **45*i*** in 4 steps (Scheme 6).[44]

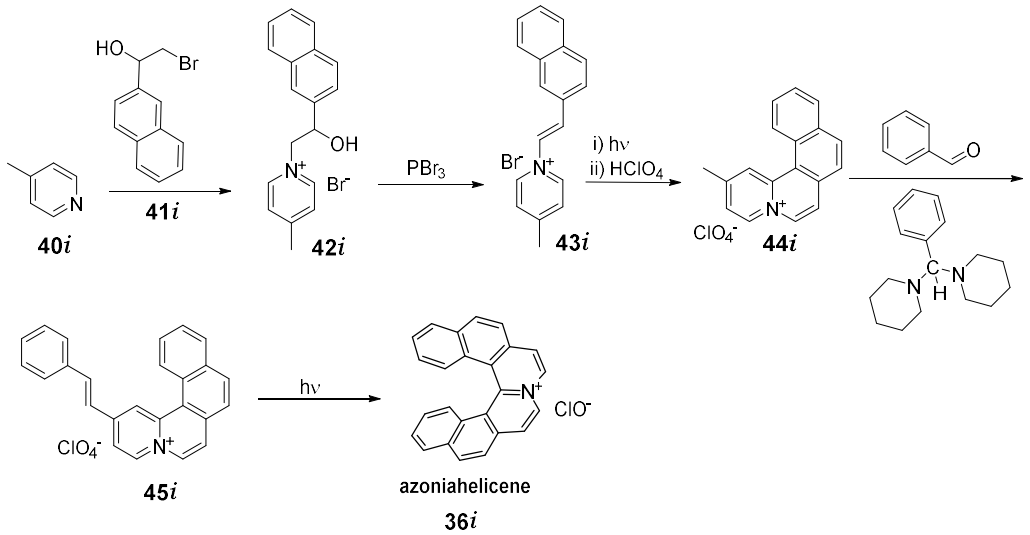

Scheme 6: *Arai's methodology for azoniahelicenes synthesis.*

Other than photochemical cyclization, several modern strategies were developed for the synthesis of azahelicenes. Stabb *et al.* reported Stille-Kelly coupling reaction (Scheme 7)[45] for azahelicene synthesis. Diaza[6]helicene **47*i*** was obtained in 52% yield in a Pd(0)

catalyzed reaction in presence of hexamethyldistannane. A similar method was independently developed by Takenaka *et al.*[46] 1-azahelicene **49*i*** was synthesized in 61% yield in Pd(II) catalyzed reaction in presence of Sn.

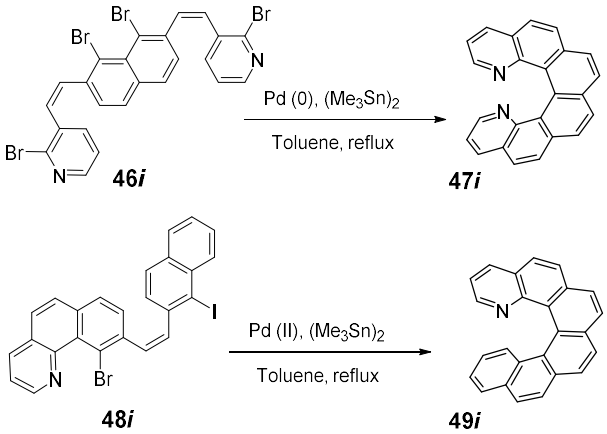

Scheme 7: *Stille-Kelly cross coupling methodology for the synthesis of azahelicenes.*

Due to easily obtained precursors *via* highly *Z*-selective Wittig reaction of halo substituents, the strategy is of considerable practical utility for the synthesis of different helicenes.

Cyclotrimerization approach developed by Stary *et al.* was also successful for the synthesis of azahelicenes (Scheme 8). Triyne precursor of type **52*i***, obtained in two consecutive steps *via* nucleophilic substitution followed by Pd/Cu catalyzed Sonogashira cross-coupling reaction was successfully cyclotrimerized to dihydrohelicene **53*i***. The bottleneck of the synthetic cascade was the final step, in which cyclotrimerized product, **53*i*** was oxidized using MnO_2 in the microwave at 150 °C. Fully aromatic 1,14-diaza[5]helicene was obtained in 41% yield. [47]

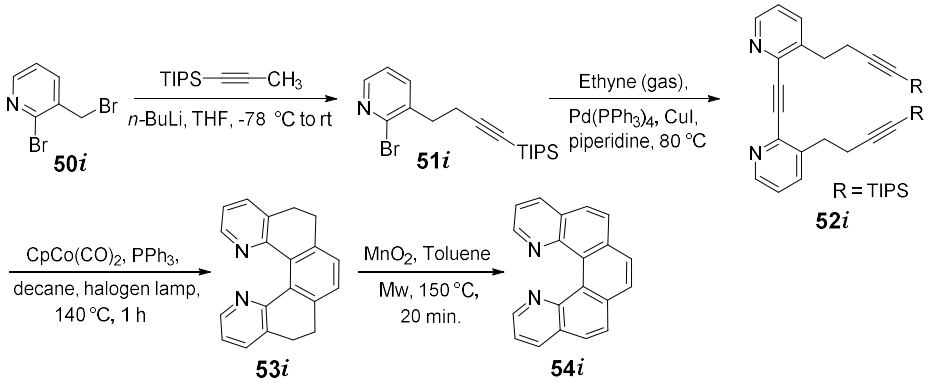

Scheme 8: *Cyclotrimerization approach for azoniahelicenes synthesis.*

Even though all above discussed methods preferentially gave *racemic* helicenes, several methods for the enantiopure synthesis such as CPL-induced asymmetric photocyclization, chemically induced asymmetric photocyclization, metal catalyzed asymmetric synthesis, asymmetric Diels-Alder reactions, asymmetric rearrangements, and synthesis using chiral additives were developed.

Several methods for the optical resolution of helicenes and helicene like molecules, such as recrystallization, direct resolution by HPLC, resolution using chiral auxiliaries, and enzymatic resolutions were developed. In our group, we developed methods for resolution of helquats *via* formation of a diastereomeric mixture from *racemic* helquat *via* anion exchange to chiral counterions such as dibenzoyl tartrate or camphor sulfonate in anion exchange process.

Two diastereomers were separated *via* washings with a preferential solvent such as MeOH or EtOH and respective pure enantiomer was obtained by breaking a pure diastereomeric salt of helquat *via* second anion exchange to achiral counterion such as bromide or triflate.[4] This method of resolution is discussed in section 2 of this thesis.

- **Properties of helicenes:**

The bond lengths between C-C and C=C in helicenes are different in comparison with typical bond length in benzene (1.393 Å).[48] The average bond length of the C-C bonds in the inner helix is lengthened to about 1.430 Å while the average length of the ones on the periphery is shortened to about 1.360 Å.[33b]

As like other aromatic compounds, helicenes are good π-donors and can form charge transfer-complexes with many π-acceptors.[49] As a result, by enthalpy driven charge transfer complex formation with a chiral π-acceptor reagent, the optical resolution of helicenes is achieved. In addition, π-π interaction also plays an important role in determining properties and self-assembly behaviour of helicene in solution and solid state.[50]

Some other interactions in crystals such as Hydrogen bonding,[51] CH-π interactions,[52] S-S interactions,[53] and H-H interactions[54] are also known to be observed in case of helicenes. In case of some helicenes, recrystallization spontaneously affords homochiral conglomerates[55] or enantioenriched crystals.[56]

High 'proton sponge' basicity is one of the property of some azahelicenes (**55*i*** to **59*i***) shown in Fig. 10 by forming linear N---H---N hydrogen bonds.[45]

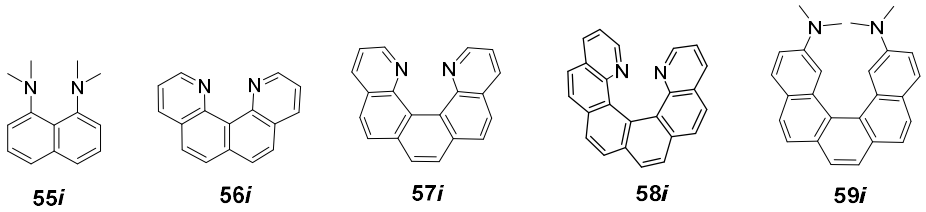

Fig. 10: *Some helical 'proton sponges'.*

The solubility of helicenes is much higher as compared to other planar polycyclic aromatic compounds. The solubility can be improved by introducing appropriate substituents-alkoxy and alkyl groups.[57]

Helicenes show a unique combination of three-dimensionality and remarkable spectral and optical properties. As a result, the considerable attention has been drawn towards their synthesis and their uses especially in the field of enantioselective catalysis,[46] sensing,[58] molecular recognition,[59] self-assembly,[51] nonlinear optics,[50b, 60] liquid crystals[61] and circularly polarized luminescence (CPL)[35] for back lighting in LCD displays.[62] Due to all these properties discussed above, the application potential of helicenes was very well explored in diverse fields such as asymmetric catalysis as chiral auxiliaries in diastereoselective reactions,[63] as organocatalyst,[64] as chiral ligands with metal catalysts for asymmetric synthesis,[65] in the field of developing molecular machines,[66] as dye materials,[67] and many more. All these applications of helicenes are the subjects of many review articles and book chapters.[33] Molecular recognition and Nonlinear optical properties of helicenes are discussed in more in context to this thesis.

- **Molecular recognition properties of helicenes:**

Noncovalent interactions such as hydrogen bonding, metal coordination, hydrophobic forces, Van der Walls forces, π- π interactions, electrostatic or electromagnetic between two or more molecules are known as molecular recognition. In addition to these direct interactions, solvents may also play important role in molecular recognition in solution. The host and guest involved in molecular recognition also possess molecular complementarily.

Chiral recognition is one of the important applications of helicenes. Nakazaki *et al.* demonstrated the use of two optically pure crown ethers **60*i*** and **61*i*** (Fig. 11), both in their *M*-configuration, for the enantiomeric separation of guest molecules in solution *via* chiral recognition.[68] Interestingly, both molecules were showing exactly opposite chiral recognition to each other.

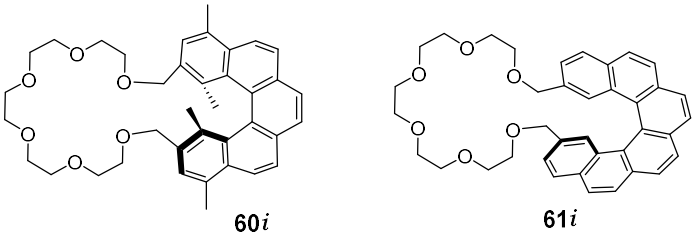

Fig. 11: *Optically pure crown ethers with helicene: showing chiral recognition in solution.*

Katz *et al.* reported a novel method to for the sensing of remote chiral centres by attaching the molecules to the chiral groove of [5]HELOL **62*i*** chlorophosphite (Scheme 9).[59b, 69]

The chiral molecules with reacting groups such as alcohols, amines or carboxylic acids in their *racemic* form were reacted with [5]HELOL chlorophosphite to form different diastereomers, which were analyzed by ^{31}P-NMR. The ratio of the peak integrals for the individual diastereomer directly gave the enantiomeric excess in the previous mixture. This method was efficient because the authors were able to synthesize [5]HELOL **62*i*** substrate on a large scale and were able to employ the method for the broad range of substrates, including alcohols, phenols, amines, and carboxylic acids.

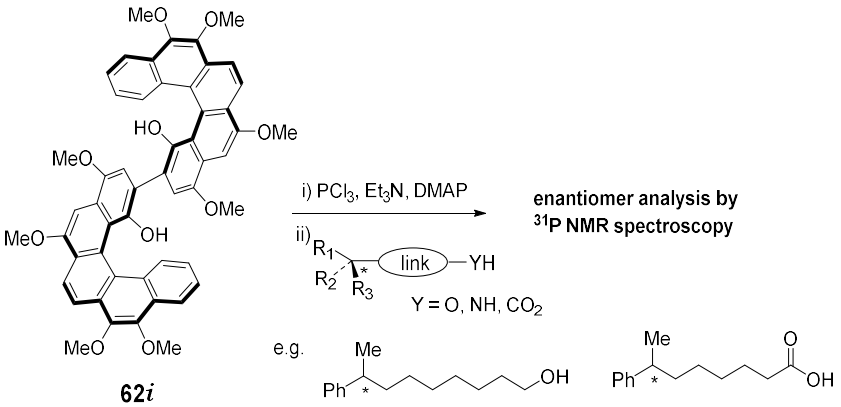

Scheme 9: *Katz method for chiral recognition of remote chiral centers.*

Molecular recognition properties of helicene were studied in the context of chiral recognition of either right-handed (*B*-form) or left-handed (*Z*-form) dsDNA. Vauthey *et al.* reported the binding properties of chiral [4]helicene derivatives **63*i*** to **65*i*** (Scheme 10) with dsDNA by fluorescence spectroscopy and linear dichroism spectroscopy, which shows higher selectivity of *M*-enantiomer over *P*. The binding constant (K_B) depends substantially on the

dye substituents and in all cases was larger in case of *M* than with *P*, by factors ranging from 1.2 to 2.3, depending on the dye (Scheme 10).[70]

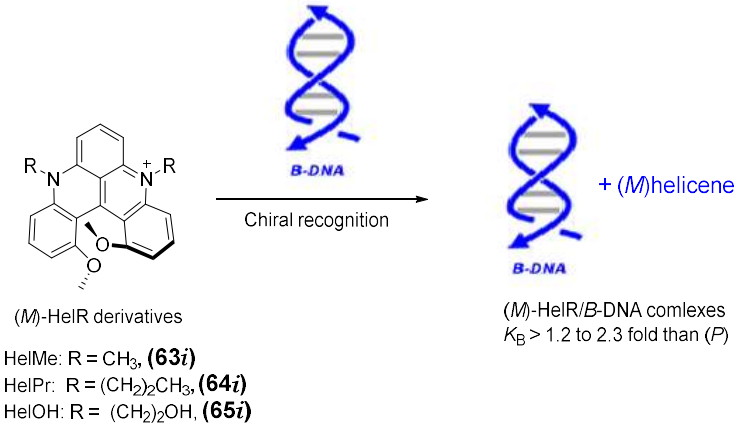

Scheme 10: *Stereo-selective binding of chiral [4]helicene with B-DNA.*

Tanaka *et al.* studied the chiral selection of *Z*-DNA using *P* and *M* enantiomers of **66*i*** (Scheme 11). The ***P*-66*i*** was found to show high selectivity towards *Z*-DNA with a K_B value five times greater than that with *M*-enantiomer. Moreover, it was also observed that the *P*-enantiomer was effectively converting *B*-DNA to *Z*-DNA [71]

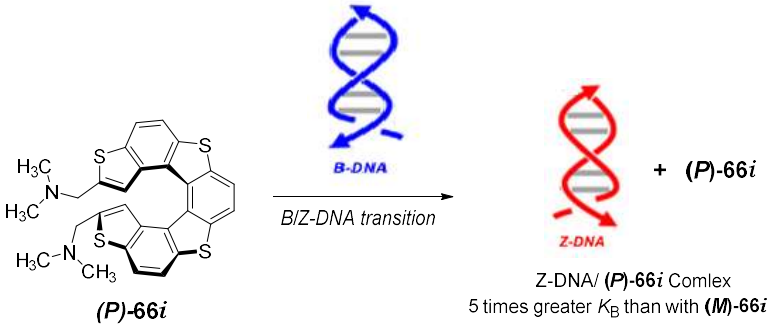

Scheme 11: *Enantiomeric pair of Tanaka's thiahelicenes* ***65i****, showing enantio-selective binding to Z-DNA.*

Sugiyama *et al.* reported another cyclic thiahelicenes molecule (**67*i***) with a short linker. The enantioselective telomerase inhibition and stabilization of G-quadruplex DNA structures was observed. They reported the dose-dependent inhibition of telomeric ladder formation, with the concentrations between 0.2 to 0.5 µM of the ***(M)*-67*i***. In contrast, no inhibition was observed in the presence of ***(P)*-67*i***, even at 10 µM concentration (Fig. 12).[72]

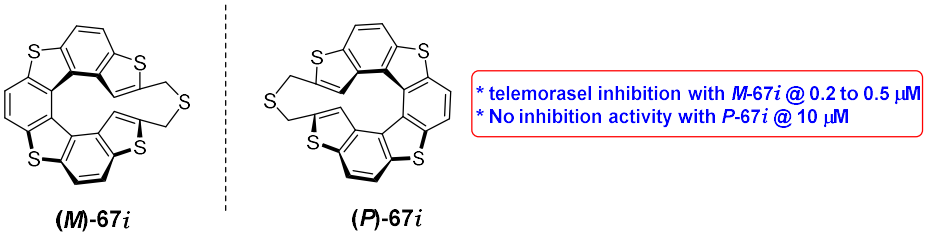

Fig. 12: *Enantiomeric pair of cyclic thiahelicene that showed stabilization of G-quadruplex DNA via selective inhibition of telomerase.*

Very recently, Sasaki *et al.* have shown the synchronized chiral recognition between [5]helicene-Spermine ligand and *B*/*Z*-DNA. The *racemic* **68*i*** was bound to B-DNA (Scheme 12). with an induction of its *P*-chirality together with the *B* to-*Z* helicity change of the duplex

DNA, $[(dC\text{-}dG)_3]_2$. The (*P*)-chirality of the bound **68*i***, in turn, transitioned to the (*M*)-chirality according to the changed chirality of the DNA to *Z* [73]

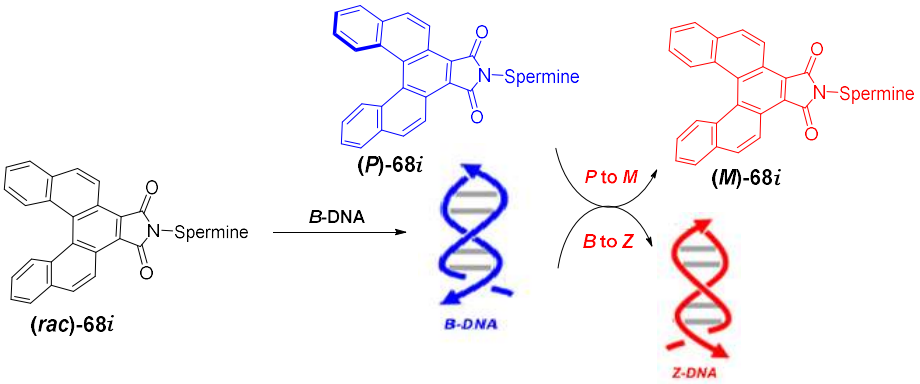

Scheme 12: *Synchronized chiral recognition between [5]helicene-Spermine ligand and B/Z-DNA.*

The field of chiral recognition of DNA, using helicene is relatively new and many developments leading to some potential applications can happen in near future.

- **Nonlinear optical (NLO) properties of helicenes:**

In day-to-day life, the optical properties of the material are independent of the intensity of the light beam. With the light of very high intensity is used, the material properties start to change according to the intensity and other characteristics of that light. The study of changing optical properties of the material after an interaction with such a high-intensity light beam is coming under a relatively young branch of Physics, called as nonlinear optics (NLO).[74, 75] The material which shows such properties due to their particular arrangement of molecular components are called as NLO material. NLO materials based on molecular compounds are of considerable interests because of their applications in advanced optoelectronic and all-optical data processing technology.[76]

In a chemist point of view, at the molecular level NLO phenomenon originated due to an interaction between polarizable electron density within a molecule and a very strong alternating electric field of a laser light beam. As a resultant induced polarization, response (*P*) of a molecule can be expressed as a power series in the applied field (*E*) according to the expression given below:[77]

$$P = \alpha E + \beta E^2 + \gamma E^3 + \ldots\ldots\ldots \qquad (eq.\ 1)$$

With the use of normal low-intensity light originated from non-laser source, the quadratic and cubic terms in eq. 1 can be neglected and a linear optical behaviour is observed. The coefficient α is known as linear molecular polarizability and is related to the refractive index of the material.

However when light originating from high power laser beam is used and the *E* approaches to the magnitude of atomic field strength, the βE^2 and γE^3 terms in equation becomes important and it gives rise to quadratic (second order) and cubic (third order) NLO effects. The coefficients β and γ are termed as molecular hyperpolarizabilities.

The equivalent form of eq. 1 at macroscopic level is given in eq. 2.

$$P = \chi^{(1)}E + \chi^{(2)}E^2 + \chi^{(3)}E^3 + \ldots\ldots\ldots \qquad (eq.\ 2)$$

Majority of molecules, which possess large β values contain three basic components:

1) A powerful σ/π electron donor group (D)

2) A powerful σ/π electron acceptor group (A)

3) A π-conjugated electron bridge connecting (D) to (A)

Few examples of such dipolar molecules[78-81] showing pronounced quadratic NLO activities are shown in Fig. 13.

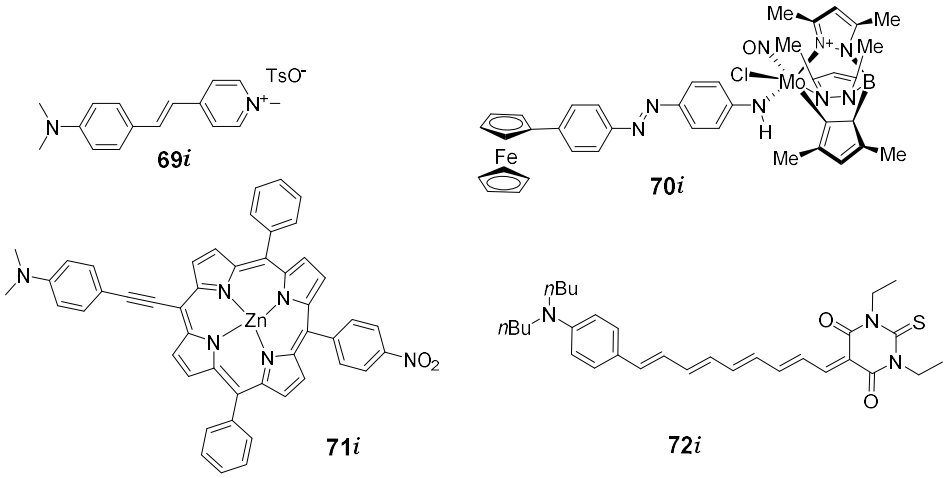

Fig.13: *Few examples of nonlinear optical materials.*

The macroscopic requirement for 2nd order hyperpolarizability, $\chi^{(2)}$ in non-centrosymmetric material featuring some degree of alignment of the dipolar molecular constituents. Therefore, the extent of potentially useful NLO activity depends on not only the structure of the molecule but its crystal packing arrangements.

Even though for the device applications thermal and photochemical stability, processability and many other factors are measured, but for common applications, the quadratic NLO properties of the materials could be adequately measured by techniques like hyper-Rayleigh scattering, second harmonic generation spectroscopy, stark spectroscopy and computational methods.

Although numerous factors must be considered for device applications (e.g., thermal and Photochemical stability, processability, etc.), the quadratic NLO properties of materials are adequately accessed on the basis of β and $\chi^{(2)}$ coefficients. $\chi^{(2)}$ coefficients values are obtained from solid-state SHG experiments, whilst β coefficients are measured in solution, and until recently the only means for achieving this was the electric-field-induced Second Harmonic Generation (EFISHG) technique.[82]

SHG is a nonlinear optical phenomenon, in which certain materials possessing required molecular arrangement and as a result showing nonlinear optical properties can modulate the property of very high-intensity light emitted from a powerful source such as a laser beam. The two light photons of same frequency after passing through such material combine and emitted as a single photon of double the frequency or half of the wavelength.[83]

In SHG spectroscopy, one focus is on measuring the doubled frequency 2ω due to an incoming electric field $E\omega$ in order to reveal information about a surface. The induced second-harmonic dipole per unit volume, $P^2 2\omega$ can be written as

$$E(2\omega) \sim P^2 2\omega = \chi^{(2)} (E\omega)(E\omega) \qquad (eq.\ 3)$$

Where, $\chi^{(2)}$ is known as the nonlinear susceptibility tensor and is a characteristic to the materials at the interface of study.[84] The generated of *E(2ω)* and corresponding $\chi^{(2}$ gives an information about the orientation of molecules at a surface/interface, the interfacial analytical chemistry of surfaces, and chemical reactions at interfaces.

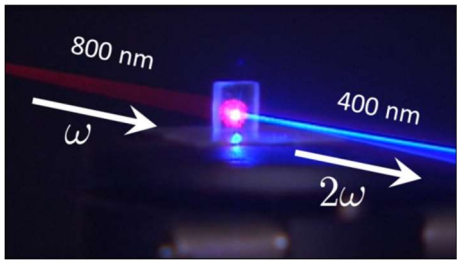

Fig.14: *Illustration of Second harmonic generation.*

Since SHG cannot be observed from an isotropic solution, pooling with a strong external electric field is used to create a partially non-centrosymmetric macroscopic structure, and analysis of the second harmonic light affords the component of β along the dipolar axis. During last few years, the versatile hyper-Rayleigh scattering (HRS) technique has also become available.[85] This relies upon the fact that microscopic anisotropy within a solution can produce incoherent harmonic scattering; this allows the determination of different directional components of β. HRS has certain advantages over EFISHG, for example, it does not require knowledge of molecular dipole moments and is applicable to charged and octopolar compounds that are not amenable to EFISHG study.

Measurements of β are typically made by the use of a 1064 nm NIR Nd^{3+}: YAG laser fundamental (532 nm second harmonic), and the resultant β1064 values are increased by resonance enhancement. By using the two-level model,[86] which is valid for dipolar molecules in which β is primarily associated with a single ICT excitation, we can calculate β_0 values. β_0 is termed the zero-frequency hyperpolarizability and is an estimate of the intrinsic molecular hyperpolarizability in the absence of resonance effects. Applications of molecular NLO materials will generally involve NIR lasers operating in the region about 1000 ± 15 nm, and β_0 values represent molecular quadratic NLO responses at such off-resonance wavelengths. The nonlinear optical properties of styryl dyes containing donor acceptor groups are discussed in section 1.4. In this section, NLO properties of helicenes and few examples are discussed below.

Chirality is an important theme of in NLO.[75] Due to the removal of mirror planes, the symmetry requirements for NLO effects can be slightly relaxed and as a result, the main requirement for NLO activity, such as polar molecular arrangement is no longer strictly necessary. Therefore, any organized bulk structure, polar or apolar with chiral components can in principle show NLO activity with this major advantage over the achiral molecules. Helicenes, which are the intrinsic chiral molecules, show NLO activity. Many groups working in helicene chemistry so far studied the NLO properties of various substituted helicenes based on theoretical studies; as a result, very few practical examples are available.

Verbiest et al. reported a new approach, in which they studied NLO properties of the novel chiral material, **73*i***. The supramolecular organization of chiral helicene material **73*i*** (Fig. 15b) was playing an important role[50b] and they proved that Langmuir-Blodgett films of a chiral helicene composed of supramolecular arrays of the molecules increase the second-order NLO susceptibility about 30 times larger than the same molecule in racemic form. The

Susceptibility components that were allowed only by chirality dominates the second-order NLO response.

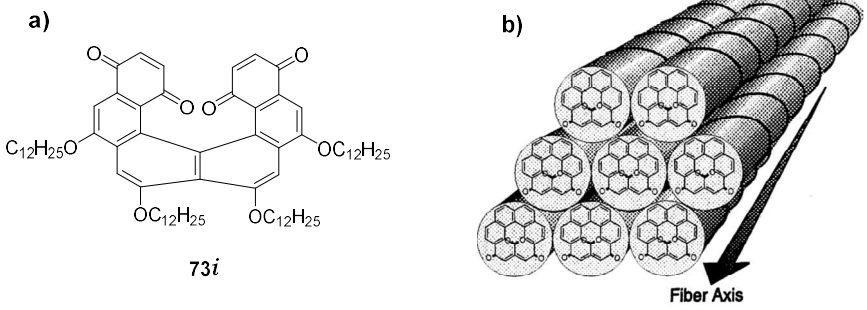

73*i*

Fig. 15: *a) Chemical structure of the helicene molecule; b) Schematic arrangement of molecules as stacked columns in solid material leading to NLO activity.*

Weber et al. reported a theoretical study using both a semi-empirical approach in the case of static and dynamic properties and Density Functional Theory (DFT), in the case of static electric properties. The nonlinear optical (NLO) properties of a set of 10 molecules were investigated to predict the couple of donor-acceptor substituents that could best enhance the optical properties of (*M*)-tetrathia-[7]-helicene, **74*i*** (Fig. 16).[60] Based on their calculations, they have shown that the best nonlinear optical properties were obtained with the nitro NO2 and the amino NH2 pair substituents.

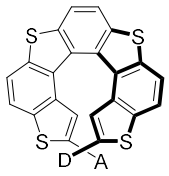

74*i*

A	D	num.
H	H	1
H	NH_2	2
NO_2	H	3
NO_2	NH_2	4
NO_2	OH	5
COOH	H	6
NO_2	Cl	7
CHO	OH	8
CHO	H	9
CF_3	NH_2	10

Fig. 16: *Basic chemical structure of the (M)-tetrathia-[7]helicene,* ***74i*** *with the list of suggested structural modifications.*

Gubler and Bosshard reviewed the molecular engineering strategies that can be used to develop new features in nonlinear optical systems and they proposed Self-assembly based on chiral molecules is one of the important approaches that opens up interesting routes in materials development.[75]

Verbiest et al. reported the second order NLO properties of the single enantiomer of helicene **75*i***, based on the orientation of a lyotropic nematic phase of the molecule by an electric field. Helicene **75*i*** in dodecane solution exhibits second-harmonic generation, the intensity of which was affected by the helicity of the irradiating circularly polarized light and it reverses the sign when the polarity of the orienting electric field reverses (Fig. 17).[87]

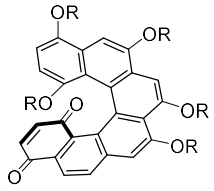

(*M*)-75*i*

Fig. 17: *Helicene* ***(M)-75i*** *studied for the NLO activity under the effect of electric field.*

So far, many research groups studied the NLO properties of helicenes *via* theoretical study and there is a lot of potential in this field to develop.

Our research group recently reported helicene like helquat dyes in their racemic form for their second-order nonlinear optical properties by measuring spectroscopic techniques and DFT calculations.[88] This study is part of this work and will be discussed in the results and discussion section of this thesis.

1.3 Viologens:

The bis-quaternary derivatives of 4,4'-bipyridyl and 2,2'-bipyridyl are known as Viologens.[89] The name originated from intensively blue colored cation radical easily available by reduction. Possibly the best-known Viologens are paraquats (e.g., **76*i***) and diquats (e.g., **77*i***), the world's most widely used herbicides.[90]

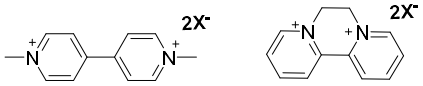

Paraquat **76*i*** Diquat **77*i***

Fig. 18: *Structures of paraquat and diquat.*

Viologens are known for their ability to change colors in solution by single electron reduction processes. A radical cation (**76*i'***) with intense blue color is formed, which may be oxidized in a reversible reaction to give back viologen. Further reduction of radical cation takes place to give a yellow colored quinoid (**76*i''***) (Scheme 13).

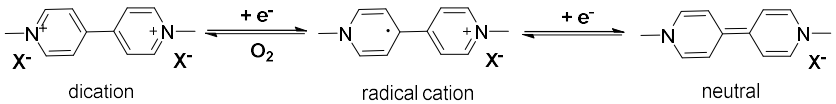

dication **76*i*** radical cation **76*i'*** neutral **76*i''***

Scheme 13: *Single electron reduction of paraquat.*

The stable, reversible redox behaviour of Viologens can be confirmed *via* cyclic voltammetry (CV), having reduction potentials of 1.09 V and -1.52 V in MeCN (vs. Fc/Fc^+, NBu_4PF_6 as supporting electrolyte). These low reductions are ideal for electron-accepting organic materials, relating to the overwhelming interest of viologens and their application to electronics. Although viologens have a variety of interesting properties, they additionally can also be modified to improve their novel electronic and photophysical properties, increasing their versatility for practical applications.[91]

Due to their highly colored, reversible redox states of Viologens makes them promising candidate several machine applications. Three common molecular machine architectures reported for Viologens includes pseudorotaxanes, rotaxanes and catenanes. Pseudorotaxanes typically consist of a rod-like species encircled by one or more

macrocycles. Rotaxanes are similar, however, contain bulky substituents on the end of the rod-like species. Catenanes differ by having interlocked macrocycles, producing a chain-like supramolecular complex. The numerical value [n] describes the number of individual species involved in the overall machine (Fig. 19).[92]

Fig. 19: *General structures of molecular machines.*

Many such molecular machines were reported by well-known research groups and one such example is the formation of pseudorotaxane complexes between curcurbit[n]uril (CB) with and Viologens, which are the suitable host-guest pair with each other. Curcurbit[n]uril (CB) are macrocyclic molecules made of glycoluril (=$C_4H_2N_4O_2$=) monomers linked by methylene bridges (-CH_2-). The oxygen atoms are located along the edges of the band and are tilted inwards, forming a partly enclosed cavity. The name is derived from the resemblance of this molecule with a pumpkin of the family of Cucurbitaceae. Viologens, due to their cationic nature, developing ideal ion-dipole interactions with the CB carbonyl rims. Song et al. synthesized 1,1'-bis[4-(4-pyridinyl)phenyl]-4,4'-bipyridinium chloride (BPPV), which was investigated with the two CBs, CB[6] and CB[7] presented to develop a [2]pseudorotaxane (single ringed) and [3]pseudorotaxane (Fig. 20).[93]

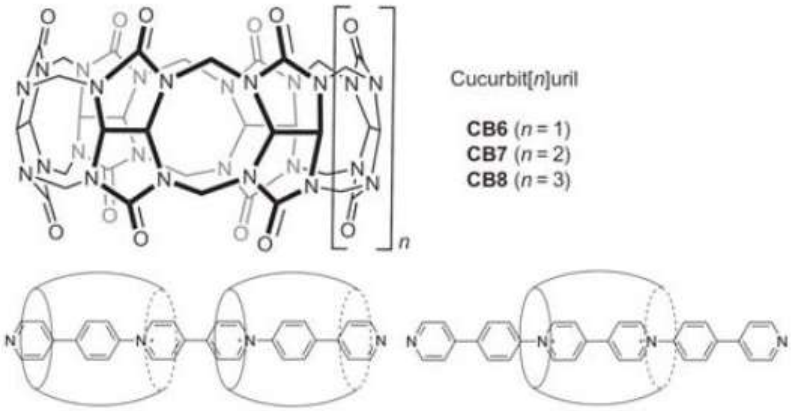

Fig. 20: *Pseudorotaxane formed by encapsulation of 1,1'-bis[4-(4-pyridinyl)phenyl]-4,4'-bipyridinium chloride (BPPV) molecule with curcurbit[n]uril.*

Other applications based on Viologens are as catalysts for direct carbohydrate fuel cells have been reported due to their ability to oxidize glucose and other carbohydrates in alkaline solutions.[94] Viologens were also reported as fast electron-transfer constitutes of data storage materials,[95] building blocks in supramolecular chemistry,[96] energy storage organic materials[97] and bioactive compounds.[98]

1.4: Cationic dyes and their applications:

- **Introduction to dyes:**

A dye is a colored substrate, which has an affinity to the other substrate to which it is being applied.[99] It is generally applied in an aqueous solution and may require a mordant to improve the fastness of the dye on the fibre.

The first human-made organic aniline dye Mauveine A **78*i*** (Fig. 21) was accidentally discovered by William Henry Perkin in 1856 during a failed attempt for the total synthesis of quinine. Other aniline dyes followed, such as fuchsine, safranin, and induline. Thousands of synthetic dyes were synthesized after that discovery.[100]

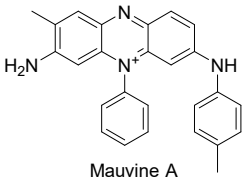

Fig. 21: *Structure of Mauvine A, first human–made organic dye.*

Based on the nature of the chromophore present, organic dyes are classified as below:
1) Azo dyes; 2) Anthraquinone dyes; 3) Indigoid dyes; 4) Polymethine dyes; 5) Pthalocyanine dyes; 6) Cationic dyes

In this thesis, the synthesis, properties and applications of cationic dyes, which are related to the present work are discussed.

- **Cationic dyes:**

Cationic dyes carry a positive charge in their molecule. The salt-forming counterion in most cases is a colorless anion of a low molecular mass inorganic or organic acid. Few examples of organic cationic dyes (**79*i*** to **83*i***)[101-105] are shown in Fig. 22.

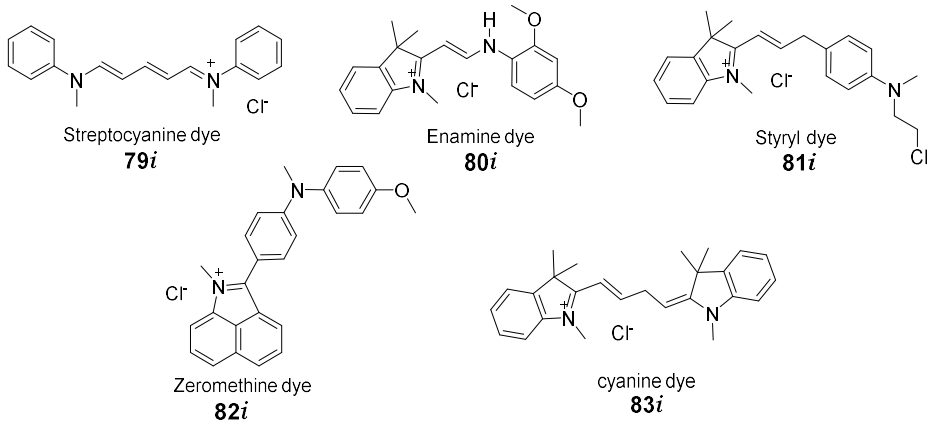

Fig. 22: *Representative examples of cationic dyes.*

a) Cyanine dyes: Cyanine is a non-systematic name of the class of functional dyes from the family of polymethine dyes. The classical cyanine dyes are mostly cationic with two terminal nitrogen heterocyclic subunits, which are separated by a polymethine bridge as shown by the generic structures in Fig. 23a.[106] Common heterocyclic units found in cyanine dyes are shown in Fig. 23b.

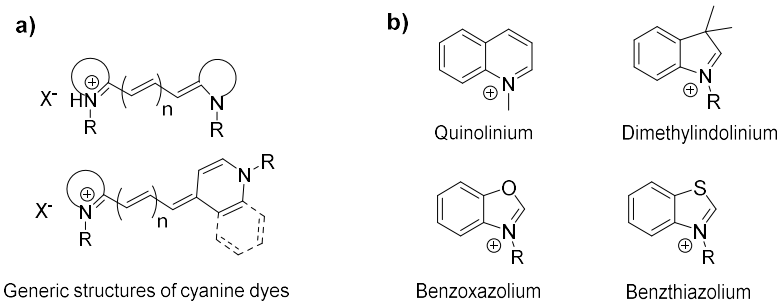

Fig. 23: *Generic structures and common heterocyclic components of cyanine dyes.*

The name cyanine is derived from an English word "cyan" conventionally means a shade of blue-green. These dyes are fluorescent molecules that embody a number of desirable qualities such as high extinction coefficients, tunable absorption/emission spectra, ease of synthesis and moderate to high quantum yields.

Various synthetic methods were reported for the synthesis of sub-classes of these dyes. Some of those methods are reviewed here. Deligeorgiev *et al.* reported the synthesis of monomethine dyes by heating together a mixture of heterocyclic salt containing 2- or 4-methyl group and 2-sulfobetaine derived from a cationic heterocyclic system and a suitable base (Scheme 14a). These are mostly known as nucleic acid binding molecular probes.[107]

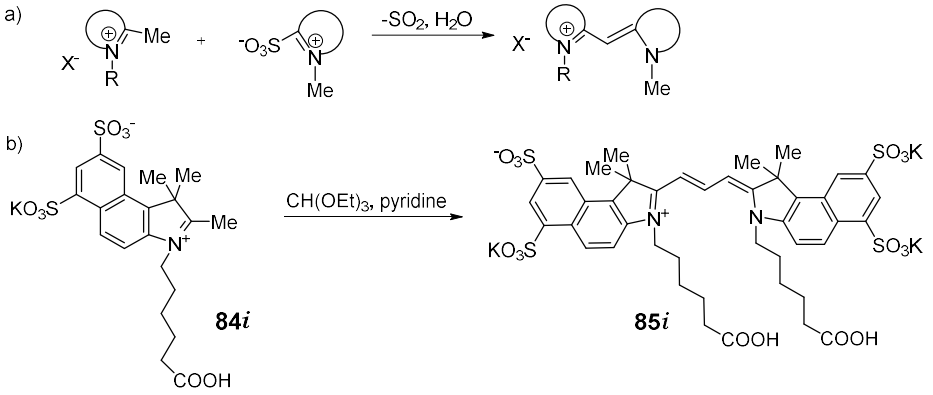

Scheme 14: *Classical approach for the synthesis of mono and trimethine dyes.*

The second approach for the synthesis of trimethine dyes (e.g. **85*i***) is shown in Scheme 14b, the condensation reaction between triethyl orthoformate and quaternary heterocyclic salt, **84*i*** substituted with activated methyl group under basic conditions.

The modern method for the synthesis includes the use of Vilsmeier-type reagent derived from *N*,*N*-dimethylformamide and HBr (Scheme 15).[108] Similarly, more recent approaches for the synthesis of pentamethine dyes are also developed.

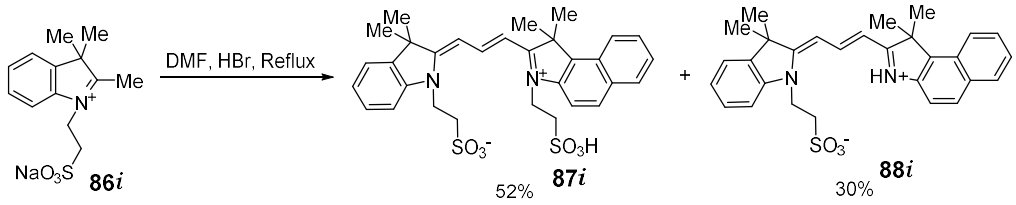

Scheme 15: *Use of Vilsmeier-type reagent for the synthesis of dyes.*

After the discovery of cyanine dyes, their first uses were limited to photographic sensitizers.[109] But other than photography, cyanine dyes now also found their applications in several other fields such as recording media,[110] laser materials,[111] solar cells,[112] and semiconductors.[113]

Currently, cyanine dyes are widely used in biotechnology due to their ability to form fluorescent complexes with nucleic acids. The structure of the dye determines the mode in which it binds to nucleic acids as well as the fluorescence properties of the resulting complexes. In addition, covalent conjugates of cyanine with nucleic acids or with nucleic acid-binding ligands allow fluorescent labelling and probing of DNA/RNA structure and function. Several examples of different types of conjugates and their applications are reported in the literature.

Symmetrical cyanine dyes Cy3 (**89*i***) and Cy5 (**90*i***),[114] which are commonly used as fluorescent DNA labels, unsymmetrical cyanine thiazole orange (**91*i***),[115] TOTO1 (**92*i***),[116] Pinacyanol (**93*i***),[117] DISC3+ (**94*i***)[118] are the common examples shown in Fig. 24.

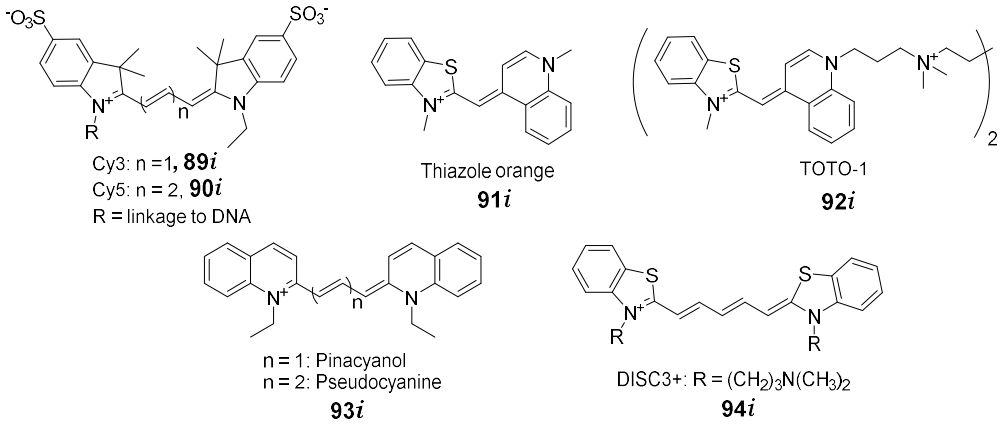

Fig. 24: *DNA binding cyanine dyes.*

Cyanine dyes typically associates noncovalently with dsDNA in one of two ways: (1) intercalation, in which the dye inserts between two adjacent base pairs resulting in a π-stacked sandwich complex, or (2) minor groove binding, in which the dye inserts lengthwise in to the narrower of the two grooves present in the DNA structure. These different dsDNA binding modes are discussed in more detail in section 1.6.

Several near infrared (NIR) cyanine dyes were reported for the fluorescent detection of proteins. Proteins in their neutral form, especially *in vivo* studies, have significant absorption and fluorescence in the visible spectral range. By moving to the longer wavelengths, the detection becomes virtually free from background interference. Such protein probes bind either by covalent or noncovalent interactions. Some common examples[119] are shown in Fig. 25.

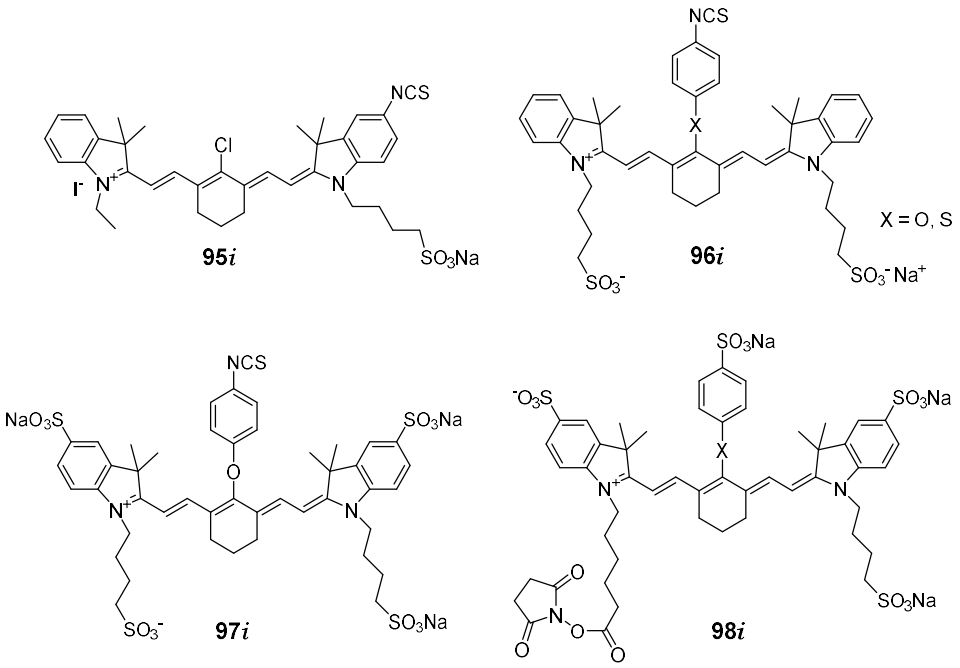

Fig. 25: *NIR cyanine dyes for covalent labeling of proteins at an amino group.*

NIR dyes had also found applications in capillary electrophoresis (CE) of proteins. The most attractive feature of covalent labelling is very low limits of detection (LODs) in CE with laser-induced fluorescence (LIF) detection.[120] Less than an attomole range of detection can be achieved when NIR dyes are used with this technique. In conjunction with immunoassays, CE-LIF is particularly beneficial. An antibody labelled with a NIR dye reduces the LOD for an antigen. The role of antibodies is to introduce specificity for only a particular antigen. The combination of the selectivity of immunoassays with the sensitivity of NIR detection makes combining the two techniques quite desirable for protein analysis.[121] The other applications of NIR emitting dyes substituted with donor-acceptor groups for bio-imaging and monitoring various functions in cells. The ability of these dyes to emit in NIR region through a turn-on activation mechanism makes them promising candidate probes for *in vivo* imaging applications.[122]

b) Styryl dyes: One of the most widely used and important class of functional dyes are the styryl dyes. The univalent radical (C_6H_5-CH=CH-), derived from styrene is called styryl radical. Charged or uncharged dyes in which, styryl moiety became the part of the molecules are called as styryl dyes.

A series of Styrylpyridinium, styrylquinolinium, and styrylbenzothiazolium dyes have been synthesized by the condensation of aryl aldehydes with methyl-substituted cationic hetero-aromatic moiety. These dyes are also referred, as hemicyanine dyes.[111] The transformation (Knoevenagel condensation) is generally reliable, selective, experimentally simple, and versatile. The environment-friendly version of this transformation includes condensation of 2- or 4-methyl substituted pyridinium, quinolinium or benzothiazolium unit with aromatic aldehydes under solvent-free conditions or microwave irradiation, in the presence of different acidic or basic reagents with excellent yields (Scheme 16).[123]

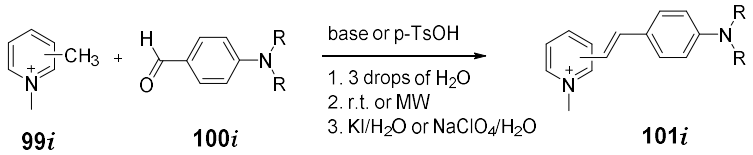

Scheme 16: *Generic scheme for the synthesis of styryl dyes.*

Many styryl dyes were reported for various applications such as novel materials, for biological imaging, dying of textiles and paper, sensitizers in silver halide based photography and many more applications. Many dyes from this class are commercial because of their wide applicability.[100]

FM® dyes are the commercial styryl dyes, which have been used to label and then monitor synaptic vesicles, secretory granules and other endocytic structures in a variety of preparations. Structures of few members of this class are shown in Fig. 26.[124]

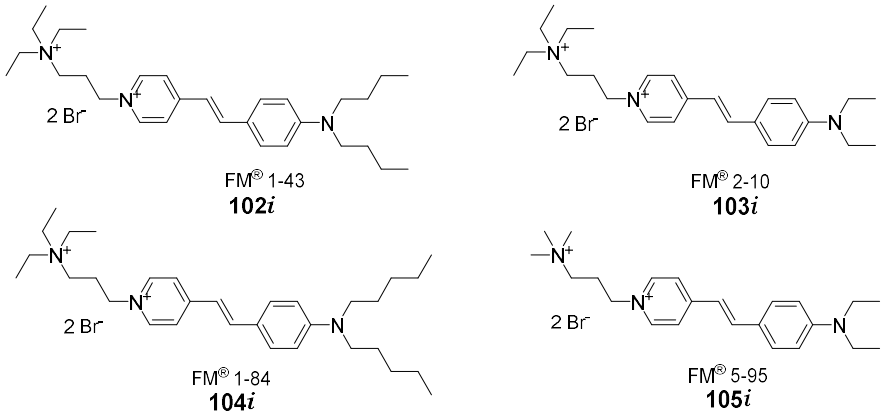

Fig. 26: *FM dye labeled synaptic vesicles in nerve terminals.*

Chang *et al.* reported number of styryl dyes for live cell imaging,[125] DNA selective probes,[126] heparin selective fluorescent chemosensors[127] and RNA selective probes[128] *via* library synthesis of styryl dyes and screening in well plate based fluorescent assay development (Fig. 27).

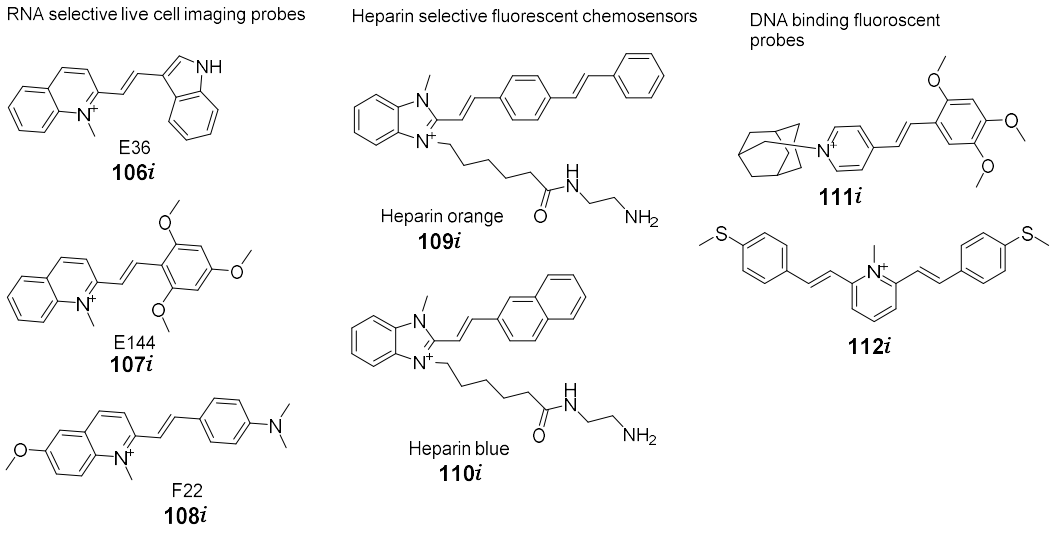

Fig. 27: *Styryl fluorescent probes from Chang's lab.*

Krieg *et al.* reported new highly fluorescent homodimeric stilbene dyes (**113*i*** to **115*i***) for the histochemical evaluation using cryotome sections and Peroxidase-staining protocol. These dyes were reported to be of potential interest because of their excitation with green light. This feature makes them complementary to the other classes of dyes, which are normally excited with either UV or blue light (Fig. 28).[129]

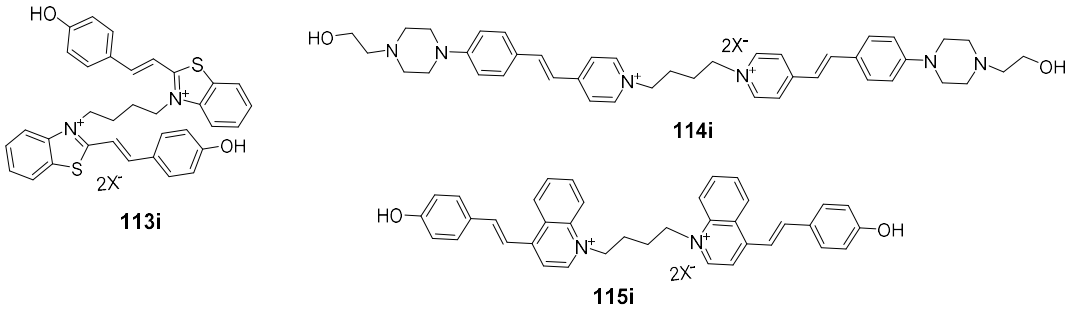

Fig. 28: *Homodimeric styryl fluorescent probes from histochemical evaluation.*

Styryl dyes are also reported to show the spectral changes in response to the voltage changes in cells. Such dyes are called as voltage sensitive dyes or potentiometric dyes (Fig. 29).[130] These voltage sensitive dyes are used for the analysis of neural network because it balances water solubility with good signal, stability, and low phototoxicity for brain tissues.[131] Depending on their chemical modifications, which change their physical properties, they are used for different experimental procedures.[133]

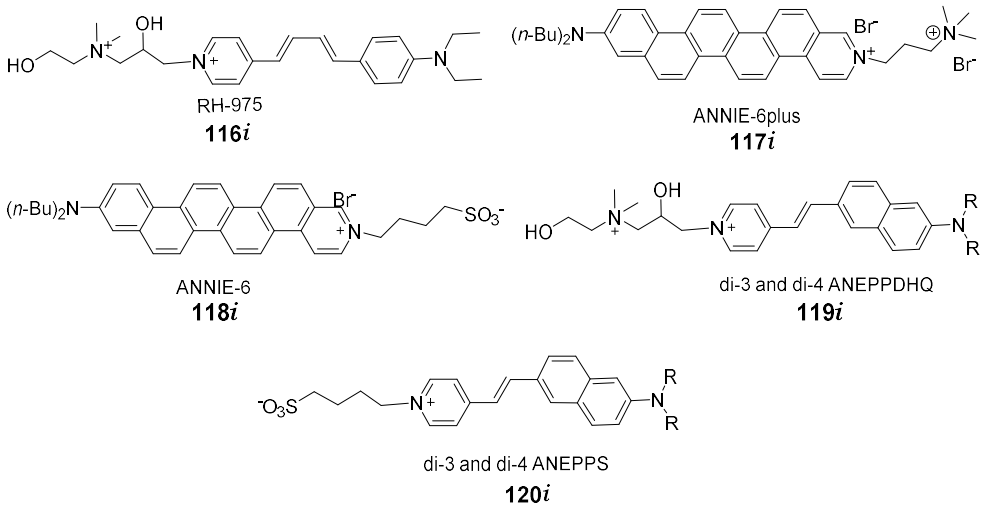

Fig. 29: *Voltage sensitive styryl dyes.*

In addition to applications as fluorescent probes and sensors, other applications of styryl dyes were also reported. Fedorova *et al.* reported a cationic styryl dye with [15]-cown-5 moiety (Fig. 30). The dye was able to sense alkaline earth metal cations *via* crown ether moiety and protons, Ag^+, and Hg^+ *via* heterocyclic moiety.[134]

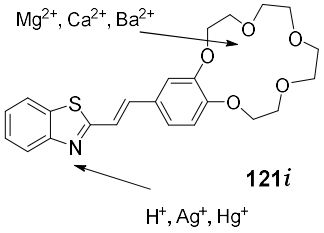

Fig. 30: *Crown ether styryl dyes for small cation sensing.*

The styryl dyes based on helical scaffolds (Fig. 31) were reported in by Arai *et al.* But no synthetic details, properties and applications were studied.[135]

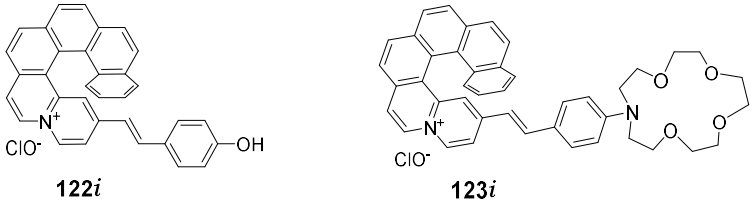

Fig. 31: *Styryl dyes originating from azoniahelicene.*

Recently our group introduced helicene like styryl dyes (Scheme 17), which were resolved into the pure enantiomers and exhibited high magnitude of ECD responses and pH switching.[8]

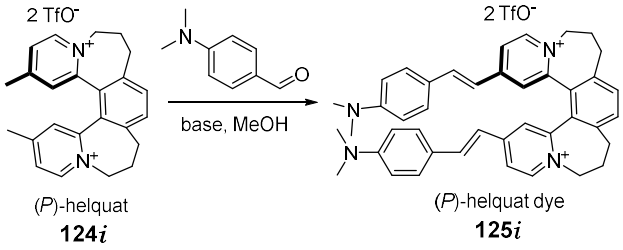

Scheme 17: *Synthesis of enantio-pure helquat dyes.*

Recently we reported G-quadruplex binding properties[136] and nonlinear optical properties of helquat styryl dyes.[88] This study is a part of the present work.

Push-pull type of molecular arrangements in some of the styryl dyes makes them ideal nonlinear optical materials. The Recent success of DAST, *p*-$MeC_6H_4SO_3$ (Fig. 32) with 10^3 higher powder SHG efficiency than urea as well as very large β_0 value from HRS measurement using 1064 nm laser ultimately lead to the fabrication of prototype NLO devices for parametric interactions and electro-optical (EO) modulations.[137] It was also observed that increasing conjugation, the nonlinear optical response of the material was also increased (e.g., **126*i***).[138]

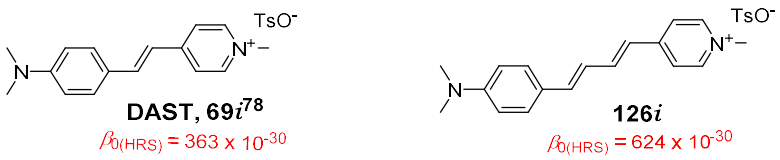

Fig.32: *Few examples of nonlinear optical materials.*

Kim *et al.* prepared an inclusion complex of a stilbazolium dye into the helical cavity of amylose, forming a rigid rod-like supramolecular complex (Fig. 33). Spin-coated thin solid

films of the material were shown to exhibit self-pooling of the chromophore leading to a respectable nonlinearity.[139]

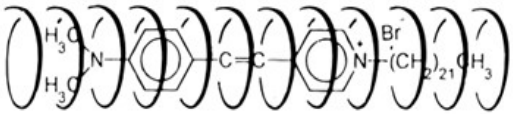

127*i*

Fig.33: *Supramolecular amylose-DASPC$_{22}$ inclusion complex.*

Recently B. *Coe et al.* reported new diquat chromophores containing stilbazolium dyes, showing higher β_0 values than DAST (Fig. 34).[140]

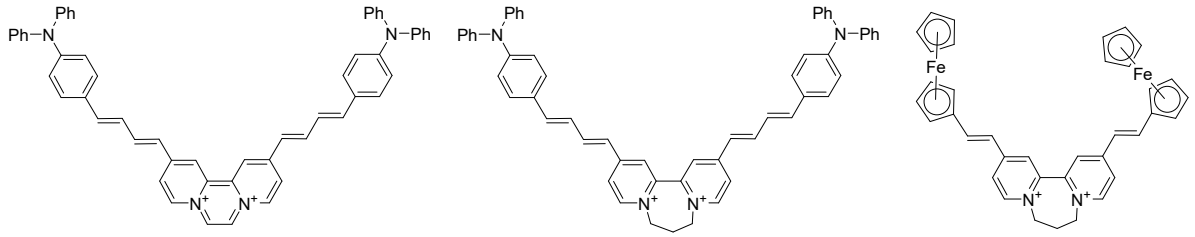

128*i*
β_0 = 876 x 10^{-30} esu

129*i*
β_0 = 916 x 10^{-30} esu

130*i*
β_0 = 206 x 10^{-30} esu

Fig.34: *Nonlinear optical materials based on diquats, showing higher β_0 value that benchmark compound DAST.*

Styryl dyes have a lot of potentials to be used for biological second harmonic imaging microscopy (SHIM). SHG does not involve the excitation of molecules like in other techniques such as fluorescence microscopy. Therefore, the molecules should not suffer the effects of phototoxicity or photobleaching. Also, since many biological structures produce strong SHG signals, the labelling of molecules with exogenous probes is not required which can also alter functions of the way a biological system. By using near infrared (NIR) wavelengths for the incident light, SHIM has the ability to construct three-dimensional images of the specimens by deeper penetration through thick tissues.[141] Structures of Some of the dyes used for SHIM are shown in Fig. 35.

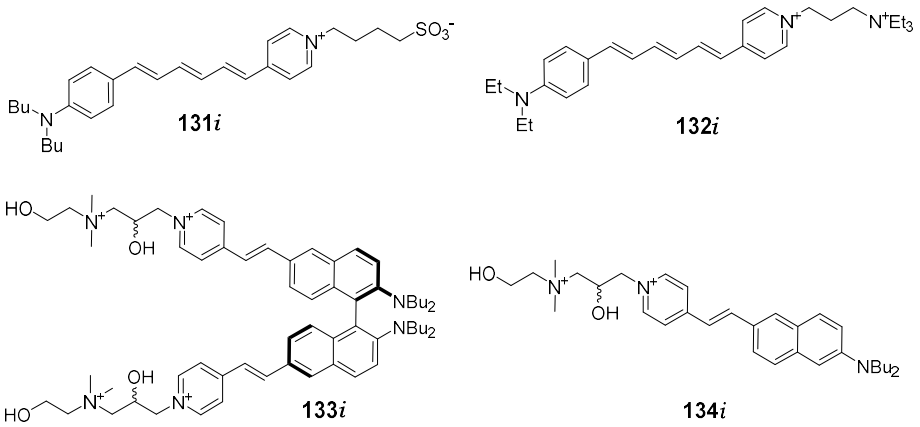

131*i*

132*i*

133*i*

134*i*

Fig.35: *Structures of some dyes used for SHIM.*

Few microscopic images taken using various styryl dyes are shown in Fig. 36 and 37.

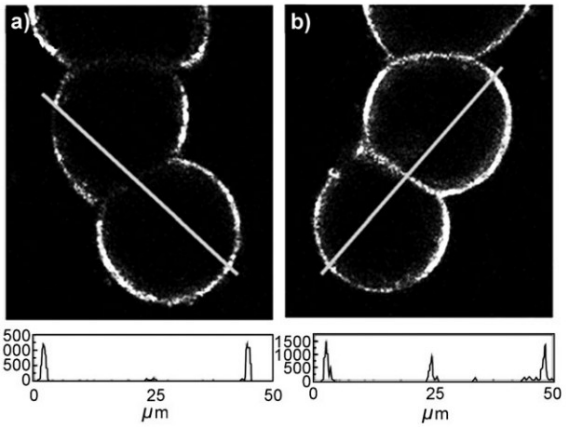

Fig.36: *SHG images of cells stained with (a) racemic dimer (**133i**), and (b) chiral dimer (**133i**) when illuminated with circularly polarized light. Intensity of line scans through cell–cell junctions are shown on plots below, demonstrating that the chiral dye (**133i**) is capable of SHG in a symmetrical bilayer environment whereas the racemate (**133i**) is not.*[142]

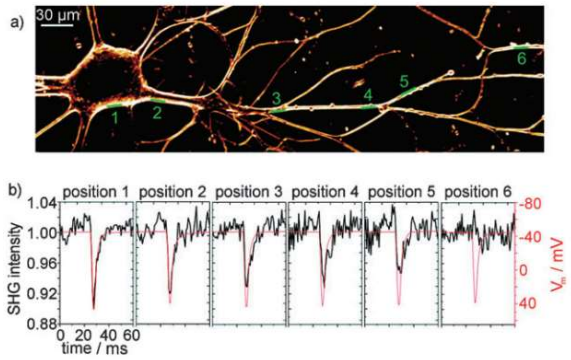

Fig.37: *(a) SHG image of a cultured squid neuron showing six positions of interest at which line scans of SHG intensity took place. (b) SHG intensity for a series of line scans at increasing distance from the soma, the point of greatest SHG response. At larger distances from the soma, SHG signal is lower but action potentials are still easily observed until position 6.*[143]

Due to relatively simple preparations and wide scope for applications of these classes of dyes are often synthesized for developing devices based on these chromophores,[144] for biological imaging and probing etc.

1.5 Heparin and its sensors:

Heparin is one of the oldest known drugs from the glycosaminoglycan (GAG) family and is in clinical use since its discovery in 1916. It was originally isolated from canine liver cells, hence its name (*hepar* or "ήπαρ" is Greek for "liver"; *hepar* + *-in*). The discovery of Heparin was even before an establishment of Food and Drug Administration of the United States in 1916, although it did not enter clinical trials until 1935.[145]

Heparin is a highly sulphated polysaccharide with the highest negative charge density of any known biomacromolecules,[146] known to bind antithrombin with a high affinity, and the binding significantly enhances antithrombin inhibition activity towards thrombin and other coagulation factors.[147] It is a linear polysaccharide consisting predominantly of 1–4 linked uronic acid and glucosamine subunits (Fig. 38).[148]

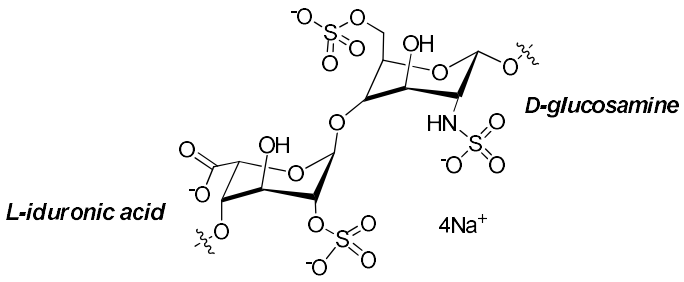

Fig. 38: *Major heparin disaccharide repeating units.*

Due to varying degrees of sulfation in disaccharide components, heparin is one the most complex member the glycosaminoglycan (GAG) family with the polymer M_r spanning ca. 2500–25 000 Da.

Even though the history and widespread use of heparin as an anticoagulant during various surgeries, it is necessary to quantify and control the heparin levels into the bloodstream of a patient. Some of the adverse effects of heparin overdosing include hemorrhages and heparin-induced thrombocytopenia (HIT).[149] To initiate the recovery of a patient, it is important to neutralize the anticoagulant effect of heparin and restore the blood clotting process.

Protamine is only licensed antidote of heparin.[150] It is usually administered to the patient for neutralizing the anticoagulant effect of heparin by electrostatic binding. However, due to nonspecificity for active and inactive forms of heparin, it can cause problems.[151] Due to all these issues there is a significant interest in finding an alternative effective and non-toxic heparin reversal agent, along with an improved methodology for determining blood heparin levels at the point of care.

Traditionally for heparin quantification, some indirect assays are used, which are measuring activated clotting time, such as aPTT or anti-Xa assay etc.[152] All these assays are expensive as well as less accurate and unreliable due to the lack of specificity and potential interference of other factors.[153] Other than clotting time-based assays, employed for this purpose are colorimetric assays, capillary electrophoresis, electrochemical methods, surface enhanced Raman spectroscopy, and unbiased sensor arrays.[154]

Therefore, it is strongly desired to develop an assay for rapid and sensitive heparin detection using an inexpensive instrumentation. In addition, the ideal method should be easily employed at the bedside of the patient and should give an accurate read-out of heparin present. The fluorescence-based techniques are highly sensitive to the environment and there are continuous developments throughout the decades with the discovery of various chemosensors for diverse chemical, biological and medical applications.

Two types of fluorescent chemosensors showing either fluorescence light-up or light-off response in presence of analytes are possible. The pioneering work towards the development of heparin fluorescent chemosensors was reported by Anslyn *et al.*[154d, 155] They reported a tripodal boronic acid-based small molecule **135*i***, which was demonstrated as fluorescence light-off (quencher) probe. (Fig. 39)

Even though it was the first successful fluorescent sensor for heparin detection in serum environment, it suffers from the emission at short wavelength (355 nm) and the auto-fluorescence in the more complex biological samples.

Egawa and co-workers reported fluorescein isothiocyanate-labelled protamine (F-protamine) as a light-off probe, [156] it was able to quantify the heparin in therapeutic level from blood serum, but was suffered from nonspecific fluorescence light-off with serum alone. Nalage *et al.* reported a pyrene functionalized kanamycin A derivative **136*i*** (Fig. 39), which was showing dual detection: either through color changes or through the fluorescence light-off response in EtOH : water (1:3) mixture as a medium.[157]

Smith *et al.* reported Mallard blue **137*i*** (Fig. 39), which was a thionine dye modified with arginine amino acids.[158] This probe was detecting heparin by showing changes in UV-vis. spectra and was reported as one of the successful sensors for detection of heparin in 100% serum.

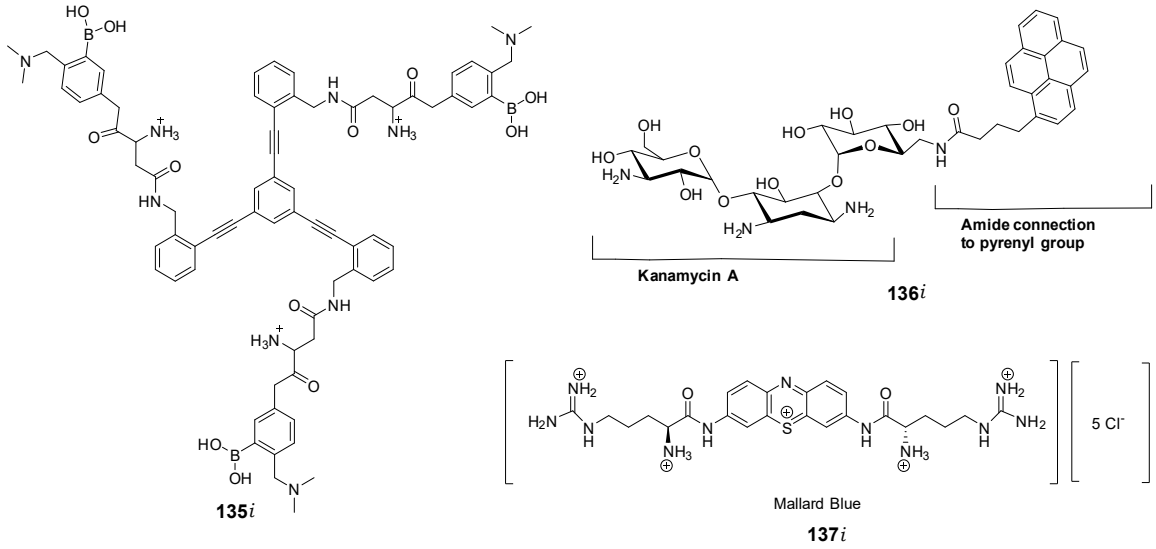

Fig. 39: *Turn-off heparin probes.*

Fluorescence quenching of light-off probe can be affected by many other components of the complex biological medium, as a result, light-up probes should be more reliable than the light-off ones to avoid false positive results.[158] In this regard, the development of sensitive and selective turn-on fluorescent probes for heparin detection is still highly desirable.

Zhang *et al.* reported a ratiometric fluorescent detection of heparin, based on aggregation-caused quenched emission (ACQ) and aggregation-induced emission (AIE) features of anthracene **138*i*** and tetraphenylethene **139*i*.**[159] This ratiometric fluorescence method was used to distinguish heparin from its analogues and quantify heparin in serum (Fig. 40).

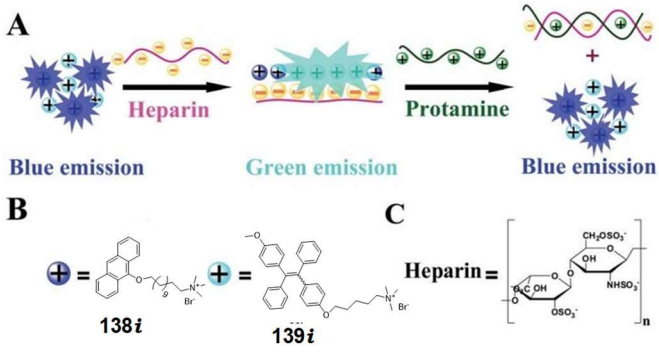

Fig. 40: *(A) Illustration of the design rationale for the fluorescence ratiometric detection of heparin based on the combination of the ACQ feature of compound **138i** and the AIE feature of compound **139i**, and the potential application to study the interaction between heparin and protamine. (B) Chemical structures of **138i** and **139i**. (C) Chemical structure of the major unit of heparin*

Wang *et al.* reported a new quinine derivative **140*i***, bearing pyrene as a fluorophore for heparin detection in an aqueous medium.[160] **140*i*** exhibits good selectivity and sensitivity for heparin over other biological molecules. Upon binding with heparin, **140*i*** shows a typical excimer emission at 489 nm along with a weak monomer emission at 376 nm. The probe can detect heparin from diluted serum (Fig. 41).

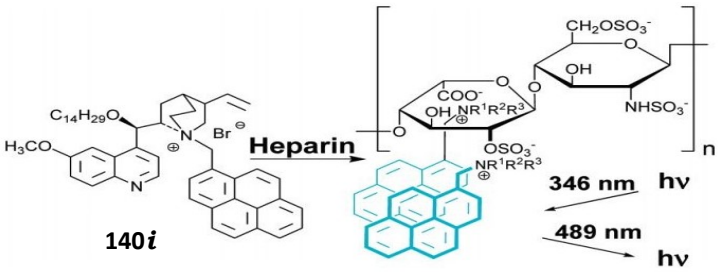

Fig. 41: *Heparin detection with quinine derivative bearing pyrene fluorophore.*

Kramer *et al.* reported a perylene diimide based dye **141*i***, with emission at long wavelength (485 nm) to overcome the problem of serum auto-fluorescence. They achieved meaningful detection of low molecular weight heparin in the presence of up to 20 vol% of serum or plasma (Fig. 42).[161]

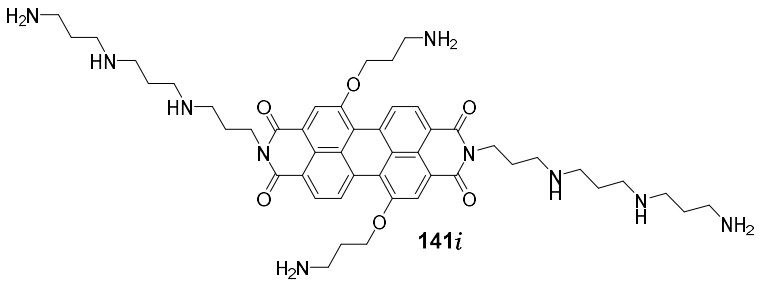

Fig. 42: *Perylene diimide based heparin probe.*

A versatile conjugated polyelectrolyte compound **142*i***, reported by Liu and co-workers, shows dual detection upon binding with heparin, either *via* fluorescence light-up or by direct colorimetric or ratiometric fashion.[162] This probe shows high selectivity for heparin over other GAGs and differentiates between heparin and other GAGs by color changes after interactions (Fig. 43).

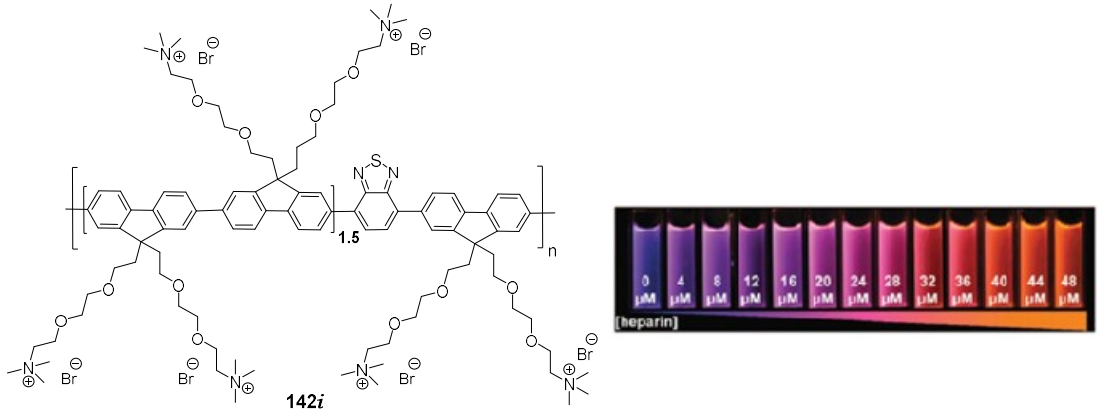

Fig. 43: *Liu's versatile probe, dual detection of heparin via fluorescence light up, as well as with naked eye detection by color changes.*

Chang and co-workers developed a high-throughput approach in search of optimized heparin chemosensors from their library of benzimidazolium dyes. They reported highly selective heparin probes heparin blue and heparin orange, which can detect and quantify UFH (Unfractionated heparin) and LMWH (Low Molecular Weight Heparin) in a clinically relevant range in 20 vol% diluted human plasma. These two probes show high selectivity for heparin over other GAGs as well as plasma proteins such as albumins, and many other analytes (Fig. 44).[163]

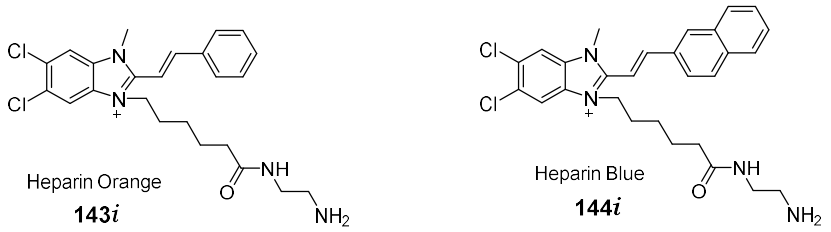

Fig. 44: *Heparin orange and heparin blue, found through a high-throughput fluorescence screening.*

Although some of the approaches detailed so far are able to respond somewhat to the presence of heparin in biological media, many of the non-colorimetric fluorescence-based assays quickly become plagued by the problem of serum auto-fluorescence. The hydrophobic regions of serum can exhibit fluorescence following excitation with shorter wavelength light and can prevent procedures from being used at high (>5%) serum levels.

There is a huge demand for simple commercially relevant systems which can achieve switch-on ratiometric sensing and operate in human serum/plasma, or even better in whole blood. Ideally, such systems should be robust and exhibit long-term stability, so that they can be built into commercial sensing systems, which can be applied at the bedside in surgery for instant read-out of heparin levels in human blood. The devices developed should be as simple as possible, in terms of use and calibration, in order to facilitate their uptake in clinical practice. In this respect, there is a huge scope in modifying currently identified fluorophores and dyes, so as they can emit even in far red or near infrared region, so that, there will be no problem of plasma/ serum autofluorescence.

1.5 dsDNA binding small molecules:

Deoxyribonucleic acid (DNA) is a molecule that carries the genetic information required for the growth, development, functioning and reproduction of all living organisms and many viruses. James Watson and Francis Crick originally elucidated the double helical anti-parallel structure of eukaryotic DNA in 1953.[164] The double-stranded helical structure is made up of the repeating units called as nucleotides, which further contains the nucleobase (Fig. 45b, blue), the deoxyribose sugar (Fig. 45b, red), and the phosphate backbone (Fig. 45b, black). The only variation found among the four DNA nucleotides is at the nucleobase part. Two types of nucleotides comprising purines (adenosine, A and guanosine, G) and pyrimidines (thymidine, T and cytosine, C). In dsDNA, the hydrogen bonding occurs between purines and pyrimidines bases, i.e. AT or GC. Although hydrogen bonding is usually a weak noncovalent bonding force, the summation of hydrogen bonding interactions along the length of DNA anti-parallel strands provides a strong and stable force keeping the strands together.

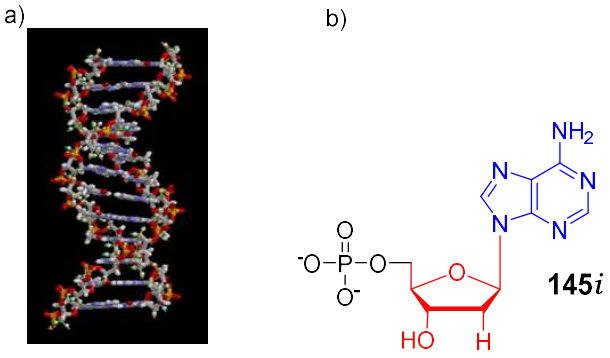

Fig. 45: *a) Double helical structure of DNA; b) structure of monomeric repeating unit (nucleotide) consisting of nucleobase (blue), deoxyribose sugar (red) and phosphate backbone (black).*

Even though B-DNA (right-handed conformation) is the most prevalent form in eukaryotic animals, the double helical structures can adopt two more conformations i.e. *A*-DNA and *Z*-DNA (Fig. 46a).[165] The conformation that the DNA adopts is depending upon many factors such as the hydration level, DNA sequence, the amount and direction of super coiling, chemical modifications of the bases, the type and concentration of metal ions, and the presence of polyamines in solution.[166]

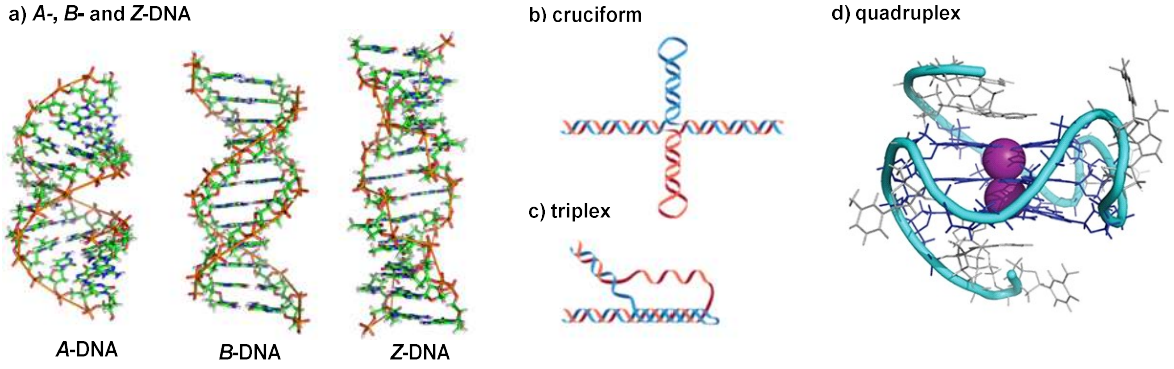

Fig. 46: *Various secondary structures of DNA.*

Depending upon particular sequences and interaction with protein, DNA can acquire a variety of alternative conformations. These secondary structures such as cruciform (Fig. 46b), triplex (Fig. 46c), and G-quadruplex (Fig. 46d) are known to exist under relevant physiological conditions. *In vivo,* functional roles of all these structures are also known.[167] This study is not the part of the present work.

Even before the secondary DNA structures and their roles in physiological and biological processes were known, the molecules interacting with dsDNA were very widely researched and are known for their therapeutic potential. For predicting the physiological/therapeutic consequences of DNA-small molecule interactions, it is necessary to understand the type of possible modes of interactions between these two partners.

DNA alkylation or covalent binding ligands are widely known in cancer chemotherapy, which are preferentially forming covalent bonds at *N*-7 position of guanine or *N*-3 of adenine. These ligands either cause the fragmentation of DNA by repair enzymes in order to replace the modified bases or can form a crosslink between two nucleobases through two binding sites, preventing further synthesis or transcription or in another mechanism, causing mutations to the DNA due to crosslinking of nucleobases. Few examples of anticancer DNA alkylating agents are shown in Fig. 47.[168-170]

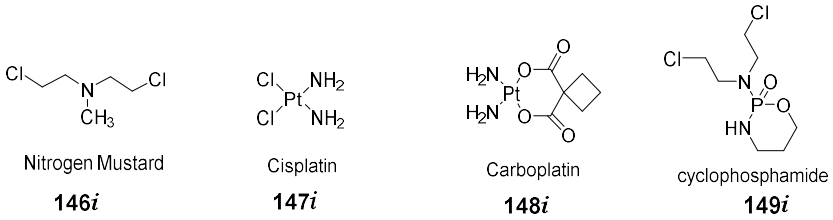

Fig 47: *DNA alkylating agents.*

Intercalation is a noncovalent type of interaction between DNA and its ligands, characterized by insertion of planar aromatic rings in between the DNA base pairs. This kind of interaction is quite strong, even though high energy is consumed for the unwinding of DNA helix and is usually independent of base pair sequences. Intercalators can affect the protein-DNA interactions because they cause severe distortion in the native conformation of the DNA. Two major types of intercalations are possible. Classical intercalation is usually seen in case of some DNA stains like ethidium bromide **9*i*** and antimalarial quinacrine **150*i*** (Fig. 48). These molecules intercalate by stacking of heteroaromatic rings present in their structure with the DNA base pairs.[171] These molecules show less sequence specificity.

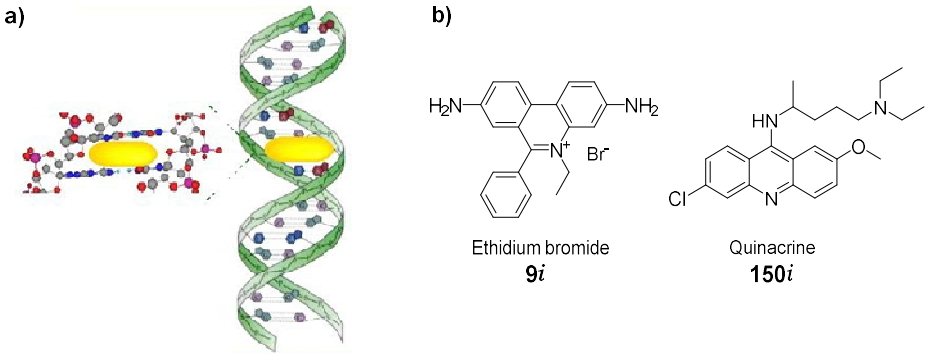

Fig. 48: *Intercalative mode of dsDNA binding: a) Pictorial illustration with a model; b) Two examples of classical DNA intercalators.*

Due to easy unstacking of the sequences in GC region, some molecules like anthracyclins, actinomycin, nogalamycin **151*i*** and daunomycin **152*i*** (Fig. 49) show preferential intercalation into the GC-rich regions.[172] Such intercalators typically have two side chains on opposite sides of planar aromatic systems. The mode of intercalation is quite complicated. The planar aromatic part is intercalated whereas the side chains interact with both minor and major groove.

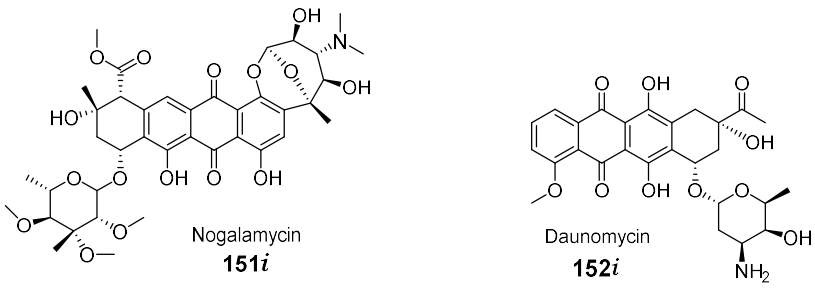

Fig. 49: *DNA intercalator molecules showing threading intercalation.*

The major and minor grooves of dsDNA are the sites for the binding of various small molecule DNA ligands. As the name suggests, the major groove is wider in comparison to a minor. Most of the small molecules interacting with dsDNA are minor groove binders and

major groove is specialized for the DNA binding proteins. Therefore, a non-protein structure containing molecules interacting with major groove are rear. Due to the evolution of minor groove binding antibiotics targeting DNA of competing organisms, a lot of attention was drawn towards minor groove binding small molecules.[173] As compared to intercalators, minor groove binders (e.g. Fig. 50b)[174] show high sequence specificity and affinity and can be neutral, mono-charged or multiply charged.

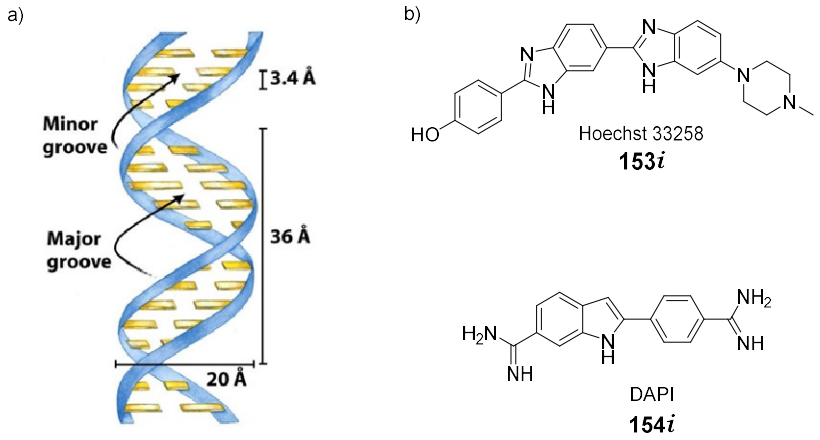

Fig. 50: *a) A dsDNA model showing major and minor grooves of dsDNA; b) Minor groove binding small molecules.*

The forces that dominate small molecule-minor groove binding interactions are electrostatic, Van der Waals, hydrophobic and hydrogen bonding forces. Most of the minor groove binding molecules are crescent shaped with a complementary shape to the groove. They usually show AT-selectivity, due to the higher electrostatic potential at AT sites as compared to GC.

More recently, the hybrid molecules with combined structural features of Intercalators and minor groove binder were introduced and getting recognition as combilexins. Such compounds showed even better sequence specificity and affinity than classical intercalators and minor groove binders. Even though these are synthetic molecules, some natural combilexin such as echinomycin,[175] actinomycin-D[176] and doxorubicin[177] were also found to behave as combilexin.

The main guiding principle behind the synthetic design of combilexin with therapeutic or DNA probing activity was to combine the AT-specificity of groove binder with the GC-specificity of an intercalator. For e.g. Bailey *et al.* reported a molecule with a combination of netropsin, a minor groove binder with an aminoacridine, an intercalator (**155*i***, Fig. 51).[178a] Few other examples of synthetic combilexin are shown in Fig. 51.[178]

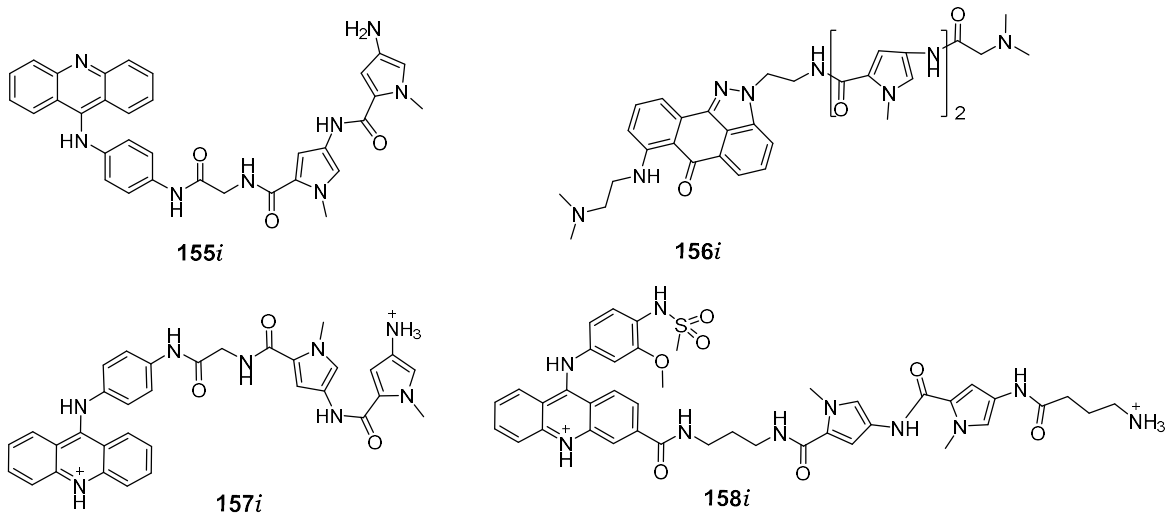

Fig. 51: *Synthetic combilexin.*

Even before the discovery of its double-stranded helical structure, DNA was a target of anticancer drug discovery. The compounds previously identified as anticancer agents were later found to target DNA either directly or through an inhibition of enzymes responsible for controlling the integrity of DNA or providing building blocks for DNA synthesis. There were several established therapeutic modalities targeting DNA: antimetabolites, which deplete nucleotides, including folic acid antagonists such as methotrexate; alkylation agents, which cause direct DNA damage, such as nitrogen mustard and its derivatives; and intercalators such as actinomycins, which bind DNA and inhibit the activity of many enzymes that use DNA as a substrate. Among the most widely and successfully used anticancer agents today are nonspecific DNA-damaging chemicals, including inhibitors of topoisomerases (TOPO) I and II, antimetabolites, alkylating agents and agents causing covalent modification of DNA (mitomycin C and platinum compounds), as well as γ-irradiation, for which the main target is also DNA.

In addition to cancer treatment, dsDNA interacting molecules also found their therapeutic uses against infectious diseases. For example, dsDNA binding small molecules such as DAPI, ethidium bromide, netropsin, and Nogalamycin efficiently inhibits the helicase and ATPase activity of *Plasmodium falciparum* helicase PfD66 and therefore can act as antimalarial drugs.[179]

In addition to therapeutic uses, dsDNA binding fluorescent probes are widely used for various microscopic and cytometry applications. Therefore, it is highly desirable to develop small molecule ligands interacting with dsDNA and other secondary structures with minimal side effects for advanced therapeutic practice as well as for diagnostic purposes such as fluorescent probes with minimal cytotoxicity and environmental friendly properties are desired.

2. Aims of the thesis:

The present thesis aims to fulfil the following tasks:

A. Synthesis of four novel *racemic* helquats **6**, **10**, **14** and **16** (Fig. 52) containing one or two active methyl groups next to the quaternary nitrogen centre and scale-up of the synthesis to accumulate these compounds on a gram scale in order to study the properties and applications.

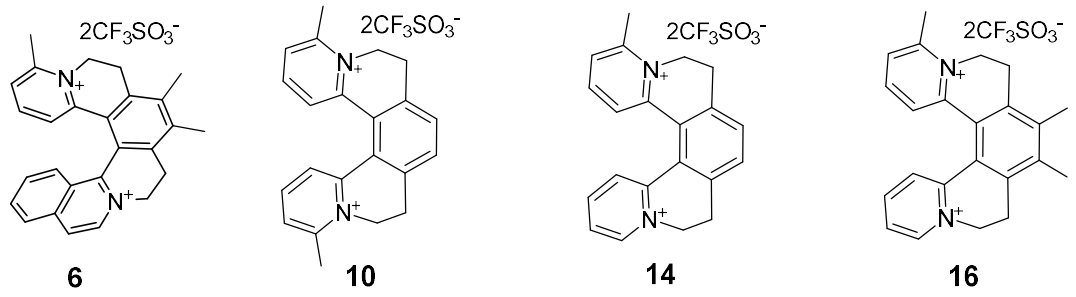

Fig. 52: *Target helquats containing active methyl groups next to quaternary center.*

B. Resolution of [6]helquat **6** and scale up the resolution in order to produce pure enantiomers (*P* and *M*) in gram scale for further explorations towards applications.

C. Synthesis of a library of helquat derivatives *via* Knoevenagel condensation between activated methyl groups attached to helquat scaffolds and various diversely substituted aromatic and heteroaromatic aldehydes. The aim of the synthesis was to run property screens with the generated library of compounds towards various directions such as in search of novel 3D nonlinear optical materials, to identify molecular recognition through fluorescence light-up with various biological targets, such as heparin and dsDNA (Scheme 18).

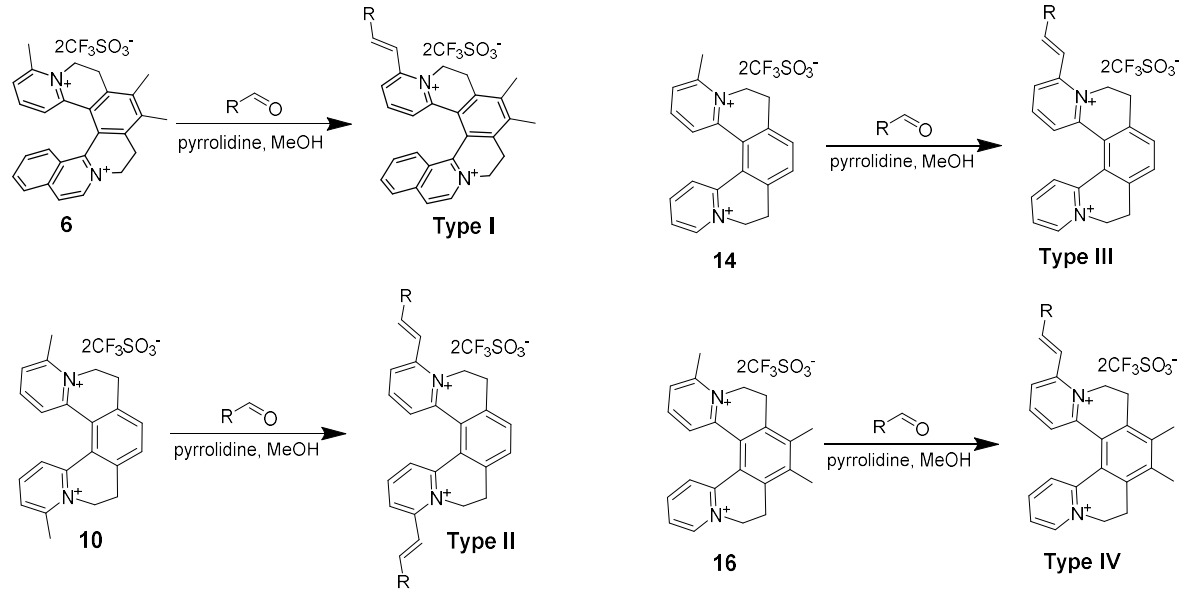

Scheme 18: *Synthesis of library of helquat dyes.*

D. Synthesize prototypical push-pull styryl dyes containing helquat **6**, substituted with electron donating aromatic or heteroaromatic chromophores for investigation of nonlinear optical properties (Fig. 53).

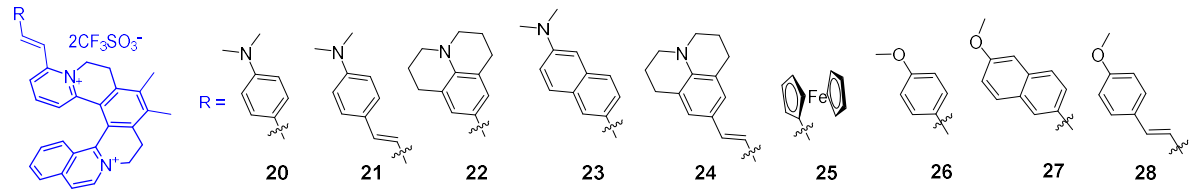

Fig. 53: *Targeted push-pull styryl dyes containing [6]helquat core.*

E. Analyze helquat derivatives of **Type I** and **II** for their molecular recognition properties towards biological targets like heparin and DNA, by selectively lighting-up fluorescence in presence of target (Fig. 54).

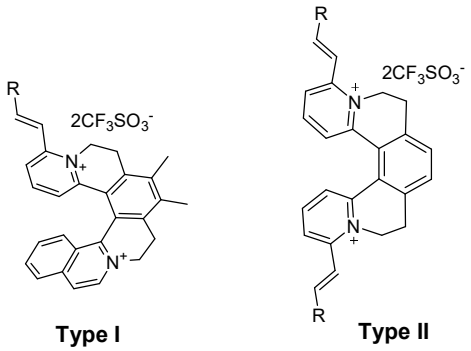

Fig. 54: *General structure of dyes screened in search of heparin chemosensors.*

3. Results and discussion:

3.1 Synthesis of helquats and helquat derivatives:

- **General Points about synthesis:**

Synthesis of four new helquats **6, 10, 14** and **16** containing activated methyl groups at position 2 with respect to quaternary nitrogen was accomplished by following previously developed three-step methodology in our group.[180]

Sonogashira cross-coupling reaction between terminal alkynes **1**, **11** or gaseous acetylene and 2-bromo-6-methylpyridine was catalyzed by Pd/Cu(I) catalyst system to give internal alkynes **3**, **7** and **12** in good to optimal yields (Scheme 19, 22 and 25).

Triyne **5**, **9**, **13** and **15** were synthesized from internal alkynes **3**, **7** and **12** respectively by S_N2 displacement of triflate from alkynyl side chains **4** and **8** (Scheme 20, 23 and 26).[180] Due to the sensitivity of alkynyl triflates and triynes to ambient light, these reactions were carried out in dark.

Helquats **6**, **10**, **14** and **16** were obtained through the final step, in which [2+2+2] cyclotrimerization of triynes 5, 9, 13 and 15 was carried out under Rh(I) catalysis (Scheme 21, 24 and 26).

Library synthesis of helquat dyes of **Type I**, **II**, **III** and **IV** was accomplished by a Knoevenagel condensation reaction between respective helquat scaffolds **6**, **10**, **14** and **16** with various substituted aromatic and heteroaromatic aldehydes in presence of alicyclic secondary amine in good to optimal yield.

The planar controls of helquat dyes of **Type V** and **VI** were synthesized by Knoevenagel condensation of respective methyl pyridinium substrates **17** and **18** with various aromatic and heteroaromatic aldehydes.

- **Synthesis of [6]helquat 6 containing active methyl group:**

The aim of this synthesis was to incorporate an activated methyl group at position 2 relative to the quaternary nitrogen atom in [6]helquat core for further functionalization using Knoevenagel condensation reaction (Fig. 55).

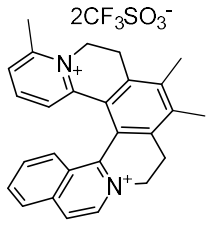

6

Fig. 55: *Structure of the [6]helquats* ***6.***

The first step in the synthesis was Pd/Cu(I) catalyzed Sonogashira cross coupling reaction between 1-ethynylisoquinoline and 2-bromo-6-methylpyridine in triethylamine as a base and high boiling solvent (Scheme 19). The study for the optimization of reaction conditions is summarized in Table 1.

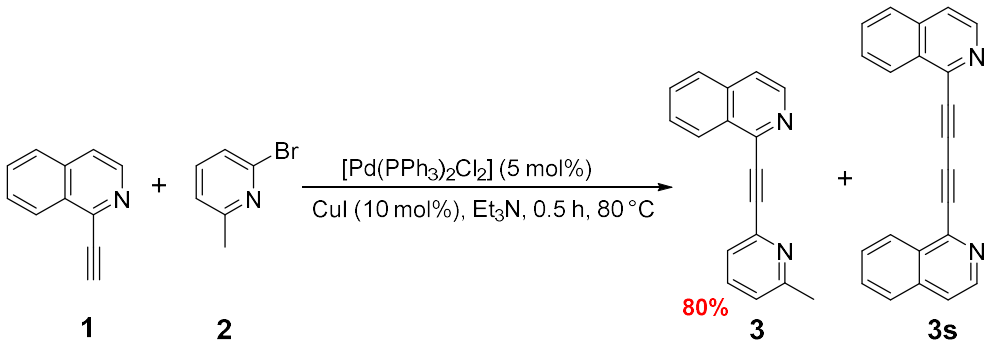

Scheme 19: *Sonogashira coupling reaction between terminal alkyne,* ***1*** *and 2-bromo-6-methylpyridine,* ***2****.*

Sr. No.	*Reaction temperature*	*Product 3 (%)*	*Recovered alkyne 1 (%)*	*Side product 3s (%)*
1.	rt	-	~ 100	-
2.	55 °C	43	~ 30	27
3.	80 °C	80	-	17

Table 1: *Optimization of reaction conditions for Sonogashira coupling.*

The reaction does not proceed at rt and after 24 h of stirring, only starting materials **1** and **2** were detected by TLC analysis (mobile phase: 50% EtOAc in *n*-hexane). After heating the reaction mixture at 55 °C for 4 h, the reaction was not completed and starting material **1** was still present according to TLC analysis. After the workup and purification by column chromatography using 50% EtOAc in *n*-hexane as a mobile phase, an internal alkyne **3** was isolated in only 43% yield with the recovery of ~30% of unreacted alkyne **1** and 27% of **3s**. In a successful attempt, complete consumption of starting material **1** takes place, when the reaction was carried out at 80 °C. Within 30 minutes, complete consumption of terminal alkyne **1** was confirmed by TLC analysis (50% EtOAc in *n*-hexane).

Attempted purification techniques involved recrystallization, trituration with solvents (boiling in *n*-heptane) and precipitation from EtOAc solution by the dropwise addition of *n*-hexane. However, only column chromatography led to pure samples of product **3.** After optimization of above-mentioned reaction conditions, heating for 30 minutes at 80 °C followed by purification of internal alkyne product **3** by column chromatography using 50% EtOAc in *n*-hexane gave the desired product in 80% yield and side product **3s** in in 17% yield.

Triyne **5** was synthesized from compound **3** (Scheme 20). Nucleophilic nitrogen atoms of **3**, displaces triflate leaving group from alkynyl side chain **4** in a S_N2 substitution reaction. As alkyne **3** is unsymmetrical, the rate of alkylation at both nitrogen is different. Due to the steric hindrance caused by methyl substituent next to the nitrogen atom of the pyridine ring, the rate of alkylation at this nitrogen was lower than the alkylation at nitrogen atom from the isoquinoline ring. The reaction proceeds through the formation of mono-quaternary product **5s**. The first alkylation takes place at the nitrogen atom from isoquinoline ring. The nucleophilicity of the nitrogen from the pyridine ring was further decreased after the formation of electron deficient isoquinolinium product **5s**. Often this reaction never goes to complete conversion to form the triyne product (**5**) and the mixture

of mono (**5s**) and bis-quaternary product (**5**) was obtained. The reaction rate was slightly increased by heating the reaction mixture to reflux in a Carius tube.

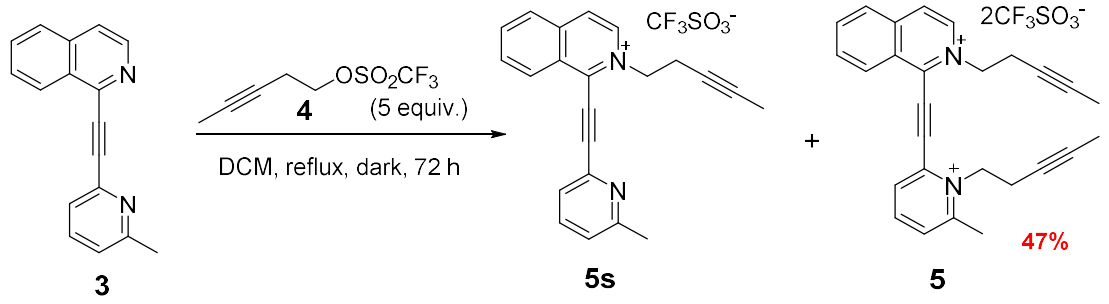

Scheme 20: *Synthesis of triyne* ***5****.*

The progress of the reaction was monitored after each 24 h by TLC analysis (mobile phase: Stoddart's magic mixture) and ^{1}H-NMR. By TLC analysis, the alkyne **3** was completely consumed, but from the spectroscopic analysis, the reaction does not proceed further, after the formation of approximately 1:1 ratio of products **5s** and **5**. Even after 72 h of reflux, the complete conversion to bis-quaternary product **5** does not take place. Due to this reason, we decided to stop the reaction, and solve the purification problem. After evaporation of volatiles, washing of the residue with various solvent combinations resulted in non-purified triyne **5**. Finally, product **5** was separated from rest of the impurities by biphasic extraction in the DCM-water system. Exclusively bis-quaternary product goes to the aqueous phase, leaving impure side product **5s** and other impurities in DCM phase. For effective separation of two phases, centrifugation was used and pure triyne **5** was obtained in 47% yield by evaporating aqueous layer on rotatory evaporator followed by trituration of yellowish brown oil with Et_2O. The attempted purifications are summarized in Table 2.

Sr.No.	*Method of purification*	*Nature/ color of the product*	*Purity by ^{1}H-NMR*
1.	EtOAc	Black, sticky residue	Impure
2.	50% EtOAc in Et_2O	Black, sticky residue	Impure
3.	THF	Black, sticky residue	Impure
4.	DCM : water extraction	Light brown sticky solid was obtained after evaporation of water layer followed by trituration with Et_2O	Pure

Table 2: *Optimization of purification procedure of triyne* ***5****.*

The final step in the synthesis of helquat **6** was [2+2+2] cyclotrimerization of triyne **5**, which was catalyzed by Wilkinson's catalyst to afford a cyclized product (Scheme 21). The workup of this step was relatively simple as compared to other steps. After completion of the reaction (analyzed by TLC analysis using Stoddart's magic mixture as a mobile phase), DMF was evaporated under reduced pressure and pure product was obtained after repeated washings with THF, until solid becomes free flowing and the THF layer after each sonication became colorless. Rh(I) catalyst goes to THF, leaving pure helquat as a solid. Finally, solid was washed several times with Et_2O and dried under high vacuum to give [6]helquat **6** as off-white solid.

The structure of helquat **6** was confirmed by spectroscopic analysis (^{1}H and ^{13}C-NMR, IR, ESI and HRMS). X-ray quality crystals of helquat **6** were grown by slow diffusion of MTBE into the methanolic solution of helquat and X-ray diffraction study of the obtained single crystals gave an idea about the structure. X-ray crystal structure of (*rac*)-helquat **6** is shown in Scheme 21.

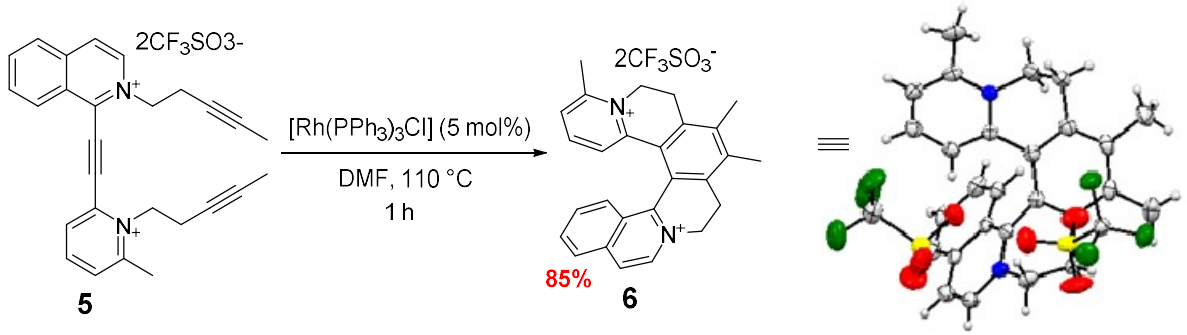

Scheme 21: *Synthesis of helquat* ***6****. Structure of the compound was confirmed by X-ray crystallography*

- **Synthesis of [5]helquats containing activated methyl groups:**

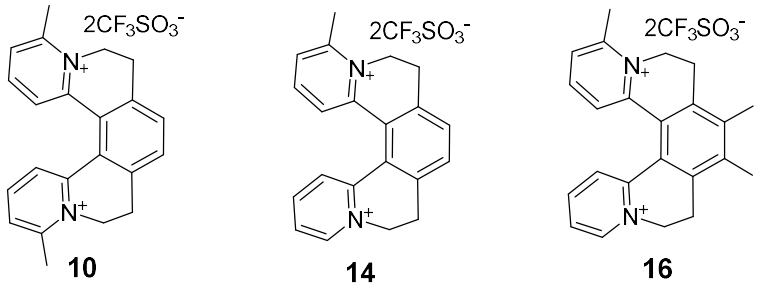

Fig. 56: *Derivatives of [5]helquat containing activated methyl groups.*

The methylated variants of [5]helquat (Fig. 56) were synthesized as new scaffolds for the library synthesis of helquat derivatives with diverse structures. The synthesized library of helquat derivatives was screened in various property screens and successful candidates were identified, which may lead us towards the application of the identified derivatives as fluorescence probe specific for specific biological targets. In addition to fluorescence library screening, the compounds were also checked for their G-quadruplex stabilizing activity as well as in live cell imaging applications in collaboration with biologists.

Alkyne **7** was prepared and purified according to the reported procedure[8] in 79% yield in a Sonogashira cross-coupling reaction between 2-bromo-6-methylpyridine **2** and gaseous acetylene catalyzed by Pd(0)/Cu(I) catalyst system (Scheme 22).

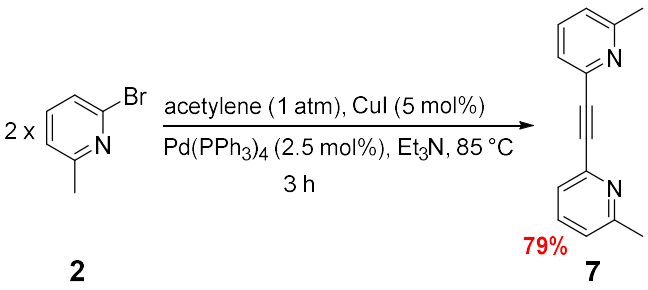

Scheme 22: *Synthesis of alkyne* ***7****.*

Triyne **9** was prepared by bis-quaternization of alkyne **7** with an excess of alkynyl triflate **8** (Scheme 23)**.** After 48 h of reflux in a Carius tube, complete conversion to triyne was observed by ^{1}H-NMR analysis.

Purification of the triyne **9** was easier as compared to triyne **5**. The solid was readily precipitated out from the reaction mixture. Excess of alkylating reagent was separated from the solid product by addition of EtOAc to the suspension followed by sonication and centrifugation of suspended solid. After first sonication and centrifugation, the dark brown supernatant was separated. Resulting solid was repeatedly washed with EtOAc *via* sonication and separation of supernatants after centrifugation. After the final washing, solid was vacuum dried and triyne **9** was obtained as an off-white solid in 83% yield.

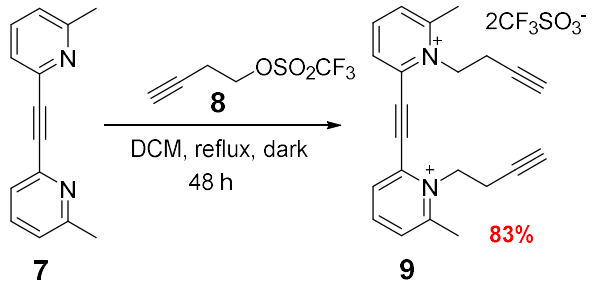

Scheme 23: *Synthesis of triyne* ***9****.*

Triyne **9** was cyclotrimerized to helquat **10** by heating DMF solution of triyne **9** in presence of Wilkinson's catalyst, [Rh(PPh$_3$)$_3$Cl] (Scheme 24). The workup of this reaction was relatively simple, similar to cyclotrimerization in case of [6]helquat **6**. After purification similar to [6]helquat **6**, [5]helquat **10** was obtained in its pure form in 73% yield.

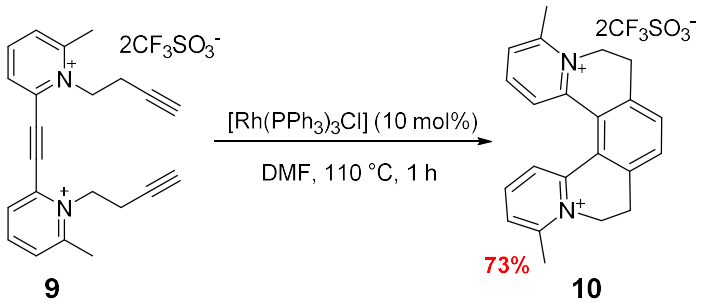

Scheme 24: *Synthesis of helquats* ***10****.*

Helquat **14** and **16** were synthesized analogously to helquat **10** in three steps.

Sonogashira cross-coupling reaction between terminal alkyne **11** and 2-bromo-6-methylpyridine **2** using previously optimized reaction conditions for the preparation and purification of alkyne **3**. Internal alkyne **12** was obtained as a brown, low melting solid in 74% yield (Scheme 25)**.**

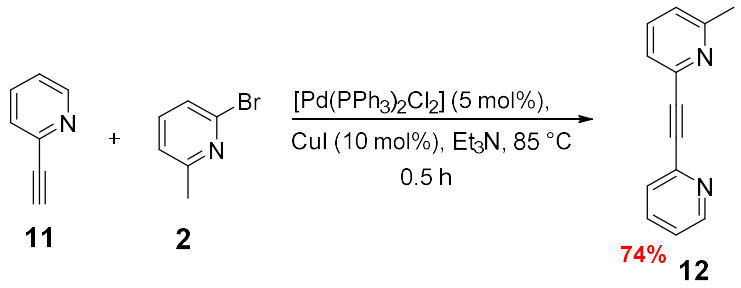

Scheme 25: *Synthesis of internal alkyne* ***12****.*

The reaction conditions for quaternization and [2+2+2] cyclotrimerization from the synthesis of helquat **10** were adopted and two new [5]helquats **14** and **16** were obtained in 69% and 59% respective overall yields over the two steps (Scheme 26).

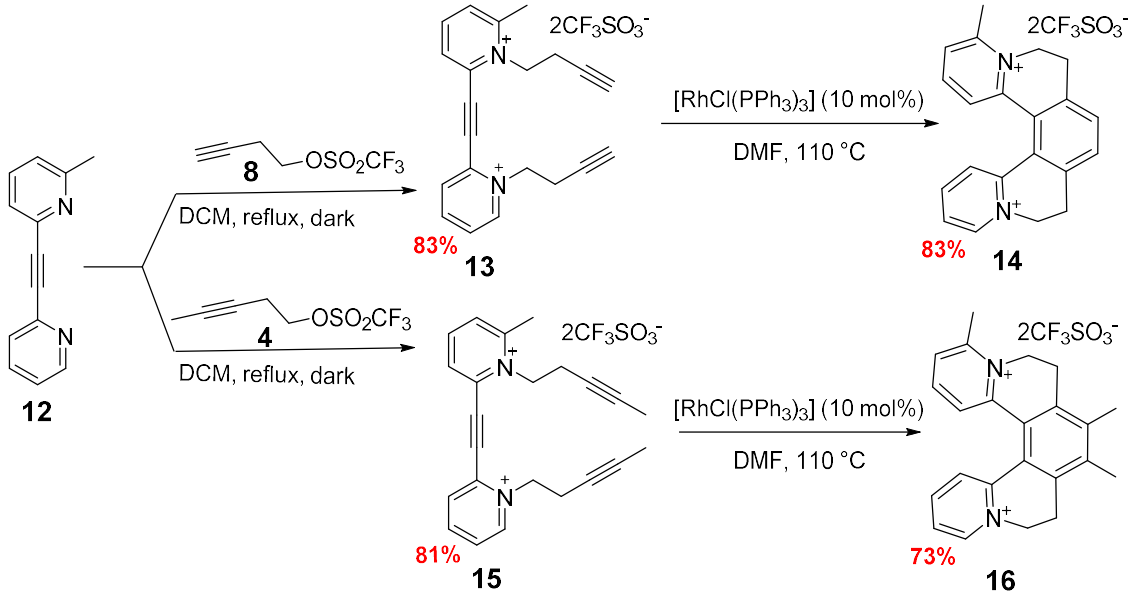

Scheme 26: *Synthesis of helquat* ***14*** *and* ***16****.*

- **Synthesis of Type I, II, III and IV helquat derivatives:**

In order to expand the existing library of helical dicationic molecules for studying their properties leading towards successful applications, a single step structure diversification protocol was developed.[8] Helquat derivatives originating from *racemic* parent helquat scaffolds **6**, **10**, **14** and **16** were synthesized by a single Knoevenagel condensation reaction. In a condensation reaction between activated methyl groups from respective parent helquats and varyingly substituted aromatic or heteroaromatic aldehydes in presence of base, helquat derivatives of **Type I**, **II**, **III** and **IV** were obtained in good to optimum yields (Scheme 27).

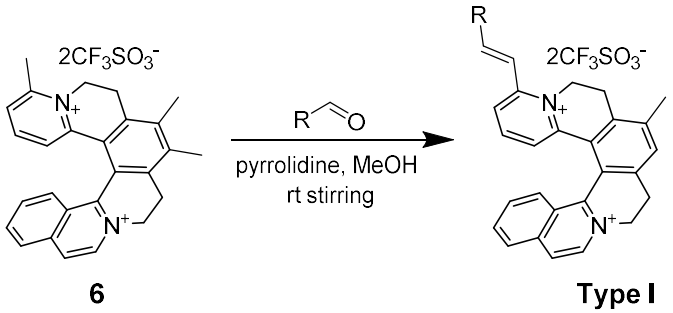

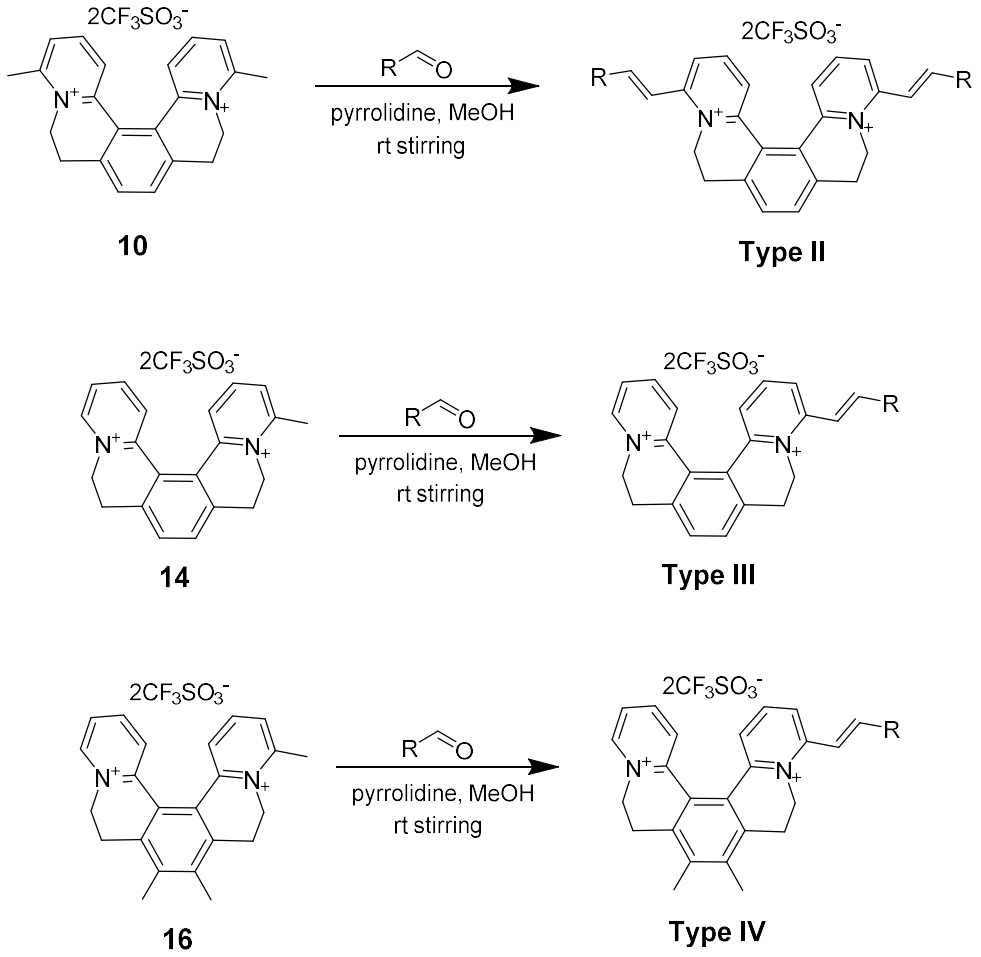

Scheme 27: *Helquat derivatization by single Knoevenagel condensation.*

Initially, all helquat derivatives of all types were synthesized in their *racemic* form and were explored in various property screens. If some specific property of the derivative was identified, then it was further explored towards finding of applications.

If needed, such compounds were synthesized in their enantiopure form as both enantiomers and were tested in comparison with the original compound.

The key characteristics of this methodology are - i) in a single step, reliable methodology, various functionalities can be attached to the helquat core; ii) products are purified by a chromatography-free method, usually by precipitation; iii) yields are moderate to high, typically more than 70% (exceptions are few dimethyl amino substituted derivatives).

Overall, it opens a very straightforward access to a structurally diverse library of helquat derivatives, which offers itself for various property screens. Number of helquat derivatives originating from **6** and **10** (**Type I** and **II**) were extensively synthesized (~ 200 and ~ 200, respectively), whereas derivatives originating from helquats **14** and **16** were mostly prepared and studied as controls or structural variant for **Type I** and **II** derivatives identified in the screens (~ 35 and ~ 15, respectively).

The reaction conditions, suitable amine catalyst and the purification process for the synthesis of **Type I** helquat derivatives were optimized by performing a model reaction of helquat **6** with 4-(*N*,*N*-dimethylamino)benzaldehyde **19** (Scheme 28) were successfully followed for the synthesis of all types of helquat derivatives with slight modifications,

depending upon the type of substrate and aldehyde. The optimized reaction and purification conditions are listed below.

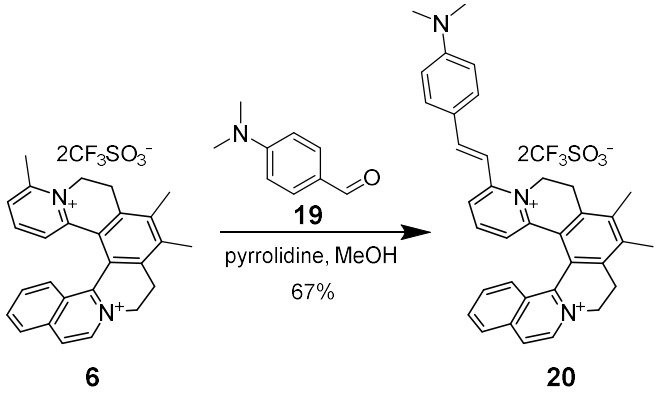

Scheme 28: *Synthesis of helquat derivatives of* ***Type I****.*

All reactions were preferentially performed at rt, while protected from ambient light and under dry conditions of solvents and glassware. Out of three screened bases (pyridine, piperidine and pyrrolidine), an excess of pyrrolidine up to 12.0 equiv. with respect to starting helquat was successful for better conversion and purity of the dye product. Even though, helquat derivatization reactions with some electron-rich aldehydes were successful using 3-5 equiv. excess of aldehyde and 1.5-3.0 equiv. of the base and it was also possible to achieve the pure products in reasonable yields, but it required reaction time up to several hours. From our previous observations, parent helquats themselves were not very stable in the strongly basic environment for a longer time and tends to get decomposed. Therefore, we decided to use an excess of base and aldehyde to shorten the reaction time from several hours to few minutes in several cases and 2-3 h in case of few alkoxy substituted and non-substituted aldehydes.

Initial attempts to purify the desired product by preparative TLC using a mixture of acetone, water and saturated KNO_3 (87.5:10:2.5) as mobile phase and the major purple dark spot was isolated but it was the impure product. Probably the product was not stable to the acidic surface of the silica.

In the next attempt, purification of the expected product by precipitation with a nonpolar solvent like Et_2O was successful when the proper ratio between MeOH and Et_2O was adjusted. It was also observed that by addition of 8 volumes higher amount of Et_2O to that of MeOH gave the product with good purity (according to ^{1}H-NMR analysis). To obtain the dye products with high purity, it was necessary to take following precautions:

1. Due to *cis-trans* isomerization of styryl double bond (as observed in case of few alkoxy substituted helquat dyes), all reactions were essentially carried out in dark, while protecting them with Alufoil cover and under argon atmosphere in dry MeOH as a solvent.

2. If the reaction time was increased, few unknown impurities were formed during the course of the reaction. It was also observed that using a large excess of aldehyde (12 equiv.); the reaction time can be minimized. Therefore many reactions were carried out under these optimized conditions.

3. For the effective purification of dye products from the unwanted impurities, complete dissolution of solid before addition of Et_2O was important.

Above optimized reaction conditions and purification protocol were used for the synthesis of **Type I** helquat derivatives. The helquat derivative **20** was fully characterized by spectroscopic analysis (^{1}H-NMR, ^{13}C-NMR, IR, ESI and HRMS analysis). The structure of the compound **20** was also confirmed by X-ray crystallography. The single crystal suitable for X-ray diffraction analysis was grown by slow diffusion of *i*-Pr_2O into the acetone solution of helquat dye **20** (Fig. 57). The conformation of styryl double bond was found to be exclusively *E* and it is in agreement with NMR spectroscopy (coupling constant, *J* = 15.9 Hz). For the condensation with few aldehydes, further optimization was needed to obtain the respective helquat derivatives in their pure form.

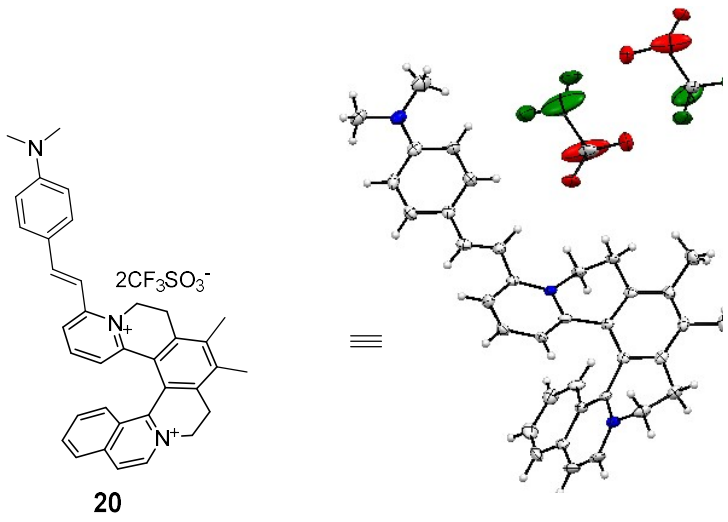

Fig. 57: *X-ray crystal structure of helquat derivative* ***20****.*

Few representative examples of **Type I** derivatives with their respective yields are shown in Fig. 58.

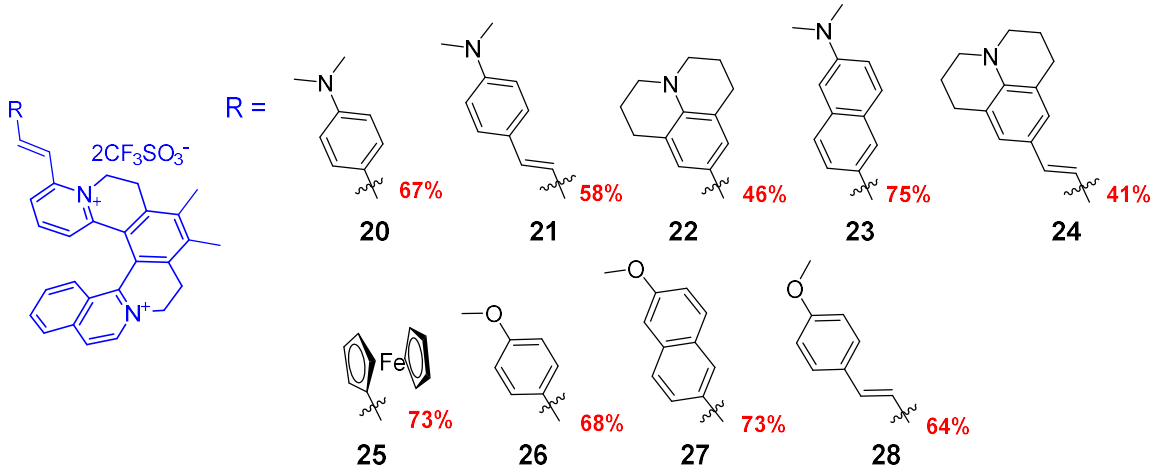

Fig. 58: *Generic structure of* ***Type I*** *derivatives (blue). Various R-group were connected to [6]helquat core with their respective yields mentioned in red.*

Helquat derivatives of **Type II**, **III** and **IV**, originating from helquat scaffolds **10**, **14** and **16**, respectively were synthesized by slightly tuning the reaction conditions and modifications in the purification procedure (Table 3).

Derivative type	Base (equiv.)	Aldehyde (equiv.)	Modifications in purification procedure
Type II	15	15	i) For few of them, MeOH was replaced with MeCN for re-dissolution of the solid during re-precipitation and purification. Less volume of Et_2O was used during precipitation. ii) For few derivatives, reaction times were higher due to the presence of two reactive methyl groups.
Type III	15	15	-
Type IV	15	15	-

Table 3: *Fine tuning of reaction conditions and purification methods to achieve* ***Type II****,* ***III*** *and* ***IV*** *helquat derivatives.*

Type II helquat derivatives originating from helquat **10** were extensively synthesized and were screened for their target-specific fluorescence light-up properties and applications based on these properties, such as fluorescent probes were developed.

For the synthesis of helquat derivatives of **Type II**, the Knoevenagel condensation methodology was successfully extended to achieve bischromophoric dyes, according to finely tuned reaction conditions and purification method described in Table 3. Reactions using a lower amount of base and aldehyde were usually sluggish, which led to longer reaction times and less clean reaction mixtures.

The generic reaction and few representative examples of **Type II** helquat derivatives with their respective yields are shown in Scheme 29.

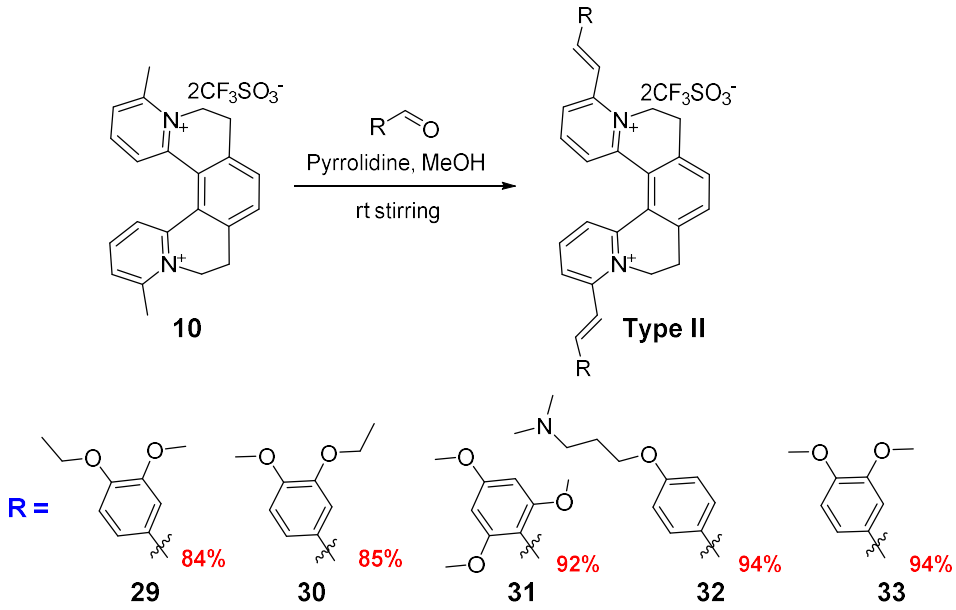

Scheme 29: *Generic scheme and few representative examples of* ***Type II*** *derivatives with their respective yields.*

Using above methodology, more than 200 derivatives of **Type II** were synthesized; some representative examples are shown in Scheme 29 with their respective yields.

Helquat derivatives of **Type III** and **IV** were synthesized from the respective substrates **14** and **16** by following reaction conditions summarized above. A small library of more than 50 compounds was synthesized (~ 35 and ~ 15, respectively).

Representative examples of these two series are shown in Scheme 30.

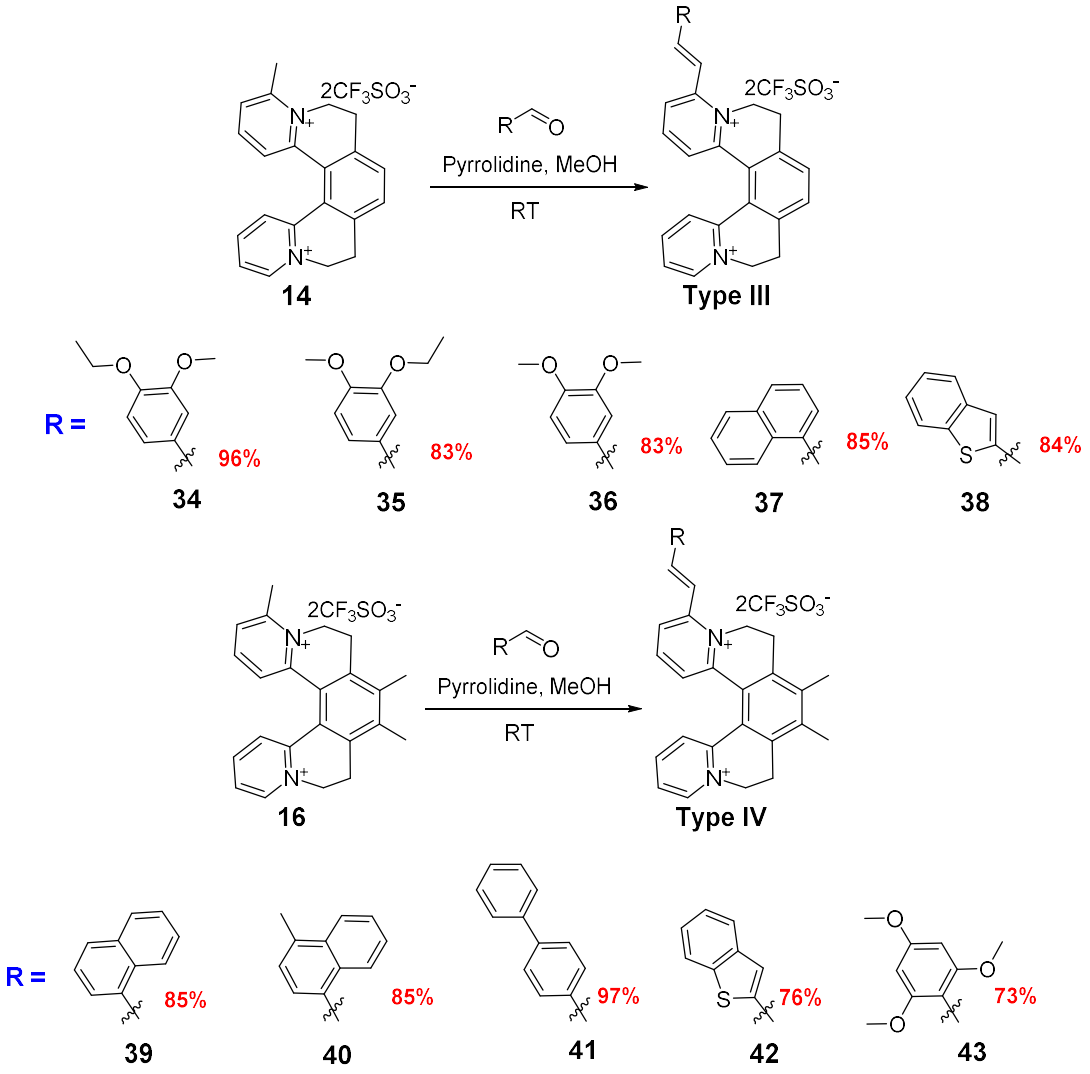

Scheme 30: *Generic scheme and representative examples of* ***Type III*** *and* ***IV*** *derivatives.*

- **Planar cationic dyes, representing controls of helquat derivatives:**

Planar dyes originating from two pyridinium substrates **17** and **18** were synthesized and screened in various experiments as controls of their helical counterparts. These dyes were prone to formation of unknown side products with increasing reaction time. Therefore, the reaction rate was increased either by refluxing EtOH solution of all reaction components in dark or in microwave reactor at 70 °C (Scheme 31).

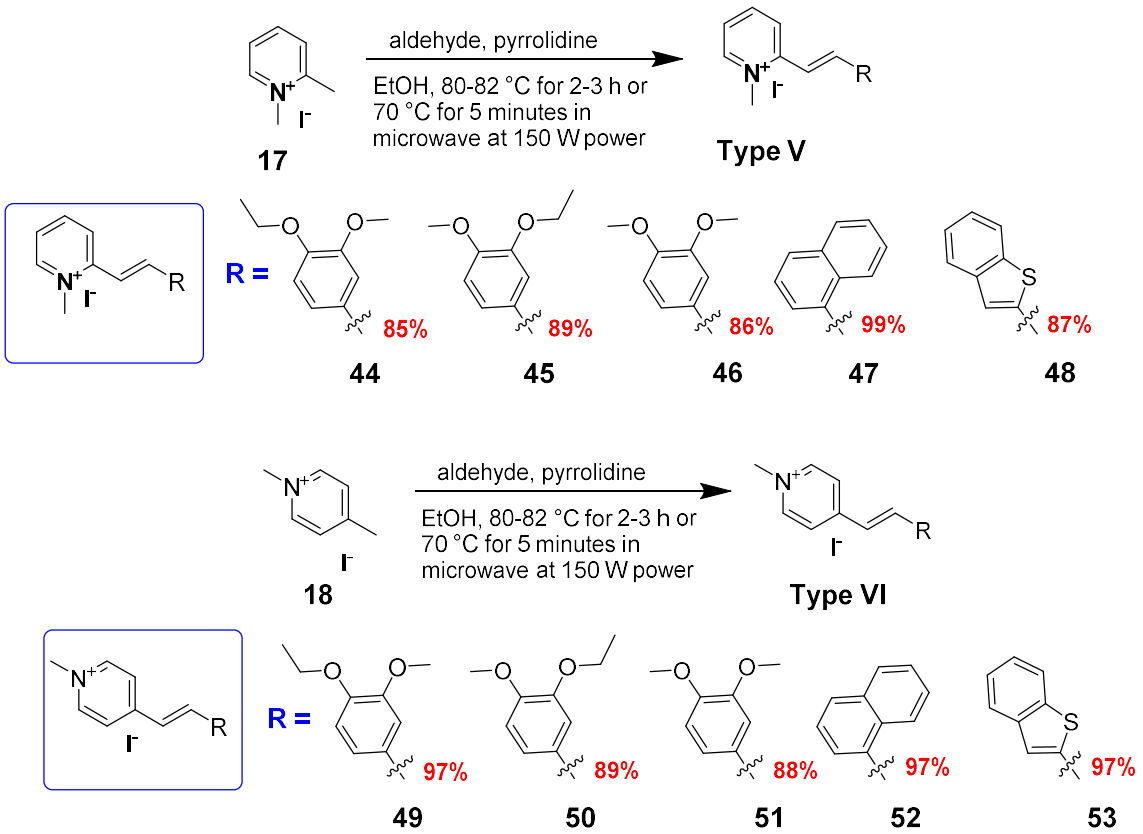

Scheme 31: *Synthesis of planar dyes of* ***Type V*** *and* ***VI****.*

3.2 Properties of helquats and their derivatives:

- **Chiroptical Properties of helquats:**

The key feature of helquats is their helical chirality. Helquats can be resolved into separate enantiomers. Our group has studied the chiral properties of helquats and developed some successful procedures for their resolutions to isolate enantiopure helquat samples in multigram scale. Out of all the helquats reported in this thesis only [6]helquat **6** can be resolved into pure enantiomers.

In our group, successful resolution of resolvable diquats (unpublished results) was achieved by direct precipitation of only one diastereomer with an addition of sodium salt of L-DBT into the aqueous solution of *racemic* dication. The second diastereomer goes to water and precipitated diastereomer was further purified by repeated washings with MeOH or EtOH. Diastereomer thus separated *via* very direct and practical protocol followed by second anion exchange from L-DBT to achiral anions (triflate or bromide) to give pure enantiomer was applied for the resolution of resolvable helquat **6**, but no diastereomer precipitation was achieved by this direct precipitation approach (Scheme 32).

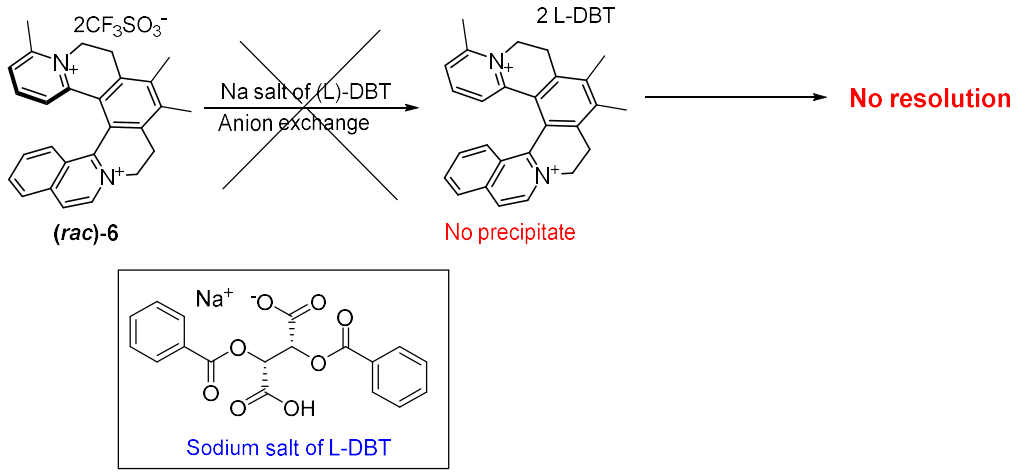

Scheme 32: *Failure of the resolution of helquat* ***6*** *by direct precipitation.*

In our group, other diquats were successfully resolved by another method, in which diastereomeric mixture was precipitated by addition of sodium borate salt of *R*-mandelic acid into the ethanolic solution of diquat. Diastereomers were separated from the mixture by EtOH washings and pure enantiomers were obtained by exchanging chiral anion to achiral anions (TfO^-, Cl^-).

In case of resolution of helquat **6**, a sticky solid was precipitated out from the ethanolic solution after 12 h of addition of the borate salt, which was analyzed by capillary electrophoresis (CE) and found to be the diastereomeric mixture. However, after several washings with EtOH, separation of diastereomers did not take place, resulting in unsuccessful resolution (Scheme 33).

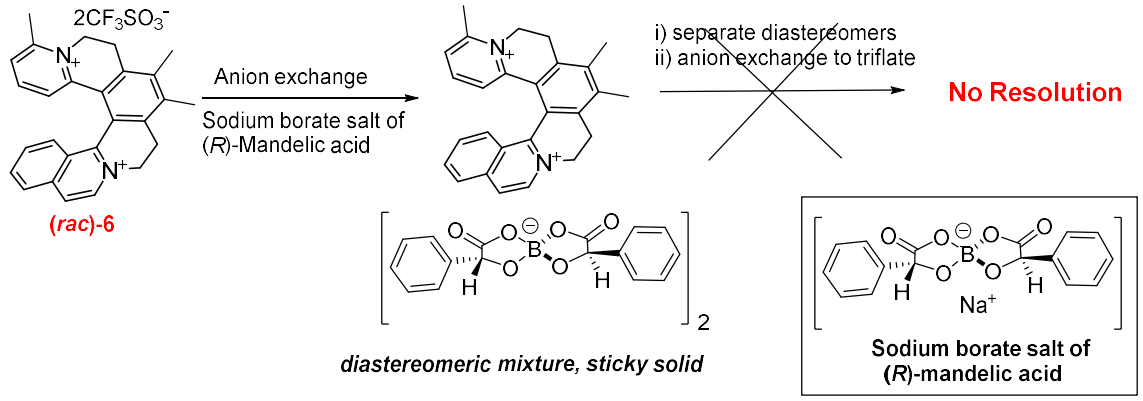

Scheme 33: *Failure of the resolution of helquat* ***6****.*

The successful resolution was achieved by following the reported procedure with other helquat scaffolds.[181]

A mixture of diastereomeric salts of both enantiomers of [6]helquat **6** was obtained by passing a methanolic solution of *racemic* helquat through a resin (anion exchange resin) column pre-loaded with L-DBT anions (Scheme 34). After confirming complete anion exchange by fluorine NMR, the attempts were made for successful separation of diastereomers.

In an initial attempt, obtained mixture of diastereomers was purified by trituration with EtOH. No separation of diastereomers was achieved using this method.

In next attempt, the diastereomeric mixture was purified using MeOH, by trituration of the mixture of the two diastereomeric salts with MeOH, which involves sonication leading to the dissolution of one diastereomeric salt in MeOH and the second diastereomer was left undissolved.

The success of the resolution was decided after analyzing the results of chiral capillary electrophoresis of final solid. The obtained solid was sufficiently enantiopure (*ee* > 98%).

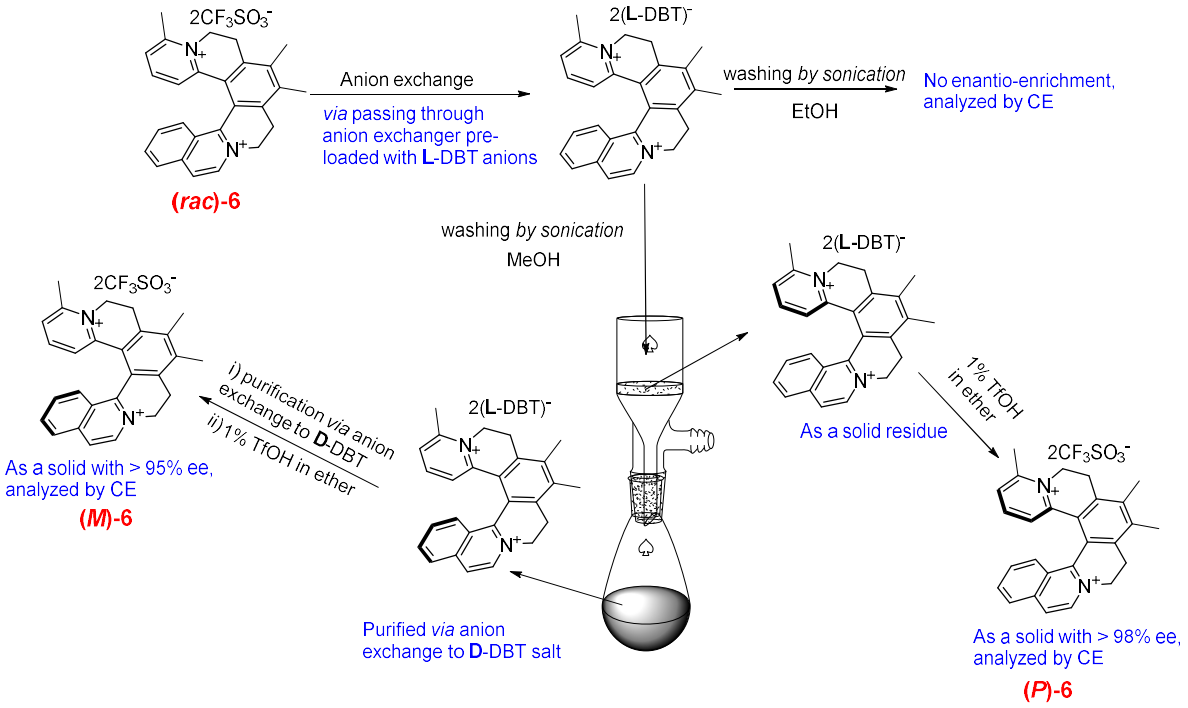

Scheme 34: *Resolution of helquat* ***6*** *via anion exchange and separation of the resulting diastereomeric salts.*

Respective pure enantiomers were obtained by breaking diastereomeric salt of pure enantiomer by second anion exchange from chiral, L-DBT counterion to achiral counterion such as triflate. The enantiopurity of obtained pure enantiomer was accessed by chiral CE analysis using cyclodextrins as chiral selectors (Fig. 59).

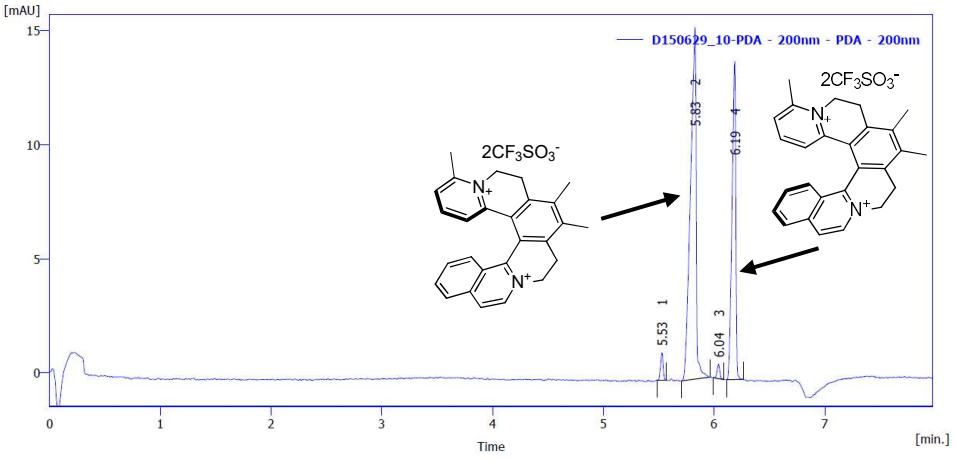

Result Table (Uncal - D150629_10-PDA - 200nm - PDA - 200nm)

	Migr. Time [min]	Area [mAU.s]	Height [mAU]	Area [%]	A/t% [%]	Efficiency [th.pl]	Resolution [-]	w [s]
1	5.529	1.9	1.2	2.09	2.25	199093		1.75
2	5.829	55.6	15.4	61.04	62.28	55321	4.046	3.50
3	6.042	1.1	0.6	1.21	1.19	237711	2.866	1.75
4	6.188	32.5	14.0	35.67	34.28	122169	2.429	2.50
	Total	91.1	31.2	100.00				9.50

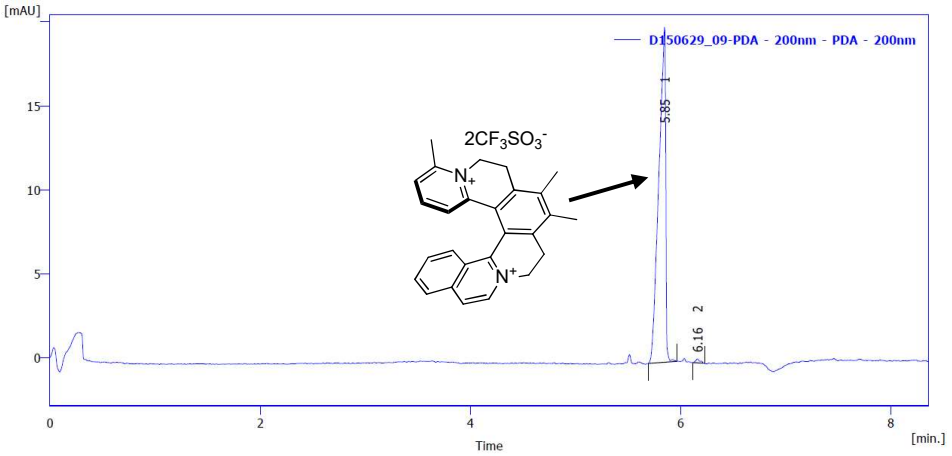

Result Table (Uncal - D150629_09-PDA - 200nm - PDA - 200nm)

	Migr. Time [min]	Area [mAU.s]	Height [mAU]	Area [%]	A/t% [%]	Efficiency [th.pl]	Resolution [-]	w [s]
1	5.846	89.8	19.9	99.21	99.25	30208		4.75
2	6.158	0.7	0.2	0.79	0.75	121020	3.052	2.50
	Total	90.5	20.2	100.00				7.25

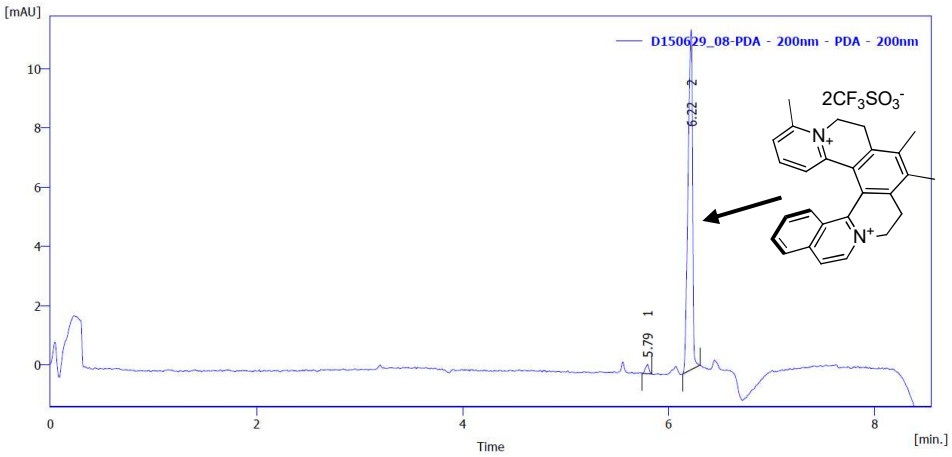

Result Table (Uncal - D150629_08-PDA - 200nm - PDA - 200nm)

	Migr. Time [min]	Area [mAU.s]	Height [mAU]	Area [%]	A/t% [%]	Efficiency [th.pl]	Resolution [-]	w [s]
1	5.792	0.8	0.3	2.16	2.32	88461		2.75
2	6.217	34.7	11.5	97.84	97.68	85642	5.233	3.00
	Total	35.4	11.8	100.00				5.75

Fig. 59: *Capillary electrophoresis charts for a)* ***(rac)-6****; b)* ***(P)-6*** *and c)* ***(M)-6*** *helquat bistriflate.*

The pure diastereomer obtained from an anion exchange to (L-DBT) was re-exchanged to the achiral, diiodide salt. The enantiopurity of this material was accessed by CE (>98%) and the X-ray quality crystals of the pure enantiomer thus obtained were grown by slow diffusion of MTBE into the MeCN solution of the enantiopure **6** diiodide. From the X-ray diffraction study of enantiopure helquat diiodide, obtained by above-mentioned root, the absolute configuration was assigned to be *P* (plus).

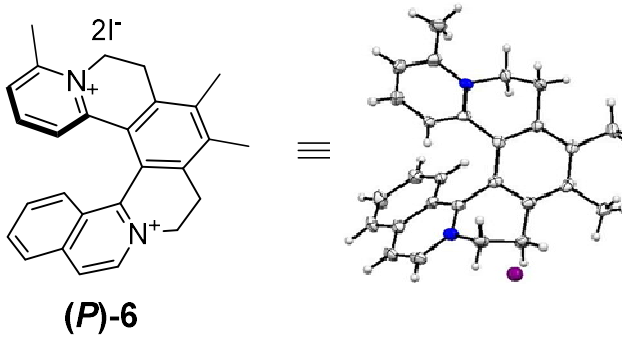

(*P*)-6

Fig. 60: *X-ray crystal structure of pure enantiomer, as a proof for the absolute configuration.*

The racemization energy and temperature of helquat **6** were determined by heating DMSO solution of 1.0 mg of pure **(*P*)-6** (0.5 mL) at 120 °C. The racemization process was monitored by chiral CE analysis of the samples taken after every 20 minutes. The decrease in *ee* of the major enantiomer with time follows the first order kinetics. When the kinetic law is transformed into the logarithmic form, the graph is linearized and the slope of the line corresponds to the desired rate constant of racemization 2k (Fig. 62). From this value, half-life of the racemization was calculated as

$$T_{1/2} = (ln\ 2)/2k \qquad \textit{(eq. 4)}$$

According to the theory of transition state, rate constant *k* can be transformed into activation Gibbs energy. This is the barrier of interconversion of one enantiomer into the other.

$$k = \frac{k_B T}{h} e^{-\Delta G^{\#}/RT} \qquad \textit{(eq. 5)}$$

Where k_B is Boltzmann constant (1.3806504 X 10^{-23} Jk^{-1}), *R* is the universal gas constant (8.314472 $Jk^{-1}mol^{-1}$), *h* is Planck constant (6.62606896 X 10^{-34} Js) *T* is thermodynamic temperature (in Kelvin).

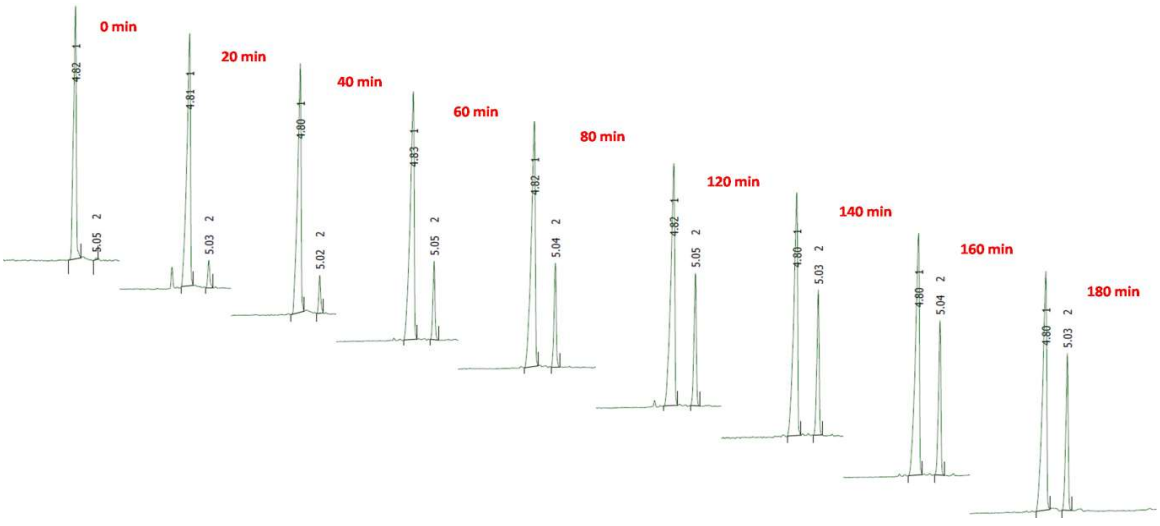

Fig. 61: *Monitoring of racemization progress at 120 °C, with increasing time %ee of major enantiomer was decreased.*

Time (minutes)	Peak 1	Peak 2	ee (%)	ln (ee %)
0	99.6	0.4	99.2	4.597
20	98.1	1.9	96.2	4.566
40	94.6	5.4	89.2	4.491
60	92.5	7.5	85.0	4.443
80	86.4	13.6	72.8	4.288
100	81.2	18.8	62.4	4.134
120	76.6	23.4	53.2	3.974
140	74.7	25.3	49.4	3.900
160	73.5	26.5	47.0	3.850
180	72.1	29.9	42.2	3.738

Table 4: *Data from CE measurement, during the racemization of helquat* ***(P)-6*** *at 120 °C.*

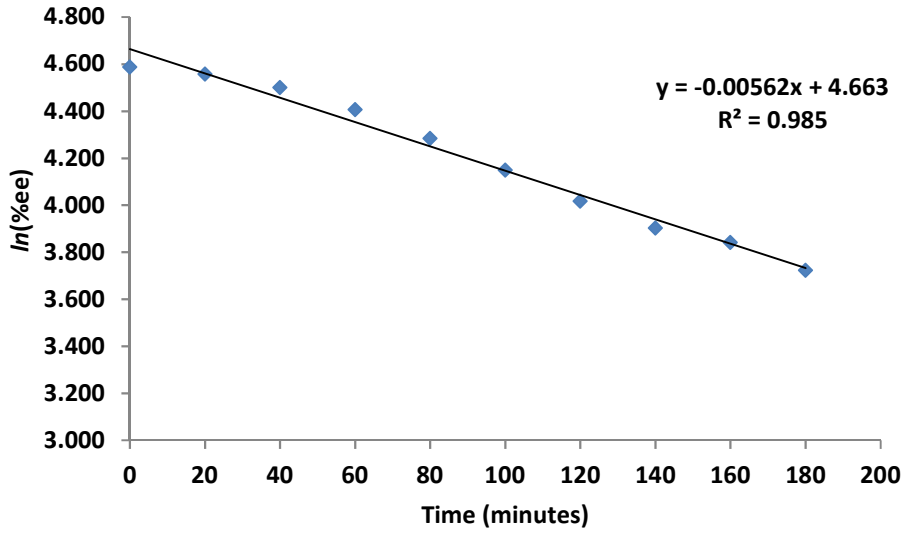

Fig. 62: *Racemization chart for* ***(P)-6*** *bis-triflate over time.*

Gibbs free energy $\Delta G^{\ddagger}$ (racemization barrier)			
$\Delta G^{\ddagger}$ (kJ/mol)	k (min^{-1})	k (s^{-1})	$T_{1/2}$ [h]
129.794	0.0028	5e-05	2.06

Table 5: *Results of racemization study of* ***(P)-6*** *bistriflate in DMSO-d_6 at 120° C.*

From the analysis of this data, we got the value of the activation free energy, $\Delta G^{\ddagger}$ = 129.8 kJ.mol^{-1} and racemization half-life at 120 °C, $T_{1/2}$ = 2 h.

- **Nonlinear optical properties of Type I helquat derivatives:**

Nonlinear optical properties of derivatives **20**–**28** were studied by Electronic spectroscopy, Hyper-Rayleigh scattering (HRS), Stark spectroscopy, and density functional theory (DFT) to assess their second-order NLO responses.

DFT and TD-DFT calculations were performed mainly to predict the molecular electronic structures and optical properties of the new cations characterized by experimental techniques. UV-vis. absorption spectra of derivatives **20**-**28** (Fig. 63) show an intense low energy absorption band due to charge transfer (ICT) from the amino/alkoxy unit to helquat fragment and less intense high-energy absorption band. By increasing conjugation between an acceptor and the donor part, the intense ICT band is shifted even higher towards the low energy region. This shifting of ICT band also depends upon the structure of donor part.

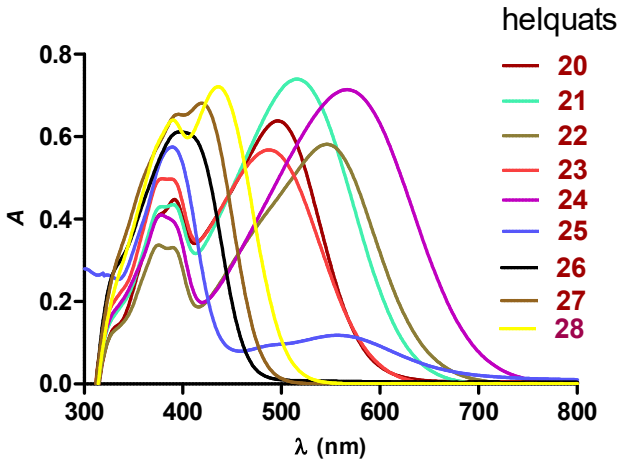

Fig.63: *UV-vis. spectra of helquat derivatives* ***20-28****.*

Helquat structure	Color	λ_{max} (nm)	ε (l.mol-1.cm^{-1})
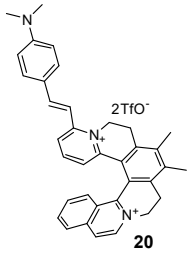 **20**	Purple	386 502	21674 31678
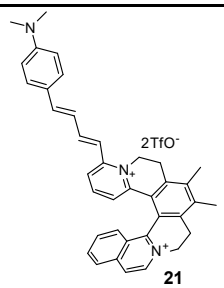 **21**	Purple	386 490	24842 28359
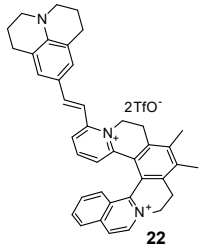 **22**	Purple	386 546	16461 29080

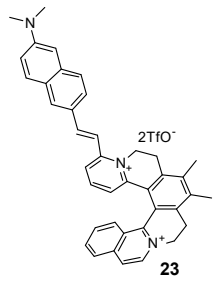 23	Red	386 523	21604 36690
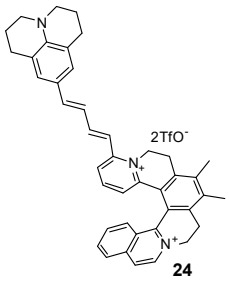 24	Deep blue	385 574	20136 35500
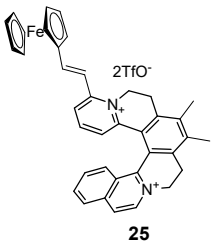 25	Blue	393 570	28504 5762
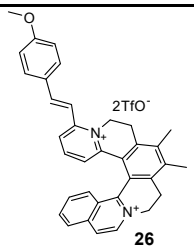 26	Yellow	391 419	30000 28000
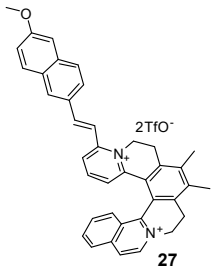 27	Lemon yellow	396 422	32000 34000
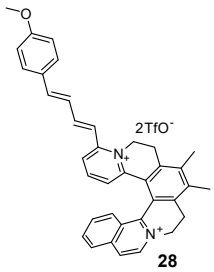 28	Orange	392 438	31000 36000

Table 6: *UV-vis. absorption properties of helquat dyes* ***20-28.***

The simulated UV-vis. spectra for dication **21** using above DFT TD-DFT method when compared with the experimental spectra confirms the above-mentioned behaviour of helquat chromophores (Fig. 64).

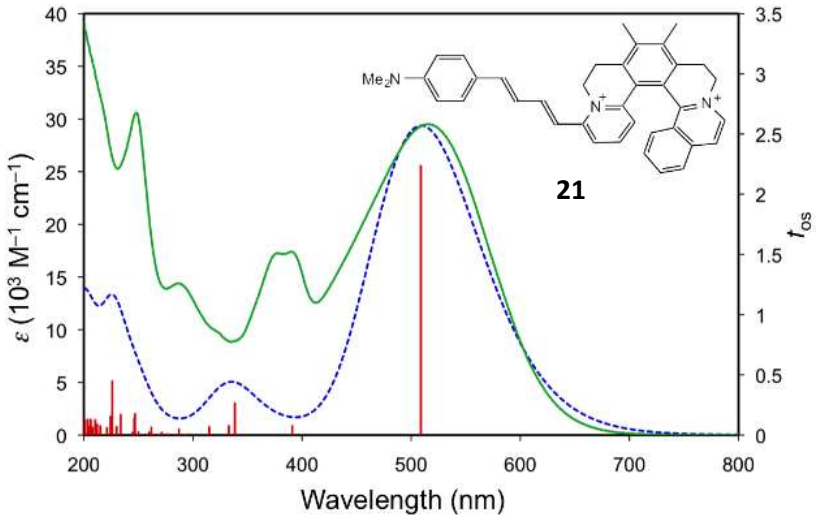

Fig. 64: *Experimental UV-vis. absorption spectra of helquat **21** (green line), with the CAM-B3LYP6-311G(d) calculated spectra. The ε-axes refer to the experimental data only and the vertical axes of the calculated data are scaled to match the main experimental absorptions. The f_{os}-axes refer to the individual calculated transitions (red).*

Molecular quadratic nonlinear optical (NLO) responses of all helquat derivatives **20**-**28** have been determined directly by using hyper-Rayleigh scattering (HRS) with 800 nm laser. The results of 800 nm *f*sHRS measurements[182] of resonant β values and β_0 (derived using the two-state model)[183] for cations **20–28** in MeCN are shown in Table 7 together with data reported for [DAS]PF_6.[184] The DFT and TD-DFT results confirm that the new chromophores are described adequately as two-state systems, i.e., a single low energy electronic transition is expected to dominate the NLO response. Helquat derivatives **20**-**28**, shows an increase in β_0[H] in the order **28** < **20** < **23** ≤ **22** < **21** ≤ **24**. The magnitude of β_0 increases either on extending the π-conjugation length or replacing a methoxy with a tertiary amino electron donor substituent. Thus the methoxy-substituted helquats show weak NLO responses than analogously substituted helquat with tertiary amino groups, possibly due to the weak electron donating strength of a methoxy group.

We have used Stark (electroabsorption) spectroscopy in PrCN glasses at 77 K to derive $\Delta\mu_{12}$ values for the low energy ICT bands of cations **20**-**28**. The results of stark spectroscopy[185] for salts **20**-**28**, along with DAS^+PF6^- are summarized in Table 7, and their representative spectra for **22**, **24** and **26** are shown below (Fig. 65).

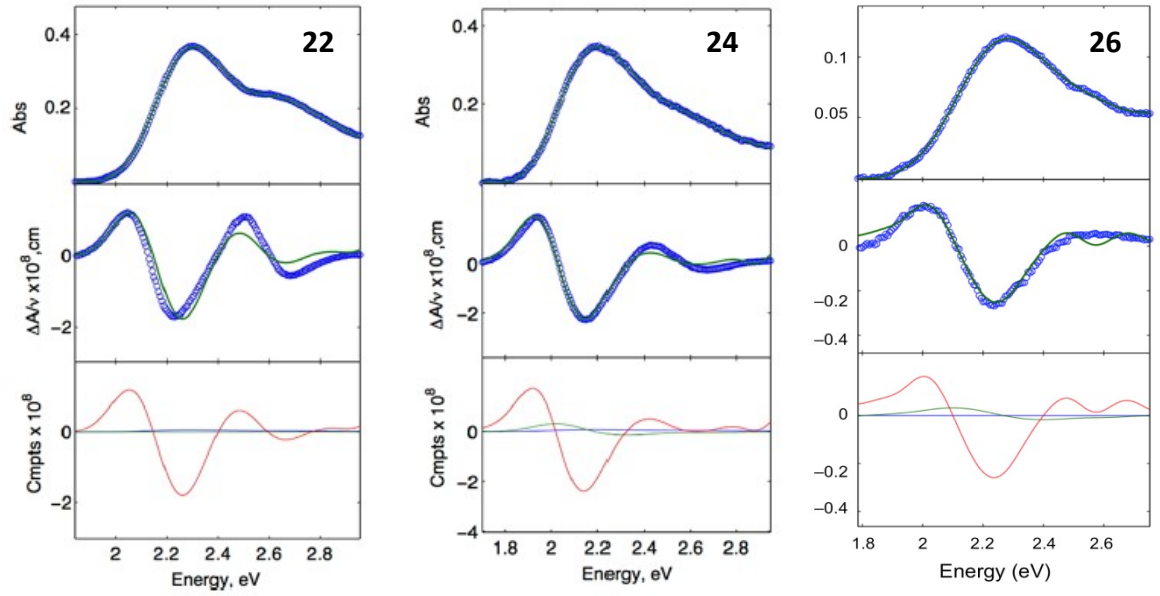

Fig. 65: *Spectral and calculated fits for salts* ***22***, ***24*** *and* ***26****. Top panel: UV–vis absorption spectrum; middle panel: electro absorption spectrum, experimental (blue), and fits (green) according to the Liptay equation[185b] and bottom panel: contribution of 0th (blue), 1st (green), and 2nd (red) derivatives of the absorption spectrum to the calculated fits.*

Salt	$\lambda_{max}{}^{a}$ *(nm)*	$\lambda_{max}{}^{b}$ *(nm)*	$E_{max}{}^{b}$ *(ev)*	$f_{os}{}^{b,c}$	$\mu_{12}{}^{b,d}$ *(D)*	$\Delta\mu_{12}{}^{b,e}$ *(D)*	$\beta_0[S]^{f}$ *(10^{-30} esu)*	$\beta_{800}{}^{g}$ *(10^{-30} esu)*	$\beta_0[H]^{h}$ *(10^{-30} esu)*
20	496	498	2.49	0.56	7.8	22.5	252	171±12	57±4
21	516	533	2.33	0.82	9.7	21.1	424	401±43	156±17
22	538	537	2.31	0.71	9.0	20.2	364	209 ±6	93±3
23	485	493	2.52	0.46	7.0	29.5	260	302±13	90±4
24	564	564	2.20	0.78	9.7	26.1	588	376±32	187±16
25	557	544	2.28	0.09	3.2	14.5	36	208±21[j]	-[i]
26	396	427	2.90	0.07	2.5	15.4	14	-[i]	-[i]
		407	3.05	0.17	3.9	13.6	26		
		383	3.24	0.11	3.0	6.0	6		
27	417	433	2.86	0.15	3.7	14.7	28	-[i]	-[i]
		412	3.01	0.17	3.9	12.8	26		
		384	3.23	0.21	4.7	0.0	2		
28	436	455	2.73	0.23	4.7	15.8	54	199±8	26±1
		428	2.90	0.34	5.6	13.0	56		
		382	3.25	0.35	5.3	8.5	28		
[DAS^{+}]^{i} PF_6^{-}	470	470	2.58	0.8	9.1	16.3	236	440±30	110±7

Table 7: *ICT absorption, Stark spectroscopic, and HRS data for salts* ***20–28****.*

[a]In MeCN at 295 K. [b]In PrCN at 77 K. [c]Obtained from $(4.32 \times 10^{-9}$ M cm$^2)\varepsilon_{max} \times fw_{1/2}$, where ε_{max} is the maximal molar extinction coefficient and $fw_{1/2}$ is the full width at half height (in wavenumbers). [d]Calculated from **eq 1.** [e]Calculated from $f_{int}\Delta\mu_{12}$ using $f_{int} = 1.33$. [f]Calculated from **eq 2.** The quoted cgs units (esu) can be converted to SI units (C^3 m^3 J^{-2}) by dividing by 2.693×10^{20} or into atomic units by dividing by 0.8640×10^{-32}. [g]Obtained from HRS measurements with an 800 nm Ti^{3+}:sapphire laser and MeCN solutions at 295 K. [h]Derived from β_{800} by application of the two-state model. [i] Could not be measured due to weak HRS signals.

In case of methoxy-substituted derivatives (**26**-**28)**, the ICT bands show almost no change on moving from MeCN to PrCN. However, small red shifts were observed in case of amino-substituted helquats (**20**-**25**) on moving from MeCN solutions to PrCN glasses. The decreases

in E_{max} on extending a vinyl to 1,3-butadienyl bridge or replacing a 4-(dimethylamino)-phenyl with julolidinyl group are maintained at 77 K. The μ_{12} values determined using eq. 6 below:

$$|\mu_{12}| = \left(\frac{f_{os}}{1.08 \times 10^{-5} E_{max}}\right)^{1/2} \quad (eq.\ 6)$$

All values were falling into a relatively narrow range with small increases on conjugation extension. In general, $\Delta\mu_{12}$ also increases in the same manner and as expected, although the value for **23** was unexpectedly low.

The β_0[S] values determined using the eq. 7 below:

$$\beta_0\,[S] = \frac{3\Delta\mu_{12}(\mu_{12})^2}{(E_{max})^2} \quad (eq.\ 7)$$

β_0 values were in order, **26 < 27 < 25 < 28 < 20 ⩽ 23 < 22 < 21 < 24** matches the HRS trend exactly. The expected increases in the NLO response on enhancing the electron donor strength or extending the conjugation are thus also shown by most of the Stark-derived data. However, the difference is within the estimated error limit of ±20%. Also, as for the HRS data, changing the helquat unit leads to variations in β_0[S] that are generally not statistically significant.

The electronic structure of the molecule **20** was predicted using DFT calculations (Fig. 65). MOs of compound **20**, were determined from gas phase transition, whereas DFT and TD-DFT calculations show the lowest energy transition from HOMO -> LUMO and HOMO -> LUMO+1. HOMO is located on the 4-(dimethylamino)styryl fragment whereas LUMO is mostly based on the helquat unit and the LUMO+1 spread over the whole molecule (Fig. 66).

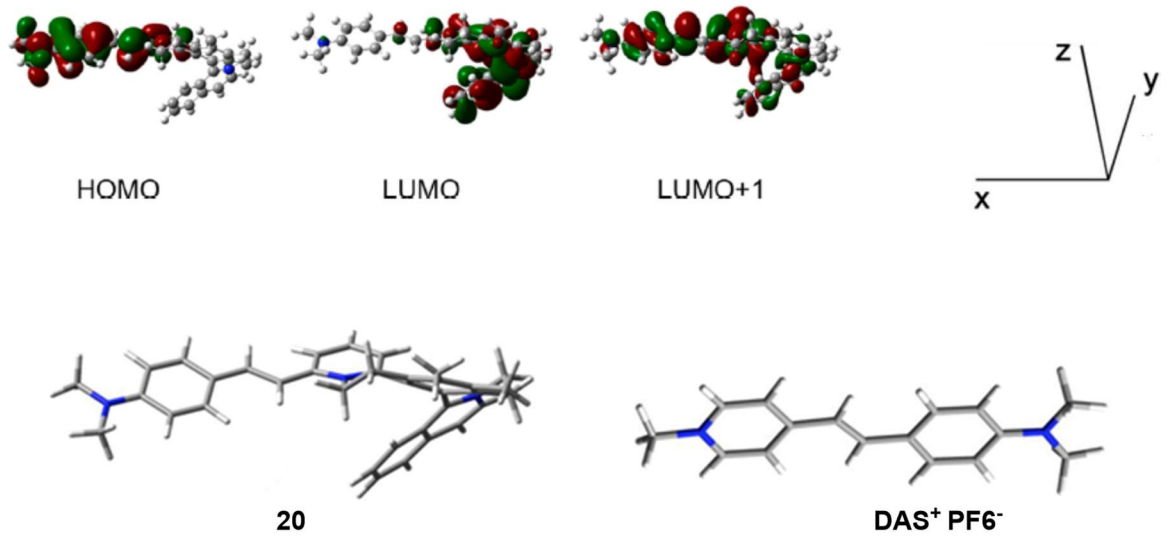

Fig. 66: *CAM-B3LYP/6-311G(d)-derived contour surface diagrams of the frontier MOs for cation **20** (isosurface value 0.03 au), optimized structures of the cation **20** and DAS+, with the axis convention used in the hyperpolarizability calculations.*

Cation	ΔE (ev)	λ (nm)	f_{os}	Major contributions
20	2.76	449	1.570	H → L (43%), H → L+1 (48%)
	3.37	368	0.136	H–1 → L (10%), H → L (37%), H → L+1 (38%)
	3.67	338	0.297	H–2 → L (28%), H–1 → L (54%)
	3.87	320	0.055	H → L+2 (73%)
	4.00	310	0.069	H–3 → L (14%), H–2 → L (49%), H–1 → L
	4.29	289	0.042	H–5 → L (35%), H–3 → L (35%)
	4.54	273	0.049	H–2 → L+1 (24%), H–1 → L+1 (34%)
	4.82	257	0.022	H → L+3 (72%)
	4.90	253	0.123	H–3 → L+1 (12%), H–2 → L+2 (20%), H–1 → L+2 (23%)
	5.04	246	0.070	H–4 → L (15%), H–4 → L+1 (35%), H → L+5 (14%), H → L+6 (23%)
	5.12	242	0.016	H–1 → L+1 (28%), H–1 → L+2 (21%)
	5.23	237	0.101	H–5 → L (20%), H–3 → L (21%), H–2 → L+2 (12%)
	5.25	236	0.075	H → L+4 (11%), H → L+5 (32%), H → L+7 (19%)
	5.32	233	0.169	H–5 → L+1 (17%), H–3 → L+2 (16%), H–2 → L+2 (17%), H–1 → L+4 (10%)
	5.37	231	0.173	H–5 → L (10%), H–5 → L+2 (12%), H–3 → L+1 (49%)
	5.51	225	0.491	H–6 → L (25%), H–5 → L+1 (14%), H–1 → L+3 (19%)
	5.58	222	0.184	H–1 → L+3 (17%), H → L+4 (30%), H → L+5 (12%)
	5.79	214	0.032	H–5 → L+1 (27%), H–3 → L+2 (17%), H → L+7 (10%)
	5.85	212	0.027	H–5 → L+3 (13%), H–2 → L+3 (32%), H–1 → L+3 (14%)
	5.93	209	0.018	H–3 → L+2 (12%), H–2 → L+3 (10%), H → L+7 (14%)
	5.96	208	0.153	H–2 → L+4 (10%), H–1 → L+4 (23%)
	6.02	206	0.058	H–9 → L (16%), H–5 → L+2 (19%)
	6.05	205	0.044	H–8 → L (11%), H–3 → L+3 (19%), H–2 → L+3 (10%)
	6.08	204	0.183	H–9 → L (10%), H–8 → L (32%), H–8 → L+1 (12%)

6.14	202	0.127	H–2 → L+4 (27%)
6.26	198	0.065	H–11 → L (16%), H–7 → L (19%), H–6 → L+2 (11%)
6.26	198	0.078	H–6 → L+1 (39%), H–6 → L+2 (16%)
6.36	195	0.087	H–12 → L (13%), H–7 → L+1 (12%), H–6 → L+3 (12%)
6.42	193	0.262	H–12 → L (19%), H–11 → L (15%), H–6 → L+3 (11%)
6.46	192	0.015	H–10 → L (12%), H–10 → L+1 (38%)
6.46	192	0.030	H → L+11 (56%), H → L+13 (16%)
6.53	190	0.015	H–6 → L+2 (14%)
6.53	190	0.124	H–12 → L (13%), H–8 → L+1 (19%)

Table 8: *Selected TD-DFT-calculated data for cation* ***20****.*

Note: Geometry optimizations and TD-DFT calculations used the CAM-B3LYP functional with the 6-311G(d) basis set, and a CPCM MeCN solvent model was included for TD-DFT. Only the main transitions within each absorption band are included. H = HOMO, L = LUMO.

atom	*x*	*y*	*z*
N	8.938623	0.17543	–0.569128
C	–1.467294	–0.645551	1.835076
H	–2.475991	–0.830667	2.173323
C	–0.389445	–1.339288	2.401899
H	–0.568716	–2.079859	3.172115
C	0.87875	–1.108696	1.958783
H	1.701071	–1.697778	2.3369
C	1.14195	–0.129418	0.975948
N	0.061826	0.591662	0.517569
C	0.269922	1.798879	–0.30703
H	0.152943	1.54192	–1.363423
H	1.288891	2.135343	–0.147571
C	–0.693994	2.896799	0.1012
H	–0.460887	3.239683	1.115219
H	–0.519047	3.743266	–0.561647
C	–2.117585	2.421636	0.002491
C	–3.177903	3.280825	–0.310579
C	–4.479914	2.769816	–0.393714
C	–4.698626	1.40977	–0.162021
C	–6.084138	0.824974	–0.050543
H	–6.788663	1.576447	0.30291
H	–6.464019	0.4605	–1.010993
C	–6.048416	–0.299107	0.965745
H	–5.724544	0.063711	1.9437
H	–7.016458	–0.780784	1.076713
N	–5.089417	–1.325069	0.498947
C	–5.452478	–2.64582	0.559874
H	–6.401234	–2.850537	1.034067

C	–4.652664	–3.607297	0.052937
H	–4.947374	–4.645841	0.131248
C	–3.474	–3.242358	–0.640819
C	–2.678155	–4.20488	–1.296248
H	–2.945761	–5.251849	–1.21663
C	–1.60634	–3.814294	–2.048495
H	–1.00767	–4.554577	–2.565512
C	–1.297992	–2.445379	–2.189819
H	–0.483378	–2.148636	–2.839268
C	–2.029658	–1.494269	–1.538114
H	–1.806993	–0.44824	–1.690834
C	–3.12434	–1.866201	–0.717962
C	–3.926166	–0.91204	–0.027005
C	–3.626714	0.533986	0.05583
C	–2.333625	1.066218	0.241808
C	–1.235647	0.290916	0.865082
C	2.439561	0.107062	0.443156
H	2.512098	0.604147	–0.513734
C	3.596725	–0.284889	1.067595
H	3.509927	–0.726301	2.056945
C	4.928874	–0.153122	0.609533
C	5.987392	–0.565757	1.450524
H	5.75365	–0.975732	2.427868
C	7.298165	–0.464695	1.080024
H	8.06357	–0.795478	1.766423
C	7.65407	0.067202	–0.188523
C	6.591031	0.481411	–1.044182
H	6.811342	0.88763	–2.020585
C	5.289038	0.373502	–0.653016
H	4.521147	0.700124	–1.345289
C	10.011352	–0.252936	0.320558
H	10.002561	0.313043	1.254694
H	10.967402	–0.083373	–0.164524
H	9.935049	–1.317778	0.551675
C	9.284704	0.720924	–1.875658
H	8.866968	0.116057	–2.683723
H	10.364463	0.724823	–1.986064
H	8.932837	1.749311	–1.984422
C	–2.934583	4.752804	–0.507418
H	–2.047658	5.099899	0.018031
H	–3.769387	5.347548	–0.141869
H	–2.807795	4.996233	–1.566974
C	–5.629666	3.680117	–0.73665
H	–6.480862	3.13746	–1.142014
H	–5.340337	4.413096	–1.488114
H	–5.977508	4.237997	0.138027

Table 9: *DFT-optimized coordinates for cation* ***20****.*

The β_{tot} value obtained *via* DFT for dyes **20** and **21** were showing an increase while moving from the gas phase to MeCN and are in correlation to the data obtained by HRS and Stark spectroscopy. β_{tot} increases substantially from 214 (for **20**) to 345 (for **21**) in the gas phase

with increasing the π-conjugation system in each pair. Whereas, by moving from gas phase to MeCN, the β_{tot} value for cation **20** was increased from 214 -> 472 and for cation **21**, it was changed from 345 to 1069.

Comparing the β_0 values for helquat dyes **20**-**28** with those of [DAS]PF_6 reveals that a number of the new dye salts show a similar level of NLO activity and that several compare favourably. In particular, **21**, and **24** show β_0[S] responses twice as large or even greater when compared with this benchmark compound. These enhancements are due to a combination of decreasing E_{max} and increasing $\Delta\mu_{12}$. These observations provide a strong incentive to pursue further crystalline materials as well as pure enantiomers (*P* and *M*) incorporating these new helquat cations in which large bulk NLO effects can be anticipated.

For this reason, the pure enantiomers of helquat **6** were synthesized and multigram quantity. Pure enantiomers of helquat dyes **20-28** will be synthesized and screened for their nonlinear optical properties in solution as well as in crystalline form.

- **Target-specific fluorescence light-up properties: search of heparin chemosensors:**

A chemical compound, recognizing the presence of a particular analyte of interest by remarkable changes in color or spectroscopic properties after interaction as compared to the sensor alone are widely studied. Such molecules are known as chemosensors and the much-desired quality of such a chemosensor must be its specificity and selectivity for the particular target of interest. Quantification of a particular analyte of interest in the complicated environment is much-desired application area of such sensors.

We were interested to screen our dyes with various important biological targets. As our dyes are cationic in nature, we expected to have electrostatic interactions with targets, which are highly negatively charged. Heparin is a member of glycosaminoglycan family and is known as a highly negatively charged molecule. It is used as an anticoagulant drug during cardiovascular surgery and many more complicated medical procedures. Taking an inspiration from the diversity-oriented approach (DOFLA)[163] developed by Chang *et al.* in search of fluorescent chemosensors, we decided to develop an assay using the experimental setup is described in the experimental section. The simple setup comprising a 96 or 384-well plate, a device for identification of preliminary hits by observing the changes that are visible with naked eyes after irradiation with UV-transilluminator and a plate reader for confirming the visually identified hits by spectroscopic measurements.

As heparin is administered at therapeutic dosing levels of 2-8 U/mL (17–67 μM) during cardiovascular surgery and 0.2–1.2 U/mL (1.7–10 μM) in post-operative and long-term care[186]. As reported in previously developed assays, for the preliminary screening 10 μM of each dye was mixed with 10 μM of heparin in HEPES (2-(4-(2-hydroxyethyl)piperazine-1-yl)ethane sulphonic acid) buffer, 10 mM (pH 7).[162, 163]The fluorescence response of each dye in absence and presence of heparin was monitored.

Before starting actual screening, the solubility of dyes containing various functional groups was determined. As most of our dyes were insoluble in HEPES buffer (pH 7), we decided to use 1 mM DMSO stock solutions of the dyes and dilute them inside the well to appropriate DMSO %, which was determined by checking the solubility of few representative dyes under four different conditions summarized in Table 10. Based upon the results, we decided to go with 10% DMSO for all preliminary screening experiments.

Structure	Solubility conditions (with % DMSO in HEPES buffer (pH 7.0)			
	0	1	5	10
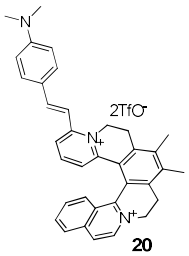 20	insoluble	soluble	soluble	soluble
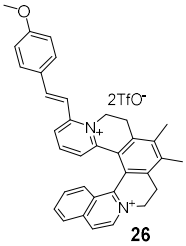 26	insoluble	soluble	soluble	soluble
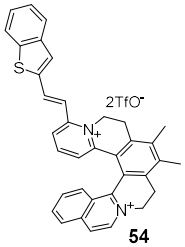 54	insoluble	insoluble	soluble	soluble
 33	insoluble	insoluble	insoluble	soluble
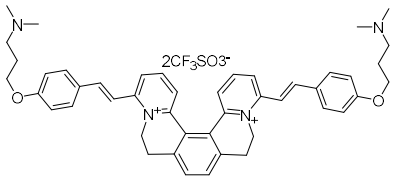 32	insoluble	insoluble	soluble	soluble
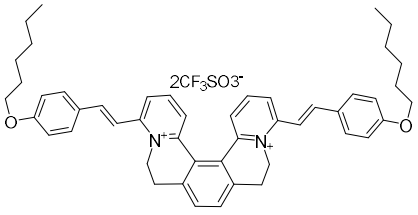 69	insoluble	insoluble	insoluble	Soluble

Table 10: *Screening of solubility conditions for helquat dyes.*

A high-throughput assay was a need to screen a library of compounds under the identical conditions in multiplicates. To identify the compounds, which shows selective florescence light-up in presence of heparin alone, two separate wells were produced for each compound, with one containing a solution of heparin in the buffer and the other for the dye alone (in absence of heparin). Each experiment was performed at least in duplicate to remove possible experimental error during the experiment preparation. After giving proper

interaction time to both the interaction partners, the preliminary assessment of the hits was performed by recording the fluorescent photograph of the whole experiment under irradiation of UV light in UV-transilluminator (commonly used device for visualization of gels). It was also observed that many compounds also show color changes in interaction with heparin. After primary identification of the compound as a preliminary hit, the result was further confirmed by measuring their relative emission spectra in presence and absence of heparin. After the preliminary screening was over, all hits were organized based on their relative fluorescence intensity increase in presence of heparin.

Entry	*Structure*	*Emission spectra*	*Relative fluorescence intensity increase*
1.	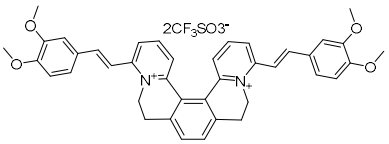 33	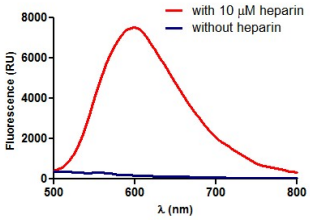	49.50
2.	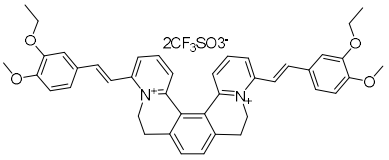 30	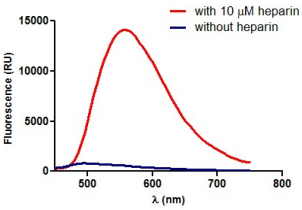	26.09
3.	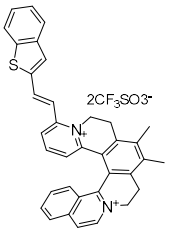 54	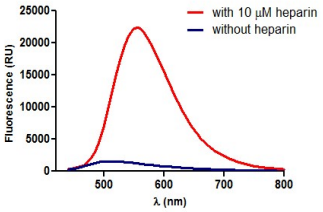	18.77
4.	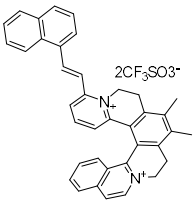 55	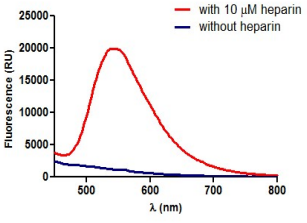	17.88
5.	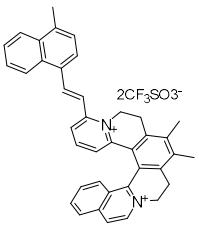 56	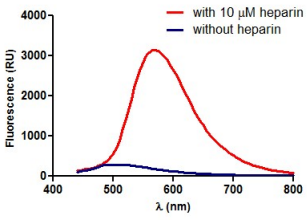	17.45

6.	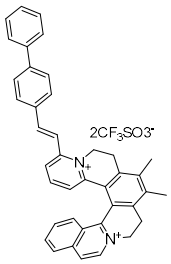 57	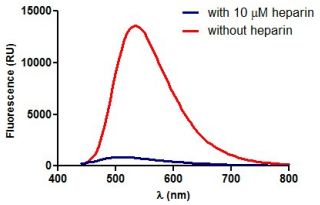	16.99
7.	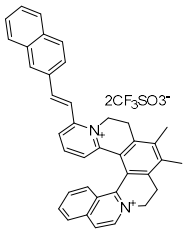 58	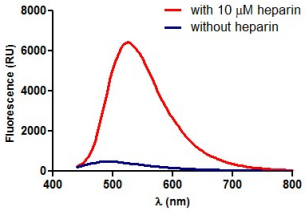	15.86
8.	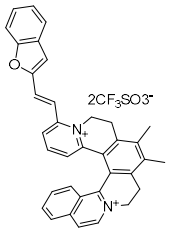 59	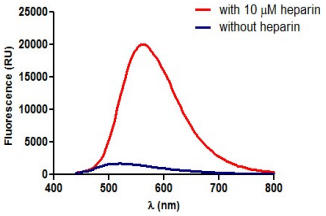	14.95
9.	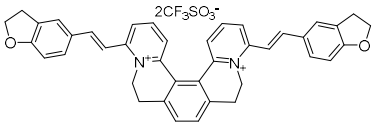 60	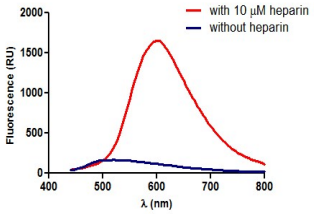	14.72
10.	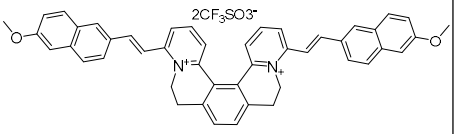 61	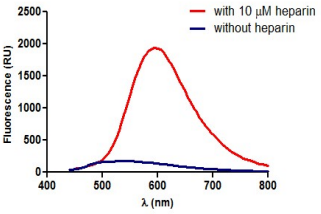	14.00
11.	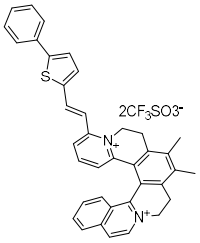 62	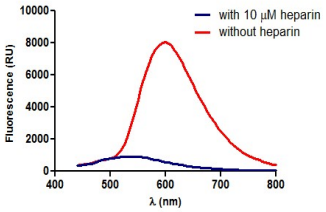	13.95

12.	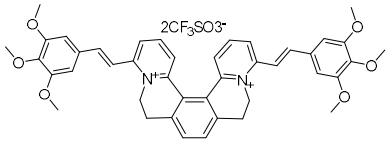 63	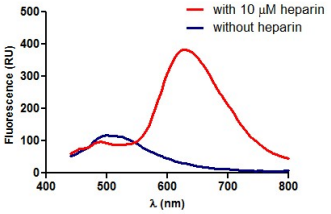	13.75
13.	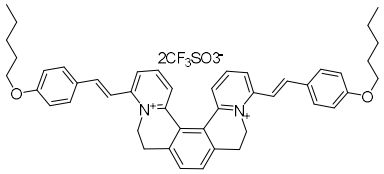 64	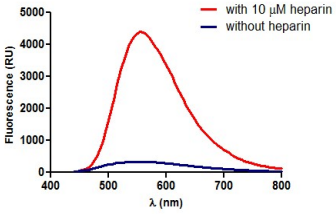	13.24
14.	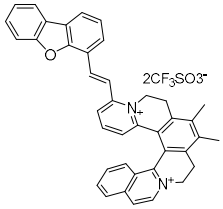 65	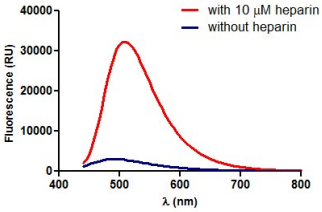	11.42
15.	 66	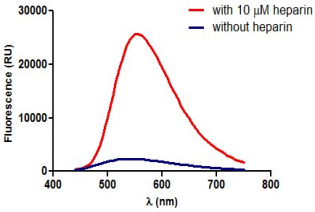	11.30
16.	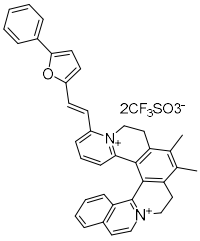 67	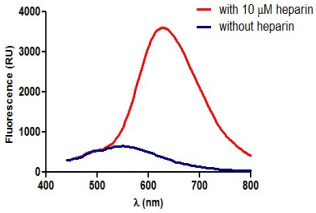	10.45
17.	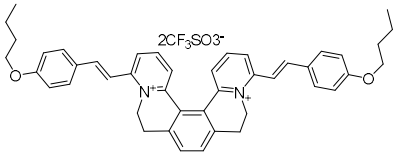 68	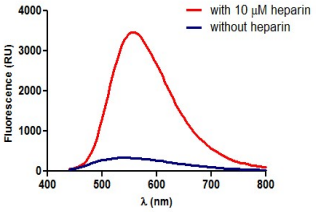	10.44
18.	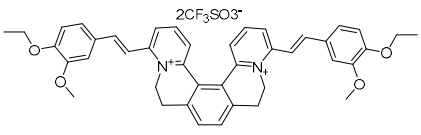 29	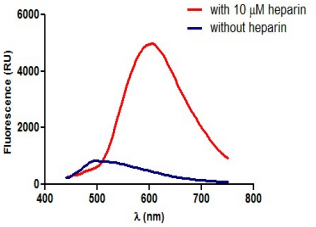	10.00

19.	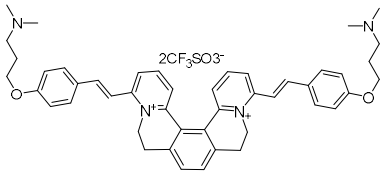 32	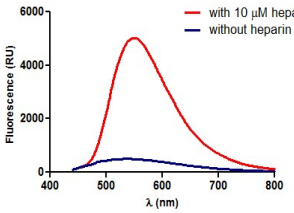	10.00
20.	 69	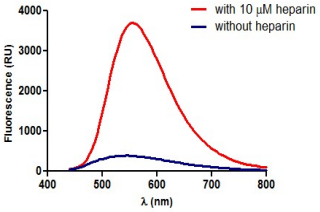	9.55
21.	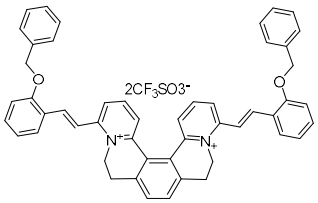 70	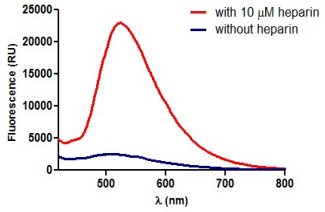	9.41
22.	 71	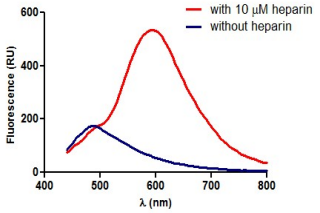	9.27
23.	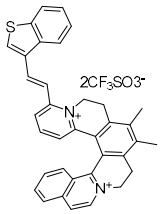 72	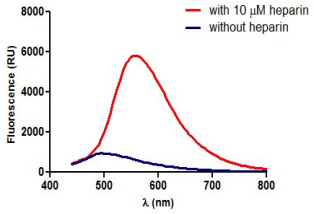	9.14
24.	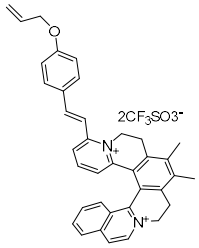 73	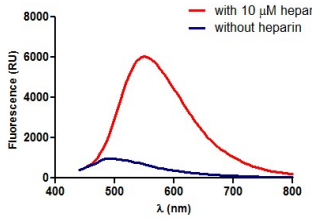	9.00

Table 11: *Hits arranged according to relative fluorescence intensity increase.*

The ideal chemosensors must interact with its target specifically, even in presence of other analytes. For this purpose, we carefully selected the analytes such as sulphated glycosaminoglycan (GAGs), which are structurally related to heparin, DNA, nucleotides, 20 % human serum, serum albumins, and many others. Out of 24 hits, two Compounds were identified to show selective fluorescence light up in presence of heparin over other analytes and accidentally found one of the hit, showing selective fluorescence light up in presence of

DNA. DNA binding properties and applications of DNA chemo-sensor obtained through the fluorescent library screening approach mentioned above were discussed in detail in the following section (Fig. 67).

In addition, few compounds show two times higher fluorescence light up in presence of chondroitin sulphate, which is another member of glycosaminoglycan family with a lot of structural similarity to heparin. In future, such compounds can be used as fluorescent probes for identification and quantification of chondroitin sulphate and oversulphated chondroitin sulphate, which are the commonly found impurities in the pharmaceutical formulations of heparin. Such a study is beyond the scope of this thesis due to some practical reasons.

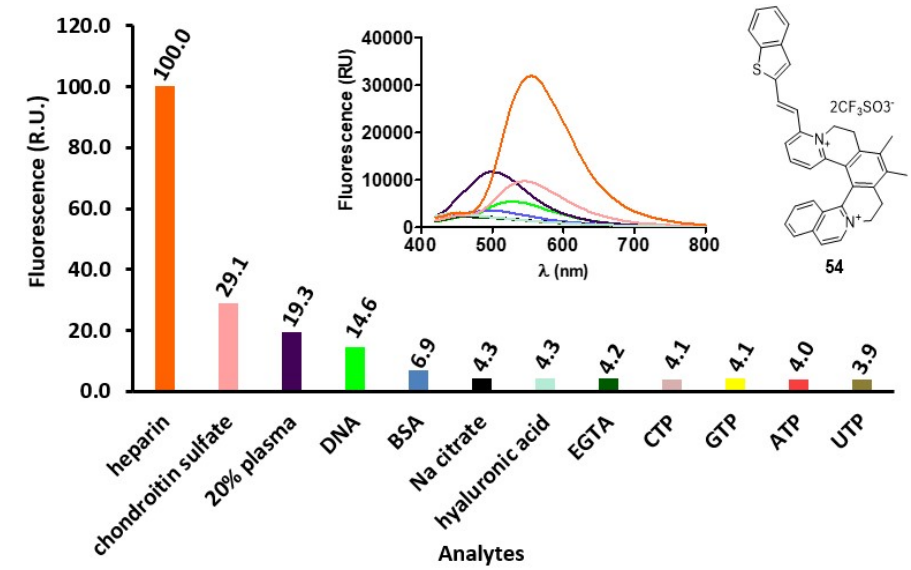

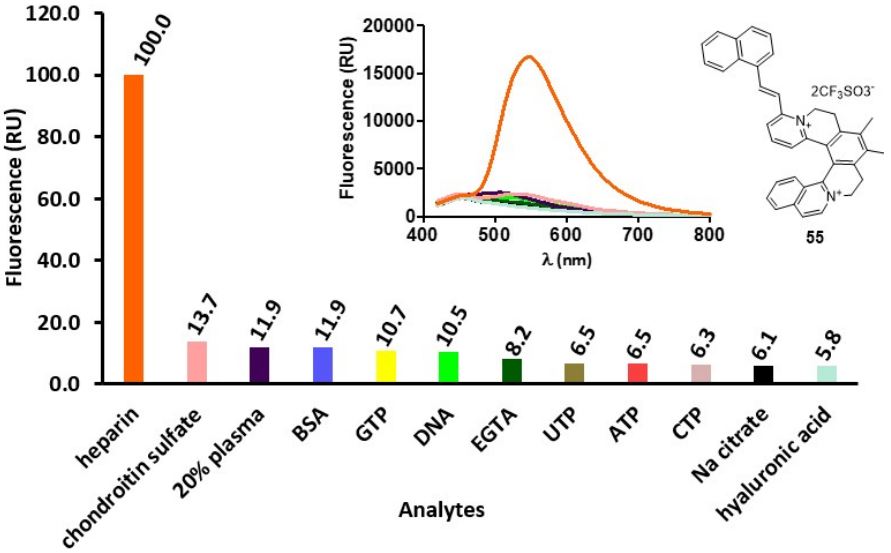

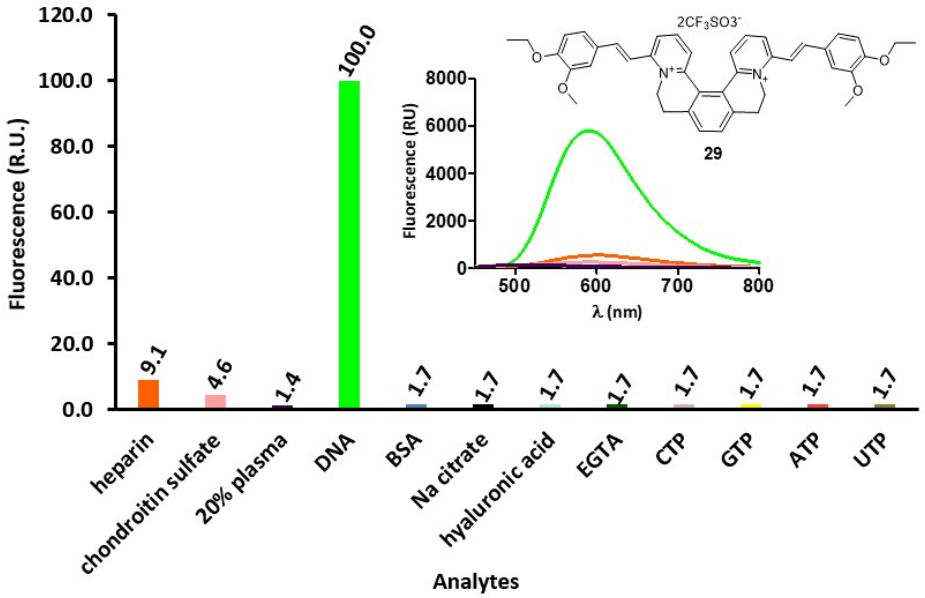

Fig. 67: *Selectivity charts of two heparin sensors,* ***54*** *and* ***55*** *and DNA sensor* ***29****.*

The next step in the assay development was to calibrate both heparin chemosensors *vs.* heparin concentrations in plasma or serum.

The plasma and serum are the complex mixtures of many components with the huge auto-fluorescence response, due to which it was quite difficult to recognize the small changes in fluorescence intensity due to the added amount of heparin. From initial calibration experiments, it was realized that, if the plasma/serum diluted, the autofluorescence could be reduced. For this reason, initially, we tested the various dilutions of the plasma and came to the conclusion with less than 20% of dilution of plasma as reported in other articles before,[163] we were able to develop the calibration with our fluorescent probes for detection of heparin present in plasma in the clinically relevant range.

In order to cope with this problem, we prepared the samples of plasma spiked with the actual concentrations observed in clinical range and then to prepare the calibration curve, with 10 times diluted samples. Therefore, the concentrations seen at calibration curves are lower by 10 times than actual. The calibration curves clearly show the potential of both probes in the quantification of UFH and LMWH in a clinical range in diluted plasma with the Lowest Limit of Detection (LOD) = 0.2 μM using both probes (Fig. 68A and 68B).

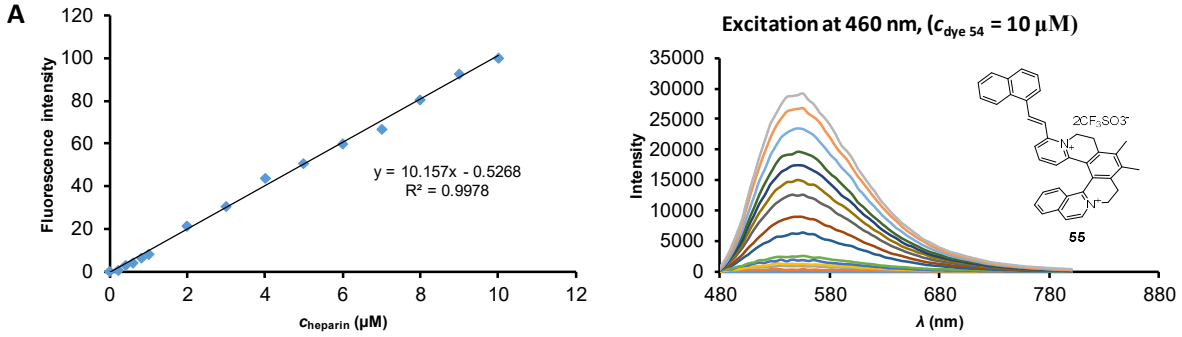

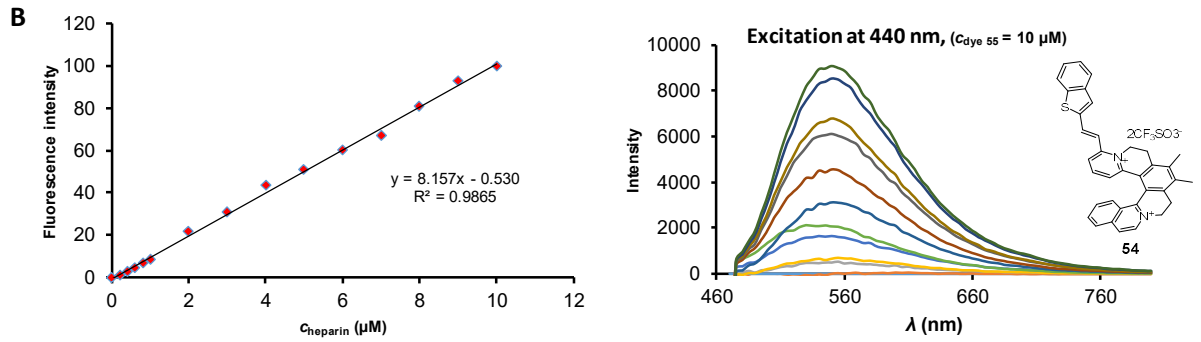

Fig. 68: *A) Calibration curve for chemosensors* ***54****; B) calibration curve for chemosensor* ***55*** *in clinically relevant concentrations of heparin.*

A small library of helquat and planar variants of two chemosensors were analyzed in search of other possible hits, but most of them show no fluorescence light up in presence as well as the absence of heparin or show nonselective fluorescence light up in presence and absence of heparin. All these results are summarized in Fig. 69.

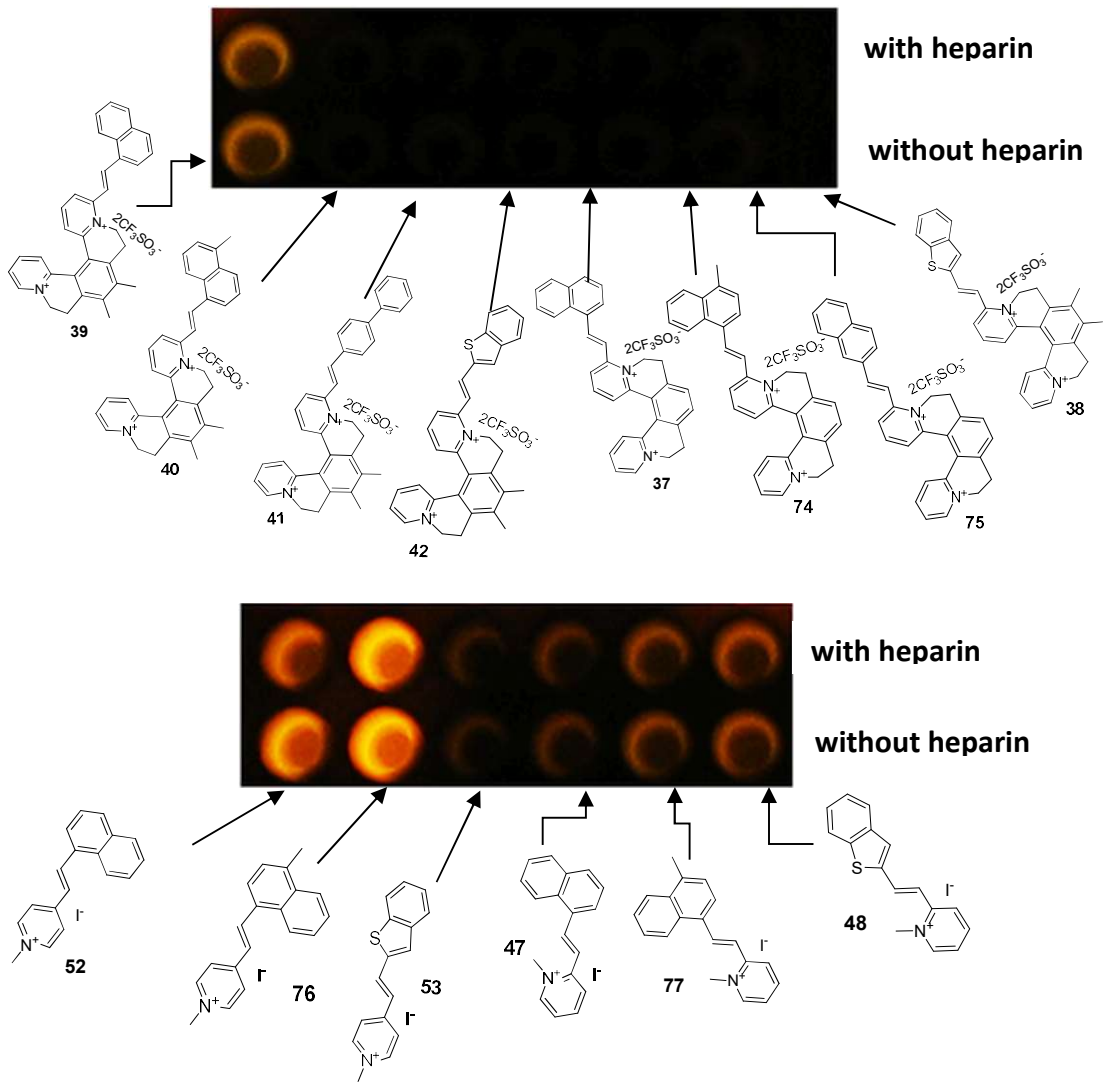

Fig. 69: *Structure Activity Relationship (SAR) study around the two chemosensor.*

We believe the molecular recognition properties of the helquat dyes with heparin are not purely due to the electrostatic interactions of the doubly positive helquat molecules and highly negative heparin molecules. Because if it would be so, the fluorescence light-up should have been observed in case of all the helquat dyes. Therefore, it needs to be inspected more deeply in collaboration with other research groups, which got expertize in the field.

Even though, at this moment, we were not able to go further with this project for actual quantification of heparin from the patient's plasma samples. However, we are in search for the research partners associated with medical hospitals, which can develop the method using our probes and can compare them with existing methods for heparin quantification.

- **Molecular Recognition: Sequence specific recognition of dsDNA, properties and applications:**

During the fluorescent library screening with various biological targets (Fig. 67), a helquat dye **29** was found. This compound was showing selective fluorescence light-up in presence of dsDNA (Fig. 70). When the quantitative fluorescence spectra of the dye in presence and absence of model DNA duplex was measured, the dye gave an emission spectra with huge increase in fluorescence intensity (λ_{max} = 590 nm) in presence of ds26 DNA, whereas very weak fluorescence response was obtained for dye alone (Fig. 73a, orange and black continuous lines respectively, for presence and absence of dsDNA). In UV-vis. absorption spectroscopy, red shifting of absorption maxima of the dye from 417 nm (unbound state) to 438 nm (in complex with dsDNA) was also observed. These two primary observations were sufficient to decide that, the dye was interacting with dsDNA. DNA binding properties of dye **29** were deeply studied using emission spectroscopy, UV-vis. spectroscopy, ECD spectroscopy, hydrodynamic study and computational methods. Due to the helical shape of the molecule, we named it as **HeliDye1**.

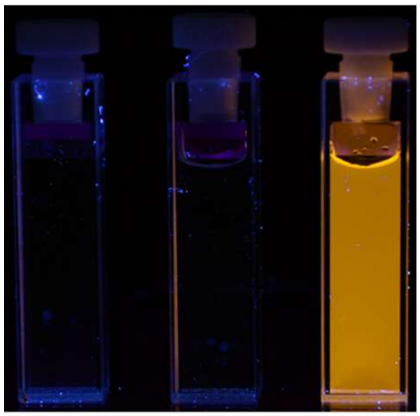

29 (HeliDye1)

Fig. 70: *Selective orange fluorescence light-up of* ***HeliDye1*** *(10 µM) in presence of ds26 (CAATCGGATCGAATTCGATCCGATTG) oligonucleotide (5 µM).*

The binding stoichiometry of **HeliDye1** : ds26 interaction was found to be in the range of 1:0.5 to 1:1. Therefore, in most of our future experiments, we used this ratio of dye : DNA as a basis.

The Structure Activity Relationship (SAR) study revealed an importance of bischromophoric helical structure with specific attachments of two alkoxy substituents, because on swapping

relative positions of ethoxy and methoxy substituents (dye **30**) or by replacing ethoxy substituent with methoxy substituent (dye **31**) the fluorescence light-up was completely lost (Fig. 71). In addition, monochromophoric helquat dyes were also inactive for fluorescence light-up in presence of dsDNA (dye **34**-**36**, Fig. 71). Planar variants of helical dyes (**44**-**46** and **49**-**51**) were completely nonselective for their light-up responses.

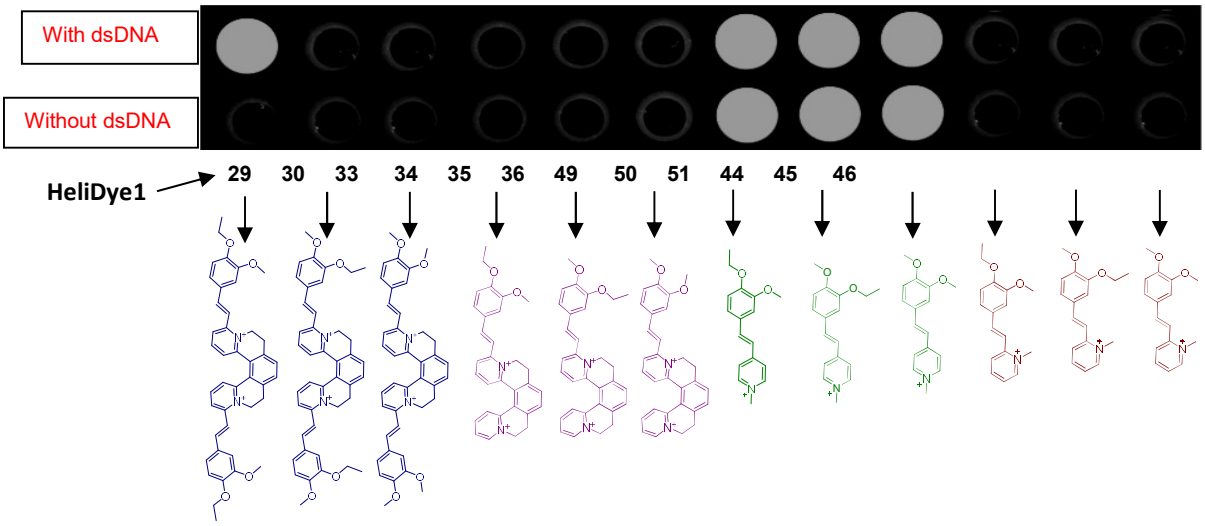

Fig. 71: *1st generation Structure Activity Relationship (SAR) study around the structure of* ***HeliDye1****.*

The fluorescence light up response of **HeliDye1** was selective towards AT-base pair containing dsDNA sequences. No fluorescence light-up was observed for **HeliDye1** alone or in presence of dsDNA lacking AT-pairs, ssDNA and total RNA (RNA isolated from cells, which may contain unknown sequences of single and double-stranded RNA templates) (Fig. 72).

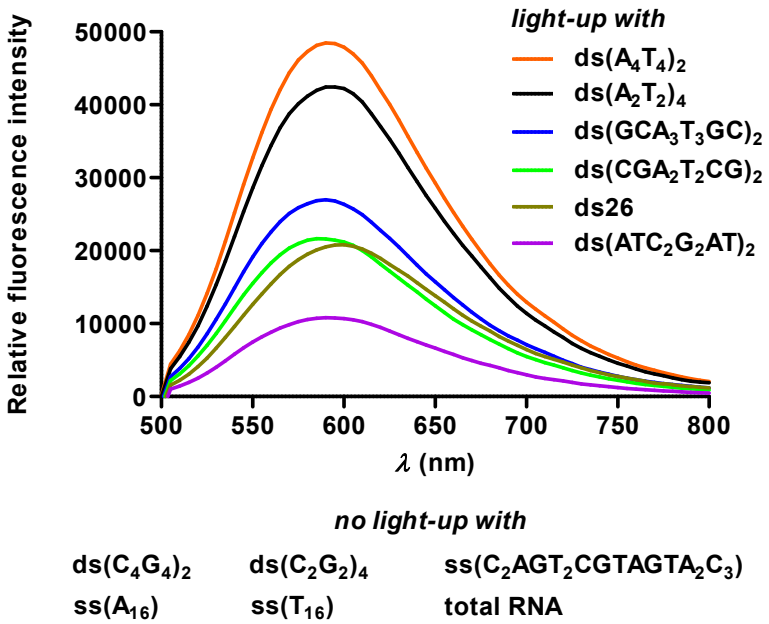

Fig. 72: *Selectivity of* ***HeliDye1*** *towards AT-rich dsDNA over GC-rich dsDNA sequences, ssDNA and RNA*

The dissociation constants of interactions between **HeliDye1** and various self-complementary and hairpin forming dsDNA sequences were determined by fluorescence titration method and are summarized in Table 12**.** An inverse relationship was observed

between the number of AT-pairs contained in the sequence and K_D value, indicating more tight binding with AT-rich dsDNA sequences.

	Sequence (5' - 3')	K_D (μM)	Number of AT pairs
	Part A: self-complementary dsDNA sequences		
1	ds(AAAATTTTAAAATTTT)	2.9 ± 0.04	8
2	ds(AATTAATTAATTAATT)	3.5 ± 0.20	8
3	ds(GCAAATTTGCGCAAATTTGC)	4.7 ± 0.20	6
4	ds(CGAATTCGCGAATTCG)	5.7 ± 0.20	4
5	ds(CGCGAATTCGCGCGCGAATTCGCG)	6.0 ± 0.10	4
6	ds(ATCCGGATATCCGGAT)	15.1± 0.10	4
	Part B: hairpin-forming dsDNA sequences		
7	ds(CAATCGGATCGAATTCGATCCGATTG)	5.9 ± 0.20	7
8	ds(GGCAAAAACGCGGTCCGCGTTTTTGCC)	9.7 ± 0.10	5
9	ds(GGCAAAACCGCGGTCCGCGGTTTTGCC)	11.2 ± 0.03	4
10	ds(GGCAAAGCCGCGGTCCGCGGCTTTGCC)	16.1 ± 0.20	3
11	ds(GGCAACGCCGCGGTCCGCGGCGTTGCC)	26.5 ± 0.30	2
12	ds(GGCAGCGCCGCGGTCCGCGGCGCTGCC)	48.2 ± 0.50	1

Table 12: *K_D values for interaction of dye **HeliDye1** with various DNA duplexes (c_{dsDNA} = 1 μM).*

The red shifting of absorption maxima was also found to be more sequences dependent and maximum shifting by 42 nm was observed in presence of ds$(A_4T_4)_2$ oligonucleotide sequence (Fig. 73C). Absorption and emission spectral changes of **HeliDye1** (10 μM) with (w) and without (w/o) different oligonucleotide sequences (5 μM) are shown in Fig. 73 and spectral properties are summarized in Table 13. The fluorescence quantum yield of **HeliDye1** in presence of various dsDNA sequences was determined using Coumarin 153 as a standard.[186]

	λ_{abs} (nm)	λ_{em} (nm)	φ^a	ϵ (l.mol^{-1}cm^{-1})
w ds26	438	590	0.010 ± 0.004	19534
w ds$(GCA_3T_3GC)_2$	435	590	0.016 ± 0.004	20578
w ds$(A_4T_4)_2$	458	590	0.030 ± 0.004	20471
w/o dsDNA	417	-	-	22921

Table 13: *Spectroscopic properties of **HeliDye1** in presence and absence of different dsDNA oligonucleotides at dye : DNA ratio 2:1 ($c_{HeliDye1}$ = 10 μM and c_{dsDNA} = 5 μM)*

[a] Coumarin 153 was used as the reference for quantum yield.[186]

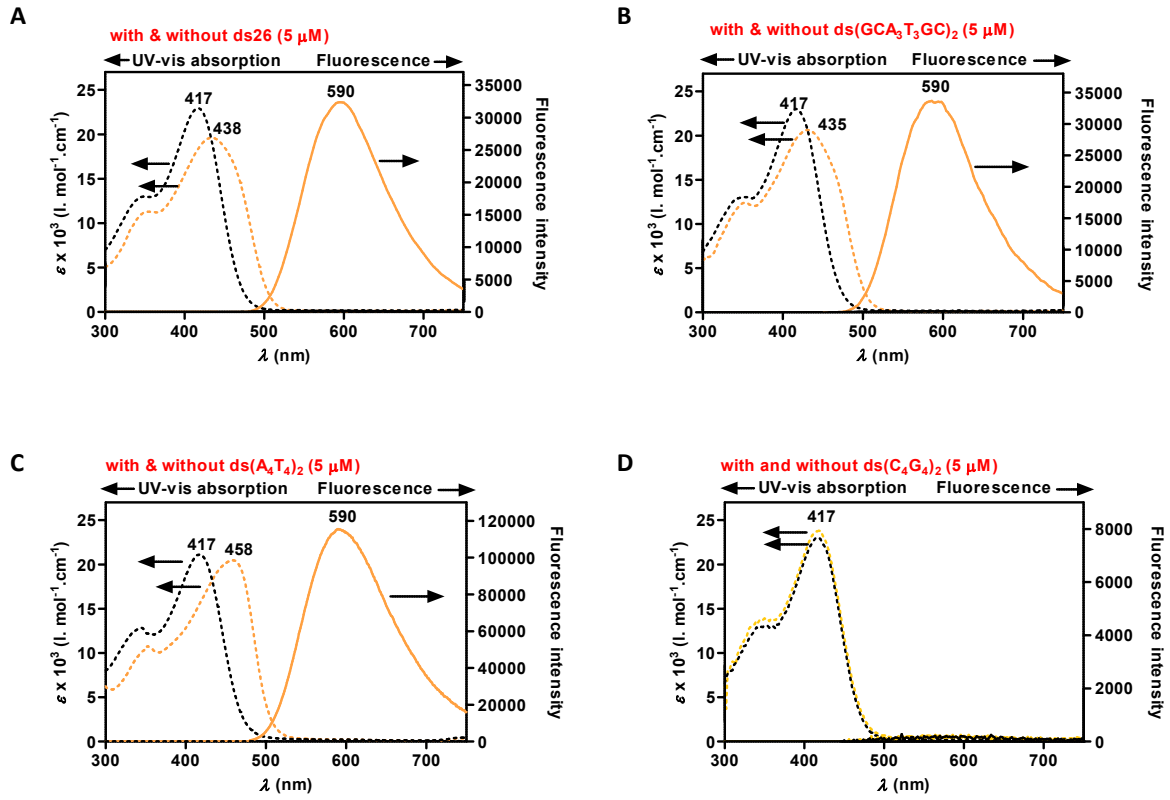

Fig. 73: *UV-Vis. absorption (left) and emission (right) spectra of* ***HeliDye1*** *(10 µM) in presence (orange line) and absence (black line) of A ds26; B ds(GCA₃T₃GC)₂; C ds(A₄T₄)₂ and D ds(C₄G₄)₂ oligonucleotides (5 µM).*

For the practical applicability of the probe, the sequence specificity of **HeliDye1** was compared with three established DNA probes, **propidium iodide (PI)**, **Hoechst-33258** and **DAPI** in a fluorescence light-up assay (Fig. 74A). Quantitative fluorescence spectra of all three probes at their respective excitation wavelengths[187] were measured in presence and absence of ds$(A_4T_4)_2$, ds$(C_4G_4)_2$, ssDNA, ssRNA, dsRNA as analytes. This experiment has proven the high specificity of **HeliDye1** as compared to **PI** and **Hoechst 33258** (Fig. 74A and B). The specificity of DAPI was also high as compared to remaining two probes, but it was showing week fluorescence response with RNA, in this respect **HeliDye1** is superior over **DAPI**.

A

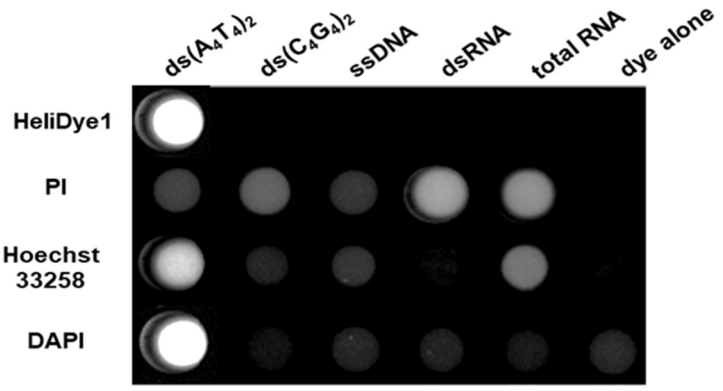

B

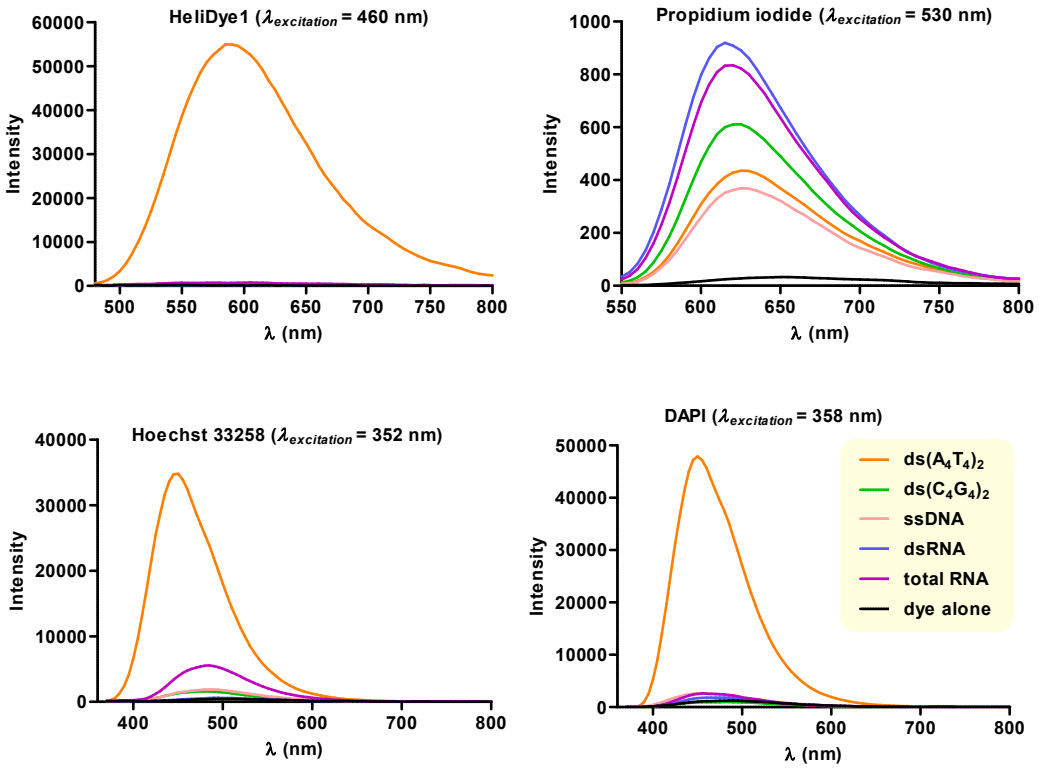

Fig. 74: *A) Picture of the well plate showing comparison in fluorescence light-up of* ***HeliDye*** *with established probes (irradiation at 365 nm UV light); B) Quantitative fluorescence spectra of* ***HeliDye1*** *and all three established probes in presence and absence of analytes at dye:DNA ratio 2:1 (c_{dye} = 10 μM and c_{dsDNA} = 5 μM).*
Note: ssDNA: ss($C_2AGT_2CGTAGTA_2C_3$); dsRNA: ds($CA_2UCG_2AUCGA_2U_2CGAUC_2GAU_2G$); total RNA: RNA isolated from cells using standard RNA isolation kit.[188]

In addition, the ability of **HeliDye1** to detect DNA duplexes bands of only specific sequences was compared with **GelRed™** stain in nondenaturing gel electrophoresis (Fig. 75).

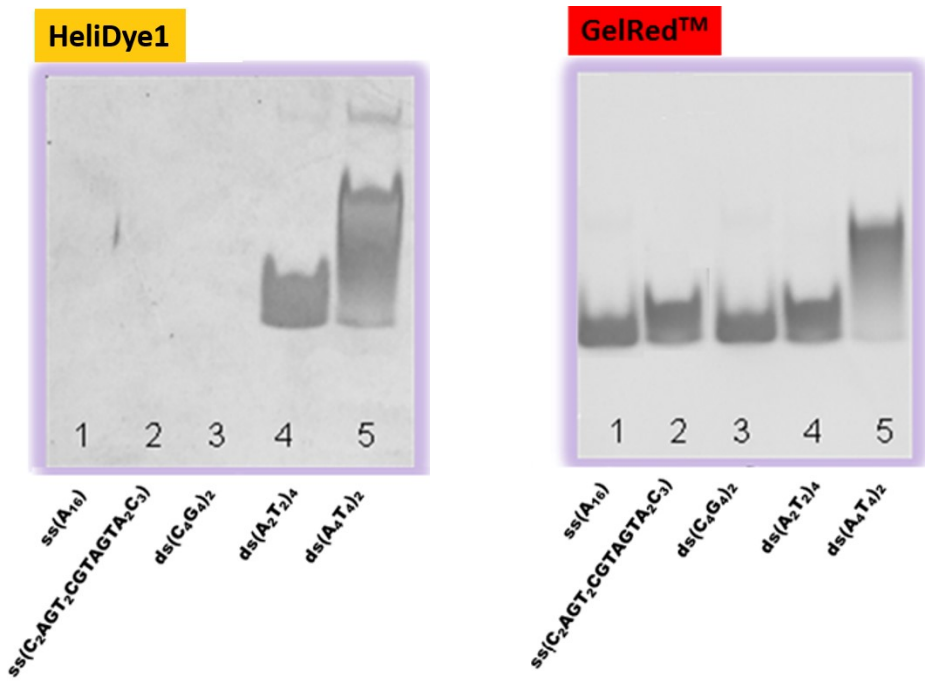

Fig. 75: *Selective staining of nucleic acid bands with* ***HeliDye1*** *(1 μM) in comparison with* ***GelRed™****.*

Electronic Circular Dichroism (ECD) spectroscopy is a technique used to study the interactions of small molecule ligands with biological targets such as proteins and nucleic acids. From our previous study, we knew that symmetrical **HeliDye1** undergoes rapid helix inversion in solution at a rate of 31 s^{-1}. Therefore, it exists as a racemate and gives no net signal in ECD spectroscopy. We measured the experimental ECD spectra of **HeliDye1** alone (10 μM), the dye : DNA complex ($c_{\mathbf{HeliDye1}}$ = 10 μM and c_{dsDNA} = 5 μM) and ds26 (5 μM) alone (Fig. 76A). (see Table 13, entry 7 for ds26 sequence). As expected, no ECD spectrum was obtained from **HeliDye1** solution in absence of DNA (magenta line). **HeliDye1** : dsDNA complex (2:1) solution gave intense induced bisignate ECD signal positioned in the visible spectral region (orange line). As DNA has no spectral contribution to ECD signal above 300 nm (blue line), the ECD bands in the visible region can be attributed exclusively to the **HeliDye1**. In order to see which enantiomer of **HeliDye1** was preferentially interacting with DNA, we computed the ECD spectra of *M*-enantiomer using DFT calculations (Fig. 76B, using BMK functional[189] with 6-31+G* basis set.[181]). By its correlation with experimental spectra, we were able to conclude that *M*-enantiomer of **HeliDye1** was preferentially interacting at this particular dye : DNA ratio.

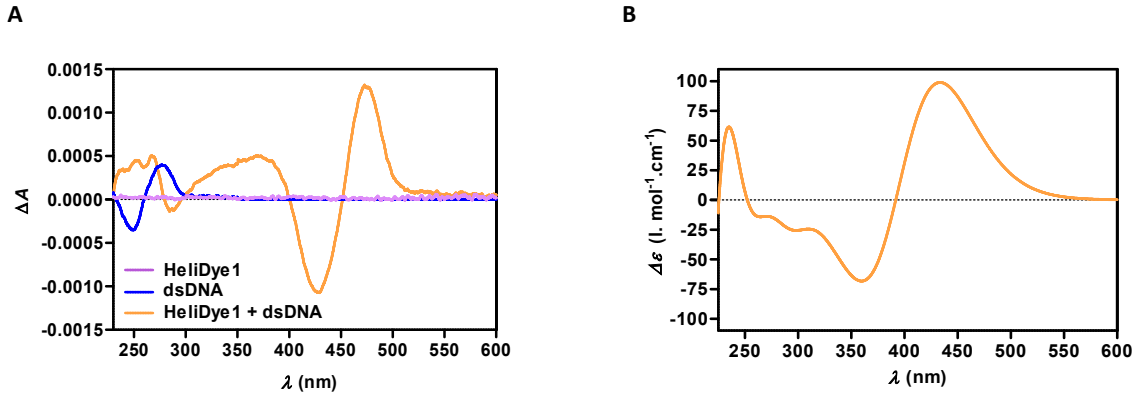

Fig. 76: *Comparison of A) experimental and B) simulated ECD spectra of* ***HeliDye1****.*

In order to study the binding mode in more details, we performed an ECD titration experiment with increasing concentrations of ds26 DNA (from 0 to 400 μM) at fixed concentration of **HeliDye1** (10 μM) (Fig. 77A) as per the previous report from Chaires *et al.*[190] Within all concentrations, the ds26 DNA existed in its most naturally abundant form (B-DNA, right-handed helix) as proven by inspecting UV region of the ECD spectra, where the ECD bands appeared with increasing DNA concentration (Fig. 77B). Therefore ECD spectral changes in the visible region should be explained only by ligand reconfiguration. From dye : DNA ratio 1:0.5 to 1:10, we could observe a decrease of ECD signal, which could be attributed possibly to the change in **HeliDye1** configuration (*M* → *P*) at higher DNA concentration, thus indicating binding of both enantiomers at two different dye : DNA ratios. At extreme ratios (> 1:20), a transition in the ECD spectral behaviour of the **HeliDye1** : DNA complex occurred. The bisignate nature of induced ECD spectrum with a positive band centered at 472 nm was transformed into a monosignate ECD negative band centered at 443 nm. Some other effects accompanied by a transition from *M* → *P* Configuration of **HeliDye1** must be responsible for such a behaviour, which we need to study more deeply.

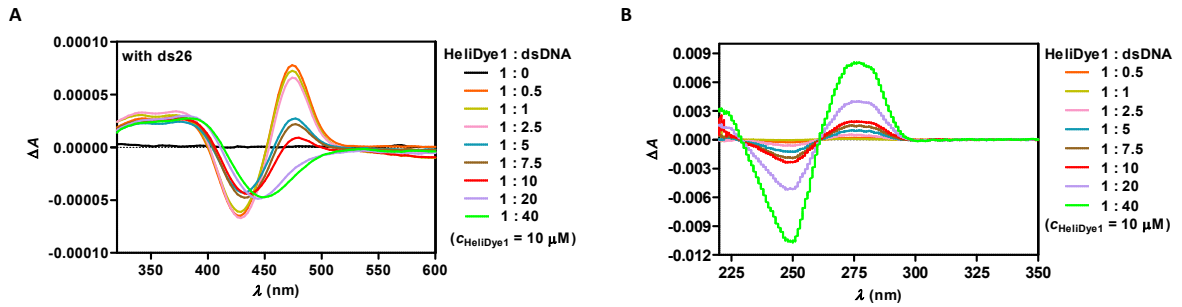

Fig. 77: *ECD titration of HeliDye1 (10 µM) with increasing concentrations of ds26 DNA (0-400 µM) in BPES buffer, A) ECD spectral region of* ***HeliDye1****,showing differential spectral behavior of P and M-enantiomers of* ***HeliDye1*** *at two extreme concentrations of ds26; B) ECD spectral region of ds26DNA, showing no conformational change in the structure of ds26 DNA.*

The consistent ECD spectral behaviour of **HeliDye1** was also observed in ECD titration experiments with different dsDNA oligonucleotide sequences. (Fig. 78A and B).

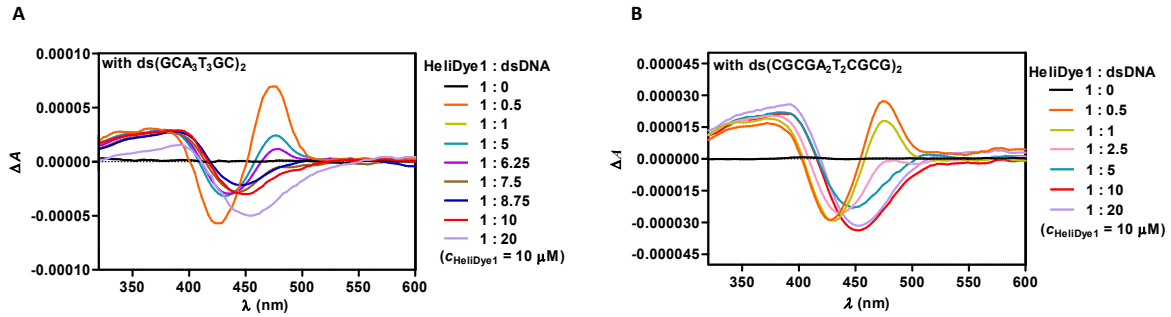

Fig. 78: *ECD titration of* ***HeliDye1*** *(10 µM) with increasing concentrations (0-200 µM) of A) ds(GCA3T3GC)2 and B) titration with ds(CGCGA2T2CGCG)2 DNA.*

Hydrodynamic study (viscosity measurement) is a classical experiment described for proposing a mode of interaction of DNA binding molecules to DNA. The Previous study reported that the viscosity of DNA solutions in complex with classical intercalator ethidium bromide increases if the concentration of ethidium was increased keeping the DNA concentration constant.[191a] It is also known that intercalators disturbs the native conformation of DNA causing lengthening of the DNA strand in the longitudinal direction, which eventually leads to an increase in the viscosity of the DNA solution. Minor groove binders, as they do not disturb the native conformation of DNA and thus have the negligible effect of their increasing concentrations on the viscosity of the DNA solutions.[191]

Effects of increasing **HeliDye1**, **PI** and **DAPI** concentrations (0-200 µM) in a set of dye : DNA complex solutions (individual set of solutions for each dye) containing 100 µM BP (base pair molarity) of calf-thymus DNA (ctDNA) were studied.

As compared to **PI**, **HeliDye** and **DAPI** affected very less the viscosity of DNA solutions with their increasing concentrations (Fig. 79). This experiment is suggesting no intercalative binding of **HeliDye1** similar to **PI**, but indicating the possibility of similar minor groove binding to that of **DAPI**.

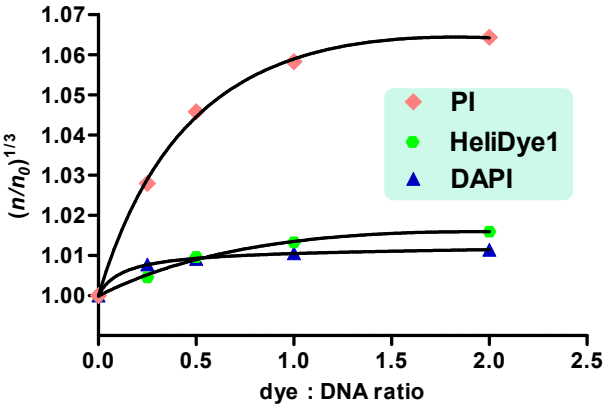

Fig. 79: *Viscosity measurements of DNA duplex (ctDNA, 100 μM BP) solution containing increasing concentrations of* ***HeliDye1****, propidium iodide (****PI****) and* ***DAPI*** *(0-200 μM).*

As the ECD titration experiments discussed above (Fig. 77) suggesting differential binding of *M* and *P*-enantiomers at different dye : dsDNA ratios, molecular docking of optimized structures of both enantiomers of **HeliDye1** with model DNA duplex ds$(GCA_3T_3GC)_2$ gave more insight into the possible mode of binding. Both intercalation and groove binding possibilities were inspected. Molecular docking was carried out to obtain potential ligand binding poses using AutoDock Vina, version 1.1.2.[192] The intercalation possibility was studied in a model where an intercalation site was formed between A5-T6, by doubling the step-to-step distance (from 3.4 to 6.8 Å) and optimization of the phosphate backbone.

The experimental results and the computational results can be correlated with each other in this way and explained with the help of Fig. 80A – D:
a) Most of the docking solutions, obtained in case of intercalation model were found to be clustered into the intercalation site, with the *M*-enantiomer of the dye was positioned in the center of the intercalation site (Fig. 80A) and the *P*-enantiomer was found to be slightly shifted to the side of the intercalation site (Fig. 80B). However, no classical intercalation was observed. Further, in molecular dynamics, this artificially created intercalation site disappeared and proposed model A and B was converted to model C and D respectively, suggesting no such binding possible.

b) In case of the model expected to check the possibility of groove binding, all obtained docking posses were clustured into the minor groove, showing a strong preference for the minor groove binding. The *M*-enantiomer of the dye fitted snugly into the groove (Fig. 80C), whereas half of the *P*-enantiomer was fitted into the groove and half of the molecule was protruded into the solvent (Fig. 80D).

The hydrodynamic behaviour and AT-sequence specificity of **HeliDye1,** similar to the known DNA minor groove binding dye DAPI opposed to known intercalator dye propidium iodide (PI) is in agreement with minor groove binding of **HeliDye1**.

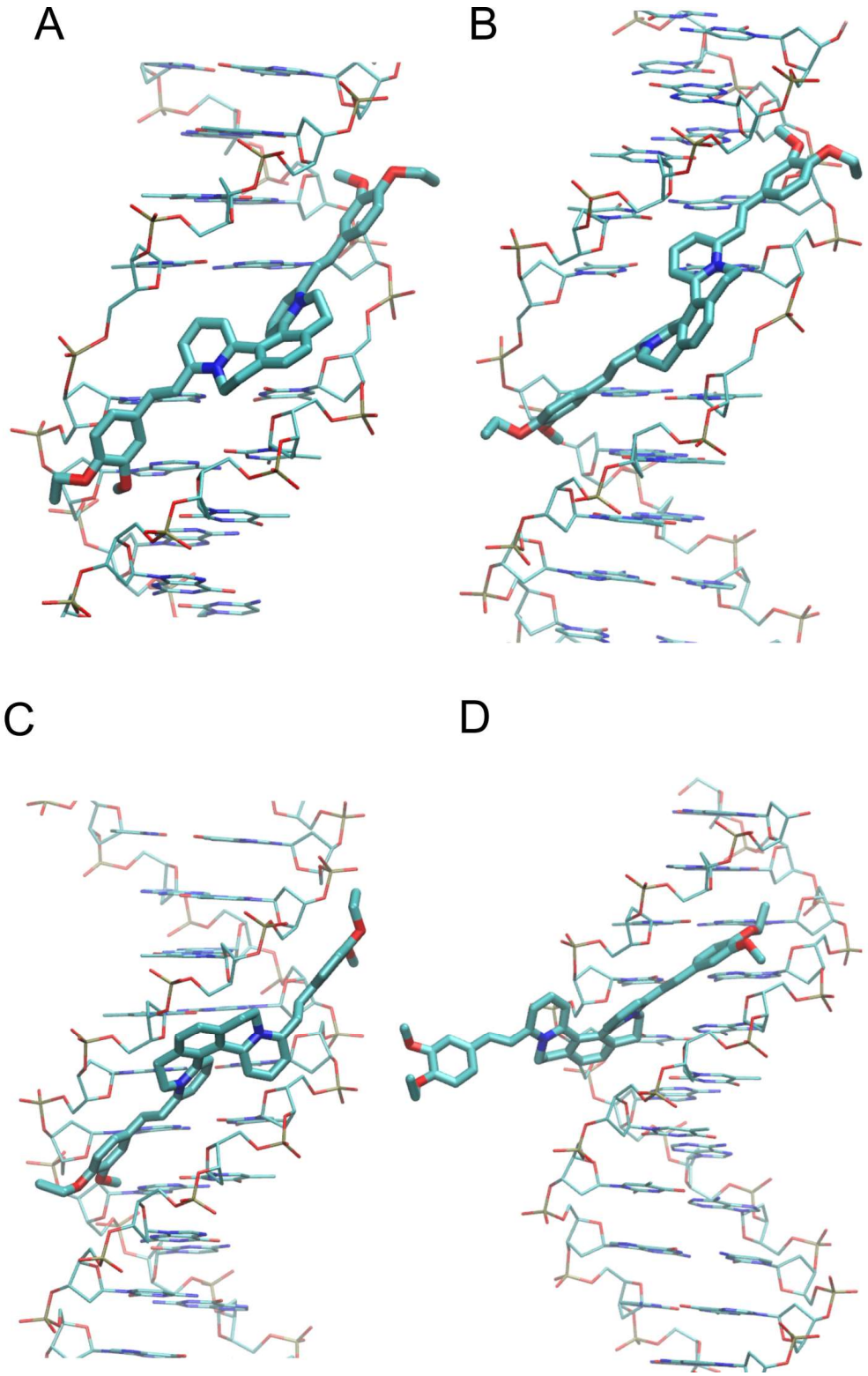

Fig. 80: *Representative binding modes of* ***HeliDye1*** *(in sticks) in AT-rich dsDNA structure as obtained from molecular docking. Panels A and C: M-enantiomer of* ***HeliDye1****. Panels B and D: P- enantiomer of* ***HeliDye1****. Panels A, B: intercalation model. Panels C, D: groove binding model. Color-coding cyan – carbon, red – oxygen, blue – nitrogen, and gold – phosphorus. Figure prepared with VMD, version 1.9.3.*[193]

Based on docking solutions, new helical dyes containing following two types of modifications in the structure of HeliDye1 were done and a short library of new helquat dyes was synthesized and tested for their DNA binding fluorescence light-up properties.

A) Modification in styryl part, while keeping helquat part intact (**78**-**80**, Fig. 81).

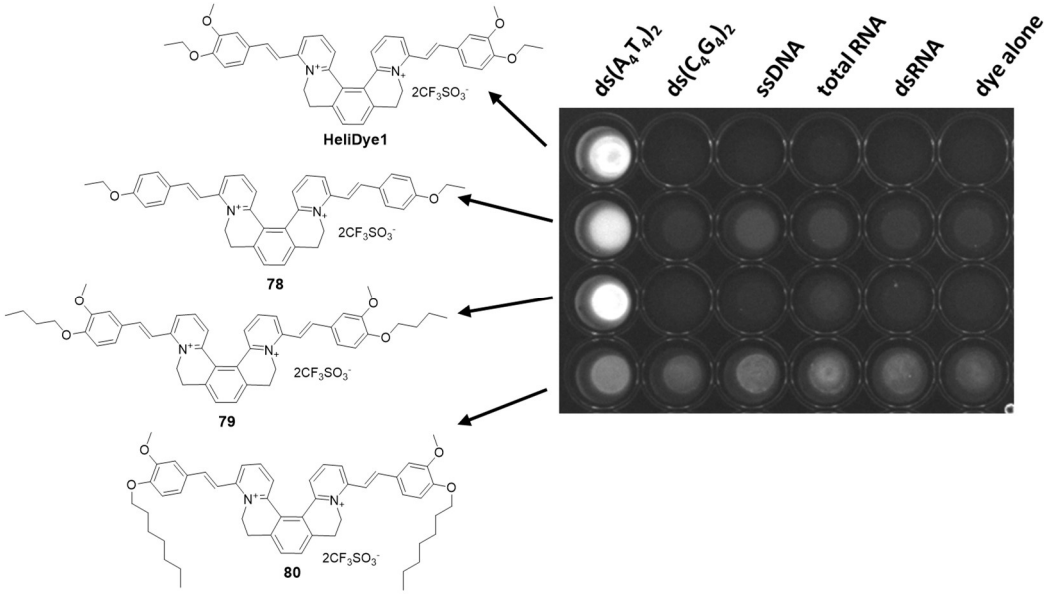

Fig. 81: *SAR study with molecules containing modifications in styryl chromophore.*

B) Helquat dyes **86**-**90** originating from various helquat cores **81**–**85**, with no modifications in styryl chromophore were synthesized (Fig. 82).

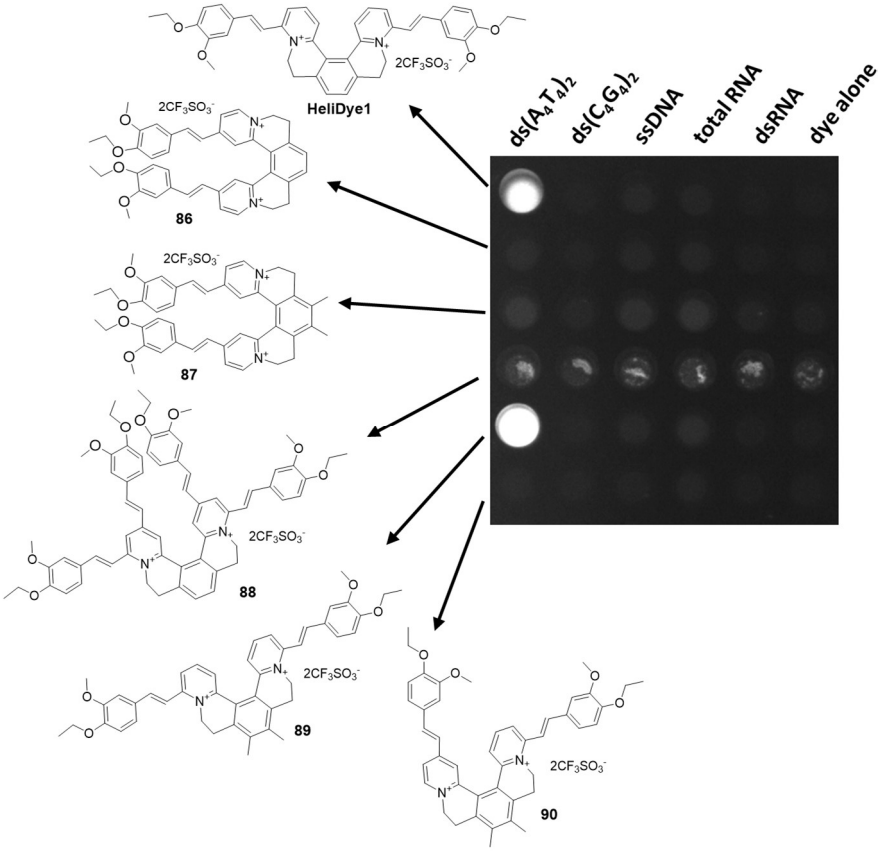

Fig. 82: *SAR study with molecules containing modifications in helical structure.*

All these modifications were screened for their performance in fluorescence light-up assay with various nucleic acid sequences. Modifications in styryl part (Fig. 81) were somehow showing similar AT-selectivity either by removing one of the methoxy substituent from the styryl chromophore (dye **78**) or by increasing the length of alkoxy chain of one of the

substituents from ethoxy to *n*-butyloxy (dye **79**), but the selectivity was completely lost in case of compound **80**, which contains *n*-heptyloxy modification in the styryl part (Fig. 81). In addition, it is important to mention that the solubility in an aqeous buffer was also getting worse with increasing the length of alkoxy side chain. Therefore, we decided to keep the basic chromophore of **HeliDye1** intact and keep our focus towards modifications in helquat cores (Fig. 82). All these helquat cores were ready in our group, which were attached with the basic styryl chromophore from **HeliDye1** through a Knoevenagel condensation reaction. However, out of all these modifications, only small modification in helquat core such as in dye **89**, in which helquat core was modified by the addition of two methyl substituents to the central aromatic ring (Fig. 82). This derivative showed strong fluorogenic response comparable to **HeliDye1** as well as similar selectivity for AT-rich dsDNA sequence. The compound **89** exhibited 2.7 times increase in fluorescence quantum yield after binding to AT-rich DNA, in comparison to **HeliDye1** (Table 14). The K_D value of interaction of dye **89** with ds(A_4T_4) was also comparable with **HeliDye1** (Table 14, last column).

In order to prove our hypothesis of chiral recognition of dsDNA target by helquat dyes, 3rd generation SAR study was performed, by synthesizing new helical dyes, in which the same styryl chromophore was present and size of ring 2 and 4 of [5]helquat skeleton was increased from six to seven carbon atoms (Fig. 83). Due to these changes, the molecule gets conformational stability[8] and two enantiomers of the new compound were obtained with *ee* > 95% (by capillary electrophoresis).

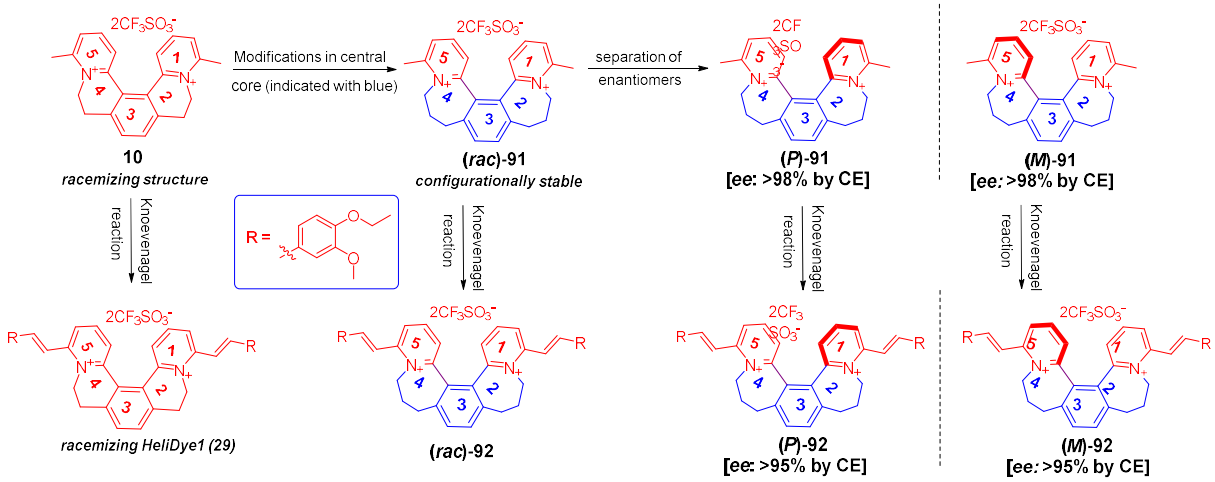

Fig. 83: *Structural modifications to the helical core of* ***HeliDye1*** *to obtain confirmationally stable helquats.*

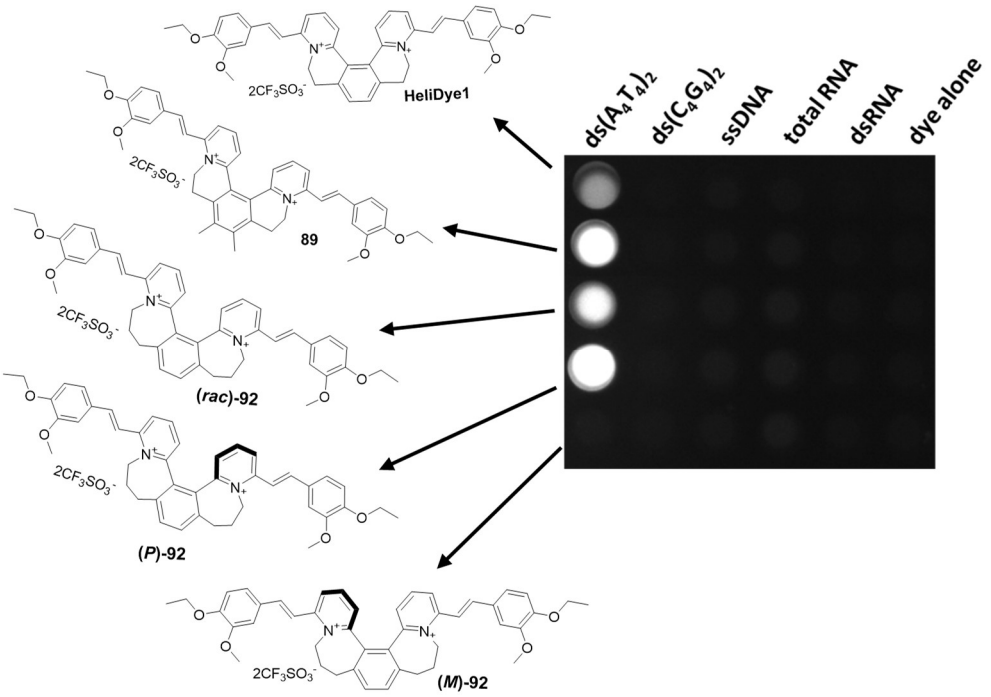

Fig. 84: *3rd generation SAR study stronger fluorescence light-up with* ***(P)-92*** *than* ***HeliDye1, 89*** *and* ***(rac)-92.*** *No fluorescence light-up of* ***(M)-92*** *with any of the analyte.*

Based on the fluorescence light-up experiment (Fig. 84), chiral recognition by *P*-enantiomer of dye **92** was observed, whereas the *M*-enantiomer, showing no fluorescence light-up in presence of any of the analyte included in the experiment.

Even though obtained results with enantiopure helquat dye **92** are contradictory to those obtained in case of **HeliDye1**, they are in strong favour of one of the hypotheses given at the beginning of this thesis, that novel specificities will be expected by the interaction of the molecules of this class with the cavities/ grooves of biological targets.

Compound	$ds(A_4T_4)_2$	λ_{abs} (nm)	λ_{em} (nm)	φ	ϵ ($l.mol^{-1}cm^{-1}$)	K_D (μM)
HeliDye1	**w**	458	590	0.030 ± 0.004	20471	2.9 ± 0.12
	w/o	417	-	-	21127	
89	**w**	455	575	0.081 ± 0.004	19220	3.2 ± 0.10
	w/o	420	-	-	21790	
(*rac*)-92	**w**	420	555	0.055 ± 0.004	19820	5.3 ± 0.10
	w/o	410	-	-	22580	
(*P*)-92	**w**	440	555	0.13 ± 0.004	21620	2.0 ± 0.10
	w/o	410	-	-	22140	
(*M*)-92	**w**	410	555	-	22330	-
	w/o	410	-	-	22970	

Table 14: *Comparison between spectroscopic properties of* ***HeliDye1****, dye* ***89****,* ***(rac)-92****,* ***(P)-92****) and* ***(M)-92*** *(all probes 10 μM) in interaction with (w) and without (w/o) $ds(A_4T_4)_2$ (5 μM). Last column with K_D (in μM) for the interaction of all these chemical modifications with $ds(A_4T_4)_2$ (1 μM), obtained by fluorescence titration.*

Currently, we are investigating in detail the possible mode of binding of dye **89** and **92** (in its *racemic* and enantiomeric form) as well other biological properties and the study will be performed, which can be considered as an outlook of the work reported in this thesis.

DNA duplex binding fluorescent molecules are useful as probes for microscopy and cell cytometry applications. Our initial microscopy experiments (Fig. 85) with **HeliDye1** (10 µM) revealed that dead cells are stained selectively leaving live cells unstained. Colocalization with GelRed™ (1:10000 as per the protocol from the supplier), an established dead cell probe, confirmed this staining pattern (Fig. 86). In addition, dot plots from flow cytometry with HGC-27 cells stained with **HeliDye1** allow to differentiate a population of dead cells that have high fluorescence as compared to a population of live cells (Fig. 86). These flow cytometry data were consistent with our findings from microscopy and thus further demonstrate the usefulness of **HeliDye1** for live/dead cell exclusion experiments.

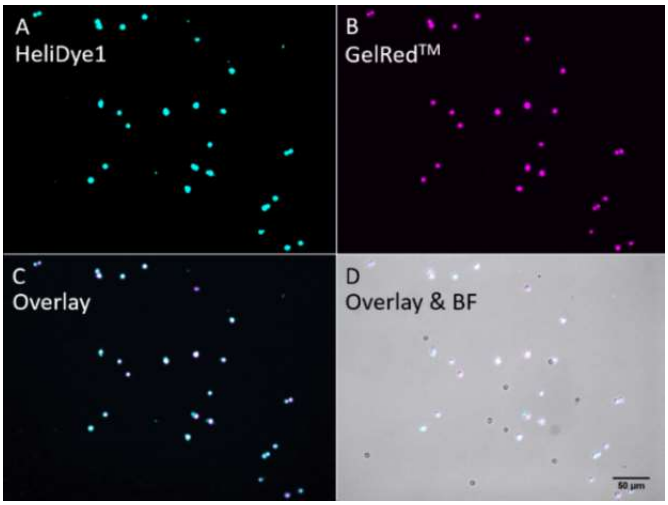

Fig. 85: *Selective staining of dead cells over live cells with* ***HeliDye1*** *(10 µM). HGC-27 cells co-stained with* ***HeliDye1*** *and* ***GelRed™****. Panel A:* ***HeliDye1*** *fluorescence channel. Panel B:* ***GelRed™*** *channel. Panel C: Overlay image obtained from* ***GelRed™*** *and* ***HeliDye1*** *fluorescence channels showing co-localization of bright spots corresponding to dead cells. Panel D: Combination of bright field (BF) image and overlay of two fluorescence channels A and B. Bright spots correspond to dead cells and dark spots to live cells.*

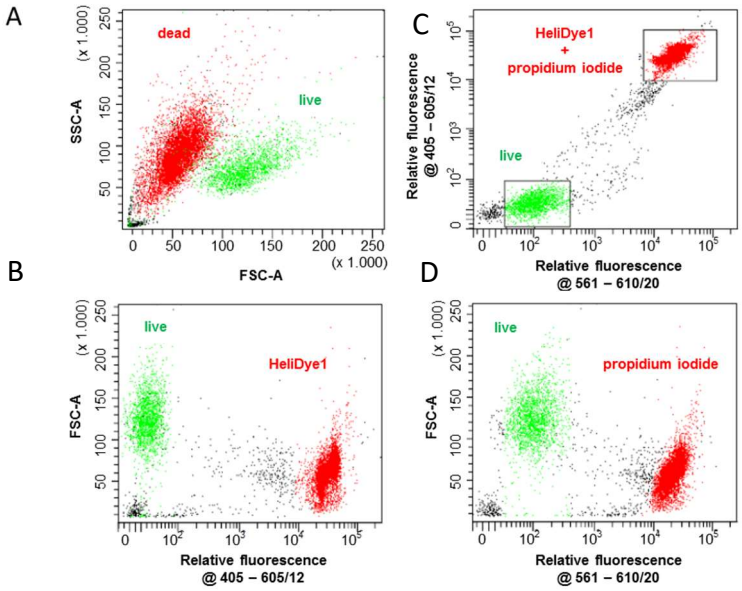

Fig. 86: *Fluorescence Activated Cell Sorting of live and dead cells (HGC-27), by* ***HeliDye1*** *(10 µM) in comparison with* ***PI*** *(1.5 µM).*

In confocal microscopy of U2OS cells (fixed cells), selective nuclei staining was observed at 1 µM concentration of **HeliDye1**. Colocalization study with **DAPI** (1 µM), confirms the selective nuclei staining (Fig. 87).

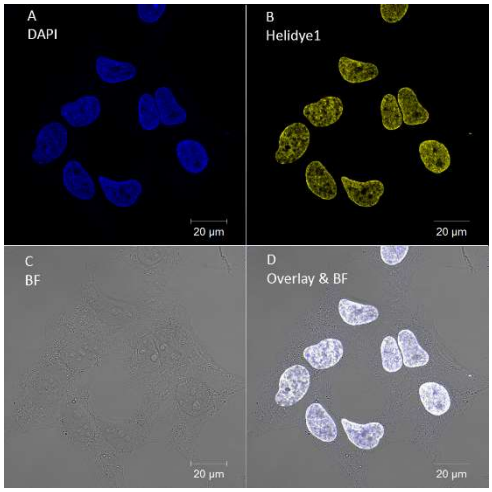

Fig. 87: *Selective nuclei staining in fixed U2OS cells using* ***HeliDye1*** *(1 µM) in colocalization with DAPI (1 µM).*

Propidium iodide (**PI**) is widely used stain for DNA quantification in flow cytometry. As it was seen that, the selectivity of **HeliDye1** towards DNA was higher than for RNA as compared to PI (Fig. 74), the use of **HeliDye1** could be advantageous for cell cycle analysis. Due to this feature of **HeliDye1**, we were able to avoid the RNase treatment completely, which is typically required in case of **PI** in order to have nice cell cycle analysis. The results are presented in Fig. 88.

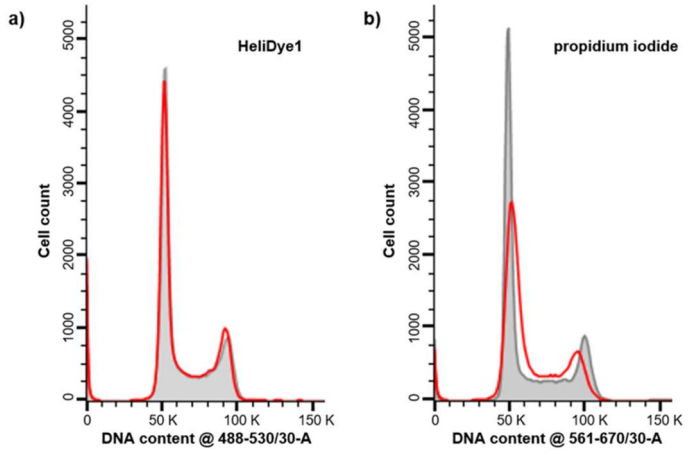

Fig. 88: *Cell cycles of HeLa cells analyzed using a)* ***HeliDye1*** *(10 µM); b)* ***PI*** *(1.5 µM). Brown histogram was obtained by standard RNase treatment prior staining with both probes. Red histogram was obtained without any RNase treatment.*

If the cell cycle analysis using **PI** was two times worse in absence of RNase treatment (Coefficient of Variation, CV value was almost double in absence of RNase treatment). Whereas, in case of cell cycle analysis using **HeliDye1**, which was mostly unaffected, even in presence and absence of RNase treatment (CV value was almost comparable).

Treatment /Cell cycle phases	G1	S2	G2/ M	G1 CV
HeliDye1 w/o RNase	43	31.1	13.4	5.5
HeliDye1 w RNase	43.9	31.2	12.3	5.7
PI w/o RNase	47	31	12.8	10.2
PI w RNase	44.7	32	12.8	5.21

Table 15: *Cell cycle analysis using HeliDye1 (10 µM) and PI (1.5 µM) as staining reagents with (w) and without (w/o) RNase treatment.*

HeliDye1 was evaluated for cytotoxic activity *in vitro* against a panel of human cancer and two non-tumour fibroblasts cell lines by using the standard 3-day MTS test. The cancer cell lines were derived from acute T-lymphoblastic leukemia CCRF-CEM, chronic myeloid leukemia K562 and their multidrug-resistant counterparts (CEM-DNR, K562-TAX) expressing the LRP and P-glycoprotein (P-gp) transporter proteins involved in tumour resistance, respectively. Additionally, solid tumour cell lines, including lung (A549) and colon (HCT116, HCT116p53-/-) adenocarcinomas, an osteosarcoma cell line (U2OS), and for comparison, two human non-cancer fibroblasts (BJ, MRC-5) and one endothelial (HUVEC) cell lines were included in the study. Importantly, **HeliDye1** showed very low cytotoxicity activity (IC_{50} > 50 µM) with all tested cell lines. Showing usefulness of the probe for most of the cell-based assays.

4. Conclusions:

Following aims of this thesis were fulfilled:

A. Helquats **6, 10, 14,** and **16** containing activated methyl groups next to quaternary nitrogen centers were successfully synthesized in multi-gram scale (Fig. 89).

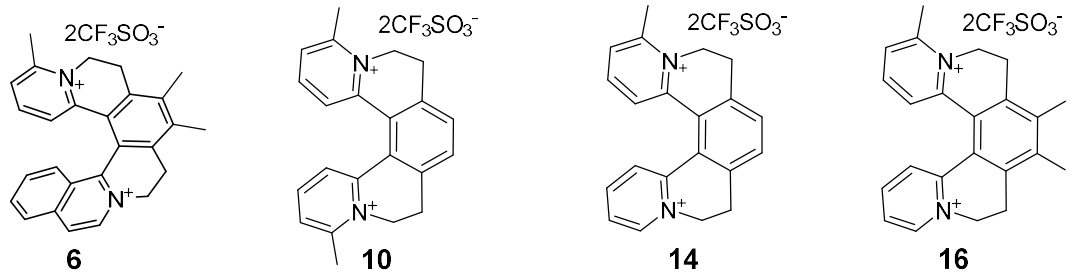

Fig. 89: *Activated methyl group containing novel helquats*

B. Resolution of methyl [6]helquat has been accomplished *via* anion exchange to form a mixture of two diastereomeric salts, which were separated by simple washing with methanol. Pure enantiomers (*P* and *M*) were obtained in multi-gram quantity by exchanging the tartrate salt to triflate (Scheme 35). The enantio-purity was determined by capillary electrophoresis and absolute configuration was determined by X-ray crystallography.

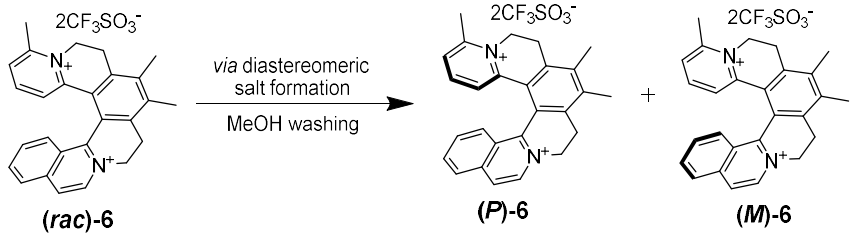

Scheme 35: *Resolution of helquat* ***6*** *via diastereomeric salt formation.*

C. A library of more than 500 compounds with diverse structures were synthesized from four different helquat scaffolds (Fig. 90) and evaluation of biological properties, to identify the therapeutic or diagnostic potential of these novel class of compounds is under investigation.

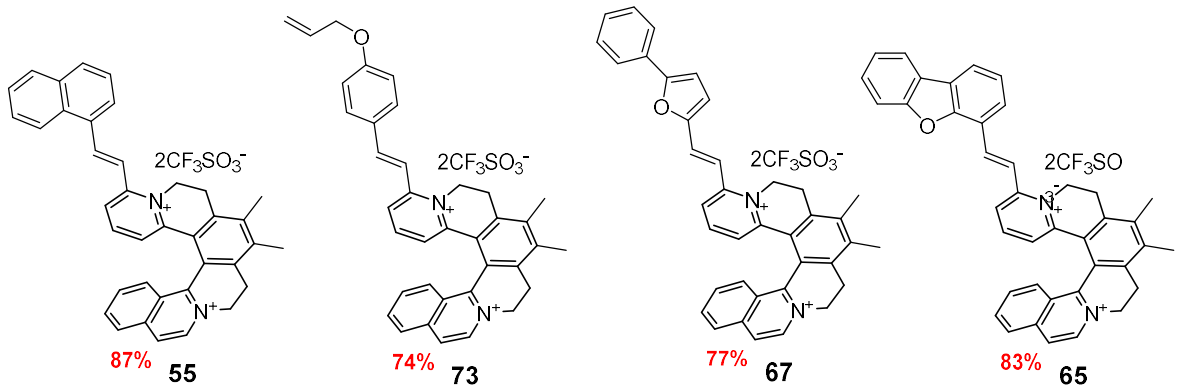

Type I derivatives

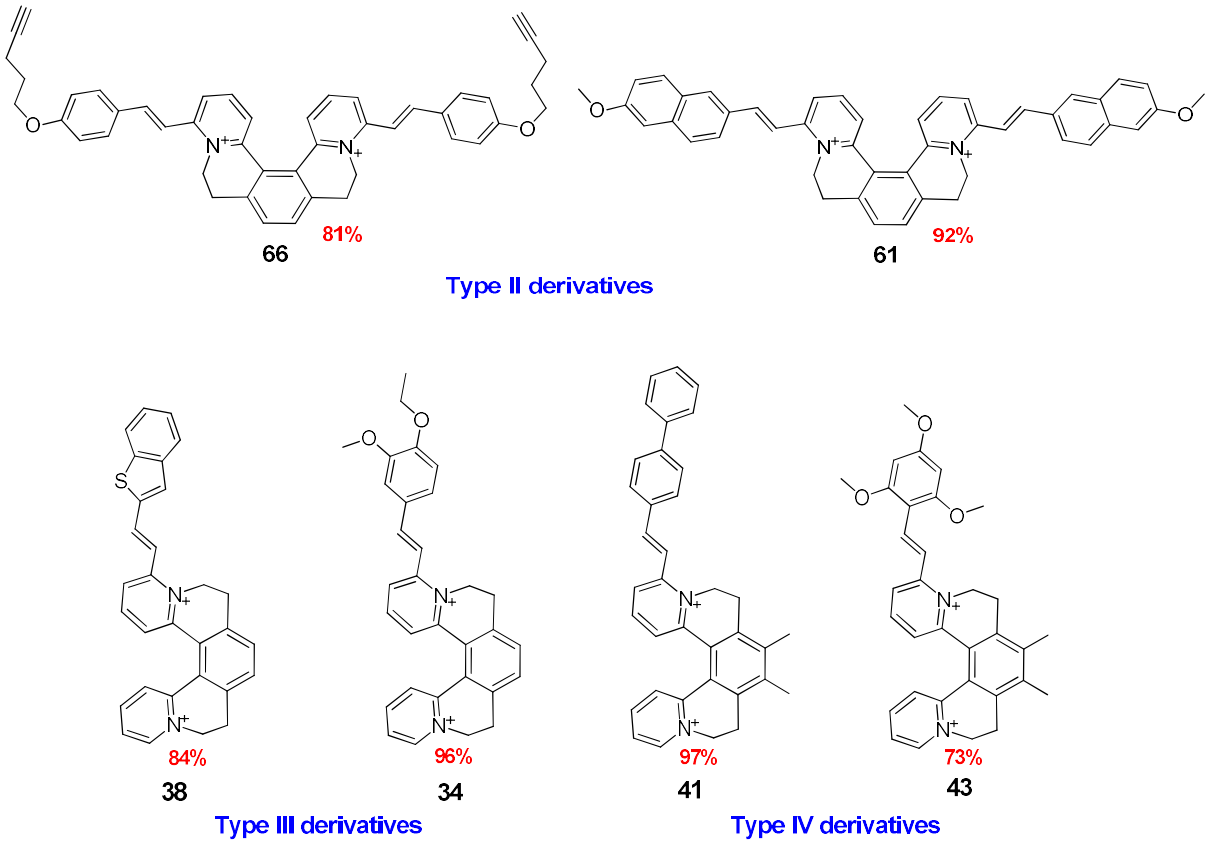

Fig. 90: *Representative examples from a library of helquat dyes.*

D. Nine compounds from **Type I** dye series were investigated for their second-order nonlinear optical responses in *racemic* forms, they were found to be better than the commercial compound DAST, with their second-order nonlinear optical responses. We will further explore the nonlinear optical properties of individual enantiomers of those nine compounds in solution and in a crystalline state (Fig. 91).

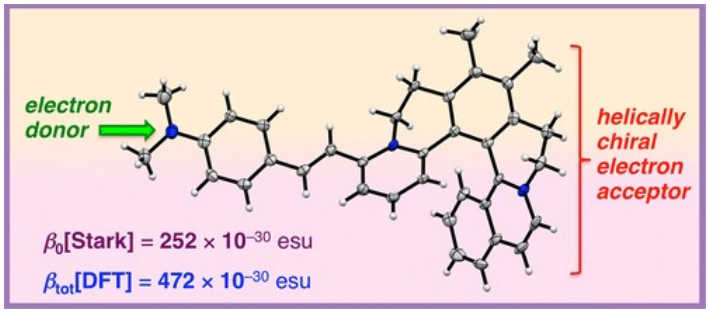

Fig. 91: *Nonlinear optical helquats.*

E. Dyes of **Type I** and **II** were screened in a high-throughput fluorescence-based assay in search of heparin chemosensors.

- Twenty four compounds were identified as preliminary hits, some of the representative examples are shown in Fig. 92:

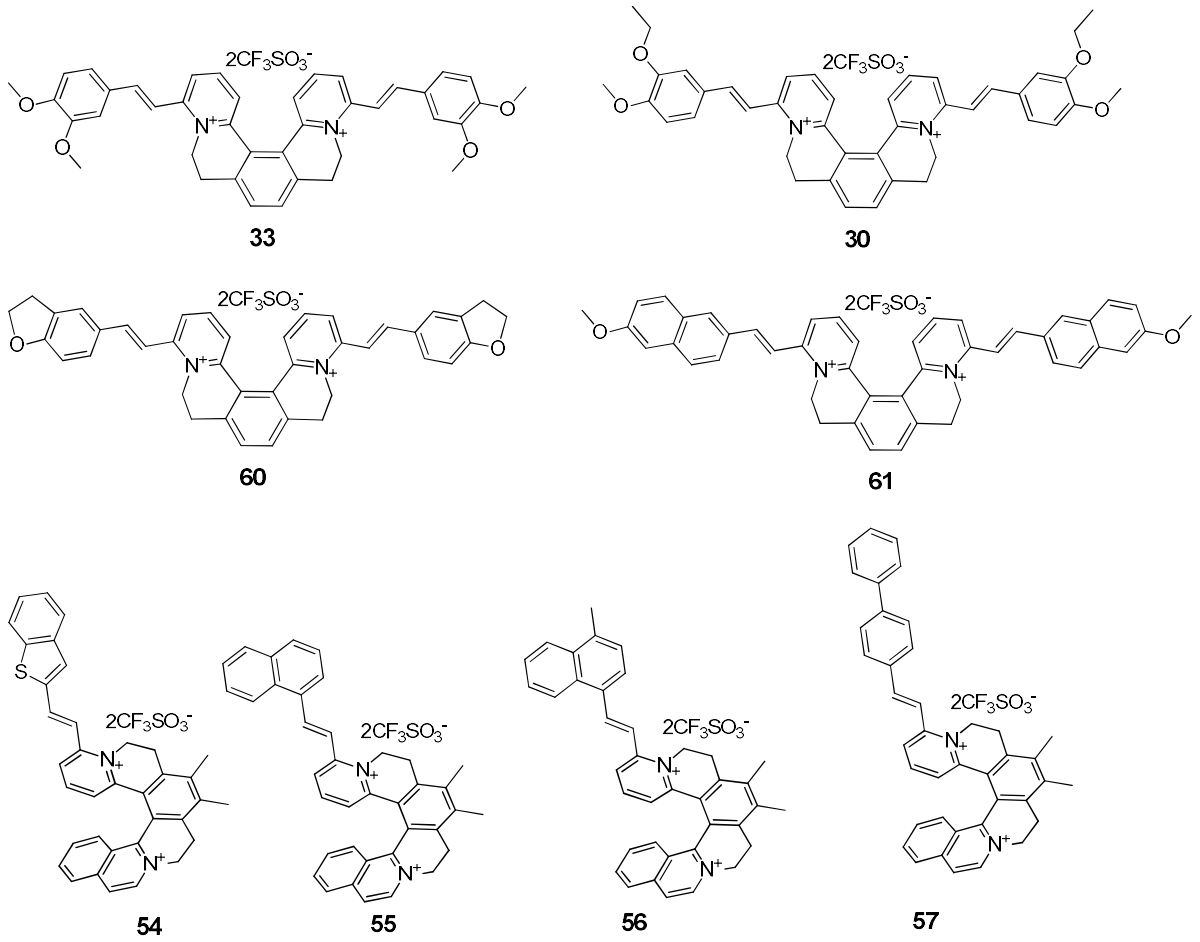

Fig. 92: *Preliminary hits for heparin chemosensors.*

- Two compounds were found to be selective for heparin over other analytes (Fig. 93).

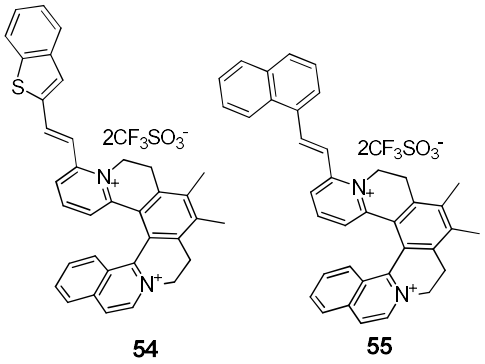

Fig. 93: *Heparin selective fluorescent probes*

- Two heparin selective fluorescent probes were validated for their capacity to quantify heparin in theoropatic and post-operative dosing level in highly competitive media such as blood plasma and serum.
- dsDNA binding dye **HeliDye1** have been discovered during the heparin screen and found to be selective for AT-rich dsDNA sequences over GC-rich sequences, ssDNA, ssRNA and dsRNA. During the SAR analysis around the structure of **HeliDye1**, three more compounds were identified to show similar selectivity and improved spectroscopic properties as compared to **HeliDye1** probe (Table 14, the fluorescence quantum yield of compound **82**, **(*rac*)-92** and **(*P*)-92** was 2.8 fold, 1.8 fold and 4.3 fold more, respectively as compared to **HeliDye1** in interaction with ds$(A_4T_4)_2$ DNA

sequence) (Fig. 94). Compound **92** was showing chiral recognition with *P*-enantiomer (K_D = 2.0 μM, Table 14), whereas *M*-enantiomer was not interacting. The biological properties and mode of interaction of newly discovered compounds will be studied in more detail.

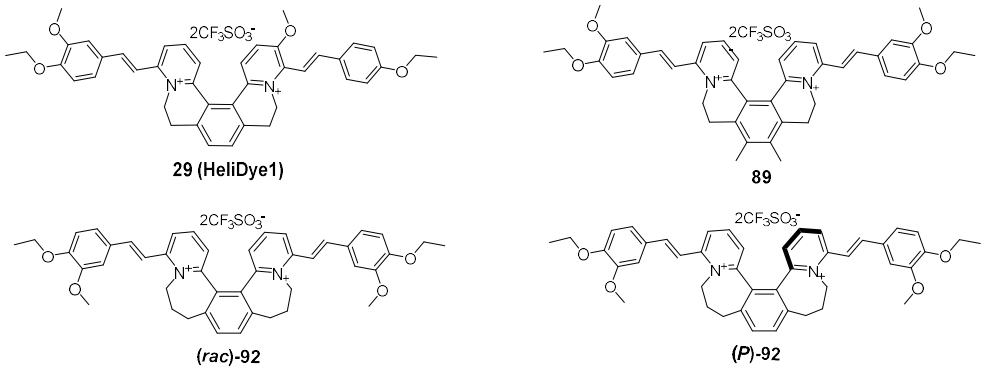

Fig. 94: *B-DNA binding helquat probes with improved spectroscopic properties.*

- DNA duplex binding properties of **HeliDye1** and other compounds were studied by UV-vis., emission, CD-spectroscopy and hydrodynamic study.
- Stereospecific recognition of minor groove of B-DNA using helquat dyes was confirmed by synthesizing enantiopure variants **(*P*)-92** and **(*M*)-92** of **HeliDye1**. Only *rac* and *P*-form of dye were found to show selective fluorescence light up in presence of AT-rich dsDNA sequences, whereas *M*-enantiomer was found to show no fluorogenic response in presence of any of the analytes, suggesting either no binding or binding with less affinity.
- A Computational study has proven the novel type of minor groove recognition of B-DNA by **HeliDye1** and binding modes of other variants are under investigation.
- Following potential applications of **HeliDye1** were successfully demonstrated
    - Nuclei staining probe in fixed cells at 1 μM concentration
    - Selectively staining of nucleic acid bands in gel electrophoresis
    - Fluorescent probe for live/dead cells exclusion
    - Fluorescent probe for cell cycle analysis

5. Experimental:

5.1 General information:

All reactions were carried out under an inert atmosphere of dry argon. Glassware was dried in an oven or by heat-gun in vacuum shortly before the experiments. Liquids and solutions were transferred *via* needle and syringe under inert atmosphere unless stated otherwise. Melting points were determined on a Wagner & Munz PolyTherm A micro melting point apparatus and are uncorrected. Thin-layer chromatography (TLC) analysis was performed on silica gel plates (Silica gel 60 F_{254}-coated aluminum sheets, Merck, cat. no. 1.05554.0001) and visualized by UV (UV lamp 254/365 nm, Spectroline® Model ENF-240C/FE). TLC analysis of dications was achieved using Stoddart's magic mixture (MeOH : NH_4Cl aq. (2 M) : $MeNO_2$, 7:2:1) as eluent on silica gel plates. Sonication was conducted with a BANDELIN SONOREX sonicator. Chemical shifts are given in δ-scale as parts per million (ppm); coupling constants (*J*) are given in Hertz (Hz). Peaks in ^1H and ^{13}C NMR spectra in acetone-d_6 were referenced relative to the solvent residual peak (CHD_2COCD_3, δ_H = 2.09 ppm) and CD_3COCD_3 (δ_C = 29.80 ppm); in $CDCl_3$ relative to the solvent peak δ_H = 7.26 ppm and δ_C = 77.00 ppm; and in DMSO-d_6 δ_H = 2.50 ppm and δ_C = 39.50 ppm. IR spectra were recorded on a Bruker EQUINOX55 (IFS55) spectrometer in KBr pellets. Abbreviations for intensities of IR bands are as follows: s for strong, vs for very strong, m for medium, w for weak, vw for very weak, br for broad, sh for shoulder. Mass spectral data were obtained at the Mass Spectrometry Facility operated by the Institute of Organic Chemistry and Biochemistry, Czech Academy of Sciences (IOCB CAS). ESI mass spectra were recorded using a Thermo Scientific LCQ Fleet mass spectrometer equipped with an electrospray ion source and controlled by Xcalibur software. The mobile phase consisted of MeOH : water (9:1) at a flow rate of 200 µL/min. The sample was dissolved, diluted with the mobile phase and injected using a 5 µL loop. Spray voltage, capillary voltage, tube lens voltage and capillary temperature were 5.5 kV, 5 V, 80 V and 275 °C, respectively. HRMS spectra were obtained with the ESI instrument.

The instruments used are listed below:

- NMR spectrometers: Bruker Avance 600 (600 MHz for ^1H, 151 MHz for ^{13}C) or Bruker Avance 400 (400 MHz for ^1H, 100.6 MHz for ^{13}C)
- For imaging of well plates: QUANTUM ST4-1100 (Viber Lourmat) imaging device
- For fluorescent imaging in cuvettes: 3UV™ transilluminator equipped with three wavelengths, 254, 312 and 365 nm.
- Microplate reader: TECAN infinite M1000 series
- UV-vis. and fluorescence spectrometer: Varian Cary 5000 series UV-vis spectrometer; Fluoromax-4 spectrofluorometer (HORIBA Scientific)
- Cell cytometry: BD FACS Aria™ cell sorter
- Fluorescence microscopy: Zeiss Axio Observer A1, 10x objective microscope; Zeiss LSM 780 confocal microscope
- Viscometer: Lovis 2000 M/ME rolling-ball viscometer, Anton Paar GmbH
- Centrifuge: Biosan LMC3000 series
- CD spectroscopy: Jasco-815 spectropolarimeter
- IR spectroscopy: Nicolet 6700
- Visualization of gels: Typhoon FLA 9500 fluorescence scanner, GE Healthcare, USA
- *NanoDrop*™ 1000 spectrophotometer, Thermo Scientific

5.2 Experimental procedures:

a) General procedure for Sonogashira coupling reaction (for internal alkyne 3 and 12):

A mixture of $[Pd(PPh_3)_2Cl_2]$ (1.6 mmol, 5 mol %), CuI (3.3 mmol, 10 mol %), and terminal alkyne **1** or **11** (32.6 mmol, 1.0 equiv.) was placed under argon into an oven-dried Schlenk flask. Freshly distilled Et_3N (6 mL/mmoL), followed by 2-bromo-6-methylpyridine (39.1 mmol, 1.2 equiv.) was added to the reaction mixture at rt. The reaction mixture was heated at 80-82 °C for 1 h until complete disappearance of **1** or **11** was detected (TLC analysis in 50% EtOAc in hexane, starting material (**1** or **11**) R_f = 0.5, product R_f = 0.25). Cooling of the reaction mixture at rt, filtration through a Celite pad, repetitive washings of Celite bed with EtOAc until no product was detected in the eluent (TLC analysis) followed by evaporation of volatiles under reduced pressure gave Sonogashira coupling product **3** or **12** in crude form. Purified product **3** or **12** was obtained by chromatographing the crude product through a column of silica gel using 1:1 mixture of hexane/EtOAc as a mobile phase. Purified products were obtained as brown solids.

b) Procedure for the synthesis of triyne 9, 13 and 15:

Internal alkynes **7** or **12** (4.8 mmol, 1.0 equiv.) was charged under argon into an oven dried Carius tube. Dry DCM (25 mL) and respective alkylating agent **4** or **8** (24 mmol, 5.0 equiv.) was added to a Carius tube at rt. The resulting solution was heated to reflux for 40 h in dark. The progress of the reaction was monitored by TLC (mobile phase Stoddart's magic mixture, starting material R_f = 0.85, product R_f = 0.48), as well as by ^{1}H-NMR analysis. After cooling, volatiles were evaporated under reduced pressure on a rotatory evaporator and resulting residue was sonicated with Et_2O (25 mL). After separation of the supernatant, the residue was sonicated in EtOAc (3 x 25 mL) and each time the supernatant was separated by centrifugation of the suspension. After drying of the solid under high vacuum, pure triynes **9**, **13** or **15** were obtained as off-white solid.

c) General procedure for the synthesis of helquat 6, 10, 14 and 16:

Cyclotrimerization of triynes **5**, **9**, **13** or **15** (2.848 mmol, 1.0 equiv.) takes place under $[Rh(PPh_3)_3Cl]$ (0.142 mmol, 5 mol %) catalysis under argon atmosphere in dry-degassed DMF in an oven dried Schlenk flask under heating at 110-112 °C. After 1 h, reaction progress was monitored by TLC analysis for complete consumption of respective triyne (mobile phase: Stoddart's magic mixture). After cooling of the reaction to rt, the reaction mixture was transferred to a round bottom flask and DMF was evaporated under reduced pressure at 50 °C water bath temperature. Brown residue obtained after evaporation of DMF was triturated with Et_2O (2 x 25 mL) and THF (3 x 25 mL) by sonication, followed by separation of supernatant by centrifugation and drying of final solid under high vacuum gave respective helquat **6**, **10**, **14** or **16** as off-white to light brown amorphous solid.

d) Procedure for the resolution of [6]helquat:

Resolution of Trimethyl[6]helquat **6** was carried out by modifying the previously described procedure.[181]

- **Procedure to prepare anion exchange resin in OH^- cycle:**

Strongly basic anion exchange resin in Cl^- cycle (soaked in water for overnight) was loaded into a column equipped with a Teflon tap and sinter s0 at the bottom of the column. For the uninterrupted smooth flow of liquid through the ion-exchange column equipped with a sinter or a piece of cotton wool plug in the bottom part of the column was used. Amount of

resin, which was used for each experiment, was measured in terms of volume of resin (in Cl^- cycle) in water (bed volume). Switching from Cl^- cycle to OH^- cycle was done by passing 2 M aq. solution of NaOH through the resin. Sufficient amount of 2 M solution of NaOH for complete exchange of chloride anions is 18 ml per 1 ml of bed volume of the resin. The fact that the exchange is complete, the absence of Cl^- anions was checked by taking a few drops of out coming basic solution to a small vial. This sample was acidified with few drops of aq. solution of HNO_3 (1:1), until the universal pH-paper test detected acidic reaction. Finally, two drops of 0.1M aq. solution of $AgNO_3$ was added. Completely clear solution (absence of AgCl precipitate) indicated the absence of Cl^- anions in the outcoming basic solution. At that point, pure water was run through the resin until the neutral reaction of out coming liquid was detected (universal pH paper test). Subsequently, water was expelled from the resin by applying small overpressure and MeOH was placed instead of it. All bubbles were removed by mixing the resin with a long needle or by stoppering the column and turning it gently upside down and back, so that all beads of the resin nicely mixed with MeOH and no bubble remained.

- **Procedure to prepare diastereomeric mixture *via* anion exchange**

A column of outer diameter 2.5 cm was put to OH- cycle. The solvent was subsequently exchanged for MeOH, then 0.2 M solution of (*R*,*R*)-(-)-*O*,*O'*-dibenzoyl-L-tartaric acid in MeOH was passed through the column until pH of the eluent becomes fairly acidic. For rough pH assessment the following method is recommended: a drop of pure MeOH is spotted on a universal pH-paper and, next to it, a drop of eluting solution is spotted. If the drop of eluting solution is more red than the drop of pure MeOH, the eluting solution is considered acidic. Overall, 85 mL of this solution was passed. Then the column was stoppered, and turned up and down repeatedly, so as to remove air bubbles and create a uniform bed of resin. Then pure MeOH was passed through the column until the pH of the eluent becomes neutral.

A methanolic solution of [*rac*-**6**][TfO^-]$_2$ (1.000 g, 1.478 mmol) (250 mL) was passed through the resin column pre-loaded with (*R*,*R*)-(-)-O,O'-dibenzoyl-L-tartrate anions. The column was repeatedly washed with pure MeOH. After regular intervals, the spot of the eluted MeOH was spotted on TLC and was observed under UV lamp for its UV response. Once no UV response was observed to the new spot on TLC, it was confirmed that complete helquat, loaded on the column was eluted and was exchanged to bis-(*R*,*R*)-(-)-*O*,*O'*-dibenzoyl-L-tartrate anions.

The combined eluent was evaporated to dryness to obtain an oily residue, which was triturated with Et_2O. Precipitated solid was filtered. After vacuum drying, the absence of fluorine signal in the ^{19}F-NMR spectrum of the solid confirms the complete exchange of bis triflate salt to diastereomeric (*R*,*R*)-(-)-*O*,*O'*-dibenzoyl-L-tartrate salt.

Two diastereomers were separated by simple washings with MeOH. The obtained mixture of diastereomeric salts was sonicated with MeOH (10 x 5 mL) and after each washing, the suspension was centrifuged, which help to separate supernatant from the solid. Each time supernatant and residual solid were sampled for CE analysis. After 10 washings, the residual solid was vacuum dried to give 924 mg of pure diastereomer with >97% ee.

The enantiopurity of the purified material was accessed by chiral capillary electrophoresis analysis. Pure enantiomer was obtained from the purified diastereomer by breaking the diastereomeric salt by anion exchange to achiral anion such as triflate.

The opposite diastereomer was recovered from the supernatant by passing it through the resin column pre-loaded with D-dibenzoyl tartrate anions and by following the similar procedure used for the isolation of the previous enantiomer in its enantiopure form, the opposite enantiomer was also obtained with satisfactory enantiopurity.

- **Procedure for anion exchange to triflate, and isolation of pure enantiomers:**

A pure diastereomeric salt of trimethyl[6]helquat, **6** with (*R*,*R*)-(-)-*O*,*O'*-dibenzoyl-L-tartrate anions (0.924 g, 0.8451 mmol) was transferred into a 50 mL centrifuge tube and dissolved in a solution of TfOH [2.3% in MeOH] (2 mL). Complete dissolution was ensured by sonication. Et_2O (40 mL) was added, the resulting solution becomes turbid and after sonication for 2-3 minutes, a dark brown oily residue was accumulated at the base of the centrifuge tube. The supernatant was separated from the residue after centrifugation of the resulting solution for 5 minutes. The dissolution, addition of Et_2O (40 mL), sonication and centrifugation was repeated for two more times, to ensure complete anion exchange. After complete anion exchange, the brownish oily residue was dissolved in MeOH (2 mL), and was re-precipitated by addition of Et_2O (40 mL). This re-dissolution and re-precipitation was repeated for two more times, still the precipitated solid becomes free flowing powder. The Obtained residue was vacuum dried as a pale yellow powder. Yield: 382 mg (76.4%).

The opposite enantiomer was obtained by following the similar procedure as a pale yellow powder. Yield: 397 mg (79.4%)

- **Racemization study with [*P*-6][TfO^-]:**

[*P*-6][TfO^-](2.5 mg, 0.004) was dissolve in DMSO (0.5 mL) in an NMR tube and was immersed in an oil bath pre-heated at 120 °C. Before heating, approximately 10 µL of the solution was taken with the help of capillary into an eppendorf for the capillary electrophoresis measurement. After commencing heating, approximately 10 µL of the sample from the NMR tube was withdrawn at an interval of 20 minutes for chiral capillary electrophoresis analysis. After analysis of all samples by CE, a racemization curve between time *vs. ln*(%*ee*) of major enantiomer and by performing some arithmetic (described in Results and discussion section), the halflife of racemization ($T_{1/2}$) and racemization barrier of interconversion of one enantiomer to other (ΔG) was determined.

e) General procedure for the synthesis of helquat dyes:

Under an argon atmosphere, helquat dye precursors **6, 10, 14,** or **16** and various aromatic, hetero-aromatic or metalloaromatic aldehydes (5 to 15 equiv.) were charged into a Schlenk flask and were placed under argon. Dry MeOH (0.1 mL/mg) followed by pyrrolidine (12 equiv.) was added to the reaction mixture. The flask was covered with Alufoil and until complete consumption of helquat dye precursor **6**, **10**, **14** or **16** analyzed by TLC analysis (mobile phase: Stoddart's magic mixture), the reaction was maintained under stirring at rt. The reaction was quenched by addition of Et_2O (8 x vol. of MeOH) into the reaction mixture. The suspension was sonicated for 2 min. and then centrifuged. The supernatant was separated from the solid. For further purification, obtained crude solid was completely dissolved in MeOH or MeCN and then precipitated by addition of Et_2O (6-8 vol. to the vol. of MeOH or MeCN). The suspension was sonicated, centrifuged and the supernatant was separated. This dissolution, precipitation procedure was repeated two more times. After drying under high vacuum, cationic styryl dyes were obtained as colored solids.

f) General procedure for the synthesis of planar dyes:

Method 1: Planar dye precursors **17 or 18** (30 mg, 0.128 mmol, 1.0 equiv.) and various aromatic, heteroaromatic or metalloaromatic aldehydes (0.640 mmol, 5.0 equiv.) were charged into a Schlenk flask under an argon atmosphere. Dry EtOH followed by pyrrolidine (15.8 μL, 13.7 mg, 0.192 mmol, 1.5 equiv.) was added to the reaction mixture. The flask was covered with Alufoil and the reaction mixture was heated at reflux until complete disappearance of the starting pyridinium substrate by TLC analysis (mobile phase: Stoddart's magic mixture). The reaction was quenched by addition of Et_2O (8 x vol. of MeOH) into the reaction mixture. The suspension was sonicated for 2 min. and then centrifuged. The supernatant was separated from the solid. The solid was further cleaned by washing with MeOH (3 x 0.5 mL) by sonication. Every time supernatant was separated from the solid and finally washed with Et_2O. Resulting solid was dried under high vacuum to give respective pyridinium dye in high yields.

Method 2: Planar dye precursor **17** or **18** (0.128 mmol, 1.0 equiv.), aromatic or heteroaromatic aldehydes (0.640 mmol, 5.0 euiv.), EtOH (1.0 ml) followed by pyrrolidine (14.7 mg, 17 μL, 0.207 mmol, 1.6 equiv.) were mixed together in a microwave glass tube and heated for 5 minutes in a microwave at microwave power 150 w. After 5 minutes complete starting consumption was confirmed by TLC analysis (eluent: Stoddart's magic mixture) and Et_2O (8 mL) was added. Precipitated solid was transferred to the storage vials and centrifuged. The supernatant was separated and solid was washed two times with MeOH (2 x 0.5 mL) and the supernatant was separated and finally with Et_2O (2 x 5 mL). Resulting solid was dried under high vacuum to give respective pyridinium dye in high yields.

g) General procedure for high-throughput fluorescence light-up assay:

A high-throughput fluorescence light up assay was designed for screening a library of helquat dyes. The experimental setup for the screening is shown in Fig. 95. In order to screen number of helquat dyes at a time, the screening was performed in a 96/384 well plate. The Well plate experiment also allows us to perform high-throughput screening of many compounds with repetition in multiplicates using a small quantity of sample as well as analytes.

DMSO stock solution (1 mM) of each dye was prepared. For screening, 1 mM DMSO stock solution of dyes and 1 mM aqueous stock solution of analyte were mixed together in a buffer in different ratios, in such a way that each well contains only one dye in presence of respective analyte. The final volume of DMSO into the test well was controlled between 1 to 10% depending upon the solubility of the dye in aqueous buffer environment. A blank well for each compound, i.e. dye alone (at the same concentration in presence of analyte) was also prepared. The well plate was protected from light. After preparing the well plate, contents were mixed together by shaking for 5 min. at rt and 500 rpm speed on a thermoshaker device and centrifuged at high speed for 30-50 seconds. At this stage, the well plate was placed inside the cabinet of an imaging device equipped with a camera at the top, the well plate was illuminated at 312 nm or 365 nm, and the picture of the well plate was recorded, while irradiating with UV light. By the visual observation of fluorescence light-up response of the dye, in presence and absence of analyte, the preliminary hits were identified. The quantitative measurement of fluorescence light up of the identified hits in presence and absence of analyte was measured at optimized excitation of the compound by using Tecan infinite® M1000 well plate reader, which confirms recognition of the analyte by the identified hit by showing fluorescence light-up in presence of analyte as compared to dye alone.

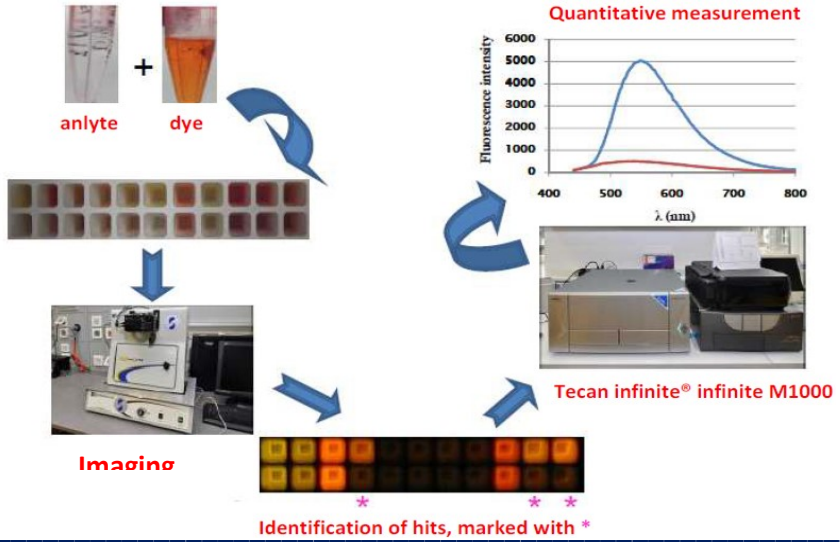

Fig. 95: *Experimental setup for fluorescence light-up experiment*

h) Procedure for determination of selectivity of identified hits for heparin or dsDNA:

The selectivity of all preliminary hits for various targets was analyzed in a competitive fluorescence light up experiment, where a solution of each analyte was mixed with each of the analyte mentioned below in a separate well.

All nucleotide triphosphates, EGTA, Na_2SO_4, glucose, Na Citrate were at 50 µM in 10 mM HEPES buffer (pH = 7.4). DNA was at 0.025 mg mL^{-1} (~50 µM). Bovine serum albumin (BSA) was at 0.5 mg mL^{-1}. Heparin, hyaluronic acid and chondroitin sulphate were at 6.5 µg mL^{-1} (~10 µM). 20% plasma solution was prepared by dilution of pooled normal human plasma in 10mM HEPES buffer (pH = 7.4). Control was 10 mM HEPES buffer (pH = 7.4).

Fluorescence light up response of each compound for each analyte was measured and the selectivity for that particular compound was decided on the basis of comparison of relative fluorescence light up intensity in each case of every analyte at maxima.

By following this general procedure, two heparin selective helquat dyes were identified as well as a dsDNA binding dye was also identified. All these identified hits were further developed for finding useful applications.

i) Procedure for blood plasma isolation:

Approximately 20 mL of blood was drawn with the help of a nurse or the general practitioner and transferred into the capillary blood collection tubes (5 mL vol., BD Vacutainer Seditainer, Catalogue number 366016). Vacutainer tubes were inverted carefully 10 times to mix blood and the anticoagulant and stored at rt until centrifugation.

The samples were centrifuged immediately by transferring the blood into sterile Falcon tubes with 10 mL volume for 15–20 minutes at 1500–1700 RCF at room temperature. The supernatant (plasma) was separated at room temperature and inspected for turbidity (if there was some turbidity, the samples were centrifuged for 15–20 min. at 1500 RCF and supernatant was filtered through the sterile filter of pore size 0.22 micron (Millipore, Catalogue Number: SLGVR25LS). The isolated plasma was aliquot to 3-4 times into the 1.5 mL sterile Eppendorf tubes with vol. for further use. Remaining aliquots were stored at 0-5 °C into the fridge.

j) Procedure for the calibration of heparin chemosensors for heparin quantification:

For developing a calibration curve for heparin quantification from plasma/serum, a concentration series from 0 µM to 100 µM was prepared by spiking 100% plasma/serum with the desired amount of heparin. The samples prepared in the previous step were diluted to achieve 10% diluted plasma (now the amount of heparin became 10 times less than the original, and these concentrations can be seen at calibration curve) were mixed with 10 µM of heparin probe **54** or **55** and fluorescence spectra from each well were recorded and the calibration curve was prepared by plotting intensity of fluorescence spectra at maxima *Vs.* heparin concentration in respective well.

k) UV-vis. absorption and fluorescence spectroscopy:

All UV-vis. and fluorescence spectra were measured in semi-micro quartz fluorescence cuvettes (Hellma Analytics) of path length 1 cm. The individual samples were prepared with or without oligonucleotide using 1 mM **HeliDye1** stock solution and 1 mM oligonucleotide stock solution as follows:

1. with oligonucleotide: Mixing of 1mM oligonucleotide stock solution (5 µL) + BPES buffer (985 µL) + **HeliDye1** 1mM stock solution (10 µL) in a 1.5 mL Eppendorf tube.

2. without oligonucleotide: Mixing of 1 mM **HeliDye1** stock solution (10 µL) + BPES buffer (990 µL) in a 1.5 mL Eppendorf tube.

UV-vis. absorption spectrum of each sample was measured in between 300–750 nm range with reference to the corresponding blank solution. For **HeliDye1** in absence of oligonucleotide, BPES buffer containing 1% DMSO was used as a reference. For each sample of HeliDye1 with oligonucleotides, respective 5 µM oligonucleotide solution in BPES buffer (containing 1% DMSO) was used as a reference solution.

After measurements of absorption spectra of each solution, fluorescence spectra of each sample was recorded at $\lambda_{excitation}$ = 460 nm. UV-vis. and fluorescence spectra for **HeliDye1** with and without respective oligonucleotide were plotted. The spectroscopic properties of **HeliDye1** in presence of various DNA oligonucleotide sequences are listed in Table 12.

l) Determination of fluorescence quantum yield (Table 12 for HeliDye1 and Table 15 for dye 90 and 93) :

Determination of the fluorescence quantum yields[186] (Φ_f) was performed using coumarin 153 (Φ_f = 0.53 at 25° C) as a standard in spectroscopy grade EtOH as a solvent. Measurements were performed in semi-micro quartz fluorescence cuvettes (Hellma Analytics) on a Fluoromax-4 spectrofluorometer equipped with a thermostated cuvette holder at 25° C. The excitation wavelength was 435 nm and the recorded spectral range was 455-750 nm for compounds and coumarin 153. The absorbance of the sample solution and the standard at the excitation wavelength were kept below 0.08. The quantum yields were calculated using the following equation:

$$\emptyset_{f,x} = \emptyset_{f,st}\, X\, \frac{F_x}{F_{st}}\, X\, \frac{1-10^{-Abss}}{1-10^{-Absx}}\, X\, \frac{n_x^2}{n_{st}^2} \qquad \textit{(eq. 8)}$$

The quantum yield, *F* is the integrated fluorescence intensity, *Abs* is the absorbance of the solution at the excitation wavelength, *n* is the refractive index of solvent; the subscripts *x*

and *st* stands for the sample and standard, respectively. Quantum yield measurements were done in triplicate with a standard deviation of ± 0.04.

m) Sequence specificity of DNA interacting dyes:

Light-up properties of DNA interacting dyes were studied with various dsDNAs, ssDNAs and RNA sequences, to determine their sequence specificity. All test nucleic acids were dissolved in nuclease-free water at 1 mM concentration and all dyes were dissolved in pure DMSO at 1 mM concentration.

In a 96 well plate, each well, 1 mM stock solution of respective nucleic acid (0.75 µL) and 1 mM DMSO stock solution of each dye (1.5 µL) were mixed with 147.75 µL of BPES buffer, to achieve 5 µM final respective nucleic acid concentrations and 10 µM final concentration of the respective dye. Fluorescence spectra of each dye at their respective excitation wavelengths[187] were measured in presence of all analytes after 5 minutes of mixing and from the fluorogenic response of each probe with all possible analytes, the sequence specificity was determined.

n) K_D values of interaction of dye 6a and various dsDNA sequences

The dissociation constants (K_D) of the interaction between **HeliDye1** and various example DNA duplexes were determined by fluorescence titration method. Each oligonucleotide (1 µM) was titrated with increasing concentrations of dye **HeliDye1** from 0 to 200 µM in BPES buffer. The dissociation curves were best-fitted using 1:1 binding with Hill slope model (nonlinear regression least square method) from Graph pad prism 5.[194] The dissociation constants for each of the dsDNA sequence are summarized in Table 13. An inverse relationship was found between number of AT-pairs and K_D.

o) Hydrodynamic study

Hydrodynamic study of drug-DNA interactions is a sensitive technique to probe the DNA duplex/ligand binding mode.[193] Viscosity measurements were performed using Rolling Ball Viscometer Lovis 2000 M/ME series, from Anton Parr GmbH. Following solutions with five different ratios of dye **HeliDye1** : dsDNA solutions were prepared, while keeping the concentration of dsDNA constant at 100 µM bp. Base pair molarity of the ctDNA stock solution was determined as follows. Concentration value of the DNA stock solution (in ng/µL) was determined by *NanoDrop*™ 1000 spectrophotometer. The base pair molarity of DNA stock solution was determined by putting the obtained value of ng/µL to the DNA calculator at molbiotools webpages.[195]

	c_{dye} (µM)	c_{dsDNA} (µM)	Ratio (dye/dsDNA)
1.	0	100	0
2.	25	100	0.25
3.	50	100	0.5
4.	100	100	1
5.	200	100	2

Table 16: *Solutions of different dye : dsDNA ratios used for viscosity measurement.*

Viscosity of each solution was measured four times, and a graph presenting $(n/n_o)^{1/3}$ *vs.* dye **HeliDye1** : dsDNA ratio was plotted. Similar experiment was performed for propidium iodide

(PI), which is a typical intercalator, and was used as a positive control. DAPI, a minor groove binder was used as a negative control.

5.3 Analytical data:

1-((6-methylpyridin-2-yl)ethynyl)isoquinoline (3)

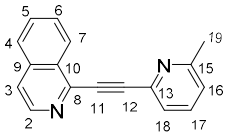

$(C_{17}H_{12}N_2)$
[244.3]

The synthesis of the compound **3** was accomplished by following *general procedure 5.2.a*.
A brown crystalline solid was obtained.
Yield: 6.370 g, 80%.
m.p. 113-116 °C. **^{1}H-NMR (600 MHz, acetone-d_6):** δ 2.61 (s, 3H, H-19), 7.39 (d, J = 7.8 Hz, 1H, H-16), 7.69 (d, J = 7.6 Hz, 1H, H-18), 7.83 (t, J = 7.7 Hz, 1H, H-17), 7.86 (ddd, J = 1.2, 6.7, 8.2 Hz, 1H, H-6), 7.89 (ddd, J = 1.4, 6.7, 8.3 Hz, 1H, H-5), 7.92 (dd, J = 1.3, 5.6 Hz, 1H, H-3), 8.08 (ddt, J = 0.8, 1.3, 8.3 Hz, 1H, H-4), 8.62 (ddd, J = 0.8, 1.4, 8.2 Hz, 1H, H-7), 8.63 (d, J = 5.6 Hz, 1H, H-2). **^{13}C-NMR (151 MHz, acetone-d_6):** δ 24.5 (C-19), 85.8 (C-11), 93.5 (C-12), 122.0 (C-3), 124.4 (C-16), 125.8 (C-18), 127.2 (C-7), 128.1 (C-4), 129.4 (C-6), 130.3 (C-10), 131.7 (C-5), 136.7 (C-9), 137.6 (C-17), 142.6 (C-13), 144.0 (C-2), 144.2 (C-8), 160.2 (C-15). **IR (KBr): ν (cm^{-1})** 1495, 1552, 1566, 1581, 1619, 2212, 3009, 3054. **MS (ESI) *m/z* (%):** 245.1 (M + 1) (100), 246.1 (20), 267.1 (10). **HRMS ESI *m/z*:** (M + 1) [$(C_{17}H_{13}N_2)^+$] calc. 245.1073, found 245.1072.

1-((6-methyl-1-(pent-3-yn-1-yl)pyridin-1-ium-2-yl)ethynyl)-2-(pent-3-yn-1-yl)isoquinolin-2-ium trifluoromethanesulfonate (5)

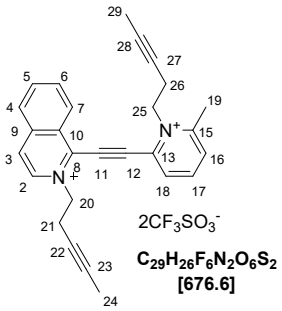

$2CF_3SO_3^-$
$C_{29}H_{26}F_6N_2O_6S_2$
[676.6]

Into an oven dried Carius tube, alkyne **3** (1.000 g, 4.093 mmol, 1.0 equiv.) and DCM (40 mL) was charged under argon. Pent-3-yn-1-yl trifluoromethanesulfonate (4.450 g, 20.586 mmol, 5.0 equiv.) was added to the reaction mixture at rt. The reaction mixture in a Carius tube was immersed into an oil bath and was heated to reflux for 65 h (reaction was monitored by ^{1}H-NMR analysis after each 24 h). The set-up was completely covered with Alufoil during the whole operation. After cooling at rt, the reaction mixture was transferred into a round bottom flask and solvent was evaporated on a rotary evaporator. The Washing of the residual containt in a flask with Et_2O (3 x 20 mL) followed by biphasic extraction in 1:0.6 water/DCM mixture (65 mL x 3), all triyne product was extracted into the aqueous phase. Evaporation of combined aqueous portion on rotatory evaporator, followed by trituration of residual oil with Et_2O (2 x 25 mL), gave **5** as a brown gummy solid.
Yield: 1.3 g, 47 %.
m.p. 151-154 °C. **^{1}H-NMR (600 MHz, acetone-d_6):** δ 1.74 (t, J = 2.6 Hz, 3H, H-29), 1.77 (t, J = 2.6 Hz, 3H, H-24), 3.27–3.30 (m, 4H, H-21 & H-27), 3.31 (s, 3H, H-19), 5.44 (t, J = 6.6 Hz, 2H, H-25), 5.50 (t, J = 6.6 Hz, 2H, H-20), 8.33 (ddd, J = 1.2, 7.0, 8.5 Hz, 1H, H-6), 8.46 (ddd, J = 1.1, 7.0, 8.4 Hz, 1H, H-5), 8.46 (dd, J = 1.6, 7.9 Hz, 1H, H-16), 8.59 (dt, J = 1.2, 8.4 Hz, 1H, H-4),

8.81 (t, *J* = 7.9 Hz, 1H, H-17), 8.90 (dd, *J* = 1.6, 7.9 Hz, 1H, H-18), 8.93 (dd, *J* = 0.8, 6.8 Hz, 1H, H-3), 9.09 (dq, *J* = 1.0, 8.5 Hz, 1H, H-7), 9.20 (d, *J* = 6.8 Hz, 1H, H-2). **^{13}C-NMR (151 MHz, acetone-d_6):** δ 3.2 (C-24), 3.2 (C-29), 20.0 (C-19), 21.8 (C-26), 22.0 (C-21), 56.5 (C-25), 61.2 (C-20), 74.2 (C-28), 74.3 (C-23), 82.0 (C-27), 82.2 (C-22), 90.1 (C-11), 99.4 (C-12), 128.6 (C-3), 129.3 (C-4), 130.0 (C-7), 131.0 (C-10), 133.6 (C-16), 134.1 (C-18), 134.4 (C-6), 136.3 (C-13), 138.5 (C-2), 138.5 (C-5), 138.6 (C-9), 138.9 (C-8), 146.3 (C-17), 160.7 (C-15). **IR (KBr): *v* (cm^{-1})** 518, 574, 639, 1031, 1172, 1265, 1491, 1509, 1564, 1581, 1602, 1611, 1619, 2223, 2291, 3092. **MS (ESI) *m/z* (%):** 295.1 (4), 296.1 (15), 311.1 (36), 312.1 (10), 377.2 (100), 378.2 (31), 395.2 (13), 527.1 [(M − $CF_3SO_3^-$)$^+$] (11). **HRMS ESI *m/z*:** calc. for [(M − $CF_3SO_3^-$)$^+$] [($C_{28}H_{26}O_3N_2F_3S$)$^+$] 527.1611, found 527.1612.

6,7,11-trimethyl-4,5,8,9-tetrahydroisoquinolino[1,2-a]pyrido[1,2-k][2,9]phenanthroline-3,10-diium trifluoromethanesulfonate (6)

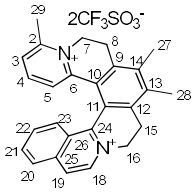

$C_{29}H_{26}F_6N_2O_6S_2$
[676.6]

Synthesis of [6]helquat **6** was accomplished by following *general procedure 5.2.c.* An off-white amorphous solid was obtained.

Yield: 1.630 g, 85 %.

m.p. 241-243 °C. **^{1}H-NMR (600 MHz, acetone-d_6):** δ 2.66 (s, 6H, H-27 & 28), 3.16 (s, 3H, H-29), 3.38 (dt, *J* = 4.8, 15.7 Hz, 1H, H-8a), 3.48 (dt, *J* = 4.5, 15.3 Hz, 1H, H-15a), 3.81 (ddd, *J* = 1.7, 3.6, 17.0 Hz, 1H, H-15b), 3.83 (ddd, *J* = 1.9, 3.7, 17.0 Hz, 1H, H-8b), 5.10 (dt, *J* = 3.7, 14.4 Hz, 1H, H-7b), 5.17 (dt, *J* = 3.6, 14.0 Hz, 1H, H-16a), 5.39 (ddd, *J* = 1.7, 4.5, 14.0 Hz, 1H, H-16b), 5.59 (ddd, *J* = 1.9, 4.8, 14.2 Hz, 1H, H-7a), 7.48 (dd, *J* = 2.7, 6.8 Hz, 1H, H-5), 7.74 (t, *J* = 7.4 Hz, 1H, H-4), 7.76 (dd, *J* = 2.7, 7.8 Hz, 1H, H-3), 7.83 (ddd, *J* = 1.2, 6.9, 8.7 Hz, 1H, H-22), 7.99 (ddd, *J* = 1.1, 6.9, 8.1 Hz, 1H, H-21), 8.09 (dq, *J* = 0.8, 8.7 Hz, 1H, H-23), 8.29 (d, *J* = 8.1 Hz, 1H, H-20), 8.55 (d, *J* = 6.7 Hz, 1H, H-19), 9.03 (d, *J* = 6.7 Hz, 1H, H-18). **^{13}C-NMR (151 MHz, acetone-d_6):** δ 16.8 (C-27), 17.0 (C-28), 21.4 (C-29), 26.0 (C-8), 26.9 (C-15), 50.2 (C-7), 56.2 (C-16), 123.8 (C-13), 125.9 (C-19), 127.0 (C-26), 128.7 (C-23), 128.8 (C-14), 128.9 (C-3), 129.2 (C-5), 129.2 (C-20), 132.8 (C-22), 136.2 (C-21), 137.6 (C-18), 138.9 (C-10), 140.0 (C-25), 141.1 (C-9), 142.0 (C-12), 142.6 (C-11), 144.4 (C-4), 148.9 (C-6), 151.7 (C-24), 157.0 (C-2). **IR (KBr): *v* (cm^{-1})** 518, 638, 1031, 1154, 1265, 1491, 1509, 1564, 1581, 1602, 1611, 1619, 3080. **MS (ESI) *m/z* (%):** 181.6 (4), 377.2 (100), 378.2 (34), 527.2 [($C_{28}H_{26}F_3N_2O_3S$)$^+$] (4). **HRMS ESI *m/z*:** calc. for [(M − $CF_3SO_3^-$)$^+$] [($C_{28}H_{26}F_3N_2O_3S$)$^+$] 527.1611, found 527.1612

1,2-bis(6-methylpyridin-2-yl)ethyne (7)

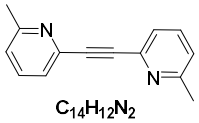

$C_{14}H_{12}N_2$
[208.3]

Synthesis was accomplished as described in literature.[8]

To the reaction mixture containing [$Pd(PPh_3)_4$] (2.85 g, 2.47 mmol, 2.5 mol%) and CuI (942 mg, 4.95 mmol, 5 mol%) in a Schlenk flask under argon was added dry Et_3N (200 mL). 2-Bromo-6- methylpyridine, **2** (11.3 mL, 17.0 g, 98.8 mmol) was added to the stirring reaction mixture *via* needle and syringe. Finally argon atmosphere was exchanged for acetylene

atmosphere by connecting a balloon with acetylene gas to the Schlenk flask and by piercing the septum with a needle for 10 seconds. The reaction mixture was stirred for 3 h at 80-82 °C. The progress of the reaction was monitored by TLC (mobile phase: 50% EtOAc in hexane, starting material, R_f = 0.88, product, R_f = 0.24). After filtration through a sinter with Celite® 512 layer and washing with EtOAc (500 mL), the volatiles were removed on a rotary evaporator and the residue was transferred to a 250 mL round-bottomed flask (using acetone for rinsing). After removing the acetone on a rotary evaporator, cyclohexane (4 x 150 mL) was added to the solid residue and the mixture was heated at 80 °C on a rotary evaporator without applying vacuum. After 1 min of rotation and heating, the insoluble residue was decanted and the hot solution was fast and carefully transferred to a new flask to complete the crystallization at rt. Crystals were separated from supernatant by vacuum filtration gave compound **7** as a yellow crystalline powder.

Yield: 8.17 g, 79%

m.p. 135-137 °C. **^{1}H-NMR (600 MHz, acetone-d_6):** δ 2.55 (bs, 6H), 7.32 (qdd, *J* = 0.6, 1.0, 7.7 Hz, 2H), 7.50 (qdd, *J* = 0.7, 1.0, 7.7 Hz, 2H), 7.77 (t, *J* = 7.7 Hz, 2H). **^{13}C-NMR (151 MHz, acetone-d_6):** δ 23.5, 87.3, 123.0, 124.6, 136.6, 141.9, 159.1. **IR (KBr):** *v* (cm^{-1}) 736, 743, 793, 1090, 1154, 1231, 1242, 1373, 1452, 1458, 1565, 1584, 2220, 2959, 2987, 3054, 3069. **MS (ESI) *m/z* (%):** 209 (100). **HRMS ESI *m/z*:** [$(C_{14}H_{13}N_2)^+$] calc.: 209.1073, found 209.1073.

6,6'-(ethyne-1,2-diyl)bis(1-(but-3-yn-1-yl)-2-methylpyridin-1-ium)trifluoromethane-sulfonate (9)

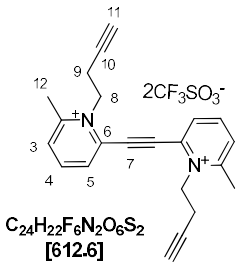

Synthesis of triyne **9** was accomplished by following the procedure *general procedure 5.2.b.* Triyne **9** was obtained as an off-white solid.

Yield: 2.4 g, 83%.

m.p. 176-178 °C. **^{1}H-NMR (600 MHz, acetonitrile-d_3):** δ 2.46 (t, 2H, H-11), 2.98 (s, 6H, H-12), 3.04 (dt, *J* = 2.7, 7.0, 7.0 Hz, 4H, H-9), 4.99 (t, *J* = 7.0 Hz, 4H, H-8), 8.06 (dd, *J* = 1.5, 8.1 Hz, 2H, H-5), 8.33(dd, *J* = 1.5, 7.9 Hz, 2H, H-3), 8.49 (t, *J* = 8.0 Hz, 2H, H-4). **^{13}C-NMR (151 MHz, acetonitrile-d_3):** 19.5 (C-9), 22.4 (C-12), 55.5 (C-8), 75.0 (C-11), 79.1 (C-10), 92.8 (C-7), 133.4 (C-5), 133.6 (C-3), 136.4 (C-6), 146.4 (C-4), 160.5 (C-2). **IR (KBr):** *v* (cm^{-1}) 632, 1025, 1128, 1157, 1195, 1220, 1252, 1272, 1282, 1435, 1468, 1526, 1574, 1629, 3069, 3099, 3251. **MS (ESI) *m/z* (%):** 261.2 (44), 313.2 (100), 314.2 (28), 345.3 (15), 463.2 (12). **HRMS ESI *m/z*:** calc. for [$(M - 2CF_3SO_3^-)^{+2}$] [$(C_{22}H_{22}N_2)^{+2}$] 157.0886, found 157.0886.

4,13-dimethyl-6,7,10,11-tetrahydrodipyrido[2,1-a:1',2'-k][2,9]phenanthroline-5,12-diium trifluoromethanesulfonate (10)

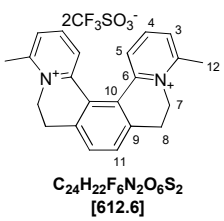

Synthesis of [5]helquat **10** was accomplished by following the *general procedure* 5.2.c. [5]helquat **10** was obtained as an off-white amorphous solid.**Yield:** 0.73 g, 73%.
m.p. 248-252 °C. **^{1}H-NMR (600 MHz, acetonitrile-d_3):** δ 2.93 (bs, 6H, H-12), 3.13-3.23 (m, 2H, H-8a), 3.27-3.38 (m, 2H, H-8b), 4.33-4.45 (m, 2H, H-7a), 5.03-5.13 (m, 2H, H-7b), 7.69 (dd, *J* = 1.0, 8.1 Hz, 2H, H-5), 7.70 (s, 2H, H-11), 7.77 (dd, *J* = 1.0, 7.9 Hz, 2H, H-3), 7.99 (t, *J* = 8.0 Hz, 2H, H-4). **^{13}C-NMR (151 MHz, acetonitrile-d_3):** δ 22.1 (C-12), 28.0 (C-8), 50.2 (C-7), 128.1 (C-10), 129.5 (C-3), 129.8 (C-5), 132.8 (C-11), 141.6 (C-9), 144.5 (C-4), 148.5 (C-6), 157.3 (C-2). **IR (KBr):** ν (cm^{-1}) 642, 831, 866, 1026, 1035, 1152, 1227, 1262, 1458, 1515, 1571, 1633, 2869, 2935, 3043, 3097, 3159. **MS (ESI) *m/z* (%):** 157.1 (33), 313.2 [$(M - 2CF_3SO_3^-)^{2+}$] (100), 463.2 [$(M - CF_3SO_3^-)^+$] (71). **HRMS ESI *m/z*:** calc. for [$(M - 2CF_3SO_3^-)^{2+}$] [$(C_{22}H_{22}N_2)^{2+}$] 157.0885, found 157.0886.

2-methyl-6-(pyridin-2-ylethynyl)pyridine (12)

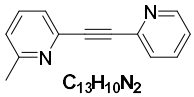

$C_{13}H_{10}N_2$
[194.2]

Synthesis of an internal alkyne **12** was accomplished by following *general procedure 5.2.a*. An internal alkyne **12** was obtained as a dark brown sticky solid.
Yield: 0.69 g, 74%.
m.p. 46-48 °C. **^{1}H-NMR (400 MHz, acetonitrile-d_3):** δ 2.52 (s, 3H), 7.24 (dd, *J* = 0.5, 7.8 Hz, 1H), 7.36 (dddd, *J* = 1.2, 7.8 Hz, 1H), 7.43 (dd, *J* = 0.5, 7.7 Hz, 1H), 7.61 (dt, *J* = 1.2, 7.8 Hz, 1H), 7.67 (t, *J* = 7.8 Hz, 1H), 7.79 (td, *J* = 1.8, 7.7 Hz, 1H), 8.61 (dt, *J* = 1.2, 5.0, 1H). **^{13}C-NMR (101 MHz, acetonitrile-d_3):** δ 24.6, 87.9, 88.6, 118.3, 124.7, 125.7, 128.6, 137.5, 137.7, 142.4, 143.4, 151.3, 160.3. **IR (KBr):** *v* (cm^{-1}) 572, 630, 737, 778, 791, 990, 1045, 1090, 1153, 1245, 1282, 1317, 1429, 1449, 1465, 1566, 1584, 2215, 2923, 3055. **MS (ESI) *m/z* (%):** 195.1 (100), 196.1 (13), 217.1 (8), 254.2 (5), 389.2 (20), 390.2 (6). **HRMS ESI *m/z*:** calc. for [$(C_{13}H_{11}N_2)^+$] 195.0917, found 195.0916.

1-(but-3-yn-1-yl)-2-((1-(but-3-yn-1-yl)pyridin-1-ium-2-yl)ethynyl)-6-methylpyridin-1-ium trifluoromethanesulfonate (13)

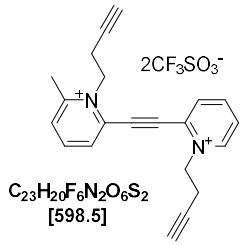

$C_{23}H_{20}F_6N_2O_6S_2$
[598.5]

Synthesis of triyne **13** was accomplished by following *general procedure 5.2.b*. Triyne **13** was obtained as an off-white amorphous powder.
Yield: 2.4 g, 83%.
m.p. 131-133 °C. **^{1}H-NMR (400 MHz, acetonitrile-d_3):** δ 2.46-2.49 (m, 2H), 2.98 (s, 3H), 3.02-3.07 (m, 4H), 4.96-5.02 (m, 4H), 8.08 (dd, *J* = 1.6, 8.0 Hz, 1H), 8.20 (dddd, *J* = 2.6, 6.2 Hz, 1H), 8.35 (dd, *J* = 1.3, 8.0 Hz, 1H), 8.49 (dd, *J* = 0.5, 8.0 Hz, 1H), 8.50 (t, *J* = 8.0 Hz, 1H), 8.70 (td, *J* = 1.4, 8.0 Hz, 1H), 8.97 (dd, J = 0.3, 6.2 Hz, 1H). **^{13}C-NMR (101 MHz, acetonitrile-d_3):** δ 19.4, 21.0, 22.3, 55.4, 59.9, 74.9, 75.3, 78.9, 79.1, 91.6, 93.4, 130.4, 133.4, 133.6, 135.2, 135.7, 136.1, 146.3, 147.5, 148.6, 160.5. **IR (KBr):** *v* (cm^{-1}) 518, 547, 573, 638, 732, 792, 814, 929, 1029, 1158, 1197, 1225, 1255, 1273, 1322, 1385, 1453, 1469, 1486, 1515, 1582, 1613, 2122, 3065, 3095, 3241, 3436. **MS (ESI) *m/z* (%):** 274.2 (32), 299.2 (50), 300.2 (22), 449.2 [(M −

$CF_3SO_3^-)^+$] (100), 450.2 (47) 451.3 (10). **HRMS ESI *m/z*:** calc. for [(M − $CF_3SO_3^-)^+$] [$(C_{22}H_{20}O_3N_2F_3S)^+$] 449.1141, found 449.1141.

4-methyl-6,7,10,11-tetrahydrodipyrido[2,1-a:1',2'-k][2,9]phenanthroline-5,12-diium trifluoromethanesulfonate (14)

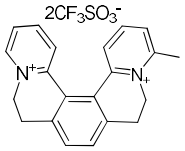

$C_{23}H_{20}F_6N_2O_6S_2$
[598.5]

Synthesis of [5]helquat **14** was accomplished by following *general procedure 5.2.c.* [5]helquat **14** was obtained as an off-white amorphous powder.

Yield: 0.83 g, 83%.

m.p. 227-229 °C. **^{1}H-NMR (400 MHz, acetonitrile-d_3):** δ 3.01 (s, 3H), 3.28-3.45 (m, 4H), 5.01-5.17 (m, 2H), 5.14-5.35 (m, 2H), 7.76 (s, 2H), 7.91 (dd, *J* = 1.4, 7.8 Hz, 1H), 7.97 (dddd, J = 1.6, 6 Hz, 1H), 8,08 (t, *J* = 7.9 Hz, 1H), 8.15 (dd, *J* = 1.3, 8.2 Hz, 1H), 8.21 (dddd, *J* = 1.6, 8.3 Hz, 1H), 8.26 (dd, *J* = 1.5, 8.3 Hz, 1H), 9.11 (dd, *J* = 0.6, 6.0 Hz, 1H). **^{13}C-NMR (101 MHz, acetonitrile-d_3):** δ 21.0, 26.9, 27.1, 49.1, 55.1, 119.5, 122.7, 126.2, 126.5, 127.0, 128.9, 130.2, 132.2, 140.6, 140.7, 143.6, 144.8, 145.7, 147.0, 147.1, 156.5. **IR (KBr):** ν (cm^{-1}) 517, 573, 632, 794, 863, 1027, 1140, 1249, 1266, 1277, 1495, 1509, 1620, 1675, 3012. **MS (ESI) *m/z* (%):** 150.1 (100), 150.6 (24), 166.1 (19), 239.1 (6), 299.2 (14), 331.2 (5), 449.1 (9). **HRMS ESI *m/z*:** calc. for [(M − $CF_3SO_3^-)^+$] [$(C_{22}H_{20}O_3N_2F_3S)^+$] 449.1141, found 449.1141.

2-methyl-1-(pent-3-yn-1-yl)-6-((1-(pent-3-yn-1-yl)pyridin-1-ium-2-yl)ethynyl)pyridin-1-ium trifluoromethanesulfonate (15)

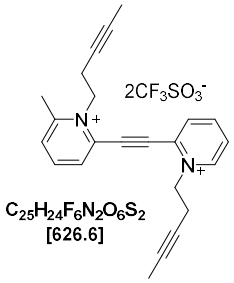

$C_{25}H_{24}F_6N_2O_6S_2$
[626.6]

Synthesis of triyne **15** was accomplished by following the *general procedure 5.2.b.* Triyne **15** was obtained as an off-white amorphous solid.

Yield: 1.3 g, 81%.

m.p. 139-141 °C. **^{1}H-NMR (400 MHz, acetonitrile-d_3):** δ 1.69 (t, *J* = 2.6 Hz, 3H), 1.71 (t, *J* = 2.6 Hz, 3H), 2.94-2.97 (m, 4H), 2.98 (s, 3H), 4.91 (t, *J* = 6.4 Hz, 2H), 4.94 (t, *J* = 6.4 Hz, 2H), 8.07 (dd, *J* = 1.6, 8.1 Hz, 1H), 8.21 (ddd, *J* = 1.5, 6.2, 7.8 Hz, 1H), 8.34 (dd, *J* = 1.5, 7.9 Hz, 1H), 8.45 (dd, *J* = 1.5, 6.6 Hz, 1H), 8.48 (t, *J* = 8.0 Hz, 1H), 8.67 (td, *J* = 1.4, 8.0 Hz, 1H), 8.94 (ddd, *J* = 0.5, 1.5, 6.1 Hz, 1H). **^{13}C-NMR (101 MHz, acetonitrile-d_3):** δ 3.3, 19.8, 21.5, 22.2, 22.2, 56.0, 60.5, 73.6, 73.9, 82.2, 82.8, 91.4, 93.2, 120.5, 123.7, 130.3, 133.3, 133.5, 135.1, 146.2, 147.4, 148.5, 160.4. **IR (KBr):** *v* (cm^{-1}) 518, 575, 640, 758, 1015, 1032, 1168, 1198, 1226, 1262, 1487, 1514, 1579, 1616, 2222, 2238, 3085. **MS (ESI) *m/z* (%):** 261.2 (10), 304.3 (8), 359.2 (22), 477.2 (13), 509.2 (100), 510.2 (27), 511.2 (11). **HRMS ESI *m/z*:** calc. for [(M – $2CF_3SO_3^-)^{2+}$]] [$(C_{23}H_{24}N_2)^{2+}$] 164.0964, found 164.0964.

4,8,9-trimethyl-6,7,10,11-tetrahydrodipyrido[2,1-a:1',2'-k][2,9]phenanthroline-5,12-diium trifluoromethanesulfonate (16)

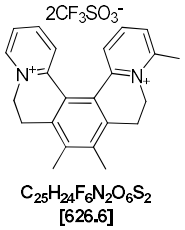

Synthesis of [5]helquat **16** was accomplished by following *general procedure 5.2.c.* [5]helquat **16** was obtained as an off-white amorphous solid.

Yield: 0.75 g, 73%.

m.p. 231-233 °C. **^{1}H-NMR (400 MHz, acetonitrile-d_3):** 2.52 (s, 6H), 3.10 (s, 3H), 3.22-3.39 (m, 2H), 3.61-3.72 (m, 2H), 4.69 (t, *J* = 14.1 Hz, 1H), 5.07 (t, *J* = 14.1 Hz, 1H), 5.28 (d, *J* = 13.2 Hz, 1H), 5.43 (d, *J* = 13.2 Hz, 1H), 7.93- 7.98 (m, 1H), 8.02 (td, *J* = 2.3, 6.4 Hz, 1H), 8.12 (s, 1H), 8.13 (d, *J* = 1.6 Hz, 1H), 8.22-8.29 (m, 2H), 9.17 (d, *J* = 6.1 Hz, 1H). **^{13}C-NMR (101 MHz, acetonitrile-d_3):** 16.8, 21.8, 21.8, 26.1, 26.3, 49.8, 55.6, 125.1, 125.9, 126.8, 129.2, 129.6, 131.5, 140.4, 140.4, 141.2, 141.2, 144.3, 145.4, 146.1, 148.8, 148.9, 156.8. **IR (KBr):** ν (cm^{-1}) 518, 574, 636, 755, 1030, 1165, 1225, 1259, 1282, 1400, 1495, 1509, 1560, 1584, 1625. **MS (ESI) *m/z* (%):** 164.1 [$(M - 2CF_3SO_3^-)^{2+}$] (100), 164.6 (25), 327.2 (4), 477.1 (3). **HRMS ESI *m/z*:** calc. for [$(M - 2CF_3SO_3^-)^{2+}$] [$(C_{23}H_{24}N_2)^{2+}$] 164.0964, found 164.0964.

(*E*)-11-(4-(dimethylamino)styryl)-6,7-dimethyl-4,5,8,9-tetrahydroisoquinolino[1,2-a]pyrido [1,2-k][2,9]phenanthroline-3,10-diium trifluoromethanesulfonate (20)

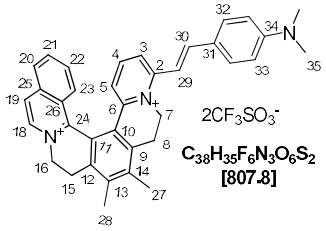

Synthesis and purification of [6]helquat dye **20** was accomplished by following *general procedure 5.2.e*, using helquat dye precursor **6** (70 mg, 0.103 mmol, 1.0 equiv.), 4-dimethylaminobenzaldehyde (48 mg, 0.322 mmol, 3.1 equiv.), pyrrolidine (100 μL, 87 mg, 1.223 mmol, 11.8 equiv.) in dry MeOH (7.0 mL) and dye **20** was obtained as a purple solid.

Yield: 0.056 g, 67%.

m.p. >350 °C. **^{1}H-NMR (600 MHz, acetone-d_6):** δ 2.66 (s, 3H, H-27), 2.66 (s, 3H, H-28), 3.15 (s, 6H, H-35), 3.34 (bddd, *J* = 4.2, 14.4, 17.3 Hz, 1H, H-8a), 3.48 (bdt, *J* = 4.0, 16.2, 16.2 Hz, 1H, H-15a), 3.82 (bdt, *J* = 3.7, 16.8, 16.8 Hz, 1H, H-8b), 3.82 (bdt, *J* = 3.5, 16.8, 16.8 Hz, 1H, H-15b), 5.12 (bdt, *J* = 3.7, 14.2, 14.2 Hz, 1H, H-7a), 5.17 (bdt, *J* = 3.5, 14.7, 14.7 Hz, 1H, H-16a), 5.40 (bdd, *J* = 4.0, 13.5 Hz, 1H, H-16b), 5.68 (bddd, *J* = 1.6, 4.2, 13.3 Hz, 1H, H-7b), 6.87- 6.90 (m, 2H, H-33), 7.3 (d, *J* = 8.0 Hz, 1H, H-5), 7.63 (t, *J* = 8.1 Hz, 1H, H-4), 7.68 (d, *J* = 15.6 Hz, 1H, H-29), 7.77-7.80 (m, 2H, H-32), 7.82 (d, *J* = 15.6 Hz, 1H, H-30), 7.84 (ddd, *J* = 1.2, 7.0, 8.5 Hz, 1H, H-22), 7.99 (bdd, *J* = 7.0, 8.2 Hz, 1H, H-21), 8.07 (bd, *J* = 8.2 Hz, 1H, H-3), 8.13 (d, *J* = 8.5 Hz, 1H, H-23), 8.29 (bd, *J* = 8.2 Hz, 1H, H-20), 8.55 (bd, *J* = 6.7 Hz, 1H, H-19), 9.04 (bd, *J* = 6.7 Hz, 1H, H-18). **^{13}C-NMR (151 MHz, acetone-d_6)**: δ 16.8 (C-28), 16.9 (C-27), 26.2 (C-8), 26.8 (C-15), 40.1 (C-35), 49.9 (C-7), 56.2 (C-16), 111.9 (C-29), 112.8 (C-33), 123.4 (C-31), 123.6 (C-13), 124.3 (C-3), 125.7 (C-19), 126.9 (C-26), 127.6 (C-5), 128.8 (C-23), 129.1 (C-20),129.2 (C-14), 131.8 (C-32), 132.6 (C-22), 136.1 (C-21), 137.4 (C-18), 138.6 (C-10), 139.8 (C-25), 140.5(C-9), 141.7 (C-12), 142.3 (C-11), 142.5 (C-4), 146.5 (C-30), 147.6 (C-6), 151.9 (C-24),

153.7 (C-34), 155.9 (C-2). **IR (KBr):** *v* (cm^{-1}) 517, 573, 638, 1030, 1164, 1269, 1530, 1555, 1591, 3076. **MS (ESI) *m/z* (%):** 194.0 (7), 247.6 (8), 254.6 (100), 255.1 (20), 375.2 (3), 508.3 (10), 658.2 [(M − $CF_3SO_3^-$)$^+$] (5). **HRMS ESI *m/z*:** calcd for [(M − $CF_3SO_3^-$)$^+$] [($C_{37}H_{35}O_3N_3F_3S$)$^+$] 658.2346, found 658.2344.

11-((1*E*,3*E*)-4-(4-(dimethylamino)phenyl)buta-1,3-dien-1-yl)-6,7-dimethyl-4,5,8,9-tetrahydro isoquinolino[1,2-a]pyrido[1,2-k][2,9]phenanthroline-3,10-diium trifluoromethanesulfonate (21)

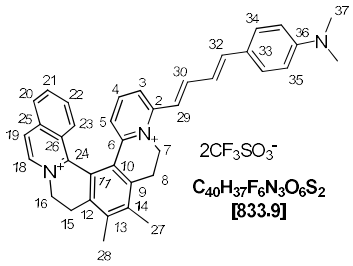

Synthesis and purification of [6]helquat dye **21** was accomplished by following *general procedure 5.2.e*, using helquat dye precursor **6** (100 mg, 0.148 mmol, 1.0 equiv.), (*E*)-3-(4-(dimethylamino)phenyl)acrylaldehyde (80 mg, 0.457 mmol, 3.1 equiv.), pyrrolidine (143 μL, 124 mg, 1.746 mmol, 11.8 equiv.) in dry MeOH (10.0 mL) and dye **21** was obtained as a purple solid.

Yield: 0.072 g, 58%.

m.p. >350 °C. **^{1}H-NMR (600 MHz, acetone-d_6):** *δ* 2.66 (s, 3H, H-27), 2.67 (s, 3H, H-28), 3.10 (s, 6H, H-37), 3.35 (bddd, *J* = 4.8, 14.8, 17.4 Hz, 1H, H-8a), 3.49 (ddd, *J* = 4.5, 14.8, 17.2 Hz, 1H, H-15a), 3.82 (ddd, *J* = 1.8, 3.7, 17.2 Hz, 1H, H-15b), 3.86 (ddd, *J* = 2.0, 3.7, 17.4 Hz, 1H, H-8b), 5.07 (dt, *J* = 3.7, 14.5, 14.5 Hz, 1H, H-7a), 5.18 (bdt, *J* = 3.7, 14.4, 14.4 Hz, 1H, H-16a), 5.40 (ddd, *J* = 1.8, 4.5, 14.0 Hz, 1H, H-16b), 5.60 (ddd, *J* = 2.0, 4.8, 13.7 Hz, 1H, H-7b), 6.81-6.84 (m, 2H, H-35), 7.16 (d, *J* = 15.3 Hz, 1H, H-32), 7.21 (dd, *J* = 10.0, 15.3 Hz, 1H, H-31), 7.30 (dd, *J* = 1.3, 8.0 Hz, 1H, H-5), 7.34 (d, *J* = 14.9 Hz, 1H, H-29), 7.52-7.55 (m, 2H, H-34), 7.64 (t, *J* = 8.1 Hz, 1H, H-4), 7.75 (dd, *J* = 10.0, 14.9 Hz, 1H, H-30), 7.81 (ddd, *J* = 1.2, 6.9, 8.8 Hz, 1H, H-22), 8.01 (ddd, *J* = 1.1, 6.9, 8.1 Hz, 1H, H-21), 8.04 (dd, *J* = 1.3, 8.2 Hz, 1H, H-3), 8.14 (dq, *J* = 0.9, 0.9, 0.9, 8.8 Hz, 1H, H-23), 8.29 (bd, *J* = 8.1 Hz, 1H, H-20), 8.55 (bd, *J* = 6.7 Hz, 1H, H-19), 9.03 (d, *J* = 6.7 Hz, 1H, H-18). **^{13}C-NMR (151 MHz, acetone-d_6):** δ 16.9 (C-27), 16.8 (C-28), 26.2 (C-8), 26.9 (C-15), 40.2 (C-37), 49.8 (C-7), 56.3 (C-16), 113.0 (C-35), 117.6 (C-29), 123.6 (C-31), 123.7 (C-13), 124.4 (C-3), 124.7 (C-33), 125.8 (C-19), 127.0 (C-26), 128.0 (C-5), 128.9 (C-23), 129.2 (C-20), 129.2 (C-14), 130.4 (C-34), 132.5 (C-22), 136.2 (C-21), 137.5 (C-18), 138.6 (C-10), 140.0 (C-25), 140.7 (C-9), 141.9 (C-12), 142. 5 (C-11), 147.6 (C-30), 142.7 (C-4), 145.1 (C-32), 147.9 (C-6), 152.0 (C-24), 152.9 (C-36), 155.3 (C-2). **IR (KBr):** ν (cm^{-1}) 518, 573, 638, 1031, 1153, 1263, 1483, 1527, 1552, 1583, 1626, 3076. **MS (ESI) *m/z* (%):** 194.1 (21), 267.7 (100), 268.2 (43), 362.3 (8), 377.3 (10), 401.4 (17), 402.4 (12), 534.5 (40), 535.5 (13), 684.5 [(M − $CF_3SO_3^-$)$^+$] (7). **HRMS ESI *m/z*:** [(M − $CF_3SO_3^-$)$^+$] [($C_{39}H_{37}O_3N_3F_3S$)$^+$] calc. 684.25022, found 684.24999.

(*E*)-11-(2-(1,2,3,5,6,7-hexahydropyrido[3,2,1-ij]quinolin-9-yl)vinyl)-6,7-dimethyl-4,5,8,9-tetrahydroisoquinolino[1,2-a]pyrido[1,2-k][2,9]phenanthroline-3,10-diium trifluoromethane- sulfonate (22)

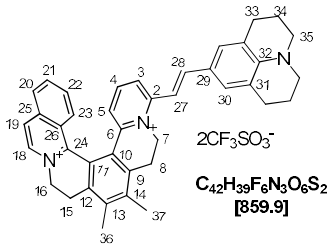

Synthesis and purification of [6]helquat dye **22** was accomplished by following *general procedure 5.2.e*, using helquat dye precursor **6** (70 mg, 0.103 mmol, 1.0 equiv.), 9-julolidinecarboxaldehyde (147 mg, 0.731 mmol, 7.1 equiv.), pyrrolidine (100 μL, 87 mg, 1.223 mmol, 11.8 equiv.) in dry MeOH (7.0 mL) and dye **22** was obtained as a purple solid.
Yield: 0.041 g, 46%.
m.p. >350 °C. **^{1}H-NMR (600 MHz, acetone-d_6):** δ 1.98-2.03 (m, 4H, H-34), 2.65 (s, 3H, H-36), 2.66 (s, 3H, H-37), 2.79-2.83 (m, 4H, H-33), 3.30 (bddd, *J* = 3.7, 14.2, 17.0 Hz, 1H, H-8a), 3.38-3.41 (m, 4H, H-35), 3.47 (bddd, *J* = 3.7, 14.5, 17.0 Hz, 1H, H-15a), 3.80 (ddd, *J* = 1.9, 4.7, 17.0 Hz, 1H, H-15b), 3.82 (ddd, *J* = 1.9, 4.9, 17.0 Hz, 1H, H-8b), 5.04 (dt, *J* = 3.7, 14.0, 14.0 Hz, 1H, H-7a), 5.16 (dt, *J* = 3.7, 14.3, 14.3 Hz, 1H, H-16a), 5.39 (ddd, *J* = 1.9, 4.7, 14.0 Hz, 1H, H-16b), 5.60 (ddd, *J* = 1.9, 4.9, 13.8 Hz, 1H, H-7b), 7.20 (dd, *J* = 1.2, 8.0 Hz, 1H, H-5), 7.34 (s, 2H, H-30), 7.55 (t, *J* = 8.1 Hz, 1H, H-4), 7.73 (d, *J* = 15.5 Hz, 1H, H-28), 7.82 (ddd, *J* = 1.2, 6.9, 8.8 Hz, 1H, H-22), 7.84 (d, *J* = 15.5 Hz, 1H, H-27), 7.98 (ddd, 1H, *J* = 1.1, 6.9, 8.1 Hz, 1H, H-21), 8.01 (dd, *J* = 1.2, 8.2 Hz, 1H, H-3), 8.11 (dq, *J* = 0.9, 0.9, 0.9, 8.8 Hz, 1H, H-23), 8.28 (bd, *J* = 8.1 Hz, 1H, H-20), 8.53 (bd, *J* = 6.8 Hz, 1H, H-19), 9.02 (d, *J* = 6.8 Hz, 1H, H-18). **^{13}C-NMR (151 MHz, acetone-d_6):** δ 16.7 (C-36), 16.9 (C-37), 22.1 (C-34), 26.2 (C-8), 26.8 (C-15), 28.3 (C-33), 49.6 (C-7),50.6 (C-35), 56.2 (C-16), 110.1 (C-27), 122.1 (C-31), 122.5 (C-29), 123.6 (C-13), 123.8 (C-3), 125.6 (C-19), 126.9 (C-5), 126.9 (C-26), 128.8 (C-23), 129.1 (C-20), 129.4 (C-14), 129.7 (C-30), 132.5 (C-22), 136.1 (C-21), 137.4 (C-18), 138.6 (C-9), 139.8 (C-25), 140.3 (C-12), 141.7 (C-10), 141.9 (C-4), 142.2 (C-11), 147.0 (C-32), 147.1 (C-28), 147.3 (C-6), 152.0 (C-24), 156.0 (C-2). **IR (KBr):** ν (cm^{-1}) 517, 573, 638, 1030, 1163, 1260, 1484, 1524, 1553, 1588, 1627, 3074. **MS (ESI) *m/z* (%):** 217.1 (4), 280.7 (100), 362.3 (7), 453.4 (10), 475.4 (6), 561.4 (7), 710.4 [(M − $CF_3SO_3^-$)$^+$] (14). **HRMS ESI *m/z*:** calc. for [(M − $CF_3SO_3^-$)$^+$] [($C_{41}H_{39}N_3O_3F_3S$)$^+$] 710.2659, found 710.2653.

(*E*)-11-(2-(6-(dimethylamino)naphthalen-2-yl)vinyl)-6,7-dimethyl-4,5,8,9-tetrahydroiso-quinoline[1,2-a]pyrido[1,2-k][2,9]phenanthroline-3,10-diium trifluoromethanesulfonate (23)

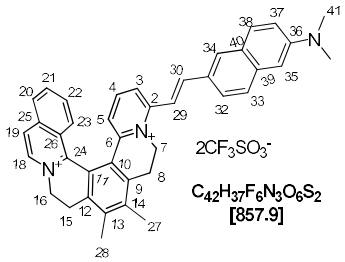

Synthesis and purification of [6]helquat dye **23** was accomplished by using helquat dye precursor **6** (75 mg, 0.111 mmol, 1.0 equiv.), 6-dimethylamino-2-naphthylaldehyde (66.3 mg, 0.333 mmol, 3.0 equiv.), pyrrolidine (108 μL, 93.2 mg, 1.310 mmol, 11.8 equiv.) in dry MeOH (7.5 mL) and dye **23** was obtained as a red solid.

Yield: 71 mg, 75%.

m.p. >350 °C. **^{1}H-NMR (600 MHz, acetonitrile-d_3):** δ 2.53 (s, 3H, H-27), 2.55 (s, 3H, H-28), 3.05 (bddd, *J* = 4.8, 14.3, 17.3 Hz, 1H, H-8a), 3.11 (s, 6H, H-41), 3.16 (bddd, *J* = 4.5, 15.1, 17.0 Hz, 1H, H-15a), 3.54 (ddd, *J* = 1.8, 3.5, 17.0 Hz, 1H, H-15b), 3.58 (bdt, *J* = 2.0, 3.8, 17.3 Hz, 1H, H-8b), 4.71 (dt, *J* = 3.8, 14.0, 14.0 Hz, 1H, H-7a), 4.79 (dt, *J* = 3.5, 14.5, 14.5 Hz, 1H, H-16a), 5.01 (ddd, *J* = 1.8, 4.5, 13.8 Hz, 1H, H-16b), 5.38 (ddd, *J* = 2.0, 4.8, 13.7 Hz, 1H, H-7b), 6.82 (dd, *J* = 1.3, 8.0 Hz, 1H, H-3), 7.01 (bd, *J* = 2.7 Hz, 1H, H-38), 7.28 (dd, *J* = 2.7, 9.0 Hz, 1H, H-37), 7.49 (t, *J* = 8.1 Hz, 1H, H-4), 7.58 (d, *J* = 15.8 Hz, 1H, H-29), 7.65 (ddd, *J* = 1.2, 6.9, 8.8 Hz, 1H, H-22), 7.74 (d, *J* = 15.8 Hz, 1H, H-30), 7.77 (d, *J* = 8.7 Hz, 1H, H-33), 7.80 (dq, *J* = 1.0, 8.8 Hz, 1H, H-23), 7.82 (bd, *J* = 9.0 Hz, 1H, H-35), 7.83 (dd, *J* = 1.3, 8.2 Hz, 1H, H-5), 7.86 (dd, *J* = 1.9, 8.7 Hz, 1H, H-32), 7.88 (ddd, *J* =1.1, 6.9, 8.1 Hz, 1H, H-21), 8.02 (bd, *J* = 1.9 Hz, 1H, H-34), 8.12 (bdt, *J* = 0.8, 0.8, 1.2, 8.1 Hz, 1H, H-20), 8.30 (bd, *J* = 6.8 Hz, 1H, H-19), 8.60 (d, *J* = 6.8 Hz, 1H, H-18). **^{13}C-NMR (151 MHz, acetonitrile-d_3):** δ 17.1 (C-27), 17.2 (C-28), 26.1 (C-8), 26.8 (C-15), 40.7 (C-41), 50.3 (C-7), 56.1 (C-16), 106.6 (C-38), 106.6 (C-39), 115.6 (C-29), 117.7 (C-36), 123.5 (C-13), 125.0 (C-32), 125.2 (C-5), 125.3 (C-20), 126.0 (C-19), 127.1 (C-26), 128.1 (C-33),128.3 (C-14), 128.3 (C-3), 128.6 (C-23), 129.1 (C-31), 131.0 (C-35), 132.4 (C-34), 132.8 (C-22), 136.5 (C-21), 137.0 (C-18), 137.9 (C-40), 138.7 (C-10), 140.0 (C-25), 141.1 (C-11), 142.3 (C-9), 142.4 (C-12), 143.1 (C-4), 146.3 (C-30), 148.1 (C-6), 151.4 (C-37), 151.9 (C-24), 155.5 (C-2). **IR (KBr):** ν (cm^{-1}) 518, 573, 639, 1031, 1154, 1263, 1484, 1508, 1560, 1599, 1622, 3081. **MS (ESI) *m/z* (%):** 194.2 (7), 279.7 (100), 280.2 (48), 375.3 (7), 558.5 (50), 559.5 [(M − $2CF_3SO_3^-$)$^{2+}$] (25), 708.5 [(M − $CF_3SO_3^-$)$^+$] (68). **HRMS ESI *m/z*:** calc. for [(M − $CF_3SO_3^-$)$^+$] [($C_{41}H_{37}O_3N_3F_3S$)$^+$] 708.2502, found 708.2505.

11-((*1E*,*3E*)-4-(1,2,3,5,6,7-hexahydropyrido[3,2,1-ij]quinolin-9-yl)buta-1,3-dien-1-yl)-6,7-dimethyl-4,5,8,9-tetrahydroisoquinolino[1,2-a]pyrido[1,2-k][2,9]phenanthroline-3,10-diium trifluoromethanesulfonate (24)

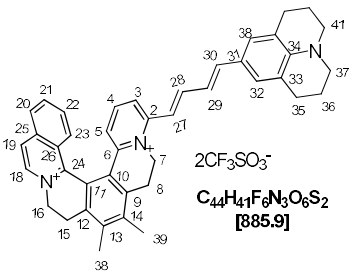

Synthesis ans purification of [6]helquat dye **24** was accomplished by following *general procedure 5.2.e*, using helquat dye precursor **6** (70 mg, 0.103 mmol, 1.0 equiv.), (*E*)-3-(1,2,3,5,6,7-hexahydropyrido[3,2,1-ij]quinolin-9-yl)acrylaldehyde (70.5 mg, 0.310 mmol, 3.0 equiv.), pyrrolidine (100 µL, 86.6 mg, 1.218 mmol, 11.8 equiv.) in dry MeOH (7.0 mL) and [6]helquat dye **24** was obtained as a blue solid.

Yield: 37.6 mg, 41%.

m.p. >350 °C. **^{1}H-NMR (600 MHz, acetone-d_6):** δ 1.96-2.01 (m, 4H, H-36), 2.65 (s, 3H, H-38), 2.66 (s, 3H, H-39), 2.77 (bt, *J* = 6.4 Hz, 4H, H-35), 3.32-3.35 (m, 4H, H-37), 3.33 (ddd, *J* = 4.8, 14.5, 17.2 Hz, 1H, H-8a), 3.47 (bddd, *J* = 4.6, 14.2, 17.0 Hz, 1H, H-15a), 3.80 (ddd, *J* = 1.8, 3.5, 17.0 Hz, 1H, H-15b), 3.84 (ddd, *J* = 1.9, 3.5, 17.2 Hz, 1H, H-8b), 5.04 (bdt, *J* = 3.5, 14.2, 14.2 Hz, 1H, H-7a), 5.16 (bdt, *J* = 3.5, 14.0, 14.0 Hz, 1H, H-16a), 5.39 (ddd, *J* = 1.8, 4.6, 13.8 Hz, 1H, H-16b), 5.55 (bddd, *J* = 1.9, 4.8, 13.9 Hz, 1H, H-7b), 7.05 (bd, *J* = 15.1 Hz, 1H, H-30), 7.08 (bd, *J* = 0.6 Hz, 2H, H-32), 7.14 (ddd, *J* = 0.7, 10.7, 15.1 Hz, 1H, H-29), 7.26 (dd, *J* = 1.3, 7.9 Hz, 1H, H-5), 7.26 (bd, *J* = 14.8 Hz, 1H, H-27), 7.59 (t, *J* = 8.1 Hz, 1H, H-4), 7.74 (dd, *J* = 10.7, 14.8 Hz, 1H, H-28), 7.80 (ddd, *J* = 1.3, 7.0, 8.8 Hz, 1H, H-22), 8.00 (ddd, *J* = 1.1, 7.0, 8.1 Hz, 1H, H-21),

8.01 (dd, *J* = 1.3, 8.4 Hz, 1H, H-3), 8.29 (ddt, *J* = 0.7, 0.7, 1.3, 8.1 Hz, 1H, H-20), 8.29 (dq, *J* = 0.9, 0.9, 0.9, 8.8 Hz, 1H, H-23), 8.54 (dd, *J* = 0.9, 6.7 Hz, 1H, H-19), 9.03 (d, *J* = 6.7 Hz, 1H, H-18). **^{13}C-NMR (151 MHz, acetone-d_6):** *δ* 16.8 (C-38), 16.9 (C-39), 22.3 (C-36), 26.1 (C-8), 26.8 (C-15), 28.3 (C-35), 49.5 (C-7), 50.5 (C-37), 56.2 (C-16), 116.4 (C-27), 121.3 (C-31), 122.1 (C-33), 122.6 (C-30), 123.6 (C-13), 124.1 (C-3), 127.5 (C-5), 125.7 (C-19), 126.9 (C-26), 128.2 (C-32), 128.8 (C-23), 129.1 (C-20), 129.2 (C-14), 132.5 (C-22), 136.1 (C-21), 137.4 (C-18), 138.5 (C-9), 139.8 (C-25), 140.4 (C-12), 141.7 (C-10), 142.2 (C-11), 142.3 (C-4), 145.9 (C-29), 145.9 (C-34), 147.6 (C-6), 147.9 (C-28), 151.9 (C-24), 155.2 (C-2). **IR (KBr):** ν (cm^{-1}) 517, 573, 638, 1030, 1163, 1260, 1484, 1524, 1553, 1588, 1627, 3074. **MS (ESI) *m/z* (%):** 186.2 (8), 194.1 (22), 279.7 (22), 293.7 (100), 294.2 (50), 401.2 (11), 586.4 (42), 736.3 [(M − $CF_3SO_3^-$)$^+$] (43). **HRMS ESI *m/z*:** calc. for [(M − $CF_3SO_3^-$)$^+$] ($C_{43}H_{41}N_3O_3F_3S$) 736.2815, found 736.2653.

(*E*)-11-(ferrocene-2-yl) vinyl)-6,7-dimethyl-4,5,8,9-tetrahydroisoquinolino[2,1-*k*]pyrido [2,1-*a*][2,9] phenanthroline-3,10-diium trifluoromethanesulfonate (25)

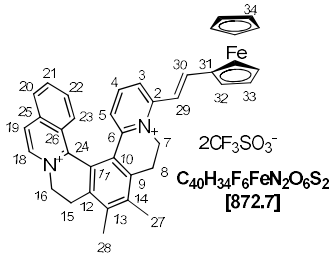

Synthesis and purification of [6]helquat dye **25** was accomplished by following *general procedure 5.2.e*, using helquat dye precursor **6** (75 mg, 0.111 mmol, 1.0 equiv.), ferrocenecarboxaldehyde (71.3 mg, 0.333 mmol, 3.0 equiv.), pyrrolidine (108 μL, 93.2 mg, 1.310 mmol, 11.8 equiv.) in dry MeOH (7.5 mL) and dye **25** was obtained as a blue solid.
Yield: 70.6 g, 73%.
m.p. >350 °C. **^{1}H-NMR (600 MHz, acetone-d_6):** *δ* 2.66 (s, 3H, H-27), 2.67 (s, 3H, H-28), 3.31-3.37 (m, 1H, 15a), 3.48 (bdt, *J* = 4.5, 15.9, 15.9 Hz, 1H, H-8a), 3.79-3.87 (m, 2H, H-8b and H-15b), 4.29 (s, 5H, H-34), 4.70 (bs, 2H, H-33), 4.92 (bs, 1H, H-32a), 4.96 (bs, 1H, H-32b), 5.12 (bdt, *J* = 3.3, 14.0, 14.0 Hz, 1H, H-7a), 5.18 (bdt, *J* = 3.5, 14.5, 14.5 Hz, 1H, H-16a), 5.39 (bdd, *J* = 4.0, 13.6 Hz, 1H, H-16b), 5.60 (bdd, *J* = 4.5, 13.7 Hz, 1H, H-7b), 7.36 (bd, *J* = 7.8 Hz, 1H, H-5), 7.54 (d, *J* = 15.4 Hz, 1H, H-29), 7.68 (bt, *J* = 7.9 Hz, 1H, H-4), 7.85 (d, *J* = 15.4 Hz, 1H, H-30), 7.86 (bt, *J* = 8.1 Hz, 1H, H-22), 8.01 (bt, *J* = 7.7 Hz, 1H, H-21), 8.07 (bd, *J* = 8.1 Hz, 1H, H-3), 8.12 (bd, *J* = 8.7 Hz, 1H, H-23), 8.29 (bd, *J* = 8.1 Hz, 1H, H-20), 8.54 (bd, *J* = 6.7 Hz, 1H, H-19), 9.02 (bd, *J* = 6.7 Hz, 1H, H-18). **^{13}C-NMR (151 MHz, acetone-d_6):** *δ* 16.8 (C-27), 16.9 (C-28), 26.1 (C-8), 26.9 (C-15), 50.2 (C-7), 56.3 (C-16), 70.1 (C-32a), 70.5 (C-32b), 70.9 (C-34), 73.0 (C-33), 80.6 (C-31), 114.7 (C-29), 123.7 (C-13), 124.8 (C-3), 125.8 (C-19), 127.0 (C-26), 128.1 (C-5), 128.9 (C-23), 129.1 (C-14), 129.2 (C-20), 132.6 (C-22), 136.1 (C-21), 137.5 (C-18), 138.7 (s, C-10), 140.0 (C-25), 140.7 (C-9), 141.8 (C-12), 142.5 (C-11), 143.1 (C-4), 147.9 (C-6), 148.1 (C-30), 151.9 (C-24), 155.3 (C-2). **IR (KBr):** *v* (cm^{-1}) 518, 573, 637, 1030, 1105, 1154, 1262, 1412, 1487, 1508, 1558, 1605, 1622, 3085. **MS (ESI) *m/z* (%):** 194.2 (12), 286.7 (17), 287.2 (100), 287.7 (47), 377.3 (17), 453.4 (15), 573.4 (40), 574.4 [(M – 2$CF_3SO_3^-$)$^{2+}$] (20), 723.5 [(M – $CF_3SO_3^-$)$^+$] (45). **HRMS ESI *m/z*:** calc. for [(M – $CF_3SO_3^-$)$^+$] [($C_{39}H_{34}O_3N_2F_3FeS$)$^+$] 723.1586; found 723.1583.

(*E*)-11-(4-Methoxystyryl)-6,7-dimethyl-4,5,8,9-tetrahydroisoquinolino[1,2-*a*]pyrido[1,2-*k*][2,9] phenanthroline-3,10-diium Trifluoromethanesulfonate (26)

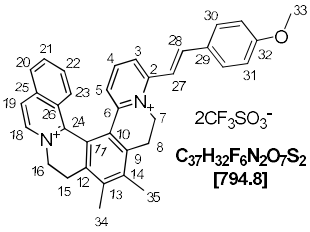

Synthesis and purification of [6]helquat dye **26** was accomplished by following *general procedure 5.2.e*, using [6]helquat dye precursor **6** (35 mg, 0.052 mmol, 1.0 equiv.), 4-methoxybenzaldehyde (354 mg, 2.6 mmol, 50.0 equiv.), pyrrolidine (53 μL, 45.9 mg, 0.645 mmol, 12.4 equiv.) in dry MeOH (3.5 mL) and [6]helquat dye **26** was obtained as a lemon yellow solid.

Yield: 28 mg, 68%.

m.p. > 350 °C. **^{1}H-NMR (600 MHz, acetone-d_6):** δ 2.66 (s, 3H, H-34), 2.66 (s, 3H, H-35), 3.38 (bddd, *J* = 4.7, 14.6, 16.8 Hz, 1H, H-8a), 3.50 (ddd, *J* = 4.6, 14.3, 16.8 Hz, 1H, H-15a), 3.84 (ddd, *J* = 1.9, 3.6, 16.8 Hz, 1H, H-8b), 3.84 (ddd, *J* = 1.9, 3.6, 16.8 Hz, 1H, H-15b), 3.94 (s, 3H, H-33), 5.18 (dt, *J* = 3.6, 14.3, 14.4 Hz, 1H, H-7a), 5.20 (dt, *J* = 3.6, 14.2, 14.2 Hz, 1H, H-16a), 5.41 (ddd, *J* = 1.9, 4.6, 14.1 Hz, 1H, H-16b), 5.74 (ddd, *J* = 1.9, 4.7, 13.7, 1H, H-7b), 7.11-7.17 (m, 2H, H-31), 7.44 (dd, *J* = 1.3, 8.0 Hz, 1H, H-5), 7.75 (t, *J* = 8.1 Hz, 1H, H-4), 7.83 (d, *J* = 15.9 Hz, 1H, H-28), 7.85 (ddd, *J* = 1.2, 6.9, 8.7 Hz, 1H, H-22), 7.88-7.91 (m, 2H, H-30), 7.90 (d, *J* = 15.9 Hz, 1H, H-27), 8.00 (ddd, *J* = 1.1, 6.9, 8.1 Hz, 1H, H-21), 8.11 (dd, *J* = 1.3, 8.2 Hz, 1H, H-3), 8.14 (dq, *J* = 0.9, 0.9, 0.9, 8.7 Hz, 1H, H-23), 8.30 (bddt, *J* = 0.7, 0.7, 1.2, 8.1 Hz, 1H, H-20), 8.57 (bd, *J* = 6.7 Hz, 1H, H-19), 9.05 (d, *J* =6.7 Hz, 1H, H-18). **^{13}C-NMR (151 MHz, acetone-d_6):** δ 16.8 (C-34), 16.9 (C-35), 26.0 (C-8), 26.7 (C-15), 50.4 (C-7), 55.9 (C-33), 56.1 (C-16), 115.4 (C-31), 116.1 (C-27), 123.7 (C-13), 125.2 (C-4), 125.8 (C-19), 126.9 (C-26), 128.6 (C-29), 128.7 (C-23), 128.8 (C-5), 128.9 (C-14), 129.1 (C-20), 131.5 (30), 132.7 (C-22), 136.1 (C-21), 137.5 (C-18), 138.7 (C10), 139.9 (C-25), 140.8 (C-9), 141.8 (C-12), 142.4 (C-11), 143.5 (C-4), 145.1 (C-28), 148.2 (C-6), 151.7 (C-24), 155.4 (C-3), 163.2 (C-32). **IR (KBr):** $\tilde{\nu}$ (cm^{-1}) 1029, 1155, 1175, 1256, 1271, 1441, 1599, 1625, 2851, 3074. **MS (ESI) *m/z* (%):** 248.1 [(M – 2 $CF_3SO_3^-$)$^{2+}$] (100), 495.2 [(M – 2$CF_3SO_3^-$)$^{2+}$] (5), 645.2 [(M – $CF_3SO_3^-$)$^+$] (5). **HRMS ESI *m/z*:** calc. for [(M – $CF_3SO_3^-$)$^+$] [($C_{36}H_{32}O_4N_2F_3S$)$^+$] 645.2029, found 645.2013.

(*E*)-11-(2-(6-Methoxynaphthalen-2-yl)vinyl)-6,7-dimethyl-4,5,8,9-tetrahydroisoquinolino-[1,2-*a*]pyrido[1,2-*k*][2,9]phenanthroline-3,10-diium Trifluoromethanesulfonate (27)

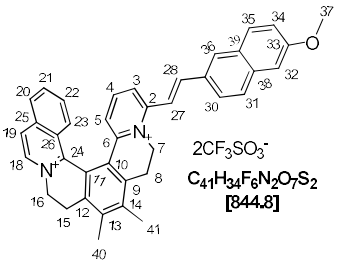

The synthesis and purification of [6]helquat dye **27** was accomplished by following *general procedure 5.2.e*, using helquat dye precursor **6** (75 mg, 0.111 mmol, 1.0 equiv.), 6-methoxy-2-naphthylaldehyde (146.7 mg, 0.788 mmol, 7.1 equiv.), pyrrolidine (108 μL, 93.5 mg, 1.315 mmol, 11.8 equiv.) in dry MeOH (7.0 mL) and [6]helquat dye **27** was obtained as a yellow amorphous solid.

Yield: 68.3 mg (73%).

m.p. > 350 °C. **^{1}H-NMR (600 MHz, acetonitrile-d_3):** δ 2.54 (s, 3H, H-40), 2.55 (s, 3H, H-41), 3.07 (ddd, *J* = 4.9, 14.8, 17.2 Hz, 1H, H-8a), 3.18 (ddd, *J* = 4.5, 14.8, 17.2 Hz, 1H, H-15a), 3.56 (ddd, *J* = 1.8, 3.6, 17.2 Hz, 1H, H-15b), 3.60 (ddd, *J* = 1.8, 3.8, 17.2 Hz, 1H, H-8b), 3.96 (s, 3H), 4.77 (dt, *J* = 3.8, 14.4, 14.4 Hz, 1H, H-7a), 4.84 (ddd, *J* = 3.6, 14.3, 14.3 Hz, 1H, H-16a), 5.04 (ddd, *J* = 1.8, 4.5, 13.8 Hz, 1H, H-16b), 5.41 (ddd, *J* = 1.8, 4.9, 14.0 Hz, 1H, H-7b), 6.92 (dd, *J* = 1.1, 8.0 Hz, 1H, H-5), 7.24 (dd, *J* = 2.6, 8.8 Hz, 1H, H-34), 7.35 (d, *J* = 2.6 Hz, 1H, H-32), 7.55 (t, *J* = 8.1 Hz, 1H, H-4), 7.68 (ddd, *J* = 1.2, 6.9, 8.7 Hz, 1H, H-22), 7.69 (d, *J* = 15.9 Hz, 1H, H-27), 7.74 (d, *J* = 15.9 Hz, 1H, H-28), 7.82 (dq, *J* =1.0, 1.0, 1.0, 8.7 Hz, 1H, H-23), 7.84 (dd, *J* = 1.1, 8.2 Hz, 1H, H-3), 7.88 (ddd, *J* =1.1, 6.9, 8.1 Hz, 1H, H-21), 7.90 (d, *J* = 8.8 Hz, 1H, H-35), 7.92 (d, *J* =8.6 Hz, 1H, H-31), 7.95 (dd, *J* = 1.8, 8.6 Hz, 1H, H-30), 8.12 (bd, *J* =8.1 Hz, 1H, H-20), 8.16 (d, *J* = 1.8 Hz, 1H, H-36), 8.30 (bd, *J* = 6.7 Hz, 1H, H-19), 8.62 (d, *J* = 6.7 Hz, 1H, H-18). **^{13}C-NMR (151 MHz, acetonitrile-d_3):** δ 16.0 (C-40), 16.1 (C-41), 25.0 (C-15), 25.8 (C-8), 49.6 (C-7), 55.1 (C-16), 55.3 (C-37), 106.6 (C-32), 116.6 (C-27), 119.6 (C-34), 122.6 (C-13), 124.4 (C-3), 124.6 (C-31), 124.9 (C-19), 126.0 (C-26), 127.5 (C-5), 127.7 (C-39), 127.8 (C-23), 128.2 (C-30), 128.7 (C-20), 130.3 (C-14), 130.4 (C-29), 130.4 (C-35), 130.4 (C-36), 131.8 (C-22), 135.5 (C-21), 136.0 (C-38), 136.3 (C-18), 137.6 (C-9), 139.0 (C-25), 140.2 (C-12), 141.4 (C-10), 141.4 (C-4), 142.6 (C-11), 144.7 (C-28), 147.3 (C-6), 150.8 (C-24), 154.2 (C-2), 159.6 (C-33). **IR (KBr):** $\tilde{\nu}$ (cm^{-1}) 518, 573, 638, 1031, 1154, 1266, 1482, 1506, 1562, 1608, 1623, 2841, 3077. **MS ESI *m/z* (%):** (15) 273.1 [(M – $CF_3SO_3^-$)$^+$] (100), 545.3 [(M – $2CF_3SO_3^-$)$^{2+}$] (25), 695.3 [(M – $CF_3SO_3^-$)$^+$]. **HRMS ESI *m/z*:** calc. for [(M – $CF_3SO_3^-$)$^+$] [($C_{40}H_{34}O_4N_2F_3S$)$^+$] 695.2186, found 695.2180.

11-((1*E*,3*E*)-4-(4-Methoxyphenyl)buta-1,3-dienyl)-6,7-dimethyl-4,5,8,9-tetrahydroisoquinolino[1,2-a]pyrido[1,2-k][2,9]phenanthroline-3,10-diium Trifluoromethanesulfonate (28)

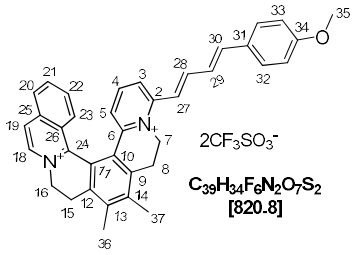

The synthesis and purification of [6]helquat dye **28** was accomplished by following the *general procedure 5.2.e*, using dye precursor **6** (100 mg, 0.148 mmol, 1.0 equiv.), 4-methoxycinnamaldehyde (170.5 mg, 1.051 mmol, 7.1 equiv.), pyrrolidine (143 μL, 124 mg, 1.744 mmol, 11.8 equiv.) in dry MeOH (10 mL) and [6]helquat dye **28** was obtained as an orange solid.

Yield: 77.6 mg (64%).

m.p. 167-169 °C. **^{1}H NMR (600 MHz, acetone-d_6):** δ 2.66 (s, 3H, H-27), 2.67 (s, 3H, H-28), 3.35 (bddd, *J* = 4.8, 14.8, 17.4 Hz, 1H, H-8a), 3.49 (ddd, *J* = 4.5, 14.8, 17.2 Hz, 1H, H-15a), 3.82 (ddd, *J* = 1.8, 3.7, 17.2 Hz, 1H, H-15b), 3.86 (ddd, *J* = 2.0, 3.7, 17.4 Hz, 1H, H-8b), 3.86 (s, 3H, H-37), 5.07 (dt, *J* = 3.7, 14.5, 14.5 Hz, 1H, H-7a), 5.18 (bdt, *J* = 3.7, 14.4, 14.4 Hz, 1H, H-16a), 5.40 (ddd, *J* = 1.8, 4.5, 14.0 Hz, 1H, H-16b), 5.60 (ddd, *J* = 2.0, 4.8, 13.7 Hz, 1H, H-7b), 6.81-6.84 (m, 2H, H-35), 7.16 (d, *J* = 15.3 Hz, 1H, H-32), 7.21 (dd, *J* = 10.0, 15.3 Hz, 1H, H-31), 7.30 (dd, *J* = 1.3, 8.0 Hz, 1H, H-5), 7.34 (d, *J* = 14.9 Hz, 1H, H-29), 7.52-7.55 (m, 2H, H-34), 7.66 (t, 1H, *J* = 8.1 Hz, 1H, H-4), 7.75 (dd, *J* = 10.0, 14.9 Hz, 1H, H-30), 7.81 (ddd, *J* = 1.2, 6.9, 8.8 Hz, 1H, H-22), 8.01 (ddd, *J* = 1.1, 6.9, 8.1 Hz, 1H, H-21), 8.04 (dd, *J* = 1.3, 8.2 Hz, 1H, H-3), 8.14 (dq, *J* = 0.9, 0.9, 0.9, 8.8 Hz, 1H, H-23), 8.29 (bd, *J* = 8.1 Hz, 1H, H-20), 8.55 (bd, *J* = 6.7 Hz, 1H, H-19), 9.03 (d, *J* = 6.7 Hz, 1H, H-18). **^{13}C NMR (151 MHz, acetone-d_6):** δ 16.8 (C-36), 16.9 (C-37), 26.0 (C-15), 26.8 (C-8), 50.1 (C-7), 55.8 (C-35), 56.2 (C-16), 115.4 (C-33), 120.1 (C-27), 123.7 (C-13), 124.8 (C-30), 125.7 (C-3), 126.4 (C-19), 126.9 (C-26), 128.7 (C-5), 128.7

(C-23), 129.0 (C-31), 129.1 (C-20), 129.7 (C-14), 130.1 (C-32), 132.6 (C-22), 136.1 (C-21), 137.5 (C-18), 138.6 (C-9), 139.9 (C-25), 140.7 (C-12), 141.8 (C-10), 142.4 (C-11), 143.0 (C-4), 143.2 (C-29), 146.4 (C-28), 148.1 (C-6), 151.7 (C-24), 154.8 (C-2), 162.1 (C-34). **IR (KBr):** $\tilde{\nu}$ (cm^{-1}) 517, 573, 638, 1030, 1155, 1259, 1485, 1577, 1589, 1626, 2483, 3074. **MS (ESI) *m/z* (%):** 261.1 [(M – $2CF_3SO_3^-$)$^{2+}$] (100), 521.2 [(M – $2CF_3SO_3^-$)$^{2+}$] (13), 671.2 [(M – $CF_3SO_3^-$)$^+$] (12). **HRMS ESI *m/z*:** calc. for [(M – $CF_3SO_3^-$)$^{2+}$] [($C_{38}H_{34}O_4N_2F_3S$)$^{2+}$] 671.2186, found 671.2183.

4,13-bis((*E*)-4-ethoxy-3-methoxystyryl)-6,7,10,11-tetrahydrodipyrido[2,1-a:1',2'-k][2,9] phenanthroline-5,12-diium trifluoromethanesulfonate (29)

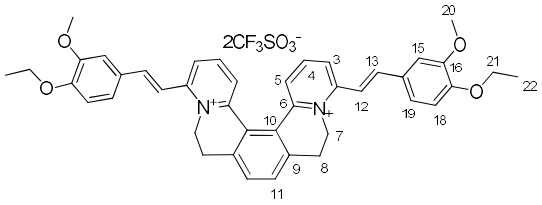

$C_{44}H_{42}F_6N_2O_{10}S_2$
[936.9]

The synthesis and purification of the [5]helquat dye **29** was accomplished by following *general procedure 5.2.e*, using helquat dye precursor **10** (50 mg, 0.082 mmol, 1.0 equiv.), 4-ethoxy-3-methoxybenzaldehyde (221.6 mg, 1.230 mmol, 15.0 equiv.), pyrrolidine (100 µL, 86.6 mg, 1.218 mmol, 14.9 equiv.) in dry MeOH (5.0 mL) and [5]helquat dye **29** was obtained as an orange solid.

Yield: 64.3 mg, 84%.

m.p. 263-265 °C. **^{1}H-NMR (600 MHz, DMSO-d_6):** δ 1.38 (t, *J* = 7.0 Hz, 6H, H-22), 3.23 (ddd, *J* = 4.5, 14.0, 17.1, 2H, H-8a), 3.36 (ddd, *J* = 2.0, 3.5, 17.1, 2H, H-8b), 3.90 (s, 6H, H-20), 4.12 (q, *J* = 7.0 Hz, 4H, H-21), 4.50 (dt, *J* = 3.5, 13.6, 13.6 Hz, 2H, H-7a), 5.40 (bdd, *J* = 2.0, 4.5, 13.4 Hz, 2H, H-7b), 7.11 (d, *J* = 8.0 Hz, 2H, H-19), 7.45 (dd, *J* = 2.1, 8.5 Hz, 2H, H-18), 7.55 (d, *J* = 2.1 Hz, 2H, H-15), 7.68 (d, *J* = 15.8 Hz, 2H, H-12), 7.79 (s, 2H), 7.85 (d, *J* = 15.8 Hz, 2H, H-13), 7.98 (dd, *J* = 1.3, 8.0 Hz, 2H, H-5), 8.15 (t, *J* = 7.9 Hz, 2H, H-4), 8.34 (dd, *J* = 1.3, 7.8 Hz, 2H, H-3). **^{13}C-NMR (151 MHz, DMSO-d_6):** δ 14.6 (C-22), 26.9 (C-8), 49.1 (C-7), 55.8 (C-20), 63.9 (C-21), 110.8 (C-15), 112.5 (C-19), 115.7 (C-12), 123.7 (C-18), 124.7 (C-3), 127.1 (C-10), 127.7 (C-14), 127.7 (C-5), 131.0 (C-11), 139.9 (C-9), 142.0 (C-4), 143.8 (C-13), 146.2 (C-6), 149.2 (C-16), 150.7 (C-17), 153.8 (C-2). **IR (KBr):** *v* (cm^{-1}) 637, 813, 822, 962, 1029, 1141, 1171, 1230, 1259, 1425, 1475, 1490, 1513, 1563, 1597, 1610, 1622, 2928, 2983, 3075. **MS (ESI) *m/z* (%):** 185.1 (23), 227.1 (91), 251.1 (17), 319.2 [(M – $2CF_3SO_3^-$)$^{2+}$] (100), 319.7 (45), 320.2 (10), 413.3 (5), 637.3 (5), 787.3 (3). **HRMS ESI *m/z*:** calc. for [(M – $2CF_3SO_3^-$)$^{2+}$] [($C_{42}H_{42}O_4N_2$)$^{2+}$] 319.1567, found 319.1566.

4,13-bis((*E*)-3-ethoxy-4-methoxystyryl)-6,7,10,11-tetrahydrodipyrido[2,1-a:1',2'-k][2,9] phenanthroline-5,12-diium trifluoromethanesulfonate (30)

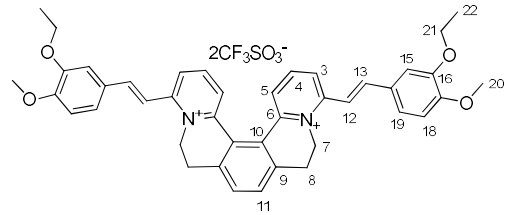

$C_{44}H_{42}F_6N_2O_{10}S_2$
[936.9]

The synthesis and purification of the [5]helquat dye **30** was accomplished by following *general procedure 5.2.e*, using helquat dye precursor **10** (50 mg, 0.082 mmol, 1.0 equiv.), 3-

ethoxy-4-methoxybenzaldehyde (221.6 mg, 1.230 mmol, 15.0 equiv.), pyrrolidine (100 µL, 86.6 mg, 1.218 mmol, 14.9 equiv.) in dry MeOH (5.0 mL) and [5]helquat dye **30** was obtained as an orange solid.

Yield: 65 mg, 85%.

m.p. 268-270 °C. **^{1}H-NMR (400 MHz, DMSO-d_6):** δ 1.40 (t, *J* = 7.0 Hz, 6H, H-22), 3.23 (ddd, *J* = 4.5, 14.0, 17.1 Hz, 2H, H-8a), 3.36 (ddd, *J* = 2.0, 3.5, 17.1, 2H, H-8b), 3.86 (s, 6H, H-20), 4.12 (q, *J* = 7.0 Hz, 4H, H-21), 4.50 (dt, *J* = 3.5, 13.6, 13.6 Hz, 2H, H-7a), 5.40 (bdd, *J* = 2.0, 4.5, 13.4 Hz, 2H, H-7b), 7.12 (d, *J* = 8.5 Hz, 2H, H-19), 7.45 (dd, *J* = 1.8, 7.4 Hz, 2H, H-18), 7.55 (d, *J* = 1.8 Hz, 2H, H-15), 7.68 (d, *J* = 15.8 Hz, 2H, H-12), 7.79 (s, 2H, H-11), 7.85 (d, *J* = 15.8 Hz, 2H, H-13), 7.98 (dd, *J* = 1.0, 8.0 Hz, 2H, H-5), 8.15 (t, *J* = 8.1 Hz, 2H, H-4), 8.34 (dd, *J* = 1.1, 8.4 Hz, 2H, H-3). **^{13}C-NMR (101 MHz, DMSO-d_6):** δ 14.7 (C-22), 26.9 (C-8), 49.2 (C-7), 55.7 (C-20), 64.1 (C-21), 111.7 (C-22), 111.8, 115.7 (C-12), 123.7 (C-18), 124.7 (C-3), 127.1 (C-10), 127.7 (C-13), 127.8 (C-14), 131.0 (C-11), 140.0 (C-9), 142.0 (C-4), 143.8 (C-13), 146.5 (C-6), 148.3 (C-16), 151.6 (C-17), 153.9 (C-3). IR (KBr): *v* (cm^{-1}) 639, 1031, 1261, 1490, 1513, 1562, 1596, 1610, 2929, 2979, 3403. **MS (ESI) *m/z* (%):** 305.1 (10), 319.2 [(M – $2CF_3SO_3^-$)$^{2+}$] (100), 319.7 (46), 320.2 (11), 637.3 (4), 787.3 (15), 788.3(10). **HRMS ESI *m/z*:** calc. for [(M – $2CF_3SO_3^-$)$^{2+}$] [($C_{42}H_{42}O_4N_2$)$^{2+}$] 319.1567, found 319.1567.

4,13-bis((*E*)-2,4,6-trimethoxystyryl)-6,7,10,11-tetrahydrodipyrido[2,1-a:1',2'-k][2,9] phenanthroline-5,12-diium trifluoromethanesulfonate (31)

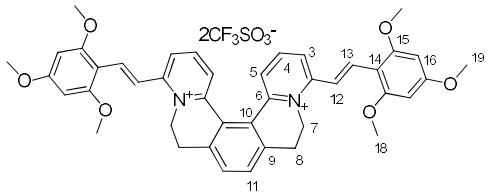

The synthesis and purification of the [5]helquat dye **31** was accomplished by following *general procedure 5.2.e*, using helquat dye precursor **10** (50 mg, 0.082 mmol, 1.0 equiv.), 2,4,6-trimethoxybenzaldehyde (241.3 mg, 1.230 mmol, 15.0 equiv.), pyrrolidine (100 µL, 86.6 mg, 1.218 mmol, 14.9 equiv.) in dry MeOH (5.0 mL) and [5]helquat dye **31** was obtained as a yellow solid.

Yield: 72.8 mg, 92%.

m.p. 314-316 °C. **^{1}H-NMR (600 MHz, DMSO-d_6):** 3.18 (ddd, *J* = 4.3, 14.0, 17.0 Hz, 2H, H-8a), 3.30 (ddd, *J* = 1.9, 3.4, 17.0 Hz, 2H, H-8b), 3.90 (s, 12H, H-18), 3.95 (s, 6H, H-19), 4.48 (dt, *J* = 3.4, 13.6 Hz, 2H, H-7a), 5.06 (ddd, *J* = 1.9, 4.3, 13.3 Hz, 2H, H-7b), 6.41 (s, 4H, H-16), 7.76 (s, 2H, H-11), 7.76 (d, *J* = 16.0 Hz, 2H, H-12), 7.83 (d, *J* = 16.0 Hz, 2H, H-13), 7.94 (dd, *J* = 1.4, 8.1 Hz, 2H, H-5), 8.08 (t, *J* = 8.1 Hz, 2H, H-4), 8.19 (dd, *J* = 1.4, 8.1 Hz, 2H). **^{13}C-NMR (151 MHz, DMSO-d_6):** 26.9 (C-8), 49.9 (C-7), 55.7 (C-19), 56.3 (C-18), 91.2 (C-16), 105.3 (C-14), 117.4 (C-12), 124.7 (C-3), 127.0 (C-5), 127.2 (C-10), 130.8 (C-11), 134.2 (C-13), 139.8 (C-9), 141.9 (C-4), 146.2 (C-6), 155.4 (C-2), 160.8 (C-15), 163.6 (C-17). **IR (KBr):** *v* (cm^{-1}) 637, 808, 1029, 1124, 1156, 1270, 1456, 1473, 1552, 1560, 1575, 1660, 3076. **MS (ESI) *m/z* (%):** 335.2 (100), 336.2 (13), 819.3 (20), 820.3 (10). **HRMS ESI *m/z*:** calc. for [(M – $2CF_3SO_3^-$)$^{2+}$] [($C_{42}H_{42}O_6N_2$)$^{2+}$] 335.1516, found 335.1517.

4,13-bis((*E*)-4-(3-(dimethylamino)propoxy)styryl)-6,7,10,11-tetrahydrodipyrido[2,1-a:1',2'-k][2,9]phenanthroline-5,12-diium trifluoromethanesulfonate (32)

$C_{48}H_{52}F_6N_4O_8S_2$
[991.1]

The synthesis and purification of the [5]helquat dye **32** was accomplished by following *general procedure 5.2.e*, using helquat dye precursor **10** (50 mg, 0.082 mmol, 1.0 equiv.), 4-(3-(dimethylamino)propoxy)benzaldehyde (255 mg, 1.230 mmol, 15.0 equiv.), pyrrolidine (100 µL, 86.6 g, 1.218 mmol, 14.9 equiv.) in dry MeOH (5.0 mL) and [5]helquat dye **32** was obtained as a yellow solid.

Yield: 76 mg, 94%.

m.p. 315-317 °C. **^{1}H-NMR (acetontrile-d_3, 400 MHz):** 1.89-1.98 (m, 4H), 2.20 (s, 12H), 2.41 (t, *J* = 7.0 Hz, 4H), 3.12-3.34 (m, 4H), 4.12 (t, *J* = 6.4 Hz, 4H), 4.41-4.50 (m, 2H), 5.21-5.26 (m, 2H), 7.06 (dd, *J* = 2.0, 6.8 Hz, 4H), 7.43 (d, *J* = 15.9 Hz, 2H), 7.65 (d, *J* = 15.8 Hz, 2H), 7.67 (dd, *J* = 7.6, 6.2 Hz, 2H), 7.70 (s, 2H), 7.78 (dd, *J* = 2.0, 6.8 Hz, 4H), 8.01 (t, *J* = 8.1 Hz, 2H), 8.11 (dd, *J* = 8.3, 1.4 Hz, 2H). **^{13}C-NMR (acetontrile-d_3, 101 MHz):** 28.1, 28.1, 45.7, 50.6, 56.7, 67.5, 116.2, 116.2, 126.3, 128.1, 128.4, 129.1, 131.4, 132.5, 141.2, 143.6, 144.9, 147.8, 156.0, 162.7. **IR (KBr):** *v* (cm^{-1}) 637, 813, 822, 962, 1029, 1141, 1171, 1230, 1259, 1425, 1475, 1490, 1513, 1563, 1597, 1610, 1622, 2928, 2983, 3075. **MS (ESI) *m/z* (%):** 281.5 (7), 303.7 (57), 346.2 (100), 346.7 (49), 347.2 (13), 521.2 (40), 522.2 (15), 606.3 (18), 607.3 (7), 692.4 (5), 841.4 (6). **HRMS ESI *m/z*:** calc. for $[(M - 2CF_3SO_3^-)^{2+}]$ $[(C_{46}H_{52}O_2N_4)^{2+}]$ 346.2040, found 346.2035.

4,13-bis((E)-3,4-dimethoxystyryl)-6,7,10,11-tetrahydrodipyrido[2,1-a:1',2'-k][2,9]phenanthroline-5,12-diium trifluoromethanesulfonate (33)

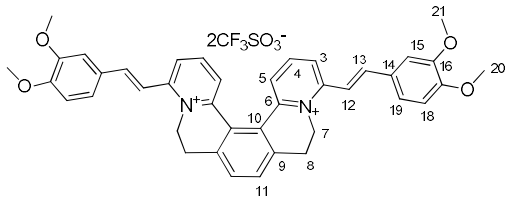

$C_{42}H_{38}F_6N_2O_{10}S_2$
[908.9]

The synthesis and purification of the [5]helquat dye **33** was accomplished by following *general procedure 5.2.e*, using helquat dye precursor **10** (50 mg, 0.082 mmol, 1.0 equiv.), 3,4-dimethoxybenzaldehyde (204.4 mg, 1.230 mmol, 15.0 equiv.), pyrrolidine (100 µL, 86.6 mg, 1.218 mmol, 14.9 equiv.) in dry MeOH (5.0 mL) and [5]helquat dye **33** was obtained as a yellow solid.

Yield: 69.7 mg, 94%.

m.p. 264-266 °C. **^{1}H-NMR (400 MHz, DMSO-d_6):** δ 3.23 (ddd, *J* = 4.5, 14.0, 17.1 Hz, 2H, H-8a), 3.36 (ddd, *J* = 2.0, 3.5, 17.1 Hz, 2H, H-8b), 3.86 (s, 6H, H-20), 3.90 (s, 6H, H-21), 4.50 (dt, *J* = 3.5, 13.6, 13.6 Hz, 2H, H-7a), 5.40 (bdd, *J* = 2.0, 4.5, 13.4 Hz, 2H, H-7b), 7.12 (d, *J* = 8.5 Hz, 2H, H-19), 7.46 (dd, *J* = 1.9, 8.5 Hz, 2H, H-18), 7.56 (d, *J* = 1.9 Hz, 2H, H-15), 7.70 (d, *J* = 15.8 Hz, 2H, H-12), 7.79 (s, 2H, H-11), 7.86 (d, *J* = 15.8 Hz, 2H, H-13), 7.99 (td, *J* = 0.3, 8.1 Hz, 2H, H-5), 8.15 (t, *J* = 8.1 Hz, 2H, H-4), 8.34 (dd, *J* = 1.3, 8.1 Hz, 2H, H-3). **^{13}C-NMR (101 MHz, DMSO-d_6):** δ 26.2 (C-8), 49.2 (C-7), 55.7 (C-20), 55.9 (C-21), 110.7 (C-15), 111.7 (C-19), 115.8 (C-12), 123.7 (C-18), 124.7 (C-3), 127.1 (C-10), 127.7 (C-14), 127.8 (C-5), 131.1 (C-11), 140.0

(C-9), 142.0 (C-4), 143.8 (C-13), 146.5 (C-6), 149.1 (C-16), 151.5 (C-17), 153.9 (C-2). **IR (KBr):** *v* (cm^{-1}) 639, 1031, 1143, 1262, 1424, 1473, 1491, 1514, 1563, 1623, 2840, 3076, 3434. **MS (ESI) *m/z* (%):** 231.2 (22), 305.2 [$(M - 2CF_3SO_3^-)^{2+}$] (100), 305.8 (58), 306.3, 461.4 (29), 462.4 (12), 609.5 (19), 611.5 (21), 612.5 (9), 723.6 (21), 759.5 (74), 760.6 (35). **HRMS ESI *m/z*:** calc. for [$(M - 2CF_3SO_3^-)^{2+}$] [$(C_{40}H_{38}O_4N_2)^{2+}$] 305.1410, found 305.1410.

(*E*)-4-(4-ethoxy-3-methoxystyryl)-6,7,10,11-tetrahydrodipyrido[2,1-a:1',2'-k][2,9] phenanthroline-5,12-diium trifluoromethanesulfonate (34)

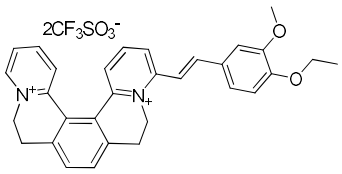

$C_{33}H_{30}F_6N_2O_8S_2$
[760.7]

The synthesis and purification of the [5]helquat dye **34** was accomplished by following *general procedure 5.2.e*, using helquat dye precursor **14** (50 mg, 0.084 mmol, 1.0 equiv.), 4-ethoxy-3-methoxybenzaldehyde (227.1 mg, 1.260 mmol, 15.0 equiv.), pyrrolidine (103 µL, 89.2 mg, 1.254 mmol, 14.9 equiv.) in dry MeOH (5.0 mL) and [5]helquat dye **34** was obtained as a yellow solid.

Yield: 61.1 mg, 96%.

m.p. 231-233 °C. **^{1}H-NMR (400 MHz, DMSO-d_6):** δ 1.37 (t, *J* = 7.0 Hz, 3H), 3.23 (ddd, *J* = 4.5, 14.0, 17.1, 2H), 3.36 (ddd, *J* = 2.0, 3.5, 17.1, 2H), 3.90 (s, 3H), 4.12 (q, *J* = 7.0 Hz, 2H), 4.45 (dt, *J* = 3.5, 13.6, 13.6 Hz, 1H), 4.83 (dt, *J* = 3.5, 13.6, 13.6 Hz, 1H), 5.04 (bdd, *J* = 2.0, 4.5, 13.4 Hz, 1H), 5.40 (bdd, *J* = 2.0, 4.5, 13.4 Hz, 1H), 7.10 (d, *J* = 8.4 Hz, 1H), 7.45 (dd, *J* = 1.9, 8.4 Hz, 1H), 7.55 (d, *J* = 1.9 Hz, 1H), 7.69 (d, *J* = 15.8 Hz, 1H), 7.77 (d, *J* = 7.8 Hz, 1H), 7.80 (d, *J* = 7.9 Hz, 1H), 7.87 (d, *J* = 15.8 Hz, 1H), 8.01-8.06 (m, 2H), 8.17 (t, *J* = 8.2 Hz, 1H), 8.20 (d, *J* = 8.2 Hz, 1H), 8.28 (t, *J* = 8.0 Hz, 1H), 8.36 (d, *J* = 8.2 Hz, 1H), 9.19 (d, *J* = 6.1 Hz, 1H). **^{13}C-NMR (101 MHz, DMSO-d_6):** 14.6, 26.9, 49.2, 54.4, 55.82, 63.9, 110.8, 112.5, 115.7, 119.1, 122.3, 123.7, 124.9, 126.1, 126.3, 127.1, 127.6, 127.7, 129.6, 131.5, 131.6, 140.1, 142.2, 143.9, 144.1, 145.8, 146.1, 146.6, 149.7, 150.7, 154.0. **IR (KBr):** *v* (cm^{-1}) 638, 1031, 1156, 1261, 1425, 1478, 1490, 1512, 1564, 1596, 1625, 2986, 3078, 3499. **MS (ESI) *m/z* (%):** 217.1 (9), 231.1 [$(M - 2CF_3SO_3^-)^{2+}$] (100), 231.6 (35), 232.1 (5), 461.2 (8), 611.2 (100), 612.2 (35). **HRMS ESI *m/z*:** calc. for [$(M - 2CF_3SO_3^-)^{2+}$] [$(C_{31}H_{30}O_2N_2)^{2+}$] 231.1148, found 231.1149.

(*E*)-4-(3-ethoxy-4-methoxystyryl)-6,7,10,11-tetrahydrodipyrido[2,1-a:1',2'-][2,9] phenanthroline-5,12-diium trifluoromethanesulfonate (35)

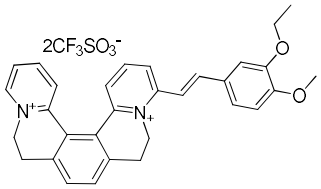

$C_{33}H_{30}F_6N_2O_8S_2$
[760.7]

The synthesis and purification of the [5]helquat dye **35** was accomplished by following *general procedure 5.2.e*, using helquat dye precursor **14** (50 mg, 0.084 mmol, 1.0 equiv.), 3-ethoxy-4-methoxybenzaldehyde (227.1 mg, 1.260 mmol, 15.0 equiv.), pyrrolidine (103 µL, 89.2 mg, 1.254 mmol, 14.9 equiv.) in dry MeOH (5.0 mL) and [5]helquat dye **35** was obtained as a yellow solid.

Yield: 52.8 mg, 83%.

m.p. 260-262 °C. **^{1}H-NMR (400 MHz, DMSO-d_6):** δ 1.40 (t, *J* = 7.0 Hz, 3H), 3.23 (ddd, *J* = 4.5, 14.0, 17.1 Hz, 2H), 3.36 (ddd, *J* = 2.0, 3.5, 17.1 Hz, 2H), 3.86 (s, 3H), 4.12 (q, *J* = 7.0 Hz, 2H), 4.45 (dt, *J* = 3.5, 13.6, 13.6 Hz, 1H), 4.83 (dt, *J* = 3.5, 13.6, 13.6 Hz, 1H), 5.04 (bdd, *J* = 2.0, 4.5, 13.4 Hz, 1H), 5.40 (bdd, *J* = 2.0, 4.5, 13.4 Hz, 1H),7.12 (d, *J* = 8.5 Hz, 1H), 7.45 (dd, *J* = 2.0, 8.5 Hz, 1H), 7.55 (d, *J* = 2.0 Hz, 1H), 7.68 (d, *J* = 15.8 Hz, 1H), 7.77 (d, *J* = 7.8 Hz, 1H), 7.81 (d, *J* = 7.8 Hz, 1H), 7.86 (d, *J* = 15.8 Hz, 1H), 8.02-8.07 (m, 2H), 8.16 (t, *J* = 8.1 Hz, 1H), 8.20 (dd, *J* = 1.3, 8.3 Hz, 1H), 8.28 (td, *J* = 1.4, 8.0 Hz, 1H), 8.36 (dd, *J* = 1.4, 8.3 Hz, 1H), 9.19 (dd, *J* = 1.0, 6.3 Hz, 1H). **^{13}C-NMR (101 MHz, DMSO-d_6):** δ 14.7, 26.8, 26.9, 49.2, 54.3, 55.7, 64.1, 111.7, 111.8, 115.7, 122.3, 123.8, 124.9, 126.1, 126.3, 127.1, 127.6, 127.8, 129.6, 131.5, 131.5, 140.1, 142.2, 143.9, 144.1, 145.7, 146.1, 146.6, 148.3, 151.6, 154.0. **IR (KBr):** *v* (cm^{-1}) 518, 640, 1031, 1143, 1162, 1261, 1436, 1478, 1490, 1513, 1564, 1596, 1612, 1625, 2984, 3076, 3438. **MS (ESI) *m/z* (%):** 231.1 [$(M - 2CF_3SO_3^-)^{2+}$] (100), 231.6 (35), 232.1 (5), 461.2 (8), 611.2 (100), 612.2 (35). **HRMS ESI *m/z*:** calc. for [$(M - 2CF_3SO_3^-)^{2+}$] [$(C_{31}H_{30}O_2N_2)^{2+}$] 231.1148, found 231.1149.

(*E*)-4-(3,4-dimethoxystyryl)-6,7,10,11-tetrahydrodipyrido[2,1-a:1',2'-k][2,9]phenanthroline -5,12-diium trifluoromethanesulfonate (36)

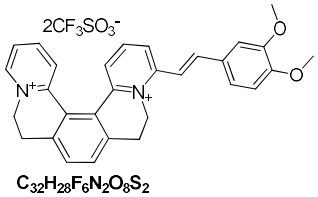

$C_{32}H_{28}F_6N_2O_8S_2$
[746.7]

The synthesis and purification of the [5]helquat dye **36** was accomplished by following *general procedure 5.2.e*, using helquat dye precursor **14** (50 mg, 0.084 mmol, 1.0 equiv.), 3,4-methoxybenzaldehyde (209.4 mg, 1.260 mmol, 15.0 equiv.), pyrrolidine (103 µL, 89.2 mg, 1.254 mmol, 14.9 equiv.) in dry MeOH (5.0 mL) and [5]helquat dye **36** was obtained as a yellow solid.

Yield: 51.8 mg, 83%.

m.p. 272-273 °C. **^{1}H-NMR (400 MHz, DMSO-d_6):** δ 3.23 (ddd, *J* = 4.5, 14.0, 17.1 Hz, 2H), 3.36 (ddd, *J* = 2.0, 3.5, 17.1 Hz, 2H), 3.86 (s, 3H), 3.90 (s, 3H), 4.45 (dt, *J* = 3.5, 13.6, 13.6 Hz, 1H), 4.83 (dt, *J* = 3.5, 13.6, 13.6 Hz, 1H), 5.04 (bdd, *J* = 2.0, 4.5, 13.4 Hz, 1H), 5.40 (bdd, *J* = 2.0, 4.5, 13.4 Hz, 1H), 7.12 (d, *J* = 8.0 Hz, 1H), 7.47 (dd, *J* = 2.0, 8.4 Hz, 1H), 7.56 (d, *J* = 2.0 Hz, 1H), 7.70 (d, *J* = 15.9 Hz, 1H), 7.77 (d, *J* = 7.8 Hz, 1H), 7.81 (d, *J* = 7.8 Hz, 1H), 7.88 (d, *J* = 15.9 Hz, 1H), 8.02-8.07 (m, 2H), 8.16 (d, *J* = 8.1 Hz, 1H), 8.20 (dd, *J* = 1.8, 8.8 Hz, 1H), 8.28 (ddd, *J* = 1.4, 7.7, 8.6 Hz, 1H), 8.37 (dd, *J* = 1.4, 8.3 Hz, 1H), 9.19 (dd, *J* = 1.4, 6.2 Hz, 1H). **^{13}C-NMR (101 MHz, DMSO-d_6):** δ 26.8, 26.9, 49.2, 54.4, 55.7, 55.9, 110.7, 111.7, 115.8, 116.8, 123.8, 124.9, 126.1, 126.3, 127.1, 127.6, 127.8, 129.6, 131.5, 131.6, 140.1, 142.2, 143.9, 144.1, 145.8, 146.1, 146.6, 149.1, 151.5, 154.0. **IR (KBr):** *v* (cm^{-1}) 519, 640, 1032, 1162, 1232, 1262, 1425, 1478, 1490, 1513, 1564, 1596, 1625, 2837, 3074, 3439. **MS (ESI) *m/z* (%):** 202.1 (5), 216.1 (14), 224.1 [$(M - 2CF_3SO_3^-)^{+2}$] (100), 224.6 (31), 225.1 (7), 447.2 (25), 448.2 (12), 479.2 (7), 597.2 (62), 598.2 (22). **HRMS ESI *m/z*:** calc. for [$(M - 2CF_3SO_3^-)^{+2}$] [$(C_{30}H_{28}O_2N_2)^{2+}$] 224.1070, found 224.1070.

(*E*)-4-(2-(naphthalen-1-yl)vinyl)-6,7,10,11-tetrahydrodipyrido[2,1-a:1',2'-k][2,9]phenanthroline-5,12-diium trifluoromethanesulfonate (37)

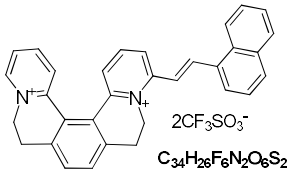

$C_{34}H_{26}F_6N_2O_6S_2$
[736.7]

The synthesis and purification of the [5]helquat dye **37** was accomplished by following *general procedure 5.2.e*, using helquat dye precursor **14** (50 g, 0.084 mmol, 1.0 equiv.), 1-naphthylaldehyde (196.8 mg, 1.260 mmol, 15.0 equiv.), pyrrolidine (103 µL, 89.2 mg, 1.254 mmol, 14.9 equiv.) in dry MeOH (5.0 mL) and [5]helquat dye **37** was obtained as a yellow solid.

Yield: 52.3 mg, 85%.

m.p. 249-251 °C. **^{1}H-NMR (acetonitrile-d_3, 400 MHz):** δ 3.15-3.37 (m, 4H), 4.48-4.60 (m, 1H), 4.82-4.91 (m, 2H), 5.27-5.31 (m, 1H), 7.62-7.71 (m, 4H), 7.73 (s, 2H), 7.84 (d, *J* = 8.0 Hz, 1H), 7.90 (ddd, *J* = 7.7, 6.1, 1.4 Hz, 1H), 7.98 (d, *J* = 8.4 Hz, 1H), 8.02 (dd, *J* = 1.4, 7.8 Hz, 1H), 8.09 (d, *J* = 8.2 Hz, 1H), 8.15 (t, *J* = 8.1, 1H), 8.12 (d, *J* = 7.3 Hz, 1H), 8.20 (td, *J* = 8.0, 1.4 Hz, 1H), 8.31 (dd, *J* = 8.2, 1.3 Hz, 1H), 8.37 (d, *J* = 8.6 Hz, 1H), 8.49 (d, *J* = 15.7 Hz, 1H), 8.81 (d, *J* = 6.2 Hz, 1H). **^{13}C-NMR (acetonitrile-d_3, 101 MHz):** δ 28.0, 28.1, 51.0, 56.1, 121.9, 124.3, 126.8, 126.8, 127.1, 127.5, 127.5, 127.6, 128.1, 128.3, 129.8, 129.9, 131.2, 132.2, 132.3, 133.0, 133.1, 133.2, 134.8, 141.5, 141.6, 141.9, 144.3, 145.9, 146.8, 147.7, 148.0, 155.5.

IR: *v* (cm^-) 804, 841, 963, 1031, 1157, 1225, 1261, 1274, 1479, 1491, 1511, 1565, 1580, 1595, 1611, 1625. **MS (ESI) *m/z* (%):** 219.2 (8), 449.4 (8), 587.5 [$(M - CF_3SO_3^-)^+$] (100), 588.5 (39), 589.5 (10), 759.5 (5). **HRMS ESI *m/z*:** calc. for [$(M - 2CF_3SO_3^-)^{2+}$] [$(C_{32}H_{26}N_2)^{2+}$] 219.1043, found 219.1044.

(*E*)-4-(2-(benzo[b]thiophen-2-yl)vinyl)-6,7,10,11-tetrahydrodipyrido[2,1-a:1',2'-k][2,9]phenanthroline-5,12-diium trifluoromethanesulfonate (38)

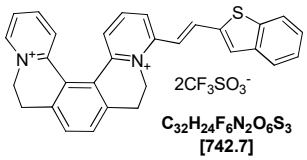

$C_{32}H_{24}F_6N_2O_6S_3$
[742.7]

The synthesis and purification of the [5]helquat dye **38** was accomplished by following *general procedure 5.2.e*, using helquat dye precursor **14** (50 mg, 0.084 mmol, 1.0 equiv.), benzo[*b*]thiophene-2-carbaldehyde (204.4 mg, 1.260 mmol, 15.0 equiv.), (103 µL, 89.2 mg, 1.254 mmol, 14.9 equiv.) in dry MeOH (5.0 mL) and [5]helquat dye **38** was obtained as a yellow solid.

Yield: 52.1 mg, 84%.

m.p. 223-225 °C. **^{1}H-NMR (acetonitrile-d_3, 400 MHz):** δ 3.21-3.43 (m, 4H), 4.49-4.56 (m, 2H), 4.81-4.90 (m, 2H), 7.38 (d, *J* = 15.7 Hz, 1H), 7.44 (ddd, *J* = 1.4, 1.4, 0.8 Hz, 1H), 7.48 (ddd, *J* = 1.6, 1.6, 0.8 Hz, 1H), 7.72 (s, 2H), 7.79 (dd, *J* = 1.4, 7.9 Hz, 1H), 7.82 (s, 1H), 7.89 (ddd, *J* = 1.4, 6.1, 7.6 Hz, 1H), 7.92-7.95 (m, 2H), 7.98 (dd, *J* = 15.7 Hz, 1H), 7.96-7.99 (m, 1H), 8.09 (t, *J* = 8.1 Hz, 1H), 8.16 (dd, *J* = 1.5, 8.3 Hz, 1H), 8.18 (dd, *J* = 1.5, 8.3 Hz, 1H), 8.80 (d, *J* = 0.8, 6.2 Hz, 1H). **^{13}C-NMR (acetonitrile-d_3, 101 MHz):** δ 28.0, 28.1, 50.9, 56.1, 119.8, 123.6, 126.0, 126.4, 126.9, 127.1, 127.5, 128.0, 128.0, 129.7, 131.2, 131.2, 133.1, 133.2, 138.2, 140.7, 140.8, 141.4, 141.5, 141.6, 144.2, 145.8, 146.7, 147.8, 148.0, 154.8. **IR:** *v* (cm^-) 726, 757, 826, 951, 1031, 1158, 1226, 1261, 1274, 1422, 1456, 1479, 1489, 1508, 1563, 1579, 1607, 1622.

MS (ESI) *m/z* (%): 222.1 (100), 593.1 (96), 594.1 (35), 595.1 (7). **HRMS ESI *m/z*:** calc. for [(M – $2CF_3SO_3^-$)$^{2+}$] [($C_{30}H_{24}N_2S$)$^{2+}$] 222.08246, found 222.08263.

(*E*)-8,9-dimethyl-4-(2-(naphthalen-1-yl)vinyl)-6,7,10,11-tetrahydrodipyrido[2,1-a:1',2'-k][2,9]phenanthroline-5,12-diium trifluoromethanesulfonate (39)

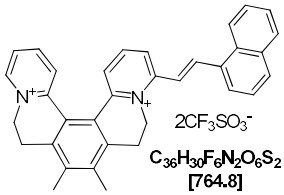

The synthesis and purification of the [5]helquat dye **39** was accomplished by following *general procedure 5.2.e*, using helquat dye precursor **16** (50 mg, 0.080 mmol, 1.0 equiv.), 1-naphthylaldehyde (187.4 mg, 1.200 mmol, 15.0 equiv.), pyrrolidine (98.5 µL, 85.3 mg, 1.200 mmol, 15.0 equiv.) in dry MeOH (5.0 mL) and [5]helquat dye **39** was obtained as a yellow solid.

Yield: 51.9 mg, 85%.

m.p. 283-285 °C. **^{1}H-NMR (acetonitrile-d_3, 400 MHz):** δ 2.44 (s, 6H), 2.99-313 (m, 2H), 3.41-3.50 (m, 2H), 4.50 (t, *J* = 14.1 Hz, 1H), 4.76 (t, *J* = 14.3 Hz, 1H), 4.95 (d, *J* = 13.3 Hz, 1H), 5.33 (d, *J*= 13.4 Hz, 1H), 7.62-7.72 (m, 5H), 7.83-7.87 (m, 2H), 8.02 (d, *J* = 7.8 Hz, 1H), 8.07-8.17 (m, 4H), 8.26 (dd, *J* = 1.3, 8.1 Hz, 1H), 8.38 (d, *J* = 8.4 Hz, 1H), 8.48 (d, *J* = 15.7 Hz, 1H), 8.76 (d, *J* = 6.8 Hz, 1H). **^{13}C-NMR (acetonitrile-d_3, 101 MHz):** δ 17.0, 17.2, 25.9, 26.7, 50.6, 56.0, 119.4, 120.6, 123.5, 125.7, 125.9, 126.4, 126.9, 128.1, 128.4, 129.2, 131.4, 132.8, 136.4, 137.0, 138.3, 138.6, 139.9, 140.6, 140.8, 141.3, 141.5, 142.3, 142.4, 143.7, 148.5, 149.5, 151.6, 154.0. **IR:** *v* (cm^-) 801, 810, 959, 1030, 1151, 1160, 1224, 1263, 1276, 1403, 1488, 1508, 1558, 1579, 1610, 1625. **MS (ESI) *m/z* (%):** 233.3 (7), 615.6 [(M – $CF_3SO_3^-$)$^+$] (100), 616.6 (40), 617.6 (10), 787.7 (5). **HRMS *m/z*:** calc. for [(M – $2CF_3SO_3^-$)$^{2+}$] [($C_{34}H_{30}N_2$)$^{2+}$] calc. 233.1199, found 233.1201.

(*E*)-8,9-dimethyl-4-(2-(4-methylnaphthalen-1-yl)vinyl)-6,7,10,11-tetrahydrodipyrido[2,1-a:1',2'-k][2,9]phenanthroline-5,12-diium trifluoromethanesulfonate (40)

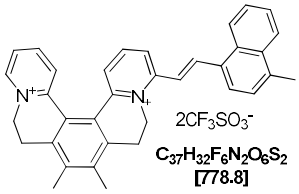

The synthesis and purification of the [5]helquat dye **40** was accomplished by following *general procedure 5.2.e*, using helquat dye precursor **16** (50 mg, 0.080 mmol, 1.0 equiv.), 4-methyl-1-naphthylaldehyde (204.2 mg, 1.200 mmol, 15.0 equiv.), pyrrolidine (98.5 µL, 85.3 mg, 1.200 mmol, 15.0 equiv.) in dry MeOH (5.0 mL) and [5]helquat dye **40** was obtained as a yellow solid.

Yield: 52.8 mg, 85%.

m.p. 242-244 °C. **^{1}H-NMR (acetonitrile-d_3, 400 MHz):** δ 2.44 (s, 6H), 2.79 (s, 3H), 2.97-3.14 (m, 2H), 3.41-3.51 (m, 2H), 4.47 (t, *J* = 13.9 Hz, 1H), 4.74 (t, *J* = 14.1 Hz, 1H), 4.93 (d, *J* = 13.4 Hz, 1H), 5.25 (d, *J* = 13.4 Hz, 1H), 7.54 (d, *J* = 7.4 Hz, 1H), 7.64-7.72 (m, 4H), 7.80 (dd, *J* = 1.0, 8.2 Hz, 1H), 7.83 (ddd, *J* = 1.5, 6.2 Hz, 1H), 8.03 (d, *J* = 7.4 Hz, 1H), 8.07 (t, *J* = 8.1 Hz, 1H), 8.14 (td, *J* = 8.1, 1.5 Hz, 1H), 8.18-8.20 (m, 1H), 8.26 (dd, *J* = 8.2, 1.3 Hz, 1H), 8.37-8.41 (m, 1H), 8.49 (d, *J* = 15.7 Hz, 1H), 8.74 (dd, *J* = 0.8, 6.2 Hz, 1H). **^{13}C-NMR (acetonitrile-d_3, 101 MHz):** δ 16.8, 16.9, 20.0, 26.2, 26.4, 50.6, 55.6, 120.7, 124.8, 125.1, 126.0, 126.1, 126.6, 126.7, 126.9, 127.4, 127.6, 127.9, 129.9, 131.3, 131.5, 132.3, 133.7, 139.6, 140.3, 140.4,

141.2, 141.3, 142.0, 143.9, 145.4, 146.1, 148.4, 148.8, 155.1. **IR:** *v* (cm^{-}) 765, 1031, 1166, 1225, 1260, 1273, 1485, 1508, 1558, 1576, 1611, 1623. **MS (ESI) *m/z* (%):** 240.3 (10), 629.5 [$(M - CF_3SO_3^-)^+$] (100), 630.5 (38), 631.6 (12), 801.6 (4). **HRMS *m/z*:** calc. for [$(M - 2CF_3SO_3^-)^{2+}$] [$(C_{35}H_{32}N_2)^{2+}$] 240.1277, found 240.1278.

(*E*)-4-(2-([1,1'-biphenyl]-4-yl)vinyl)-8,9-dimethyl-6,7,10,11-tetrahydrodipyrido[2,1-a:1',2'-k][2,9]phenanthroline-5,12-diium trifluoromethanesulfonate (41)

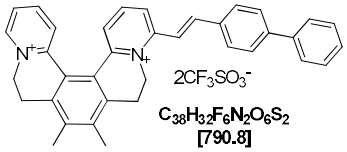

The synthesis and purification of the [5]helquat dye **41** was accomplished by following *general procedure 5.2.e*, using helquat dye precursor **16** (50 mg, 0.080 mmol, 1.0 equiv.), [1,1'-biphenyl]-4-carbaldehyde (218.6 mg, 1.200 mmol, 15.0 equiv.), pyrrolidine (98.5 µL, 85.3 mg, 1.200 mmol, 15.0 equiv.) in dry MeOH (5.0 mL) and [5]helquat dye **41** was obtained as a yellow solid.

Yield: 61.2 g, 97%.

m.p. 269-273 °C. **^{1}H-NMR (acetonitrile-d_3, 400 MHz):** δ 2.44 (s, 3H), 2.45 (s, 3H), 2.96-3.13 (m, 2H), 3.41-3.49 (m, 2H), 4.46 (t, *J* = 14.0 Hz, 1H), 4.73 (t, *J* = 14.1 Hz, 1H), 4.93 (d, *J* = 13.4 Hz, 1H), 5.32 (d, *J* = 13.6 Hz, 1H), 7.42-7.46 (m, 1H), 7.50-7.55 (m, 2H), 7.63 (dd, *J* = 8.1, 1.3 Hz, 1H), 7.64 (d, *J* = 16.0 Hz, 1H), 7.72-7.77 (m, 3H), 7.79 (dd, J = 1.2, 8.3 Hz, 1H), 7.82 (d, *J* = 8.6 Hz, 1H), 7.83-7.85 (m, 2H), 7.91-7.94 (m, 2H), 8.04 (t, J = 8.1 Hz, 1H), 8.10 (dd, *J* = 1.5, 8.5 Hz, 1H), 8.12 (dd, *J* = 8.4, 1.4 Hz, 1H), 8.74 (dd, J = 0.7, 6.2 Hz, 1H). **^{13}C-NMR (acetonitrile-d_3, 101 MHz):** δ 16.8, 16.9, 26.2, 26.3, 50.5, 55.6, 118.9, 125.1, 126.0, 126.3, 126.8, 128.0, 128.6, 129.2, 129.9, 130.1, 131.5, 135.0, 140.3, 140.4, 140.7, 141.1, 141.2, 143.9, 144.2, 144.3,145.4, 146.1, 148.5, 148.8, 155.1. **IR:** *v* (cm^{-}) 699, 833, 1006, 1030, 1160, 1224, 1261, 1275, 1412, 1450, 1488, 1509, 1577, 1559, 1603, 1610, 1625. **MS (ESI) *m/z* (%):** 246.1 (100), 246.6 (40), 247.1 (7), 491.2 (8), 641.2 (100), 642.2 (41), 643.2 (9). **HRMS ESI *m/z*:** calc. for [$(M - 2CF_3SO_3^-)^{2+}$] [$(C_{36}H_{32}N_2)^{2+}$] 246.1277, found 246.1277.

(*E*)-4-(2-(benzo[b]thiophen-2-yl)vinyl)-8,9-dimethyl-6,7,10,11-tetrahydrodipyrido[2,1-a:1',2'-k][2,9]phenanthroline-5,12-diium trifluoromethanesulfonate (42)

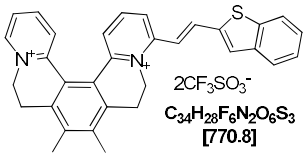

The synthesis and purification of the [5]helquat dye **42** was accomplished by following *general procedure 5.2.e*, using helquat dye precursor **16** (50 mg, 0.080 mmol, 1.0 equiv.), benzo[*b*]thiophene-2-carbaldehyde (194.6 mg, 1.200 mmol, 15.0 equiv.), pyrrolidine (98.5 µL, 85.3 mg, 1.200 mmol, 15.0 equiv.) in dry MeOH (5.0 mL) and [5]helquat dye **42** was obtained as a yellow solid.

Yield: 46.7 mg, 76%.

m.p. 309-311 °C. **^{1}H-NMR (acetonitrile-d_3, 400 MHz):** δ 2.43 (s, 3H), 2.44 (s, 3H), 2.96-3.13 (m, 2H), 3,43-3.50 (m, 2H), 4.47 (t, *J* = 13.9 Hz, 1H), 4.74 (t, *J* = 14.1 Hz, 1H), 4.93 (d, *J* = 13.4 Hz, 1H), 5.25 (d, *J* = 13.4 Hz, 1H), 7.39 (d, *J* = 15.7 Hz, 1H), 7.44-7.52 (m, 2H), 7.66 (dd, *J* = 8.0, 1.4 Hz, 1H), 7.84 (ddd, *J* = 7.6, 6.1, 1.4 Hz, 1H), 7.81 (s, 1H), 7.79 (ddd, *J* = 8.4, 1.5, 0.5 Hz, 1H), 7.92-8.01 (m, 3H), 8.04 (t, *J* = 8.1, 1H), 8.10 (td, *J* = 1.52, 7.98 Hz, 1H), 8.12 (dd, *J* = 1.4, 8.2 Hz, 1H), 8.74 (dd, *J* = 0.9, 6.2 Hz, 1H). **^{13}C-NMR (acetonitrile-d_3, 101 MHz):** δ 16.8, 16.9,

26.2, 26.3, 50.6, 55.6, 119.7, 123.6, 125.1, 126.0, 126.3, 126.4, 126.9, 128.0, 130.1, 131.1, 131.5, 131.5, 138.0, 140.3, 140.4, 140.7, 140.8, 141.2, 141.3, 141.5, 143.9, 145.4, 146.1, 148.6, 148.7, 154.2. **IR:** *v* (cm^{-}) 728, 757, 832, 1031, 1158, 1224, 1261, 1272, 1401, 1457, 1485, 1508, 1556, 1577, 1621. **MS (ESI) *m/z* (%):** 236.1 [$(M - 2CF_3SO_3^-)^{2+}$] (100), 236.6 (35), 237.1 (4), 593.1 (7), 621.1 (75), 622.1 (27), 623.1 (5). **HRMS *m/z:*** calc. for [$(M - 2CF_3SO_3^-)^{2+}$] [$(C_{32}H_{28}N_2S)^{2+}$] 236.0981, found 236.0982.

(*E*)-8,9-dimethyl-4-(2,4,6-trimethoxystyryl)-6,7,10,11-tetrahydrodipyrido[2,1-a:1',2'-k][2,9]phenanthroline-5,12-diium trifluoromethanesulfonate (43)

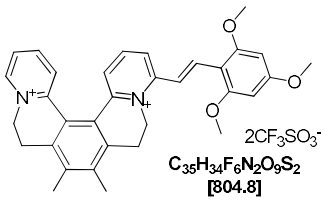

The synthesis and purification of the [5]helquat dye **43** was accomplished by following *general procedure 5.2.e*, using helquat dye precursor **16** (50 mg, 0.080 mmol, 1.0 equiv.), 2,4,6-trimethoxybenzaldehyde (235.4 mg, 1.200 mmol, 15.0 equiv.), pyrrolidine (98.5 µL, 85.3 mg, 1.200 mmol, 15.0 equiv.) in dry MeOH (5.0 mL) and [5]helquat dye **43** was obtained as a yellow solid.

Yield: 46.9 mg, 73.2%.

m.p. 315-317 °C. **^{1}H-NMR (acetonitrile-d_3, 400 MHz):** δ 2.43 (s, 3H), 2.44 (s, 3H), 2.96-3.13 (m, 2H), 3,43-3.50 (m, 2H), 3.90 (s, 3H), 3.97 (s, 6H), 4.47 (t, *J* = 13.9 Hz, 1H), 4.74 (t, *J* = 14.1 Hz, 1H), 4.93 (d, *J* = 13.4 Hz, 1H), 5.25 (d, *J* = 13.4 Hz, 1H), 6.33 (s, 2H), 7.50 (dd, *J* = 1.3, 7.9 Hz, 1H), 7.74 (dd, *J* = 1.3, 8.4 Hz, 1H), 7.82 (ddd, *J* = 1.4, 6.2, 7.6 Hz, 1H), 7.86 (d, *J* = 16.0 Hz, 1H), 7.91 (d, *J* = 8.1 Hz, 1H), 7.96 (d, *J* = 16.0 Hz, 1H), 8.04 (dd, *J* = 1.4, 8.3 Hz, 1H), 8.09 (td, *J* = 1.5, 8.1 Hz, 1H), 8.73 (dd, *J* = 1.4, 6.2 Hz, 1H). **^{13}C-NMR (acetonitrile-d_3, 101 MHz):** δ 16.8, 26.3, 26.4, 49.8, 55.6, 56.4, 57.0, 92.0, 106.8, 117.8, 120.1, 125.0, 125.4, 126.3, 126.8, 128.6, 131.4, 136.3, 140.2, 140.3, 140.8, 141.1, 143.1, 145.3, 146.0, 147.8, 148.9, 157.5, 162.5, 165.3. **IR:** *v* (cm^{-}) 517, 573, 637, 856, 1030, 1157, 1223, 1261, 1440, 2844. **MS (ESI) *m/z* (%):** 253.1 (59), 253.6 (20), 505.2 (18), 655.2 (100), 656.2 (32). **HRMS ESI *m/z***: calc. for [$(M - 2CF_3SO_3^-)^{2+}$] [$(C_{33}H_{33}N_2O_3)^{2+}$] 505.24857, found 505.24835.

(*E*)-4-(4-ethoxy-3-methoxystyryl)-1-methylpyridin-1-ium iodide (44)

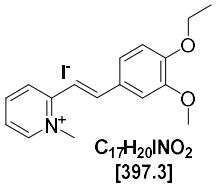

The synthesis and purification of pyridinium dye **44** was accomplished using *general procedure 5.2.f. method 1*. Pyridinium dye **44** was obtained as a yellow amorphous solid.

Yield: 43.1 mg, 85%.

m.p. 235-237 °C. **^{1}H-NMR (400 MHz, DMSO- d_6):** δ 1.36 (t, *J* = 7.0 Hz, 3H), 3.87 (s, 3H), 4.10 (q, *J* = 7.0 Hz, 2H), 4.37 (s, 3H), 7.07 (d, *J* = 8.4 Hz, 1H), 7.38 (dd, *J* = 2.0, 8.4 Hz, 1H), 7.45 (d, *J* = 15.9 Hz, 1H), 7.49 (d, *J* = 2.0 Hz, 1H), 7.85 (td, *J* = 2.2, 6.5 Hz, 1H), 7.91 (d, *J* = 15.9 Hz, 1H), 8.43-8.50 (m, 2H), 8.86 (dt, *J* = 0.9, 6.2 Hz, 1H). **^{13}C-NMR (101 MHz, DMSO- d_6):** δ 14.6, 46.0, 55.8, 63.9, 110.7, 112.4, 114.7, 123.7, 124.4, 124.4, 127.6, 143.4, 143.9, 145.8, 149.1, 150.7, 152.8. **IR (KBr) *v* (cm^{-1}):** 517, 537, 569, 643, 800, 921, 1032, 1145, 1185, 1233, 1427, 1442, 1459, 1484, 1516, 1565, 1577, 1539, 1613, 1631, 2832, 3033, 3428. **MS (ESI) *m/z* (%):** 270.2

(100), 271.2 (19), 450.2 (5). **HRMS ESI *m/z*:** calc. for [(M – I^-)$^+$] [($C_{17}H_{20}O_2N$)$^+$] 270.1489, found 270.1489.

(*E*)-4-(3-ethoxy-4-methoxystyryl)-1-methylpyridin-1-ium iodide (45)

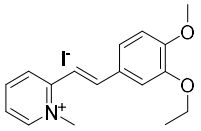

$C_{17}H_{20}INO_2$
[397.3]

The synthesis and purification of pyridinium dye **45** was accomplished using *general procedure 5.2.f. method 1*. Pyridinium dye **45** was obtained as a yellow amorphous solid.
Yield: 45.1 mg, 89%.
m.p. 233-235 °C. **^{1}H-NMR (400 MHz, DMSO-d_6):** δ 1.38 (t, *J* = 7.0 Hz, 3H), 3.84 (s, 3H), 4.11 (q, *J* = 7.0 Hz, 2H), 4.36 (s, 3H), 7.09 (d, *J* = 8.4 Hz, 1H), 7.39 (dd, *J* = 2.0, 8.4 Hz, 1H), 7.44 (d, *J* = 15.9 Hz, 1H), 7.48 (d, *J* = 2.0 Hz, 1H), 7.85 (td, *J* = 2.8, 6.2 Hz, 1H), 7.90 (d, *J* = 15.9 Hz, 1H), 8.41-8.51 (m, 2H), 8.86 (dt, *J* = 0.9, 6.2 Hz, 1H). **^{13}C-NMR (101 MHz, DMSO- d_6):** δ 14.7, 46.0, 55.7, 64.0, 111.7, 111.8, 114.7, 123.7, 124.4, 124.4, 127.7, 143.4, 143.9, 145.8, 148.3, 151.6, 152.8. **IR (KBr):** *v* (cm^{-1}): 543, 637, 773, 814, 855, 900, 974, 1022, 1041, 1148, 1171, 1181, 1238, 1268, 1331, 1440, 1461, 1514, 1566, 1577, 1592, 1616, 1631, 2036, 2838, 2931, 2980, 3034, 3070, 3431. **MS (ESI) *m/z* (%):** 270.2 (100), 271.2 (22), 539.3 (5), 667.2 (3). **HRMS ESI *m/z*:** calc. for [(M – I^-)$^+$] [($C_{17}H_{20}O_2N$)$^+$] 270.1489, found 270.1489.

(*E*)-4-(3,4-dimethoxystyryl)-1-methylpyridin-1-ium iodide (46)

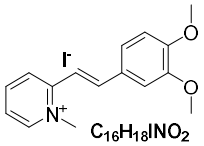

$C_{16}H_{18}INO_2$
[383.2]

The synthesis and purification of pyridinium dye **46** was accomplished using *general procedure 5.2.f. method 1*. Pyridinium dye **46** was obtained as a yellow amorphous solid.
Yield: 42.1 g, 86%.
m.p. 235-237 °C. **^{1}H-NMR (400 MHz, DMSO- d_6):** δ 3.84 (s, 3H), 3.87 (s, 3H), 4.36 (s, 3H), 7.09 (d, *J* = 8.4 Hz, 1H), 7.40 (dd, *J* = 2.0, 8.4 Hz, 1H), 7.46 (d, *J* = 15.9 Hz, 1H), 7.49 (d, *J* = 2.0 Hz, 1H), 7.85 (td, *J* = 2.5, 6.4 Hz, 1H), 7.91 (d, *J* = 15.9 Hz, 1H), 8.40-8.53 (m, 2H), 8.86 (dt, *J* = 0.9, 6.2 Hz, 1H). **^{13}C-NMR (101 MHz, DMSO- d_6):** δ 46.0, 55.7, 55.9, 110.6, 111.7, 114.8, 123.7, 124.4, 124.4, 127.7, 143.4, 143.93, 145.82, 149.06, 151.43, 152.77. **IR (KBr):** *v* (cm^{-1}) 543, 589, 617, 637, 773, 814, 900, 1022, 1041, 1109, 1148, 1171, 1181, 1238, 1268, 1331, 1401, 1440, 1461, 1514, 1566, 1577, 1592, 1616, 1631, 2036, 2836, 2931, 2971, 2980, 3034, 3070, 3142, 3431**. MS (ESI) *m/z* (%):** 256.2 (100), 257.2 (22). **HRMS ESI *m/z*:** calc. for [(M – I^-)$^+$] [($C_{16}H_{18}O_2N$)$^+$] 256.13321, found 256.13323.

(*E*)-1-methyl-2-(2-(naphthalen-1-yl)vinyl)pyridin-1-ium iodide (47)

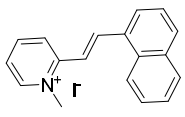

$C_{18}H_{16}IN$
[373.2]

The synthesis and purification of pyridinium dye **47** was accomplished using *general procedure 5.2.f. method 2*. Pyridinium dye **47** was obtained as a yellow amorphous solid.
Yield: 47.1 mg, 99%.

m.p. 254-256 °C. **^{1}H-NMR (DMSO-d_6, 400 MHz):** δ 4.43 (s, 3H), 7.60-7.73 (m, 4H), 7.97 (ddd, *J* = 1.5, 6.2, 7.6 Hz, 1H), 8.01-8.06 (m, 1H), 8.10 (d, *J* = 8.2 Hz, 1H), 8.22 (dt, *J* = 0.8, 7.3 Hz, 1H), 8.53-8.56 (m, 1H), 8.58 (dd, *J* = 1.4, 7.9 Hz, 1H), 8.74 (d, *J* = 15.8 Hz, 1H), 8.84 (dd, *J* = 1.4, 8.2 Hz, 1H), 8.96 (dt, *J* = 0.8, 6.2 Hz, 1H). **^{13}C-NMR (DMSO-d_6, 101 MHz):** δ 46.1, 120.1, 121.4, 123.7, 125.4, 125.7, 125.7, 126.5, 127.1, 128.7, 131.0, 131.0, 131.9, 133.3, 139.3, 144.4, 146.1, 152.1.
IR (KBr): *v* (cm^{-1}) 794, 832, 1143, 1170, 1459, 1510, 1517, 1575, 1597, 1638**. MS (ESI) *m/z* (%):** 246.1 (100), 247.1 (21), 491.3 (5). **HRMS ESI *m/z*:** calc. for [(M – I^-)$^+$] [($C_{18}H_{16}N$)$^+$] 246.1277, found 246.1277.

(*E*)-2-(2-(benzo[b]thiophen-2-yl)vinyl)-1-methylpyridin-1-ium iodide (48)

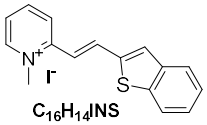

The synthesis and purification of pyridinium dye **48** was accomplished using *general procedure 5.2.f. method 2*. Pyridinium dye **48** was obtained as a yellow amorphous solid.
Yield: 42.1 g, 87%.
m.p. 221-223 °C. **^{1}H-NMR (DMSO-d_6, 400 MHz):** δ 4.39 (s, 3H), 7.31 (d, *J* = 15.7 Hz, 1H), 7.40-7.52 (m, 2H), 7.89-7.99 (m, 3H), 8.00-8.08 (m, 2H), 8.29 (d, *J* = 15.8 Hz, 1H), 8.45-8.57 (m, 2H), 8.94 (d, *J* = 6.7 Hz, 1H). **^{13}C-NMR (DMSO-d_6, 101 MHz):** δ 46.0, 118.5, 122.8, 125.0, 121.1, 125.3, 125.4, 126.7, 129.5, 136.0, 139.3, 139.8, 139.9, 144.4, 146.2, 151.5. **IR:** *v* (cm^-) 491, 509, 708, 725, 745, 1129, 1152, 1177, 1259, 1456, 1505, 1520, 1588, 1609, 1627. **MS (ESI) *m/z* (%):** 252.1 (100), 253.1 (24), 254.1 (10), 414.4 (5). **HRMS ESI *m/z*:** calc. for [(M - I^-)$^+$] [($C_{16}H_{14}NS$)$^+$] 252.0842, found 252.0842.

(*E*)-4-(4-ethoxy-3-methoxystyryl)-1-methylpyridin-1-ium iodide (49)

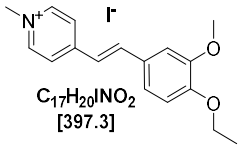

The synthesis and purification of pyridinium dye **49** was accomplished using *general procedure 5.2.f. method 1*. Pyridinium dye **49** was obtained as a yellow amorphous solid.
Yield: 49.2 mg, 97%.
m.p. 268-271 °C. **^{1}H-NMR (400 MHz, DMSO-d_6):** δ 1.35 (t, *J* = 7.0 Hz, 3H), 3.85 (s, 3H), 4.09 (q, *J* = 7.0 Hz, 2H), 4.23 (s, 3H), 7.05 (d, *J* = 8.4 Hz, 1H), 7.27 (d, *J* = 2.0, 8.4 Hz, 1H), 7.39 (d, *J* = 2.0 Hz, 2H), 7.42 (d, *J* = 16.3 Hz, 1H), 7.96 (d, *J* = 16.3 Hz, 1H), 8.15 (d, *J* = 6.8 Hz, 2H), 8.80 (d, *J* = 6.8 Hz, 1H). **^{13}C-NMR (101 MHz, DMSO-d_6):** δ 14.6, 46.7, 55.6, 63.8, 110.0, 112.5, 120.7, 122.9, 123.1, 127.8, 141.0, 144.9, 149.1, 150.4, 152.9. **IR (KBr):** *v* (cm^{-1}) 514, 616, 803, 867, 1036, 1141, 1168, 1268, 1426, 1474, 1519, 1579, 1594, 1616, 1645, 2910, 3002, 3028. **MS (ESI) *m/z* (%):** 270.2 (100), 271.2 (13). **HRMS ESI *m/z*:** calc. for [(M - I^-)$^+$] [($C_{17}H_{20}O_2N$)$^+$] calc. 270.14886, found 270.14889.

(*E*)-4-(3-ethoxy-4-methoxystyryl)-1-methylpyridin-1-ium iodide (50)

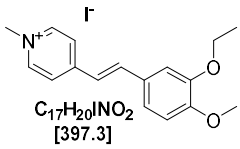

The synthesis and purification of pyridinium dye **50** was accomplished using *general procedure 5.2.f. method 1*. Pyridinium dye **50** was obtained as a yellow amorphous solid.
Yield: 45.1 mg, 89%.
m.p. 263-265 °C. **^{1}H-NMR (400 MHz, DMSO-d_6):** δ 1.37 (t, *J* = 7.0 Hz, 3H), 3.83 (s, 3H), 4.10 (q, *J* = 7.0 Hz, 2H), 4.22 (s, 3H), 7.07 (d, *J* = 8.4 Hz, 1H), 7.28 (dd, *J* = 2.0, 8.4 Hz, 1H), 7.37 (d, *J* = 2.0 Hz, 1H), 7.41 (d, *J* = 16.3 Hz, 1H), 7.94 (d, *J* = 16.3 Hz, 1H), 8.13 (d, *J* = 6.8 Hz, 2H), 8.79 (d, *J* = 6.8 Hz, 2H). **^{13}C-NMR (101 MHz, DMSO-d_6):** δ 14.7, 46.7, 55.6, 63.9, 111.0, 111.8, 120.8, 122.9, 123.1, 128.0, 141.0, 144.9, 148.3, 151.2, 152.9. **IR (KBr):** *v* (cm^{-1}) 516, 614, 978, 1043, 1140, 1265, 1314, 1432, 1469, 1517, 1580, 1594, 1616, 1643, 2929, 2977, 3028, 3439. **MS (ESI) *m/z* (%):** 270.1 (100), 271.2 (22). **HRMS ESI *m/z*:** calc. for $[(M - I^-)^+]$ $[(C_{17}H_{20}O_2N)^+]$ 270.14886, found 270.14891.

(*E*)-4-(3,4-dimethoxystyryl)-1-methylpyridin-1-ium iodide (51)

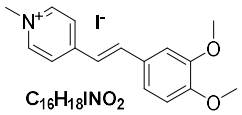

The synthesis and purification of pyridinium dye **51** was accomplished using *general procedure 5.2.f. method 1*. Pyridinium dye **51** was obtained as a yellow amorphous solid.
Yield: 43 mg, 88%.
m.p. 265-267 °C. **^{1}H-NMR (400 MHz, DMSO-d_6):** δ 3.83 (s, 3H), 3.85 (s, 3H), 4.23 (s, 3H), 7.07 (d, *J* = 8.4 Hz, 1H), 7.29 (dd, *J* = 2.0, 8.4 Hz, 1H), 7.40 (d, *J* = 2.0 Hz, 1H), 7.45 (d, *J* = 16.2 Hz, 1H), 7.96 (d, *J* = 16.2 Hz, 1H), 8.15 (d, *J* = 6.5 Hz, 2H), 8.81 (d, *J* = 6.5 Hz, 2H). **^{13}C-NMR (101 MHz, DMSO-d_6):** δ 46.8, 55.6, 55.7, 109.9, 111.7, 120.8, 122.9, 123.1, 128.0, 141.0, 144.9, 149.1, 151.1, 152.9. **IR (KBr):** *v* (cm^{-1}) 514, 618, 766, 829, 865, 968, 1020, 1142, 1163, 1186, 1209, 1238, 1271, 1423, 1446, 1487, 1517, 1595, 1615, 1644, 2831, 2911, 2988, 3075, 3439. **MS (ESI) *m/z* (%):** 256.2 $[(M - I^-)]$ (100), 257.2 (20). **HRMS ESI *m/z*:** calc. for $[(M - I^-)^+]$ $[(C_{16}H_{18}O_2N)^+]$ 256.1332, found 256.1332.

(*E*)-1-methyl-4-(2-(naphthalen-1-yl)vinyl)pyridin-1-ium iodide (52)

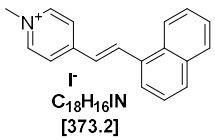

The synthesis and purification of pyridinium dye **52** was accomplished using *general procedure 5.2.f. method 2*. Pyridinium dye **52** was obtained as a yellow amorphous solid.
Yield: 46.2 mg, 97%.
m.p. 289-291 °C. **^{1}H-NMR (DMSO-d_6, 400 MHz):** δ 4.29 (s, 3H), 7.60-7.70 (m, 4H), 8.02 (dd, *J* = 8.0, 1.4 Hz, 1H), 8.06 (d, *J* = 8.1 Hz, 1H), 8.10 (dd, *J* = 7.4, 1.1 Hz, 1H), 8.45 (d, *J* = 6.9 Hz, 2H), 8.59 (d, *J* = 8.5 Hz, 1H), 8.82 (d, *J* = 16.1 Hz, 1H), 8.92 (d, *J* = 6.6 Hz, 2H).
^{13}C-NMR (DMSO-d6, 101 MHz): δ 47.0, 123.7, 124.0, 124.9, 125.8, 125.8, 126.4, 127.0, 128.7, 130.7, 131.0, 132.1, 133.4, 136.8, 145.1, 152.3. **IR:** *v* (cm^-) 744, 798, 826, 1142, 1188, 1459, 1511, 1519, 1571, 1618, 1639. **MS (ESI) *m/z* (%):** 246.1 $[(M - I^-)]$ (100), 247.1 (21). **HRMS ESI *m/z:*** calc. for $[(M - I^-)]$ $[(C_{18}H_{16}N)^+]$ 246.1277, found: 246.1278.

(*E*)-4-(2-(benzo[b]thiophen-2-yl)vinyl)-1-methylpyridin-1-ium iodide (53)

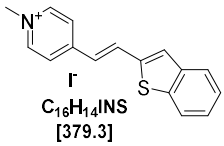

The synthesis and purification of pyridinium dye **53** was accomplished using *general procedure 5.2.f. method 2*. Pyridinium dye **53** was obtained as a yellow amorphous solid.
Yield: 47.0 mg, 97%.
m.p. 254-256 °C. **^{1}H-NMR (DMSO-d_6, 400 MHz):** δ 4.26 (s, 3H), 7.25 (d, *J* = 16.0 Hz, 1H), 7.38-7.49 (m, 2H), 7.81 (s, 1H), 7.89-7.97 (m, 1H), 7.98-8.07 (m, 1H), 8.27 (d, *J* = 6.9 Hz, 2H), 8.35 (d, *J* = 16.1 Hz, 1H), 8.88 (d, *J* = 6.9 Hz, 2H). **^{13}C-NMR (DMSO-d_6, 101 MHz):** δ 47.0, 122.8, 123.6, 124.5, 124.8, 125.2, 126.6, 129.1, 134.1, 139.4, 139.6, 140.4, 145.1, 151.7. **IR:** *v* (cm^-) 707, 726, 752, 1147, 1454, 1504, 1523, 1587, 1613, 1641. **MS (ESI) *m/z* (%):** 252.1 [$(M - I^-)^+$] (100), 253.1 (18), 414.1 (3). **HRMS ESI *m/z*:** calc. for [$(M - I^-)^+$] [$(C_{16}H_{14}NS)^+$] 252.0842, found 252.0842.

(*E*)-11-(2-(benzo[b]thiophen-2-yl)vinyl)-6,7-dimethyl-4,5,8,9-tetrahydroisoquinolino[1,2-a]pyrido[1,2-k][2,9]phenanthroline-3,10-diium trifluoromethanesulfonate (54)

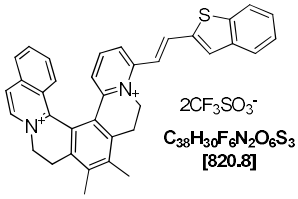

The synthesis and purification of [6]helquat dye **54** was accomplished by following the *general procedure 5.2.e*, using helquat dye precursor **6** (20 mg, 0.030 mmol, 1.0 equiv.), benzo[*b*]thiophene-2-carbaldehyde (73 mg, 0.450 mmol, 15.0 equiv.), pyrrolidine (30 µL, 26 mg, 0.366 mmol, 12.2 equiv.) in dry MeOH (2.0 mL) and dye **54** was obtained as a yellow solid.
Yield: 19 mg, 78%.
m.p. 216-218 °C. **^{1}H-NMR (acetonitrile-d_3, 400 MHz):** δ 2.54 (s, 3H), 2.55 (s, 3H), 3.05 (ddd, *J* = 4.9, 14.3, 17.1 Hz, 1H), 3.16 (ddd, *J* = 4.6, 14.6, 17.2 Hz, 1H), 3.54 (ddd, *J* = 1.8, 3.5, 17.2 Hz, 1H), 3.58 (ddd, *J* = 1.9, 3.8, 17.1 Hz, 1H), 4.70 (dt, *J* = 3.8, 14.0 Hz, 1H), 4.79 (dt, *J* = 3.5, 14.3 Hz, 1H), 5.01 (ddd, *J* = 1.8, 4.6, 13.9 Hz, 1H), 5.38 (ddd, *J* = 1.9, 4.9, 13.8 Hz, 1H), 6.92 (dd, *J* = 1.2, 8.2 Hz, 1H), 7.42 (d, *J* = 15.6 Hz, 1H), 7.45-7.53 (m, 2H), 7.55 (t, *J* = 4.1, 1H), 7.67 (ddd, *J* = 1.3, 6.9, 8.6 Hz, 1H), 7.77 (dq, *J* = 1.3, 8.2 Hz, 1H), 7.79 (s, 2H), 7.86-7.94 (m, 3H), 7.99 (ddd, *J* = 0.7, 1.6, 7.3 Hz, 1H), 8.12 (dd, *J* = 1.1, 8.3 Hz, 1H), 8.31 (d, *J* = 6.7 Hz, 1H), 8.61 (d, *J* = 6.7 Hz, 1H). **^{13}C-NMR (acetonitrile-d_3, 101 MHz):** 17.0, 17.2, 25.9, 26.7, 50.6, 56.0, 119.4, 120.6, 123.5, 123.7, 125.7, 125.9, 126.4, 126.9, 128.1, 128.4, 129.2, 129.2, 131.4, 132.8, 136.4, 137.0, 138.3, 138.6, 139.9, 140.6, 140.8, 141.3, 141.5, 142.3, 142.4, 143.7, 148.5, 149.5, 151.6, 154.0. **IR (KBr):** *v* (cm^{-1}) 728, 757, 828, 1031, 1157, 1226, 1265, 1379, 1410, 1457, 1484, 1507, 1554, 1563, 1574, 1606, 1622. **MS (ESI) *m/z* (%):** 261.1 (100), 261.6 (42), 262.1 [$(M - CF_3SO_3^-)^{2+}$] (6), 521.2 [$(M - CF_3SO_3^-)^{2+}$] (9), 671.2 [$(M - CF_3SO_3^-)^+$] (55), 672.2 (23). **HRMS ESI *m/z*:** calc. for [$(M - 2CF_3SO_3^-)^{2+}$] [$(C_{36}H_{30}N_2S)^{2+}$] 261.1059, found 261.1060.

(*E*)-6,7-dimethyl-11-(2-(naphthalen-1-yl)vinyl)-4,5,8,9-tetrahydroisoquinolino[1,2-a]pyrido[1,2-k][2,9]phenanthroline-3,10-diium trifluoromethanesulfonate (55)

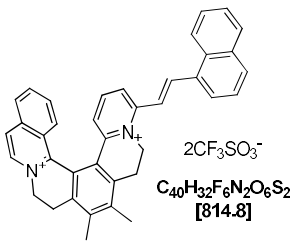

The synthesis and purification of [6]helquat dye **55** was accomplished by *general procedure 5.2.e*, using helquat dye precursor **6** (20 mg, 0.030 mmol, 1.0 equiv.), 1-naphthylaldehyde (70.3 mg, 0.450 mmol, 15.0 equiv.), pyrrolidine (30 µL, 26 mg, 0.366 mmol, 12.2 equiv.) in dry MeOH (2.0 mL) and helquat dye **55** was obtained as a yellow solid.

Yield: 21 mg, 87%.

m.p. > 350 °C. **^{1}H-NMR (600 MHz, acetone-d_6):** δ 2.63 (s, 3H), 2.64 (s, 3H), 3.34 (ddd, *J* = 4.2, 14.4, 17.3 Hz, 1H), 3.48 (dt, *J* = 4.0, 16.2 Hz, 1H), 3.82 (dt, *J* = 3.7, 16.8 Hz, 1H), 3.82 (dt, *J* = 3.5, 16.8 Hz, 1H), 5.12 (dt, *J* = 3.7, 14.2 Hz, 1H), 5.17 (dt, *J* = 3.5, 14.7 Hz, 1H), 5.40 (dd, *J* = 4.0, 13.5 Hz, 1H), 5.68 (ddd, *J* = 1.6, 4.2, 13.3 Hz, 1H), 7.52 (d, *J* = 8.0 Hz, 1H), 7.61-7.66 (m, 2H), 7.68 (t, *J* = 7.7 Hz, 1H), 7.82 (t, *J* = 8.0 Hz, 1H), 7.84 (ddd, *J* = 3.3, 8.7 Hz, 1H), 7.98 (ddd, *J* = 1.04, 7.0 Hz, 1H), 8.03-8.05 (m, 1H), 8.10 (dd, *J* = 0.28, 5.6 Hz, 1H), 8.13 (d, *J* = 2.0 Hz, 1H), 8.14 (dd, *J* = 0.9, 8.7 Hz, 1H), 8.27 (d, *J* = 7.7 Hz, 1H), 8.28 (d, *J* = 8.6 Hz, 1H), 8.33 (dd, *J* = 1.1, 8.1 Hz, 1H), 8.42 (d, *J* = 7.7 Hz, 1H), 8.55 (d, *J* = 6.6 Hz, 1H), 8.64 (d, *J* = 15.7 Hz, 1H), 9.03 (d, *J* = 6.7 Hz, 1H). **^{13}C-NMR (151 MHz, acetone-d_6):** δ 16.9, 17.0, 26.1, 26.8, 50.8, 56.2, 121.5, 123.8, 124.2, 125.9, 126.3, 126.6, 126.7, 127.0, 127.4, 128.1, 128.8, 128.9, 129.2, 129.6, 129.8, 132.2, 132.4, 132.8, 132.9, 134.8, 136.2, 137.6, 138.7, 140.0, 141.0, 141.6, 141.9, 142.6, 144.1, 148.6, 151.6, 154.8. **IR:** *v* (cm^-) 517, 573, 638, 1030, 1168, 1264, 1484, 1524, 1553, 1588, 1627, 3074. **MS (ESI) *m/z* (%):** 258.1 (100), 258.6 (42), 258.1 (9), 377.2 (6), 413.3 (13), 515.2 (6), 516.2 [$(M - 2CF_3SO_3^-)^{2+}$] (2), 665.2 [$(M - CF_3SO_3^-)^+$] (4). **HRMS ESI *m/z*:** calc. for [$(M - CF_3SO_3^-)^+$] [$(C_{39}H_{32}O_3N_2F_3S)^+$] 665.2080, found 665.2079.

(*E*)-6,7-dimethyl-11-(2-(4-methylnaphthalen-1-yl)vinyl)-4,5,8,9-tetrahydroisoquinolino[1,2-a] pyrido[1,2-k][2,9]phenanthroline-3,10-diium trifluoromethanesulfonate (56)

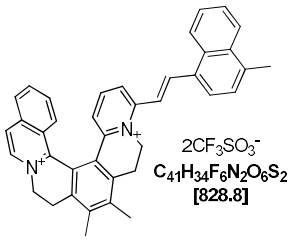

The synthesis and purification of [6]helquat dye **56** was accomplished by following the *general procedure 5.2.e*, using helquat dye precursor **6** (20 mg, 0.030 mmol, 1.0 equiv.), 4-methyl-1-naphthylaldehyde (76.6 mg, 0.450 mmol, 15.0 equiv.), pyrrolidine (30 µL, 26 mg, 0.366 mmol, 12.2 equiv.) in dry MeOH (2.0 mL) and [6]helquat **56** was obtained as a yellow solid.

Yield: 14.9 g, 61%.

m.p. 314-316 °C. **^{1}H-NMR (400 MHz, acetonitrile-d_3):** δ 2.54 (s, 3H), 2.55 (s, 3H), 2.79 (s, 3H), 3.05 (ddd, *J* = 4.9, 14.3, 17.1 Hz, 1H), 3.16 (ddd, *J* = 4.6, 14.6, 17.2 Hz, 1H), 3.54 (ddd, *J* = 1.8, 3.5, 17.2 Hz, 1H), 3.58 (ddd, *J* = 1.9, 3.8, 17.1 Hz, 1H), 4.70 (dt, *J* = 3.8, 14.0 Hz, 1H), 4.79 (dt, *J* = 3.5, 14.3 Hz, 1H), 5.01 (ddd, *J* = 1.8, 4.6, 13.9 Hz, 1H), 5.38 (ddd, *J* = 1.9, 4.9, 13.8 Hz, 1H), 6.95 (dd, *J* = 8.0 Hz, 1H), 7.56 (d, *J* = 8.1 Hz, 1H), 7.60 (d, *J* = 8.1 Hz, 1H), 7.67-7.71 (m, 4H), 7.82 (dd, *J* = 1.0, 8.8 Hz, 1H), 7.90 (ddd, *J* = 1.1, 6.9, 8.2 Hz, 1H), 7.95 (dd, *J* = 1.3, 8.2 Hz, 1H), 8.05 (d, *J* = 7.4 Hz, 1H), 8.13 (d, *J* = 8.3 Hz, 1H), 8.16-8.20 (m, 1H), 8.31-8.36 (m, 2H), 8.39 (d, *J* = 15.7 Hz, 1H), 8.62 (d, *J* = 6.7 Hz, 1H). **^{13}C-NMR (101 MHz, acetonitrile-d_3):** δ 17.0, 17.1, 20.1, 25.9, 26.7, 50.6, 56.1, 120.4, 123.5, 124.7, 125.9, 126.1, 126.2, 126.6, 126.7, 127.0, 127.4, 127.6, 128.0, 128.5, 128.6, 129.0, 129.2, 131.3, 132.3, 132.8, 133.7, 136.4, 137.0, 138.6, 139.7, 139.9, 141.2, 142.3, 142.4, 143.7, 148.2, 151.6, 154.9. **IR:** *v* (cm^-) 517, 573, 639, 743, 771, 804, 961, 1031, 1159, 1223, 1245, 1272, 1488, 1507, 1562, 1576, 1611, 1628. **MS (ESI) *m/z* (%):** 265.1 [$(M - 2CF_3SO_3^-)^{2+}$] (100), 265.6 (41), 529.3 (25), 679.2 (72), 680.2 (30),

697.2 (10). **HRMS ESI *m/z*:** calc. for [(M – $2CF_3SO_3^-)^{2+}$] [$(C_{39}H_{33}N_2)^{2+}$] 529.2638, found 529.2638.

(*E*)-11-(2-(biphenyl-4-yl)vinyl)-6,7-dimethyl-4,5,8,9-tetrahydroisoquinolino[1,2-a]pyrido-[1,2-k][2,9]- phenanthroline-3,10-diiumbistrifluoromethanesulfonate (57)

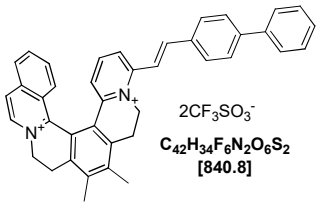

The synthesis and purification of [6]helquat dye **57** was accomplished by following the *general procedure 5.2.e*, using helquat dye precursor **6** (20 mg, 0.030 mmol, 1.0 equiv.), [1,1'-biphenyl]-4-carbaldehyde (82 mg, 0.450 mmol, 15.0 equiv.), pyrrolidine (30 µL, 26 mg, 0.366 mmol, 12.2 equiv.) in dry MeOH and [6]helquat dye **57** was obtained as a yellow solid.
Yield: 22.9 mg, 92%.
m.p. 311-313 °C. **^{1}H-NMR (600 MHz, acetonitrile-d_3):** δ 2.54 (s, 3H), 2.55 (s, 3H), 3.05 (ddd, *J* = 4.9, 14.3, 17.1 Hz, 1H), 3.16 (ddd, *J* = 4.6, 14.6, 17.2 Hz, 1H), 3.54 (ddd, *J* = 1.8, 3.5, 17.2 Hz, 1H), 3.58 (ddd, *J* = 1.9, 3.8, 17.1 Hz, 1H), 4.70 (dt, *J* = 3.8, 14.0 Hz, 1H), 4.79 (dt, *J* = 3.5, 14.3 Hz, 1H), 5.01 (ddd, *J* = 1.8, 4.6, 13.9 Hz, 1H), 5.38 (ddd, *J* = 1.9, 4.9, 13.8 Hz, 1H), 6.91 (d, *J* = 8.0 Hz, 1H), 7.42-7.55 (m, 4H), 7.57-7.68 (m, 3H), 7.71-7.91 (m, 9H), 8.12 (d, *J* = 8.3 Hz, 1H), 8.31 (d, *J* = 6.8 Hz, 1H), 8.61 (d, *J* = 6.8 Hz, 1H). **^{13}C–NMR (151 MHz, acetonitrile-d_3):** δ 17.1, 17.2, 26.0, 26.8, 50.6, 56.1, 121.1, 123.2, 123.6, 125.7, 126.0, 127.0, 128.0, 128.5, 128.7, 128.7, 129.1, 129.2, 129.3, 130.2, 132.9, 134.9, 136.5, 137.1, 138.7, 140.0, 140.7, 142.3, 142.4, 142.5, 143.8, 144.4, 144.8, 148.4, 151.7, 155.0. **IR:** *v* (cm^-) 517, 573, 638, 756, 770, 826, 1006, 1031, 1151, 1262, 132, 1379, 1411, 1436, 1447, 1508, 1562, 1610, 1628, 3081, 3435. **MS (ESI) *m/z* (%):** 235.6 (6), 268.2 (7), 271.1 (100), 271.6 (44), 541.3 (12), 542.3 [(M – $2CF_3SO_3^-)^{2+}$] (5), 691.2 [(M – $CF_3SO_3^-)^+$] (6). **HRMS ESI *m/z*:** calc. for [(M – $CF_3SO_3^-)^+$] [$(C_{41}H_{34}O_3N_2F_3S)^+$] 691.2237, found 691.2235.

(*E*)-6,7-dimethyl-11-(2-(naphthalen-2-yl)vinyl)-4,5,8,9-tetrahydroisoquinolino[1,2-a]pyrido [1,2-k][2,9]phenanthroline-3,10-diium trifluoromethanesulfonate (58)

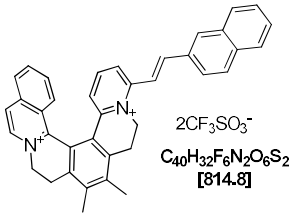

The synthesis and purification of [6]helquat dye **58** was accomplished by following the *general procedure 5.2.e*, using helquat dye precursor **6** (20 mg, 0.030 mmol, 1.0 equiv.), 2-naphthylaldehyde (70.3 mg, 0.450 mmol, 15.0 equiv.), pyrrolidine (30 µL, 26 mg, 0.366 mmol, 12.2 equiv.) in dry MeOH (2.0 mL) and [6]helquat dye **58** was obtained as a yellow solid.
Yield: 21 mg, 87%.
m.p. 312-313 °C. **^{1}H-NMR (acetonitrile-d_3, 600 MHz):** δ 2.54 (s, 3H), 2.55 (s, 3H), 3.05 (ddd, *J* = 4.9, 14.3, 17.1 Hz, 1H), 3.16 (ddd, *J* = 4.6, 14.6, 17.2 Hz, 1H), 3.54 (ddd, *J* = 1.8, 3.5, 17.2 Hz, 1H), 3.58 (ddd, *J* = 1.9, 3.8, 17.1 Hz, 1H), 4.70 (dt, *J* = 3.8, 14.0 Hz, 1H), 4.79 (dt, *J* = 3.5, 14.3 Hz, 1H), 5.01 (ddd, *J* = 1.8, 4.6, 13.9 Hz, 1H), 5.38 (ddd, *J* = 1.9, 4.9, 13.8 Hz, 1H), 6.91 (d, *J* = 8.1 Hz, 1H), 7.56 (t, *J* = 8.1 Hz, 1H), 7.61 (dd, *J* = 2.5, 9.6 Hz, 1H), 7.63 (t, *J* = 3.7 Hz, 1H), 7.68 (dd, *J* = 7.1, 1.3 Hz, 1H), 7.76 (s, 2H), 7.81 (d, *J* = 8.7 Hz, 1H), 7.87 (td, *J* = 1.2, 7.1 Hz, 1H), 7.89

(dd, *J* = 1.0, 7.0 Hz, 1H), 7.97-8.06 (m, 4H), 8.13 (d, *J* = 8.2 Hz, 1H), 8.23 (d, *J* = 1.5 Hz, 1H), 8.31 (d, *J* = 6.7 Hz, 1H), 8.61 (d, *J* = 6.7 Hz, 1H). **^{13}C-NMR (acetonitrile-*d*$_3$, 151 MHz):** *δ* 17.0, 17.4, 26.0, 26.8, 50.6, 56.1, 118.9, 120.5, 123.6, 124.6, 125.7, 125.9, 126.9, 128.2, 128.5, 128.6, 128.9 128.9, 129.0, 129.2, 129.7, 130.0, 131.6, 132.8, 133.4, 134.3, 135. 136.4, 137.0, 138.6, 139.9, 141.2, 142.3, 143.7, 145.2, 148.3, 151.7, 154.9. **IR:** *v* (cm^{-}) 517, 573, 638, 756, 770, 826, 1006, 1031, 1151, 1262, 1329, 1379, 1411, 1436, 1447, 1508, 1562, 1610, 1628, 3081, 3435. **MS (ESI) *m/z* (%):** 258.1 (100), 258.6 (42), 258.1 (9), 377.2 (6), 413.3 (13), 515.2 (6), 516.2 [(M – 2$CF_3SO_3^-$)$^{2+}$] (2), 655.2 [(M – $CF_3SO_3^-$)$^+$] (4). **HRMS ESI *m/z*:** calc. for [(M – $CF_3SO_3^-$)$^+$] [($C_{39}H_{32}O_3N_2F_3S$)$^+$] 665.2080, found 665.2079.

(*E*)-11-(2-(benzofuran-2-yl)vinyl)-6,7-dimethyl-4,5,8,9-tetrahydroisoquinolino[1,2-a]pyrido[1,2-k][2,9]phenanthroline-3,10-diium trifluoromethanesulfonate (59)

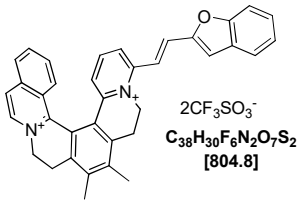

The synthesis and purification of [6]helquat dye **59** was accomplished by following the *general procedure 5.2.e*, using helquat dye precursor **6** (20 mg, 0.030 mmol, 1.0 equiv.), benzofuran-2-carbaldehyde (65.7 mg, 0.450 mmol, 15.0 equiv.), pyrrolidine (30 µL, 26 mg, 0.366 mmol, 12.2 equiv.) in dry MeOH (2.0 mL) and helquat dye **59** was obtained as a yellow solid.

Yield: 18.1 mg, 76%.

m.p. 321-323 °C. **^{1}H-NMR (acetonitrile-*d*$_3$, 400 MHz):** *δ* 2.54 (s, 3H), 2.55 (s, 3H), 3.05 (ddd, *J* = 4.9, 14.3, 17.1 Hz, 1H), 3.16 (ddd, *J* = 4.6, 14.6, 17.2 Hz, 1H), 3.54 (ddd, *J* = 1.8, 3.5, 17.2 Hz, 1H), 3.58 (ddd, *J* = 1.9, 3.8, 17.1 Hz, 1H), 4.70 (dt, *J* = 3.8, 14.0 Hz, 1H), 4.79 (dt, *J* = 3.5, 14.3 Hz, 1H), 5.01 (ddd, *J* = 1.8, 4.6, 13.9 Hz, 1H), 5.38 (ddd, *J* = 1.9, 4.9, 13.8 Hz, 1H), 6.94 (dd, *J* = 1.3, 8.0 Hz, 1H), 7.31 (s, 1H), 7.36 (ddd, *J* = 1.0, 7.3, 8.1 Hz, 1H), 7.50 (ddd, *J* = 1.3, 7.3, 8.4 Hz, 1H), 7.55 (t, *J* = 8.08, 1H), 7.57 (d, *J* = 15.6 Hz, 1H), 7.63 (dq, *J* = 0.9, 8.4 Hz, 1H), 7.65 (ddd, *J* = 1.23, 6.9 Hz, 1H), 7.67 (d, *J* = 15.6 Hz, 1H), 7.74-7.77 (m, 1H), 7.78-7.81 (m, 2H), 7.88 (ddd, *J* = 1.2, 6.9, 8.2 Hz, 1H), 8.12 (d, *J* = 8.4 Hz, 1H), 8.31 (d, *J* = 6.7 Hz, 1H), 8.62 (d, *J* = 6.7 Hz, 1H).

^{13}C-NMR (acetonitrile-*d*$_3$, 101 MHz): *δ* 17.0, 17.1, 25.8, 26.7, 50.6, 56.0, 106.0, 112.2, 113.9, 114.0, 120.5, 123.5, 123.7, 124.9, 128.4, 128.5, 128.5, 129.2, 129.2, 129.3, 129.5, 131.5, 132.9, 136.4, 137.0, 138.5, 139.9, 141.3, 142.3, 142.5, 143.7, 148.5, 151.6, 153.5, 154.0, 156.7. **IR (KBr):** *v* (cm^{-1}) 518, 573, 638, 755, 888, 1031, 1100, 1157, 1224, 1263, 1276, 1349, 1379, 1411, 1449, 1485, 1507, 1551, 1565, 1607, 1627. **MS (ESI) *m/z* (%):** 253.1 [(M – 2$CF_3SO_3^-$)$^{2+}$] (100), 253.6 (40), 254.1 (7), 655.2 [(M – $CF_3SO_3^-$)$^+$] (23), 656.2 (7). **HRMS ESI *m/z*:** calc. for [(M – 2$CF_3SO_3^-$)$^{2+}$] [($C_{36}H_{30}ON_2$)$^{2+}$] 253.1174, found 253.1174.

4,13-bis((*E*)-2-(2,3-dihydrobenzofuran-5-yl)vinyl)-6,7,10,11-tetrahydrodipyrido[2,1-a:1',2'-k] [2,9]phenanthroline-5,12-diium trifluoromethanesulfonatetrifluoromethanesulfonate (60)

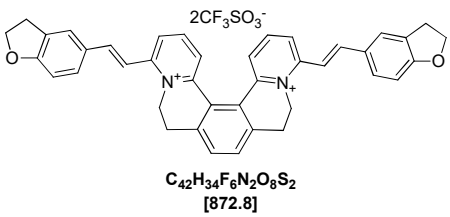

The synthesis and purification of the [5]helquat dye **60** was accomplished according to *general procedure 5.2.e*, using helquat dye precursor **10** (50 mg, 0.082 mmol, 1.0 equiv.), 2,3-dihydrobenzofuran-5-carbaldehyde (182.3 mg, 1.230 mmol, 15.0 equiv.), pyrrolidine (100 µL, 86.6 mg, 1.218 mmol, 14.9 equiv.) in dry MeOH (5.0 mL) and [5]helquat dye **60** was obtained as a yellow solid.

Yield: 64.1 g, 90%.

m.p. 204-206 °C. **^{1}H-NMR (acetonitrile-d_3, 400 MHz):** δ 3.16-3.19 (m, 4H), 3.29 (t, *J* = 8.5 Hz, 4H), 4.45-4.53 (m, 2H), 4.67 (t, *J* = 8.5 Hz, 4H), 5.18-5.26 (m, 2H), 6.89 (d, *J* = 8.3 Hz, 2H), 7.40 (d, *J* = 15.9 Hz, 2H), 7.58 (dd, *J* = 1.9, 8.3 Hz, 2H), 7.64 (d, *J* = 15.9 Hz, 2H), 7.69 (s, 2H), 7.72 (dd, *J* = 1.4, 8.1 Hz, 2H), 7.76 (d, *J* = 1.7 Hz, 2H), 8.00 (t, *J* = 8.1 Hz, 2H), 8.11 (dd, *J* = 1.4, 8.3 Hz, 2H). **^{13}C-NMR (acetonitrile-d_3, 101 MHz):** δ 28.2, 29.7, 50.5, 73.2, 110.6, 115.6, 126.2, 128.1, 128.7, 129.0, 130.3, 131.3, 131.4, 132.4, 141.2, 143.5, 145.4, 147.7, 156.0, 164.1. **IR (KBr):** *v* (cm^{-1}) 935, 1031, 1154, 1231, 1260, 1276, 1326, 1473, 1493, 1561, 1588, 1601, 1625. **MS (ESI) *m/z* (%):** 287.1 [$(M - 2CF_3SO_3^-)^{2+}$] (100), 287.6 (43), 288.1 (8), 723.2 [$(M - CF_3SO_3^-)^+$] (6). **HRMS ESI *m/z*:** calc. for [$(M - 2CF_3SO_3^-)^{2+}$] [$(C_{40}H_{34}O_2N_2)^{2+}$] 287.13047, found 287.13055.

4,13-bis((*E*)-2-(6-methoxynaphthalen-2-yl)vinyl)-6,7,10,11-tetrahydrodipyrido[2,1-a:1',2'-k] [2,9]phenanthroline-5,12-diium trifluoromethanesulfonate (61)

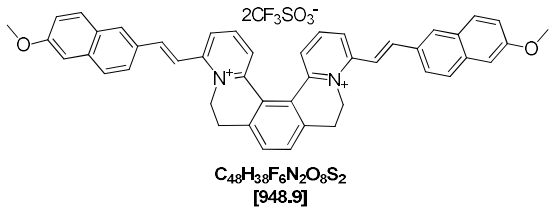

The synthesis and purification of the [5]helquat dye **61** was accomplished according to *general procedure 5.2.e*, using helquat dye precursor **10** (50 mg, 0.082 mmol, 1.0 equiv.), 6-methoxy-2-naphtylaldehyde (229.0 mg, 1.230 mmol, 15.0 equiv.), pyrrolidine (100 µL, 86.6 mg, 1.218 mmol, 14.9 equiv.) in dry MeOH (5.0 mL) and [5]helquat dye **61** was obtained as a yellow solid.

Yield: 71.2 mg, 92%.

m.p. 264-266 °C. **^{1}H-NMR (acetonitrile-d_3, 400 MHz):** δ 3.12-3.34 (m, 4H), 3.95 (s, 6H), 4.48-4.56 (m, 2H), 5.26-5.34 (m, 2H), 7.25 (dd, *J* = 9.0, 2.5 Hz, 2H), 7.36 (d, *J* = 2.5 Hz, 2H), 7.66 (d, *J* = 15.9 Hz, 2H), 7.72 (d, *J* = 4.1 Hz, 2H), 7.74 (dd, *J* = 1.32, 8.0 Hz, 2H), 7.85 (d, *J* = 15.9 Hz, 2H), 7.91 (d, *J* = 3.8 Hz, 2H), 7.93 (d, *J* = 3.4 Hz, 2H), 7.97-8.01 (m, 2H), 8.07 (t, *J* = 8.1 Hz, 2H), 8.19 (d, *J* = 1.6 Hz, 2H), 8.20 (dd, *J* = 1.3, 8.2 Hz, 2H). **^{13}C-NMR (acetonitrile-d_3, 101 MHz):** δ 28.1, 50.7, 56.2, 56.3, 107.3, 120.7, 125.4, 126.6, 128.1, 128.8, 129.5, 129.6, 131.2, 131.3, 131.4, 132.6, 137.2, 141.3, 143.8, 145.3, 147.9, 155.7, 160.4. **IR (KBr):** *v* (cm^{-1}) 812, 965, 1030, 1156, 1224, 1265, 1272, 1392, 1441, 1474, 1482, 1502, 1563, 1600, 1608, 1619, 2841. **MS (ESI) *m/z* (%):** 241.1 (18), 325.1 [$(M - 2CF_3SO_3^-)^{2+}$] (100), 325.6 (50), 326.1 (13), 481.2 (8), 649.3 (13), 799.2 [$(M - CF_3SO_3^-)^+$] (93), 800.2 (47), 801.3 (10). **HRMS ESI *m/z*:** calc. for [$(M - 2CF_3SO_3^-)^{2+}$] [$(C_{46}H_{38}O_2N_2)^{2+}$] calc. 325.14612, found 325.14632.

(*E*)-6,7-dimethyl-11-(2-(5-phenylthiophen-2-yl)vinyl)-4,5,8,9-tetrahydroisoquinolino[1,2-a] pyrido[1,2-k][2,9]phenanthroline-3,10-diium trifluoromethanesulfonate (62)

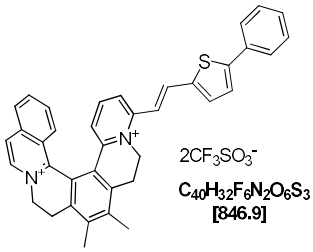

The synthesis and purification of [6]helquat dye **62** was accomplished according to the *general procedure 5.2.e* using [6]helquat dye precursor **6** (20 mg, 0.030 mmol, 1.0 equiv.), 5-phenylthiophene-2-carbaldehyde (84.7 mg, 0.450 mmol, 15.0 equiv.), pyrrolidine (30 µL, 26 mg, 0.366 mmol, 12.2 equiv.) in dry MeOH (2.0 mL) and [6]helquat dye **62** was obtained as a yellow solid.

Yield: 17.8 mg, 72%.

m.p. 329-331 °C. **^{1}H-NMR (400 MHz, acetonitrile-d_3):** δ 2.53 (s, 3H), 2.54 (s, 3H), 3.05 (ddd, *J* = 4.9, 14.3, 17.1 Hz, 1H), 3.16 (ddd, *J* = 4.6, 14.6, 17.2 Hz, 1H), 3.54 (ddd, *J* = 1.8, 3.5, 17.2 Hz, 1H), 3.58 (ddd, *J* = 1.9, 3.8, 17.1 Hz, 1H), 4.70 (dt, *J* = 3.8, 14.0 Hz, 1H), 4.79 (dt, *J* = 3.5, 14.3 Hz, 1H), 5.01 (ddd, *J* = 1.8, 4.6, 13.9 Hz, 1H), 5.38 (ddd, *J* = 1.9, 4.9, 13.8 Hz, 1H), 6.87 (dd, *J* = 1.5, 8.3 Hz, 1H), 7.36 (d, *J* = 15.6 Hz, 1H), 7.41-7.43 (m, 1H), 7.48-7.56 (m, 5H), 7.66 (ddd, *J* = 1.3, 6.9, 7.2 Hz, 1H), 7.76-7.80 (m, 5H), 7.88 (ddd, J = 1.3, 6.9, 7.2 Hz, 1H), 8.12 (d, *J* = 8.4 Hz, 1H), 8.30 (d, *J* = 6.7 Hz, 1H), 8.61 (d, J = 6.7 Hz, 1H). **^{13}C-NMR (101 MHz, acetonitrile-d_3):** δ 17.0, 17.1, 25.9, 26.7, 50.4, 56.0, 116.6, 120.5, 123.4, 123.7, 125.2, 125.9, 126.1, 126.9, 128.4, 128.6, 128.7, 129.2, 130.0, 130.3, 132.8, 134.1, 135.2, 136.4, 137.0, 137.7, 138.5, 139.9, 140.1, 141.1, 141.8, 142.2, 142.4, 143.3, 148.2, 149.9, 151.6, 154.5. **IR:** *v* (cm^-) 1032, 1163, 1227, 1264, 1412, 1432, 1571, 1610, 1629, 2363, 3090. **MS (ESI) *m/z* (%):** 274.1 (100), 274.6 (43), 547.2 [$(M - 2CF_3SO_3^-)^{2+}$] (45), 548.2 (20), 697.2 [$(M - CF_3SO_3^-)^+$] (10). **HRMS *m/z*:** calc. for [$(M - 2CF_3SO_3^-)^{2+}$] [$(C_{38}H_{31}N_2S)^{2+}$] 547.22025, found 547.22017.

4,13-bis((*E*)-3,4,5-trimethoxystyryl)-6,7,10,11-tetrahydrodipyrido[2,1-a:1',2'-k][2,9] phenanthroline-5,12-diium trifluoromethanesulfonate (63)

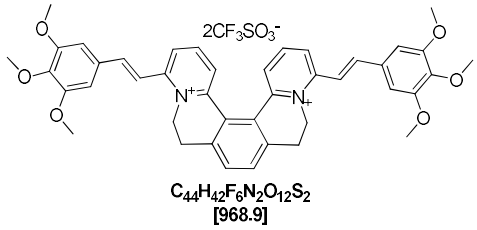

The synthesis and purification of [5]helquat dye **63** was accomplished according to *general procedure 5.2.e*, using helquat dye precursor **10** (50 mg, 0.082 mmol, 1.0 equiv.), 3,4,5-trimethoxybenzaldehyde (241.3 mg, 1.230 mmol, 15.0 equiv.), pyrrolidine (100 µL, 86.6 mg, 1.218 mmol, 14.9 equiv.) in dry MeOH (5 mL) and [5]helquat dye **63** was obtained as a yellow solid.

Yield: 74.4 mg, 94%.

m.p. 280-282 °C. **^{1}H-NMR (acetonitrile-d_3, 400 MHz):** δ 3.14-3.36 (m, 4H), 3.83 (s, 6H), 3.93 (s, 12H), 4.52 (t, *J* = 13.8 Hz, 2H), 5.28 (d, *J* = 13.2 Hz, 2H), 7.12 (s, 4H), 7.55 (d, *J* = 15.9 Hz, 2H), 7.62 (d, *J* = 15.9 Hz, 2H), 7.72 (s, 2H), 7.75 (dd, *J* = 1.5, 7.9 Hz, 2H), 8.06 (t, *J* = 8.0 Hz, 2H), 8.12 (dd, *J* = 1.5, 8.2 Hz, 2H). **^{13}C-NMR (acetonitrile-d_3, 101 MHz):** δ 28.1, 50.9, 57.0, 61.1, 107.1, 126.6, 128.1, 129.5, 131.4, 132.6, 141.3, 141.7, 143.9, 145.1, 147.9, 154.8, 154.8, 155.7. **IR (KBr):** *v* (cm^{-1}): 518, 573, 638, 756, 1031, 1158, 1231, 1262, 1272, 1405,

1431, 1479, 1489, 1510, 1565, 1589, 1608, 1623, 1962. **MS (ESI) *m/z* (%):** 253.1 (7), 335.2 [(M – $2CF_3SO_3^-)^{2+}$] (100), 335.7 (42), 336.2 (10), 669.3 [(M – $2CF_3SO_3^-)^{2+}$] (5), 819.3 [(M – $CF_3SO_3^-)^+$] (27), 820.3 (15). **HRMS ESI *m/z*:** calc. for [(M – $2CF_3SO_3^-)^{2+}$] [$(C_{42}H_{42}O_6N_2)^{2+}$] 335.1516, found 335.1517.

4,13-bis((*E*)-4-(pentyloxy)styryl)-6,7,10,11-tetrahydrodipyrido[2,1-a:1',2'-k][2,9]phenanthroline-5,12-diium trifluoromethanesulfonate (64)

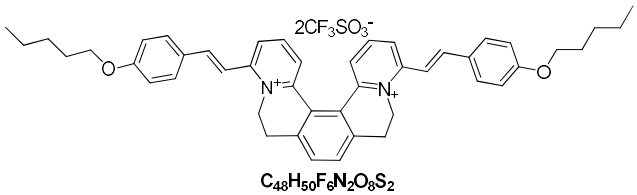

The synthesis and purification of [5]helquat dye **64** was accomplished according to *general procedure 5.2.e*, using [5]helquat dye precursor **10** (50 mg, 0.082 mmol, 1.0 equiv.), 4-(pentyloxy)benzaldehyde (236.5 mg, 1.230 mmol, 15.0 equiv.), pyrrolidine (100 µL, 86.6 mg, 1.218 mmol, 14.9 equiv.) in dry MeOH (5 mL) and [5]helquat dye **64** was obtained as a yellow solid.

Yield: 62.7 mg, 80.4%.

m.p. 289-291 °C. **^{1}H-NMR (acetonitrile-d_3, 400 MHz):** δ 0.95 (t, *J* = 7.1 Hz, 6H), 1.34-1.51 (m, 8H), 1.77-1.84 (m, 4H), 3.12-3.33 (m, 4H), 4.08 (t, *J* = 6.6 Hz, 4H), 4.57 (m, 2H), 5.22-5.26 (m, 2H), 7.04 (dd, *J* = 2.0, 6.8 Hz, 4H), 7.43 (d, *J* = 15.9 Hz, 2H), 7.65-7.70 (m, 6H), 7.77 (dd, *J* = 2.0, 6.8 Hz, 4H), 8.02 (t, *J* = 8.1 Hz, 2H), 8.11 (dd, *J* = 8.3, 1.4 Hz, 2H). **^{13}C-NMR (acetonitrile-d_3, 101 MHz):** δ 14.3, 23.1, 28.1, 28.9, 29.6, 50.6, 69.3, 116.1, 116.2, 126.3, 128.1, 128.3, 129.1, 131.4, 132.5, 141.2, 143.6, 144.9, 147.8, 156.0, 162.7. **IR (KBr):** *v* (cm^{-1}) 518, 573, 639, 755, 828, 968, 1031, 1156, 1176, 1230, 1256, 1277, 1427, 1473, 1490, 1512, 1563, 1600, 1623. **MS (ESI) *m/z* (%):** 331.4 (70), 331.9 (37), 661.8 (4), 811.9 [(M – $CF_3SO_3^-)^+$] (100), 812.9 (50), 813.9 (15). **HRMS ESI *m/z*:** calc. for [(M – $2CF_3SO_3^-)^{2+}$] [$(C_{46}H_{50}O_2N_2)^{2+}$] 331.1931, found 331.1933.

(*E*)-11-(2-(dibenzo[b,d]furan-4-yl)vinyl)-6,7-dimethyl-4,5,8,9-tetrahydroisoquinolino[1,2-a]pyrido[1,2-k][2,9]phenanthroline-3,10-diium trifluoromethanesulfonate (65)

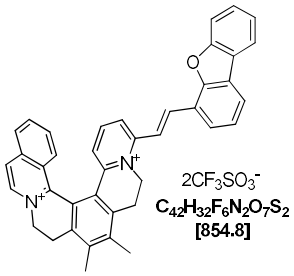

The synthesis and purification of [6]helquat dye **65** was accomplished according to *general procedure 5.2.e*, using dye precursor **6** (20 mg, 0.030 mmol, 1.0 equiv.), dibenzo[*b*,*d*]furan-4-carbaldehyde (88.3 mg, 0.450 mmol, 15.0 equiv.), pyrrolidine (30 µL, 26 mg, 0.366 mmol, 12.2 equiv.) in dry MeOH (2.0 mL) and dye **65** was obtained as a yellow solid.

Yield: 21 mg, 83%.

m.p. 312-314 °C. **^{1}H-NMR (acetonitrile-d_3, 400 MHz):** δ 2.55 (s, 3H), 2.56 (s, 3H), 3.05 (ddd, *J* = 4.9, 14.3, 17.1 Hz, 1H), 3.16 (ddd, *J* = 4.6, 14.6, 17.2 Hz, 1H), 3.54 (ddd, *J* = 1.8, 3.5, 17.2 Hz, 1H), 3.58 (ddd, *J* = 1.9, 3.8, 17.1 Hz, 1H), 4.70 (dt, *J* = 3.8, 14.0 Hz, 1H), 4.79 (dt, *J* = 3.5, 14.3 Hz, 1H), 5.01 (ddd, *J* = 1.8, 4.6, 13.9 Hz, 1H), 5.38 (ddd, *J* = 1.9, 4.9, 13.8 Hz, 1H), 6.98 (dd, *J*= 1.3, 8.0 Hz, 1H), 7.48-7.57 (m, 2H), 7.58-7.66 (m, 2H), 7.69 (ddd, *J* = 1.23, 6.9 Hz, 1H), 7.81-

7.86 (m, 4H), 7.88 (dd, *J* = 1.23, 5.2 Hz, 1H), 7.90 (dd, *J* = 1.22, 5.26 Hz, 1H), 8.14 (d, *J* = 8.3 Hz, 1H), 8.17 (ddd, *J* = 0.7, 1.4, 7.8, Hz, 1H), 8.22 (dd, *J* = 1.2, 7.7 Hz, 1H), 8.28 (d, *J* = 16.1 Hz, 1H), 8.33 (d, *J* = 6.7 Hz, 1H), 8.63 (d, *J* = 6.7 Hz, 1H). **^{13}C-NMR (acetonitrile-*d*$_3$, 101 MHz):** *δ* 17.0, 17.2, 25.9, 26.7, 50.7, 56.1, 112.8, 120.5, 120.9, 121.9, 122.4, 123.5, 123.7, 124.4, 124.6, 124.8, 125.8, 126.0, 126.1, 126.2, 127.0, 128.5, 128.5, 129.2, 129.7, 132.9, 136.4, 137.0, 138.4, 138.6, 139.8, 140.0, 141.3, 142.3, 142.5, 143.9, 148.4, 151.6, 155.0, 157.1. **IR:** *v* (cm^{-}) 761, 832, 1031, 1157, 1188, 1224, 1263, 1275, 1380, 1411, 1455, 1475, 1485, 1507, 1560, 1574, 1609, 1625**. MS (ESI) *m/z* (%):** 278.1 [$(M - 2CF_3SO_3^-)^{2+}$] (100), 278.6 (44), 279.1 (7), 376.2 (12), 376.7 (7), 705.2 [$(M - CF_3SO_3^-)^+$] (8). **HRMS *m/z*:** calc. for [$(M - 2CF_3SO_3^-)^{2+}$] [$(C_{40}H_{32}ON_2)^{2+}$] 278.1252, found 278.1253.

4,13-bis((*E*)-4-(pent-4-yn-1-yloxy)styryl)-6,7,10,11-tetrahydrodipyrido[2,1-a:1',2'-k][2,9] phenanthroline-5,12-diium trifluoromethanesulfonate (66)

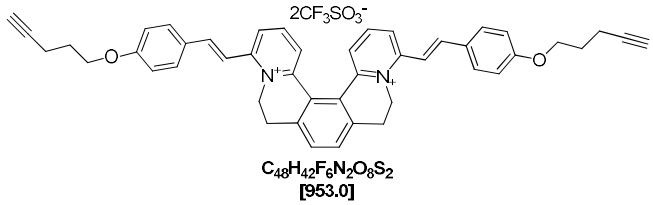

The synthesis and purification of [5]helquat dye **66** was accomplished by following *general procedure 5.2.e*, using [5]helquat dye precursor **10** (50 mg, 0.082 mmol, 1.0 equiv.), 4-(pent-4-yn-1-yloxy)benzaldehyde (231.5 mg, 1.230 mmol, 15.0 equiv.), pyrrolidine (100 µL, 86.6 mg, 1.218 mmol, 14.9 equiv.) in dry MeOH (5 mL) and [5]helquat dye **66** was obtained as a yellow solid.

Yield: 63 mg, 81%.

m.p. 213-215 °C. **^{1}H-NMR (acetonitrile-*d*$_3$, 400 MHz):** *δ* 2.00 (p, *J* = 6.4 Hz, 4H), 2.22 (t, *J* = 2.7 Hz, 2H), 2.41 (td, *J* = 7.1, 2.7 Hz, 4H), 3.12-3.33 (m, 4H), 4.17 (t, *J* = 6.2 Hz, 4H), 4.43-4.51 (m, 2H), 5.23-5.27 (m, 2H), 7.05-7.10 (dd, *J* = 2.0, 6.8 Hz, 4H), 7.44 (d, *J* = 15.9 Hz, 2H), 7.65 (d, *J* = 15.9 Hz, 2H), 7.68 (d, *J* = 7.8 Hz, 2H), 7.70 (s, 2H), 7.77-7.80 (dd, *J* = 2.2, 6.8 Hz, 4H), 8.02 (t, *J* = 8.1 Hz, 2H), 8.12 (dd, *J* = 8.3, 1.4 Hz, 2H). **^{13}C-NMR (acetonitrile-*d*$_3$, 101 MHz):** *δ* 15.5, 28.1, 28.8, 50.6, 67.6, 70.3, 84.3, 116.2, 116.4, 126.3, 128.1, 128.5, 129.2, 131.4, 132.5, 141.2, 143.6, 144.9, 147.8, 155.9, 162.4. **IR (KBr):** *v* (cm^{-1}) 650, 828, 968, 1031, 1156, 1176, 1230, 1257, 1276, 1427, 1474, 1490, 1512, 1563, 1600, 1625, 2116, 3260. **MS (ESI) *m/z* (%):** 327.2 [$(M - 2CF_3SO_3^-)^{2+}$] (100), 327.7 (37), 328.2 (13), 653.3 (8), 803.3 (50), 804.3 [$(M - CF_3SO_3^-)^+$] (25), 805.3 (5). **HRMS ESI *m/z*:** calc. for [$(M - 2CF_3SO_3^-)^{2+}$] [$(C_{46}H_{42}O_2N_2)^{2+}$] 327.1618, found 327.1620.

(*E*)-6,7-dimethyl-11-(2-(5-phenylfuran-2-yl)vinyl)-4,5,8,9-tetrahydroisoquinolino[1,2-a] pyrido [1,2-k][2,9]phenanthroline-3,10-diium trifluoromethanesulfonate (67)

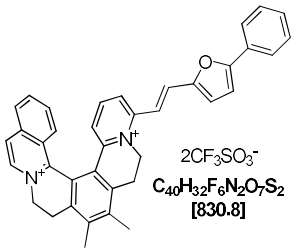

The synthesis and purification of helquat dye **67** was accomplished according to *general procedure 5.2.e*, using [6]helquat dye precursor **6** (20 mg, 0.030 mmol, 1.0 equiv.), 5-phenylfuran-2-carbaldehyde (77.5 mg, 0.450 mmol, 15.0 equiv.), pyrrolidine (30 µL, 26 mg,

0.366 mmol, 12.2 equiv.) in dry MeOH (2.0 mL) and [6[helquat dye **67** was obtained as a yellow solid.

Yield: 18.9 mg, 77%.

m.p. 230-232 °C. **^{1}H-NMR (acetonitrile-d_3, 400 MHz):** δ 2.55 (s, 3H), 2.56 (s, 3H), 3.05 (ddd, *J* = 4.9, 14.3, 17.1 Hz, 1H), 3.16 (ddd, *J* = 4.6, 14.6, 17.2 Hz, 1H), 3.54 (ddd, *J* = 1.8, 3.5, 17.2 Hz, 1H), 3.58 (ddd, *J* = 1.9, 3.8, 17.1 Hz, 1H), 4.70 (dt, *J* = 3.8, 14.0 Hz, 1H), 4.79 (dt, *J* = 3.5, 14.3 Hz, 1H), 5.01 (ddd, *J* = 1.8, 4.6, 13.9 Hz, 1H), 5.38 (ddd, *J* = 1.9, 4.9, 13.8 Hz, 1H), 6.86 (dd, *J* = 1.3, 8.1 Hz, 1H), 7.05 (s, 2H), 7.42-7.49 (m, 2H), 7.50-7.57 (m, 4H), 7.66 (ddd, *J* = 1.2, 6.9, 8.5 Hz, 1H), 7.76 (dd, *J* = 8.3, 1.3 Hz, 1H), 7.78 (dq, *J* = 0.9, 8.7 Hz, 1H), 7.88 (ddd, *J* = 1.1, 6.9, 8.2 Hz, 1H), 7.95-7.97 (m, 2H), 8.12 (dt, *J* = 0.8, 8.4 Hz, 1H), 8.29 (d, *J* = 7.6 Hz, 1H), 8.61 (d, *J* = 6.7 Hz, 1H). **^{13}C-NMR (acetonitrile-d_3, 101 MHz):** δ 17.0, 17.1, 25.9, 26.7, 50.3, 56.0, 110.1, 115.0, 120.9, 123.4, 124.9, 125.5, 125.6, 125.9, 126.9, 128.5, 128.5, 128.7, 129.2, 130.1, 130.5, 130.8, 132.8, 136.4, 136.5, 137.0, 138.5, 139.9, 141.1, 142.2, 142.3, 143.1, 148.2, 151.7, 154.6, 158.2. **IR:** *v* (cm^-) 518, 573, 638, 695, 1031, 1156, 1224, 1262, 1366, 1379, 1411, 1475, 1484, 1507, 1519, 1562, 1581, 1607, 1625. **MS (ESI) *m/z* (%):** 266.1 [(M – $2CF_3SO_3^-)^{2+}$] (100), 266.6 (43), 267.1 (7), 681.2 [(M – $2CF_3SO_3^-)^{2+}$] (5). **HRMS *m/z*:** calc. for [(M – $2CF_3SO_3^-)^{2+}$] [$(C_{38}H_{32}ON_2)^{2+}$] 266.1252, found 266.1253.

4,13-bis((*E*)-4-butoxystyryl)-6,7,10,11-tetrahydrodipyrido[2,1-a:1',2'-k][2,9] phenanthroline-5,12-diium trifluoromethanesulfonate (68)

$C_{46}H_{46}F_6N_2O_8S_2$
[933.0]

The synthesis and purification of [5]helquat dye **68** was accomplished according to *general procedure 5.2.e*, using dye precursor **10** (50 mg, 0.082 mmol, 1.0 equiv.), 4-butoxybenzaldehyde (219.2 mg, 1.230 mmol, 15.0 equiv.), pyrrolidine (100 µL, 86.6 mg, 1.218 mmol, 14.9 equiv.) in dry MeOH (5 mL) and [5]helquat dye **68** was obtained as a yellow solid.

Yield: 57.2 mg, 75%.

m.p. 231-233 °C. **^{1}H-NMR (acetonitrile-d_3, 400 MHz):** δ 0.99 (t, *J* = 7.4 Hz, 6H), 1.46-1.55 (m, 4H), 1.78 (p, *J* = 7.0 Hz, 4H), 3.08-3.34 (m, 4H), 4.09 (t, *J* = 6.5 Hz, 4H), 4.41-4.50 (m, 2H), 5.21-5.25 (m, 2H), 7.06 (dd, *J* = 2.0, 6.8 Hz, 4H), 7.43 (d, *J* = 15.9 Hz, 2H), 7.65 (d, *J* = 15.8 Hz, 2H), 7.67 (dd, *J* = 0.8, 8.0 Hz, 2H), 7.70 (s, 2H), 7.78 (dd, *J* = 2.0, 6.8 Hz, 4H), 8.01 (t, *J* = 8.1 Hz, 2H), 8.11 (dd, *J* = 8.2, 1.3 Hz, 2H). **^{13}C-NMR (acetonitrile-d_3, 101 MHz):** δ 14.1, 19.9, 28.1, 31.9, 50.6, 69.0, 116.1, 116.2, 126.3, 128.1, 128.3, 129.1, 131.4, 132.5, 141.2, 143.6, 144.9, 147.8, 156.0, 162.7. **IR (KBr):** *v* (cm^{-1}) 828, 970, 1031, 1156, 1176, 1227, 1257, 1277, 1427, 1474, 1490, 1512, 1563, 1600, 1623. **MS (ESI) *m/z* (%):** 185.1 (50), 227.1 (86), 228.1 (10), 317.2 [(M – $2CF_3SO_3^-)^{2+}$] (100), 317.7 (50), 318.2 (11), 783.3 [(M – $2CF_3SO_3^-)^{2+}$] (21), 784.3 (10). **HRMS ESI *m/z*:** calc. for [(M – $2CF_3SO_3^-)^{2+}$] [$(C_{44}H_{46}O_2N_2)^{2+}$] 317.17742, found 317.17716.

4,13-bis((*E*)-4-(hexyloxy)styryl)-6,7,10,11-tetrahydrodipyrido[2,1-a:1',2'-k][2,9]phenanthroline-5,12-diium trifluoromethanesulfonate (69)

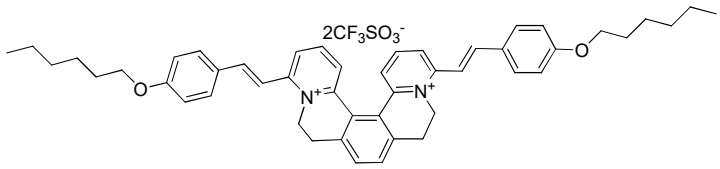

$C_{50}H_{54}F_6N_2O_8S_2$
[989.1]

The synthesis and purification of [5]helquat dye **69** was accomplished according to *general procedure 5.2.e*, using dye precursor **10** (50 mg, 0.082 mmol, 1.0 equiv.), 4-hexyloxybenzaldehyde (253.7 mg, 1.230 mmol, 15.0 equiv.), pyrrolidine (100 µL, 86.6 mg, 1.218 mmol, 14.9 equiv.) in dry MeOH (5 mL) and [5]helquat dye **69** was obtained as a yellow solid.

Yield: 61.3 mg, 76%.

m.p. 267-269 °C. **^{1}H-NMR (acetonitrile-d_3, 400 MHz):** δ 0.92 (t, J = 7.1 Hz, 6H), 1.29-1.54 (m, 12H), 1.79 (p, J = 6.8 Hz, 4H), 3.08-3.34 (m, 4H), 4.08 (t, J = 6.6 Hz, 4H), 4.41-4.50 (m, 2H), 5.21-5.25 (m, 2H), 7.04 (d, J = 6.8 Hz, 2H), 7.06 (d, J = 6.8 Hz, 2H), 7.43 (d, J = 15.9 Hz, 2H), 7.65-7.69 (m, 4H), 7.70 (s, 2H), 7.76 (d, J = 6.8, 2H), 7.78 (d, J = 6.8 Hz, 2H), 8.01 (t, J = 8.1 Hz, 2H), 8.11 (dd, J = 1.4, 8.3 Hz, 2H). **^{13}C-NMR (acetonitrile-d_3, 101 MHz):** δ 14.3, 23.3, 26.4, 28.1, 29.8, 32.3, 50.6, 69.3, 116.1, 116.2, 126.3, 128.3, 129.1, 131.4, 131.5, 132.5, 141.2, 143.6, 145.0, 147.8, 156.0, 162.7. **IR (KBr):** ν (cm^{-1}) 513, 573, 639, 755, 828, 969, 1031, 1156, 1176, 1229, 1256, 1276, 1427, 1474, 1490, 1513, 1563, 1600, 1623, 1870, 2934, 2954.

MS (ESI) *m/z* (%): 261.1 (5), 303.2 (5), 345.2 [$(M - 2CF_3SO_3^-)^{2+}$] (100), 345.7 (53), 346.2 (14), 689.4 [$(M - 2CF_3SO_3^-)^{2+}$] (4), 839.4 [$(M - CF_3SO_3^-)^{+}$] (45), 840.4 (25), 841.4 (7). **HRMS ESI *m/z*:** calc. for [$(M - 2CF_3SO_3^-)^{2+}$] [$(C_{48}H_{54}O_2N_2)^{2+}$] 345.2087, found 345.2088.

4,13-bis((*E*)-2-(benzyloxy)styryl)-6,7,10,11-tetrahydrodipyrido[2,1-a:1',2'-k][2,9]phenanthroline-5,12-diium trifluoromethanesulfonate (70)

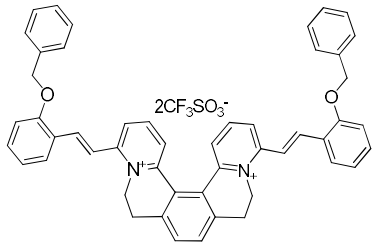

$C_{52}H_{42}F_6N_2O_8S_2$
[1001.0]

The synthesis and purification of [5]helquat dye **70** was accomplished according to *general procedure 5.2.e*, using dye precursor **10** (50 mg, 0.082 mmol, 1.0 equiv.), 2-benzyloxybenzaldehyde (261.0 mg, 1.230 mmol, 15.0 equiv.), pyrrolidine (100 µL, 86.6 mg, 1.218 mmol, 14.9 equiv.) in dry MeOH (5 mL) and [5]helquat dye **70** was obtained as a lemon yellow solid.

Yield: 76.0 mg, 93%.

m.p. 311-313 °C. **^{1}H-NMR (acetonitrile-d_3, 400 MHz):** δ 2.83–3.28 (m, 4H), 4.14-4.22 (m, 2H), 4.91-4.96 (m, 2H), 5.28 (s, 4H), 7.13 (td, J = 0.9, 7.5 Hz, 2H), 7.25 (dd, J = 0.9, 8.5 Hz, 2H), 7.37-7.52 (m, 8H), 7.57-7.60 (m, 4H), 7.64 (d, J = 7.8 Hz, 2H), 7.70 (s, 2H), 7.73 (d, J = 16.0 Hz, 2H), 7.76 (dd, J = 1.6, 7.7 Hz, 2H), 7.83 (d, J = 16.0 Hz, 2H), 8.00 (t, J = 8.1 Hz, 2H), 8.08 (dd, J = 1.4, 8.2 Hz, 2H). **^{13}C-NMR (acetonitrile-d_3, 101 MHz):** δ 28.0, 50.3, 71.6, 114.1, 120.2, 122.3, 124.5, 126.4, 127.6, 129.3, 129.4, 129.4, 129.8, 131.8, 132.6, 133.5, 137.7, 140.9,

141.0, 143.9, 147.8, 156.1, 158.9. **IR (KBr):** *v* (cm^{-1}) 513, 573, 639, 755, 828, 969, 1031, 1156, 1176, 1229, 1256, 1276, 1427, 1474, 1490, 1513, 1563, 1600, 1623, 1870, 2934, 2954. **MS (ESI) *m/z* (%):** 185.1 (25), 227.1 (86), 228.1 (8), 351.2 [$(M - 2CF_3SO_3^-)^{2+}$] (100), 351.7 (52), 352.2 (14), 701.3 (5), 851.3 [$(M - CF_3SO_3^-)^+$] (21), 852.3 (11). **HRMS ESI *m/z*:** calc. for [$(M - 2CF_3SO_3^-)^{2+}$] [$(C_{50}H_{42}O_2N_2)^{2+}$] 351.16177, found 351.16200.

4,13-bis((*E*)- 2,4,5-trimethoxystyryl -6,7,10,11-tetrahydrodipyrido[2,1-a:1',2'-k][2,9] phenanthroline-5,12-diium trifluoromethanesulfonate (71)

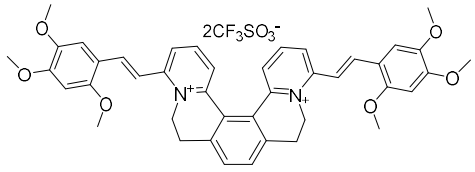

$C_{44}H_{42}F_6N_2O_{12}S_2$
[968.9]

The synthesis and purification of [5]helquat dye **71** was accomplished according to *general procedure 5.2.e*, using dye precursor **10** (50 mg, 0.082 mmol, 1.0 equiv.), 2,4,5-trimethoxybenzaldehyde (241.3 mg, 1.230 mmol, 15.0 equiv.), pyrrolidine (100 µL, 86.6 mg, 1.218 mmol, 14.9 equiv.) in dry MeOH (5 mL) and [5]helquat dye **71** was obtained as a yellow solid.

Yield: 67.2 mg, 85%.

m.p. 298-300 °C. **^{1}H-NMR (acetonitrile-d_3, 400 MHz):** δ 3.10-3.33 (m, 4H), 3.89 (s, 6H), 3.94 (s, 6H), 3.96 (s, 6H), 4.42-4.51 (m, 2H), 5.20-5.23 (m, 2H), 6.74 (s, 2H), 7.34 (s, 2H), 7.52 (d, *J* = 15.9 Hz, 2H), 7.64 (dd, *J* = 1.3, 8.0 Hz, 2H), 7.69 (s, 2H), 7.91 (d, *J* = 15.9 Hz, 2H), 7.98 (t, *J* = 8.1 Hz, 2H), 8.09 (dd, *J* = 8.3, 1.4 Hz, 2H). **^{13}C-NMR (101 MHz, acetonitrile-d_3):** δ 28.2, 50.4, 56.8, 57.2, 57.3, 98.4, 112.5, 115.7, 116.1, 126.1, 128.2, 128.7, 132.4, 140.1, 141.2, 143.3, 144.7, 147.6, 154.7, 155.7, 156.5. **IR (KBr):** *v* (cm^{-1}) 969, 1031, 1152, 1230, 1265, 1440, 1458, 1472, 1489, 1510, 1558, 1602, 1621, 2837. **MS (ESI) *m/z* (%):** 227.1 (5), 320.1 (5), 335.2 [$(M - 2CF_3SO_3^-)^{2+}$] (100), 335.7 (46), 819.3 [$(M - CF_3SO_3^-)^+$] (18), 820.3 (8). **HRMS ESI *m/z*:** calc. for [$(M - 2CF_3SO_3^-)^{2+}$] [$(C_{42}H_{42}O_6N_2)^{2+}$] 335.15160, found 335.15164.

(*E*)-11-(2-(benzo[b]thiophen-3-yl)vinyl)-6,7-dimethyl-4,5,8,9-tetrahydroisoquinolino[1,2-a] pyrido[1,2-k][2,9]phenanthroline-3,10-diium trifluoromethanesulfonate (72)

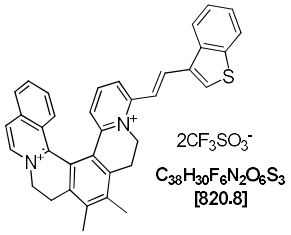

$C_{38}H_{30}F_6N_2O_6S_3$
[820.8]

The synthesis and purification of [6]helquat dye **72** was accomplished by using helquat dye precursor **6** (20 mg, 0.030 mmol, 1.0 equiv.), benzo[b]thiophene-3-carbaldehyde (73 mg, 0.450 mmol, 15.0 equiv.), pyrrolidine (30 µL, 26 mg, 0.366 mmol, 12.2 equiv.) in dry MeOH (2.0 mL) and helquat dye **72** was obtaind as a yellow solid.

Yield: 16 mg, 66%.

m.p. 286-288 °C. **^{1}H-NMR (400 MHz, acetonitrile-d_3):** δ 2.54 (s, 3H), 2.55 (s, 3H), 3.05 (ddd, *J* = 4.9, 14.3, 17.1 Hz, 1H), 3.16 (ddd, *J* = 4.6, 14.6, 17.2 Hz, 1H), 3.54 (ddd, *J* = 1.8, 3.5, 17.2 Hz, 1H), 3.58 (ddd, *J* = 1.9, 3.8, 17.1 Hz, 1H), 4.70 (dt, *J* = 3.8, 14.0 Hz, 1H), 4.79 (dt, *J* = 3.5, 14.3 Hz, 1H), 5.01 (ddd, *J* = 1.8, 4.6, 13.9 Hz, 1H), 5.38 (ddd, *J* = 1.9, 4.9, 13.8 Hz, 1H), 6.93 (dd, *J* =

1.3, 8.1 Hz, 1H), 7.50 (ddd, *J* = 1.2, 6.9 Hz, 1H), 7.57 (dd, *J* = 1.1, 7.1 Hz, 1H), 7.59 (dd, *J* = 1.1, 7.1 Hz, 1H), 7.68 (ddd, *J* = 1.2, 7.0 Hz, 1H), 7.72 (d, *J* = 16.0 Hz, 1H), 7.80 (dq, *J* = 1.0, 8.7 Hz, 1H), 7.87 (d, *J* = 0.8 Hz, 1H), 7.89-7.90 (m, 1H), 7.91 (dd, *J* = 1.2, 3.8 Hz, 1H), 8.05 (dq, *J* = 0.7, 8.06 Hz, 1H), 8.13 (d, *J* = 8.3 Hz, 1H), 8.22 (dt, *J* = 1.0, 7.8 Hz, 1H), 8.29 (d, *J* = 6.6 Hz, 1H), 8.31 (d, *J* = 6.6 Hz, 1H), 8.62 (d, *J* = 6.8 Hz, 1H). **^{13}C-NMR (101 MHz, acetonitrile-d_3):** δ 17.0, 17.2, 25.9, 26.7, 50.6, 56.0, 119.4, 120.6, 123.5, 123.7, 125.7, 125.9, 126.4, 126.9, 128.1, 128.4, 129.2, 129.2, 131.4, 132.8, 136.4, 137.0, 138.3, 138.6, 139.9, 140.6, 140.8, 141.3, 141.5, 142.3, 142.4, 143.7, 148.5, 149.5, 151.6, 154.0. **IR:** *v* (cm^-) 735, 818, 1031, 1157, 1224, 1263, 1379, 1411, 1461, 1483, 1505, 1556, 1573, 1608, 1625. **MS (ESI) *m/z* (%):** 261.1 [(M – $2CF_3SO_3^-$)$^{2+}$] (100), 261.6 (43), 262.1 (5), 521.2 (10), 671.2 [(M – $CF_3SO_3^-$)$^+$] (55), 672.2 (23), 673.3 (5). **HRMS *m/z*:** calc. for [(M – $2CF_3SO_3^-$)$^{2+}$] [($C_{36}H_{30}N_2S$)$^{2+}$] 261.1059, found 261.1060.

(*E*)-11-(4-(allyloxy)styryl)-6,7-dimethyl-4,5,8,9-tetrahydroisoquinolino[1,2-a]pyrido[1,2-k][2,9] phenanthroline-3,10-diium trifluoromethanesulfonate (73)

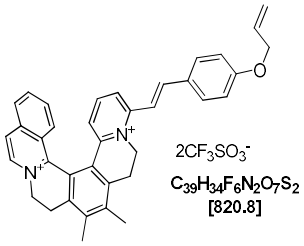

The synthesis and purification was accomplished according to *general procedure 5.2.e,* using [6]helquat dye precursor **6** (20 mg, 0.030 mmol, 1.0 equiv.), 4-(allyloxy)benzaldehyde (73 mg, 0.450 mmol, 15.0 equiv.), pyrrolidine (30 µL, 26 mg, 0.366 mmol, 12.2 equiv.) in dry MeOH (2.0 mL) and [6]helquat dye **73** was obtained as a yellow solid.
Yield: 18 mg, 74%.
m.p. 234-236 °C. **^{1}H-NMR (400 MHz, acetonitrile-d_3):** δ 2.54 (s, 3H), 2.55 (s, 3H), 3.05 (ddd, *J* = 4.9, 14.3, 17.1 Hz, 1H), 3.16 (ddd, *J* = 4.6, 14.6, 17.2 Hz, 1H), 3.54 (ddd, *J* = 1.8, 3.5, 17.2 Hz, 1H), 3.58 (ddd, *J* = 1.9, 3.8, 17.1 Hz, 1H), 4.67 (t, *J* = 1.5, 5.3 Hz, 2H), 4.70 (dt, *J* = 3.8, 14.0 Hz, 1H), 4.79 (dt, *J* = 3.5, 14.3 Hz, 1H), 5.01 (ddd, *J* = 1.8, 4.6, 13.9 Hz, 1H), 5.32 (dq, *J* = 1.5, 11.0 Hz, 1H), 5.38 (ddd, *J* = 1.9, 4.9, 13.8 Hz, 1H), 5.45 (dq, *J* = 1.7, 17.0 Hz, 1H), 6.06-6.15 (m, 1H), 6.81-6.86 (m, 1H), 7.09 (dd, *J* = 2.2, 6.7 Hz, 2H), 7.45-7.52 (m, 2H), 7.56 (d, *J* = 16.0 Hz, 1H), 7.61-7.66 (m, 1H), 7.75-7.79 (m, 4H), 7.87 (ddd, *J* = 1.1, 6.9, 8.2 Hz, 1H), 8.11 (d, *J* = 8.3 Hz, 1H), 8.30 (d, *J* = 6.7 Hz, 1H), 8.60 (dd, *J* = 3.9, 6.8 Hz, 1H). **^{13}C-NMR (acetonitrile-d_3, 101 MHz):** δ 17.0, 17.2, 25.9, 26.7, 50.3, 56.0, 69.8, 116.0, 116.4, 123.4, 125.2, 125.9, 126.9, 128.4, 128.5, 128.6, 128.7, 129.2, 131.4, 132.7, 134.2, 136.4, 136.9, 138.6, 139.9, 141.0, 142.2, 142.3, 143.3, 145.1, 148.1, 151.7, 155.3, 162.2. **IR:** *v* (cm^-) 735, 818, 1031, 1157, 1224, 1263, 1379, 1411, 1461, 1483, 1505, 1556, 1573, 1608, 1625. **MS (ESI) *m/z* (%):** 240.6 (58), 261.6 (22), 521.3 (40), 522.3 [(M – $2CF_3SO_3^-$)$^{2+}$] (16), 671.2 [(M – $CF_3SO_3^-$)$^+$] (100), 672.3 (40), 673.2 (10). HRMS m/z: calc. for [(M – $2CF_3SO_3^-$)$^{2+}$] [($C_{37}H_{33}ON_2$)$^{2+}$] 521.2587, found 521.2587.

(*E*)-4-(2-(4-methylnaphthalen-1-yl)vinyl)-6,7,10,11-tetrahydrodipyrido[2,1-a:1',2'-k][2,9] phenanthroline-5,12-diium trifluoromethanesulfonate (74)

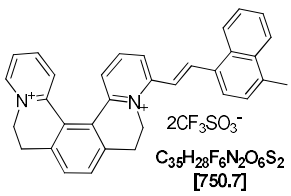

The synthesis and purification of [5]helquat dye **74** was accomplished according to *general procedure 5.2.e*, using dye precursor **14** (50 mg, 0.084 mmol, 1.0 equiv.), 4-methyl-1-naphthylaldehyde (214.4 mg, 1.260 mmol, 15.0 equiv.), pyrrolidine (103.4 µL, 89.6 mg, 1.260 mmol, 15.0 equiv.) in dry MeOH (5.0 mL) and dye **74** was obtained as a yellow solid.
Yield: 52.0 mg, 83%.
m.p. 294-296 °C. **^{1}H-NMR (acetonitrile-d_3, 400 MHz):** δ 2.78 (s, 3H), 3.23-3.33 (m, 4H), 4.50-4.54 (m, 1H), 4.82-4.90 (m, 2H), 5.28-5.31 (m, 1H), 7.54 (d, *J* = 7.4 Hz, 1H), 7.66-7.72 (m, 3H), 7.73 (s, 2H), 7.81 (dd, *J* = 8.1, 1.4 Hz, 1H), 7.90 (ddd, *J* = 7.7, 6.1, 1.4 Hz, 1H), 7.95 (dd, *J* = 1.2, 8.3 Hz, 1H), 8.04 (d, *J* = 7.4 Hz, 1H), 8.13 (t, *J* = 8.1 Hz, 1H), 8.17 (dd, *J* = 1.9, 7.8 Hz, 1H), 8.20 (dd, *J* = 1.9, 7.8 Hz, 1H), 8.31 (dd, *J* = 8.2, 1.4 Hz, 1H), 8.37-8.41 (m, 1H), 8.49 (d, *J* = 15.6 Hz, 1H), 8.80 dd, *J* = 0.9, 6.2 Hz, 1H). **^{13}C-NMR (acetonitrile-d_3, 101 MHz):** δ 20.0, 28.0, 28.1, 50.1, 56.1, 120.9, 124.8, 126.1, 126.7, 127.1, 127.4, 127.4, 127.5, 127.6, 128.0, 128.1, 129.6, 131.2, 131.3, 132.3, 133.1, 133.1, 133.7, 139.6, 141.5, 141.5, 142.2, 144.2, 145.8, 146.7, 147.7, 148.0, 155.7. **IR:** *v* (cm^-) 763, 836, 1031, 1160, 1226, 1259, 1272, 1478, 1490, 1511, 1565, 1580, 1595, 1612, 1624. **MS (ESI) *m/z* (%):** 226.1 [$(M - 2CF_3SO_3^-)^{2+}$] (100), 226.6 (37), 227.1 (23), 451.2 [$(M - 2CF_3SO_3^-)^{2+}$] (8), 601.2 [$(M - CF_3SO_3^-)^+$] (55), 602.2 (21). **HRMS *m/z*:** calc. for [$(M - 2CF_3SO_3^-)^{2+}$] [$(C_{33}H_{28}N_2)^{2+}$] 226.1121, found 226.1122.

(*E*)-4-(2-(naphthalen-2-yl)vinyl)-6,7,10,11-tetrahydrodipyrido[2,1-a:1',2'-k][2,9] phenanthroline-5,12-diium trifluoromethanesulfonate (75)

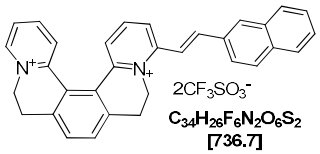

A reaction mixture of helquat dye precursor **14** (25 mg, 0.042 mmol, 1.0 equiv.), 2-naphthylaldehyde (32.8 mg, 0.210 mmol, 5.0 equiv.), EtOH (1 mL) and pyrrolidine (10.4 µL, 9.0 mg, 0.126 mmol, 3.0 equiv.) was placed into a sealed microwave glass tube and was heated in a microwave reactor at 70 °C 5 minutes (microwave power = 150 W). After 5 minutes, TLC analysis (mobile phase: Stoddart's magic mixture) has shown complete consumption of starting helquat **14.** The reaction was quenched by addition of Et_2O (8.0 mL). After centrifugation for 5 minutes, supernatant was separated and the compound was further purified according to the *general procedure 5.2.e*. After drying of the solid under high vacuum, helquat dye **75** was obtained as a greenish yellow solid.
Yield: 27.1 mg, 88.0%.
m.p. 294-296 °C. **^{1}H-NMR (DMSO-d_6, 400 MHz):** δ 3.20-3.29 (m, 2H), 3.34-3.41 (m, 2H), 4.52 (t, *J* = 13.9 Hz, 1H), 4.85 (t, *J* = 13.5 Hz, 1H), 5.05 (d, *J* = 13.0 Hz, 1H), 5.47 (d, *J* = 13.3 Hz, 1H), 7.63 (t, *J* = 9.4 Hz, 1H), 7.65 (dd, *J* = 1.4, 7.4 Hz, 1H), 7.79 (d, *J* = 7.9 Hz, 1H), 7.82 (d, *J* = 7.9 Hz, 1H), 7.97-8.11 (m, 6H), 8.13 (dd, *J* = 1.3, 8.1 Hz, 1H), 8.18-8.38 (m, 5H), 8.47 (dd, *J* = 1.4, 8.2 Hz, 1H), 9.20 (d, *J* = 5.9 Hz, 1H). **^{13}C-NMR (DMSO-d_6, 101 MHz):** δ 26.8, 28.9, 49.4, 54.3, 118.1, 119.1, 122.3, 124.1, 125.3, 126.2, 126.3, 127.1, 127.7, 127.8, 128.2, 128.6, 128.7, 129.6, 130.3, 131.6, 131.7, 132.6, 132.9, 133.9, 140.2, 142.6, 143.4, 144.1, 145.8, 146.4, 146.5, 153.6. **IR:** *v* (cm^-) 518, 573, 637, 755, 793, 825, 1031, 1177, 1260, 1363, 1436, 1509, 1564, 1595, 1624. **MS (ESI) *m/z* (%):** 219.1 [$(M - 2\ CF_3SO_3^-)^{2+}$] (100), 219.6 (42), 437.2 (35), 438.3 (16), 469.2 (10), 587.2 (11). **HRMS ESI *m/z*:** calc. for [$(M - 2\ CF_3SO_3^-)^{2+}$] [$(C_{32}H_{26}N_2)^{2+}$] 219.1043, found 219.1043.

(*E*)-1-methyl-4-(2-(naphthalen-1-yl)vinyl)pyridin-1-ium iodide (76)

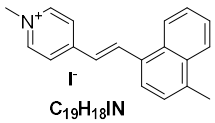

$C_{19}H_{18}IN$
[387.3]

Synthesis and purification of dye **76** as a dark yellow solid was accomplished using *general procedure 5.2.f. method 2.*

Yield: 43 mg, 87%.

m.p. 239-241 °C. **^{1}H-NMR (DMSO-d_6, 400 MHz):** δ 2.72 (s, 3H), 4.28 (s, 3H), 7.51 (dd, *J* = 1.0, 7.5 Hz, 1H), 7.58 (d, *J* = 16.0 Hz, 1H), 7.63-7.72 (m, 2H), 8.01 (d, *J* = 7.5 Hz, 1H), 8.08-8.14 (m, 1H), 8.42 (d, *J* = 6.6 Hz, 2H), 8.55-8.64 (m, 1H), 8.81 (d, *J* = 16.0 Hz, 1H), 8.89 (d, *J* = 6.4 Hz, 2H). **^{13}C-NMR (DMSO-d_6, 101 MHz):** δ 19.5, 46.9, 123.8, 124.2, 124.7, 124.8, 124.9, 126.4, 126.7, 130.4, 130.7, 131.1, 132.3, 137.0, 137.5, 145.0, 152.5. **IR:** *v* (cm^-) 757, 820, 1158, 1189, 1442, 1519, 1595, 1575, 1617, 1640. **MS (ESI) *m/z* (%):** 260.1 (100), 261.2 (25). **HRMS ESI *m/z*:** calc. for $[(M - I^-)^+]$ $[(C_{19}H_{18}N)^+]$: 260.1434, found: 260.1432.

(*E*)-1-methyl-2-(2-(naphthalen-1-yl)vinyl)pyridin-1-ium iodide (77)

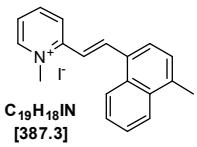

$C_{19}H_{18}IN$
[387.3]

Synthesis and purification of dye **77** as a lemon yellow solid was accomplished using *general procedure 5.2.f. method 2.*

Yield: 43 mg, 87%.

m.p. 271-273 °C. **^{1}H-NMR (DMSO-d_6, 400 MHz):** δ 2.74 (s, 3H), 4.42 (s, 3H), 7.54 (d, *J* = 7.5 Hz, 1H), 7.63 (d, *J* = 15.8 Hz, 1H), 7.65-7.71 (m, 2H), 7.94 (ddd, *J* = 1.4, 6.1, 7.6 Hz, 1H), 8.05-8.21 (m, 2H), 8.48-8.60 (m, 2H), 8.74 (d, *J* = 15.7 Hz, 1H), 8.83 (dd, *J* = 1.4, 8.4 Hz, 1H), 8.94 (dd, *J* = 1.4, 6.3 Hz, 1H). **^{13}C-NMR (DMSO- d_6, 101 MHz):** δ 19.5, 46.9, 119.1, 124.2, 124.9, 125.2, 125.5, 125.6, 126.4, 126.6, 126.8, 130.2, 131.1, 132.3, 137.8, 139.4, 144.2, 146.0, 152.2. **IR:** *v* (cm^-) 741, 803, 1148, 1178, 1462, 1511, 1575, 1610, 1618, 1640. **MS (ESI) *m/z* (%):** 260.1 $[(M - I^-)^+]$ (100), 261.2 (23). **HRMS ESI *m/z*:** calc. for $[(M - I^-)^+]$ $[(C_{19}H_{18}N)]$ 260.1434, found 260.1435.

4,13-bis((*E*)-4-ethoxystyryl)-6,7,10,11-tetrahydrodipyrido[2,1-a:1',2'-k][2,9] phenanthroline-5,12-diium trifluoromethanesulfonate (78)

$C_{42}H_{38}F_6N_2O_8S_2$
[876.9]

Synthesis and purification of [5]helquat dye **78** following *general procedure 5.2.e*, using dye precursor **10** (50 mg, 0.082 mmol, 1.0 equiv.), 4-ethoxybenzaldehyde (184.7 mg, 1.230 mmol, 15.0 equiv.), pyrrolidine (100 µL, 86.6 mg, 1.218 mmol, 14.9 equiv.) in dry MeOH (5 mL) gave **78** as a yellow solid after purification and drying of the solid.

Yield: 63 mg, 88%.

m.p. 213-215 °C. **^{1}H-NMR (acetonitrile-d_3, 400 MHz):** δ 1.41 (t, *J* = 7.0 Hz, 6H), 3.03-3.36 (m, 4H), 4.14 (q, *J* = 7.0 Hz, 4H), 4.43-4.50 (m, 2H), 5.21-5.26 (m, 2H), 7.03 (dd, *J* = 2.0, 6.7 Hz, 2H), 7.05 (dd, *J* = 2.0, 6.7 Hz, 2H), 7.44 (d, *J* = 15.9 Hz, 2H), 7.66 (d, *J* = 15.9 Hz, 2H), 7.67-7.69

(m, 2H), 7.70 (s, 2H), 7.77 (dd, *J* = 2.0, 6.7 Hz, 2H), 7.79 (dd, *J* = 2.0, 6.7 Hz, 2H), 8.02 (t, *J* = 8.1 Hz, 2H), 8.11 (dd, *J* = 1.4, 8.2 Hz, 2H). **^{13}C-NMR (acetonitrile-*d*$_3$, 101 MHz):** *δ* 15.0, 28.1, 50.6, 64.8, 116.1, 116.2, 122.7, 126.3, 128.1, 128.3, 129.1, 131.4, 132.5, 141.2, 145.0, 147.8, 156.0, 162.5. **IR:** *v* (cm^{-}) 518, 573, 638, 755, 827, 1031, 1155, 1177, 1225, 1230, 1256, 1276, 1427, 1475, 1490, 1513, 1564, 1600, 1624, 3074. **MS (ESI) *m/z* (%):** 246.1 (5), 261.1 (24), 275.1 (29), 289.1 [(M – 2$CF_3SO_3^-$)$^{2+}$] (100), 289.6 (43), 290.1 (8), 577.3 (8), 727.2 [(M – $CF_3SO_3^-$)$^{+}$] (36) 728.2 (15). **HRMS ESI *m/z*:** calc. for [(M – 2$CF_3SO_3^-$)$^{2+}$] [($C_{40}H_{38}O_2N_2$)$^{2+}$] 289.14612, found 289.14627.

4,13-bis((*E*)-4-butoxy-3-methoxystyryl)-6,7,10,11-tetrahydrodipyrido[2,1-a:1',2'-k][2,9] phenanthroline-5,12-diium trifluoromethanesulfonate (79)

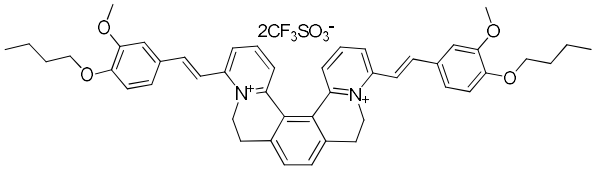

$C_{48}H_{50}F_6N_2O_{10}S_2$
[993.0]

Synthesis and purification of dye **79** using dye precursor **10** (25 mg, 0.041 mmol, 1.0 equiv.), 4-butyloxy-3-methoxybenzaldehyde (128.1 mg, 0.615 mmol, 15.0 equiv.), pyrrolidine (50 µL, 43.3 mg, 0.609 mmol, 14.9 equiv.) in dry MeOH (2.5 mL) was accomplished and [5]helquat dye **79** was obtained as a lemon yellow solid.

Yield: 14.2 mg, 35%.

m.p. 219-221 °C. **^{1}H-NMR (acetonitrile-*d*$_3$, 400 MHz):** *δ* 0.99 (t, *J* = 7.4 Hz, 6H), 1.42-1.58 (m, 4H), 1.79 (dq, *J* = 6.6, 8.5 Hz, 4H), 3.03-3.38 (m, 4H), 3.94 (s, 6H), 4.09 (t, *J* = 6.6 Hz, 4H), 4.43-4.50 (m, 2H), 5.21-5.26 (m, 2H), 7.05 (d, *J* = 8.4 Hz, 2H), 7.34 (dd, *J* = 2.1, 8.4 Hz, 2H), 7.43 (d, *J* = 2.1 Hz, 2H), 7.46 (d, *J* = 15.9 Hz, 2H), 7.65 (d, *J* = 15.9 Hz, 2H), 7.69 (d, *J* = 1.3 Hz, 2H), 7.71 (s, 2H), 8.02 (t, *J* = 8.1 Hz, 2H), 8.12 (dd, *J* = 8.3, 1.4 Hz, 2H). **^{13}C-NMR (acetonitrile-*d*$_3$, 101 MHz):** *δ* 14.1, 20.0, 28.1, 31.9, 50.6, 56.7, 69.5, 111.4, 113.6, 116.3, 124.8, 126.3, 128.1, 128.5, 129.1,132.5, 141.3, 143.6, 145.3, 147.8, 150.8, 152.7, 156.0. **IR:** *v* (cm^{-}) 518, 573, 638, 755, 827, 1031, 1155, 1177, 1225, 1230, 1256, 1276, 1427, 1475, 1490, 1513, 1564, 1600, 1624, 3074. **MS (ESI) *m/z* (%):** 347.2 [(M – 2$CF_3SO_3^-$)$^{2+}$] (100), 347.7 (57), 348.2 (15), 807.4 (8), 843.3 [(M – $CF_3SO_3^-$)$^{+}$] (29), 844.4 (15). **HRMS ESI *m/z*:** calc. for [(M – 2$CF_3SO_3^-$)$^{2+}$] [($C_{46}H_{50}O_4N_2$)$^{2+}$] 347.18798, found 347.18807.

4,13-bis((*E*)-4-heptyloxy-3-methoxystyryl)-6,7,10,11-tetrahydrodipyrido[2,1-a:1',2'-k][2,9] phenanthroline-5,12-diium trifluoromethanesulfonate (80)

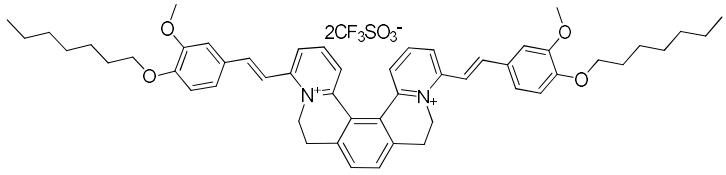

$C_{54}H_{62}F_6N_2O_{10}S_2$
[1077.2]

Synthesis and purification of dye **80** using dye precursor **10** (25 mg, 0.041 mmol, 1.0 equiv.), 4-heptyloxy-3-methoxybenzaldehyde (154 mg, 0.615 mmol, 15.0 equiv.), pyrrolidine (50 µL, 43.3 mg, 0.609 mmol, 14.9 equiv.) in dry MeOH (5 mL) was accomplished according to *general procedure 5.2.e* and [5]helquat dye **80** was obtained as a yellow solid.

Yield: 15 mg, 34%.

m.p. 219-221 °C. **^{1}H-NMR (acetonitrile-*d*$_3$, 400 MHz):** *δ* 0.90 (t, *J* = 7.4 Hz, 6H), 1.27-1.53 (m, 16H), 1.73-1.87 (m, 4H), 3.03-3.38 (m, 4H), 3.94 (s, 6H), 4.09 (t, *J* = 6.6 Hz, 4H), 4.43-4.50 (m,

2H), 5.21-5.26 (m, 2H), 7.05 (d, *J* = 8.4 Hz, 2H), 7.34 (dd, *J* = 2.1, 8.4 Hz, 2H), 7.43 (d, *J* = 2.1 Hz, 2H), 7.46 (d, *J* = 15.9 Hz, 2H), 7.65 (d, *J* = 15.9 Hz, 2H), 7.69 (d, *J* = 1.3 Hz, 2H), 7.71 (s, 2H), 8.02 (t, *J* = 8.1 Hz, 2H), 8.12 (dd, *J* = 8.3, 1.4 Hz, 2H). **^{13}C-NMR (acetonitrile-d_3, 101 MHz):** *δ* 14.4, 23.3, 26.7, 28.1, 29.7, 29.9, 32.5, 50.6, 56.7, 69.8, 111.4, 113.6, 116.3, 124.8, 126.3, 128.1, 128.5, 129.1,132.5, 141.3, 143.6, 145.3, 147.8, 150.8, 152.7, 156.0. **IR:** *v* (cm^-) 518, 573, 638, 755, 827, 1031, 1155, 1177, 1225, 1230, 1256, 1276, 1427, 1475, 1490, 1513, 1564, 1600, 1624, 3074. **MS (ESI) *m/z* (%):** 389.2 [$(M - 2CF_3SO_3^-)^{2+}$] (100), 389.7 (67), 390.2 (23), 891.5 [$(M - 2CF_3SO_3^-)^{2+}$] (10), 927.4 [$(M - CF_3SO_3^-)^+$] (14). **HRMS *m/z*:** calc. for [$(M - 2CF_3SO_3^-)^{+2}$] [$(C_{52}H_{62}O_4N_2)^{2+}$] 389.2349, found 389.2351.

2,15-bis((E)-4-ethoxy-3-methoxystyryl)-6,7,10,11-tetrahydrodipyrido[2,1-a:1',2'-k][2,9] phenanthroline-5,12-diium trifluoromethanesulfonate (86)

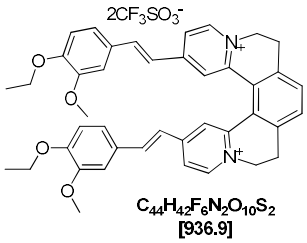

Synthesis and purification of dye **86** using dye precursor **81** (50 mg, 0.082 mmol, 1.0 equiv.), 4-ethoxy-3-methoxybenzaldehyde (221.6 mg, 1.230 mmol, 15.0 equiv.), pyrrolidine (100 µL, 86.6 mg, 1.218 mmol, 14.9 equiv.) in dry MeOH (5 mL) was accomplished according to *general procedure 5.2.e* and [5]helquat dye **86** was obtained as lemon yellow solid.
Yield: 0.052 g, 68.0%.
m.p. 280-282 °C. **^{1}H-NMR (DMSO-d_6, 400 MHz):** *δ* 1.33 (t, *J* = 7.0 Hz, 6H), 3.33-3.36 (m, 4H), 3.76 (s, 6H), 4.04 (q, *J* = 7.0 Hz, 4H), 4.66-4.74 (m, 2H), 4.93-4.99 (m, 2H), 6.98 (d, *J* = 1.0 Hz, 4H), 7.03 (d, *J* = 16.0 Hz, 2H), 7.06 (d, *J* = 1.2 Hz, 2H), 7.34 (d, *J* = 16.2 Hz, 2H), 7.79 (s, 2H), 8.08 (dd, *J* = 2.0, 6.6 Hz, 2H), 8.31 (d, *J* = 2.0 Hz, 2H), 9.08 (d, *J* = 6.6 Hz, 2H). **^{13}C-NMR (DMSO-d_6, 101 MHz):** *δ* 53.2, 66.8, 93.1, 94.6, 103.4, 149.1, 151.6, 159.2, 160.5, 162.5, 164.8, 165.6, 166.8, 171.6, 179.6, 180.8, 184.3, 185.4, 188.7, 190.4, 192.7. **IR:** *v* (cm^-) 517, 573, 638, 859, 1030, 1106, 1161, 1224, 1256, 1424, 1481, 1560, 1615, 1628, 2830. **MS (ESI) *m/z* (%):** 290.1 (10), 319.2 (53), 319.7 (23), 637.3 [$(M - 2CF_3SO_3^-)^{2+}$] (14), 787.3 [$(M - CF_3SO_3^-)^+$] (100), 788.3 (43), 815.3 (14). **HRMS *m/z*:** calc. for [$(M - 2CF_3SO_3^-)^{2+}$] [$(C_{42}H_{41}O_4N_2)^{2+}$] 638.30608, found 638.30624.

2,15-bis((E)-4-ethoxy-3-methoxystyryl)-8,9-dimethyl-6,7,10,11-tetrahydrodipyrido[2,1-a:1',2'-k][2,9]phenanthroline-5,12-diium trifluoromethanesulfonate (87)

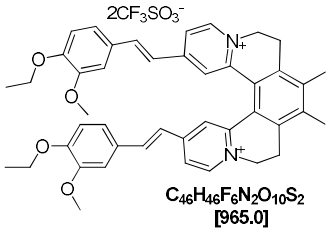

A reaction mixture containing helquat dye precursor **82** (25 mg, 0.039 mmol, 1.0 equiv.), 4-ethoxy-3-methoxybenzaldehyde (35.2 mg, 0.195 mmol, 5.0 equiv.), EtOH (1 mL) and pyrrolidine (9.6 µL, 8.3 mg, 0.117 mmol, 3.0 equiv.) was heated at 70 °C in a microwave reactor for 5 minutes (microwave power = 150 W). After 5 minutes, TLC analysis (mobile phase: Stoddart's magic mixture) has shown complete consumption of starting helquat **82.** The reaction was quenched by addition of Et_2O (8.0 mL). After centrifugation for 5 minutes,

supernatant was separated and the compound was further purified by *general procedure 5.2.e,* followed by drying under high vacuum gave **87** as a yellow solid.

Yield: 29 mg, 77.0%.

m.p. 280-282 °C. **^{1}H-NMR (DMSO-d_6, 400 MHz):** δ 1.37 (t, J = 7.0 Hz, 6H), 2.45 (s, 6H), 3.00-3.16 (m, 2H), 3.32-3.55 (m, 2H), 3.81 (s, 6H), 4.07 (q, J = 7.0 Hz, 4H), 4.68 (td, J = 3.7, 13.7, 14.1 Hz, 1H), 4.70 (td, J = 14.1, 13.7, 3.7 Hz, 1H), 4.84 (dd, J = 13.4, 4.6 Hz, 1H), 4.86 (dd, J = 13.4, 4.6 Hz, 1H), 6.92 (d, J = 8.3 Hz, 2H), 6.98 (d, J = 16.2 Hz, 2H), 7.04 (dd, J = 2.1, 8.3 Hz, 2H), 7.09 (d, J = 2.0 Hz, 2H), 7.31 (d, J = 16.2 Hz, 2H), 7.76 (d, J = 1.9 Hz, 2H), 7.85 (dd, J = 2.0, 6.6 Hz, 2H), 8.59 (d, J = 6.6 Hz, 2H). **^{13}C-NMR (DMSO-d_6, 101 MHz):** δ 14.6, 16.4, 25.3, 52.9, 55.5, 63.8, 110.0, 112.5, 120.4, 122.3, 122.7, 124.3, 125.5, 127.5, 138.8, 139.4, 140.8, 144.6, 146.6, 149.1, 150.4, 152.1. **IR:** v (cm$^-$) 518, 573, 638, 735, 1030, 1143, 1226, 1265, 1424, 1467, 1476, 1512, 1565, 1612, 1631, 2855. **MS (ESI) *m/z* (%):** 333.2 [(M – $2CF_3SO_3^-$)$^{+2}$] (100), 333.8 (67), 334.3 (18), 665.5 [(M – $2CF_3SO_3^-$)$^{2+}$] (5), 815.6 (10). **HRMS *m/z*:** calc. for [(M – $2CF_3SO_3^-$)$^{2+}$] ($C_{44}H_{45}N_2O_4$) calc. 665.3374, found 665.3375.

2,4-bis((E)-4-ethoxy-3-methoxystyryl)-6,7,10,11-tetrahydrodipyrido[2,1-a:1',2'-k][2,9] phenanthroline-5,12-diium trifluoromethanesulfonate (88)

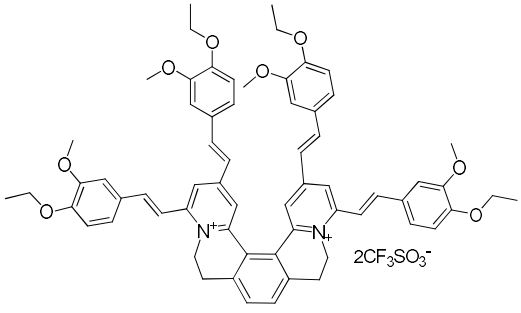

Synthesis and purification of dye **88** using dye precursor **83** (20 mg, 0.031 mmol, 1.0 equiv.), 4-ethoxy-3-methoxybenzaldehyde (167.6 mg, 0.930 mmol, 30.0 equiv.)**,** pyrrolidine (50 µL, 43.3 mg, 0.609 mmol, 19.6 equiv.) in dry MeOH (2 mL) was accomplished according to *general procedure 5.2.e* and [5]helquat dye **88** was obtained as yellow solid.

Yield: 35.9 mg, 89.0%.

m.p. > 350 °C. **^{1}H-NMR (DMSO-d_6, 400 MHz):** δ 1.31 (t, J = 6.9 Hz, 6H), 1.39 (t, J = 6.9 Hz, 6H), 3.22-3.40 (m, 4H), 3.67 (s, 6H), 3.92 (s, 6H), 4.02 (q, J = 7.0 Hz, 4H), 4.14 (q, J = 7.0 Hz, 4H), 4.44-4.52 (m, 2H), 5.30-5.36 (m, 2H), 6.96 (d, J = 8.3 Hz, 2H), 7.00-7.03 (m, 4H), 7.03 (d, J = 16.0 Hz, 2H), 7.13 (d, J = 8.5 Hz, 2H), 7.38 (d, J = 16.2 Hz, 2H), 7.45 (dd, J = 8.4, 1.9 Hz, 2H), 7.54 (d, J = 2.0 Hz, 2H), 7.68 (d, J = 15.8 Hz, 2H), 7.82 (s, 2H), 7.89 (d, J = 15.7 Hz, 2H), 8.04 (d, J = 1.7 Hz, 2H), 8.36 (d, J = 1.8 Hz, 2H). **^{13}C-NMR (DMSO-d_6, 101 MHz):** δ 14.6, 14.7, 27.2, 48.5, 55.3, 55.8, 63.8, 63.9, 110.3, 110.6, 112.6, 112.6, 116.1, 119.9, 120.5, 121.8, 123.4, 127.4, 127.6, 127.7, 131.0, 132.8, 137.0, 139.7, 140.2, 142.8, 146.0, 149.0, 149.2, 150.2, 150.6, 153.3. **IR:** v (cm$^-$) 763, 836, 1031, 1160, 1226, 1259, 1272, 1478, 1490, 1511, 1565, 1580, 1595, 1612, 1624. **MS (ESI) *m/z* (%):** 414.2 (10), 495.2 (100), 495.7 (70), 496.2 (22), 815.3 (5), 1139.4 [(M – $CF_3SO_3^-$)$^+$] (10). **HRMS *m/z*:** calc. for [(M – $2CF_3SO_3^-$)$^{2+}$] [($C_{64}H_{65}O_8N_2$)$^{2+}$] 989.4735, found 989.4738.

4,13-bis((*E*)-4-ethoxy-3-methoxystyryl)-8,9-dimethyl-6,7,10,11-tetrahydrodipyrido[2,1-a:1',2'-k][2,9]phenanthroline-5,12-diium trifluoromethanesulfonate (89)

$C_{46}H_{46}F_6N_2O_{10}S_2$
[965.0]

Synthesis and purification of dye **89** using dye precursor **84** (50 mg, 0.078 mmol, 1.0 equiv.), 4-ethoxy-3-methoxybenzaldehyde (210.8 mg, 1.170 mmol, 15.0 equiv.), pyrrolidine (96 µL, 83.2 mg, 1.170 mmol, 15.7 equiv.) in dry MeOH (5 mL) was accomplished according to *general procedure 5.2.e* and [5]helquat dye **89** was obtained as a lemon yellow solid.
Yield: 60.2 mg, 80.0%.
m.p. 341-343 °C. **^{1}H-NMR (DMSO-d_6, 400 MHz):** δ 1.38 (t, *J* = 6.9 Hz, 6H), 2.43 (s, 6H), 3.00-3.10 (m, 2H), 3.38-3.49 (m, 2H), 3.89 (s, 6H), 4.12 (q, *J* = 6.9 Hz, 4H), 4.43-4.51 (m, 2H), 5.40-5.46 (m, 2H), 7.11 (d, *J* = 8.4 Hz, 2H), 7.44 (dd, *J* = 2.0, 8.4 Hz, 2H), 7.55 (d, *J* = 2.0 Hz, 2H), 7.70 (d, *J* = 15.9 Hz, 2H), 7.84 (d, *J* = 15.8 Hz, 2H), 7.88 (d, *J* = 1.3 Hz, 2H), 8.09 (t, *J* = 8.1 Hz, 2H), 8.29 (dd, *J* = 1.3, 8.3 Hz, 2H). **^{13}C-NMR (DMSO-d_6, 101 MHz):** δ 14.6, 16.1, 25.2, 48.9, 55.8, 63.9, 110.7, 112.5, 115.6, 123.6, 124.1, 125.1, 127.7, 128.0, 138.5, 138.7, 141.8, 143.5, 147.2, 149.2, 150.7, 153.3. **IR:** *v* (cm^-) 763, 836, 1031, 1160, 1226, 1259, 1272, 1478, 1490, 1511, 1565, 1580, 1595, 1612, 1624. **MS (ESI) *m/z* (%):** 318.1 (10), 333.2 (76), 333.7 (37), 334.2 (7), 665.3 [$(M - 2CF_3SO_3^-)^{2+}$] (14), 787.3 (7), 815.3 [$(M - 2CF_3SO_3^-)^+$] (100), 816.3 (47), 817.3 (11). **HRMS *m/z*:** calc. for [$(M - 2CF_3SO_3^-)^{2+}$] [$(C_{44}H_{45}O_4N_2)^{2+}$] 665.3374, found 665.3375.

2,4-bis((E)-4-ethoxy-3-methoxystyryl)-6,7,10,11-tetrahydrodipyrido[2,1-a:1',2'-k][2,9] phenanthroline-5,12-diium trifluoromethanesulfonate (90)

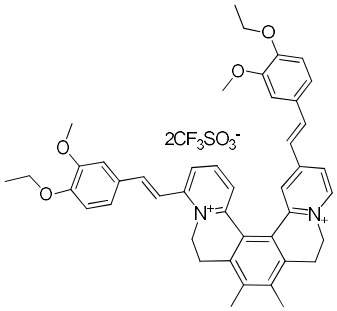

$C_{46}H_{46}F_6N_2O_{10}S_2$
[965.0]

Synthesis and purification of dye **90** using dye precursor **85** (50 mg, 0.078 mmol, 1.0 equiv.), 4-ethoxy-3-methoxybenzaldehyde (210.8 mg, 1.170 mmol, 15.0 equiv.), pyrrolidine (96.1 µL, 83.2 mg, 1.170 mmol, 15.0 equiv.) in dry MeOH (5 mL) was accomplished according to *general procedure 5.2.e* and [5]helquat dye **90** was obtained as a golden yellow solid.
Yield: 51.2 mg, 68.0%.
m.p. 318-320 °C. **^{1}H-NMR (DMSO-d_6, 400 MHz):** δ 1.31 (t, *J* = 6.9 Hz, 3H), 1.38 (t, *J* = 7.0 Hz, 3H), 2.42 (s, 3H), 2.43 (s, 3H), 2.99-3.13 (m, 2H), 3.47 (dd, *J* = 15.1, 18.6 Hz, 1H), 3.49 (dd, *J* = 15.1, 18.6 Hz, 1H), 3.68 (s, 3H), 3.91 (s, 3H), 4.03 (q, *J* = 7.0 Hz, 2H), 4.13 (q, *J* = 7.0 Hz, 2H), 4.44-4.58 (m, 1H), 4.68 (t, *J* = 13.5 Hz, 1H), 4.94 (d, *J* = 12.3 Hz, 1H), 5.48 (d, *J* = 13.2 Hz, 1H), 6.98 (d, *J* = 8.4 Hz, 1H), 7.03 (d, *J* = 8.8 Hz, 1H), 7.06 (d, *J* = 5.4 Hz, 1H), 7.10 (dd, *J* = 2.0, 8.4 Hz, 1H), 7.13 (d, *J* = 8.4 Hz, 1H), 7.36 (d, *J* = 16.2 Hz, 1H), 7.45 (dd, *J* = 8.4, 2.1 Hz, 1H), 7.55

(d, *J* = 2.1 Hz, 1H), 7.72 (d, *J* = 15.9 Hz, 1H), 7.89 (d, *J* = 1.9 Hz, 1H), 7.93 (d, *J* = 15.8 Hz, 1H), 8.02 (dd, *J* = 2.0, 6.7 Hz, 1H), 8.03 (dd, *J* = 1.2, 7.9 Hz, 1H), 8.14 (t, *J* = 8.1 Hz, 1H), 8.37 (dd, *J* = 1.3, 8.3 Hz, 1H), 8.99 (d, *J* = 6.6 Hz, 1H). **^{13}C-NMR (DMSO-d_6, 101 MHz):** *δ* 14.6, 14.7, 16.3, 25.2, 49.1, 52.8, 55.4, 55.8, 63.8, 63.9, 110.6, 110.8, 112.5, 112.7, 115.6, 119.1, 120.5, 120.9, 122.0, 122.3, 123.7, 123.9, 124.4, 125.0, 125.5, 127.5, 127.7, 127.9, 138.7, 138.7, 138.9, 139.1, 141.0, 141.7, 143.4, 144.4, 146.5, 147.3, 149.0, 149.2, 150.3, 150.7, 152.0, 153.5. **IR:** *v* (cm^-) 763, 836, 1031, 1160, 1226, 1259, 1272, 1478, 1490, 1511, 1565, 1580, 1595, 1612, 1624. **MS (ESI) *m/z* (%):** 333.2 (100), 333.7 [$(M - 2CF_3SO_3^-)^{2+}$] (60), 334.2 (18), 665.4 [$(M - 2CF_3SO_3^-)^{2+}$] (8), 815.3 [$(M - CF_3SO_3^-)^+$] (10). **HRMS *m/z*:** calc. for [$(M - 2CF_3SO_3^-)^{2+}$] [$(C_{44}H_{45}O_4N_2)^{2+}$] 665.3374, found 665.3375.

4,15-Bis((*E*)-4-ethoxy-3-methoxystyryl)-6,7,8,11,12,13-hexahydrodipyrido[1,2-a:1', 2'-a'] benzo[2,1-c:3,4-c']bisazepindiium trifluoromethansulfonate [(*rac*)-92]

$C_{46}H_{46}F_6N_2O_{10}S_2$
965.0

Synthesis and purification of dye (***rac*)-92** using dye precursor **(*rac*)-91** (20 mg, 0.031 mmol, 1.0 equiv.), 4-ethoxy-3-methoxybenzaldehyde (83.8 mg, 0.465 mmol, 15.0 equiv.)**,** pyrrolidine (38 µL, 33.0 mg, 0.464 mmol, 15.0 equiv.) in dry MeOH (1.0 mL) was accomplished according to *general procedure 5.2.e* and [5]helquat dye **(*rac*)-92** was obtained as lemon yellow solid.

Yield: 26.2 mg, 87.0%.

m.p. 280-282 °C. **^{1}H-NMR (DMSO-d_6, 400 MHz):** *δ* 1.37 (t, *J* = 6.9 Hz, 6H), 2.24-2.45 (m, 4H), 2.66-2.77 (m, 2H), 3.03 (dd, *J* = 6.1, 13.5 Hz, 1H), 3.05 (dd, *J* = 6.1, 13.5 Hz, 1H), 3.89 (s, 6H), 4.12 (q, *J* = 7.0 Hz, 4H), 4.32-4.41 (m, 2H), 5.17-5.22 (m, 2H), 7.10 (d, *J* = 8.4 Hz, 2H), 7.39 (dd, *J* = 1.3, 7.8 Hz, 2H), 7.48 (dd, *J* = 2.0, 8.5 Hz, 2H), 7.54 (d, *J* = 15.7 Hz, 2H), 7.57 (d, *J* = 1.0 Hz, 2H), 7.77 (s, 2H), 7.90 (d, *J* = 15.7 Hz, 2H), 8.12 (t, *J* = 8.1 Hz, 2H), 8.41 (dd, *J* = 1.3, 8.6 Hz, 2H). **^{13}C-NMR (DMSO-d_6, 101 MHz):** *δ* 14.6, 28.2, 30.5, 52.5, 55.9, 63.9, 111.2, 112.5, 115.0, 123.8, 125.3, 127.6, 128.7, 131.1, 132.5, 138.5, 142.8, 144.8, 149.1, 150.9, 151.5, 154.1. **IR:** *v* (cm^-) 763, 836, 1031, 1160, 1226, 1259, 1272, 1478, 1490, 1511, 1565, 1580, 1595, 1612, 1624. **MS (ESI) *m/z* (%):** 333.1 (100), 333.6 (73), 334.1 (20), 503.2 (5), 815.3 (17), 816.3 (10). **HRMS *m/z*:** calc. for [$(M - 2CF_3SO_3^-)^{2+}$] [$(C_{44}H_{46}O_4N_2)^{2+}$] 333.1723, found 333.1726.

4,15-Bis((*E*)-4-ethoxy-3-methoxystyryl)-6,7,8,11,12,13-hexahydrodipyrido[1,2-a:1', 2'-a'] benzo[2,1-c:3,4-c']bisazepindiium trifluoromethansulfonate (*P*)- 92

$C_{46}H_{46}F_6N_2O_{10}S_2$
965.0

Synthesis and purification of dye **(*P*)-92** using dye precursor **(*P*)-91** (20 mg, 0.031 mmol, 1.0 equiv.), 4-ethoxy-3-methoxybenzaldehyde (83.8 mg, 0.465 mmol, 15.0 equiv.), pyrrolidine (38 µL, 33.0 mg, 0.464 mmol, 15.0 equiv.) in dry MeOH (1.0 mL) was accomplished according to *general procedure 5.2.e* and [5]helquat dye **(*P*)-92** was obtained as a yellow solid.

Yield: 25 mg, 83.0%.

m.p. 280-282 °C. **^{1}H-NMR (DMSO-d_6, 400 MHz):** δ 1.37 (t, *J* = 6.9 Hz, 6H), 2.24-2.45 (m, 4H), 2.66-2.77 (m, 2H), 3.03 (dd, *J* = 6.1, 13.5 Hz, 1H), 3.05 (dd, *J* = 6.1, 13.5 Hz, 1H), 3.89 (s, 6H), 4.12 (q, *J* = 7.0 Hz, 4H), 4.32-4.41 (m, 2H), 5.17-5.22 (m, 2H), 7.10 (d, *J* = 8.4 Hz, 2H), 7.39 (dd, *J* = 1.3, 7.8 Hz, 2H), 7.48 (dd, *J* = 2.0, 8.5 Hz, 2H), 7.54 (d, *J* = 15.7 Hz, 2H), 7.57 (d, *J* = 1.0 Hz, 2H), 7.77 (s, 2H), 7.90 (d, *J* = 15.7 Hz, 2H), 8.12 (t, *J* = 8.1 Hz, 2H), 8.41 (dd, *J* = 1.3, 8.6 Hz, 2H). **^{13}C-NMR (DMSO-d_6, 101 MHz):** δ 14.6, 28.2, 30.5, 52.5, 55.9, 63.9, 111.2, 112.5, 115.0, 123.8, 125.3, 127.6, 128.7, 131.1, 132.5, 138.5, 142.8, 144.8, 149.1, 150.9, 151.5, 154.1. **IR:** *v* (cm^-) 763, 836, 1031, 1160, 1226, 1259, 1272, 1478, 1490, 1511, 1565, 1580, 1595, 1612, 1624. **MS (ESI) *m/z* (%):** 333.1 (100), 333.6 (73), 334.1 (20), 503.2 (5), 815.3 (17), 816.3 (10). **HRMS *m/z*:** calc. for $[(M - 2\ CF_3SO_3^-)^{2+}]$ $[(C_{44}H_{46}O_4N_2)^{2+}]$ 333.1723, found 333.1726. **Chiral purity:** >95% *ee* by CE (Capillary electrophoresis).

4,15-Bis((*E*)-4-ethoxy-3-methoxystyryl)-6,7,8,11,12,13-hexahydrodipyrido[1,2-a:1', 2'-a'] benzo[2,1-c:3,4-c']bisazepindiium trifluoromethansulfonate (*M*)- 92

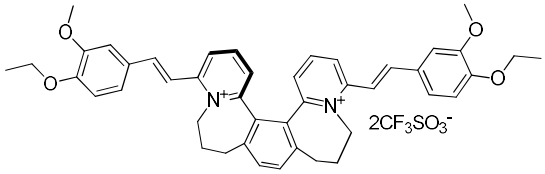

$C_{46}H_{46}F_6N_2O_{10}S_2$
[965.0]

Synthesis and purification of dye **(*M*)-92** using dye precursor **(*M*-91)** (20 mg, 0.031 mmol, 1.0 equiv.), 4-ethoxy-3-methoxybenzaldehyde (83.8 mg, 0.465 mmol, 15.0 equiv.), pyrrolidine (38 µL, 33.0 mg, 0.464 mmol, 15.0 equiv.) in dry MeOH (1.0 mL) was accomplished according to *general procedure 5.2.e* and [5]helquat dye **(*M*)-92** was obtained as a yellow solid.

Yield: 22 g, 73.0%.

m.p. 280-282 °C. δ 1.37 (t, *J* = 6.9 Hz, 6H), 2.24-2.45 (m, 4H), 2.66-2.77 (m, 2H), 3.03 (dd, *J* = 6.1, 13.5 Hz, 1H), 3.05 (dd, *J* = 6.1, 13.5 Hz, 1H), 3.89 (s, 6H), 4.12 (q, *J* = 7.0 Hz, 4H), 4.32-4.41 (m, 2H), 5.17-5.22 (m, 2H), 7.10 (d, *J* = 8.4 Hz, 2H), 7.39 (dd, *J* = 1.3, 7.8 Hz, 2H), 7.48 (dd, *J* = 2.0, 8.5 Hz, 2H), 7.54 (d, *J* = 15.7 Hz, 2H), 7.57 (d, *J* = 1.0 Hz, 2H), 7.77 (s, 2H), 7.90 (d, *J* = 15.7 Hz, 2H), 8.12 (t, *J* = 8.1 Hz, 2H), 8.41 (dd, *J* = 1.3, 8.6 Hz, 2H). **^{13}C-NMR (DMSO-d_6, 101 MHz):** δ 14.6, 28.2, 30.5, 52.5, 55.9, 63.9, 111.2, 112.5, 115.0, 123.8, 125.3, 127.6, 128.7, 131.1, 132.5, 138.5, 142.8, 144.8, 149.1, 150.9, 151.5, 154.1. **IR:** *v* (cm^-) 763, 836, 1031, 1160, 1226, 1259, 1272, 1478, 1490, 1511, 1565, 1580, 1595, 1612, 1624. **MS (ESI) *m/z* (%):** 333.1 (100), 333.6 (73), 334.1 (20), 503.2 (5), 815.3 (17), 816.3 (10). **HRMS *m/z*:** calc. for $[(M - 2\ CF_3SO_3^-)^{2+}]$ $[(C_{44}H_{46}O_4N_2)^{2+}]$ 333.1723, found 333.1726. **Chiral purity:** >95% *ee* by CE.

5.4 X-ray crystallography:

Crystallographic data were collected on a diffractometer equipped with a CCD detector using a monochromatized MoKα radiation (λ = 0.71073 Å) at a temperature of 150(2) K. The structure was solved by direct methods (SHELXS){ref} and refined by full matrix least squares based on F 2 (SHELXL97).){ref} The hydrogen atoms on carbons were fixed into idealized positions (riding model) and assigned temperature factors either Hiso(H) = 1.2 Ueq(pivot atom) or Hiso(H) = 1.5 Ueq for methyl moiety.

5.4.1 X-ray data for [6]helquat 6.

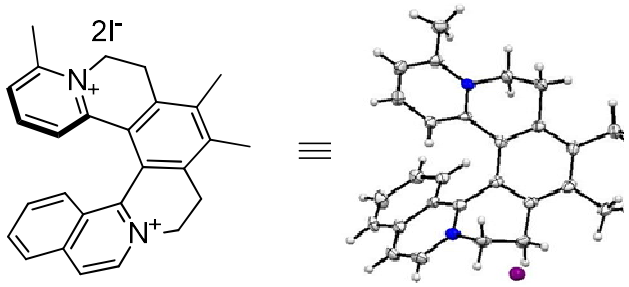

Crystal data for [(*P*)-6][I]$_2$: $C_{27}H_{26}N_2$•2(I), M_r = 632.30; Monoclinic, space group $P2_{1/n}$ (No 14), *a* = 7.8813 (2) Å, *b* = 16.2049 (4) Å, *c* = 19.5829 (5) Å, *β* = 99.067 (1)°; V = 2469.79 (11) Å3 , Z = 4, D_x = 1.700 Mg m-3 ; dimensions of yellow bar 0.44 × 0.12 × 0.11 mm, ϑ_{max} = 27.5°; numerical absorption correction (μ = 2.56 mm^{-1}) T_{min} = 0.401, T_{max} = 0.769; 31665 diffractions collected, 5678 independent (R_{int} =0.025) and 5069 observed according to the $I > 2\sigma(I)$ criterion. The refinement converged (Δ/σ_{max}= 0.002) to *R* = 0.022 for observed reflections and wR(F^2) = 0.047, *GOF* = 1.02 for 283 parameters and all 5678 reflections. The final difference map displayed no peaks of chemical significance ($\Delta\rho_{max}$ =1.02, $\Delta\rho_{min}$ -0.83 e.Å^{-3}).

5.4.2 X-ray data for [6]helquat dye 20:

CCDC 1012247

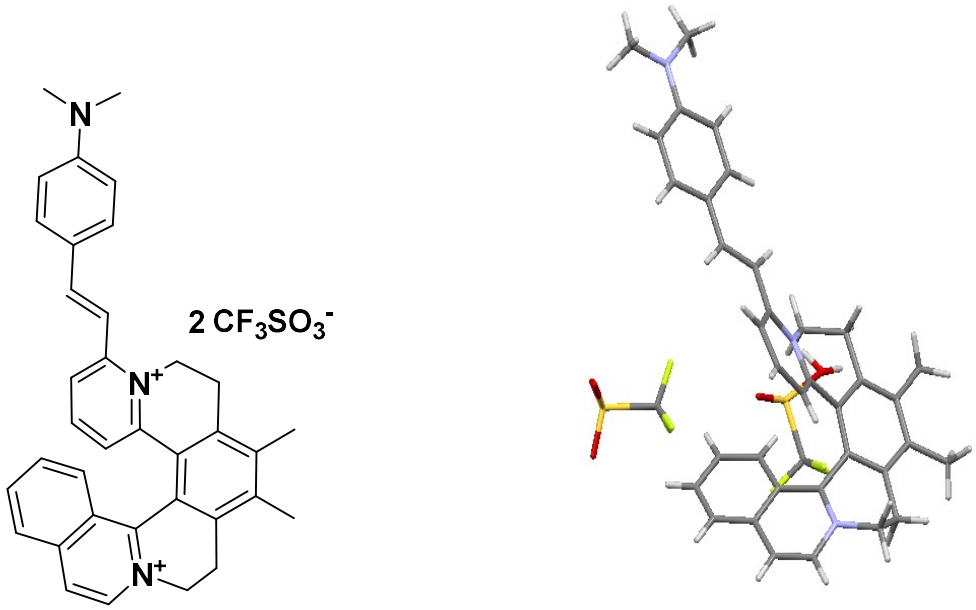

[6]Helquat dye **6** (2 mg) was dissolved in acetone (0.2 mL). Single crystals suitable for X-ray analysis were grown *via* slow diffusion of *i*-Pr2O into the solution at room temperature (22–25 °C) in the dark over 10 days.

Crystal data for CCDC 1012247: 2($C_{36}H_{35}N_3$)•4(CF_3O_3S)•H_2O, *M*r = 1633.64; Triclinic, *P*1 (No 1), *a* = = 9.7985(3) Å, *b* = 10.1396(4) Å, *c* = 19.4403(7) Å, *α* = 89.593(1)°, *β* = 83.894(1)° , *γ* = 68.851(1) °, *V* = 1790.12(11) Å3 , Z = 1, *D*x = 1.515 Mg m–3, red plate of dimensions 0.51 ×

0.43 × 0.17 mm, multi-scan absorption correction (μ = 0.24 mm–1) *T*min = 0.890, *T*max = 0.962; a total of 44178 measured reflections (θmax= 27.5˚), from which 16387 were unique (*R*int = 0.026) and 14165 observed according to the $I > 2\sigma(I)$ criterion. The refinement converged (Δ/σmax= 0.001) to *R* = 0.071 for observed reflections and *wR*(*F*2) = 0.201, GOF = 1.01 for 1001 parameters and all 16387 reflections. The final difference Fourier map displayed no peaks of chemical significance; positive ones are in the vicinity of the triflate moiety, due to its disorder (Δρmax = 1.70, Δρmin = –0.61 eÅ–3). S5

The structure was refined in the noncentrosymmetric space group *P*1, however two helquat cations follow closely the centrosymmetric space group *P*-1 (both enantiomers are present). In this space group, the triflate anions would appeared to be vastly disordered; therefore, low symmetry was selected for final refinement. One isolated peak of positive electron density was assigned to a water molecule, but its hydrogen atoms could not be found on the difference map and were therefore placed in positions suitable for hydrogen bonds.

5.4.3 X-ray data for [6]helquat dye 28:

CCDC 1532598

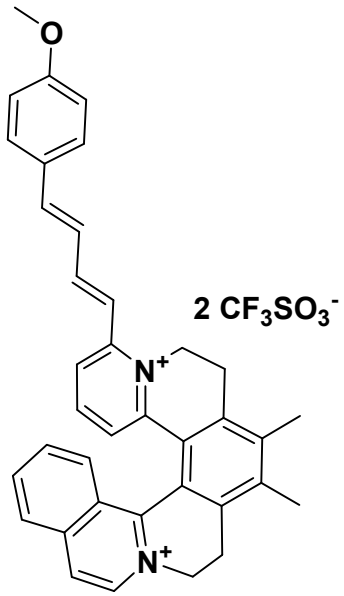

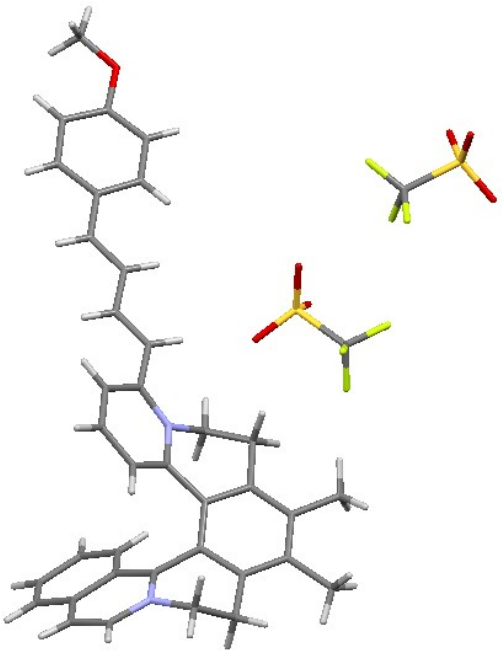

The solid (2 mg) was dissolved in MeOH (0.2 ml). Single crystals suitable for X-ray analysis were grown *via* slow diffusion of *i*-Pr_2O into MeOH solution at room temperature (22-25°C) in dark at within 8 -10 days.

Crystal data for 1532598: , M_r = 820.80; Triclinic, *P-1* (No 2), *a* = 8.1458 (13) Å, *b* = 14.503 (3) Å, *c* = 15.696 (3) Å, α = 89.660 (5) °, *β* = 89.057 (6)°, γ = 76.492 (6), *V* = 1802.8 (5) $Å^3$, Z = 2, D_x = 1.512 Mg m^{-3}, yellow plate of dimensions 0.30 × 0.24 × 0.12 mm, multi-scan absorption correction (μ = 0.23 mm^{-1}), T_{min} = 0.93, T_{max} = 0.97; a total of 13233 measured reflections (ϑ_{max}= 25˚), from which 6369 were unique (R_{int} = 0.072) and 4063 observed according to the $I > 2\sigma(I)$ criterion. The refinement converged (Δ/σ_{max}= 0.003) to *R* = 0.073 for observed reflections and *wR*(F^2) = 0.206, GOF = 1.03 for 508 parameters and all 6369 reflections. The final difference Fourier map displayed no peaks of chemical significance, ($\Delta\rho_{max}$ = 0.51, $\Delta\rho_{min}$ = -0.35 e.$Å^{-3}$).

5.4.4 X-ray data for HeliDye1 (29)

CCDC 1412114

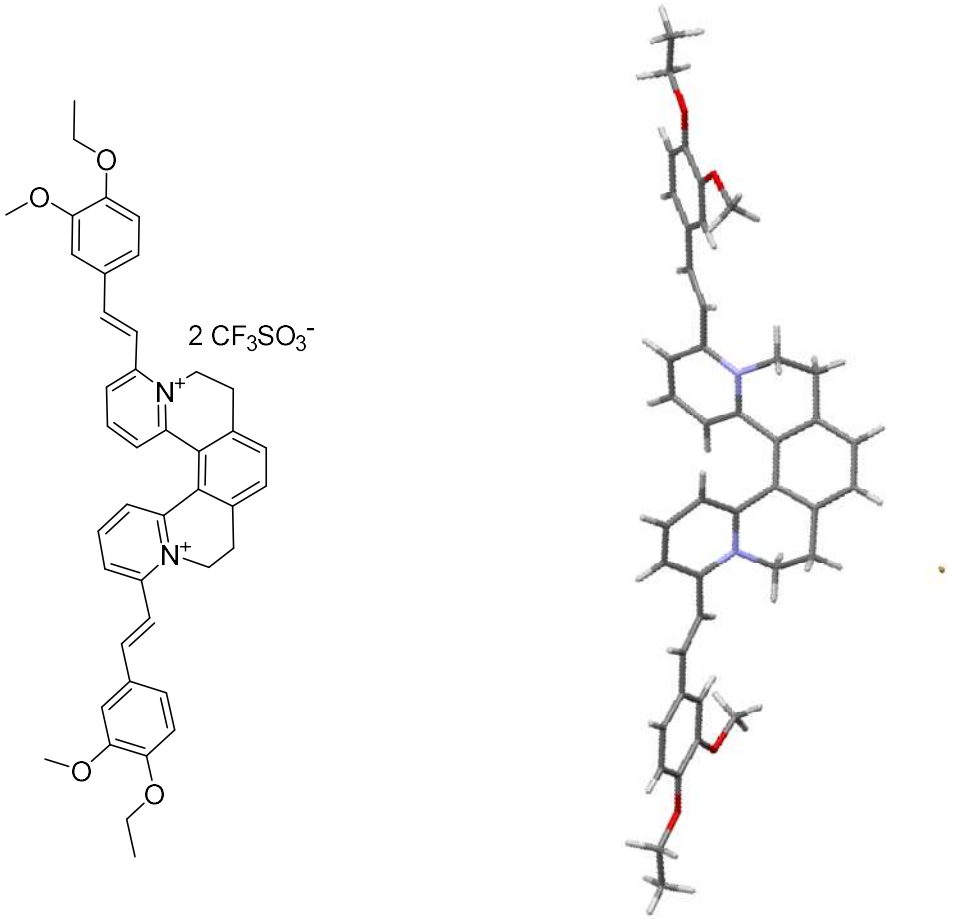

The displacement ellipsoids in this illustration were set to 50% probability level.

Dibromide salt of **29** (2 mg) was dissolved in MeOH (0.2 mL). Single crystals suitable for X-ray analysis were grown *via* slow diffusion of *i*-Pr_2O into the methanolic solution at rt (22-25°C) in the dark within 8-10 days.

CCDC 1412114. Crystal data: $C_{42}H_{42}N_2O_4 \bullet 2Br$, M_r = 798.60, Monoclinic, *C*2/*c* (No 15), *a* = 45.657 (4) Å, *b* = 12.2162 (12) Å, *c* = 7.4051 (6) Å, *β* = 93.046 (3)°, *V* = 4124.4 (7)Å^3, Z = 4, D_x = 1.286 Mg m^{-3}, yellow plate of dimensions 0.38 × 0.18 × 0.06 mm, numerical absorption correction (μ = 2.01 mm^{-1}) T_{min} = 0.515, T_{max} = 0.896, a total of 13287 measured reflections (ϑ_{max}= 26˚), from which 4050 were unique (R_{int} = 0.039) and 2859 observed according to the $I > 2\sigma(I)$ criterion. The refinement converged (Δ/σ_{max}= 0.001) to *R* = 0.048 for observed reflections and $wR(F^2)$ = 0.116, GOF = 1.01 for 228 parameters and all 4050 reflections. The final difference Fourier map displayed no peaks of chemical significance, ($\Delta\rho_{max}$ = 0.74, $\Delta\rho_{min}$ = -0.34 e.Å^{-3}). PLATON/ SQUEEZE procedure was used to correct the diffraction data for the presence of the disordered methanol solvent.

6. References:

1 L. Adriaenssens, L. Severa, T. Salova, I. Cisarova, R. Pohl, D. Saman, S. V. Rocha, N. S. Finney, L. Pospisil, P. Slavicek and F. Teply, *Chem. Eur. J.*, 2009, **15**, 1072.

2 R. H. Martin, *Angew. Chem. Int. Ed.*, 1974, **13**, 649.

3 (a) H. Weidel and M. Russo, *Monatshefte für Chemie und verwandte Teile anderer Wissenschaften*, **3**, 850; (b) L. Michaelis, *Biochem. Zeitschrift*, 1932, **250**, 564; (c) L. A. Summers, *The Bipyridinium Herbicides*, Academic Press, 1980; (d) P. Monk, *viologens*, Wiley, 1998.

4 (a) J. Vavra, L. Severa, P. Svec, I. Cisarova, D. Koval, P. Sazelova, V. Kasicka and F. Teply, *Eur. J. Org. Chem.,* 2012, 489; (c) J. Vavra, L. Severa, I. Cisarova, B. Klepetarova, D. Saman, D. Koval, V. Kasicka and F. Teply, *J. Org. Chem.*, 2013, **78**, 1329.

5 L. Pospisil, F. Teply, M. Gal, L. Adriaenssens, M. Horacek and L. Severa, *Phys. Chem. Chem. Phys.*, 2010, **12**, 1550.

6 L. Adriaenssens, L. Severa, D. Koval, I. Cisarova, M. M. Belmonte, E. C. Escudero-Adan, P. Novotna, P. Sazelova, J. Vavra, R. Pohl, D. Saman, M. Urbanova, V. Kasicka and F. Teply, *Chem. Sci.*, 2011, **2**, 2314.

7 L. Severa, M. Oncak, D. Koval, R. Pohl, D. Saman, I. Cisarova, P. E. Reyes-Gutierrez, P. Sazelova, V. Kasicka, F. Teply and P. Slavicek, *Angew. Chem. Int. Ed.*, 2012, **51**, 11972.

8 P. E. Reyes-Gutierrez, M. Jirasek, L. Severa, P. Novotna, D. Koval, P. Sazelova, J. Vavra, A. Meyer, I. Cisarova, D. Saman, R. Pohl, P. Stepanek, P. Slavicek, B. J. Coe, M. Hajek, V. Kasicka, M. Urbanova and F. Teply, *Chem. Commun.*, 2015, **51**, 1583.

9 M. R. Sonawane, in *Faculty of Science: Department of Organic Chemistry* Charles University in Prague, Prague, 2014, p. 242.

10 (a) P. Belenky, K. L. Bogan and C. Brenner, *Trends Biochem. Sci.*, 2007, **32**, 12; (b) A. D. Vinogradov, *Biochim. Biophys. Acta.*, 2008, **1777**, 729.

11 (a) Cicero A. F., Baggioni A., Adv. Exp. Med. Biol., 2016, **928**, 27; (b) Yin J., Xing H., Ye J., Metabolism, 2008, **57**, 712.

12 L. Grycová, J. Dostál and R. Marek, *Phytochemistry*, 2007, **68**, 150.

13 F. R. Stermitz, P. Lorenz, J. N. Tawara, L. A. Zenewicz and K. Lewis, *Proc. Natl. Acad. Sci. U.S.A.*, 2000, **97**, 1433.

14 Wu H. L.; Hsu C. Y.; Liu W. H.; Yung B. Y. *Int. J. Cancer*, 1999, **81**, 923.

15 M. Freile, F. A. Giannini, M. Sortino, M. Zamora, A. Juárez, S. Zacchino and R. D. Enriz, *Acta Farmacéutica Bonaerense,* 2006, **25**, 83.

16 A. Shirwaikar, A. Shirwaikar, K. Rajendran and I. S. R. Punitha, *Biol. Pharm. Bull.,* 2006, **29**, 1906.

17 J. L. Vennerstrom and D. L. Klayman, *J. Med. Chem.*, 1988, **31**, 1084.

18 S. K. Kulkarni and A. Dhir, *European J. Pharmacol.*, 2008, **589**, 163.

19 (a) R. K.Y. Zee-Cheng, K. D. Paull and C. C. Cheng, *J. Med. Chem.*, 1974, **17**, 347; (b) R. K. Y. Zee-Cheng and C. C. Cheng, *J. Med. Chem.*, 1976, **19**, 882.

20 (a) M. Franceschin, L. Rossetti, A. D'Ambrosio, S. Schirripa, A. Bianco, G. Ortaggi, M. Savino, C. Schultes and S. Neidle, *Bioorg. Med. Chem. Lett.*, 2006, **16**, 1707; (b) W.-J. Zhang, T.-M. Ou, Y.-J. Lu, Y.-Y. Huang, W.-B. Wu, Z.-S. Huang, J.-L. Zhou, K.-Y. Wong and L.-Q. Gu, *Bioorg. Med. Chem. Lett.*, 2007, **15**, 5493.

21 (a) B. Zamiri, K. Reddy, R. B. Jr. Macgregor, C. E. Pearson, *J. Biol. Chem.*, 2014, **289**, 4653; (b) L. Aixiao, M. Francois, B. Florent, D. Michel, W. Baoshan, Z. Xiang, W. Ping, *Eur. J. Med. Chem.*, 2010, **45**, 983; (c) E. Salvati, C. Leonetti, A. Rizzo , M. Scarsella, M. Mottolese, R. Galati, I. Sperduti, M. F. Stevens, M. D'Incalci, M. Blasco, G. Chiorino, S. Bauwens, B. Horard, E. Gilson, A. Stoppacciaro, G. Zupi, A. Biroccio, *J. Clin. Invest.*, 2007, **117**, 3236; (d) W. J. Chung, B. Heddi, F. Hamon, M. P. Teulade-Fichou, A. T. Phan, *Angew. Chem. Int. Ed.*, 2014, **53**, 999; (e) D. Verga, F. Hamon, F. Poyer, S. Bombard, M. P. Teulade-Fichou, *Angew. Chem. Int. Ed.*, 2014, **53**, 994.

22 M. Earle, P. Wasserscheid, P. Schulz, H. Olivier-Bourbigou, F. Favre, M. Vaultier, A. Kirschning, V. Singh, A. Riisager, R. Fehrmann and S. Kuhlmann, in *Ionic Liquids in Synthesis*, Wiley-VCH Verlag GmbH & Co. KGaA, 2008, pp. 265.

23 J.-f. Liu, G.-b. Jiang, J.-f. Liu and J. Å. Jönsson, *Trends Anal. Chem.; TrAC*, 2005, **24**, 20.

24 M. Antonietti, D. Kuang, B. Smarsly and Y. Zhou, *Angew. Chem. Int. Ed.*, 2004, **43**, 4988.

25 (a) P. Wasserscheid and W. Keim, *Angew. Chem. Int. Ed.*, 2000, **39**, 3772; (b) R. Sheldon, *Chem. Commun.*, 2001, 2399; (c) V. I. Pârvulescu and C. Hardacre, *Chem. Rev.*, 2007, **107**, 2615.

26 (a) C. E. Song, *Chem. Commun.*, 2004, 1033; (b) P. Domínguez de María, *Angew. Chem. Int. Ed.*, 2008, **47**, 6960.

27 C. Reichardt, *Chem. Rev.*, 1994, **94**, 2319.

28 C. L. Bird and A. T. Kuhn, *Chem. Soc. Rev.*, 1981, **10**, 49.

29 M. I. Knyazhanskii, Y. R. Tymyanskii, V. M. Feigelman and A. R. Katritzky, *Heterocycles*, 1987, **26**, 2963.

30 (a) C. R. Bock, T. J. Meyer and D. G. Whitten, *J. Am. Chem. Soc.*, 1974, **96**, 4710; (b) H. Dürr and S. Bossmann, *Acc. Chem. Res.*, 2001, **34**, 905.

31 C. M. Ronconi, J. F. Stoddart, V. Balzani, M. Baroncini, P. Ceroni, C. Giansante and M. Venturi, *Chem. Eur. J.*, 2008, **14**, 8365.

32 Z. Gan, A. Okui, Y. Kawashita and M. Hayashi, *Chem. Lett.*, 2008, **37**, 1302.

33 (a) H. Wynberg, *Acc. Chem. Res.*, 1971, **4**, 65; (b) W. H. Laarhoven and W. J. C. Prinsen, in *Stereochemistry*, eds. F. Vögtle and E. Weber, Springer Berlin Heidelberg, Berlin, Heidelberg, 1984, pp. 63; (c) F. Vögtle, *Fascinating molecules in organic chemistry*, John Wiley & Sons Inc, 1992; (d) Y. Shen and C.-F. Chen, *Chem. Rev.*, 2012, **112**, 1463.

34 M. Flammang-Barbieux, J. Nasielski and R. H. Martin, *Tetrahedron Lett.*, 1967, **8**, 743.

35 K. E. S. Phillips, T. J. Katz, S. Jockusch, A. J. Lovinger and N. J. Turro, *J. Am. Chem. Soc.*, 2001, **123**, 11899.

36 (a) M. Gingras and F. Dubois, *Tetrahedron Lett.*, 1999, **40**, 1309; (b) A. Rajca, H. Wang, M. Pink and S. Rajca, *Angew. Chem.,* 2000, **112**, 4655; (c) A. Rajca, H. Wang, M. Pink and S. Rajca, *Angew. Chem. Int. Ed.*, 2000, **39**, 4481.

37 (a) D. C. Harrowven, M. I. T. Nunn and D. R. Fenwick, *Tetrahedron Lett.,* 2002, **43**, 7345; (b) D. C. Harrowven, M. I. T. Nunn and D. R. Fenwick *Tetrahedron Lett.*, 2002, **43**, 3189.

38 S. K. Collins, A. Grandbois, M. P. Vachon and J. Côté, *Angew. Chem. Int. Ed.*, 2006, **45**, 2923.

39 (a) C. Romero, D. Peña, D. Pérez and E. Guitián, *J. Org. Chem.*, 2008, **73**, 7996; (b) D. Peña, D. Pérez, E. Guitián and L. Castedo, *Org. Lett.*, 1999, **1**, 1555; (c) D. Peña, A. Cobas, D. Pérez, E. Guitián and L. Castedo, *Org. Lett.*, 2003, **5**, 1863; (d) D. Peña, A. Cobas, D. Pérez, E. Guitián and L. Castedo, *Org. Lett.*, 2000, **2**, 1629.

40 (a) F. Teplý, I. G. Stará, I. Starý, A. Kollárovič, D. Šaman, L. Rulíšek and P. Fiedler, *J. Am. Chem. Soc.*, 2002, **124**, 9175; (b) I. G. Stara, I. Stary, A. Kollarovic, F. Teply, D. Saman and P. Fiedler, *Collect. Czech. Chem. Commun.*, 2003, **68**, 917; (c) F. Teplý, I. G. Stará, I. Starý, A. Kollárovič, D. Šaman, Š. Vyskočil and P. Fiedler, *J. Am. Chem. Soc.*, 2003, **68**, 5193.

41 (a) S. Han, D. R. Anderson, A. D. Bond, H. V. Chu, R. L. Disch, D. Holmes, J. M. Schulman, S. J. Teat, K. P. C. Vollhardt and G. D. Whitener, *Angewandte Chemie International Edition*, 2002, **41**, 3227; (b) S. Han, A. D. Bond, R. L. Disch, D. Holmes, J. M. Schulman, S. J. Teat, K. P. C. Vollhardt and G. D. Whitener, *Angew. Chem. Int. Ed.*, 2002, **41**, 3223.

42 K. Tanaka, N. Fukawa, T. Suda and K. Noguchi, *Angew. Chem. Int. Ed.*, 2009, **48**, 5470.

43 M. R. Crittall, H. S. Rzepa and D. R. Carbery, *Org. Lett.*, 2011, **13**, 1250.

44 S. Arai, M. Ishikura and T. Yamagishi, *J. Chem. Soc., Perkin Trans.*, 1998, 1561.

45 H. A. Staab, M. Diehm and C. Krieger, *Tetrahedron Lett.*, 1994, **35**, 8357.

46 (a) N. Takenaka, R. S. Sarangthem and B. Captain, *Angew. Chem. Int. Ed.*, 2008, **47**, 9708; (b) J. Chen and N. Takenaka, *Chem. Eur. J.*, 2009, **15**, 7268; (c) M. Šámal, J. Míšek, I. G. Stará and I. Starý, *Collect. Czech. Chem. Commun.*, 2009, **74**, 1151; (d) A. Terfort, H. Görls and H. Brunner, *Synthesis*, 1997, **1997**, 79; (e) M. T. Reetz and S. Sostmann, *J. Organomet.*

Chem., 2000, **603**, 105; (f) M. T. Reetz, E. W. Beuttenmüller and R. Goddard, *Tetrahedron Lett.*, 1997, **38**, 3211.

47 J. Misek, F. Teply, I. G. Stara, M. Tichy, D. Saman, I. Cisarova, P. Vojtisek and I. Stary, *Angew Chem. Int. Ed.*, 2008, **47**, 3188.

48 F. H. Allen, O. Kennard, D. G. Watson, L. Brammer, A. G. Orpen and R. Taylor, *J. Chem. Soc., Perkin Trans. 2*, 1987, S1.

49 (a) M. S. Newman, W. B. Lutz and D. Lednicer, *J. Am. Chem. Soc.*, 1955, **77**, 3420; (b) J. M. Brown, I. P. Field and P. J. Sidebottom, *Tetrahedron Lett.*, 1981, **22**, 4867.

50 (a) B. Busson, M. Kauranen, C. Nuckolls, T. J. Katz and A. Persoons, *Phy. Rev. Lett.*, 2000, **84**, 79; (b) T. Verbiest, S. V. Elshocht, M. Kauranen, L. Hellemans, J. Snauwaert, C. Nuckolls, T. J. Katz and A. Persoons, *Science*, 1998, **282**, 913; (c) R. Amemiya and M. Yamaguchi, *Chem. Rec.,* 2008, **8**, 116; (d) R. Amemiya and M. Yamaguchi, *Org. Biomol. Chem.*, 2008, **6**, 26.

51 E. Murguly, R. McDonald and N. R. Branda, *Org. Lett.*, 2000, **2**, 3169.

52 (a) Y. Kitahara and K. Tanaka, *Chem. Commun.*, 2002, 932; (b) J. E. Field, T. J. Hill and D. Venkataraman, *J. Org. Chem.*, 2003, **68**, 6071.

53 T. Caronna, R. Sinisi, M. Catellani, L. Malpezzi, S. V. Meille and A. Mele, *Chem. Commun.*, 2000, 1139.

54 D. J. Wolstenholme, C. F. Matta and T. S. Cameron, *J. Phy. Chem. A*, 2007, **111**, 8803.

55 (a) J. Vávra, L. Severa, I. Císařová, B. Klepetářová, D. Šaman, D. Koval, V. Kašička and F. Teplý, *J. Org. Chem.*, 2013, **78**, 1329; (b) R. H. Martin and M. J. Marchant, *Tetrahedron*, 1974, **30**, 343.

56 (a) H. Wynberg and M. B. Groen, *J. Am. Chem. Soc.*, 1968, **90**, 5339; (b) R. H. Martin, M. Flammang-Barbieux, J. P. Cosyn and M. Gelbcke, *Tetrahedron Lett.*, 1968, **9**, 3507.

57 (a) T. J. Katz, L. Liu, N. D. Willmore, J. M. Fox, A. L. Rheingold, S. Shi, C. Nuckolls and B. H. Rickman, *J. Am. Chem. Soc.*, 1997, **119**, 10054; (b) K. Paruch, L. Vyklický, D. Z. Wang, T. J. Katz, C. Incarvito, L. Zakharov and A. L. Rheingold, *J. Org. Chem.*, 2003, **68**, 8539.

58 M. T. Reetz and S. Sostmann, *Tetrahedron*, 2001, **57**, 2515.

59 (a) L. Owens, C. Thilgen, F. Diederich and C. B. Knobler, *Helv. Chimica Acta*, 1993, **76**, 2757; (b) D. J. Weix, S. D. Dreher and T. J. Katz, *J. Am. Chem. Soc.*, 2000, **122**, 10027.

60 C. A. Daul, I. Ciofini and V. Weber, *Int. J. Quantum Chem.*, 2003, **91**, 297.

61 C. Nuckolls and T. J. Katz, *J. Am. Chem. Soc.*, 1998, **120**, 9541.

62 A. Montali, C. Bastiaansen, P. Smith and C. Weder, *Nature*, 1988, **392**, 261.

63 (a) B. B. Hassine, M. Gorsane, J. Pecher and R. H. Martin, *Bull. Soc. Chim. Belg.*, 1985, **94**, 597; (b) B. B. Hassine, M. Gorsane, J. Pecher and R. H. Martin, *Bull. Soc. Chim. Belg.*, 1985, **94**, 759; (c) B. B. Hassine, M. Gorsane, F. Geerts-Evrard, J. Pecher, R. H. Martin and D. Castelet, *Bull. Soc. Chim. Belg.*, 1986, **95**, 547; (d) B. B. Hassine, M. Gorsane, J. Pecher and R. H. Martin, *Bull. Soc. Chim. Belg.*, 1986, **95**, 557; (e) B. B. Hassine, M. Gorsane, J. Pecher and R. H. Martin, *Bull. Soc. Chim. Belg.*, 1987, **96**, 801.

64 S. D. Dreher, T. J. Katz, K.-C. Lam and A. L. Rheingold, *J. Org. Chem.*, 2000, **65**, 815.

65 (a) I. G. Sanchez, M. Samal, J. Nejedly, M. Karras, J. Klivar, J. Rybacek, M. Budesinsky, L. Bednarova, B. Seidlerova, I. G. Stara and I. Stary, *Chem. Commun.*, 2017, **53,** 4370; (b) Z. Krausova, P. Sehnal, B. P. Bondzic, S. Chercheja, P. Eilbracht, I. G. Stara, D. Saman and I. Stary, *Eur. J. Org. Chem.* 2011, 3849; (c) K. Yamamoto, T. Shimizu, K. Igawa, K. Tomooka, G. Hirai, H. Suemune and K. Usui, *Sci. Rep.*, 2016, **6**, 36211.

66 (a) K. Tanaka, *Chem. Commun.*, 1998, 1141; (b) K. Tanaka, H. Osuga and Y. Kitahara, *J. Chem. Soc., Perkin Trans., 2*, 2000, 2492; (c) *J. Org. Chem.*, 2002, **67**, 1795; (c) J.-i. Nishida, T. Suzuki, M. Ohkita and T. Tsuji, *Angew. Chem. Int. Ed.*, 2001, **40**, 3251; (d) T. Suzuki, Y. Ishigaki, T. Iwai, H. Kawai, K. Fujiwara, H. Ikeda, Y. Kano and K. Mizuno, *Chem. Eur. J.*, 2009, **15**, 9434.

67 (a) Y. Ooyama, G. Ito, H. Fukuoka, T. Nagano, Y. Kagawa, I. Imae, K. Komaguchi and Y. Harima, *Tetrahedron*, 2010, **66**, 7268; (b) Y. Ooyama, A. Ishii, Y. Kagawa, I. Imae and Y. Harima, *New J. Chem.*, 2007, **31**, 2076; (c) Y. Ooyama, Y. Shimada, Y. Kagawa, I. Imae and Y. Harima, *Org. Biomol. Chem.*, 2007, **5**, 2046; (d) Y. Ooyama, Y. Shimada, Y. Kagawa, Y. Yamada, I. Imae, K. Komaguchi and Y. Harima, *Tetrahedron Lett.*, 2007, **48**, 9167.

68 M. Nakazaki, K. Yamamoto, T. Ikeda, T. Kitsuki, Y. Okamoto, *J. Chem. Soc., Chem. Commun.*, 1983, 787.

69 D. Z. Wang and T. J. Katz, *J. Org. Chem.*, 2005, **70**, 8497.

70 O. Kel, A. Fürstenberg, N. Mehanna, C. Nicolas, B. Laleu, M. Hammarson, B. Albinsson, J. Lacour and E. Vauthey, *Chem. Eur. J.*, 2013, **19**, 7173.

71 (a) Y. Xu, Y. X. Zhang, H. Sugiyama, T. Umano, H. Osuga and K. Tanaka, *J. Am. Chem. Soc.*, 2004, **126**, 6566; (b) Y. Xu, H. Sugiyama, K. Tanaka and H. Osuga, *Nucleic Acids Symp. Ser.*, 2004, **48**, 87.

72 (a) K.-i. Shinohara, Y. Sannohe, S. Kaieda, K.-i. Tanaka, H. Osuga, H. Tahara, Y. Xu, T. Kawase, T. Bando and H. Sugiyama, *J. Am. Chem. Soc.*, 2010, **132**, 3778; (b) Y. Xu, S. Yamazaki, H. Osuga and H. Sugiyama, *Nucleic Acids Symp. Ser.*, 2006, **50**, 183.

73 K. Kawara, G. Tsuji, Y. T. and S. Sasaki, *Chem. Eur. J.*, 2017, **23**, 1763.

74 T. Verbiest and A. Persoons, in Materials Chirality: Topics in Stereochemistry, Eds. M. M. Green, R. J. M. Nolte, E. W. Meijer, S. E. Denmark, J. Siegel, Wiley: New York, 2003; Vol. 24, pp 519−570.

75 U. Gubler and C. Bosshard, *Nat. Mater.*, 2002, **1**, 209.

76 (a) *Nonlinear optical properties of organic molecules and crystals*, D. S. Chemla and J. Zyss, Eds., 1987; Vol. 1 and 2; (b) *Molecular Nonlinear Optics: Materials, Physics and Devices*; J. Zyss, Ed.: Academic Press: Boston, 1994; (c) *Nonlinear Optics*, C. Bosshard, K. Sutter, P. Pretre, J. Hulliger, M. Florsheimer, P. Kaatz, P. Gunter, Eds., Gordon & Breach: Amsterdam, The Netherlands, 1995; Vol. 1; (c) *Nonlinear Optics of Organic Molecules and Polymers*, H. S. Nalwa, S. Miyatra, Eds., CRC Press: BocaRaton, FL., 1997.

77 B. J. Coe, *Chem. Eur. J.*, 1999, **5**, 2464.

78 S. R. Marder, J. W. Perry, W. P. Schaefer, *Science*, 1989, **245**, 626.

79 B. J. Coe, J. -D. Foulon, T. A. Hamor, C. J. Jones, J. A. McCleverty, D. Bloor, G. H. Cross, T. L. Axon, *J. Chem. Soc., Dalt. Trans.*, 1994, **23**, 3427.

80 S. M. LeCours, H. –W. Guan, S. G. DiMagno, C. H. Wang, M. J. Therien, *J. Am. Chem. Soc.*, 1996, **118**, 1497.

81 M. Blanchard-Desce, V. Alain, P. V. Bedworth, S. R. Marder, A. Fort, C. Runser, M. Barzoukas, S. Lebus, R. Wortmann, *Chem. Eur. J.*, 1997, **3**, 1091.

82 G. R. Meredith, *Rev. Sci. Instruments*, 1982, **53**, 48.

83 P. Franken, A. Hill, C. Peters, G. Weinreich, *Phys. Rev. Lett.*, 1961, **7**, 118.

84 Y. R. Shen, Nature, 1989, **337**, 519.

85 E. Hendrickx, K. Clays, A. Persoons, *Acc. Chem. Res*., 1998, **31**, 675.

86 J. L. Oudar, J. Zyss, *Phys. Rev. A*, 1982, **26**, 2016.

87 T. Verbiest, S. Sioncke, A. Persoons, L. VyKlicky, T. J. Katz, *Angew. Chem. Int. Ed.*, 2002, **41**, 3882

88 (a) L. E. R. Buckley, B. J. Coe, D. Rusanova, V. D. Joshi, S. Sanchez,́ M. Jirasek,́ J. Vavra,́ D. Khobragade, L. Severa, I. Císarovaˇ, D. Šaman, R. Pohl, K. Clays, G. Depotter, B. S. Brunschwig and F. Teply, *J. Phys. Chem. A*, 2017, **121**, 5842; (b) B. J. Coe, D. Rusanova, V. D. Joshi, S. Sanchez,́ J. Vavra,́ D. Khobragade, L. Severa, I. Císarovaˇ, D. Šaman, R. Pohl, K. Clays, G. Depotter, B. S. Brunschwig and F. Teply, *J. Org. Chem.*, 2016, **81**, 1912; (c) L. E. R. Buckley, B. J. Coe, D. Rusanova, V. D. Joshi, S. Sanchez,́ J. Vavra,́ D. Khobragade, L. Severa, M. Jirasek,́ I. Císarovaˇ, D. Šaman, R. Pohl, K. Clays, G. Depotter, B. S. Brunschwig and F. Teply, *Dalton Trans.*, 2017, **46**, 1052.

89 N. M., J. J. and K. B. 2006., eds., *Viologens, IUPAC Compendium of Chemical Terminology (Online Ed.). doi:10.1351/goldbook.V06624*, 2006.

90 R. C. Brian, R. F. Homer, J. Stubbs and R. L. Jones, *Nature*, 1958, **181**, 446.

91 L. Striepe and T. Baumgartner, *Chem. Eur. J.*, 2017, Doi: 10.1002/chem.201703348.

92 E. A. Neal, S. M. Goldup, *Chem. Commun.*, 2014, **50**, 5128.

93 Y. Song, X. Huang, H. Hua, Q. Wang, *Dyes Pigm.*, 2017, **137**, 229.

94 D. R. Wheeler, J. Nichols, D. Hansen, M. Andrus, S. Choi and G. D. Watt, *J. Electrochem. Soc.*, 2009, **156**, B1201.

95 B. L. Allwood, F. H. Kohnke, A. M. Z. Slawin, J. F. Stoddart and D. J. Williams, *J. Chem. Soc., Chem. Commun.*, 1985, 311.

96 M. Lahav, K. T. Ranjit, E. Katz and I. Willner, *Chem. Commun.*, 1997, 259.

97 (a) J. Winsberg, T. Hagemann, T. Janoschka, M. D. Hager, U. S. Schubert, *Angew. Chem. Int. Ed*., 2017, **56**, 686; (b) A. Ghosh, S. Mitra, *RSC Adv.*, 2015, **5**, 105632.

98 S. Asaftei and E. De Clercq, *J. Med. Chem.*, 2010, **53**, 3480.

99 H. Mustroph, in *Ullmann's Encyclopedia of Industrial Chemistry*, Wiley-VCH Verlag GmbH & Co. KGaA, 2000.

100 K. Hunger, *Industrial dyes: chemistry, properties, applications*, John Wiley & Sons, 2007.

101 A. E. Siegrist: .Die Anwendung optischer Aufheller in der Papierindustrie., *Papier (Darmstadt),* 1954*,* **8**, 109.

102 R. Zweidler: .Einführung in die Chemie der optischen Aufheller., *Textilveredlung*, 1969, **4,** 75.

103 T. Förster: *Fluoreszenz organischer Verbindungen*, Vandenhoek und Ruprecht, Göttingen, 1951.

104 F. P. Schäfer: *Dye Lasers*, Springer Verlag, Berlin 1973.

105 (a) H. Gold: ‘‘Fluorescent Brightening Agents’’ K. Venkataraman (ed.) in ‘‘*The Chemistry of Synthetic Dyes’’*, vol. V, Academic Press, New York.London 1971, 535; (b) M. Zahradnik: *The Production and Application of Fluorescent Brightening Agents*, John Wiley & Sons, Chichester 1982.

106 L. Strekowski, *Heterocyclic polymethine dyes: synthesis, properties and applications*, Springer, 2008.

107 T. G. Deligeorgiev, D. A. Zaneva, H. E. Katerinopoulos and V. N. Kolev, *Dyes Pigm.*, 1999, **41**, 49.

108 (a) S. R. Mujumdar, R. B. Mujumdar, C. M. Grant and A. S. Waggoner, *Bioconjug. Chem.*, 1996, **7**, 356; (b) B. Chipon, G. Clavé, C. Bouteiller, M. Massonneau, P.-Y. Renard and A. Romieu, *Tetrahedron Lett.*, 2006, **47**, 8279.

109 T. Tani, *J. Imaging sci. Technol.*, 1995, **39**, 31.

110 Z. Dai, L. Qun and B. Peng, *Dyes Pigm.*, 1998, **36**, 243.

111 R. Reisfeld, A. Weiss, T. Saraidarov, E. Yariv and A. Ishchenko, *Polymers Adv. Tech.*, 2004, **15**, 291.

112 (a) M. Liang, W. Xu, F. Cai, P. Chen, B. Peng, J. Chen and Z. Li, *J. Phy. Chem. C*, 2007, **111**, 4465; (b) Q. Zhang, C. S. Dandeneau, X. Zhou and G. Cao, *Adv. Mater.*, 2009, **21**, 4087.

113 (a) C. Nasr, S. Hotchandani, P. V. Kamat, S. Das, K. G. Thomas and M. George, *Langmuir*, 1995, **11**, 1777; (b) F. Tang, H. Shi, D. Gu, X. Tang and F. Gan, in *Optical Science, Engineering and Instrumentation'97*, International Society for Optics and Photonics, 1997, pp. 210.

114 R. B. Mujumdar, L. A. Ernst, S. R. Mujumdar, C. J. Lewis and A. S. Waggoner, *Bioconjug. Chem.*, 1992, **4**, 105.

115 L. G. Lee, C. H. Chen and L. A. Chiu, *Cytometry*, 1986, **7**, 508.

116 T. Deligeorgiev, I. Timcheva, V. Maximova, N. Gadjev, A. Vassilev, J.-P. Jacobsen and K.-H. Drexhage, *Dyes Pigm.*, 2004, **61**, 79.

117 B. Nordén and F. Tjerneld, *Biophys. Chem.*, 1976, **6**, 31.

118 H. Ihmels and D. Otto, in *Supermolecular dye chemistry*, Springer, 2005, pp. 161.

119 R. J. Williams, M. Lipowska, G. Patonay and L. Strekowski, *Anal. Chem.*, 1993, **65**, 601;

120 M. J. Baars and G. Patonay, *Anal. Chem.*, 1999, **71**, 667.

121 J. Sowell, R. Parihar and G. Patonay, *J. Chromatogr. B: Biomed. Sci. Appl.*, 2001, **752**, 1.

122 N. Karton-Lifshin, L. Albertazzi, M. Bendikov, P. S. Baran and D. Shabat, *J. Am. Chem. Soc.*, 2012, **134**, 20412.

123 (a) W. König, *J. Prakt. Chem.*, 1912, **86**, 166; (b) H. Barbier and *Bull. Soc. Chim. Fr.*, 1920, **27**, 427.

124 A. Vasilev, T. Deligeorgiev, N. Gadjev, S. Kaloyanova, J. J. Vaquero, J. Alvarez-Builla and A. G. Baeza, *Dyes Pigm.*, 2008, **77**, 550.

125 (a) M. A. Gaffield and W. J. Betz, *Nat. Protoc.*, 2007, **1**, 2916; (b) S. O. Rizzoli, D. A. Richards and W. J. Betz, *J. Neurocytol.*, 2003, **32**, 539;

(c) https://tools.thermofisher.com/content/sfs/manuals/mp34653.pdf, 2005.
126 G. R. Rosania, J. W. Lee, L. Ding, H.-S. Yoon and Y.-T. Chang, *J. Am. Chem. Soc.*, 2003, **125**, 1130.
127 (a) J. W. Lee, M. Jung, G. R. Rosania and Y.-T. Chang, *Chem. Commun.*, 2003, 1852; (b) S. Feng, Y. Kyung Kim, S. Yang and Y.-T. Chang, *Chem. Commun.*, 2010, **46**, 436.
128 S. Wang and Y.-T. Chang, *Chem. Commun.* 2008, 1173.
129 Q. Li, Y. Kim, J. Namm, A. Kulkarni, G. R. Rosania, Y.-H. Ahn and Y.-T. Chang, *Chem. Biol.*, 2006, **13**, 615.
130 R. Krieg, A. Eitner and K.-J. Halbhuber, *Acta Histochem.*, 2011, **113**, 682.
131 L. M. Loew, *Pure Appl. Chem.*, 1996, **68**, 1405.
132 A. Obaid, L. Loew, J. Wuskell and B. Salzberg, *J. Neurosci. Methods*, 2004, **134**, 179.
133 P. Yan, C. D. Acker, W.-L. Zhou, P. Lee, C. Bollensdorff, A. Negrean, J. Lotti, L. Sacconi, S. D. Antic and P. Kohl, *Proc. Natl. Acad. Sci. U.S.A.*, 2012, **109**, 20443.
134 Y. V. Fedorov, O. A. Fedorova, E. N. Andryukhina, S. P. Gromov, M. V. Alfimov, L. G. Kuzmina, A. V. Churakov, J. A. K. Howard and J. J. Aaron, *New J. Chem.*, 2003, **27**, 280.
135 *Cyclophane Chemistry for the 21st Century*, 2002.
136 F. Teply, M. Hajek, E. Kuzmova, J. Kozak, V. Komarova, P. Hubalkova, P. E. Reyes-Gutierrez, M. Jirasek, M. R. Sonawane and V. D. Joshi, WO/2015/180701, 2015.
137 (a) F. Pan, G. Knöpfle, C. Bosshard, S. Follonier, R. Spreiter, M. S. Wong, P. Günter, *Appl. Phys. Lett.*, 1996, **69**, 13; (b) U. Meier, M. Bösch, C. Bosshard, F. Pan, P. Günter, *J. Appl. Phys.*, 1998, **83**, 3486; (c) M. Thakur, J. J. Xu, A. Bhowmik, L. G. Zhou, *Appl. Phys. Lett.*, 1999, **74**, 635; (d) F. Pan, K. McCallion, M. Chiapetta, *Appl. Phys. Lett.*, 1999, **74**, 492; e) A. K. Bhowmik, S. Tan, A. C. Ahyi, A. Mishra, M. Thakur, *Polym. Mater. Sci. Eng.*, 2000, **83**, 169.
138 T. Verbiest, S. Houbrechts, M. Kauranen, K. Clays and A. Persoons, *J. Mater. Chem.*, 1997, **7**, 2175.
139 O. -K. Kim, L. -S. Choi, H. -Y. Zhang, X. H. He and Y. -H. Shih, *J. Am. Chem. Soc.*, 1996, **118**, 12220.
140 (a) B. J. Coe, J. Fielden, S. P. Foxon, I. Asselberghs, K. Clays, V. Cleuvenbergen, B. Brunschwig, *Organometallics*, 2011, **30**, 5731; (b) B. J. Coe, J. Fielden, S. P. Foxon, M. Helliwell, B. S. Brunschwig, I. Asselberghs, K. Clays, J. Olesiak, K. Matczyszyn, M. J. Samoc, *Phys. Chem. A*, 2010, **114**, 12028; (c) B. J. Coe, J. Fielden, S. P. Foxon, M. Helliwell, M. Helliwell, B. S. Brunschwig, I. Asselberghs, K. Clays, J. Garín, J. J. Orduna, *J. Am. Chem. Soc.*, 2010, **132**, 10498; (d) B. J. Coe, J. A. Harris, B. S. Brunschwig, J. Garín, J. J. Orduna, *J. Am. Chem. Soc.*, 2005, **127**, 3284.
141 J. E. Reeve, H. L. Anderson and K. Clays, *Phys. Chem. Chem. Phys.*, 2010, **12**, 13484.
142 P. Yan, A. C. Millard, M. Wei and L. M. Loew, *J. Am. Chem. Soc.*, 2006, **128**, 11030.
143 L. Sacconi, D. A. Dombeck and W. W. Webb, *Proc. Natl. Acad. Sci. U. S. A.*, 2006, **103**, 3124.
144 http://www.rainbowphotonics.com/prod_dast.php
145 R. J. Linhardt, *Chemistry and industry*, 1991.
146 (a) I. Capila and R. J. Linhardt, *Angew. Chem. Int. Ed.*, 2002, **41**, 390; (b) J. R. Bishop, M. Schuksz and J. D. Esko, *Nature*, 2007, **446**, 1030; (c) C. Guo, B. Wang, L. Wang and B. Xu, *Chem. Commun.*, 2012, **48**, 12222.
147 (a) J. D. Esko and S. B. Selleck, *Annu. Rev. Biochem.*, 2002, **71**, 435; (b) C. Guo, X. Fan, H. Qiu, W. Xiao, L. Wang and B. Xu, *Phys. Chem. Chem. Phy.*, 2015, **17**, 13301.
148 (a) R. Barbucci, A. Magnani, S. Lamponi and A. Albanese, *Polymers Adv. Tech.*, 1996, **7**, 675; (b) D. L. Rabenstein, *Nat. Prod. Rep.*, 2002, **19**, 312; (c) S. Middeldorp, *Thromb. Res.*, 2008, **122**, 753.
149 (a) B. Girolami and A. Girolami, in *Seminars in thrombosis and hemostasis*, Copyright© 2006 by Thieme Medical Publishers, Inc., 333 Seventh Avenue, New York, NY 10001, USA., 2006, pp. 803; (b) T. E. Warkentin, M. N. Levine, J. Hirsh, P. Horsewood, R. S. Roberts, M. Gent and J. G. Kelton, *N. Engl. J. Med.*, 1995, **332**, 1330.
150 R. Balhorn, *Genome Biol.*, 2007, **8**, 227.

151 (a) M. Nybo and J. Madsen, *J.-J. Cai, D.-C. Jiang, D. Jia, S.-Y. Yan and Y.-Q. Wang, Clin. Ther.*, 2010, **32**, 1729; (b) Y.-Q. Chu, L.-J. Cai, D.-C. Jiang, D. Jia, S.-Y. Yan and Y.-Q. Wang, *Clin. Ther.*, 2010, **32**, 1729.

152 (a) G. J. Despotis, G. Gravlee, K. Filos and J. Levy, *J. Am. Soc. Anesthesiol.*, 1999, **91**, 1122; (b) P. Raymond, M. Ray, S. Callen and N. Marsh, *Perfusion*, 2003, **18**, 269; (c) J. W. Vandiver and T. G. Vondracek, *Pharmacotherapy: J. Human Pharmacol. Drug Ther.*, 2012, **32**, 546.

153 M. N. Levine, J. Hirsh, M. Gent, A. G. Turpie, M. Cruickshank, J. Weitz, D. Anderson and M. Johnson, *Arch. Intern. Med.*, 1994, **154**, 49.

154 (a) H. Qi, L. Zhang, L. Yang, P. Yu and L. Mao, *Anal. Chem.*, 2013, **85**, 3439; (b) J. Guo and S. Amemiya, *Anal. Chem.*, 2006, **78**, 6893; (c) G. Qu, G. Zhang, Z. Wu, A. Shen, J. Wang and J. Hu, *Biosens. Bioelectron.*, 2014, **60**, 124; (d) Z. Zhong and E. V. Anslyn, *J. Am. Chem. Soc.*, 2002, **124**, 9014; (e) G. A. Crespo, M. G. Afshar and E. Bakker, *Angew. Chem. Int. Ed.*, 2012, **51**, 12575.

155 A. T. Wright, Z. Zhong and E. V. Anslyn, *Angew. Chem. Int. Ed.*, 2005, **44**, 5679.

156 Y. Egawa, R. Hayashida, T. Seki and J.-i. Anzai, *Talanta*, 2008, **76**, 736.

157 S. V. Nalage, S. V. Bhosale, S. K. Bhargava and S. V. Bhosale, *Tetrahedron Lett.*, 2012, **53**, 2864.

158 S. M. Bromfield, A. Barnard, P. Posocco, M. Fermeglia, S. Pricl and D. K. Smith, *J. Am. Chem. Soc.*, 2013, **135**, 2911.

159 X. Gu, G. Zhang and D. Zhang, Analyst, 2012, **137**, 365.

160 L. Zeng, P. Wang, H. Zhang, X. Zhuang, Q. Dai and W. Liu, *Org. Lett.*, 2009, **11**, 4294.

161 H. Szelke, S. Schubel, J. Harenberg and R. Kramer, *Chem. Commun.*, 2010, **46**, 1667.

162 K.-Y. Pu and B. Liu, *Macromolecules*, 2008, **41**, 6636.

163 S. Wang and Y. –T. Chang, *Chem. Commun.*, 2008, **0**, 1173.

164 J. D. Watson and F. H. C. Crick, *Nature*, 1953, **171**, 737.

165 A. Ghosh and M. Bansal, *Acta Cryst. D*, 2003, **59**, 620.

166 H. S. Basu, B. G. Feuerstein, D. A. Zarling, R. H. Shaffer and L. J. Marton, *J. Biomol. Struct. Dyn.*, 1988, **6**, 299.

167 M. L. Bochman, K. Paeschke and V. A. Zakian, *Nat. Rev. Genet.*, 2012, **13**, 770.

168 G. B. Bauer and L. F. Povirk, *Nucleic Acids Res.*, 1997, **25**, 1211.

169 L. H. Hurley, *Nat. Rev. Cancer*, 2002, **2**, 188.

170 J. Reedijk, *Proc. Natl. Acad. Sci. USA*, 2003, **100**, 3611.

171 B. Clement and F. Jung, *Drug Metab. Dispos.*, 1994, **22**, 486.

172 L. D. Williams, M. Egli and Q. Gao, *Proc. Natl. Acad. Sci. USA*, 1990, **87**, 2225.

173 M. Palumbo, *Advances in DNA Sequence-Specific Agents*, Elsevier, 1997.

174 a) S. A Latt, G. Stetten, L. A. Juergens, H. F. Willard and C. D. Scher, *J. Histochem. Cytochem.*, 1975, **23**, 493; (b) J. Kapuscinski and W. Szer, *Nucleic Acids Res.*, 1979, **6**, 3519.

175 C. Bailly and J. P. Henichart, *Bioconjugate Chem.*, 1991, **2**, 379.

176 S. Kamitori and F. Takusagawa, *J. Am. Chem. Soc.*, 1994, **116**, 4154.

177 C. A. Frederick, L. D. Williams, G. Ughetto, G. A. Van der Marel, J. H. Van Boom, A. Rich and A. H. J. Wang, *Biochemistry*, 1990, **29**, 2538.

178 (a) C. Bailly, M. Collyn-D'Hooghe, D. Lantoine, C. Fournier, B. Hecquet, P. Fosse, J.-M. Saucier, P. Colson, C. Houssier and J. -P. Henichar, *Biochem. Pharmacol.*, 1992, **43**, 457; (b) R. Zhanga, X. Wua, L. J. Guziecb, F. S. Guziec Jr.b, G. –L. Cheea, J. C. Yalowichc and B. B. Hasinoff, *Bioorg. Med. Chem.*, 2010, **18**, 3974; (c) C. Bourdouxhe-Housiaux, P. Colson, C. Houssier, M. J. Waring and C. Bailly, *Biochemistry,* 1996, **35***,* 14.

179 Z. Zhenyu and H. Piet, *Curr. Med. Chem.*, 2001, **8**, 517.

180 (a) L. Adriaenssens, L. Severa, T. Salova, I. Cisarova, R. Pohl, D. Saman, S. V. Rocha, N. S. Finney, L. Pospisil, P. Slavicek and F. Teply, *Chem. Eur. J.*, 2009, **15**, 1072; (b) F. Teply, *Chem. Listy*, 2011, **105**, 506; (c) L. Severa, L. Adriaenssens, J. Vavra, D. Saman, I. Cisarova, P. Fiedler and F. Teply, *Tetrahedron*, 2010, **66**, 3537.

181 L. Severa, D. Koval, P. Novotna, M. Oncak, P. Sazelova, D. Saman, P. Slavicek, M. Urbanova, V. Kasicka and F. Teply, *New J.Chem.*, 2010, **34**, 1063.
182 G. Olbrechts, K. Clays and A. Persoons, *J. Opt. Soc. Am. B*, 2000, **17**, 1867.
183 J. L. Oudar and D. S. Chemla, *J. Chem. Phy.*, 1977, **66**, 2664.
184 (a) K. Clays and B. J. Coe, *Chem. Mater.*, 2003, **15**, 642; (b) B. J. Coe, J. A. Harris, I. Asselberghs, K. Wostyn, K. Clays, A. Persoons, B. S. Brunschwig, S. J. Coles, T. Gelbrich, M. E. Light, M. B. Hursthouse and K. Nakatani, *Adv. Funct. Mat.*, 2003, **13**, 347.
185 (a) G. U. Bublitz and and S. G. Boxer, *Annu. Rev. Phys. Chem.*, 1997, **48**, 213; (b) W. Liptay, *Excited states*, 1974, **1**, 129.
185 (a) J. C. Sauceda, R. M. Duke and M. Nitz, *ChemBioChem*, 2007, **8**, 391; (b) J. C. van Kerkhof, P. Bergveld and R. B. M. Schasfoort, *Biosens. Bioelectron.*, 1995, **10**, 269.
186 C. Würth, M. Grabolle, J. Pauli, M. Spieles and U. Resch-Genger, *Nat. Protoc.*, 2013, **8**, 1535.
187 https://www.thermofisher.com/cz/en/home/references/molecular-probes-the-handbook.html
188 *RNeasy Mini Handbook*, 2012, 23.
189 A. D. Boese and J. M. L. Martin, *J. Chem. Phys.*, 2004, **121**, 3405.
190 N. C. Garbett, P. A. Ragazzon and J. B. Chaires, *Nat. Protoc.*, 2007, **2**, 3166.
191 (a) P. C. Dedon, in *Curr. Protoc. Nucleic Acid Chem.*, 2001, ed. S. L. Beaucage, Chapter 8, Unit 8.1; (b) D. Suh and J. B. Chaires, *Bioorg. Med. Chem.*, 1995, **3**, 723.
192 O. Trott and A. J. Olson, *J. Comput. Chem.*, 2010, **31**, 455.
193 W. Humphrey, A. Dalke and K. Schulten, *J. Mol. Graph.*, 1996, **14**, 33.
194 G. Prism, *San Diego, CA, USA*, 1994.
195 http://www.molbiotools.com/dnacalculator.html.